

**Ongoing Face Recognition
Vendor Test (FRVT)**
Part 1: Verification

Patrick Grother
Mei Ngan
Kayee Hanaoka
Joyce C. Yang
Austin Hom

*Information Access Division
Information Technology Laboratory*

This publication is available free of charge from:
<https://www.nist.gov/programs-projects/face-recognition-vendor-test-frvt-ongoing>

2022/03/18

ACKNOWLEDGMENTS

The authors are grateful for the long-standing support and collaboration of the the Department of Homeland Security's Science & Technology Directorate (S&T) and the Office of Biometric Identity Management (OBIM).

Additionally, the authors are grateful to staff in the NIST Biometrics Research Laboratory for infrastructure supporting rapid evaluation of algorithms.

DISCLAIMER

Specific hardware and software products identified in this report were used in order to perform the evaluations described in this document. In no case does identification of any commercial product, trade name, or vendor, imply recommendation or endorsement by the National Institute of Standards and Technology, nor does it imply that the products and equipment identified are necessarily the best available for the purpose.

INSTITUTIONAL REVIEW BOARD

The National Institute of Standards and Technology's Research Protections Office reviewed the protocol for this project and determined it is not human subjects research as defined in Department of Commerce Regulations, 15 CFR 27, also known as the Common Rule for the Protection of Human Subjects (45 CFR 46, Subpart A).

FRVT STATUS

This report is a draft NIST Interagency Report, and is open for comment. It is the thirty sixth edition of the report since the first was published in June 2017. Prior editions of this report are maintained on the FRVT [website](#), and may contain useful information about older algorithms and datasets no longer used in FRVT.

FRVT remains open: All [four tracks](#) of the FRVT are open to new algorithm submissions.

2022-03-18 changes since 2022-02-23:

- ▷ We have added support for the detection of multiple people in a single image (see Section [1.2](#)). Specifically the API allows an algorithm to extract features from one or more faces it detects in an image. NIST scores such cases as a correct match when any detected face matches the reference photo, and as a false positive when either face matches a non-mated reference photo. The expected effect of doing this will be to improve reported false non-match rates, and to minimally elevate false match rates. This technique was only applied to images of type “border” and “kiosk”.
- ▷ We have added results for first algorithms from four developers: IntelliVIX, Kasikorn Labs, Lebentech Biometrics, and Wicket.
- ▷ We have added results for new algorithms from 10 returning developers: Chunghwa Telecom, Cloudmatrix, Beijing DeepSense Technologies, FarBar Inc, Imagus Technology Pty, Intellivision, Maxvision Technology, NHN Corp, Seventh Sense Artificial Intelligence, and Verigram.
- ▷ We have retired results for 4 algorithms per our policy to only list results for two algorithms per developer. Results for retired algorithms appear in prior versions of this report in the [archive](#).

2022-02-23 changes since 2022-01-24:

- ▷ We have added results for first algorithms from four developers: AFIS and Biometrics Consulting, Digidata, Graymatics, Hangzhuo Allu Network Information Technology, KnowUTech LLC, Sukshi Technology Innovation, T4iSB, and TuringTech.vip
- ▷ We have added results for new algorithms from 18 returning developers: Cognitec Systems GmbH, GeoVision Inc, Glory, Herta Security, Intel Research Group, InsightFace AI, Kakao Enterprise, N-Tech Lab, Omnidarde Ltd, Papilon Savunma, Paravision, Reveal Networks Inc, Reveal Media Ltd, Shenzhen Inst Adv Integrated Tech CAS, Suprema AI Inc, Toshiba, Universidade de Coimbra, and Yuan High-Tech Development
- ▷ We have retired results for 14 algorithms per our policy to only list results for two algorithms per developer. Results for retired algorithms appear in prior versions of this report in the [archive](#).

2022-01-24 changes since 2022-01-20:

- ▷ We have added results for new algorithms from one returning developer: Vocord.

2022-01-20 changes since 2021-12-18:

- ▷ We have added results for first algorithms from four developers: Armatura, Beyne.AI, One More Security, and VinBigData

- ▷ We have added results for new algorithms from 19 returning developers: AuthenMetric, BOE Technology Group, Cybercore, Cyberlink, Dahua Technology, FaceTag Co, Innovatrics, Megvii, Mobbeel Solutions, Neurotechnology, Oz Forensics, Rank One Computing, Regula Forensics, Samsung S1, Securif AI, Sensetime Group, TigerIT Americas, Videmo Intelligent Videoanalyse, and YooniK.
- ▷ We have retired results for 14 algorithms per our policy to only list results for two algorithms per developer. Results for retired algorithms appear in prior versions of this report in the [archive](#).

: **2021-12-16** changes since 2021-11-22:

- ▷ We have added results for first algorithms from five developers: Alfabeta, Cloudmatrix, Euronovate SA, FaceOnLive Inc, and Mobiclip Technology.
- ▷ We have added results for new algorithms from ten returning developers: ACI Software, ITMO University, NEO Systems, Guangzhou Pixel Solutions, Panasonic R+D Center Singapore, Qnap Security, Scanovate, Tevian, Unissey, and Vietnam Posts and Telecommunications Group.
- ▷ We have retired results for eight algorithms per our policy to only list results for two algorithms per developer. Results for retired algorithms appear in prior versions of this report in the [archive](#).
- ▷ We have revamped Figure 19 showing performance on 20 pairs of open-source images. It now color-codes false negatives and positives against a default threshold value.

2021-11-22 changes since 2021-10-28:

- ▷ We have added results to the [website](#) for kiosk-collected images where the design and geometry configuration mean that many images have considerable downward pitch angle. In some images, the face is partially cropped. Some images have other background faces.
- ▷ We have stopped using child exploitation images in FRVT, as we lost access to the imagery. All results for that set have been removed from the [website](#), and will be removed from future PDF reports.
- ▷ We have added results for first algorithms from seven new developers: CUDO Communication, Daon, KuKe3D Technology, Mantra Softtech India, Maxvision Technology, Multi-Modality Intelligence, and Samsung-SDS.
- ▷ We have added results for new algorithms from seven returning developers: Acer Incorporated, Cloudwalk-Moontime Smart Technology, Gorilla Technology, ID3 Technology, Incode Technologies, NSENSE Corp., and SQIsoft.
- ▷ We have retired results for six algorithms per our policy to only list results for two algorithms per developer. Results for retired algorithms appear in prior versions of this report in the [archive](#).

2021-10-28 changes since 2021-09-08:

- ▷ We have substantially revised the algorithm-specific report cards that are linked from the [FRVT results page](#). (Example: [HTML](#)).
- ▷ We have added results for first algorithms from eight new developers: Beijing Mendaxia Technology, Beijing Hisign Technology, Biocube Matrics, Clearview AI, Reveal Media, Toppan ID Gate, Verigram, and Viettel High Technology.
- ▷ We have added results for new algorithms from thirty returning developers: 20Face, 3divi, Canon Inc Chunghwa Telecom, Corsight, Decatur Industries, Deepglint, Dermalog, FaceTag, Fiberhome Telecommunication Technologies, GeoVision, ICM Airport Technics, Imagus Technology, InsightFace AI, Kakao

Enterprise, Kookmin University, Line Corporation, N-Tech Lab, NotionTag Technologies, Realnetworks, Suprema ID, Taiwan-Certificate Authority, Toshiba, Tripleize, Trueface.ai, Veridas Digital Authentication, Visidon, VisionLabs, YooniK, and Yuan High-Tech Development.

- ▷ We have retired results for twenty algorithms per our policy to only list results for two algorithms per developer. Results for retired algorithms appear in prior versions of this report in the [archive](#).

2021-09-08 changes since 2021-08-02:

- ▷ We have added results for first algorithms from seven new developers: Griaule, SQISoft, Qnap Security, Techsign, Smart Engines, Verihubs, and Wuhan Tianyu Information Industry.
- ▷ We have added results for new algorithms from sixteen returning developers: ADVANCE.AI, AuthenMetric, CloudSmart Consulting, Code Everest Pvt, Cognitec Systems, Thales Gemalto Cogent, Intel Research Group, Omnidarde, Oz Forensics, Rank One Computing, Samsung S1 Corp, Securif AI, Tevian, TigerIT Americas, Universidade de Coimbra, and Vigilant Solutions
- ▷ We have retired results for eleven algorithms per our policy to only list results for two algorithms per developer. Results for retired algorithms appear in prior versions of this report in the [archive](#).

2021-08-02 changes since 2021-06-25:

- ▷ We have added results for first algorithms from eight new developers: Bee the Data, Closeli Inc, Coretech Knowledge Inc, Deepsense (France), ioNetworks Inc, Kakao Pay Corp, Seventh Sense Artificial Intelligence, and SK Telecom.
- ▷ We have added results for new algorithms from fifteen returning developers: Alchera Inc, Adera Global PTE, Aware, Bresee Technology, Cyberlink Corp, Expasoft LLC, Fujitsu Research and Development Center, Gorilla Technology, Idemia, Neurotechnology, NEO Systems, NHN Corp, Paravision, Panasonic R+D Center Singapore, and Shenzhen University-Macau University of Science and Technology.
- ▷ We have retired results for twelve algorithms per our policy to only list results for two algorithms per developer. Results for retired algorithms appear in prior versions of this report in the [archive](#).

2021-06-25 changes since 2021-05-21:

- ▷ We have added results for first algorithms from six new developers: Alice Biometrics, BOE Technology Group, Fincore, Neosecu, Sodec App, and Yuntu Data and Technology.
- ▷ We have added results for new algorithms from seven returning developers: Incode Technologies, HyperVerge, Mobbeel Solutions, Guangzhou Pixel Solutions, Remark Holdings, Sensetime, and Vietnam Posts and Telecommunications Group.
- ▷ We have retired results for four algorithms per our policy to only list results for two algorithms per developer. Results for retired algorithms appear in prior versions of this report in the [archive](#).

2021-05-21 changes since 2021-04-26:

- ▷ We have added results for first algorithms from five new developers: Ekin Smart City Technologies, Suprema ID, Tripleize, Taiwan-Certificate Authority, and Vision Intelligence Center of Meituan.
- ▷ We have added results for new algorithms from eight returning developers: ID3 Technology, Imagus Technology, Momentum Digital, N-Tech Lab, NSENSE, Shanghai Jiao Tong University, Vision-Box, and Yuan High-Tech Development

- ▷ We have retired results for seven algorithms per our policy to only list results for two algorithms per developer. Results for retired algorithms appear in prior versions of this report in the [archive](#).

2021-04-26 changes since 2021-04-16:

- ▷ We have added results for first algorithms from three new developers: Quantasoft, Rendip, and NEO Systems.
- ▷ We have added results for new algorithms from four returning developers: 3Divi, Realnetworks, Veridas Digital Authentication Solutions, and Universidade de Coimbra.
- ▷ We have retired results for three algorithms per our policy to only list results for two algorithms per developer. Results for retired algorithms appear in prior versions of this report in the [archive](#).

2021-04-16 changes since 2021-03-19:

- ▷ We have added results for first algorithms from six new developers: 20Face, Beijing DeepSense Technologies, BitCenter UK, Enface, FaceTag, InsightFace AI, Line Corporation, Lema Labs, Nanjing Kiwi Network Technology, Omnidarde, Regula Forensics, and Suprema.
- ▷ We have added results for new algorithms from ten returning developers: CloudSmart Consulting, Dermalog, GeoVision, Neurotechnology, Panasonic R+D Center Singapore, Samsung S1, Securif AI, Trueface.ai, Vigilant Solutions, and Visidon.
- ▷ We have retired results for ten algorithms per our policy to only list results for two algorithms per developer. Results for retired algorithms appear in prior versions of this report in the [archive](#).

2021-03-19 changes since 2021-03-05:

- ▷ We have added results for first algorithms from six new developers: Ajou University, AuthenMetric, Code Everest, Corsight, Papilon Savunma, and NHN Corp
- ▷ We have added results for new algorithms from seven returning developers: Alchera, Deepglint, Fiber-home Telecommunication Technologies, Kakao Enterprise, Kookmin University, Megvii/Face++, and NotionTag Technologies.
- ▷ We have updated many of the hyperlinked HTML report-cards to include seven figures on demographic dependence. Figures of this kind first appeared, and are documented in, the December 2019 document, [NIST Interagency Report 8280](#) on demographic differentials in face recognition. The figures quantify false negative dependence on demographics using “visa-border” comparisons, and false positive dependence using comparisons of “application” photos that uniformly of quality and similar to visa photos.

2021-03-05 changes since 2021-01-19:

- ▷ We have added results for first algorithms from three new developers: IVA Cognitive, Mobbeel, and MoreDian Technology.
- ▷ We have added results for new algorithms from returning developers: Ability Enterprise - Andro Video, ACI Software, Adera Global, AnyVision, BioID Technologies, China Electronics Import-Export, Cognitec Systems, Fujitsu Research and Development Center, Glory, Guangzhou Pixel Solutions, Hengrui AI Technology, Incode Technologies, Intel Research, iQIYI, Mobai, Oz Forensics, Paravision, VisionLabs, and Xforward AI Technology.

- ▷ We have added a new “resources” tab to the main [webpage](#). It includes sortable columns for data related to speed, model size, storage, and memory consumption.
- ▷ We have retired results for 13 algorithms per our policy to only list results for two algorithms per developer. Results for retired algorithms appear in prior versions of this report in the [archive](#).

2021-01-19 changes since 2020-12-18:

- ▷ This report adds results for first algorithms from four developers: Herta Security, Irex AI, Shenzhen University-Macau University of Science and Technology, and Vietnam Posts and Telecommunications Group. See Table 6 for more information.
- ▷ The report also includes results for thirteen developers who have previously submitted algorithms: Bresee Technology, Canon (previously Canon Information Technology (Beijing)), Cyberlink, CSA IntelliCloud Technology, Dahua Technology, ID3 Technology, Imagus Technology (Vixvizon), Moontime Smart Technology, N-Tech Lab, Thales Cogent, Veridas Digital Authentication Solutions, Vocord, and Yuan High-Tech Development.
- ▷ We have retired results for ten algorithms per our policy to only list results for two algorithms per developer. Results for retired algorithms appear in prior versions of this report in the [archive](#).

2020-12-18 changes since 2020-10-09:

- ▷ This report adds results for first algorithms from ten developers: BitCenter UK, CloudSmart Consulting, Cubox, Institute of Computing Technology, Naver Corp, Minivision, NSENSE Corp, Viettel Group, Visage Technologies, and Xiamen University. See Table 6 for more information.
- ▷ The report also includes results for eighteen developers who have previously submitted algorithms: ADVANCE.AI, Awidit Systems, Chosun University, Dermalog, GeoVision, ICM Airport Technics, Idemia, Institute of Information Technologies, Kakao Enterprise, Neurotechnology, Panasonic R+D Center Singapore, Rank One Computing, Sensetime Group, Shanghai Jiao Tong University, TigerIT Americas LLC, Vigilant Solutions, Winsense, and YooniK
- ▷ We have retired results for twelve algorithms per our policy to only list results for two algorithms per developer. Results for retired algorithms appear in prior versions of this report in the [archive](#).

Changes since September 18, 2020:

- ▷ This report adds results for first algorithms from five developers: Aigen, Cortica, Kookmin University, Securif AI and Vinai.
- ▷ The report also includes results for three developers who have previously submitted algorithms: Fujitsu Laboratories, Hengrui AI, and X-Forward AI.
- ▷ In the per-algorithm report-cards linked from tables and the main webpage, we have added a chart to showing reduction in error rates over the course of FRVT i.e. from 2017 onwards for all algorithms supplied by that developer. Similarly we have added a chart showing error rate reductions for our test of protective face mask verification.
- ▷ We plan to continue evaluating algorithms on various mask datasets. We hold that algorithms should be capable of detecting masks and verifying identity of all combinations of masked and unmasked faces. We have accordingly increased the amount of time allowed to extract those features from 1.0 to 1.5 seconds.

Changes since August 25, 2020:

- ▷ This report adds results for first algorithms from eight new developers. Akurat Satu Indonesia, Cybercore, Decatur Industries, Innef Labs, Satellite Innovation/Eocortex, Expasoft, and Mobai.
- ▷ The report includes results for seven developers who have previously submitted algorithms: 3Divi, BioID Technologies, Incode Technologies, Innovatrics, iSAP Solution, Synology, and Tevian.
- ▷ We have retired results for five algorithms per our policy to only list results for two algorithms per developer. Results for retired algorithms appear in prior versions of this report in the [archive](#).

Changes since July 27, 2020:

- ▷ We have introduced per-algorithm report sheets. These are HTML documents linked from the accuracy tables in this report (i.e. Table 26) and on the FRVT 1:1 [homepage](#). The sheets contain interactive graphics allowing, for example, mouseover exploration of FNMR(T) and FMR(T). Some of their content had previously appeared in this document.
- ▷ This report adds results for algorithms from six new developers. ACI Software, Bresee Technology, Fiberhome Telecommunication Technologies, Imageware Systems, Oz Forensics, and Pensees.
- ▷ The report includes results for thirteen developers who have previously submitted algorithms: Canon Information Technology (Beijing), Cyberlink, Dahua Technology, Gorilla Technology, ID3 Technology, Intel Research Group, iQIYI Inc, Momentum Digital, Netbridge Technology, Tech5 SA, Shenzhen AiMall Tech, Vigilant Solutions, and VisionLabs.
- ▷ We have retired results for nine algorithms per our policy to only list results for two algorithms per developer. Results for retired algorithms appear in prior versions of this report in the [archive](#).

Changes since May 18, 2020:

- ▷ The report is the first FRVT update since the pandemic closed it from March to June 2020.
- ▷ This report includes results for algorithms from nine new developers: GeoVision Inc, Su Zhou NaZhi-TianDi Intelligent Technology, YooniK, AYF Technology, PXL Vision AG, Yuan High-Tech Development, Beihang University-ERCACAT, ICM Airport Technics, and Staqu Technologies
- ▷ This report includes results for algorithms from 15 returning developers Acer Incorporated, Antheus Technologia, Chosun University, Chunghwa Telecom, Idemia, Moontime Smart Technology, Neurotechnology, Guangzhou Pixel Solutions, Panasonic R+D Center Singapore, Rank One Computing, Scanovate, Shanghai Universiy - Shanghai Film Academy, Synesis, Trueface.ai, and Veridas Digital Authentication Solutions
- ▷ We have retired results for ten algorithms per our policy to only list results for two algorithms per developer. Results for retired algorithms appear in prior versions of this report in the [archive](#).
- ▷ We separated timing and other resource consumption from the main participation table. The new Table 16 includes template generation durations for four kinds of images, not just mugshots.
- ▷ We have published a separate report, [NIST Interagency Report 8311](#) on accuracy of pre-pandemic algorithms on subjects wearing face masks. We plan to track improvements in accuracy on masked images going forward. In particular, we invite submission of algorithms that can detect whether a person is wearing a mask, extract features from the full face or the exposed periocular region, and do appropriate comparison. We do not intend to evaluate algorithms that assume 100% of images will be of masked individuals.

Changes since March 25, 2020:

- ▷ The report is a maintenance release - it does not add any new algorithms, and FRVT has been closed to new algorithms since mid March 2020.
- ▷ We modified the primary accuracy summary, Table 26, as follows:
 - ▷▷ For visa images, the column for FNMR at FMR = 0.0001 has been removed. The visa images are so highly controlled that the error rates for the most accurate algorithms are dominated by false rejection of very young children and by the presence of a few noisy greyscale images. For now, two visa columns remain: FNMR at $FMR = 10^{-6}$ and, for matched covariates, FNMR at $FMR = 10^{-4}$.
 - ▷▷ We have inserted a new column labelled "BORDER" giving accuracy for comparison of moderately poor webcam border-crossing photos that exhibit pose variations, poor compression, and low contrast due to strong background illumination. The accuracies are the worst from all cooperative image datasets used in FRVT.
- ▷ Accordingly, we updated the failure-to-template rates in Table 33.
- ▷ We withdrew a figure showing how false matches are concentrated in certain visa images used in cross-comparison, because it didn't attempt to include demographic information.

Changes since February 27, 2020:

- ▷ The report adds results algorithms from two new developers: Beijing Alleyes Technology, and the Chinese University of Hong Kong. Results for newly submitted algorithms from two other developers will appear in the next report.
- ▷ The report adds results for algorithms from thirteen returning developers: ASUSTek Computer, Aware, Cyberlink Corp, Gorilla Technology, Innovative Technology, Kakao Enterprise, Lomonosov Moscow State University, Panasonic R+D Center Singapore, Shenzhen AiMall Technology, Shenzhen Intellifusion Technologies, Synology, Tech5 SA, and Via Technologies.
- ▷ Per policy to only list results for two algorithms per developer, we have dropped results for algorithms from Aware, Cyberlink, Gorilla Technology, Kakao Enterprise, Lomonosov Moscow State University, Panasonic R+D Center Singapore, and Tech5 SA.

Changes since January 20, 2020:

- ▷ The report adds results for five new developers: Ability Enterprise (Andro Video), Chosun University, Fujitsu Research and Development Center, University of Coimbra, and Xforward AI Technology.
- ▷ The report adds results for algorithms from six returning developers: AlphaSSTG, Incode Technologies, Kneron, Shanghai Jiao Tong University, Vocord, and X-Laboratory.
- ▷ We have corrected template comparison timing numbers for algorithms submitted September 2019 to January 2020. The values reported previously were slower due to a software bug.
- ▷ We have dropped results for algorithms from Vocord and Incode per policy to only list results for two algorithms per developer.
- ▷ The [FRVT 1:1 homepage](#) has been updated with latest accuracy results.
- ▷ The [FRVT 1:N homepage](#) now includes an update to the September 2019 NIST Interagency Report 8271. The new report adds results for one-to-many search algorithms submitted to NIST from June 2019 to January 2020.

Changes since January 6, 2020:

- ▷ Section 2 has been updated to better describe the Visa and Border images. The caption for Table 26 has been updated to better relate the accuracy values to particular image comparisons.
- ▷ The report adds results for five new developers: Acer, Advance.AI, Expasoft, Netbridge Technology, and Videmo Intelligent Videoanalyse.
- ▷ The report adds results for algorithms from 7 returning developers: China Electronics Import-Export Corp, Intel Research Group, ITMO University, Neurotechnology, N-Tech Lab, Rokid, and VisionLabs.
- ▷ We have dropped results from this edition of the report per policy to only list results for two algorithms per developer: N-Tech Lab, Neurotechnology, ITMO, Visionlabs, and CEIEC.
- ▷ The [FRVT homepage](#) has been updated with latest accuracy results.

Changes since November 11, 2019:

- ▷ Table 16 has been updated to include runtime memory usage. This is the first time such a quantity has been reported. The value is the peak size of the resident set size logged during enrollment of single images.
- ▷ We have migrated summary results table to a new platform that supports sortable tables:
<https://pages.nist.gov/frvt/html/frvt11.html>
- ▷ The report adds results for four new developers: Antheus Technologia, BioID Technologies SA, Canon Information Tech. (Beijing), Samsung S1 (listed in the tables as S1), and Taiwan AI Labs.
- ▷ The report adds results for algorithms from 13 returning developers: Anke Investments, Chunghwa Telecom, Deepglint, Institute of Information Technologies, iQIYI, Kneron, Ping An Technology, Paravision, KanKan Ai, Rokid Corporation, Shanghai Universiy - Shanghai Film Academy, Veridas Digital Authentication Solutions, and Videonetics Technology.
- ▷ We have dropped results from this edition of the report per policy to only list results for two algorithms per developer: remarkai-000, veridas-001, sensetime-001, iit-000, anke-003, and everai-002. Results for these are available in prior editions of this report linked from the FRVT page.
- ▷ We issued [NIST Interagency Report 8280: FRVT Part 3: Demographics](#) on 2019-12-19. It includes results for many of the algorithms covered by this report.

Changes since October 16, 2019:

- ▷ The report adds results for ten new developers: Ai-Union Technology, ASUSTek Computer, DiDi ChuXing Technology, Innovative Technology, Luxand, MVision, Pyramid Cyber Security + Forensic, Scanovate, Shenzhen AiMall Tech, and TUPU Technology.
- ▷ The report adds results for 12 returning developers: CTBC Bank Glory Gorilla Technology Guangzhou Pixel Solutions Imagus Technology Incode Technologies Lomonosov Moscow State University Rank One Computing Samtech InfoNet Shanghai Ulucu Electronics Technology Synesis, and Winsense.
- ▷ We have dropped results from this edition of the report per policy to only list results for two algorithms per developer: glory-000, gorilla-002, incode-003, rankone-006, and synesis-004.
- ▷ Results for five recently submitted algorithms will appear in the next report.

Changes since September 11, 2019:

- ▷ The report adds results for five new participants: Awidit Systems (Awiros), Momenmtum Digital (Sertis), Trueface AI, Shanghai Jiao Tong University, and X-Laboratory.
- ▷ The reports adds results for five new algorithms from returning developers: Cyberlink, Hengrui AI Technology, Idemia, Panasonic R+D Singapore, and Tevian. This causes three algorithm, to be de-listed from the report per policy to list results for two algorithms per developer.

Changes since July 31 2019:

- ▷ The HTML table on the [FRVT 1:1 homepage](#) has been updated to include a column for cross-domain Visa-Border verification. Results for this new dataset appeared in the July 29 report under the name "CrossEV" - these are now renamed "Visa-Border".
- ▷ The [FRVT 1:1 homepage](#) lists algorithms according to lowest mean rank accuracy:

$$\begin{aligned} &\text{Rank(FNMR}_{\text{VISA}} \text{ at FMR = 0.000001}) + \\ &\text{Rank(FNMR}_{\text{VISA-BORDER}} \text{ at FMR = 0.000001}) + \\ &\text{Rank(FNMR}_{\text{MUGSHOT}} \text{ at FMR = 0.00001 after 14 years}) + \\ &\text{Rank(FNMR}_{\text{WILD}} \text{ at FMR = 0.00001}) \end{aligned}$$

This ordering rewards high accuracy across all datasets.
- ▷ The main results in Table 26 is now in landscape format to accomodate extra columns for the Visa-Border set, and mugshot comparisons after at least 12 years.
- ▷ The report adds results for nine new participants: Alpha SSTG, Intel Research, ULSee, Chungwa Telecon, iSAP Solution, Rokid, Shenzhen EI Networks, CSA Intellilcloud, Shenzhen Intellifusion Technologies.
- ▷ The reports adds results for six new algorithms from returning developers: Innovatrics, Dahua Technology, Tech5 SA, Intellivision, Nodeflux and Imperial College, London. One algorithm, from Imperial has been retired, per policy to list results for two algorithms per developer.
- ▷ The cross-country false match rate heatmaps have been replotted to reveal more structure by listing countries by region instead of alphabetically.
- ▷ The next version of this report will be posted around October 18, 2019.

Changes since July 3 2019:

- ▷ The HTML table on the [FRVT 1:1 homepage](#) has been updated to list the 20 most accurate developers rather than algorithms, choosing the most accurate algorithm from each developer based on visa and mugshot results. Also, the algorithms are ordered in terms of lowest mean rank across mugshot, visa and wild datasets, rewarding broad accuracy over a good result on one particular dataset.
- ▷ This report includes results for a new dataset - see the column labelled "visa-border" in Table 5. It compares a new set of high quality visa-like portraits with a set webcam border-crossing photos that exhibit moderately poor pose variations and background illumination. The two new sets are described in sections 2.2 and 2.3. The comparisons are "cross-domain" in that the algorithm must compare "visa" and "wild" images. Results for other algorithms will be added in future reports as they become available.
- ▷ This report adds results for algorithms from 9 developers submitted in early July 2019. These are from 3DiVi, Camvi, EverAI-Paravision, Facesoft, Farbar (F8), Institute of Information Technologies, Shanghai U. Film Academy, Via Technologies, and Ulucu Electronics Tech. Six of these are new participants.
- ▷ Several other algorithms have been submitted and are being evaluated. Results will be released in the next report, scheduled for September 5. That report will include results for new datasets.

- ▷ Older algorithms from Everai, Camvi and 3DiVi, have been retired, per the policy to list only two algorithms per developer.

Changes since June 2019:

- ▷ This report adds results for algorithms from 18 developers submitted in early June 2019. These are from CTBC Bank, Deep Glint, Thales Cogent, Ever AI Paravision, Gorilla Technology, Imagus, Incode, Kneron, N-Tech Lab, Neurotechnology, Notiontag Technologies, Star Hybrid, Videonetics, Vigilant Solutions, Winsense, Anke Investments, CEIEC, and DSK. Nine of these are new participants.
- ▷ Several other algorithms have been submitted and are being evaluated. Results will be released in the next report, scheduled for August 1.
- ▷ Older algorithms from Everai, Thales Cogent, Gorilla Technology, Incode, Neurotechnology, N-Tech Lab and Vigilant Solutions have been retired, per the policy to list only two algorithms per developer.

Changes since April 2019:

- ▷ This report adds results for nine algorithms from nine developers submitted in early June 2019. These are from Tencent Deepsea, Hengrui, Kedacom, Moontime, Guangzhou Pixel, Rank One Computing, Synesis, Sensetime and Vocord.
- ▷ Another 23 algorithms have been submitted and are being evaluated. Results will be released in the next report, scheduled for July 3.
- ▷ Older algorithms for Rank One, Synesis, and Vocord have been retired, per the policy to list only two algorithms per developer.

Changes since February 2019:

- ▷ This report adds results for 49 algorithms from 42 developers submitted in early March 2019.
- ▷ This report omits results for algorithms that we retired. We retired for three reasons: 1. The developer submitted a new algorithm, and we only list two. 2. The algorithm needs a GPU, and we no longer allow GPU-based algorithms. 3. Inoperable algorithms.
- ▷ Previous results for retired algorithms are available in older editions of this report linked [here](#).
- ▷ The mugshot database used from February 2017 to January 2019 has been replaced with an extract of the mugshot database documented in NIST Interagency Report 8238, November 2018. The new mugshot set is described in section [2.4](#) and is adopted because:
 - ▷▷ It has much better identity label integrity, so that false non-match rates are substantially lower than those reported in FRVT 1:1 reports to date - see Figure [81](#).
 - ▷▷ It includes images collected over a 17 year period such that ageing can be much better characterized - - see Figure [294](#).
- ▷ Using the new mugshot database, Figure [294](#) shows accuracy for four demographic groups identified in the biographic metadata that accompanies the data: black females, black males, white females and white males.
- ▷ The report adds Figure [19](#) with results for the twenty human-difficult pairs used in the May 2018 paper *Face recognition accuracy of forensic examiners, superrecognizers, and face recognition algorithms* by Phillips et al. [[1](#)].
- ▷ The report uses an update to the wild image database that corrects some ground truth labels.
- ▷ Some results for the child exploitation database are not complete. They are typically updated less frequently than for other image sets.

Contents

ACKNOWLEDGMENTS	1
DISCLAIMER	1
INSTITUTIONAL REVIEW BOARD	1
1 METRICS	48
1.1 CORE ACCURACY	48
1.2 MULTI-TEMPLATE SCORING METHODOLOGY	48
2 DATASETS	49
2.1 VISA IMAGES	49
2.2 APPLICATION IMAGES	49
2.3 BORDER CROSSING IMAGES	49
2.4 MUGSHOT IMAGES	50
2.5 WILD IMAGES	50
3 RESULTS	50
3.1 TEST GOALS	50
3.2 TEST DESIGN	51
3.3 FAILURE TO ENROLL	54
3.4 RECOGNITION ACCURACY	62
3.5 GENUINE DISTRIBUTION STABILITY	295
3.5.1 EFFECT OF BIRTH PLACE ON THE GENUINE DISTRIBUTION	295
3.5.2 EFFECT OF AGEING	330
3.5.3 EFFECT OF AGE ON GENUINE SUBJECTS	356
3.6 IMPOSTOR DISTRIBUTION STABILITY	392
3.6.1 EFFECT OF BIRTH PLACE ON THE IMPOSTOR DISTRIBUTION	392
3.6.2 EFFECT OF AGE ON IMPOSTORS	396

List of Tables

1 PARTICIPANT INFORMATION	20
2 PARTICIPANT INFORMATION	21
3 PARTICIPANT INFORMATION	22
4 PARTICIPANT INFORMATION	23
5 PARTICIPANT INFORMATION	24
6 PARTICIPANT INFORMATION	25
7 ALGORITHM SUMMARY	26
8 ALGORITHM SUMMARY	27
9 ALGORITHM SUMMARY	28
10 ALGORITHM SUMMARY	29
11 ALGORITHM SUMMARY	30
12 ALGORITHM SUMMARY	31
13 ALGORITHM SUMMARY	32
14 ALGORITHM SUMMARY	33
15 ALGORITHM SUMMARY	34
16 ALGORITHM SUMMARY	35
17 FALSE NON-MATCH RATE	36
18 FALSE NON-MATCH RATE	37
19 FALSE NON-MATCH RATE	38
20 FALSE NON-MATCH RATE	39

21	FALSE NON-MATCH RATE	40
22	FALSE NON-MATCH RATE	41
23	FALSE NON-MATCH RATE	42
24	FALSE NON-MATCH RATE	43
25	FALSE NON-MATCH RATE	44
26	FALSE NON-MATCH RATE	45
27	FAILURE TO ENROL RATES	55
28	FAILURE TO ENROL RATES	56
29	FAILURE TO ENROL RATES	57
30	FAILURE TO ENROL RATES	58
31	FAILURE TO ENROL RATES	59
32	FAILURE TO ENROL RATES	60
33	FAILURE TO ENROL RATES	61

List of Figures

1	PERFORMANCE SUMMARY: FNMR VS. TEMPLATE SIZE TRADEOFF	46
2	PERFORMANCE SUMMARY: FNMR VS. TEMPLATE TIME TRADEOFF	47
3	EXAMPLE IMAGES	51
(A)	VISA	51
(B)	MUGSHOT	51
(C)	WILD	51
(D)	BORDER	51
4	PERFORMANCE ON 20 HUMAN-DIFFICULT PAIRS	63
5	PERFORMANCE ON 20 HUMAN-DIFFICULT PAIRS	64
6	PERFORMANCE ON 20 HUMAN-DIFFICULT PAIRS	65
7	PERFORMANCE ON 20 HUMAN-DIFFICULT PAIRS	66
8	PERFORMANCE ON 20 HUMAN-DIFFICULT PAIRS	67
9	PERFORMANCE ON 20 HUMAN-DIFFICULT PAIRS	68
10	PERFORMANCE ON 20 HUMAN-DIFFICULT PAIRS	69
11	PERFORMANCE ON 20 HUMAN-DIFFICULT PAIRS	70
12	PERFORMANCE ON 20 HUMAN-DIFFICULT PAIRS	71
13	PERFORMANCE ON 20 HUMAN-DIFFICULT PAIRS	72
14	PERFORMANCE ON 20 HUMAN-DIFFICULT PAIRS	73
15	PERFORMANCE ON 20 HUMAN-DIFFICULT PAIRS	74
16	PERFORMANCE ON 20 HUMAN-DIFFICULT PAIRS	75
17	PERFORMANCE ON 20 HUMAN-DIFFICULT PAIRS	76
18	PERFORMANCE ON 20 HUMAN-DIFFICULT PAIRS	77
19	PERFORMANCE ON 20 HUMAN-DIFFICULT PAIRS	78
20	ERROR TRADEOFF CHARACTERISTIC: VISA IMAGES	79
21	ERROR TRADEOFF CHARACTERISTIC: VISA IMAGES	80
22	ERROR TRADEOFF CHARACTERISTIC: VISA IMAGES	81
23	ERROR TRADEOFF CHARACTERISTIC: VISA IMAGES	82
24	ERROR TRADEOFF CHARACTERISTIC: VISA IMAGES	83
25	ERROR TRADEOFF CHARACTERISTIC: VISA IMAGES	84
26	ERROR TRADEOFF CHARACTERISTIC: VISA IMAGES	85
27	ERROR TRADEOFF CHARACTERISTIC: VISA IMAGES	86
28	ERROR TRADEOFF CHARACTERISTIC: VISA IMAGES	87
29	ERROR TRADEOFF CHARACTERISTIC: VISA IMAGES	88
30	ERROR TRADEOFF CHARACTERISTIC: VISA IMAGES	89
31	ERROR TRADEOFF CHARACTERISTIC: VISA IMAGES	90
32	ERROR TRADEOFF CHARACTERISTIC: VISA IMAGES	91
33	ERROR TRADEOFF CHARACTERISTIC: VISA IMAGES	92
34	ERROR TRADEOFF CHARACTERISTIC: VISA IMAGES	93
35	ERROR TRADEOFF CHARACTERISTIC: VISA IMAGES	94

36	ERROR TRADEOFF CHARACTERISTIC: VISA IMAGES	95
37	ERROR TRADEOFF CHARACTERISTIC: VISA IMAGES	96
38	ERROR TRADEOFF CHARACTERISTIC: VISA IMAGES	97
39	ERROR TRADEOFF CHARACTERISTIC: VISA IMAGES	98
40	ERROR TRADEOFF CHARACTERISTIC: VISA IMAGES	99
41	ERROR TRADEOFF CHARACTERISTIC: VISA IMAGES	100
42	ERROR TRADEOFF CHARACTERISTIC: VISA IMAGES	101
43	ERROR TRADEOFF CHARACTERISTIC: VISA IMAGES	102
44	ERROR TRADEOFF CHARACTERISTIC: VISA IMAGES	103
45	ERROR TRADEOFF CHARACTERISTIC: VISA IMAGES	104
46	ERROR TRADEOFF CHARACTERISTIC: VISA IMAGES	105
47	ERROR TRADEOFF CHARACTERISTIC: VISA IMAGES	106
48	ERROR TRADEOFF CHARACTERISTIC: VISA IMAGES	107
49	ERROR TRADEOFF CHARACTERISTIC: VISA IMAGES	108
50	ERROR TRADEOFF CHARACTERISTIC: VISA IMAGES	109
51	ERROR TRADEOFF CHARACTERISTIC: VISA IMAGES	110
52	ERROR TRADEOFF CHARACTERISTIC: VISA IMAGES	111
53	ERROR TRADEOFF CHARACTERISTIC: VISA IMAGES	112
54	ERROR TRADEOFF CHARACTERISTIC: VISA IMAGES	113
55	ERROR TRADEOFF CHARACTERISTIC: VISA IMAGES	114
56	ERROR TRADEOFF CHARACTERISTIC: VISA IMAGES	115
57	ERROR TRADEOFF CHARACTERISTIC: VISA IMAGES	116
58	ERROR TRADEOFF CHARACTERISTIC: VISA IMAGES	117
59	ERROR TRADEOFF CHARACTERISTIC: VISA IMAGES	118
60	ERROR TRADEOFF CHARACTERISTIC: VISA IMAGES	119
61	ERROR TRADEOFF CHARACTERISTIC: MUGSHOT IMAGES	120
62	ERROR TRADEOFF CHARACTERISTIC: MUGSHOT IMAGES	121
63	ERROR TRADEOFF CHARACTERISTIC: MUGSHOT IMAGES	122
64	ERROR TRADEOFF CHARACTERISTIC: MUGSHOT IMAGES	123
65	ERROR TRADEOFF CHARACTERISTIC: MUGSHOT IMAGES	124
66	ERROR TRADEOFF CHARACTERISTIC: MUGSHOT IMAGES	125
67	ERROR TRADEOFF CHARACTERISTIC: MUGSHOT IMAGES	126
68	ERROR TRADEOFF CHARACTERISTIC: MUGSHOT IMAGES	127
69	ERROR TRADEOFF CHARACTERISTIC: MUGSHOT IMAGES	128
70	ERROR TRADEOFF CHARACTERISTIC: MUGSHOT IMAGES	129
71	ERROR TRADEOFF CHARACTERISTIC: MUGSHOT IMAGES	130
72	ERROR TRADEOFF CHARACTERISTIC: MUGSHOT IMAGES	131
73	ERROR TRADEOFF CHARACTERISTIC: MUGSHOT IMAGES	132
74	ERROR TRADEOFF CHARACTERISTIC: MUGSHOT IMAGES	133
75	ERROR TRADEOFF CHARACTERISTIC: MUGSHOT IMAGES	134
76	ERROR TRADEOFF CHARACTERISTIC: MUGSHOT IMAGES	135
77	ERROR TRADEOFF CHARACTERISTIC: MUGSHOT IMAGES	136
78	ERROR TRADEOFF CHARACTERISTIC: MUGSHOT IMAGES	137
79	ERROR TRADEOFF CHARACTERISTIC: MUGSHOT IMAGES	138
80	ERROR TRADEOFF CHARACTERISTIC: MUGSHOT IMAGES	139
81	ERROR TRADEOFF CHARACTERISTIC: MUGSHOT IMAGES	140
82	ERROR TRADEOFF CHARACTERISTIC: WILD IMAGES	141
83	ERROR TRADEOFF CHARACTERISTIC: WILD IMAGES	142
84	ERROR TRADEOFF CHARACTERISTIC: WILD IMAGES	143
85	ERROR TRADEOFF CHARACTERISTIC: WILD IMAGES	144
86	ERROR TRADEOFF CHARACTERISTIC: WILD IMAGES	145
87	ERROR TRADEOFF CHARACTERISTIC: WILD IMAGES	146
88	ERROR TRADEOFF CHARACTERISTIC: WILD IMAGES	147
89	ERROR TRADEOFF CHARACTERISTIC: WILD IMAGES	148
90	ERROR TRADEOFF CHARACTERISTIC: WILD IMAGES	149
91	ERROR TRADEOFF CHARACTERISTIC: WILD IMAGES	150
92	ERROR TRADEOFF CHARACTERISTIC: WILD IMAGES	151

93	ERROR TRADEOFF CHARACTERISTIC: WILD IMAGES	152
94	ERROR TRADEOFF CHARACTERISTIC: WILD IMAGES	153
95	ERROR TRADEOFF CHARACTERISTIC: WILD IMAGES	154
96	ERROR TRADEOFF CHARACTERISTIC: WILD IMAGES	155
97	ERROR TRADEOFF CHARACTERISTIC: WILD IMAGES	156
98	ERROR TRADEOFF CHARACTERISTIC: WILD IMAGES	157
99	FALSE MATCH RATES WITHIN AND ACROSS DEMOGRAPHIC GROUPS	158
100	FALSE MATCH RATES WITHIN AND ACROSS DEMOGRAPHIC GROUPS	159
101	FALSE MATCH RATES WITHIN AND ACROSS DEMOGRAPHIC GROUPS	160
102	FALSE MATCH RATES WITHIN AND ACROSS DEMOGRAPHIC GROUPS	161
103	FALSE MATCH RATES WITHIN AND ACROSS DEMOGRAPHIC GROUPS	162
104	FALSE MATCH RATES WITHIN AND ACROSS DEMOGRAPHIC GROUPS	163
105	FALSE MATCH RATES WITHIN AND ACROSS DEMOGRAPHIC GROUPS	164
106	FALSE MATCH RATES WITHIN AND ACROSS DEMOGRAPHIC GROUPS	165
107	FALSE MATCH RATES WITHIN AND ACROSS DEMOGRAPHIC GROUPS	166
108	FALSE MATCH RATES WITHIN AND ACROSS DEMOGRAPHIC GROUPS	167
109	FALSE MATCH RATES WITHIN AND ACROSS DEMOGRAPHIC GROUPS	168
110	FALSE MATCH RATES WITHIN AND ACROSS DEMOGRAPHIC GROUPS	169
111	FALSE MATCH RATES WITHIN AND ACROSS DEMOGRAPHIC GROUPS	170
112	FALSE MATCH RATES WITHIN AND ACROSS DEMOGRAPHIC GROUPS	171
113	FALSE MATCH RATES WITHIN AND ACROSS DEMOGRAPHIC GROUPS	172
114	FALSE MATCH RATES WITHIN AND ACROSS DEMOGRAPHIC GROUPS	173
115	FALSE MATCH RATES WITHIN AND ACROSS DEMOGRAPHIC GROUPS	174
116	FALSE MATCH RATES WITHIN AND ACROSS DEMOGRAPHIC GROUPS	175
117	FALSE MATCH RATES WITHIN AND ACROSS DEMOGRAPHIC GROUPS	176
118	FALSE MATCH RATES WITHIN AND ACROSS DEMOGRAPHIC GROUPS	177
119	SEX AND RACE EFFECTS: MUGSHOT IMAGES	178
120	SEX AND RACE EFFECTS: MUGSHOT IMAGES	179
121	SEX AND RACE EFFECTS: MUGSHOT IMAGES	180
122	SEX AND RACE EFFECTS: MUGSHOT IMAGES	181
123	SEX AND RACE EFFECTS: MUGSHOT IMAGES	182
124	SEX AND RACE EFFECTS: MUGSHOT IMAGES	183
125	SEX AND RACE EFFECTS: MUGSHOT IMAGES	184
126	SEX AND RACE EFFECTS: MUGSHOT IMAGES	185
127	SEX AND RACE EFFECTS: MUGSHOT IMAGES	186
128	SEX AND RACE EFFECTS: MUGSHOT IMAGES	187
129	SEX AND RACE EFFECTS: MUGSHOT IMAGES	188
130	SEX AND RACE EFFECTS: MUGSHOT IMAGES	189
131	SEX AND RACE EFFECTS: MUGSHOT IMAGES	190
132	SEX AND RACE EFFECTS: MUGSHOT IMAGES	191
133	SEX AND RACE EFFECTS: MUGSHOT IMAGES	192
134	SEX AND RACE EFFECTS: MUGSHOT IMAGES	193
135	SEX AND RACE EFFECTS: MUGSHOT IMAGES	194
136	SEX AND RACE EFFECTS: MUGSHOT IMAGES	195
137	SEX AND RACE EFFECTS: MUGSHOT IMAGES	196
138	SEX AND RACE EFFECTS: MUGSHOT IMAGES	197
139	SEX AND RACE EFFECTS: MUGSHOT IMAGES	198
140	SEX EFFECTS: VISA IMAGES	199
141	SEX EFFECTS: VISA IMAGES	200
142	SEX EFFECTS: VISA IMAGES	201
143	SEX EFFECTS: VISA IMAGES	202
144	SEX EFFECTS: VISA IMAGES	203
145	SEX EFFECTS: VISA IMAGES	204
146	SEX EFFECTS: VISA IMAGES	205
147	SEX EFFECTS: VISA IMAGES	206
148	SEX EFFECTS: VISA IMAGES	207
149	SEX EFFECTS: VISA IMAGES	208

150	SEX EFFECTS: VISA IMAGES	209
151	SEX EFFECTS: VISA IMAGES	210
152	SEX EFFECTS: VISA IMAGES	211
153	SEX EFFECTS: VISA IMAGES	212
154	SEX EFFECTS: VISA IMAGES	213
155	SEX EFFECTS: VISA IMAGES	214
156	SEX EFFECTS: VISA IMAGES	215
157	SEX EFFECTS: VISA IMAGES	216
158	SEX EFFECTS: VISA IMAGES	217
159	SEX EFFECTS: VISA IMAGES	218
160	SEX EFFECTS: VISA IMAGES	219
161	SEX EFFECTS: VISA IMAGES	220
162	SEX EFFECTS: VISA IMAGES	221
163	SEX EFFECTS: VISA IMAGES	222
164	SEX EFFECTS: VISA IMAGES	223
165	SEX EFFECTS: VISA IMAGES	224
166	SEX EFFECTS: VISA IMAGES	225
167	SEX EFFECTS: VISA IMAGES	226
168	SEX EFFECTS: VISA IMAGES	227
169	SEX EFFECTS: VISA IMAGES	228
170	SEX EFFECTS: VISA IMAGES	229
171	SEX EFFECTS: VISA IMAGES	230
172	SEX EFFECTS: VISA IMAGES	231
173	SEX EFFECTS: VISA IMAGES	232
174	FALSE MATCH RATE CALIBRATION: MUGSHOT IMAGES	233
175	FALSE MATCH RATE CALIBRATION: MUGSHOT IMAGES	234
176	FALSE MATCH RATE CALIBRATION: MUGSHOT IMAGES	235
177	FALSE MATCH RATE CALIBRATION: MUGSHOT IMAGES	236
178	FALSE MATCH RATE CALIBRATION: MUGSHOT IMAGES	237
179	FALSE MATCH RATE CALIBRATION: MUGSHOT IMAGES	238
180	FALSE MATCH RATE CALIBRATION: MUGSHOT IMAGES	239
181	FALSE MATCH RATE CALIBRATION: MUGSHOT IMAGES	240
182	FALSE MATCH RATE CALIBRATION: MUGSHOT IMAGES	241
183	FALSE MATCH RATE CALIBRATION: MUGSHOT IMAGES	242
184	FALSE MATCH RATE CALIBRATION: MUGSHOT IMAGES	243
185	FALSE MATCH RATE CALIBRATION: MUGSHOT IMAGES	244
186	FALSE MATCH RATE CALIBRATION: MUGSHOT IMAGES	245
187	FALSE MATCH RATE CALIBRATION: MUGSHOT IMAGES	246
188	FALSE MATCH RATE CALIBRATION: MUGSHOT IMAGES	247
189	FALSE MATCH RATE CALIBRATION: MUGSHOT IMAGES	248
190	FALSE MATCH RATE CALIBRATION: MUGSHOT IMAGES	249
191	FALSE MATCH RATE CALIBRATION: MUGSHOT IMAGES	250
192	FALSE MATCH RATE CALIBRATION: MUGSHOT IMAGES	251
193	FALSE MATCH RATE CALIBRATION: MUGSHOT IMAGES	252
194	FALSE MATCH RATE CALIBRATION: MUGSHOT IMAGES	253
195	FALSE MATCH RATE CALIBRATION: VISA IMAGES	254
196	FALSE MATCH RATE CALIBRATION: VISA IMAGES	255
197	FALSE MATCH RATE CALIBRATION: VISA IMAGES	256
198	FALSE MATCH RATE CALIBRATION: VISA IMAGES	257
199	FALSE MATCH RATE CALIBRATION: VISA IMAGES	258
200	FALSE MATCH RATE CALIBRATION: VISA IMAGES	259
201	FALSE MATCH RATE CALIBRATION: VISA IMAGES	260
202	FALSE MATCH RATE CALIBRATION: VISA IMAGES	261
203	FALSE MATCH RATE CALIBRATION: VISA IMAGES	262
204	FALSE MATCH RATE CALIBRATION: VISA IMAGES	263
205	FALSE MATCH RATE CALIBRATION: VISA IMAGES	264
206	FALSE MATCH RATE CALIBRATION: VISA IMAGES	265

207	FALSE MATCH RATE CALIBRATION: VISA IMAGES	266
208	FALSE MATCH RATE CALIBRATION: VISA IMAGES	267
209	FALSE MATCH RATE CALIBRATION: VISA IMAGES	268
210	FALSE MATCH RATE CALIBRATION: VISA IMAGES	269
211	FALSE MATCH RATE CALIBRATION: VISA IMAGES	270
212	FALSE MATCH RATE CALIBRATION: VISA IMAGES	271
213	FALSE MATCH RATE CALIBRATION: VISA IMAGES	272
214	FALSE MATCH RATE CALIBRATION: VISA IMAGES	273
215	FALSE MATCH RATE CALIBRATION: VISA IMAGES	274
216	FALSE MATCH RATE CALIBRATION: VISA IMAGES	275
217	FALSE MATCH RATE CALIBRATION: VISA IMAGES	276
218	FALSE MATCH RATE CALIBRATION: VISA IMAGES	277
219	FALSE MATCH RATE CALIBRATION: VISA IMAGES	278
220	FALSE MATCH RATE CALIBRATION: VISA IMAGES	279
221	FALSE MATCH RATE CALIBRATION: VISA IMAGES	280
222	FALSE MATCH RATE CALIBRATION: VISA IMAGES	281
223	FALSE MATCH RATE CALIBRATION: VISA IMAGES	282
224	FALSE MATCH RATE CALIBRATION: VISA IMAGES	283
225	FALSE MATCH RATE CALIBRATION: VISA IMAGES	284
226	FALSE MATCH RATE CALIBRATION: VISA IMAGES	285
227	FALSE MATCH RATE CALIBRATION: VISA IMAGES	286
228	FALSE MATCH RATE CALIBRATION: VISA IMAGES	287
229	FALSE MATCH RATE CALIBRATION: VISA IMAGES	288
230	FALSE MATCH RATE CALIBRATION: VISA IMAGES	289
231	FALSE MATCH RATE CALIBRATION: VISA IMAGES	290
232	FALSE MATCH RATE CALIBRATION: VISA IMAGES	291
233	FALSE MATCH RATE CALIBRATION: VISA IMAGES	292
234	FALSE MATCH RATE CALIBRATION: VISA IMAGES	293
235	FALSE MATCH RATE CALIBRATION: VISA IMAGES	294
236	EFFECT OF COUNTRY OF BIRTH ON FNMR	296
237	EFFECT OF COUNTRY OF BIRTH ON FNMR	297
238	EFFECT OF COUNTRY OF BIRTH ON FNMR	298
239	EFFECT OF COUNTRY OF BIRTH ON FNMR	299
240	EFFECT OF COUNTRY OF BIRTH ON FNMR	300
241	EFFECT OF COUNTRY OF BIRTH ON FNMR	301
242	EFFECT OF COUNTRY OF BIRTH ON FNMR	302
243	EFFECT OF COUNTRY OF BIRTH ON FNMR	303
244	EFFECT OF COUNTRY OF BIRTH ON FNMR	304
245	EFFECT OF COUNTRY OF BIRTH ON FNMR	305
246	EFFECT OF COUNTRY OF BIRTH ON FNMR	306
247	EFFECT OF COUNTRY OF BIRTH ON FNMR	307
248	EFFECT OF COUNTRY OF BIRTH ON FNMR	308
249	EFFECT OF COUNTRY OF BIRTH ON FNMR	309
250	EFFECT OF COUNTRY OF BIRTH ON FNMR	310
251	EFFECT OF COUNTRY OF BIRTH ON FNMR	311
252	EFFECT OF COUNTRY OF BIRTH ON FNMR	312
253	EFFECT OF COUNTRY OF BIRTH ON FNMR	313
254	EFFECT OF COUNTRY OF BIRTH ON FNMR	314
255	EFFECT OF COUNTRY OF BIRTH ON FNMR	315
256	EFFECT OF COUNTRY OF BIRTH ON FNMR	316
257	EFFECT OF COUNTRY OF BIRTH ON FNMR	317
258	EFFECT OF COUNTRY OF BIRTH ON FNMR	318
259	EFFECT OF COUNTRY OF BIRTH ON FNMR	319
260	EFFECT OF COUNTRY OF BIRTH ON FNMR	320
261	EFFECT OF COUNTRY OF BIRTH ON FNMR	321
262	EFFECT OF COUNTRY OF BIRTH ON FNMR	322
263	EFFECT OF COUNTRY OF BIRTH ON FNMR	323

264	EFFECT OF COUNTRY OF BIRTH ON FNMR	324
265	EFFECT OF COUNTRY OF BIRTH ON FNMR	325
266	EFFECT OF COUNTRY OF BIRTH ON FNMR	326
267	EFFECT OF COUNTRY OF BIRTH ON FNMR	327
268	EFFECT OF COUNTRY OF BIRTH ON FNMR	328
269	EFFECT OF COUNTRY OF BIRTH ON FNMR	329
270	ERROR TRADEOFF CHARACTERISTIC: MUGSHOT IMAGES	331
271	ERROR TRADEOFF CHARACTERISTIC: MUGSHOT IMAGES	332
272	ERROR TRADEOFF CHARACTERISTIC: MUGSHOT IMAGES	333
273	ERROR TRADEOFF CHARACTERISTIC: MUGSHOT IMAGES	334
274	ERROR TRADEOFF CHARACTERISTIC: MUGSHOT IMAGES	335
275	ERROR TRADEOFF CHARACTERISTIC: MUGSHOT IMAGES	336
276	ERROR TRADEOFF CHARACTERISTIC: MUGSHOT IMAGES	337
277	ERROR TRADEOFF CHARACTERISTIC: MUGSHOT IMAGES	338
278	ERROR TRADEOFF CHARACTERISTIC: MUGSHOT IMAGES	339
279	ERROR TRADEOFF CHARACTERISTIC: MUGSHOT IMAGES	340
280	ERROR TRADEOFF CHARACTERISTIC: MUGSHOT IMAGES	341
281	ERROR TRADEOFF CHARACTERISTIC: MUGSHOT IMAGES	342
282	ERROR TRADEOFF CHARACTERISTIC: MUGSHOT IMAGES	343
283	ERROR TRADEOFF CHARACTERISTIC: MUGSHOT IMAGES	344
284	ERROR TRADEOFF CHARACTERISTIC: MUGSHOT IMAGES	345
285	ERROR TRADEOFF CHARACTERISTIC: MUGSHOT IMAGES	346
286	ERROR TRADEOFF CHARACTERISTIC: MUGSHOT IMAGES	347
287	ERROR TRADEOFF CHARACTERISTIC: MUGSHOT IMAGES	348
288	ERROR TRADEOFF CHARACTERISTIC: MUGSHOT IMAGES	349
289	ERROR TRADEOFF CHARACTERISTIC: MUGSHOT IMAGES	350
290	ERROR TRADEOFF CHARACTERISTIC: MUGSHOT IMAGES	351
291	ERROR TRADEOFF CHARACTERISTIC: MUGSHOT IMAGES	352
292	ERROR TRADEOFF CHARACTERISTIC: MUGSHOT IMAGES	353
293	ERROR TRADEOFF CHARACTERISTIC: MUGSHOT IMAGES	354
294	ERROR TRADEOFF CHARACTERISTIC: MUGSHOT IMAGES	355
295	EFFECT OF SUBJECT AGE ON FNMR	357
296	EFFECT OF SUBJECT AGE ON FNMR	358
297	EFFECT OF SUBJECT AGE ON FNMR	359
298	EFFECT OF SUBJECT AGE ON FNMR	360
299	EFFECT OF SUBJECT AGE ON FNMR	361
300	EFFECT OF SUBJECT AGE ON FNMR	362
301	EFFECT OF SUBJECT AGE ON FNMR	363
302	EFFECT OF SUBJECT AGE ON FNMR	364
303	EFFECT OF SUBJECT AGE ON FNMR	365
304	EFFECT OF SUBJECT AGE ON FNMR	366
305	EFFECT OF SUBJECT AGE ON FNMR	367
306	EFFECT OF SUBJECT AGE ON FNMR	368
307	EFFECT OF SUBJECT AGE ON FNMR	369
308	EFFECT OF SUBJECT AGE ON FNMR	370
309	EFFECT OF SUBJECT AGE ON FNMR	371
310	EFFECT OF SUBJECT AGE ON FNMR	372
311	EFFECT OF SUBJECT AGE ON FNMR	373
312	EFFECT OF SUBJECT AGE ON FNMR	374
313	EFFECT OF SUBJECT AGE ON FNMR	375
314	EFFECT OF SUBJECT AGE ON FNMR	376
315	EFFECT OF SUBJECT AGE ON FNMR	377
316	EFFECT OF SUBJECT AGE ON FNMR	378
317	EFFECT OF SUBJECT AGE ON FNMR	379

318	EFFECT OF SUBJECT AGE ON FNMR	380
319	EFFECT OF SUBJECT AGE ON FNMR	381
320	EFFECT OF SUBJECT AGE ON FNMR	382
321	EFFECT OF SUBJECT AGE ON FNMR	383
322	EFFECT OF SUBJECT AGE ON FNMR	384
323	EFFECT OF SUBJECT AGE ON FNMR	385
324	EFFECT OF SUBJECT AGE ON FNMR	386
325	EFFECT OF SUBJECT AGE ON FNMR	387
326	EFFECT OF SUBJECT AGE ON FNMR	388
327	EFFECT OF SUBJECT AGE ON FNMR	389
328	EFFECT OF SUBJECT AGE ON FNMR	390
329	WORST CASE REGIONAL EFFECT FNMR	393
330	IMPOSTOR DISTRIBUTION SHIFTS FOR SELECT COUNTRY PAIRS	395

	Location	Developer Name	Short Name	Seq. Num.	Validation Date
1	NL	20Face	20face-000	000	2021-04-12
2	NL	20Face	20face-001	001	2021-09-29
3	US	3Divi	3divi-006	006	2021-04-14
4	US	3Divi	3divi-007	007	2021-09-27
5	TH	ACI Software	acisw-003	003	2020-08-03
6	TH	ACI Software	acisw-007	007	2021-11-15
7	SG	ADVANCE.AI	advance-002	002	2019-12-19
8	SG	ADVANCE.AI	advance-003	003	2021-08-05
9	US	AFIS and Biometrics Consulting	afisbiometrics-000	000	2022-01-27
10	TW	ASUSTek Computer Inc	asusaics-000	000	2019-10-24
11	TW	ASUSTek Computer Inc	asusaics-001	001	2020-02-25
12	CN	AYF Technology	ayftech-001	001	2020-07-06
13	TW	Ability Enterprise - Andro Video	androvideo-000	000	2021-01-25
14	TW	Acer Incorporated	acer-001	001	2020-06-30
15	TW	Acer Incorporated	acer-002	002	2021-11-10
16	SG	Adera Global PTE	adera-002	002	2021-02-16
17	SG	Adera Global PTE	adera-003	003	2021-07-12
18	TH	Ai First	aifirst-001	001	2019-11-21
19	TW	AiUnion Technology	aiunionface-000	000	2019-10-22
20	TH	Aigen	aigen-001	001	2020-10-06
21	TH	Aigen	aigen-002	002	2021-03-15
22	KR	Ajou University	ajou-001	001	2021-03-08
23	ID	Akurat Satu Indonesia	ptakuratsatu-000	000	2020-09-11
24	KR	Alchera Inc	alchera-002	002	2021-03-05
25	KR	Alchera Inc	alchera-003	003	2021-07-13
26	ID	Alfabeta	alfabeta-001	001	2021-12-02
27	ES	Alice Biometrics	alice-000	000	2021-06-15
28	RU	Alivia / Innovation Sys	isystems-001	001	2018-06-12
29	RU	Alivia / Innovation Sys	isystems-002	002	2018-10-18
30	IN	AllGoVision	allgovision-000	000	2019-03-01
31	CN	AlphaSTG	alphaface-001	001	2019-09-03
32	CN	AlphaSTG	alphaface-002	002	2020-02-20
33	GB	Amplified Group	amplifiedgroup-001	001	2019-03-01
34	CN	Anke Investments	anke-004	004	2019-06-27
35	CN	Anke Investments	anke-005	005	2019-11-21
36	BR	Antheus Technologia	antheus-000	000	2019-12-05
37	BR	Antheus Technologia	antheus-001	001	2020-06-25
38	GB	AnyVision	anyvision-004	004	2018-06-15
39	GB	AnyVision	anyvision-005	005	2021-02-03
40	US	Armatura LLC	armatura-001	001	2022-01-04
41	CN	AuthenMetric	authenmetric-003	003	2021-08-09
42	CN	AuthenMetric	authenmetric-004	004	2022-01-03
43	US	Aware	aware-005	005	2020-02-27
44	US	Aware	aware-006	006	2021-07-03
45	IN	Awidit Systems	awiros-001	001	2019-09-23
46	IN	Awidit Systems	awiros-002	002	2020-10-28
47	JP	Ayonix	ayonix-000	000	2017-06-22
48	CN	BOE Technology Group	boetech-001	001	2021-06-22
49	CN	BOE Technology Group	boetech-002	002	2021-12-21
50	ES	Bee the Data	beethedata-000	000	2021-07-26
51	CN	Beihang University-ERCACAT	ercacat-001	001	2020-07-06
52	CN	Beijing Alleyes Technology	alleyes-000	000	2020-03-09
53	CN	Beijing DeepSense Technologies	deepsense-000	000	2021-03-19
54	CN	Beijing DeepSense Technologies	deepsense-001	001	2022-03-11
55	CN	Beijing Hisign Technology	hisign-001	001	2021-09-24
56	CN	Beijing Mendaxia Technology	mendaxiatech-000	000	2021-09-15
57	CN	Beijing Vion Technology Inc	vion-000	000	2018-10-19
58	KZ	Beyne.AI	beyneai-000	000	2022-01-03
59	CH	BioID Technologies SA	bioidechswiss-001	001	2020-08-28
60	CH	BioID Technologies SA	bioidechswiss-002	002	2021-02-17
61	IN	Biocube Matrics	biocube-001	001	2021-09-08
62	UK	BitCenter UK	farfaces-001	001	2021-04-09
63	CN	Bitmain	bm-001	001	2018-10-17
64	CN	Bresee Technology	bresee-001	001	2020-12-30
65	CN	Bresee Technology	bresee-002	002	2021-06-30
66	CN	CSA IntelliCloud Technology	intellicloudai-001	001	2019-08-13
67	CN	CSA IntelliCloud Technology	intellicloudai-002	002	2020-12-17
68	TW	CTBC Bank	ctbcbank-000	000	2019-06-28
69	TW	CTBC Bank	ctbcbank-001	001	2019-10-28
70	KR	CUDO Communication	cudocommunication-001	001	2021-10-20

Table 1: Summary of participant information included in this report.

	Location	Developer Name	Short Name	Seq. Num.	Validation Date
71	US	Camvi Technologies	camvi-002	002	2018-10-19
72	US	Camvi Technologies	camvi-004	004	2019-07-12
73	CN	Canon Inc	canon-002	002	2020-12-29
74	JP	Canon Inc	canon-003	003	2021-09-15
75	CN	China Electronics Import-Export Corp	ceiec-003	003	2020-01-06
76	CN	China Electronics Import-Export Corp	ceiec-004	004	2021-01-18
77	CN	China University of Petroleum	upc-001	001	2019-06-05
78	CN	Chinese University of Hong Kong	cuhkee-001	001	2020-03-18
79	KR	Chosun University	chosun-001	001	2020-07-01
80	KR	Chosun University	chosun-002	002	2020-11-25
81	TW	Chunghwa Telecom	chtface-004	004	2021-10-08
82	TW	Chunghwa Telecom	chtface-005	005	2022-03-09
83	US	Clearview AI Inc	clearviewai-000	000	2021-09-22
84	CN	Closeli Inc	closeli-001	001	2021-07-15
85	US	CloudSmart Consulting LLC	csc-002	002	2021-03-24
86	US	CloudSmart Consulting LLC	csc-003	003	2021-08-26
87	TW	Cloudmatrix	cloudmatrix-000	000	2021-10-22
88	TW	Cloudmatrix	cloudmatrix-001	001	2022-02-16
89	CN	Cloudwalk - Hengrui AI Technology	cloudwalk-hr-003	003	2020-09-25
90	CN	Cloudwalk - Hengrui AI Technology	cloudwalk-hr-004	004	2021-02-10
91	CN	Cloudwalk - Moontime Smart Technology	cloudwalk-mt-003	003	2020-12-22
92	CN	Cloudwalk - Moontime Smart Technology	cloudwalk-mt-004	004	2021-11-09
93	IN	Code Everest Pvt	facex-001	001	2021-03-08
94	IN	Code Everest Pvt	facex-002	002	2021-08-24
95	DE	Cognitec Systems GmbH	cognitec-003	003	2021-07-30
96	DE	Cognitec Systems GmbH	cognitec-004	004	2022-02-10
97	TW	Coretech Knowledge Inc	coretech-000	000	2021-07-12
98	IL	Corsight	corsight-001	001	2021-03-11
99	IL	Corsight	corsight-002	002	2021-09-01
100	IL	Cortica	cor-001	001	2020-09-24
101	KR	Cubox	cubox-001	001	2020-12-07
102	KR	Cubox	cubox-002	002	2021-08-24
103	JP	Cybercore	cybercore-000	000	2020-08-26
104	JP	Cybercore	cybercore-001	001	2021-12-15
105	US	Cyberextruder	cyberextruder-001	001	2017-08-02
106	US	Cyberextruder	cyberextruder-002	002	2018-01-30
107	TW	Cyberlink Corp	cyberlink-007	007	2021-07-16
108	TW	Cyberlink Corp	cyberlink-008	008	2022-01-07
109	CN	DSK	dsk-000	000	2019-06-28
110	CN	Dahua Technology	dahua-006	006	2020-12-30
111	CN	Dahua Technology	dahua-007	007	2021-12-20
112	IE	Daon	daon-000	000	2021-11-03
113	US	Decatur Industries Inc	decatur-000	000	2020-08-18
114	US	Decatur Industries Inc	decatur-001	001	2021-09-27
115	CN	Deepglint	deepglint-003	003	2021-03-03
116	CN	Deepglint	deepglint-004	004	2021-09-17
117	FR	Deepsense	dps-000	000	2021-07-16
118	DE	Dermalog	dermalog-008	008	2021-03-25
119	DE	Dermalog	dermalog-009	009	2021-10-06
120	CN	DiDi ChuXing Technology	didiglobalface-001	001	2019-10-23
121	IN	Digidata	didata-000	000	2022-01-27
122	GB	Digital Barriers	digitalbarriers-002	002	2019-03-01
123	TR	Ekin Smart City Technologies	ekin-002	002	2021-05-04
124	RU	Enface	enface-000	000	2021-04-09
125	RU	Enface	enface-001	001	2021-12-17
126	CH	Euronovate SA	euronovate-001	001	2021-11-15
127	RU	Expasoft LLC	expasoft-001	001	2020-09-03
128	RU	Expasoft LLC	expasoft-002	002	2021-07-26
129	DE	FaceOnLive Inc	faceonlive-001	001	2021-11-23
130	GB	FaceSoft	facesoft-000	000	2019-07-10
131	KR	FaceTag Co	facetag-000	000	2021-03-22
132	KR	FaceTag Co	facetag-002	002	2022-01-06
133	TW	FarBar Inc	f8-001	001	2019-07-11
134	TW	FarBar Inc	f8-002	002	2022-03-02
135	CN	Fiberhome Telecommunication Technologies	fiberhome-nanjing-003	003	2021-03-12
136	CN	Fiberhome Telecommunication Technologies	fiberhome-nanjing-004	004	2021-09-14
137	UK	Fincore Ltd	fincore-000	000	2021-06-07
138	CN	Fujitsu Research and Development Center	fujitsulab-002	002	2021-02-24
139	CN	Fujitsu Research and Development Center	fujitsulab-003	003	2021-07-12
140	US	Gemalto Cogent	cogent-005	005	2020-12-29

Table 2: Summary of participant information included in this report.

	Location	Developer Name	Short Name	Seq. Num.	Validation Date
141	US	Gemalto Cogent	cogent-006	006	2021-07-28
142	TW	GeoVision Inc	geo-002	002	2021-04-01
143	TW	GeoVision Inc	geo-004	004	2022-02-10
144	JP	Glory	glory-003	003	2021-01-15
145	JP	Glory	glory-004	004	2022-02-08
146	TW	Gorilla Technology	gorilla-007	007	2021-06-28
147	TW	Gorilla Technology	gorilla-008	008	2021-11-08
148	US	Graymatics	graymatics-001	001	2022-01-13
149	US	Griaule	griaule-000	000	2021-08-20
150	CN	Guangzhou Pixel Solutions	pixelall-006	006	2021-06-17
151	CN	Guangzhou Pixel Solutions	pixelall-007	007	2021-12-01
152	CN	Hangzhuo Allu Network Information Technology	hzailu-001	001	2022-01-27
153	ES	Herta Security	hertasecurity-000	000	2021-01-05
154	ES	Herta Security	hertasecurity-001	001	2022-01-18
155	CN	Hikvision Research Institute	hik-001	001	2019-03-01
156	IN	HyperVerge Inc	hyperverge-001	001	2020-12-13
157	IN	HyperVerge Inc	hyperverge-002	002	2021-05-27
158	AU	ICM Airport Technics	icm-002	002	2020-11-13
159	AU	ICM Airport Technics	icm-003	003	2021-09-06
160	FR	ID3 Technology	id3-006	006	2020-12-17
161	FR	ID3 Technology	id3-008	008	2021-11-10
162	RU	ITMO University	itmo-007	007	2020-01-06
163	RU	ITMO University	itmo-008	008	2021-11-19
164	RU	IVA Cognitive	ivacognitive-001	001	2021-01-29
165	FR	Idemia	idemia-007	007	2020-12-04
166	FR	Idemia	idemia-008	008	2021-07-07
167	US	Imageware Systems	iws-000	000	2020-08-12
168	AU	Imagus Technology Pty	imagus-004	004	2021-09-20
169	AU	Imagus Technology Pty	imagus-005	005	2022-03-03
170	GB	Imperial College London	imperial-000	000	2019-03-01
171	GB	Imperial College London	imperial-002	002	2019-08-28
172	US	Incode Technologies Inc	incode-009	009	2021-06-22
173	US	Incode Technologies Inc	incode-010	010	2021-10-22
174	IN	Innef Labs	inneflabs-000	000	2020-09-04
175	GB	Innovative Technology	innovativetechnologyltd-001	001	2019-10-22
176	GB	Innovative Technology	innovativetechnologyltd-002	002	2020-02-26
177	SK	Innovatrics	innovatrics-007	007	2020-08-19
178	SK	Innovatrics	innovatrics-008	008	2021-12-15
179	CN	InsightFace AI	insightface-001	001	2021-09-27
180	CN	InsightFace AI	insightface-002	002	2022-01-31
181	CN	Institute of Computing Technology	icthtc-000	000	2020-11-29
182	RU	Institute of Information Technologies	iit-002	002	2019-12-04
183	RU	Institute of Information Technologies	iit-003	003	2020-12-01
184	IS	Intel Research Group	intelresearch-004	004	2021-08-24
185	IS	Intel Research Group	intelresearch-005	005	2022-02-13
186	KR	IntelliVIX	intellivix-001	001	2022-02-25
187	US	Intellivision	intellivision-002	002	2019-08-23
188	US	Intellivision	intellivision-003	003	2022-03-07
189	US	IrexAI	irex-000	000	2020-12-17
190	IL	Is It You	isityou-000	000	2017-06-26
191	KR	Kakao Enterprise	kakao-005	005	2021-03-09
192	KR	Kakao Enterprise	kakao-007	007	2022-01-12
193	KR	Kakao Pay Corp	kakaoipay-001	001	2021-07-06
194	TH	Kasikorn Labs	kasikornlabs-000	000	2022-03-02
195	SG	Kedacom International Pte	kedacom-000	000	2019-06-03
196	US	Kneron Inc	kneron-003	003	2019-07-01
197	US	Kneron Inc	kneron-005	005	2020-02-21
198	US	KnowUTech LLC	knowutech-000	000	2022-02-13
199	KR	Kookmin University	kookmin-002	002	2021-03-05
200	CN	KuKe3D Technology	kuke3d-001	001	2021-10-28
201	BR	Lebentech Biometrics	lebentech-000	000	2022-02-16
202	IN	Lema Labs	lemalabs-001	001	2021-04-13
203	JP	Line Corporation	line-000	000	2021-03-31
204	JP	Line Corporation	line-001	001	2021-09-26
205	RU	Lomonosov Moscow State University	intsy whole-001	001	2019-10-22
206	RU	Lomonosov Moscow State University	intsy whole-002	002	2020-03-12
207	IN	Lookman Electroplast Industries	lookman-002	002	2018-06-13
208	IN	Lookman Electroplast Industries	lookman-004	004	2019-06-03
209	US	Luxand Inc	luxand-000	000	2019-11-07
210	RU	MVision	mvision-001	001	2019-11-12

Table 3: Summary of participant information included in this report.

	Location	Developer Name	Short Name	Seq. Num.	Validation Date
211	IN	Mantra Softtech India	mantra-000	000	2021-10-28
212	CN	Maxvision Technology	maxvision-000	000	2021-10-27
213	CN	Maxvision Technology	maxvision-001	001	2022-03-03
214	CN	Megvii/Face++	megvii-003	003	2021-03-08
215	CN	Megvii/Face++	megvii-004	004	2021-11-19
216	GB	MicroFocus	microfocus-001	001	2018-06-13
217	GB	MicroFocus	microfocus-002	002	2018-10-17
218	CN	Minivision	minivision-000	000	2020-10-28
219	NO	Mobai	mobai-000	000	2020-08-26
220	NO	Mobai	mobai-001	001	2021-02-17
221	ES	Mobbet Solutions	mobbet-001	001	2021-06-16
222	ES	Mobbet Solutions	mobbet-002	002	2021-12-16
223	KR	Mobipin Technology	mobipintech-000	000	2021-11-23
224	TH	Momentum Digital	sertis-000	000	2019-10-07
225	TH	Momentum Digital	sertis-002	002	2021-05-13
226	CN	MoreDian Technology	moredian-000	000	2021-02-24
227	CN	Multi-Modality Intelligence	multimodality-000	000	2021-10-19
228	RU	N-Tech Lab	ntechlab-011	011	2021-09-13
229	RU	N-Tech Lab	ntechlab-012	012	2022-01-20
230	CA	NEO Systems	neosystems-002	002	2021-07-03
231	CA	NEO Systems	neosystems-003	003	2021-11-11
232	KR	NHN Corp	nhn-002	002	2021-07-15
233	KR	NHN Corp	nhn-003	003	2022-02-22
234	KR	NSENSE Corp	nsensecorp-002	002	2021-05-06
235	KR	NSENSE Corp	nsensecorp-003	003	2021-10-29
236	CN	Nanjing Kiwi Network Technology	kiwitech-000	000	2021-03-19
237	KR	Naver Corp	clova-000	000	2020-10-21
238	KR	Neosecu Co	openface-001	001	2021-06-15
239	TW	Netbridge Technology Incoporation	netbridgetech-001	001	2020-01-08
240	TW	Netbridge Technology Incoporation	netbridgetech-002	002	2020-08-11
241	LT	Neurotechnology	neurotechnology-012	012	2021-07-26
242	LT	Neurotechnology	neurotechnology-013	013	2022-01-07
243	ID	Nodeflux	nodeflux-002	002	2019-08-13
244	IN	NotionTag Technologies Private Limited	notiontag-001	001	2021-03-04
245	IN	NotionTag Technologies Private Limited	notiontag-002	002	2021-09-17
246	US	Omnigarde Ltd	omnigarde-001	001	2021-08-23
247	US	Omnigarde Ltd	omnigarde-002	002	2022-01-19
248	KR	One More Security	omsecurity-000	000	2021-12-15
249	RU	Oz Forensics LLC	oz-003	003	2021-08-09
250	RU	Oz Forensics LLC	oz-004	004	2021-12-13
251	CH	PXL Vision AG	pxl-001	001	2020-06-30
252	SG	Panasonic R+D Center Singapore	psl-008	008	2021-07-21
253	SG	Panasonic R+D Center Singapore	psl-009	009	2021-12-08
254	TR	Papilon Savunma	papsav1923-001	001	2021-03-10
255	TR	Papilon Savunma	papsav1923-002	002	2022-01-20
256	US	Paravision	paravision-008	008	2021-06-30
257	US	Paravision (EverAI)	paravision-010	010	2022-02-02
258	SG	Pensees Pte	pensees-001	001	2020-08-17
259	IN	Pyramid Cyber Security + Forensic (P)	pyramid-000	000	2019-11-04
260	TW	Qnap Security	qnap-000	000	2021-08-09
261	TW	Qnap Security	qnap-001	001	2021-12-09
262	CZ	Quantasoft	quantasoft-003	003	2021-04-19
263	US	Rank One Computing	rankone-011	011	2021-08-27
264	US	Rank One Computing	rankone-012	012	2021-12-27
265	US	Realnetworks Inc	realnetworks-005	005	2021-09-27
266	US	Realnetworks Inc	realnetworks-006	006	2022-02-09
267	US	Regula Forensics	regula-000	000	2021-04-13
268	US	Regula Forensics	regula-001	001	2021-12-14
269	CN	Remark Holdings	remarkai-001	001	2019-03-01
270	CN	Remark Holdings	remarkai-003	003	2021-06-22
271	SG	Rendip	rendip-000	000	2021-04-19
272	UK	Reveal Media Ltd	revealmedia-005	005	2021-09-24
273	UK	Reveal Media Ltd	revealmedia-006	006	2022-01-26
274	CN	Rokid Corporation	rokid-000	000	2019-08-01
275	CN	Rokid Corporation	rokid-001	001	2019-12-13
276	KR	SK Telecom	sktelecom-000	000	2021-07-09
277	KR	SQISoft	sqisoft-001	001	2021-07-27
278	KR	SQISoft	sqisoft-002	002	2021-11-03
279	DE	Saffe	saffe-001	001	2018-10-19
280	DE	Saffe	saffe-002	002	2019-03-01

Table 4: Summary of participant information included in this report.

	Location	Developer Name	Short Name	Seq. Num.	Validation Date
281	KR	Samsung S1 Corp	s1-003	003	2021-08-24
282	KR	Samsung S1 Corp	s1-004	004	2022-01-04
283	KR	Samsung-SDS	samsungsds-000	000	2021-10-28
284	IN	Samtech InfoNet Limited	samtech-001	001	2019-10-15
285	RU	Satellite Innovation/Eocortex	eocortex-000	000	2020-08-26
286	IL	Scanovate	scanovate-002	002	2020-06-26
287	IL	Scanovate	scanovate-003	003	2021-11-15
288	RO	Securif AI	securifai-003	003	2021-08-03
289	RO	Securif AI	securifai-004	004	2021-12-21
290	CN	Sensetime Group	sensetime-005	005	2021-05-24
291	CN	Sensetime Group	sensetime-006	006	2021-12-28
292	SG	Seventh Sense Artificial Intelligence	seventhsense-000	000	2021-06-29
293	SG	Seventh Sense Artificial Intelligence	seventhsense-001	001	2022-03-04
294	US	Shaman Software	shaman-000	000	2017-12-05
295	US	Shaman Software	shaman-001	001	2018-01-13
296	CN	Shanghai Jiao Tong University	sjtu-003	003	2020-11-02
297	CN	Shanghai Jiao Tong University	sjtu-004	004	2021-05-13
298	CN	Shanghai Ulucu Electronics Technology	uluface-002	002	2019-07-10
299	CN	Shanghai Ulucu Electronics Technology	uluface-003	003	2019-11-12
300	CN	Shanghai University - Shanghai Film Academy	shu-002	002	2019-12-10
301	CN	Shanghai University - Shanghai Film Academy	shu-003	003	2020-06-24
302	CN	Shanghai Yitu Technology	yitu-003	003	2019-03-01
303	CN	Shenzhen AiMall Tech	aimall-002	002	2020-03-12
304	CN	Shenzhen AiMall Tech	aimall-003	003	2020-08-12
305	CN	Shenzhen EI Networks	einetworks-000	000	2019-08-13
306	CN	Shenzhen Inst Adv Integrated Tech CAS	siat-002	002	2018-06-13
307	CN	Shenzhen Inst Adv Integrated Tech CAS	siat-005	005	2022-02-08
308	CN	Shenzhen Intellifusion Technologies	intellifusion-001	001	2019-08-22
309	CN	Shenzhen Intellifusion Technologies	intellifusion-002	002	2020-03-18
310	CN	Shenzhen University-Macau University of Science and Technology	sztu-000	000	2020-12-17
311	CN	Shenzhen University-Macau University of Science and Technology	sztu-001	001	2021-07-13
312	RU	Smart Engines	smartengines-000	000	2021-08-25
313	DE	Smilart	smilart-002	002	2018-02-06
314	DE	Smilart	smilart-003	003	2019-03-01
315	TR	Sodec App Inc	sodec-000	000	2021-06-02
316	IN	Staqu Technologies	st aqu-000	000	2020-07-15
317	CN	Star Hybrid Limited	starhybrid-001	001	2019-06-19
318	CN	Su Zhou NaZhiTianDi intelligent technology	nazhiai-000	000	2020-06-25
319	IN	Sukshi Technology Innovation	sukshi-000	000	2022-02-13
320	KR	Suprema AI Inc	suprema-001	001	2021-09-23
321	KR	Suprema AI Inc	suprema-002	002	2022-02-11
322	KR	Suprema ID Inc	supremaid-001	001	2021-05-04
323	RU	Synesis	synesis-006	006	2019-10-10
324	RU	Synesis	synesis-007	007	2020-06-24
325	TW	Synology Inc	synology-000	000	2019-10-23
326	TW	Synology Inc	synology-002	002	2020-08-20
327	BR	T4iSB	t4isb-000	000	2022-01-28
328	CN	TUPU Technology	tuputech-000	000	2019-10-11
329	TW	Taiwan AI Labs	ailabs-001	001	2019-12-18
330	TW	Taiwan-Certificate Authority Incorporation	twface-000	000	2021-05-14
331	TW	Taiwan-Certificate Authority Incorporation	twface-001	001	2021-09-14
332	CH	Tech5 SA	tech5-004	004	2020-03-09
333	CH	Tech5 SA	tech5-005	005	2020-07-24
334	TR	Techsign	techsign-000	000	2021-08-25
335	CN	Tencent Deepsea Lab	deepsea-001	001	2019-06-03
336	RU	Tevian	tevian-007	007	2021-08-06
337	RU	Tevian	tevian-008	008	2021-12-06
338	US	TigerIT Americas LLC	tiger-005	005	2021-07-29
339	US	TigerIT Americas LLC	tiger-006	006	2021-12-13
340	RU	Tinkoff Bank	tinkoff-001	001	2021-05-13
341	CN	TongYi Transportation Technology	tongyi-005	005	2019-06-12
342	TW	Toppan ID Gate	toppanidgate-000	000	2021-09-28
343	JP	Toshiba	toshiba-004	004	2021-09-27
344	JP	Toshiba	toshiba-005	005	2022-02-09
345	JP	Tripleize	aize-001	001	2021-04-23
346	JP	Tripleize	aize-002	002	2021-10-08
347	US	Trueface.ai	trueface-002	002	2021-03-29
348	US	Trueface.ai	trueface-003	003	2021-09-30
349	CN	TuringTech.vip	turingtechvip-001	001	2022-02-03
350	CN	ULSee Inc	ulsee-001	001	2019-07-31

Table 5: Summary of participant information included in this report.

	Location	Developer Name	Short Name	Seq. Num.	Validation Date
351	FR	Unissey	unissey-001	001	2021-11-29
352	PT	Universidade de Coimbra	visteam-002	002	2021-08-20
353	PT	Universidade de Coimbra	visteam-003	003	2022-01-31
354	US	VCognition	vcog-002	002	2017-06-12
355	ES	Veridas Digital Authentication Solutions S.L.	veridas-006	006	2021-04-15
356	ES	Veridas Digital Authentication Solutions S.L.	veridas-007	007	2021-09-02
357	KZ	Verigram	verigram-000	000	2021-09-06
358	KZ	Verigram	verigram-001	001	2022-03-09
359	ID	Verihubs	verihubs-inteligensia-000	000	2021-07-27
360	TW	Via Technologies Inc	via-000	000	2019-07-08
361	TW	Via Technologies Inc	via-001	001	2020-01-08
362	DE	Videmo Intelligent Videoanalyse	videmo-000	000	2019-12-19
363	DE	Videmo Intelligent Videoanalyse	videmo-001	001	2021-12-22
364	IN	Videonetics Technology Pvt	videonetics-001	001	2019-06-19
365	IN	Videonetics Technology Pvt	videonetics-002	002	2019-11-21
366	VN	Vietnam Posts and Telecommunications Group	vnpt-002	002	2021-06-08
367	VN	Vietnam Posts and Telecommunications Group	vnpt-003	003	2021-12-01
368	VN	Viettel Group	vts-000	000	2020-11-04
369	VN	Viettel High Technology	viettelhightech-000	000	2021-08-04
370	US	Vigilant Solutions	vigilantsolutions-010	010	2021-04-07
371	US	Vigilant Solutions	vigilantsolutions-011	011	2021-08-07
372	VN	VinAI Research VietNam	vinai-000	000	2020-09-24
373	VN	VinBigData	vinbigdata-001	001	2022-01-06
374	SE	Visage Technologies	visage-000	000	2020-12-09
375	FI	Visidon	vd-002	002	2021-04-12
376	FI	Visidon	vd-003	003	2021-10-12
377	CN	Vision Intelligence Center of Meituan	meituan-000	000	2021-05-14
378	PT	Vision-Box	visionbox-001	001	2019-03-01
379	PT	Vision-Box	visionbox-002	002	2021-04-29
380	RU	VisionLabs	visionlabs-010	010	2021-01-25
381	RU	VisionLabs	visionlabs-011	011	2021-10-13
382	RU	Vcord	vcord-009	009	2020-12-28
383	RU	Vcord	vcord-010	010	2021-12-20
384	US	Wicket	wicket-000	000	2022-02-14
385	CN	Winsense	winsense-001	001	2019-10-16
386	CN	Winsense	winsense-002	002	2020-11-20
387	CN	Wuhan Tianyu Information Industry	wuhantianyu-001	001	2021-08-05
388	CN	X-Laboratory	x-laboratory-000	000	2019-09-03
389	CN	X-Laboratory	x-laboratory-001	001	2020-01-21
390	CN	Xforward AI Technology	xforwardai-001	001	2020-09-25
391	CN	Xforward AI Technology	xforwardai-002	002	2021-02-10
392	CN	Xiamen Meiya Pico Information	meiya-001	001	2019-03-01
393	CN	Xiamen University	xm-000	000	2020-10-19
394	PT	YooniK	yoonik-002	002	2021-09-06
395	PT	YooniK	yoonik-003	003	2022-01-06
396	TW	Yuan High-Tech Development	yuan-003	003	2021-09-17
397	TW	Yuan High-Tech Development	yuan-004	004	2022-01-14
398	CN	Yuntu Data and Technology	ytu-000	000	2021-06-16
399	CN	Zhuhai Yisheng Electronics Technology	yisheng-004	004	2018-06-12
400	CN	iQIYI Inc	iqface-000	000	2019-06-04
401	CN	iQIYI Inc	iqface-003	003	2021-02-23
402	TW	iSAP Solution Corporation	isap-001	001	2019-08-07
403	TW	iSAP Solution Corporation	isap-002	002	2020-09-01
404	TW	ioNetworks Inc	ionetworks-000	000	2021-07-20

Table 6: Summary of participant information included in this report.

	ALGORITHM	CONFIG	LIBRARY	TEMPLATE								COMPARISON ⁴									
				NAME	DATA	DATA	MEMORY	SIZE	GENERATION TIME (ms) ⁴				TIME (ns) ⁵								
									(KB) ¹	(KB) ²	(MB) ³	(B)	MUGSHOT	480x720	960x1440	1600x2400	3000x4500	GENUINE	IMPOSTOR		
1	20face-000	117155	324083	195	905	144	2048 ± 0	34	232 ± 1	24	223 ± 1	19	226 ± 4	17	222 ± 1	12	224 ± 1	375	44880 ± 134	374	44462 ± 163
2	20face-001	226824	324119	322	1940	361	4096 ± 0	45	279 ± 2	28	266 ± 1	21	266 ± 1	20	267 ± 1	15	267 ± 0	297	5553 ± 54	295	5541 ± 65
3	3divi-006	273866	52656	78	472	132	2048 ± 0	190	654 ± 1	158	651 ± 0	140	660 ± 1	123	678 ± 2	125	759 ± 13	97	775 ± 19	96	770 ± 22
4	3divi-007	483115	24723	255	1285	112	2048 ± 0	174	615 ± 1	148	616 ± 1	126	623 ± 1	112	644 ± 1	115	727 ± 5	81	707 ± 31	85	712 ± 25
5	acer-001	36650	66086	64	417	28	512 ± 0	31	199 ± 0	25	237 ± 28	20	229 ± 26	19	242 ± 37	14	259 ± 21	226	2453 ± 44	228	2461 ± 62
6	acer-002	43922	624858	31	187	149	2048 ± 0	27	184 ± 0	19	184 ± 0	13	185 ± 0	10	185 ± 0	10	186 ± 0	262	3370 ± 47	262	3350 ± 54
7	acisw-003	282029	35664	45	282	401	18467 ± 8	35	232 ± 1	29	267 ± 22	79	488 ± 28	218	990 ± 24	334	2977 ± 129	403	847908 ± 16757	403	851850 ± 17018
8	acisw-007	267619	36111	46	286	255	2048 ± 0	50	283 ± 0	39	293 ± 3	50	414 ± 0	39	404 ± 0	40	484 ± 1	152	1316 ± 22	152	1297 ± 23
9	ader-a-002	0	749797	200	921	392	5120 ± 0	389	1394 ± 11	347	1381 ± 1	344	1393 ± 1	321	1403 ± 1	275	1464 ± 2	217	2163 ± 32	217	2158 ± 28
10	ader-a-003	0	749778	198	917	391	5120 ± 0	384	1381 ± 12	348	1385 ± 1	345	1394 ± 1	318	1401 ± 1	276	1469 ± 1	216	2148 ± 34	216	2130 ± 32
11	advance-002	257173	20434	50	295	96	2048 ± 0	246	811 ± 2	203	803 ± 2	156	696 ± 2	130	699 ± 4	111	718 ± 1	115	987 ± 10	113	988 ± 45
12	advance-003	258867	78699	96	518	269	2048 ± 0	158	586 ± 0	133	584 ± 0	111	583 ± 0	93	588 ± 0	73	591 ± 1	196	1813 ± 17	192	1788 ± 26
13	afisbiometrics-000	545886	32882	230	1088	21	512 ± 0	353	1219 ± 1	297	1135 ± 1	282	1137 ± 2	251	1137 ± 1	208	1147 ± 1	158	1400 ± 29	155	1357 ± 32
14	aifirst-001	224157	808777	81	485	186	2048 ± 0	160	587 ± 2	127	568 ± 2	112	584 ± 3	98	601 ± 6	123	755 ± 5	132	1099 ± 14	134	1087 ± 45
15	aigen-001	256958	595227	237	1136	142	2048 ± 0	399	1448 ± 9	360	1451 ± 8	364	1759 ± 6	362	2594 ± 4	348	5691 ± 44	277	3772 ± 57	276	3736 ± 56
16	aigen-002	205300	1316138	190	874	270	2048 ± 0	159	586 ± 24	132	582 ± 4	220	920 ± 4	345	1758 ± 5	347	5427 ± 17	273	3678 ± 44	271	3646 ± 48
17	ailabs-001	1054663	338989	249	1252	110	2048 ± 0	197	664 ± 4	197	774 ± 50	285	1145 ± 12	350	1972 ± 74	345	5205 ± 272	394	104034 ± 661	394	103415 ± 7722
18	aimall-002	370156	25210	291	1576	237	2048 ± 0	235	776 ± 4	251	927 ± 27	229	940 ± 21	209	955 ± 34	180	1003 ± 75	391	72811 ± 7399	390	71216 ± 6286
19	aimall-003	504324	171935	318	1913	63	1024 ± 0	195	662 ± 1	187	740 ± 51	173	752 ± 62	147	741 ± 46	136	807 ± 47	369	34565 ± 93	370	34598 ± 118
20	aiunionface-000	241642	840295	61	402	234	2048 ± 0	183	637 ± 13	192	754 ± 41	256	1025 ± 28	262	1179 ± 29	293	1639 ± 47	126	1072 ± 19	132	1080 ± 47
21	aize-001	268456	168970	279	1436	240	2048 ± 0	100	437 ± 10	79	440 ± 8	99	542 ± 17	151	756 ± 27	289	1583 ± 53	206	1937 ± 22	202	1919 ± 23
22	aize-002	257106	182517	115	586	124	2048 ± 0	111	467 ± 1	92	479 ± 1	175	756 ± 1	333	1477 ± 1	343	4617 ± 41	49	597 ± 16	54	598 ± 14
23	ajou-001	363257	31734	70	442	233	2048 ± 0	132	530 ± 0	113	536 ± 0	95	535 ± 0	84	549 ± 0	69	577 ± 0	50	597 ± 19	53	596 ± 13
24	alchera-002	405409	22275	247	1233	114	2048 ± 0	306	968 ± 1	261	976 ± 2	243	979 ± 1	217	988 ± 1	185	1025 ± 2	268	3488 ± 63	266	3430 ± 63
25	alchera-003	487718	24613	267	1376	245	2048 ± 0	266	854 ± 3	223	862 ± 2	201	870 ± 1	183	882 ± 2	160	918 ± 1	265	3426 ± 57	263	3383 ± 53
26	alfabeta-001	128232	21780	6	73	31	512 ± 0	41	271 ± 0	34	276 ± 0	66	459 ± 2	186	886 ± 2	324	2547 ± 9	35	470 ± 25	37	458 ± 20
27	alice-000	1741293	19355	306	1732	363	4096 ± 0	299	950 ± 2	253	933 ± 1	234	949 ± 1	225	1011 ± 3	232	1264 ± 8	342	14975 ± 201	341	14890 ± 229
28	alleyes-000	507636	997090	187	857	148	2048 ± 0	238	784 ± 1	260	970 ± 61	241	974 ± 62	205	943 ± 69	193	1057 ± 23	151	1298 ± 34	153	1303 ± 51
29	allgovision-000	172509	155862	108	561	160	2048 ± 0	78	384 ± 8	62	395 ± 17	49	413 ± 14	61	471 ± 14	108	710 ± 21	366	29903 ± 406	367	29735 ± 194
30	alphaface-001	259849	81636	98	527	222	2048 ± 0	170	612 ± 1	144	613 ± 3	123	612 ± 1	103	619 ± 1	89	640 ± 2	119	1008 ± 10	119	1002 ± 19
31	alphaface-002	768995	70692	278	1434	241	2048 ± 0	179	628 ± 2	189	746 ± 19	172	751 ± 18	157	779 ± 22	142	828 ± 40	110	945 ± 25	111	935 ± 17
32	amplifiedgroup-001	0	47053	9	81	56	866 ± 2	9	93 ± 0	-	-	-	-	-	-	-	385	57803 ± 4210	383	56365 ± 1196	
33	androvideo-000	174847	585063	62	403	209	2048 ± 0	44	277 ± 0	37	285 ± 0	27	314 ± 0	33	372 ± 1	80	620 ± 0	243	2860 ± 28	243	2847 ± 22
34	anke-004	349388	410776	146	706	313	2056 ± 0	177	625 ± 1	149	627 ± 2	134	635 ± 3	117	653 ± 2	176	982 ± 8	67	633 ± 22	68	632 ± 34
35	anke-005	328553	429160	235	1134	303	2056 ± 0	161	590 ± 2	139	594 ± 5	119	601 ± 3	111	638 ± 4	140	821 ± 24	77	685 ± 19	81	687 ± 26
36	antheus-000	119453	41994	17	116	45	520 ± 0	13	109 ± 1	20	187 ± 1	15	189 ± 1	12	195 ± 1	13	236 ± 2	314	6901 ± 268	314	6936 ± 103
37	antheus-001	119453	41962	18	118	46	520 ± 0	16	120 ± 1	27	265 ± 13	70	468 ± 22	276	1223 ± 27	325	2660 ± 87	310	6218 ± 47	309	6216 ± 45
38	anyvision-004	401001	630797	232	1102	66	1024 ± 0	67	355 ± 1	-	-	-	-	-	-	-	202	1891 ± 51	196	1829 ± 85	
39	anyvision-005	190979	116595	208	963	64	1024 ± 0	309	985 ± 1	265	997 ± 1	253	1004 ± 1	219	995 ± 1	178	995 ± 1	89	733 ± 14	90	733 ± 16
40	armatura-001	0	374608	238	1151	229	2048 ± 0	208	688 ± 1	171	689 ± 1	154	693 ± 1	136	708 ± 3	124	756 ± 13	15	270 ± 17	18	268 ± 11
41	asusaics-000	257418	245320	123	605	126	2048 ± 0	119	484 ± 13	107	506 ± 21	197	850 ± 26	346	1789 ± 61	350	6305 ± 188	295	5455 ± 78	294	5422 ± 112
42	asusaics-001	257418	245330	120	595	373	4096 ± 0	263	842 ± 17	269	1008 ± 20	339	1377 ± 28	361	2423 ± 90	356	7284 ± 277	324	8618 ± 42	324	8638 ± 136
43	authenmetric-003	293599	39492	212	982	128	2048 ± 0	312	992 ± 1	267	1006 ± 1	252	1003 ± 2	223	1002 ± 1	187	1036 ± 1	185	1757 ± 19	185	1755 ± 19
44	authenmetric-004	381165	39492	242	1214	267	2048 ± 0	285	910 ± 1	244	909 ± 1	216	915 ± 1	196	921 ± 2	180	1724 ± 14	177	1691 ± 29	-	-

Notes

- 1 The configuration size does not capture static data included in libraries.
- 2 The library size is the combined total of all files provided in the submission lib folder. These libraries e.g. OpenCV may or may not be installed on any end user's platform natively and would not need to be installed with the algorithm. Some developers put neural network models in their libraries.
- 3 The memory usage is the peak resident set size reported by the ps system call during template generation.
- 4 The median template creation times are measured on Intel®Xeon®CPU E5-2630 v4 @ 2.20GHz processors.
- 5 The comparison durations, in nanoseconds, are estimated using std::chrono::high_resolution_clock which on the machine in (2) counts 1ns clock ticks. Precision is somewhat worse than that however. The \pm value is the median absolute deviation times 1.48 for Normal consistency.

	ALGORITHM	CONFIG	LIBRARY	TEMPLATE								COMPARISON ⁴									
				NAME	DATA	DATA	MEMORY	SIZE	GENERATION TIME (ms) ⁴				TIME (ns) ⁵								
									(KB) ¹	(KB) ²	(MB) ³	(B)	MUGSHOT	480x720	960x1440	1600x2400	3000x4500	GENUINE	IMPOSTOR		
45	aware-005	300017	26320	251 aware-005	1265	88	1572 ± 0	280	886 ± 23	278	1038 ± 21	277	1121 ± 22	299	1337 ± 58	308	2195 ± 144	165	1475 ± 63	161	1427 ± 115
46	aware-006	298543	14124	206 aware-006	943	14	352 ± 0	341	1148 ± 3	302	1146 ± 2	297	1190 ± 2	291	1306 ± 20	301	1754 ± 84	234	2598 ± 42	234	2559 ± 60
47	awiros-001	15499	87480	12 awiros-001	88	17	512 ± 0	109	97 ± 6	798 ± 4	9	138 ± 6	18	225 ± 7	65	556 ± 8	128	1079 ± 44	127	1050 ± 45	
48	awiros-002	289016	203723	109 awiros-002	562	231	2048 ± 0	115	479 ± 0	105	500 ± 0	94	534 ± 0	102	618 ± 0	167	946 ± 1	207	1966 ± 31	207	1957 ± 25
49	ayftech-001	195423	43580	156 ayftech-001	731	27	512 ± 0	88	408 ± 23	91	476 ± 52	186	814 ± 108	347	1827 ± 384	346	5412 ± 1029	59	615 ± 16	108	885 ± 44
50	ayonix-000	58505	5252	69	73	1036 ± 0	2	18 ± 2	-	-	-	-	-	-	-	62	621 ± 23	64	620 ± 26		
51	beethedata-000	227849	1087592	107 beethedata-000	555	230	2048 ± 0	109	465 ± 0	90	467 ± 0	72	468 ± 0	60	467 ± 0	40	467 ± 0	214	2121 ± 34	215	2110 ± 38
52	beynei-000	256958	591433	233 beynei-000	1124	228	2048 ± 0	103	451 ± 8	82	449 ± 1	177	767 ± 7	341	1603 ± 25	344	4669 ± 124	276	3730 ± 57	273	3668 ± 54
53	biocube-001	25030	6192987	74 biocube-001	458	357	4096 ± 0	49	282 ± 22	38	292 ± 24	92	521 ± 57	124	684 ± 59	235	1282 ± 68	355	21787 ± 96	355	21812 ± 109
54	bioidechswiss-001	1178769	120811	281 bioidechswiss-001	1455	30	512 ± 0	305	966 ± 4	326	1270 ± 270	318	1294 ± 96	322	1409 ± 157	303	1793 ± 79	235	2610 ± 25	235	2624 ± 32
55	bioidechswiss-002	744786	114842	215 bioidechswiss-002	993	26	512 ± 0	288	917 ± 2	252	930 ± 2	233	952 ± 2	207	947 ± 3	194	1058 ± 11	218	2177 ± 29	220	2170 ± 31
56	bm-001	287734	38076	24 bm-001	148	164 ± 0	101	444 ± 88	-	-	-	-	-	-	-	201	1887 ± 31	200	1877 ± 26		
57	boetech-001	261376	88710	270 boetech-001	1384	172	2048 ± 0	40	271 ± 1	30	268 ± 1	22	273 ± 0	22	286 ± 1	17	318 ± 1	388	68519 ± 1921	388	67648 ± 822
58	boetech-002	294347	88710	285 boetech-002	1489	220	2048 ± 0	56	305 ± 4	41	296 ± 1	25	302 ± 1	23	313 ± 1	21	348 ± 2	389	68921 ± 2137	389	69473 ± 2104
59	bresee-001	287880	23227	243 bresee-001	1214	153	2048 ± 0	355	1223 ± 3	313	1216 ± 1	331	1331 ± 1	278	1227 ± 1	249	1360 ± 1	370	37240 ± 655	371	37167 ± 584
60	bresee-002	313627	30902	324 bresee-002	1956	135	2048 ± 0	225	743 ± 4	300	1143 ± 2	286	1146 ± 2	254	1148 ± 2	219	1176 ± 2	188	1778 ± 22	187	1775 ± 23
61	camvi-002	236278	225285	157 camvi-002	737	61	1024 ± 0	202	677 ± 7	183	726 ± 36	200	869 ± 28	247	1129 ± 43	331	2785 ± 113	58	612 ± 26	58	603 ± 20
62	camvi-004	280733	615819	199 camvi-004	919	248	2048 ± 0	229	759 ± 10	222	861 ± 17	247	986 ± 34	288	1279 ± 51	333	2891 ± 158	111	948 ± 40	112	963 ± 31
63	canon-002	446491	130232	193 canon-002	891	349	4096 ± 0	374	1308 ± 2	335	1315 ± 1	328	1326 ± 2	301	1345 ± 1	272	1452 ± 1	309	6211 ± 25	308	6194 ± 25
64	canon-003	2550850	101378	391 canon-003	5472	395	6180 ± 0	364	1263 ± 3	324	1263 ± 1	313	1283 ± 1	297	1320 ± 1	280	1482 ± 2	287	4783 ± 17	284	4780 ± 19
65	ceiec-003	260371	88707	68 ceiec-003	430	207	2048 ± 0	251	817 ± 4	235	883 ± 57	208	897 ± 60	189	899 ± 72	165	944 ± 72	222	2256 ± 38	222	2241 ± 54
66	ceiec-004	2634746	67011	63 ceiec-004	408	212	2048 ± 0	318	1024 ± 1	272	1027 ± 1	258	1027 ± 1	227	1030 ± 1	191	1055 ± 1	198	1844 ± 26	197	1836 ± 20
67	chosun-001	765615	707	86 chosun-001	491	169	2048 ± 0	237	783 ± 2	210	826 ± 4	363	1662 ± 13	367	3679 ± 67	364	11694 ± 243	116	998 ± 25	125	1035 ± 11
68	chosun-002	234001	31875	71 chosun-002	450	105	2048 ± 0	36	248 ± 3	31	273 ± 3	360	1495 ± 14	368	7920 ± 90	365	80302 ± 1349	63	623 ± 17	71	634 ± 13
69	chtface-004	409656	311027	284 chtface-004	1487	147	2048 ± 0	60	332 ± 0	44	323 ± 1	31	329 ± 1	26	335 ± 1	24	377 ± 1	181	1727 ± 17	180	1720 ± 16
70	chtface-005	408364	311100	274 chtface-005	1412	102	2048 ± 0	58	322 ± 0	42	316 ± 1	29	325 ± 2	24	324 ± 1	30	411 ± 2	203	1907 ± 19	201	1898 ± 23
71	clearviewai-000	342491	211852	355 clearviewai-000	2750	120	2048 ± 0	393	1402 ± 1	354	1403 ± 1	348	1412 ± 1	325	1420 ± 1	265	1418 ± 1	170	1592 ± 37	168	1561 ± 37
72	closeli-001	420342	9851	163 closeli-001	773	342	4096 ± 0	262	839 ± 1	217	843 ± 1	195	841 ± 1	173	845 ± 1	151	865 ± 1	294	5404 ± 17	293	5400 ± 25
73	cloudmatrix-000	309939	542141	152 cloudmatrix-000	727	263	2048 ± 0	228	754 ± 10	190	750 ± 2	174	754 ± 4	155	764 ± 1	133	793 ± 2	379	49192 ± 206	379	49275 ± 176
74	cloudmatrix-001	10390	542121	39 云矩阵-001	249	116	2048 ± 0	15	114 ± 1	10	117 ± 0	8	118 ± 0	7	123 ± 1	9	169 ± 1	380	50263 ± 212	380	50243 ± 237
75	cloudwalk-hr-003	383739	144263	214 cloudwalk-hr-003	984	320	2057 ± 0	167	606 ± 0	135	588 ± 0	115	594 ± 0	101	612 ± 1	-	317	6982 ± 80	316	6972 ± 84	
76	cloudwalk-hr-004	502916	520169	272 cloudwalk-hr-004	1394	276	2049 ± 0	273	873 ± 1	231	877 ± 1	205	876 ± 1	182	879 ± 1	157	902 ± 3	333	11652 ± 127	332	11608 ± 123
77	cloudwalk-mt-003	490365	494959	262 cloudwalk-mt-003	1342	277	2049 ± 0	291	923 ± 1	246	918 ± 1	226	926 ± 1	197	925 ± 1	163	936 ± 1	332	11620 ± 179	334	11661 ± 128
78	cloudwalk-mt-004	1384602	512628	389 cloudwalk-mt-004	5426	238	2048 ± 0	292	923 ± 2	247	919 ± 1	218	918 ± 0	195	919 ± 0	161	927 ± 1	334	11744 ± 170	333	11631 ± 126
79	clova-000	198420	6824	76 clova-000	464	141	2048 ± 0	99	437 ± 0	77	431 ± 0	58	435 ± 0	52	452 ± 2	49	508 ± 7	189	1794 ± 16	193	1795 ± 19
80	cogent-005	1876796	75276	357 cogent-005	2806	331	2523 ± 0	354	1221 ± 2	318	1236 ± 1	314	1289 ± 2	326	1420 ± 4	290	1602 ± 5	361	24854 ± 69	361	24858 ± 71
81	cogent-006	1078167	58108	289 cogent-006	1547	76	1062 ± 0	233	768 ± 0	200	789 ± 1	190	831 ± 2	199	930 ± 1	174	971 ± 1	192	1802 ± 17	194	1797 ± 23
82	cognitec-003	471458	62502	176 cognitec-003	817	279	2052 ± 0	73	366 ± 9	66	403 ± 9	47	408 ± 9	45	424 ± 9	50	509 ± 13	264	3417 ± 51	267	3433 ± 53
83	cognitec-004	705645	62678	114 cognitec-004	585	296	2052 ± 0	107	463 ± 9	102	497 ± 9	85	504 ± 10	75	521 ± 10	81	631 ± 12	250	3028 ± 197	251	3059 ± 238
84	cor-001	1194948	11240	248 cor-001	1249	323	2060 ± 0	214	699 ± 3	224	863 ± 76	198	865 ± 80	179	872 ± 89	169	952 ± 39	399	270145 ± 2259	399	282686 ± 11788
85	coretech-000	186423	43964	60 coretech-000	393	30	512 ± 0	166	602 ± 15	159	659 ± 12	283	1139 ± 24	256	1149 ± 25	215	1165 ± 23	23	333 ± 14	23	321 ± 13
86	corsight-001	1437763	31525	330 corsight-001	2040	324	2064 ± 0	370	1291 ± 3	328	1285 ± 1	317	1293 ± 1	290	1303 ± 2	253	1379 ± 3	398	249340 ± 1713	398	248929 ± 1909
87	corsight-002	1474921	32093	331 corsight-002	2061	327	2080 ± 0	369	1290 ± 1	329	1287 ± 1	315	1290 ± 1	292	1307 ± 2	258	1388 ± 4	362	24953 ± 637	360	24263 ± 578
88	csc-002	0	519768	268 corsight-002	1376	51	544 ± 0	113	473 ± 0	100	494 ± 0	74	481 ± 1	66	490 ± 1	53	514 ± 5	29	367 ± 11	29	371 ± 10

Notes

- 1 The configuration size does not capture static data included in libraries.
- 2 The library size is the combined total of all files provided in the submission lib folder. These libraries e.g. OpenCV may or may not be installed on any end user's platform natively and would not need to be installed with the algorithm. Some developers put neural network models in their libraries.
- 3 The memory usage is the peak resident set size reported by the ps system call during template generation.
- 4 The median template creation times are measured on Intel®Xeon®CPU E5-2630 v4 @ 2.20GHz processors.
- 5 The comparison durations, in nanoseconds, are estimated using std::chrono::high_resolution_clock which on the machine in (2) counts 1ns clock ticks. Precision is somewhat worse than that however. The ± value is the median absolute deviation times 1.48 for Normal consistency.

	ALGORITHM	CONFIG	LIBRARY	TEMPLATE								COMPARISON ⁴									
				NAME		DATA		MEMORY		SIZE		GENERATION TIME (ms) ⁴				TIME (ns) ⁵					
				(KB) ¹	(KB) ²	(MB) ³	(B)	MUGSHOT	480x720	960x1440	1600x2400	3000x4500	GENUINE	IMPOSTOR							
89	csc-003	0	400435	298	1609	50	544 ± 0	124	499 ± 0	104	500 ± 1	83	502 ± 0	71	508 ± 1	57	535 ± 4	31	393 ± 8	32	397 ± 7
90	ctcbcbank-000	257208	599238	112	570	122	2048 ± 0	150	568 ± 43	141	606 ± 38	153	690 ± 53	137	711 ± 50	143	831 ± 51	269	3551 ± 87	286	4805 ± 209
91	ctcbcbank-001	275511	599238	121	603	259	2048 ± 0	188	652 ± 35	199	781 ± 30	204	875 ± 43	188	898 ± 51	186	1030 ± 47	278	3926 ± 45	277	3924 ± 56
92	cubox-001	369627	75427	128	649	232	2048 ± 0	283	907 ± 1	242	902 ± 1	212	903 ± 0	194	917 ± 0	162	931 ± 0	154	1379 ± 37	160	1417 ± 38
93	cubox-002	542254	90975	325	1964	271	2048 ± 0	289	921 ± 1	245	921 ± 1	222	922 ± 1	201	933 ± 1	181	1003 ± 1	209	2008 ± 72	209	1969 ± 57
94	cudocommunication-001	385258	341277	226	1077	204	2048 ± 0	293	925 ± 1	249	923 ± 1	227	928 ± 1	200	932 ± 0	171	964 ± 1	230	2534 ± 20	232	2537 ± 20
95	cuuhkee-001	787853	74917	345	2515	290	2052 ± 0	307	977 ± 31	-	-	-	-	-	-	237	2719 ± 60	241	2783 ± 56		
96	cybercore-000	86008	55441	36	200	24	512 ± 0	192	655 ± 3	170	689 ± 71	139	649 ± 6	113	648 ± 8	98	680 ± 6	341	14800 ± 75	343	15757 ± 782
97	cybercore-001	166096	7791	347	2574	119	2048 ± 0	121	487 ± 0	96	486 ± 0	78	488 ± 0	65	487 ± 0	48	502 ± 0	382	52119 ± 111	382	52127 ± 111
98	cyberextruder-001	121211	13629	30	178	6	256 ± 0	282	893 ± 25	-	-	-	-	-	-	129	1083 ± 16	131	1079 ± 19		
99	cyberextruder-002	168909	13924	35	194	191	2048 ± 0	135	532 ± 6	-	-	-	-	-	-	194	1803 ± 14	190	1779 ± 22		
100	cyberlink-007	380046	102446	307	1743	396	6212 ± 0	218	725 ± 1	186	732 ± 1	168	734 ± 1	145	736 ± 1	130	767 ± 1	20	304 ± 19	21	304 ± 16
101	cyberlink-008	380047	102470	308	1748	397	6212 ± 0	220	729 ± 1	182	725 ± 0	165	727 ± 0	143	732 ± 0	126	760 ± 0	14	263 ± 17	17	255 ± 13
102	dahua-006	831641	119261	386	5068	203	2048 ± 0	391	1398 ± 2	353	1397 ± 1	347	1404 ± 1	320	1402 ± 1	261	1402 ± 1	12	249 ± 13	18	250 ± 11
103	dahua-007	1578737	119418	397	7237	350	4096 ± 0	388	1393 ± 2	345	1373 ± 1	340	1378 ± 1	311	1378 ± 1	252	1379 ± 2	28	367 ± 102	33	434 ± 108
104	daon-000	280726	2307	329	2013	325	2065 ± 0	145	562 ± 3	131	581 ± 5	180	791 ± 9	170	838 ± 15	192	1055 ± 32	344	16052 ± 88	344	16041 ± 85
105	decatur-000	350495	171271	196	907	376	4100 ± 0	317	1024 ± 2	-	-	-	-	-	-	330	11439 ± 80	330	11418 ± 112		
106	decatur-001	342866	25374	286	1507	282	2052 ± 0	330	1103 ± 2	283	1064 ± 2	268	1063 ± 2	236	1067 ± 2	198	1084 ± 2	56	610 ± 19	57	602 ± 8
107	deepglint-003	838065	262081	341	2374	393	6144 ± 0	343	1159 ± 1	301	1145 ± 1	287	1148 ± 1	255	1148 ± 1	214	1163 ± 1	346	17227 ± 41	346	17210 ± 51
108	deepglint-004	1073382	261571	366	3084	197	2048 ± 0	402	1470 ± 1	365	1474 ± 1	359	1485 ± 1	332	1474 ± 1	281	1492 ± 2	303	5961 ± 34	304	5955 ± 29
109	deepsea-001	147497	336250	57	358	65	1024 ± 0	180	630 ± 7	191	752 ± 37	171	746 ± 30	141	727 ± 32	139	820 ± 32	159	1401 ± 37	162	1467 ± 50
110	deeepsense-000	357113	936618	398	7618	168	2048 ± 0	198	664 ± 3	157	645 ± 1	141	660 ± 2	126	687 ± 2	137	808 ± 3	36	480 ± 22	38	459 ± 34
111	deeepsense-001	73173	1288355	387	5314	16	512 ± 0	338	1142 ± 2	303	1164 ± 3	295	1183 ± 3	272	1201 ± 3	244	1323 ± 2	225	2356 ± 35	225	2354 ± 42
112	dermalog-008	0	937895	385	4989	36	512 ± 0	83	404 ± 2	67	410 ± 3	55	424 ± 5	47	430 ± 5	43	477 ± 5	33	468 ± 31	28	328 ± 13
113	dermalog-009	0	319363	131	664	38	512 ± 0	63	349 ± 0	50	351 ± 0	34	352 ± 0	30	357 ± 0	27	389 ± 0	38	487 ± 34	31	385 ± 29
114	didiglobalface-001	259849	70680	97	527	219	2048 ± 0	169	612 ± 1	153	633 ± 3	133	634 ± 3	115	650 ± 15	95	666 ± 4	113	973 ± 20	114	988 ± 20
115	digidata-000	133370	30249	41	257	164	2048 ± 0	72	361 ± 0	54	360 ± 0	37	361 ± 0	31	363 ± 0	25	380 ± 0	213	2084 ± 37	211	2039 ± 42
116	digitalbarriers-002	83002	598577	320	1930	305	2056 ± 0	32	209 ± 11	26	250 ± 19	48	411 ± 37	161	808 ± 72	310	2236 ± 123	337	13409 ± 228	338	13267 ± 206
117	dps-000	0	2211812	221	1058	365	4096 ± 0	268	868 ± 2	239	893 ± 6	353	1445 ± 9	364	2910 ± 38	359	9345 ± 17	164	1473 ± 37	164	1479 ± 37
118	dsk-000	11967	782905	40	252	35	512 ± 0	54	304 ± 47	43	317 ± 33	251	1001 ± 96	363	2660 ± 170	362	10451 ± 832	320	7152 ± 115	318	7134 ± 111
119	einetworks-000	372608	219883	191	880	310	2056 ± 0	186	645 ± 3	-	-	-	-	-	-	289	4876 ± 66	290	5156 ± 77		
120	ekin-002	51434	278	21	139	335	3072 ± 0	349	1186 ± 13	309	1180 ± 12	293	1181 ± 11	270	1191 ± 11	224	1207 ± 8	281	4294 ± 80	297	5569 ± 112
121	enface-000	369598	153781	130	662	62	1024 ± 0	144	555 ± 4	125	558 ± 4	145	669 ± 6	216	987 ± 15	315	2349 ± 54	318	7059 ± 62	317	6980 ± 65
122	enface-001	370710	173609	134	670	60	1024 ± 0	142	550 ± 4	123	555 ± 3	144	668 ± 7	213	981 ± 15	319	2416 ± 59	312	6734 ± 68	312	6766 ± 69
123	eocortex-000	255937	59432	38	224	107	2048 ± 0	55	305 ± 22	48	341 ± 25	62	440 ± 47	57	464 ± 45	51	513 ± 44	109	923 ± 11	110	918 ± 11
124	ercacat-001	811623	58012	358	2816	286	2052 ± 0	325	1052 ± 3	-	-	-	-	-	-	232	2551 ± 62	229	2501 ± 81		
125	euronovate-001	0	1774966	260	1308	79	1177 ± 0	321	1034 ± 2	304	1165 ± 3	289	1160 ± 3	261	1177 ± 3	218	1172 ± 2	393	81294 ± 591	393	81631 ± 931
126	expasoft-001	39057	983064	22	142	250	2048 ± 0	7	70 ± 0	57	74 ± 0	57	77 ± 0	4	73 ± 0	4	74 ± 0	174	1660 ± 35	175	1676 ± 48
127	expasoft-002	38760	59825	27	168	215	2048 ± 0	5	34 ± 0	34	34 ± 0	34	34 ± 0	2	34 ± 0	2	34 ± 0	325	8870 ± 78	325	8838 ± 77
128	f8-001	272977	19668	252	1276	109	2048 ± 0	255	822 ± 39	-	-	-	-	-	-	343	15262 ± 139	342	15277 ± 212		
129	f8-002	28278	215616	11	83	192	2048 ± 0	6	39 ± 0	4	41 ± 0	4	75 ± 0	14	197 ± 1	105	702 ± 1	340	14765 ± 131	340	14790 ± 133
130	faceonlive-001	0	71529	52	302	312	2056 ± 0	24	179 ± 0	15	179 ± 0	17	190 ± 0	16	217 ± 0	20	343 ± 1	125	1064 ± 37	124	1033 ± 35
131	facesoft-000	370120	10612	167	796	275	2048 ± 0	201	675 ± 18	163	669 ± 3	151	686 ± 3	121	675 ± 5	101	687 ± 2	221	2239 ± 28	223	2277 ± 96
132	facetag-000	1232331	4022	210	965	55	684 ± 0	66	355 ± 17	56	369 ± 8	249	989 ± 33	360	2408 ± 91	357	7930 ± 316	390	72003 ± 625	391	71912 ± 612

Notes

- 1 The configuration size does not capture static data included in libraries.
- 2 The library size is the combined total of all files provided in the submission lib folder. These libraries e.g. OpenCV may or may not be installed on any end user's platform natively and would not need to be installed with the algorithm. Some developers put neural network models in their libraries.
- 3 The memory usage is the peak resident set size reported by the ps system call during template generation.
- 4 The median template creation times are measured on Intel®Xeon®CPU E5-2630 v4 @ 2.20GHz processors.
- 5 The comparison durations, in nanoseconds, are estimated using std::chrono::high_resolution_clock which on the machine in (2) counts 1ns clock ticks. Precision is somewhat worse than that however. The ± value is the median absolute deviation times 1.48 for Normal consistency.

	ALGORITHM	CONFIG	LIBRARY	TEMPLATE								COMPARISON ⁴					
				NAME		DATA		MEMORY		SIZE		GENERATION TIME (ms) ⁴				TIME (ns) ⁵	
				(KB) ¹	(KB) ²	(MB) ³	(B)	MUGSHOT	480x720	960x1440	1600x2400	3000x4500	GENUINE	IMPOSTOR			
133	facetag-002	819806	4021	¹⁵¹ 726	¹⁹⁶ 2048 ± 0	¹³⁸ 544 ± 1		¹¹⁷ 544 ± 0	⁹⁸ 542 ± 0	⁸² 545 ± 0	⁶⁴ 554 ± 0	¹⁸² 1730 ± 25	¹⁸² 1733 ± 25				
134	facex-001	305074	930372	³⁶⁵ 2931	²⁵³ 2048 ± 0	⁹² 422 ± 4		⁷⁷ 434 ± 4	⁹¹ 520 ± 7	¹⁴⁶ 737 ± 13	²⁹⁵ 1670 ± 27	¹⁹⁹ 1871 ± 23	¹⁹⁸ 1846 ± 29				
135	facex-002	305074	928334	³⁶⁷ 3095	⁹⁵ 2048 ± 0	⁹³ 426 ± 5		⁷⁴ 429 ± 4	⁸⁹ 516 ± 8	¹⁴² 730 ± 12	³⁰⁰ 1738 ± 36	⁶⁵ 631 ± 25	⁶² 614 ± 19				
136	farfaces-001	346494	44581	⁴² 261	²³ 512 ± 0	³⁴⁵ 1179 ± 1		³⁰⁸ 1180 ± 1	²⁹² 1180 ± 0	²⁶⁵ 1185 ± 1	²²⁵ 1209 ± 2	¹⁰⁶ 855 ± 25	¹⁰⁵ 860 ± 31				
137	fiberhome-nanjing-003	352895	1482309	¹⁸⁴ 845	¹⁵⁴ 2048 ± 0	³³⁶ 1136 ± 7		²⁹⁶ 1134 ± 4	²⁸¹ 1132 ± 3	²⁵² 1139 ± 3	²⁰⁹ 1154 ± 5	¹³¹ 1097 ± 38	¹³³ 1083 ± 42				
138	fiberhome-nanjing-004	443779	1482313	²¹⁸ 1048	³⁵⁵ 4096 ± 0	³⁷⁸ 1321 ± 5		³³² 1304 ± 3	³²² 1307 ± 2	²⁹⁴ 1308 ± 3	²⁴⁶ 1326 ± 5	¹⁵⁰ 1276 ± 40	¹⁵⁰ 1265 ± 38				
139	fincore-000	256615	19409	¹⁰¹ 535	¹⁸⁷ 2048 ± 0	¹²⁸ 508 ± 3		¹⁰⁰ 505 ± 0	⁸⁰ 508 ± 1	⁷³ 513 ± 2	⁵⁸ 535 ± 1	¹⁸⁶ 1765 ± 31	¹⁸⁶ 1763 ± 22				
140	fujitsulab-002	0	1088887	²⁹⁹ 1613	³⁸¹ 4104 ± 0	³⁵⁸ 1237 ± 2		³¹⁵ 1222 ± 2	³⁰³ 1236 ± 1	²⁷⁹ 1251 ± 2	²⁴⁷ 1327 ± 2	²⁴¹ 2836 ± 25	²⁴² 2809 ± 44				
141	fujitsulab-003	662263	318209	³⁹⁶ 6907	³⁸³ 4104 ± 0	³⁰¹ 951 ± 20		²⁵⁵ 941 ± 19	²³⁷ 952 ± 19	²¹² 971 ± 20	¹⁸⁹ 1045 ± 21	²⁴² 2855 ± 16	²⁴⁴ 2849 ± 19				
142	geo-002	369903	98667	²¹⁶ 1018	²¹⁶ 2048 ± 0	²⁴¹ 791 ± 1		²⁰¹ 793 ± 0	¹⁸¹ 794 ± 0	¹⁵⁸ 795 ± 1	¹³⁴ 803 ± 1	²⁶³ 3407 ± 45	²⁶⁵ 3422 ± 65				
143	geo-004	168980	107714	²⁵⁴ 1280	¹²³ 2048 ± 0	³⁶⁵ 1268 ± 1		³²⁷ 1279 ± 1	³¹¹ 1274 ± 0	²⁸³ 1259 ± 1	²³⁹ 1296 ± 1	¹²¹ 1023 ± 20	¹²³ 1028 ± 22				
144	glory-003	0	536910	²⁷³ 1400	³⁸⁷ 4234 ± 0	¹²² 489 ± 0		¹²⁶ 565 ± 0	¹⁶⁷ 732 ± 0	³⁴⁹ 1876 ± 2	³⁵⁸ 8941 ± 20	³⁰⁵ 6020 ± 90	³⁰⁷ 6003 ± 72				
145	glory-004	0	999639	³³⁷ 2181	³⁸⁶ 4182 ± 0	²⁰⁹ 688 ± 0		¹⁹⁴ 759 ± 1	²³¹ 941 ± 1	³⁵³ 2134 ± 4	³⁶⁰ 9360 ± 47	²⁹¹ 4982 ± 66	²⁸⁹ 4990 ± 63				
146	gorilla-007	441058	708166	³⁰⁰ 1691	³⁹⁸ 6288 ± 0	¹⁶³ 592 ± 1		¹³⁷ 592 ± 1	¹²¹ 603 ± 1	¹⁰⁷ 625 ± 2	¹¹³ 722 ± 9	²⁷⁴ 3686 ± 37	²⁷⁵ 3709 ± 36				
147	gorilla-008	450175	707000	³¹¹ 1789	⁴⁰⁰ 8338 ± 0	¹⁶⁵ 595 ± 1		¹³⁶ 590 ± 0	¹¹⁸ 600 ± 1	¹⁰⁵ 621 ± 2	¹¹² 720 ± 9	²⁸⁴ 4530 ± 44	²⁸² 4524 ± 38				
148	graymatics-001	13095	70406	¹⁹ 127	³⁷¹ 4096 ± 0	²⁹ 191 ± 1		²¹ 203 ± 1	¹¹⁴ 592 ± 5	³⁴³ 1698 ± 9	³⁵⁴ 7150 ± 34	³⁷² 39874 ± 309	³⁷² 39762 ± 295				
149	griaule-000	0	598214	²²⁰ 1054	²⁸⁸ 2052 ± 0	⁹¹ 416 ± 6		⁷² 425 ± 7	¹⁷⁹ 770 ± 14	³⁴⁴ 1749 ± 43	³⁵² 6406 ± 189	²⁷⁹ 3987 ± 42	²⁷⁸ 3938 ± 38				
150	hertasecurity-000	0	780014	⁹⁵ 516	³ 256 ± 0	¹¹ 99 ± 0		⁸ 98 ± 0	⁷ 100 ± 0	⁶ 107 ± 0	⁶ 139 ± 0	⁸³ 710 ± 31	⁷⁷ 667 ± 28				
151	hertasecurity-001	0	944427	²⁴⁰ 1183	³² 512 ± 0	⁶⁴ 346 ± 0		⁴⁹ 345 ± 0	³³ 349 ± 0	²⁸ 354 ± 0	²⁶ 388 ± 0	¹⁸⁷ 1770 ± 45	¹⁸¹ 1726 ± 48				
152	hik-001	667866	9290	³⁹⁴ 6597	⁸³ 1408 ± 0	¹⁸⁷ 651 ± 0		¹⁶² 667 ± 8	¹⁴⁸ 677 ± 16	¹²⁵ 686 ± 13	¹¹⁸ 737 ± 12	³⁹ 488 ± 19	³⁹ 477 ± 22				
153	hisign-001	732412	167488	²⁹⁰ 1553	³²⁶ 2080 ± 0	³⁷³ 1306 ± 1		³³⁷ 1320 ± 1	³²⁴ 1315 ± 1	²⁹⁶ 1312 ± 1	²⁴⁵ 1325 ± 1	⁷ 201 ± 10	⁶ 185 ± 13				
154	hyperverge-001	260819	88624	⁹⁰ 507	¹³⁰ 2048 ± 0	²⁰⁴ 682 ± 20		¹⁷³ 695 ± 17	³⁰⁰ 1196 ± 37	³⁵⁹ 2400 ± 68	³⁵⁵ 7178 ± 204	³⁰⁷ 6026 ± 40	³⁰⁶ 5984 ± 38				
155	hyperverge-002	2951900	198832	³²⁶ 1975	⁶⁸ 1024 ± 0	²⁹⁵ 938 ± 1		²³² 941 ± 1	²⁰⁶ 945 ± 1	¹⁷⁵ 975 ± 1	³⁰⁶ 6023 ± 37	³⁰⁵ 5966 ± 40					
156	hzailu-001	0	372018	¹¹⁰ 563	³⁰⁸ 2056 ± 0	³³⁴ 1126 ± 1		²⁹⁵ 1128 ± 1	²⁸⁰ 1130 ± 1	²⁴⁸ 1132 ± 1	²¹² 1159 ± 1	¹⁰⁸ 894 ± 19	¹⁰⁹ 899 ± 22				
157	icm-002	621586	903	⁸⁰ 484	²⁵⁶ 2048 ± 0	³²⁰ 1031 ± 7		-	-	-	-	³⁵⁹ 24052 ± 118	³⁵⁸ 24049 ± 124				
158	icm-003	1513988	940	⁸⁸ 500	²²⁷ 2048 ± 0	²⁰³ 681 ± 6		¹⁶⁴ 672 ± 4	¹⁶² 714 ± 11	¹⁶⁸ 837 ± 41	²⁵⁴ 1381 ± 131	³⁶⁰ 24351 ± 161	³⁵⁹ 24227 ± 146				
159	icthtc-000	172459	1471004	³¹³ 1805	¹⁷³ 2048 ± 0	⁶³ 338 ± 11		⁴⁷ 338 ± 9	⁵⁹ 437 ± 16	¹³³ 705 ± 24	²⁹⁹ 1719 ± 44	²⁹³ 5284 ± 63	²⁹² 5290 ± 54				
160	id3-006	210116	7706	²¹³ 982	⁴⁷ 520 ± 0	²⁰⁵ 683 ± 0		²⁸⁶ 1088 ± 1	²⁹⁸ 1192 ± 1	²⁷⁵ 1209 ± 1	²³³ 1270 ± 1	²⁹⁶ 5547 ± 34					
161	id3-008	242416	8151	²²⁴ 1068	⁹ 264 ± 0	²⁵² 819 ± 0		³¹¹ 1209 ± 2	³²⁰ 1297 ± 2	²⁹⁸ 1329 ± 1	²⁷⁰ 1433 ± 1	²⁹⁹ 5658 ± 44	²⁹⁹ 5624 ± 40				
162	idemria-007	353242	67485	²¹⁹ 1051	¹⁸ 468 ± 0	⁷⁹ 384 ± 0		⁶¹ 389 ± 0	⁴⁴ 393 ± 1	⁴⁰ 405 ± 2	³⁵ 441 ± 8	²⁵⁸ 3243 ± 63	²⁵⁸ 3202 ± 63				
163	idemria-008	374017	69922	²⁴¹ 1194	¹³ 348 ± 0	¹⁰⁵ 457 ± 1		⁸⁷ 461 ± 0	⁶⁸ 466 ± 1	⁶² 476 ± 2	⁵² 513 ± 10	²⁵³ 3080 ± 41	²⁴⁹ 3046 ± 56				
164	iit-002	259579	52070	¹⁵⁴ 731	¹⁶⁷ 2048 ± 0	¹²⁹ 514 ± 1		¹⁰⁹ 531 ± 2	¹⁰² 547 ± 1	⁸⁸ 583 ± 1	¹¹⁶ 733 ± 2	¹²² 1023 ± 7	¹²⁰ 1011 ± 66				
165	iit-003	261288	53791	¹⁷⁸ 817	¹³⁶ 2048 ± 0	¹¹⁸ 482 ± 0		⁹⁹ 493 ± 0	⁸⁷ 509 ± 0	⁸⁰ 541 ± 0	⁹³ 661 ± 0	²² 324 ± 17	²⁴ 326 ± 8				
166	imagus-004	254405	380049	¹⁴³ 697	²³⁶ 2048 ± 0	¹⁷⁶ 624 ± 1		¹³⁴ 587 ± 10	¹²⁸ 626 ± 3	⁹⁶ 592 ± 3	¹¹⁰ 717 ± 6	⁹³ 760 ± 22	⁸⁴ 703 ± 28				
167	imagus-005	38886	534579	¹⁵⁶ 731	¹⁷⁷ 2048 ± 0	⁹⁷ 433 ± 4		⁵⁹ 381 ± 3	⁴³ 383 ± 3	³⁴ 373 ± 1	³¹ 411 ± 1	⁸⁸ 731 ± 63	⁶⁷ 632 ± 32				
168	imperial-000	370120	10623	¹⁶⁸ 796	¹³⁹ 2048 ± 0	²⁰⁰ 669 ± 1		¹⁶⁵ 675 ± 3	¹⁴⁹ 683 ± 17	¹²² 676 ± 2	¹⁰² 689 ± 2	²¹⁵ 2130 ± 32	²¹³ 2052 ± 100				
169	imperial-002	472327	16134	³¹⁴ 1826	¹⁹⁵ 2048 ± 0	¹⁵¹ 569 ± 1		¹³⁰ 581 ± 15	¹⁰⁹ 575 ± 5	⁸⁶ 576 ± 2	⁷¹ 588 ± 3	²²³ 2278 ± 90	²¹⁷ 2131 ± 44				
170	incode-009	266103	21014	²⁰⁴ 939	²²¹ 2048 ± 0	¹²⁵ 503 ± 0		⁹⁸ 490 ± 1	⁸² 498 ± 0	⁷⁰ 505 ± 0	⁵⁹ 537 ± 0	¹³⁴ 1102 ± 28	¹³⁷ 1113 ± 29				
171	incode-010	627808	21014	³⁴⁹ 2628	¹⁷⁶ 2048 ± 0	³⁴⁶ 1180 ± 2		³⁰⁶ 1178 ± 1	²⁹⁴ 1182 ± 1	²⁶⁴ 1184 ± 1	²²⁷ 1221 ± 1	¹⁴⁰ 1164 ± 32	¹⁴¹ 1144 ± 32				
172	ineffulabs-000	370588	162172	⁶⁹ 439	¹⁷⁸ 2048 ± 0	³¹⁵ 1006 ± 3		²⁷¹ 1025 ± 3	²⁵⁹ 1030 ± 4	²³¹ 1041 ± 2	²⁰⁶ 1135 ± 3	³⁰⁰ 5782 ± 41	³⁰² 5741 ± 45				
173	innovativetechnologyltd-001	177232	335757	⁵⁴ 341	¹⁴⁵ 2048 ± 0	⁹⁶ 433 ± 7		⁸¹ 446 ± 8	⁶⁰ 439 ± 4	⁵³ 452 ± 4	⁴⁶ 485 ± 7	²⁰⁰ 1877 ± 42	²⁰³ 1924 ± 97				
174	innovativetechnologyltd-002	173939	372324	¹⁹⁷ 912	¹⁵¹ 2048 ± 0	¹⁹³ 661 ± 2		¹⁸⁴ 726 ± 4	²⁴⁴ 981 ± 27	²²⁰ 997 ± 40	¹²⁹ 766 ± 3	¹⁹⁷ 1841 ± 50	¹⁹⁹ 1857 ± 59				
175	innovatrics-007	0	493269	³²¹ 1937	⁷⁷ 1064 ± 0	⁴⁰⁴ 1485 ± 7		³⁶⁷ 1785 ± 184	³⁶⁶ 2078 ± 24	³⁵² 2123 ± 15	³⁰⁹ 2210 ± 42	³⁰⁴ 5978 ± 88	³⁰¹ 5690 ± 102				
176	innovatrics-008	307323	59842	²⁷⁶ 1424	⁴⁸ 538 ± 0	²³⁶ 778 ± 6		¹⁹⁸ 767 ± 3	¹⁷⁸ 770 ± 3	¹⁵⁹ 803 ± 3	¹⁴⁸ 853 ± 10	²⁴⁸ 3021 ± 66	²³⁷ 2673 ± 88				

Notes

	ALGORITHM	CONFIG	LIBRARY	TEMPLATE								COMPARISON ⁴									
				NAME	DATA	DATA	MEMORY	SIZE	GENERATION TIME (ms) ⁴				TIME (ns) ⁵								
									(KB) ¹	(KB) ²	(MB) ³	(B)	MUGSHOT	480x720	960x1440	1600x2400	3000x4500	GENUINE	IMPOSTOR		
177	insightface-001	776777	16606	376	3852	272	2048 ± 0	382	1366 ± 2	342	1368 ± 3	336	1372 ± 3	310	1375 ± 5	257	1386 ± 4	136	1119 ± 29	135	1108 ± 34
178	insightface-002	800572	16606	375	3819	158	2048 ± 0	390	1396 ± 2	350	1389 ± 4	346	1403 ± 3	319	1402 ± 2	264	1413 ± 3	141	1169 ± 40	138	1118 ± 38
179	intellicloudai-001	220831	868246	129	655	273	2048 ± 0	112	468 ± 2	84	456 ± 1	69	466 ± 3	69	492 ± 1	82	632 ± 2	124	1056 ± 4	128	1051 ± 72
180	intellicloudai-002	259047	58559	371	3584	377	4100 ± 0	264	847 ± 1	218	847 ± 2	196	849 ± 1	175	853 ± 1	153	878 ± 4	103	822 ± 28	102	818 ± 23
181	intellifusion-001	271872	289387	161	762	201	2048 ± 0	230	764 ± 38	198	774 ± 39	182	797 ± 42	160	803 ± 34	135	805 ± 33	135	1112 ± 28	139	1128 ± 41
182	intellifusion-002	762731	385841	205	941	364	4096 ± 0	300	950 ± 2	290	1096 ± 42	272	1088 ± 33	259	1168 ± 31	216	1171 ± 10	178	1713 ± 57	174	1665 ± 87
183	intellivision-002	43692	14505	10	81	314	2056 ± 0	59	322 ± 1	52	355 ± 2	39	372 ± 1	43	422 ± 2	75	600 ± 1	338	13525 ± 134	337	12782 ± 278
184	intellivision-003	64023	133748	169	799	317	2056 ± 0	87	407 ± 3	64	398 ± 2	51	418 ± 2	51	450 ± 1	72	591 ± 4	329	11069 ± 56	329	11066 ± 75
185	intellivox-001	256654	111858	182	842	200	2048 ± 0	76	378 ± 1	57	379 ± 1	41	381 ± 1	36	384 ± 1	33	421 ± 3	133	1100 ± 16	136	1109 ± 22
186	intelresearch-004	646918	85290	317	1856	252	2048 ± 0	377	1319 ± 2	338	1322 ± 3	329	1330 ± 3	302	1345 ± 3	263	1411 ± 5	282	4696 ± 63	283	4692 ± 66
187	intelresearch-005	398137	85290	239	1158	261	2048 ± 0	379	1328 ± 1	340	1334 ± 2	332	1344 ± 2	304	1356 ± 2	267	1423 ± 4	283	4524 ± 87	281	4461 ± 74
188	intsysmsu-001	384409	172480	166	789	134	2048 ± 0	171	614 ± 2	146	615 ± 2	137	642 ± 2	149	750 ± 3	211	1159 ± 4	61	621 ± 8	60	611 ± 31
189	intsysmsu-002	765921	172298	165	786	67	1024 ± 0	164	593 ± 1	202	793 ± 2	188	827 ± 1	180	875 ± 104	238	1293 ± 3	43	549 ± 25	43	548 ± 29
190	ionetworks-000	287609	51236	56	351	129	2048 ± 0	95	430 ± 0	78	435 ± 0	57	433 ± 0	48	432 ± 0	37	444 ± 0	315	6913 ± 102	319	7150 ± 160
191	iqface-000	268819	596337	145	704	389	4750 ± 32	137	538 ± 26	101	494 ± 2	100	543 ± 3	144	734 ± 4	260	1393 ± 4	402	636433 ± 38446	402	632654 ± 85615
192	iqface-003	370803	963398	175	817	390	4763 ± 37	131	529 ± 1	110	532 ± 2	117	599 ± 8	174	850 ± 2	296	1694 ± 2	401	575924 ± 2601	401	576553 ± 2051
193	irex-000	741899	47419	333	2086	336	3080 ± 0	265	852 ± 2	220	850 ± 1	203	874 ± 2	203	939 ± 1	229	1249 ± 5	8	201 ± 11	9	208 ± 8
194	isap-001	99049	204201	18	369	4096 ± 0	10 ± 0	-	-	-	-	-	-	-	-	-	32	459 ± 17	36	456 ± 11	
195	isap-002	256765	49931	48	288	217	2048 ± 0	234	769 ± 3	273	1027 ± 2	206	877 ± 2	154	761 ± 1	158	912 ± 2	251	3045 ± 94	246	2973 ± 66
196	isityou-000	48010	36621	14	110	402	19200 ± 0	14	113 ± 5	-	-	-	-	-	-	-	397	237517 ± 1318	397	237374 ± 1279	
197	isystems-001	274621	639268	231	1091	93	2048 ± 0	51	291 ± 9	-	-	-	-	-	-	-	45	557 ± 16	47	564 ± 22	
198	isystems-002	358984	803389	296	1595	246	2048 ± 0	256	822 ± 8	-	-	-	-	-	-	-	90	749 ± 31	69	632 ± 28	
199	itmo-007	415979	245376	339	2199	156	2048 ± 0	224	741 ± 2	-	-	-	-	-	-	-	231	2551 ± 50	231	2529 ± 80	
200	itmo-008	726866	318238	269	1377	356	4096 ± 0	320	1060 ± 1	281	1058 ± 1	267	1059 ± 1	238	1072 ± 4	201	1104 ± 1	270	3578 ± 25	270	3580 ± 28
201	ivacognitive-001	256958	62791	207	947	161	2048 ± 0	371	1292 ± 3	330	1289 ± 4	316	1292 ± 4	289	1292 ± 3	243	1321 ± 4	280	4228 ± 41	279	4226 ± 41
202	iws-000	30875	3063	87	77	19	512 ± 0	43	277 ± 5	36	283 ± 1	80	494 ± 3	215	984 ± 3	335	2987 ± 39	117	999 ± 40	116	992 ± 22
203	kakao-005	414316	152216	292	1581	280	2052 ± 0	327	1068 ± 1	285	1073 ± 1	270	1079 ± 0	239	1077 ± 1	200	1089 ± 1	212	2067 ± 26	212	2043 ± 34
204	kakao-007	526993	129545	380	9353	159	2048 ± 0	302	952 ± 1	258	961 ± 1	238	958 ± 1	211	962 ± 1	173	968 ± 1	123	1056 ± 16	126	1047 ± 28
205	kakaopay-001	397864	179869	136	684	341	4096 ± 0	102	448 ± 0	115	542 ± 0	97	542 ± 0	81	542 ± 0	62	553 ± 0	66	633 ± 22	66	630 ± 22
206	kasikornlabs-000	256471	61000	140	693	115	2048 ± 0	284	908 ± 36	232	878 ± 22	239	969 ± 39	263	1184 ± 54	317	2382 ± 145	367	31669 ± 188	368	31714 ± 182
207	kedacom-000	245292	37401	403	23574	11	292 ± 0	126	506 ± 3	120	547 ± 10	125	614 ± 9	92	588 ± 10	94	665 ± 24	75	684 ± 14	79	682 ± 16
208	kiwitech-000	369711	21375	172	808	98	2048 ± 0	162	591 ± 0	138	594 ± 0	116	595 ± 1	97	596 ± 0	77	609 ± 0	184	1755 ± 20	183	1734 ± 16
209	kneron-003	58366	1747	32	188	131	2048 ± 0	46	281 ± 3	35	280 ± 1	28	315 ± 13	32	365 ± 7	228	1224 ± 30	292	5237 ± 63	291	5274 ± 99
210	kneron-005	375374	13633	73	457	199	2048 ± 0	130	518 ± 2	108	522 ± 4	105	556 ± 5	152	757 ± 19	302	1760 ± 25	204	1922 ± 11	204	1926 ± 20
211	knowutech-000	808045	32886	259	1303	84	1536 ± 0	396	1419 ± 2	344	1372 ± 1	338	1377 ± 1	312	1382 ± 2	256	1386 ± 2	276	3743 ± 31	274	3693 ± 38
212	kookmin-002	371771	30734	180	827	188	2048 ± 0	323	1038 ± 2	280	1047 ± 1	264	1045 ± 1	235	1061 ± 1	202	1116 ± 1	69	638 ± 19	72	636 ± 20
213	kuke3d-001	403462	68786	99	530	346	4096 ± 0	248	814 ± 2	205	811 ± 2	185	814 ± 2	162	814 ± 1	145	834 ± 1	311	6413 ± 57	311	6413 ± 51
214	lebentech-000	0	10360	15	110	37	512 ± 0	32	22 ± 0	122	20 ± 0	122	20 ± 0	123	20 ± 0	123	20 ± 0	101	801 ± 42	103	825 ± 51
215	lemalabs-001	748400	198794	354	2738	182	2048 ± 0	245	810 ± 0	206	812 ± 0	184	813 ± 0	164	819 ± 0	147	844 ± 1	336	11930 ± 35	336	11913 ± 37
216	line-000	264443	407003	117	590	174	2048 ± 0	157	586 ± 0	142	612 ± 0	122	609 ± 1	100	611 ± 0	79	618 ± 1	240	2753 ± 19	240	2745 ± 23
217	line-001	944355	407058	340	2373	127	2048 ± 0	260	833 ± 10	213	830 ± 3	189	828 ± 4	169	838 ± 8	144	833 ± 4	236	2696 ± 23	238	2677 ± 35
218	lookman-002	138200	25410	401	16518	53	548 ± 0	22	173 ± 1	-	-	-	-	-	-	-	57	610 ± 19	61	612 ± 22	
219	lookman-004	244775	37401	402	23548	52	548 ± 0	127	507 ± 5	118	545 ± 12	124	613 ± 12	95	590 ± 11	90	656 ± 16	107	871 ± 29	107	878 ± 29
220	luxand-000	0	57908	266	1366	74	1040 ± 0	84	407 ± 23	76	433 ± 11	63	444 ± 14	56	464 ± 14	67	562 ± 25	104	828 ± 28	104	828 ± 32

Notes

- 1 The configuration size does not capture static data included in libraries.
- 2 The library size is the combined total of all files provided in the submission lib folder. These libraries e.g. OpenCV may or may not be installed on any end user's platform natively and would not need to be installed with the algorithm. Some developers put neural network models in their libraries.
- 3 The memory usage is the peak resident set size reported by the ps system call during template generation.
- 4 The median template creation times are measured on Intel®Xeon®CPU E5-2630 v4 @ 2.20GHz processors.
- 5 The comparison durations, in nanoseconds, are estimated using std::chrono::high_resolution_clock which on the machine in (2) counts 1ns clock ticks. Precision is somewhat worse than that however. The ± value is the median absolute deviation times 1.48 for Normal consistency.

Table 11: Summary of algorithms and properties included in this report. The red superscripts give ranking for the quantity in that column.

	ALGORITHM	CONFIG	LIBRARY	TEMPLATE								COMPARISON ⁴									
				NAME	DATA	DATA	MEMORY	SIZE	GENERATION TIME (ms) ⁴				TIME (ns) ⁵								
									(KB) ¹	(KB) ²	(MB) ³	(B)	MUGSHOT	480x720	960x1440	1600x2400	3000x4500	GENUINE	IMPOSTOR		
221	mantra-000	471458	62566	159	749	285	2052 ± 0	89	413 ± 18	97	487 ± 19	81	494 ± 18	72	511 ± 18	74	598 ± 19	255	3151 ± 51	254	3127 ± 63
222	maxvision-000	133114	56426	312	1791	26	512 ± 0	70	359 ± 0	53	356 ± 0	36	359 ± 0	29	356 ± 0	23	370 ± 1	227	2461 ± 20	226	2452 ± 17
223	maxvision-001	256146	61793	362	2880	111	2048 ± 0	42	275 ± 3	33	274 ± 2	23	277 ± 4	21	280 ± 4	18	325 ± 3	84	714 ± 13	87	717 ± 13
224	megvii-003	4430290	42790	384	4878	360	4096 ± 0	351	1210 ± 1	316	1223 ± 0	334	1356 ± 4	339	1582 ± 7	327	2727 ± 23	396	225342 ± 3574	396	225413 ± 6344
225	megvii-004	3962505	44019	383	4436	374	4097 ± 0	368	1287 ± 1	343	1369 ± 2	323	1310 ± 2	314	1384 ± 3	271	1436 ± 5	377	46801 ± 204	377	46832 ± 207
226	meituhan-000	259514	333178	105	554	218	2048 ± 0	98	436 ± 4	80	441 ± 1	127	626 ± 5	242	1098 ± 15	337	3126 ± 53	70	638 ± 17	70	633 ± 16
227	meiya-001	280055	264913	91	507	278	2049 ± 0	175	622 ± 12	-	-	-	-	-	-	-	-	323	8356 ± 615	323	8134 ± 97
228	mendaxiatech-000	1941475	45484	369	3195	375	4097 ± 0	359	1243 ± 2	321	1255 ± 1	337	1373 ± 2	340	1598 ± 3	326	2689 ± 8	378	46872 ± 275	378	46872 ± 217
229	microfocus-001	104524	27242	33	190	256	± 0	39	264 ± 18	-	-	-	-	-	-	-	-	11	215 ± 8	11	217 ± 10
230	microfocus-002	96288	27362	29	176	4256	± 0	37	259 ± 18	-	-	-	-	-	-	-	-	24	337 ± 34	13	230 ± 25
231	minivision-000	836697	16597	381	4013	351	4096 ± 0	322	1035 ± 1	276	1033 ± 2	261	1035 ± 1	229	1037 ± 1	195	1059 ± 2	228	2466 ± 26	227	2460 ± 25
232	mobai-000	365451	80573	164	786	394	6144 ± 0	231	766 ± 8	227	869 ± 6	301	1205 ± 31	348	1867 ± 45	341	3549 ± 190	345	16458 ± 333	345	16423 ± 1473
233	mobai-001	265297	60164	100	534	152	2048 ± 0	168	612 ± 3	145	614 ± 3	152	687 ± 9	184	886 ± 31	297	1707 ± 103	155	1386 ± 25	156	1377 ± 26
234	mobbl-001	231160	58706	37	223	99	2048 ± 0	26	183 ± 32	18	184 ± 25	35	354 ± 76	167	823 ± 396	330	2781 ± 1166	335	11832 ± 109	335	11851 ± 88
235	mobbl-002	242920	60119	49	288	183	2048 ± 0	196	663 ± 6	160	660 ± 5	142	662 ± 5	119	663 ± 5	97	676 ± 5	331	11616 ± 78	331	11588 ± 97
236	mobiptime-000	370514	303291	234	1130	239	2048 ± 0	360	1245 ± 1	317	1234 ± 1	308	1264 ± 1	308	1360 ± 1	298	1707 ± 1	339	14506 ± 214	339	14433 ± 197
237	moreedian-000	525259	21374	202	932	100	2048 ± 0	212	694 ± 0	174	698 ± 0	158	699 ± 0	131	700 ± 0	109	713 ± 1	193	1803 ± 11	189	1779 ± 23
238	multimodality-000	0	503924	273	1417	97	2048 ± 0	90	416 ± 0	71	420 ± 0	54	423 ± 0	46	427 ± 0	39	463 ± 0	108	848 ± 25	100	800 ± 28
239	mvision-001	227502	149531	150	723	22	512 ± 0	210	691 ± 21	176	702 ± 19	157	697 ± 24	135	708 ± 29	107	710 ± 27	137	1123 ± 40	142	1154 ± 38
240	nazhiai-000	547484	16141	351	2716	242	2048 ± 0	206	683 ± 3	169	687 ± 2	192	835 ± 27	172	840 ± 31	146	834 ± 34	220	2230 ± 34	218	2133 ± 81
241	neosystems-002	599441	349942	246	1222	247	2048 ± 0	335	1135 ± 2	369	1855 ± 3	367	2258 ± 5	356	2238 ± 3	311	2247 ± 3	348	18752 ± 167	349	18610 ± 213
242	neosystems-003	599442	349942	244	1215	91	2048 ± 0	339	1143 ± 2	368	1836 ± 7	368	2260 ± 3	358	2273 ± 6	312	2273 ± 3	351	19130 ± 223	351	19167 ± 186
243	netbridge-tech-001	133108	205875	92	508	344	4096 ± 0	8	85 ± 1	6	83 ± 0	6	84 ± 0	5	92 ± 0	5	113 ± 4	326	9280 ± 74	326	9446 ± 512
244	netbridge-tech-002	257687	49931	51	299	117	2048 ± 0	261	838 ± 6	216	838 ± 2	193	839 ± 1	171	839 ± 3	148	859 ± 3	244	2893 ± 65	250	3050 ± 123
245	neurotechnology-012	147830	51395	174	814	5	256 ± 0	80	384 ± 0	60	387 ± 0	46	404 ± 1	50	435 ± 1	70	583 ± 7	3	119 ± 7	3	116 ± 7
246	neurotechnology-013	474749	85552	364	2894	43	514 ± 0	313	1000 ± 1	268	1006 ± 2	255	1022 ± 2	234	1053 ± 2	220	1195 ± 8	2	109 ± 4	1	110 ± 4
247	nhn-002	363471	817674	133	667	372	4096 ± 0	337	1141 ± 3	298	1138 ± 2	284	1141 ± 2	257	1151 ± 6	222	1203 ± 2	383	56608 ± 579	384	56549 ± 606
248	nhn-003	933665	432730	282	1464	345	4096 ± 0	356	1229 ± 2	323	1261 ± 1	307	1263 ± 3	287	1279 ± 2	251	1375 ± 3	381	50560 ± 105	381	50592 ± 142
249	nodeflux-002	774668	690213	77	466	180	2048 ± 0	217	708 ± 4	178	709 ± 4	163	716 ± 5	140	716 ± 7	117	736 ± 3	267	3475 ± 62	264	3408 ± 143
250	notiontag-001	92753	427967	111	566	54	584 ± 0	294	929 ± 35	287	1092 ± 39	369	3709 ± 81	369	10233 ± 180	-	-	373	43636 ± 286	373	43724 ± 330
251	notiontag-002	271987	967207	359	2840	330	2120 ± 0	104	453 ± 2	83	453 ± 3	64	453 ± 3	54	458 ± 2	41	471 ± 3	354	20278 ± 194	354	20195 ± 186
252	nsensecorp-002	187421	122407	106	554	244	2048 ± 0	62	333 ± 0	46	333 ± 0	32	337 ± 0	27	338 ± 0	22	351 ± 0	376	45965 ± 213	376	45988 ± 158
253	nsensecorp-003	199895	117041	148	710	205	2048 ± 0	194	661 ± 0	161	664 ± 0	143	662 ± 1	118	659 ± 1	92	659 ± 0	374	44658 ± 51	375	44654 ± 72
254	ntechlab-011	786933	209458	395	6867	82	1280 ± 0	342	1148 ± 2	299	1142 ± 1	288	1159 ± 1	267	1185 ± 1	237	1290 ± 3	4	179 ± 11	5	173 ± 11
255	ntechlab-012	570796	212350	390	5451	333	2560 ± 0	375	1309 ± 1	339	1323 ± 1	330	1331 ± 1	307	1360 ± 1	274	1460 ± 3	10	211 ± 8	10	211 ± 7
256	omnigarde-001	200523	32882	75	464	18	512 ± 0	296	941 ± 0	234	883 ± 1	207	886 ± 1	187	891 ± 1	154	898 ± 0	160	1405 ± 31	157	1379 ± 26
257	omnigarde-002	368860	32882	160	757	57	1024 ± 0	372	1303 ± 1	319	1246 ± 1	304	1249 ± 1	280	1253 ± 1	231	1261 ± 1	239	2686 ± 32	239	2686 ± 32
258	omnisecurity-000	45945	844976	25	150	58	1024 ± 0	285	185 ± 1	23	206 ± 2	18	203 ± 1	111	195 ± 1	11	193 ± 1	37	481 ± 42	35	456 ± 20
259	openface-001	0	40111	13	100	166	2048 ± 0	19	148 ± 1	13	154 ± 0	38	365 ± 3	42	409 ± 9	78	616 ± 31	55	608 ± 14	59	604 ± 13
260	oz-003	484147	519652	400	11949	299	2053 ± 0	383	1375 ± 12	349	1388 ± 3	365	1773 ± 16	351	2039 ± 6	339	3209 ± 5	392	73905 ± 456	392	73892 ± 444
261	oz-004	373982	1075452	399	8071	300	2053 ± 0	259	832 ± 7	228	871 ± 6	210	899 ± 10	240	1078 ± 12	291	1608 ± 10	387	61654 ± 418	386	61749 ± 450
262	papsav1923-001	279210	52652	79	473	260	2048 ± 0	178	626 ± 1	150	628 ± 1	130	630 ± 1	114	648 ± 2	121	744 ± 3	87	725 ± 25	89	731 ± 28
263	papsav1923-002	491185	24727	236	1136	294	2052 ± 0	242	792 ± 1	262	978 ± 1	263	1042 ± 1	258	1158 ± 1	294	1641 ± 19	143	1209 ± 29	140	1206 ± 38
264	paravision-008	542190	204400	280	1448	359	4096 ± 0	215	699 ± 0	175	700 ± 0	159	701 ± 0	132	702 ± 1	106	702 ± 0	28	337 ± 17	26	330 ± 13

Notes

- 1 The configuration size does not capture static data included in libraries.
- 2 The library size is the combined total of all files provided in the submission lib folder. These libraries e.g. OpenCV may or may not be installed on any end user's platform natively and would not need to be installed with the algorithm. Some developers put neural network models in their libraries.
- 3 The memory usage is the peak resident set size reported by the ps system call during template generation.
- 4 The median template creation times are measured on Intel®Xeon®CPU E5-2630 v4 @ 2.20GHz processors.
- 5 The comparison durations, in nanoseconds, are estimated using std::chrono::high_resolution_clock which on the machine in (2) counts 1ns clock ticks. Precision is somewhat worse than that however. The ± value is the median absolute deviation times 1.48 for Normal consistency.

Table 12: Summary of algorithms and properties included in this report. The red superscripts give ranking for the quantity in that column.

	ALGORITHM	CONFIG	LIBRARY	TEMPLATE								COMPARISON ⁴									
				NAME		DATA		MEMORY		SIZE		GENERATION TIME (ms) ⁴									
				(KB) ¹	(KB) ²	(MB) ³	(B)	MUGSHOT	480x720	960x1440	1600x2400	3000x4500	GENUINE	IMPOSTOR							
265	paravision-010	688291	205854	335	2150	380	4100 ± 0	182	634 ± 0	155	635 ± 0	135	635 ± 0	109	635 ± 0	86	635 ± 1	169	1577 ± 35	169	1571 ± 32
266	pensees-001	1619431	408932	319	1922	399	8200 ± 0	332	1108 ± 3	359	1448 ± 17	350	1439 ± 10	331	1464 ± 5	287	1546 ± 9	256	3151 ± 34	255	3143 ± 25
267	pixelall-006	0	746305	203	934	332	2560 ± 0	316	1024 ± 3	274	1028 ± 2	260	1033 ± 1	228	1032 ± 1	190	1054 ± 2	91	754 ± 14	88	722 ± 10
268	pixelall-007	0	444912	264	1349	264	2048 ± 0	319	1026 ± 4	279	1038 ± 2	273	1089 ± 2	241	1087 ± 2	203	1124 ± 2	82	708 ± 14	83	701 ± 19
269	psl-008	954351	524525	374	3807	338	3144 ± 0	395	1412 ± 4	357	1415 ± 3	349	1416 ± 2	324	1418 ± 2	266	1418 ± 2	13	259 ± 22	16	252 ± 22
270	psl-009	411027	411504	388	5369	385	4168 ± 0	385	1382 ± 2	346	1381 ± 1	341	1383 ± 1	313	1383 ± 2	255	1385 ± 1	21	316 ± 14	20	289 ± 14
271	ptakuratsatu-000	0	585434	263	1347	49	538 ± 0	275	875 ± 3	225	863 ± 48	228	928 ± 9	210	958 ± 17	197	1066 ± 26	302	5900 ± 103	300	5687 ± 167
272	pxl-001	110116	78231	26	168	40	512 ± 0	12	101 ± 5	9	104 ± 5	16	189 ± 12	41	408 ± 27	277	1470 ± 144	298	5598 ± 45	298	5590 ± 68
273	pyramid-000	372608	219883	170	804	301	2056 ± 0	153	583 ± 2	-	-	-	-	-	-	319	7147 ± 59	321	7586 ± 425		
274	qnap-000	186731	15598	44	272	163	2048 ± 0	219	726 ± 9	85	457 ± 1	65	458 ± 0	58	464 ± 1	44	482 ± 2	73	660 ± 25	75	654 ± 29
275	qnap-001	196210	13399	47	286	143	2048 ± 0	172	614 ± 1	147	615 ± 1	129	627 ± 1	106	623 ± 1	83	634 ± 2	71	649 ± 11	73	648 ± 14
276	quantasoft-003	370518	211354	222	1058	157	2048 ± 0	181	632 ± 2	154	634 ± 0	132	632 ± 0	108	631 ± 1	85	634 ± 0	9	201 ± 7	8	203 ± 8
277	rankone-011	0	179209	23	146	7	261 ± 0	148	567 ± 1	124	557 ± 1	107	567 ± 1	89	586 ± 1	99	682 ± 3	17	283 ± 14	12	220 ± 19
278	rankone-012	0	264182	20	134	8	261 ± 0	146	564 ± 3	122	554 ± 1	106	564 ± 1	90	586 ± 1	103	695 ± 1	16	273 ± 17	14	231 ± 14
279	realnetworks-005	172253	56755	142	697	306	2056 ± 0	33	211 ± 4	22	205 ± 3	24	290 ± 6	74	515 ± 17	240	1312 ± 78	144	1213 ± 17	147	1207 ± 16
280	realnetworks-006	466225	56771	294	1588	309	2056 ± 0	184	638 ± 4	151	630 ± 3	146	672 ± 5	134	706 ± 5	131	774 ± 5	34	469 ± 19	40	478 ± 25
281	regula-000	262444	29384	124	610	249	2048 ± 0	350	1187 ± 1	294	1126 ± 1	279	1129 ± 0	249	1132 ± 1	213	1159 ± 1	41	491 ± 16	42	500 ± 22
282	regula-001	256075	25980	211	976	193	2048 ± 0	367	1284 ± 1	314	1220 ± 1	302	1222 ± 1	277	1226 ± 1	230	1255 ± 1	27	361 ± 10	27	342 ± 25
283	remarkai-001	241857	868314	153	730	295	2052 ± 0	258	831 ± 6	219	849 ± 18	266	1055 ± 25	271	1198 ± 34	283	1519 ± 38	148	1229 ± 20	101	805 ± 56
284	remarkai-003	280516	58559	378	3896	379	4100 ± 0	310	986 ± 1	264	993 ± 1	250	992 ± 1	221	999 ± 3	183	1019 ± 2	99	787 ± 20	98	793 ± 22
285	rendip-000	0	437653	135	682	137	2048 ± 0	108	464 ± 2	86	458 ± 0	73	473 ± 0	63	483 ± 1	66	556 ± 4	46	576 ± 13	48	573 ± 11
286	revealmedia-005	293933	202465	162	763	378	4100 ± 0	94	428 ± 0	73	428 ± 0	56	430 ± 0	49	433 ± 0	36	442 ± 0	210	2023 ± 38	210	2009 ± 26
287	revealmedia-006	293933	200912	158	741	284	2052 ± 0	77	381 ± 0	58	381 ± 0	42	382 ± 0	35	384 ± 0	29	394 ± 0	64	626 ± 35	56	600 ± 2
288	rokid-000	258612	396624	245	1218	319	2056 ± 0	139	546 ± 3	116	542 ± 2	101	545 ± 1	70	522 ± 3	68	563 ± 4	266	3457 ± 62	268	3463 ± 77
289	rokid-001	641223	413733	225	1071	322	2060 ± 0	280	911 ± 2	241	901 ± 5	209	899 ± 2	190	900 ± 3	156	901 ± 3	261	3345 ± 50	261	3346 ± 149
290	s1-003	145509	95446	177	817	353	4096 ± 0	298	947 ± 0	257	959 ± 0	236	952 ± 0	208	952 ± 1	170	955 ± 1	272	3657 ± 19	272	3652 ± 16
291	s1-004	246514	202623	144	700	140	2048 ± 0	249	815 ± 0	207	818 ± 1	187	818 ± 1	165	820 ± 1	141	828 ± 1	259	3245 ± 100	256	3161 ± 88
292	saffe-001	85973	62488	28	168	80	1280 ± 0	47	281 ± 1	-	-	-	-	-	-	149	1274 ± 19	151	1277 ± 26		
293	saffe-002	260622	28285	186	855	165	2048 ± 0	250	817 ± 11	204	805 ± 15	183	809 ± 19	163	815 ± 29	138	813 ± 23	85	717 ± 7	86	714 ± 29
294	samsungds-000	0	307431	228	1083	103	2048 ± 0	57	316 ± 0	45	326 ± 5	30	328 ± 4	25	327 ± 1	19	343 ± 0	357	23722 ± 295	357	23874 ± 305
295	samtech-001	288082	219883	122	605	304	2056 ± 0	52	294 ± 3	-	-	-	-	-	-	322	7694 ± 59	322	7678 ± 91		
296	scanovate-002	256986	457227	185	850	181	2048 ± 0	213	696 ± 32	179	713 ± 33	169	738 ± 28	156	779 ± 32	217	1172 ± 53	249	3021 ± 38	253	3120 ± 163
297	scanovate-003	135585	89469	171	808	118	2048 ± 0	155	585 ± 1	143	613 ± 12	113	591 ± 1	99	610 ± 2	100	684 ± 1	245	2926 ± 22	245	2925 ± 20
298	securifai-003	303794	13512	361	2868	384	4104 ± 0	141	549 ± 7	121	550 ± 7	103	549 ± 7	83	546 ± 6	60	546 ± 6	179	1714 ± 26	179	1713 ± 37
299	securifai-004	282177	12027	127	636	121	2048 ± 0	269	869 ± 1	226	867 ± 1	199	867 ± 1	178	867 ± 1	152	865 ± 1	177	1711 ± 19	178	1705 ± 29
300	senstime-005	765353	37673	393	6133	70	1028 ± 0	381	1361 ± 27	333	1304 ± 1	326	1319 ± 1	309	1360 ± 1	282	1514 ± 1	147	1223 ± 28	145	1184 ± 29
301	senstime-006	765353	37673	392	5994	69	1028 ± 0	380	1352 ± 17	334	1311 ± 1	327	1323 ± 1	305	1357 ± 1	284	1523 ± 2	142	1179 ± 28	144	1157 ± 29
302	sertis-000	265572	68770	66	427	198	2048 ± 0	227	754 ± 0	193	759 ± 0	176	764 ± 0	153	760 ± 0	128	763 ± 0	166	1497 ± 29	170	1582 ± 38
303	sertis-002	460790	68929	271	1391	175	2048 ± 0	348	1181 ± 1	305	1178 ± 0	296	1183 ± 0	269	1187 ± 0	226	1221 ± 0	130	1086 ± 32	129	1076 ± 31
304	seventhSense-000	369850	1561668	179	824	281	2052 ± 0	362	1250 ± 3	322	1257 ± 1	305	1261 ± 1	282	1259 ± 1	234	1272 ± 2	191	1800 ± 35	191	1787 ± 32
305	seventhSense-001	369850	3183365	173	811	289	2052 ± 0	363	1255 ± 2	331	1294 ± 15	312	1277 ± 3	286	1275 ± 2	236	1288 ± 3	205	1936 ± 26	206	1943 ± 34
306	shaman-000	0	120033	89	507	367	4096 ± 0	189	653 ± 16	-	-	-	-	-	-	30	380 ± 25	30	379 ± 31		
307	shaman-001	0	174446	94	511	352	4096 ± 0	53	294 ± 2	-	-	-	-	-	-	68	635 ± 19	34	441 ± 25		
308	shu-002	731250	148309	192	890	340	4096 ± 0	226	751 ± 2	196	769 ± 4	221	922 ± 4	327	1431 ± 9	340	3489 ± 47	404	2930763 ± 47355	404	2929759 ± 39149

Notes
 1 The configuration size does not capture static data included in libraries.
 2 The library size is the combined total of all files provided in the submission lib folder. These libraries e.g. OpenCV may or may not be installed on any end user's platform natively and would not need to be installed with the algorithm. Some developers put neural network models in their libraries.
 3 The memory usage is the peak resident set size reported by the ps system call during template generation.
 4 The median template creation times are measured on Intel®Xeon®CPU E5-2630 v4 @ 2.20GHz processors.
 5 The comparison durations, in nanoseconds, are estimated using std::chrono::high_resolution_clock which on the machine in (2) counts 1ns clock ticks. Precision is somewhat worse than that however. The ± value is the median absolute deviation times 1.48 for Normal consistency.

	ALGORITHM	CONFIG	LIBRARY	TEMPLATE								COMPARISON ⁴						
				NAME	DATA	DATA	MEMORY	SIZE	GENERATION TIME (ms) ⁴				TIME (ns) ⁵					
									(KB) ¹	(KB) ²	(MB) ³	(B)	MUGSHOT	480x720	960x1440	1600x2400	3000x4500	GENUINE
309	shu-003	428774	146940	⁹³ 511	¹⁴⁶ 2048 ± 0	²⁵³ 820 ± 6	²¹² 828 ± 3	²³⁰ 941 ± 9	²⁹³ 1308 ± 15	³³⁶ 3045 ± 44	²²⁹ 2506 ± 26	²³⁰ 2512 ± 38						
310	siat-002	486842	7738	³⁴² 2434	²⁹⁸ 2052 ± 0	¹⁵² 579 ± 0	-	-	-	-	-	⁹⁶ 769 ± 13	⁹³ 750 ± 13					
311	siat-005	380936	16935	²⁵⁸ 1298	¹⁸⁴ 2048 ± 0	⁸² 403 ± 0	⁶⁵ 400 ± 0	⁴⁵ 401 ± 0	³⁸ 403 ± 1	³⁴ 422 ± 7	⁴⁷ 577 ± 13	⁴⁹ 580 ± 17						
312	sjtu-003	480795	148243	¹⁰² 538	²²⁶ 2048 ± 0	²⁵⁴ 821 ± 2	²⁰⁸ 820 ± 2	²²³ 923 ± 3	²⁷³ 1201 ± 3	³¹⁶ 2373 ± 9	¹⁶⁸ 1560 ± 20	¹⁶⁷ 1560 ± 14						
313	sjtu-004	1953267	241108	³⁵² 2727	³⁸⁸ 4608 ± 0	³⁵⁷ 1236 ± 2	³¹² 1209 ± 2	³¹⁹ 1294 ± 4	³³⁷ 1554 ± 5	³²⁹ 2738 ± 8	²⁵² 3057 ± 14	²⁵² 3070 ± 20						
314	sktelecom-000	527132	298496	²⁶¹ 1311	⁸⁵ 1536 ± 0	³³³ 1110 ± 1	²⁹¹ 1113 ± 1	²⁷⁵ 1114 ± 1	²⁴⁴ 1120 ± 1	²¹⁰ 1155 ± 1	³⁶⁵ 26583 ± 128	³⁶⁴ 26508 ± 126						
315	smartengines-000	1711	3025	³ 50	¹⁰ 288 ± 0	²¹ 168 ± 7	¹⁶ 180 ± 1	¹⁴ 188 ± 3	¹⁵ 217 ± 3	¹⁶ 275 ± 1	⁶ 197 ± 5	⁴ 167 ± 11						
316	smilart-002	111826	87805	⁴³ 263	⁵⁹ 1024 ± 0	²³ 176 ± 16	-	-	-	-	-	³⁴⁹ 18784 ± 136	³⁵⁰ 18795 ± 151					
317	smilart-003	67339	91670	³⁴ 192	³⁴ 512 ± 0	²⁵ 180 ± 12	¹⁷ 181 ± 10	²⁶ 313 ± 22	¹²⁰ 665 ± 49	³¹³ 2299 ± 196	¹⁵⁶ 1395 ± 74	¹²² 1027 ± 66						
318	sodec-000	836592	13142	³⁶⁸ 3186	³⁶⁸ 4096 ± 0	³²⁴ 1041 ± 2	²⁷⁵ 1032 ± 1	²⁶² 1035 ± 1	²³⁰ 1037 ± 2	¹⁹⁶ 1061 ± 2	¹⁹⁰ 1794 ± 37	¹⁸⁸ 1775 ± 23						
319	sqisoft-001	278968	386291	¹³⁸ 688	³⁰² 2056 ± 0	¹¹⁴ 477 ± 5	³⁴¹ 1348 ± 18	³³³ 1353 ± 26	³⁰⁰ 1340 ± 14	²⁵⁹ 1393 ± 28	¹⁰⁰ 797 ± 22	⁹⁷ 788 ± 22						
320	sqisoft-002	278039	386291	¹³² 666	³¹⁵ 2056 ± 0	¹¹⁰ 466 ± 8	⁸⁹ 466 ± 2	⁷¹ 468 ± 11	⁵⁵ 461 ± 6	⁴² 472 ± 4	⁹² 758 ± 11	⁹⁴ 760 ± 23						
321	stagu-000	879661	624676	²²³ 1064	³⁷⁰ 4096 ± 0	²⁴⁷ 813 ± 25	-	-	-	-	-	²⁴⁶ 2979 ± 31	²⁴⁸ 3007 ± 75					
322	starhybrid-001	100509	289356	¹⁸³ 845	¹²⁵ 2048 ± 0	⁶⁹ 358 ± 82	⁵¹ 355 ± 49	⁴⁰ 379 ± 58	³⁷ 401 ± 79	²⁸ 393 ± 67	¹²⁷ 1075 ± 51	¹³⁰ 1078 ± 53						
323	sukshi-000	94035	688738	⁵⁸ 372	⁴⁰³ 32768 ± 0	⁸⁶ 407 ± 11	⁶⁸ 413 ± 8	⁸⁴ 504 ± 8	¹²⁷ 689 ± 11	²⁸⁸ 1574 ± 28	³²⁸ 9817 ± 50	³²⁷ 9787 ± 62						
324	suprema-001	373423	41460	³⁰⁵ 1731	²⁵⁸ 2048 ± 0	²⁴⁰ 788 ± 1	²¹¹ 826 ± 2	²¹⁵ 914 ± 2	²⁵³ 1146 ± 7	³²¹ 2443 ± 4	²⁵⁷ 3212 ± 16	²⁵⁹ 3220 ± 22						
325	suprema-002	373808	41473	³⁰⁴ 1731	¹⁹⁴ 2048 ± 0	²³⁹ 787 ± 3	²¹⁵ 833 ± 3	²²⁴ 924 ± 4	²⁶⁶ 1185 ± 6	³²³ 2479 ± 3	²⁶⁰ 3255 ± 17	²⁶⁰ 3253 ± 14						
326	supremaid-001	258193	23479	¹⁰³ 541	²⁶⁶ 2048 ± 0	¹¹⁶ 479 ± 1	⁹⁴ 481 ± 0	⁷⁵ 481 ± 0	⁶⁷ 490 ± 0	⁵⁶ 522 ± 0	⁸⁰ 704 ± 19	⁷⁴ 652 ± 19						
327	synesis-006	731941	21817	²⁸³ 1472	³⁸² 4104 ± 0	¹⁴⁰ 549 ± 1	¹¹⁹ 546 ± 1	¹⁰⁴ 552 ± 1	⁸⁵ 558 ± 2	⁸⁸ 639 ± 28	⁷⁹ 697 ± 32	⁸² 688 ± 31						
328	synesis-007	1442961	24145	³⁴³ 2443	³³⁷ 3080 ± 0	³⁵² 1215 ± 5	³²⁵ 1268 ± 30	³²¹ 1306 ± 67	²⁹³ 1311 ± 58	²⁶⁸ 1423 ± 52	⁷⁶ 684 ± 32	⁸⁰ 686 ± 25						
329	synology-000	221021	25809	⁷² 453	¹⁰⁸ 2048 ± 0	⁸⁵ 407 ± 14	⁶⁹ 415 ± 14	¹⁵⁵ 694 ± 31	³¹⁷ 1396 ± 58	³⁴² 4568 ± 211	³⁵³ 19720 ± 203	³⁵² 19767 ± 379						
330	synology-002	256713	25943	⁸³ 488	²⁰² 2048 ± 0	²⁸¹ 886 ± 4	²³⁷ 892 ± 3	²¹⁹ 920 ± 2	²²² 1000 ± 5	²⁴¹ 1317 ± 12	¹⁶³ 1466 ± 32	¹⁶⁵ 1496 ± 45						
331	sztu-000	338637	15871	²⁵⁶ 1298	²⁵⁷ 2048 ± 0	¹³⁴ 531 ± 0	¹¹¹ 532 ± 0	⁹³ 533 ± 0	⁷⁸ 537 ± 0	⁶¹ 548 ± 0	⁴⁸ 585 ± 11	⁵¹ 592 ± 13						
332	sztu-001	338650	15871	²⁵⁷ 1298	¹⁸⁵ 2048 ± 0	¹³⁶ 535 ± 0	¹¹⁴ 537 ± 0	⁹⁶ 538 ± 0	⁷⁹ 540 ± 0	⁶³ 553 ± 0	⁵² 599 ± 10	⁵⁵ 598 ± 10						
333	t4isb-000	234227	115237	⁵⁵ 343	⁹² 2048 ± 0	³¹⁴ 1006 ± 5	²⁶⁶ 1001 ± 1	²⁵⁴ 1006 ± 1	²²⁴ 1009 ± 1	¹⁸⁴ 1022 ± 2	²⁷¹ 3586 ± 34	²⁶⁹ 3534 ± 34						
334	tech5-004	2410272	118858	³⁵³ 2733	¹² 321 ± 0	²⁷² 872 ± 2	²⁹² 1117 ± 164	²⁷⁶ 1114 ± 182	²⁵⁰ 1134 ± 179	¹⁷⁹ 999 ± 44	⁵¹ 597 ± 13	⁵² 592 ± 16						
335	tech5-005	1178769	120517	²⁷⁷ 1426	²⁰ 512 ± 0	³⁶⁶ 1272 ± 109	²⁷⁷ 1038 ± 63	²⁶⁵ 1046 ± 39	²⁴⁵ 1124 ± 38	²⁴⁸ 1351 ± 44	²³³ 2573 ± 37	²³³ 2545 ± 32						
336	techsign-000	0	1101622	³²³ 1955	¹⁸⁰ 2048 ± 0	⁷⁴ 366 ± 1	⁶³ 398 ± 1	²⁹⁰ 1172 ± 3	³⁶⁶ 3065 ± 18	³⁶³ 10460 ± 65	²⁸⁶ 4758 ± 112	²⁸⁵ 4789 ± 93						
337	tevian-007	779934	19523	³⁰³ 1714	⁷¹ 1032 ± 0	¹⁵⁴ 583 ± 1	¹²⁹ 579 ± 0	¹¹⁰ 580 ± 0	⁹¹ 588 ± 1	⁸⁷ 636 ± 0	²⁹⁰ 4894 ± 65	²⁸⁸ 4841 ± 83						
338	tevian-008	847177	19519	³⁷⁰ 3490	⁷² 1032 ± 0	²⁷⁹ 884 ± 2	²⁴³ 903 ± 1	²¹¹ 903 ± 1	¹⁹² 911 ± 1	¹⁶⁶ 946 ± 1	²⁸⁸ 4828 ± 40	²⁸⁷ 4811 ± 41						
339	tiger-005	342866	253734	²⁸⁸ 1531	²⁹⁷ 2052 ± 0	³²⁸ 1097 ± 2	²⁸⁴ 1065 ± 2	²⁶⁹ 1066 ± 2	²³⁷ 1067 ± 3	¹⁹⁹ 1088 ± 3	⁶⁰ 620 ± 19	⁶³ 615 ± 16						
340	tiger-006	421186	394688	¹⁴⁷ 707	²⁹³ 2052 ± 0	³⁸⁷ 1392 ± 16	³⁵⁵ 1411 ± 10	³⁵² 1444 ± 10	³³⁵ 1531 ± 11	³⁰⁴ 1848 ± 10	¹⁹⁵ 1810 ± 20	¹⁹⁵ 1801 ± 13						
341	tinkoff-001	274660	389272	¹¹⁹ 592	²⁷⁴ 2048 ± 0	³⁴⁴ 1176 ± 3	³⁰⁷ 1179 ± 3	²⁹¹ 1178 ± 3	²⁶⁰ 1169 ± 2	²²³ 1203 ± 3	²⁸² 4361 ± 74	²⁸⁰ 4364 ± 75						
342	tongyi-005	1140701	138919	³³⁴ 2121	³²⁹ 2089 ± 0	²⁰ 165 ± 1	-	-	-	-	-	³⁵⁰ 18924 ± 65	³⁵³ 20158 ± 103					
343	toppanidgate-000	671181	711850	³¹⁰ 1786	³⁵⁵ 4096 ± 0	²⁸⁷ 915 ± 1	²⁴⁵ 916 ± 1	²¹⁷ 916 ± 1	¹⁹³ 917 ± 1	¹⁵⁹ 917 ± 1	³⁶³ 25262 ± 84	³⁶² 25264 ± 97						
344	toshiba-004	599297	27880	²⁹⁷ 1595	³¹⁶ 2056 ± 0	³⁹⁸ 1447 ± 3	³⁶¹ 1453 ± 2	³⁵⁶ 1457 ± 9	³²⁹ 1457 ± 3	²⁷⁹ 1479 ± 4	¹²⁰ 1020 ± 25	¹¹⁷ 998 ± 32						
345	toshiba-005	599298	61113	²⁹⁵ 1593	³¹⁸ 2056 ± 0	⁴⁰⁰ 1456 ± 4	³⁶² 1454 ± 2	³⁵⁷ 1461 ± 2	³²⁸ 1455 ± 2	²⁷³ 1459 ± 2	¹⁷¹ 1613 ± 34	¹⁷¹ 1607 ± 28						
346	trueface-002	253947	123116	⁸² 486	⁹⁰ 2000 ± 0	⁷¹ 360 ± 0	⁵⁵ 361 ± 0	⁵³ 423 ± 0	⁹⁴ 590 ± 1	-	⁵ 192 ± 14	⁷ 186 ± 19						
347	trueface-003	346530	24308	³⁷⁹ 3915	²⁵⁴ 2048 ± 0	³³¹ 1107 ± 22	¹⁶⁷ 677 ± 3	¹⁶⁶ 732 ± 7	¹⁹¹ 905 ± 5	-	¹⁰³ ± 11	² 112 ± 29						
348	putepatch-000	11476	17185	²³ 33	²¹¹ 2048 ± 0	¹⁷ 122 ± 4	¹¹ 120 ± 1	¹⁰ 142 ± 2	¹³ 196 ± 5	³² 411 ± 14	³⁵⁸ 23893 ± 406	³⁶³ 25279 ± 406						
349	turingtechvip-001	399874	54535	¹²⁶ 617	¹³³ 2048 ± 0	³⁸⁶ 1384 ± 4	³⁵¹ 1391 ± 1	³⁴³ 1393 ± 1	³²³ 1411 ± 1	²⁷⁸ 1476 ± 2	¹⁸³ 1733 ± 19	¹⁸⁴ 1734 ± 20						
350	twface-000	661735	11782	³⁴⁸ 2610	²¹⁴ 2048 ± 0	²⁷⁰ 871 ± 1	²²⁹ 873 ± 1	²⁰² 873 ± 2	¹⁸¹ 876 ± 2	¹⁵⁵ 898 ± 1	¹⁶⁷ 1504 ± 29	¹⁶⁶ 1510 ± 34						
351	twface-001	671511	11782	³⁶⁰ 2855	¹⁰⁴ 2048 ± 0	²⁹⁰ 923 ± 1	²⁵⁰ 925 ± 2	²²⁵ 926 ± 1	¹⁹⁸ 929 ± 2	¹⁶⁴ 940 ± 2	¹⁵⁷ 1400 ± 32	¹⁵⁸ 1402 ± 37						
352	ulsee-001	370519																

				TEMPLATE								COMPARISON ⁴		
NAME		DATA	LIBRARY	GENERATION TIME (ms) ⁴								TIME (ns) ⁵		
		(KB) ¹	(KB) ²	(MB) ³	(B)	MUGSHOT	480x720	960x1440	1600x2400	3000x4500	GENUINE	IMPOSTOR		
353	uluface-002	0	480761	²²⁹ 1088	²³⁵ 2048 ± 0	²⁷⁴ 873 ± 42	²²¹ 855 ± 9	²⁴² 978 ± 24	²⁸⁴ 1271 ± 40	³¹⁴ 2333 ± 68	³⁵² 19207 ± 1114	³⁴⁸ 18501 ± 274		
354	uluface-003	97357	529422	²⁵⁰ 1264	³³⁴ 3072 ± 0	³⁰⁴ 965 ± 11	²⁵⁹ 968 ± 10	²⁷¹ 1087 ± 20	³¹⁵ 1387 ± 36	³²² 2469 ± 86	³⁶⁴ 26057 ± 195	³⁶⁶ 26865 ± 566		
355	unissey-001	0	1956593	²⁹³ 1584	³⁶² 4096 ± 0	²⁷⁷ 880 ± 3	²³⁸ 892 ± 3	³⁵⁵ 1452 ± 8	³⁶⁵ 3048 ± 12	³⁶¹ 10017 ± 387	¹⁶² 1463 ± 35	¹⁶³ 1471 ± 34		
356	upc-001	0	89914	²²⁷ 1077	⁷⁵ 1052 ± 0	¹⁴³ 551 ± 15	¹⁷⁷ 703 ± 56	¹⁶⁴ 724 ± 51	¹⁵⁰ 751 ± 49	¹⁵⁰ 863 ± 33	²⁵⁴ 3114 ± 44	²⁵⁷ 3165 ± 97		
357	vcog-002	3229434	118946	³⁷² 3666	⁴⁰⁴ 61504 ± 5	⁶⁸ 357 ± 25	-	-	-	-	⁴⁰⁰ 296154 ± 3077	⁴⁰⁰ 296436 ± 4183		
358	vd-002	254498	34389	¹³⁹ 688	⁴⁴ 516 ± 0	²⁰⁷ 684 ± 5	¹⁶⁸ 679 ± 4	¹⁴⁷ 676 ± 5	¹²⁹ 693 ± 5	¹²² 754 ± 5	¹⁹ 300 ± 14	²² 319 ± 32		
359	vd-003	254505	44051	¹⁴¹ 696	²⁹¹ 2052 ± 0	²¹¹ 691 ± 5	¹⁷² 690 ± 5	¹⁵⁰ 683 ± 4	¹²⁸ 691 ± 5	¹¹⁴ 722 ± 5	¹¹⁸ 1003 ± 11	¹¹⁸ 1001 ± 7		
360	veridas-006	355669	896424	³²⁸ 1990	²⁶² 2048 ± 0	²⁷⁸ 880 ± 8	²³⁶ 885 ± 8	³¹⁰ 1271 ± 18	³⁵⁷ 2242 ± 38	³⁵³ 6414 ± 156	³⁸⁴ 56940 ± 149	³⁸⁷ 66077 ± 194		
361	veridas-007	355105	891492	³⁴⁶ 2527	²²⁵ 2048 ± 0	²⁷¹ 872 ± 9	²³⁰ 875 ± 8	³⁰⁶ 1261 ± 18	³⁵⁵ 2238 ± 38	³⁵¹ 6374 ± 147	⁷² 655 ± 16	⁷⁶ 660 ± 19		
362	verigram-000	256209	7798	³¹⁵ 1842	¹³⁸ 2048 ± 0	²⁴² 807 ± 1	²⁰⁹ 821 ± 1	²⁴⁰ 972 ± 2	³⁰⁶ 1358 ± 3	³³² 2848 ± 13	¹⁴⁰ 1222 ± 17	¹⁴⁸ 1219 ± 17		
363	verigram-001	282155	11773	³⁵⁰ 2638	²⁶³ 2048 ± 0	¹⁹⁹ 664 ± 2	¹⁶⁶ 675 ± 2	¹⁹¹ 833 ± 4	²⁷⁴ 1202 ± 7	³²⁸ 2733 ± 32	¹⁷⁵ 1664 ± 60	¹⁷³ 1648 ± 56		
364	verihubs-inteligensia-000	209562	51877	⁶⁷ 427	¹⁹⁰ 2048 ± 0	¹⁴⁹ 567 ± 0	³⁶⁶ 1558 ± 8	³⁶² 1560 ± 8	³³⁸ 1568 ± 8	²⁹² 1621 ± 8	³⁵⁶ 22351 ± 91	³⁵⁶ 22371 ± 81		
365	via-000	124422	11151	²⁰⁹ 964	²⁵¹ 2048 ± 0	²¹⁶ 707 ± 8	¹⁸⁸ 740 ± 5	²¹³ 906 ± 41	²⁰⁴ 941 ± 40	¹⁸⁸ 1040 ± 5	¹¹² 966 ± 28	¹²¹ 1021 ± 44		
366	via-001	370255	11151	³⁰¹ 1697	²⁰⁸ 2048 ± 0	³⁰³ 964 ± 3	²⁷⁰ 1011 ± 3	²⁵⁷ 1026 ± 4	²³² 1045 ± 3	²⁰⁷ 1137 ± 28	¹¹⁴ 983 ± 31	¹¹⁵ 989 ± 40		
367	videmo-000	139643	39470	⁵⁹ 390	¹⁷⁹ 2048 ± 0	¹⁸ 142 ± 5	¹² 150 ± 4	¹¹ 150 ± 6	⁸ 151 ± 4	⁷ 155 ± 8	⁴² 513 ± 16	⁴³ 523 ± 38		
368	videmo-001	212051	95063	⁵³ 304	¹⁰¹ 2048 ± 0	³⁰ 199 ± 0	¹⁴ 164 ± 0	¹² 164 ± 0	⁹ 164 ± 0	⁸ 165 ± 0	¹⁸ 296 ± 17	¹⁹ 288 ± 16		
369	videonetics-001	30875	5963	⁴ 61	²⁹ 512 ± 0	³⁸ 262 ± 3	³² 273 ± 1	⁶¹ 439 ± 3	¹⁶⁶ 820 ± 3	³¹⁸ 2393 ± 43	¹³⁸ 1153 ± 38	¹⁴⁰ 1142 ± 65		
370	videonetics-002	121981	6289	¹⁶ 115	²⁸³ 2052 ± 0	⁴⁸ 282 ± 5	⁴⁰ 295 ± 1	⁸⁸ 513 ± 4	²²⁰ 1029 ± 3	³³⁸ 3151 ± 46	¹⁴⁵ 1219 ± 57	¹⁴⁹ 1262 ± 56		
371	viettelhightech-000	259471	215557	⁶⁵ 419	²²³ 2048 ± 0	¹⁰⁶ 461 ± 1	⁸⁸ 461 ± 2	⁶⁷ 461 ± 1	⁵⁹ 467 ± 2	⁴⁷ 494 ± 0	⁵³ 599 ± 11	⁵⁰ 591 ± 13		
372	vigilantsolutions-010	348798	49973	¹⁸ 840	⁸⁶ 1548 ± 0	¹⁷³ 615 ± 0	¹⁵² 631 ± 0	¹³¹ 632 ± 0	¹¹⁰ 636 ± 0	⁹¹ 659 ± 0	⁴⁰ 490 ± 13	⁴¹ 488 ± 11		
373	vigilantsolutions-011	255661	49973	¹¹⁸ 591	⁸⁷ 1548 ± 0	⁸¹ 402 ± 0	⁷⁰ 418 ± 0	⁵² 418 ± 0	⁴⁴ 422 ± 0	³⁸ 445 ± 0	²⁶ 339 ± 20	²⁸ 366 ± 37		
374	vinai-000	402391	866522	²¹⁷ 1032	⁹⁴ 2048 ± 0	³²⁹ 1099 ± 1	²⁸⁹ 1095 ± 1	²⁷⁴ 1093 ± 1	²⁴³ 1099 ± 1	²⁰⁴ 1126 ± 1	²⁴⁷ 2996 ± 20	²⁴⁷ 2993 ± 26		
375	vinbigdata-001	271405	44746	¹¹⁶ 589	²¹⁰ 2048 ± 0	³⁹² 1400 ± 5	³⁵² 1393 ± 2	³⁴² 1391 ± 2	³¹⁰ 1393 ± 1	²⁶² 1404 ± 1	¹⁵³ 1351 ± 50	¹⁵⁴ 1310 ± 38		
376	vion-000	228219	7533	⁸⁷ 498	²⁹² 2052 ± 0	⁶¹ 333 ± 1	-	-	-	-	³⁷¹ 39839 ± 3561	³⁶⁵ 26830 ± 2241		
377	visage-000	49218	70150	⁷³ 73	³³ 512 ± 0	⁴² 27 ± 0	²²⁷ ± 0	²³¹ ± 0	³⁸ ± 0	³ 63 ± 0	²¹⁹ 2220 ± 14	²²¹ 2218 ± 14		
378	visionbox-001	256869	190645	¹¹³ 579	¹⁵⁵ 2048 ± 0	³⁰⁸ 983 ± 7	²⁸⁸ 1093 ± 46	³³⁵ 1360 ± 68	³⁵⁴ 2181 ± 105	³⁴⁹ 5955 ± 281	¹³⁹ 1161 ± 22	¹⁴³ 1154 ± 20		
379	visionbox-002	259063	135281	¹²⁵ 612	³²¹ 2059 ± 0	¹¹⁷ 482 ± 1	⁹⁵ 482 ± 0	⁷⁶ 484 ± 1	⁶⁸ 492 ± 1	⁵⁴ 517 ± 3	²⁰⁸ 1969 ± 44	²⁰⁵ 1931 ± 42		
380	visionlabs-010	1067280	19357	¹⁹⁴ 902	⁴¹ 513 ± 0	²²¹ 730 ± 0	¹⁸⁰ 717 ± 1	¹⁶⁰ 709 ± 0	¹³⁸ 713 ± 1	¹¹⁹ 739 ± 0	⁵⁴ 600 ± 41	⁶⁵ 626 ± 35		
381	visionlabs-011	1067280	19353	¹⁸⁸ 862	⁴² 513 ± 0	²²² 731 ± 1	¹⁸¹ 717 ± 1	¹⁶¹ 710 ± 1	¹³⁹ 714 ± 1	¹²⁰ 741 ± 1	⁴⁴ 556 ± 26	⁴⁶ 559 ± 25		
382	visteam-002	186440	30888	¹⁰⁴ 547	³⁴⁷ 4096 ± 0	²⁵⁷ 829 ± 5	²¹⁴ 832 ± 6	¹⁹⁴ 839 ± 7	¹⁷⁶ 853 ± 6	¹⁸² 1013 ± 14	³¹⁶ 6952 ± 118	³¹³ 6970 ± 120		
383	visteam-003	215359	33730	⁸⁵ 489	³⁵⁴ 4096 ± 0	³⁶¹ 1249 ± 4	³²⁰ 1251 ± 4	³⁰⁹ 1266 ± 5	²⁸⁵ 1272 ± 5	²⁵⁰ 1370 ± 9	³¹³ 6816 ± 111	³¹³ 6816 ± 105		
384	vnpt-002	271649	3203296	⁸⁴ 489	¹⁷⁰ 2048 ± 0	²²³ 739 ± 2	¹⁸⁵ 731 ± 2	¹⁷⁰ 740 ± 1	¹⁴⁸ 742 ± 2	¹²⁷ 763 ± 2	⁹⁵ 766 ± 13	⁹⁵ 762 ± 13		
385	vnpt-003	369956	297799	¹⁴⁹ 714	³⁶⁶ 4096 ± 0	³⁷⁶ 1315 ± 4	³³⁶ 1315 ± 4	³²⁵ 1318 ± 2	³⁰³ 1350 ± 3	²⁶⁹ 1428 ± 3	³²¹ 7397 ± 31	³²⁰ 7384 ± 29		
386	vocord-009	1380132	201560	³⁸² 4162	⁸⁹ 1920 ± 0	⁴⁰³ 1472 ± 2	³⁶⁴ 1472 ± 1	³⁶¹ 1549 ± 1	³⁴² 1667 ± 2	³⁰⁷ 2064 ± 2	²¹¹ 2052 ± 50	²¹⁴ 2056 ± 39		
387	vocord-010	902552	206873	³⁷⁷ 3858	⁷⁸ 1088 ± 0	⁴⁰¹ 1459 ± 2	³⁶³ 1459 ± 1	³⁵⁸ 1463 ± 2	³³⁴ 1484 ± 1	²⁸⁵ 1535 ± 3	²³⁸ 2724 ± 31	²³⁶ 2653 ± 45		
388	vts-000	256589	169760	³⁰² 1704	¹⁷¹ 2048 ± 0	¹²⁰ 486 ± 1	⁹³ 481 ± 0	⁷⁷ 484 ± 0	⁶⁴ 485 ± 1	⁵⁵ 517 ± 0	³⁹⁵ 124209 ± 352	³⁹⁵ 123652 ± 358		
389	wicket-000	826392	641802	³³² 2071	²⁰⁶ 2048 ± 0	³⁹⁷ 1419 ± 2	³⁵⁸ 1429 ± 3	³⁵¹ 1444 ± 4	³³⁰ 1460 ± 3	²⁸⁶ 1537 ± 6	³⁸⁶ 60976 ± 232	³⁸⁵ 61096 ± 323		
390	winsense-001	264428	32035	²⁰¹ 922	⁸¹ 1280 ± 0	²³² 766 ± 7	²⁸² 1058 ± 47	²⁴⁵ 983 ± 97	²³³ 1053 ± 119	²⁴² 1320 ± 84	¹⁷² 1631 ± 28	²⁰⁸ 1964 ± 171		
391	winsense-002	281379	25780	³⁰⁹ 1781	¹⁵⁰ 2048 ± 0	¹²³ 494 ± 2	¹⁰³ 498 ± 1	⁹⁰ 519 ± 1	⁷⁷ 537 ± 1	⁸⁴ 634 ± 1	¹⁷⁶ 1683 ± 8	¹⁷⁶ 1685 ± 7		
392	wuhantianyu-001	465118	66457	¹⁸⁹ 866	²¹³ 2048 ± 0	¹⁸⁵ 642 ± 1	¹⁵⁶ 642 ± 1	¹³⁸ 644 ± 0	¹¹⁶ 652 ± 0	¹⁰⁴ 697 ± 0	³²⁷ 9502 ± 151	³²⁸ 9920 ± 253		
393	x-laboratory-000	520020	197310	²⁸⁷ 1524	³¹¹ 2056 ± 0	²⁴⁴ 808 ± 7	²⁴⁰ 897 ± 113	²¹⁴ 907 ± 103	¹⁸⁵ 886 ± 103	⁹⁶ 673 ± 39	⁸⁶ 725 ± 19	⁹² 749 ± 34		
394	x-laboratory-001	625140	398792	³¹⁶ 1844	³⁰⁷ 2056 ± 0	¹⁵⁶ 586 ± 2	¹⁴⁰ 596 ± 5	¹²⁰ 603 ± 6	¹⁰⁴ 620 ± 7	¹³² 793 ± 14	¹⁰² 813 ± 28	¹⁰⁶ 872 ± 32		
395	xforwardai-001	340100	51163	³³⁶ 2173	²⁴³ 2048 ± 0	³⁴⁷ 1180 ± 2	³¹⁰ 1182 ± 1	²⁹⁹ 1194 ± 1	²⁶⁸ 1186 ± 2	²²¹ 1203 ± 1	⁹⁸ 779 ± 17	⁹⁹ 797 ± 13		
396	xforwardai-002	707715	51163	³²⁷ 1989	³⁴⁸ 4096 ± 0	²⁹⁷ 944 ± 1	²⁵⁰ 942 ± 1	²³³ 943 ± 4	²⁰² 935 ± 1	¹⁷² 967 ± 1	¹⁶¹ 1406 ± 8	¹⁵⁹ 1405 ± 13		

Notes

- 1 The configuration size does not capture static data included in libraries.
- 2 The library size is the combined total of all files provided in the submission lib folder. These libraries e.g. OpenCV may or may not be installed on any end user's platform natively and would not need to be installed with the algorithm. Some developers put neural network models in their libraries.
- 3 The memory usage is the peak resident set size reported by the ps system call during template generation.
- 4 The median template creation times are measured on Intel®Xeon®CPU E5-2630 v4 @ 2.20GHz processors.
- 5 The comparison durations, in nanoseconds, are estimated using std::chrono::high_resolution_clock which on the machine in (2) counts 1ns clock ticks. Precision is somewhat worse than that however. The ± value is the median absolute deviation times 1.48 for Normal consistency.

Table 15: Summary of algorithms and properties included in this report. The red superscripts give ranking for the quantity in that column.

	ALGORITHM	CONFIG	LIBRARY	TEMPLATE								COMPARISON ⁴									
				NAME	DATA	DATA	MEMORY	SIZE	GENERATION TIME (ms) ⁴				TIME (ns) ⁵								
									(KB) ¹	(KB) ²	(MB) ³	(B)	MUGSHOT	480x720	960x1440	1600x2400	3000x4500	GENUINE	IMPOSTOR		
397	xm-000	578041	148920	137	688	287	2052 ± 0	276	878 ± 2	233	882 ± 1	248	988 ± 2	281	1258 ± 3	320	2434 ± 7	173	1634 ± 17	172	1632 ± 20
398	yisheng-004	486351	38653	253	1279	339	3704 ± 0	75	378 ± 12	-	-	-	-	-	-	78	693 ± 137	44	526 ± 34		
399	yitu-003	1525719	138919	373	3737	328	2082 ± 0	267	860 ± 0	-	-	-	-	-	-	347	18305 ± 71	347	18286 ± 62		
400	yoonik-002	453720	265415	356	2755	106	2048 ± 0	340	1145 ± 4	293	1123 ± 2	278	1124 ± 2	246	1125 ± 2	205	1126 ± 3	94	761 ± 32	91	736 ± 32
401	yoonik-003	346691	265415	338	2196	113	2048 ± 0	311	991 ± 3	263	980 ± 1	246	984 ± 4	214	982 ± 1	177	983 ± 1	74	684 ± 45	78	678 ± 41
402	yitu-000	1477360	44032	344	2484	268	2048 ± 0	133	530 ± 0	112	533 ± 0	136	640 ± 0	177	861 ± 2	306	1949 ± 8	368	31797 ± 131	369	31794 ± 133
403	yuan-003	370419	147783	363	2885	224	2048 ± 0	394	1405 ± 2	356	1413 ± 3	354	1446 ± 3	336	1547 ± 5	305	1878 ± 5	224	2320 ± 32	224	2287 ± 34
404	yuan-004	428665	50011	265	1353	343	4096 ± 0	147	567 ± 0	128	569 ± 0	108	573 ± 0	87	579 ± 0	76	607 ± 0	301	5816 ± 35	303	5800 ± 31

Notes

- 1 The configuration size does not capture static data included in libraries.
- 2 The library size is the combined total of all files provided in the submission lib folder. These libraries e.g. OpenCV may or may not be installed on any end user's platform natively and would not need to be installed with the algorithm. Some developers put neural network models in their libraries.
- 3 The memory usage is the peak resident set size reported by the ps system call during template generation.
- 4 The median template creation times are measured on Intel®Xeon®CPU E5-2630 v4 @ 2.20GHz processors.
- 5 The comparison durations, in nanoseconds, are estimated using std::chrono::high_resolution_clock which on the machine in (2) counts 1ns clock ticks. Precision is somewhat worse than that however. The ± value is the median absolute deviation times 1.48 for Normal consistency.

Table 16: Summary of algorithms and properties included in this report. The red superscripts give ranking for the quantity in that column.

	Algorithm	FALSE NON-MATCH RATE (FNMR)										LESS CONSTRAINED, NON-COOP.					
		CONSTRAINED, COOPERATIVE								WILD							
		Name	VISAMC	VISA	MUGSHOT	MUGSHOT12+YRS	VISABORDER	BORDER	BORDER	1E-05							
	FMR	0.0001	1E-06	1E-05	1E-05	1E-06	1E-06	1E-06	1E-05	0.0001							
1	20face-000	0.1268	347	0.1828	342	0.1748	350	0.2768	350	0.1765	339	0.1864	282	0.0927	310	0.0405	245
2	20face-001	0.0521	325	0.0732	325	0.1414	345	0.2549	348	0.0769	320	0.1354	278	0.0419	274	0.0295	148
3	3divi-006	0.0064	152	0.0094	150	0.0047	130	0.0066	135	0.0091	139	0.0191	149	0.0113	136	0.0289	127
4	3divi-007	0.0024	36	0.0038	40	0.0028	40	0.0034	36	0.0046	53	0.0101	67	0.0082	80	0.0300	161
5	acer-001	0.0294	304	0.0504	310	0.0240	302	0.0463	304	0.0436	299	0.0622	247	0.0360	267	0.0307	171
6	acer-002	0.0169	275	0.0262	276	0.0103	232	0.0167	243	0.0182	236	0.0281	192	0.0159	192	0.0297	154
7	acisw-003	0.9682	402	0.9971	402	0.7892	388	0.8738	388	0.8752	383	0.8275	344	0.6698	366	0.4470	374
8	acisw-007	0.4276	377	0.5493	378	0.8425	389	0.9185	389	0.8424	378	0.9976	372	0.9930	386	0.4963	378
9	ader-a-002	0.0052	117	0.0071	113	0.0047	128	0.0064	130	0.0087	132	0.0159	122	0.0136	164	0.0990	313
10	ader-a-003	0.0043	97	0.0059	95	0.0036	86	0.0043	71	0.0076	111	0.0151	110	0.0128	156	0.0989	312
11	advance-002	0.0089	197	0.0137	199	0.0073	191	0.0115	193	0.0400	292	0.0722	254	0.0593	292	0.0498	269
12	advance-003	0.0060	148	0.0087	143	0.0052	144	0.0067	136	0.0389	291	0.4914	313	0.1291	317	0.0508	271
13	afisbiometrics-000	0.0051	116	0.0073	118	0.0030	53	0.0050	92	0.0044	46	0.0077	31	0.0057	22	0.0282	81
14	aifirst-001	0.0119	237	0.0170	230	0.0084	210	0.0127	205	0.0131	197	0.0212	160	0.0138	167	0.0432	254
15	aigen-001	0.0124	242	0.0219	253	0.0143	271	0.0217	266	0.0236	261	0.8960	348	0.3255	342	0.0681	294
16	aigen-002	0.0192	286	0.0343	291	0.0256	303	0.0402	299	0.0389	290	0.9196	351	0.3876	348	0.1096	320
17	ailabs-001	0.0158	269	0.0276	282	0.0192	289	0.0317	291	0.0352	284	0.0608	244	0.0434	278	0.0338	209
18	aimall-002	0.0119	235	0.0167	228	0.0224	298	0.0411	300	0.0233	258	0.0373	221	0.0235	242	0.0327	198
19	aimall-003	0.0033	61	0.0041	49	0.0033	75	0.0035	42	0.0056	79	0.0109	74	0.0087	93	0.0312	180
20	aiunionface-000	0.0104	220	0.0154	218	0.0082	208	0.0122	196	0.0141	204	0.0243	175	0.0169	200	0.0306	168
21	aize-001	0.0223	294	0.0344	292	0.0199	290	0.0313	289	0.0367	286	0.0522	237	0.0359	266	0.0446	259
22	aize-002	0.0210	292	0.0327	287	0.0280	306	0.0489	307	0.0504	305	0.0692	251	0.0434	277	0.0854	307
23	ajou-001	0.0093	205	0.0147	209	0.0071	188	0.0126	200	0.0173	234	0.0274	187	0.0186	215	0.0348	217
24	alchera-002	0.0107	223	0.0157	219	0.0104	236	0.0229	269	0.0144	209	0.0246	176	0.0198	226	0.0328	200
25	alchera-003	0.0044	98	0.0055	85	0.0031	58	0.0039	58	0.0042	40	0.0077	33	0.0065	35	0.0339	211
26	alfabeta-001	0.4867	385	0.5831	382	0.6855	377	0.8156	381	0.8253	377	0.7765	339	0.6416	365	0.3427	365
27	alice-000	0.0119	238	0.0192	242	0.0106	240	0.0170	244	0.0167	226	0.0265	183	0.0150	184	0.0288	119
28	alleyes-000	0.0058	139	0.0090	146	0.0055	153	0.0087	172	0.0068	103	0.0105	72	0.0076	67	0.0282	80
29	allgovern-000	0.0346	314	0.0527	313	0.0232	299	0.0339	292	0.0372	289	0.0620	246	0.0443	281	0.0607	286
30	alphaface-001	0.0065	156	0.0097	159	0.0039	100	0.0063	129	0.0083	125	-	-	-	0.0280	65	
31	alphaface-002	0.0052	119	0.0075	124	0.0030	48	0.0044	74	1.0000	395	0.0115	84	0.0084	86	0.0279	54
32	amplifiedgroup-001	0.5034	387	0.5848	383	0.6973	381	0.8316	382	0.7807	372	0.7724	337	0.6354	362	0.4250	371
33	androvideo-000	0.0243	296	0.0438	306	0.0239	301	0.0365	296	0.0483	304	0.1870	283	0.0635	295	0.1163	322
34	anke-004	0.0080	187	0.0154	217	0.0073	190	0.0112	191	0.0102	165	0.0178	140	0.0118	143	0.0288	121
35	anke-005	0.0070	163	0.0109	178	0.0059	165	0.0094	178	0.0105	168	0.0142	100	0.0102	116	0.0289	126
36	antheus-000	0.2564	360	0.3776	364	0.7240	383	0.8699	385	0.8899	384	0.9872	362	0.9483	380	0.7668	385
37	antheus-001	0.1311	348	0.2306	349	0.5113	369	0.6797	370	0.8748	382	0.9908	366	0.9649	383	0.7586	384
38	anyvision-004	0.0267	301	0.0385	299	0.0258	304	0.0487	306	0.0234	260	0.0301	197	0.0191	219	0.0470	263
39	anyvision-005	0.0023	34	0.0037	38	0.0027	38	0.0035	41	0.0049	60	0.0084	43	0.0069	50	0.0285	98
40	armatura-001	0.0033	60	0.0042	53	0.0031	56	0.0037	48	0.0056	78	0.0110	75	0.0092	102	0.0815	305
41	asusaics-000	0.0125	244	0.0209	248	0.0085	211	0.0134	212	0.0143	207	0.7189	331	0.0285	255	0.0295	147
42	asusaics-001	0.0125	245	0.0210	249	0.0085	213	0.0134	213	0.0143	208	0.7437	334	0.0289	256	0.0295	146
43	authenmetric-003	0.0036	77	0.0053	82	0.0039	105	0.0051	95	0.0095	153	0.9930	367	0.5932	360	0.0290	131
44	authenmetric-004	0.0027	47	0.0042	54	0.0033	72	0.0036	45	0.0083	128	0.9879	364	0.4058	350	0.0290	135

Table 17: FNMR is the proportion of mated comparisons below a threshold set to achieve the FMR given in the header on the fourth row. FMR is the proportion of impostor comparisons at or above that threshold. The light grey values give rank over all algorithms in that column. The pink columns use only same-sex impostors; others are selected regardless of demographics. The exception, in the green column, uses "matched-covariates" i.e. impostors of the same sex, age group, and country of birth. The second pink column includes effects of extended ageing. Missing entries for border, visa, mugshot and wild images generally mean the algorithm did not run to completion. The VISA columns compare images described in section 2.1. The MUGSHOT columns compare images described in section 2.4. The VISA-BORDER column compare images described in section 2.2 with those of section 2.3. The BORDER column compares images described in section 2.3. The WILD columns compare images described in section 2.5.

	Algorithm	FALSE NON-MATCH RATE (FNMR)										LESS CONSTRAINED, NON-COOP.					
		CONSTRAINED, COOPERATIVE								WILD							
		Name	VISAMC	VISA	MUGSHOT	MUGSHOT12+YRS	VISABORDER	BORDER	BORDER	1E-06	1E-05						
	FMR	0.0001	1E-06	1E-05	1E-05	1E-06	1E-06	1E-06	1E-05	0.0001							
45	aware-005	0.0457	322	0.0643	320	0.0603	329	0.1094	331	0.0613	311	0.1075	271	0.0491	283	0.0314	184
46	aware-006	0.0487	323	0.0819	329	0.0529	324	0.1090	330	0.1011	331	0.1058	267	0.0502	285	0.0317	187
47	awiros-001	0.4044	374	0.4622	371	0.5530	370	0.6518	368	0.2008	343	0.1994	287	0.1386	320	0.5584	380
48	awiros-002	0.1990	354	0.2561	352	0.3319	359	0.4411	359	0.3821	357	0.9938	368	0.2634	336	0.0997	314
49	ayftech-001	0.0946	340	0.1941	343	0.2438	355	0.3625	355	0.1558	336	0.1589	280	0.0936	311	0.0785	301
50	ayonix-000	0.4351	380	0.4872	372	0.6150	375	0.7510	375	0.6557	366	0.6361	324	0.4981	354	0.3635	366
51	beethedata-000	0.0127	247	0.0195	243	0.0092	223	0.0157	234	0.0171	231	0.0306	199	0.0204	227	0.0285	100
52	beyneai-000	0.0071	169	0.0107	175	0.0104	237	0.0131	210	0.0170	230	0.9837	361	0.6171	361	0.0597	285
53	biocube-001	0.5596	391	0.6834	389	0.7700	387	0.8712	386	0.8446	379	0.9661	358	0.7922	373	0.2377	351
54	bioidtechswiss-001	0.0054	127	0.0072	115	0.0069	183	0.0124	199	0.0060	87	0.0094	56	0.0065	40	0.0313	182
55	bioidtechswiss-002	0.0049	106	0.0067	107	0.0064	172	0.0116	194	0.0067	101	0.0117	86	0.0086	91	0.0279	45
56	bm-001	0.7431	397	0.9494	398	0.9586	394	0.9843	392	0.9049	385	0.9021	350	0.8395	376	0.9935	394
57	boetech-001	0.0662	332	0.0802	328	0.0493	321	0.0791	321	0.0682	316	0.1074	270	0.0758	304	0.1719	336
58	boetech-002	0.0535	327	0.0565	317	0.0114	255	0.0136	215	0.0403	293	0.0650	248	0.0606	293	0.1697	335
59	bresee-001	0.0085	195	0.0143	206	0.0086	217	0.0153	232	0.0108	173	0.0168	131	0.0115	140	0.0355	229
60	bresee-002	0.0079	186	0.0101	166	0.0065	177	0.0079	157	0.0129	192	0.0263	182	0.0224	238	0.0327	199
61	camvi-002	0.0125	246	0.0221	254	0.0089	221	0.0145	225	0.0142	205	0.2650	298	0.0166	199	0.0288	118
62	camvi-004	0.0171	278	0.0316	286	0.0042	116	0.0049	90	0.0097	158	0.6636	326	0.0141	171	0.0284	91
63	canon-002	0.0034	70	0.0050	74	0.0026	27	0.0033	35	0.0043	43	0.0182	143	0.0065	39	0.0279	51
64	canon-003	0.0041	93	0.0059	93	0.0030	47	0.0040	61	0.0040	33	0.0073	24	0.0059	25	0.0274	20
65	ceiec-003	0.0071	171	0.0107	174	0.0061	168	0.0079	159	0.0160	218	0.0316	202	0.0260	250	0.0308	176
66	ceiec-004	0.0038	82	0.0051	75	0.0045	126	0.0053	99	0.0062	94	0.3939	308	0.0104	123	0.0325	195
67	chosun-001	0.0525	326	0.0936	331	0.0742	334	0.1263	336	0.0978	330	1.0000	391	0.9354	379	0.4446	373
68	chosun-002	0.0390	317	0.0646	321	0.0339	314	0.0576	314	0.0455	302	0.6904	328	0.1746	328	0.0696	296
69	chtface-004	0.0046	103	0.0062	99	0.0052	143	0.0080	160	0.0088	136	0.0152	111	0.0106	126	0.0306	170
70	chtface-005	0.0033	63	0.0049	69	0.0029	44	0.0041	63	0.0044	45	0.0317	203	0.0066	43	0.0306	169
71	clearviewai-000	0.0010	4	0.0019	9	0.0024	8	0.0028	19	0.0030	11	0.0058	9	0.0050	8	0.0271	5
72	closeli-001	0.0136	249	0.0163	222	0.0039	102	0.0054	101	0.0072	107	1.0000	384	0.0094	106	0.0318	188
73	cloudmatrix-000	0.0192	287	0.0340	290	0.0133	265	0.0220	267	0.9837	389	1.0000	387	0.0281	254	0.0668	291
74	cloudmatrix-001	0.0668	333	0.1141	335	0.0539	325	0.0905	324	0.3509	353	0.9819	360	0.9010	378	0.0636	288
75	cloudwalk-hr-003	0.0026	43	0.0041	48	0.0040	109	0.0058	113	0.0060	92	0.9992	375	0.0094	104	0.7206	383
76	cloudwalk-hr-004	0.0009	1	0.0018	5	0.0034	77	0.0028	23	0.0052	67	0.9992	376	0.0093	103	0.1625	334
77	cloudwalk-mt-003	0.0013	12	0.0022	11	0.0026	22	0.0027	16	0.0039	29	0.0076	27	0.0067	44	0.0347	214
78	cloudwalk-mt-004	0.0009	3	0.0013	1	0.0024	10	0.0021	2	0.0028	8	0.0054	5	0.0050	9	0.0285	103
79	clova-000	0.0099	214	0.0150	212	0.0094	227	0.0147	228	0.0136	199	0.0213	162	0.0152	187	0.0307	172
80	cogent-005	0.0060	144	0.0112	182	0.0064	175	0.0070	140	0.0095	152	0.0184	146	0.0135	162	0.0423	251
81	cogent-006	0.0046	102	0.0059	96	0.0036	82	0.0047	80	0.0058	84	0.0113	81	0.0091	99	0.0343	213
82	cognitec-003	0.0038	81	0.0052	77	0.0054	152	0.0057	111	0.0225	255	0.0416	226	0.0388	270	0.0348	218
83	cognitec-004	0.0036	72	0.0053	79	0.0053	145	0.0056	106	0.0098	159	0.0202	158	0.0154	188	0.0352	227
84	cor-001	0.0075	179	0.0113	184	0.0055	156	0.0084	166	0.0091	141	0.0148	106	0.0092	101	0.0277	36
85	coretech-000	0.7699	399	1.0000	403	1.0000	405	-	1.0000	404	1.0000	402	1.0000	397	1.0000	398	
86	corsight-001	0.0040	88	0.0057	91	0.0033	74	0.0047	79	0.0045	49	0.0095	59	0.0063	33	0.0276	27
87	corsight-002	0.0053	121	0.0068	110	0.0030	51	0.0041	64	0.0039	31	0.0079	35	0.0054	19	0.0276	32
88	csc-002	0.0099	215	0.0132	197	0.0077	196	0.0142	222	0.0126	190	0.0195	152	0.0146	178	0.1779	339

Table 18: FNMR is the proportion of mated comparisons below a threshold set to achieve the FMR given in the header on the fourth row. FMR is the proportion of impostor comparisons at or above that threshold. The light grey values give rank over all algorithms in that column. The pink columns use only same-sex impostors; others are selected regardless of demographics. The exception, in the green column, uses “matched-covariates” i.e. impostors of the same sex, age group, and country of birth. The second pink column includes effects of extended ageing. Missing entries for border, visa, mugshot and wild images generally mean the algorithm did not run to completion. The VISA columns compare images described in section 2.1. The MUGSHOT columns compare images described in section 2.4. The VISA-BORDER column compare images described in section 2.2 with those of section 2.3. The BORDER column compares images described in section 2.3. The WILD columns compare images described in section 2.5.

Algorithm	FALSE NON-MATCH RATE (FNMR)															
	CONSTRAINED, COOPERATIVE											LESS CONSTRAINED, NON-COOP.				
	Name	VISAMC	VISA	MUGSHOT	MUGSHOT12+YRS	VISABORDER	BORDER	BORDER	WILD							
	FMR	0.0001	1E-06	1E-05	1E-05	1E-06	1E-06	1E-05			0.0001					
89 <i>csc-003</i>	0.0053	122	0.0065	104	0.0037	90	0.0047	82	0.0074	109	0.0124	93	0.0112	135	0.1773	338
90 <i>ctbcbank-000</i>	0.0168	273	0.0250	270	0.0146	274	0.0224	268	0.0211	252	0.8964	349	0.3779	347	1.0000	406
91 <i>ctbcbank-001</i>	0.0155	267	0.0235	263	0.0148	279	0.0243	274	0.0207	249	0.9279	353	0.3469	344	1.0000	400
92 <i>cubox-001</i>	0.0064	153	0.0080	132	0.0037	89	0.0055	103	0.0060	88	0.0111	77	0.0077	68	0.0300	159
93 <i>cubox-002</i>	0.0034	69	0.0041	46	0.0025	17	0.0025	10	0.0033	17	0.0064	14	0.0058	24	0.0480	266
94 <i>cudocommunication-001</i>	0.4777	383	1.0000	404	0.4373	364	0.5360	362	1.0000	405	1.0000	403	1.0000	398	1.0000	399
95 <i>cuhkee-001</i>	0.0036	74	0.0045	61	0.0031	62	0.0046	77	0.0051	66	0.0095	60	0.0079	71	0.1492	329
96 <i>cybercore-000</i>	0.0728	335	0.1110	333	0.1521	347	0.2375	345	0.1874	342	0.1907	284	0.1178	316	0.1191	324
97 <i>cybercore-001</i>	0.3759	372	0.5677	380	0.6928	380	0.7926	377	0.8118	375	0.9291	356	0.7080	369	0.3811	367
98 <i>cyberextruder-001</i>	0.1972	352	0.2547	351	0.4686	368	0.6387	367	0.3807	356	0.3806	306	0.2582	332	0.1747	337
99 <i>cyberextruder-002</i>	0.0811	338	0.1336	336	0.1465	346	0.2266	344	0.2086	346	1.0000	393	1.0000	401	0.1000	315
100 <i>cyberlink-007</i>	0.0032	56	0.0053	80	0.0041	112	0.0043	69	0.0052	70	0.0243	174	0.0084	87	0.0280	61
101 <i>cyberlink-008</i>	0.0042	95	0.0056	89	0.0038	98	0.0048	84	0.0053	71	0.0099	64	0.0074	62	0.0274	17
102 <i>dahua-006</i>	0.0027	44	0.0039	42	0.0031	60	0.0039	59	0.0039	30	0.0067	19	0.0058	23	0.0280	58
103 <i>dahua-007</i>	0.0017	20	0.0023	15	0.0026	25	0.0032	33	0.0033	15	0.0060	10	0.0054	18	0.0278	40
104 <i>daon-000</i>	0.0095	208	0.0117	186	0.0068	180	0.0077	154	0.0092	145	0.0174	136	0.0137	166	0.0331	203
105 <i>decatur-000</i>	0.0714	334	0.1115	334	0.0608	330	0.1106	332	0.0866	324	1.0000	388	0.0714	301	0.0658	290
106 <i>decatur-001</i>	0.0424	319	0.0711	323	0.0237	300	0.0458	303	0.0447	300	1.0000	382	0.9969	389	0.0280	64
107 <i>deepglint-003</i>	0.0027	45	0.0038	41	0.0030	50	0.0032	32	0.0043	42	0.0082	40	0.0076	66	0.0279	47
108 <i>deepglint-004</i>	0.0025	41	0.0034	34	0.0039	103	0.0061	125	0.0050	64	0.0091	51	0.0082	79	0.0285	105
109 <i>deepsea-001</i>	0.0136	252	0.0215	251	0.0142	270	0.0214	265	0.0163	222	0.0250	178	0.0192	220	0.0347	216
110 <i>deepsense-000</i>	0.0145	258	0.0265	278	0.0113	253	0.0196	258	0.0151	212	0.0215	164	0.0129	157	0.0290	130
111 <i>deepsense-001</i>	0.0013	11	0.0019	8	0.0024	15	0.0025	9	0.0027	6	0.0115	85	0.0053	14	0.0285	99
112 <i>dermalog-008</i>	0.0096	211	0.0166	227	0.0086	214	0.0133	211	0.0165	224	0.0586	241	0.0226	239	0.0277	35
113 <i>dermalog-009</i>	0.0067	159	0.0094	152	0.0051	141	0.0069	138	0.0116	182	0.0312	200	0.0177	207	0.0270	4
114 <i>didiglobalface-001</i>	0.0055	130	0.0092	148	0.0030	49	0.0045	75	0.0088	135	0.0119	90	0.0085	89	0.0282	78
115 <i>digidata-000</i>	0.0967	341	0.1410	338	0.2596	356	0.3462	354	0.0293	277	0.0363	217	0.0212	232	0.0310	177
116 <i>digitalbarriers-002</i>	0.3360	369	0.3690	362	0.0877	337	0.1557	337	0.0971	329	0.0951	263	0.0497	284	0.0436	256
117 <i>dps-000</i>	0.0115	230	0.0176	234	0.0149	281	0.0185	253	0.0173	233	0.0275	189	0.0180	210	0.1067	318
118 <i>dsk-000</i>	0.1526	349	0.2169	348	0.3787	361	0.5426	364	0.3115	349	0.3089	302	0.1994	329	0.2201	347
119 <i>einetworks-000</i>	0.0099	216	0.0180	236	0.0088	220	0.0140	220	0.0130	194	0.0225	170	0.0147	180	0.0293	140
120 <i>ekin-002</i>	0.1168	344	0.2042	345	0.1530	348	0.2524	347	0.1777	341	0.2773	299	0.1347	319	0.4801	377
121 <i>enface-000</i>	0.0028	49	0.0049	70	0.0043	118	0.0072	142	0.0058	85	0.0150	108	0.0090	98	0.0290	137
122 <i>enface-001</i>	0.0072	175	0.0107	173	0.0071	185	0.0138	217	0.0068	104	0.0515	235	0.0094	107	0.0284	95
123 <i>eocortex-000</i>	0.3485	370	0.6943	390	0.1122	339	0.1574	338	0.2155	348	0.2257	294	0.1606	327	0.2546	357
124 <i>ercacat-001</i>	0.0036	75	0.0044	59	0.0033	71	0.0047	83	0.0106	170	0.0202	157	0.0184	213	0.0258	1
125 <i>euronovate-001</i>	0.2786	363	0.3608	361	0.4489	366	0.6105	366	0.5010	362	0.5392	318	0.3769	346	0.4333	372
126 <i>expasoft-001</i>	0.0328	311	0.0488	308	0.0211	294	0.0342	294	0.0629	314	0.6483	325	0.2816	339	0.0552	280
127 <i>expasoft-002</i>	0.0170	276	0.0274	280	0.0787	336	0.0768	320	0.1629	337	0.9996	378	0.9631	382	0.0337	207
128 <i>f8-001</i>	0.0249	298	0.0336	288	0.0178	287	0.0232	270	0.0303	280	0.0615	245	0.0408	273	0.0475	265
129 <i>f8-002</i>	0.0340	313	0.0591	319	0.0213	296	0.0374	297	0.0452	301	0.0760	255	0.0502	286	0.1601	333
130 <i>faceonlive-001</i>	0.0269	302	0.0359	295	0.0387	317	0.0721	319	0.0246	270	0.0349	214	0.0220	235	0.0548	278
131 <i>facesoft-000</i>	0.0085	194	0.0112	183	0.0064	174	0.0107	188	0.0091	140	0.0171	133	0.0107	127	0.0275	22
132 <i>facetag-000</i>	0.2836	364	0.4081	368	0.2933	358	0.4303	358	0.3448	351	0.6312	323	0.3530	345	0.2087	346

Table 19: FNMR is the proportion of mated comparisons below a threshold set to achieve the FMR given in the header on the fourth row. FMR is the proportion of impostor comparisons at or above that threshold. The light grey values give rank over all algorithms in that column. The pink columns use only same-sex impostors; others are selected regardless of demographics. The exception, in the green column, uses “matched-covariates” i.e. impostors of the same sex, age group, and country of birth. The second pink column includes effects of extended ageing. Missing entries for border, visa, mugshot and wild images generally mean the algorithm did not run to completion. The VISA columns compare images described in section 2.1. The MUGSHOT columns compare images described in section 2.4. The VISA-BORDER column compare images described in section 2.2 with those of section 2.3. The BORDER column compares images described in section 2.3. The WILD columns compare images described in section 2.5.

	Algorithm	FALSE NON-MATCH RATE (FNMR)										LESS CONSTRAINED, NON-COOP.					
		CONSTRAINED, COOPERATIVE								WILD							
		Name	VISAMC	VISA	MUGSHOT	MUGSHOT12+YRS	VISABORDER	BORDER	BORDER	1E-06	1E-05						
	FMR	0.0001	1E-06	1E-05	1E-05	1E-05	1E-06	1E-06	1E-05	0.0001	0.0001						
133	facetag-002	0.0098	213	0.0147	210	0.0064	176	0.0110	189	0.0116	181	0.0190	148	0.0119	147	0.0675	293
134	facex-001	1.0000	404	1.0000	405	1.0000	398	-		1.0000	406	1.0000	405	1.0000	395	1.0000	396
135	facex-002	0.0803	336	0.1404	337	0.1283	341	0.1979	342	0.1440	335	0.1952	286	0.1299	318	0.2377	350
136	farfaces-001	0.4890	386	0.5860	384	0.5650	371	0.7268	373	0.8015	374	0.7511	335	0.5892	359	0.1976	344
137	fiberhome-nanjing-003	0.0090	198	0.0139	203	0.0082	207	0.0144	223	0.0110	175	0.0174	134	0.0107	128	0.0272	11
138	fiberhome-nanjing-004	0.0037	80	0.0056	90	0.0031	57	0.0043	70	0.0043	44	0.0083	41	0.0061	31	0.0272	9
139	fincore-000	0.0309	309	0.0502	309	0.0281	307	0.0510	309	0.0521	307	0.0815	257	0.0522	287	0.0681	295
140	fujitsulab-002	0.0091	203	0.0124	191	0.0105	238	0.0156	233	0.0169	229	0.0345	213	0.0146	179	0.0282	74
141	fujitsulab-003	0.0045	100	0.0065	105	0.0057	161	0.0083	164	0.0080	118	0.0154	116	0.0101	113	0.0280	56
142	geo-002	0.0171	279	0.0187	240	0.0035	81	0.0051	97	0.0064	96	0.0117	87	0.0083	84	0.0302	164
143	geo-004	0.0030	50	0.0041	47	0.0025	20	0.0030	27	0.0035	22	0.0065	16	0.0053	16	0.0286	108
144	glory-003	0.0076	181	0.0125	194	0.0077	198	0.0103	185	0.0130	193	0.0205	159	0.0143	175	0.0763	299
145	glory-004	0.0077	182	0.0123	188	0.0074	194	0.0098	182	0.0122	187	0.0193	150	0.0134	161	0.0743	298
146	gorilla-007	0.0074	177	0.0111	181	0.0065	178	0.0126	201	0.0100	163	0.0151	109	0.0102	115	0.0278	37
147	gorilla-008	0.0058	138	0.0091	147	0.0049	134	0.0079	158	0.0079	117	0.0126	95	0.0091	100	0.0278	44
148	graymatics-001	0.1039	343	0.1620	340	0.1344	343	0.1917	340	0.1648	338	0.5160	316	0.2689	337	0.3057	363
149	griaule-000	0.0071	170	0.0099	161	0.0050	137	0.0072	141	0.0160	216	0.0304	198	0.0267	252	0.0338	208
150	hertasecurity-000	0.0630	331	0.0780	327	0.0503	323	0.0898	323	0.0738	317	0.0693	253	0.0420	275	0.0575	283
151	hertasecurity-001	0.0249	297	0.0309	285	0.0105	239	0.0161	236	0.0245	268	0.0447	229	0.0359	265	0.0486	268
152	hik-001	0.0096	210	0.0125	192	0.0093	226	0.0164	241	0.0108	174	0.0937	261	0.0127	154	0.0271	6
153	hisign-001	0.0036	78	0.0050	73	0.0034	76	0.0046	76	0.0079	116	0.0153	115	0.0133	159	0.0286	111
154	hyperverge-001	1.0000	405	1.0000	406	1.0000	401	-		1.0000	400	1.0000	400	1.0000	404	1.0000	403
155	hyperverge-002	0.0050	109	0.0066	106	0.0035	80	0.0051	94	0.0062	93	0.0107	73	0.0074	63	0.0276	31
156	hzailu-001	0.0122	239	0.0164	224	0.0095	229	0.0196	257	0.0079	114	0.0118	88	0.0090	97	0.0392	240
157	icm-002	0.0143	256	0.0249	269	0.0144	272	0.0256	275	0.0236	263	0.0386	223	0.0263	251	0.0339	210
158	icm-003	0.0138	253	0.0222	255	0.0149	280	0.0282	284	0.0227	256	0.0384	222	0.0257	248	0.0333	205
159	ichthc-000	0.0260	300	0.0396	300	0.0207	293	0.0339	293	0.0291	276	0.0474	232	0.0346	262	0.0459	262
160	id3-006	0.0072	173	0.0103	168	0.0049	135	0.0074	148	0.0095	151	0.0165	130	0.0119	146	0.9938	395
161	id3-008	0.0039	84	0.0055	86	0.0032	67	0.0042	66	0.0081	122	0.0155	117	0.0134	160	0.8856	389
162	idemia-007	0.0024	37	0.0039	43	0.0032	69	0.0038	55	0.0046	52	0.0092	53	0.0070	54	0.0288	124
163	idemia-008	0.0023	33	0.0032	28	0.0023	5	0.0028	18	0.0034	20	0.0067	18	0.0056	21	0.0290	134
164	iit-002	0.0111	227	0.0177	235	0.0085	212	0.0140	219	0.0193	245	0.0332	208	0.0260	249	0.1373	326
165	iit-003	0.0082	193	0.0151	215	0.0053	147	0.0084	167	0.0122	186	0.0199	155	0.0137	165	0.0407	246
166	imagus-004	0.0063	150	0.0094	155	0.0055	155	0.0081	162	0.0098	160	0.0157	120	0.0111	132	0.0283	87
167	imagus-005	0.0276	303	0.0420	302	0.0302	311	0.0629	315	0.0288	275	0.0447	228	0.0235	243	0.0265	2
168	imperial-000	0.0067	160	0.0108	177	0.0080	204	0.0134	214	0.0087	133	0.0581	239	0.0102	117	0.0281	69
169	imperial-002	0.0058	136	0.0081	135	0.0055	154	0.0085	169	0.0083	126	0.0157	118	0.0103	118	0.0273	14
170	incode-009	0.0044	99	0.0067	109	0.0034	79	0.0051	93	0.0049	61	0.0091	50	0.0067	45	0.0296	152
171	incode-010	0.0041	92	0.0063	101	0.0028	42	0.0043	68	0.0047	57	0.0077	32	0.0061	30	0.0296	153
172	innefulabs-000	0.0122	240	0.0199	244	0.0112	252	0.0197	259	0.0222	254	0.0372	220	0.0271	253	0.0348	219
173	innovativetechnologyltd-001	0.0578	329	0.0938	332	0.0501	322	0.0981	325	0.0592	310	0.0779	256	0.0422	276	0.0449	261
174	innovativetechnologyltd-002	0.0451	321	0.0716	324	0.0541	326	0.1009	328	0.0506	306	0.0682	249	0.0371	268	0.0804	304
175	innovatrics-007	0.0040	91	0.0054	84	0.0057	160	0.0078	155	0.0079	115	0.0123	91	0.0088	94	0.0282	79
176	innovatrics-008	0.0047	104	0.0064	103	0.0038	97	0.0052	98	0.0053	72	0.0088	48	0.0069	51	0.0287	112

Table 20: FNMR is the proportion of mated comparisons below a threshold set to achieve the FMR given in the header on the fourth row. FMR is the proportion of impostor comparisons at or above that threshold. The light grey values give rank over all algorithms in that column. The pink columns use only same-sex impostors; others are selected regardless of demographics. The exception, in the green column, uses “matched-covariates” i.e. impostors of the same sex, age group, and country of birth. The second pink column includes effects of extended ageing. Missing entries for border, visa, mugshot and wild images generally mean the algorithm did not run to completion. The VISA columns compare images described in section 2.1. The MUGSHOT columns compare images described in section 2.4. The VISA-BORDER column compare images described in section 2.2 with those of section 2.3. The BORDER column compares images described in section 2.3. The WILD columns compare images described in section 2.5.

	Algorithm	FALSE NON-MATCH RATE (FNMR)									
		CONSTRAINED, COOPERATIVE								LESS CONSTRAINED, NON-COOP.	
		Name	ViSAMC	VISA	MUGSHOT	MUGSHOT12+YRS	VISA BORDER	BORDER	BORDER	WILD	
	FMR	0.0001	1E-06	1E-05	1E-05	1E-05	1E-06	1E-06	1E-05	0.0001	
177	insightface-001	0.0009	2	0.0014	2	0.0027	31	0.0024	5	0.0035	21
178	insightface-002	0.0011	6	0.0019	7	0.0027	35	0.0026	11	0.0036	26
179	intellicloudai-001	0.0142	255	0.0234	261	0.0092	225	0.0145	224	0.0162	220
180	intellicloudai-002	0.0059	143	0.0085	138	0.0060	167	0.0069	139	0.0108	172
181	intellifusion-001	0.0072	172	0.0094	153	0.0056	159	0.0085	170	0.0111	177
182	intellifusion-002	0.0059	142	0.0077	127	0.0040	108	0.0074	147	0.0085	131
183	intellivision-002	0.1000	342	0.1775	341	0.0610	331	0.1009	327	0.0805	322
184	intellivision-003	0.1177	345	0.2006	344	0.0760	335	0.1244	335	0.1069	332
185	intellivix-001	0.0064	155	0.0087	142	0.0046	127	0.0063	128	0.0072	106
186	intelresearch-004	0.0025	39	0.0035	35	0.0032	65	0.0038	53	0.0049	62
187	intelresearch-005	0.0016	17	0.0023	14	0.0028	39	0.0034	38	0.0042	41
188	intsysmsu-001	0.9543	401	0.9888	400	0.9923	395	-	0.9977	390	0.9955
189	intsysmsu-002	0.0130	248	0.0254	272	0.0137	268	0.0267	282	0.0160	217
190	ionetworks-000	0.0060	147	0.0087	140	0.0044	119	0.0058	115	0.0080	121
191	iqface-000	0.0091	202	0.0143	205	0.0075	195	0.0110	190	0.0171	232
192	iqface-003	0.0058	137	0.0079	130	0.0051	142	0.0058	116	0.0104	167
193	irex-000	0.0052	118	0.0099	162	0.0056	158	0.0083	165	0.0137	202
194	isap-001	0.5092	388	0.6588	386	0.6899	379	0.7978	378	0.7200	368
195	isap-002	0.0114	229	0.0186	239	0.0087	218	0.0151	231	0.0156	215
196	isityou-000	0.5682	392	0.7033	392	1.0000	402	-	1.0000	398	1.0000
197	isystems-001	0.0149	264	0.0245	267	0.0138	269	0.0210	263	0.0209	251
198	isystems-002	0.0118	233	0.0182	237	0.0111	249	0.0162	239	0.0166	225
199	itmo-007	0.0080	188	0.0125	193	0.0107	241	0.0185	251	0.0167	227
200	itmo-008	0.0090	199	0.0150	213	0.0058	163	0.0059	120	0.0187	241
201	ivacognitive-001	0.0189	284	0.0351	293	0.0123	260	0.0235	271	0.0198	247
202	iws-000	0.4824	384	0.5801	381	0.6859	378	0.8155	380	0.8251	376
203	kakao-005	0.0040	86	0.0059	94	0.0036	88	0.0057	110	0.0085	130
204	kakao-007	0.0019	26	0.0028	24	0.0024	7	0.0026	12	0.0033	16
205	kakaipay-001	0.0152	266	0.0252	271	0.0145	273	0.0270	283	0.0232	257
206	kasikornlabs-000	0.0112	228	0.0184	238	0.0086	215	0.0137	216	0.0130	195
207	kedacom-000	0.0055	129	0.0081	136	0.0111	251	0.0120	195	0.0415	295
208	kiwitech-000	0.0076	180	0.0105	170	0.0081	206	0.0128	207	0.0096	154
209	kneron-003	0.0542	328	0.0902	330	0.0346	315	0.0562	312	0.0919	326
210	kneron-005	0.0157	268	0.0259	274	0.0126	263	0.0212	264	0.0406	294
211	knowutech-000	0.0039	85	0.0055	87	0.0028	43	0.0042	65	0.0042	38
212	kookmin-002	0.0054	128	0.0077	126	0.0043	117	0.0065	132	0.0123	188
213	kuke3d-001	0.0058	135	0.0104	169	0.0083	209	0.0093	177	0.0270	273
214	lebentech-000	0.5940	393	0.7032	391	0.8854	391	0.9511	390	0.9089	386
215	lemalabs-001	0.0111	226	0.0175	232	0.0088	219	0.0142	221	0.0143	206
216	line-000	0.0172	280	0.0236	264	0.0109	245	0.0194	256	0.0183	237
217	line-001	0.0025	40	0.0040	44	0.0026	30	0.0034	40	0.0045	50
218	lookman-002	0.0297	306	0.0547	316	0.0339	313	0.0562	311	0.0614	312
219	lookman-004	0.0074	178	0.0099	163	0.0124	262	0.0149	229	0.0430	298
220	luxand-000	0.2056	355	0.2814	355	0.4053	363	0.5365	363	0.3497	352

Table 21: FNMR is the proportion of mated comparisons below a threshold set to achieve the FMR given in the header on the fourth row. FMR is the proportion of impostor comparisons at or above that threshold. The light grey values give rank over all algorithms in that column. The pink columns use only same-sex impostors; others are selected regardless of demographics. The exception, in the green column, uses “matched-covariates” i.e. impostors of the same sex, age group, and country of birth. The second pink column includes effects of extended ageing. Missing entries for border, visa, mugshot and wild images generally mean the algorithm did not run to completion. The VISA columns compare images described in section 2.1. The MUGSHOT columns compare images described in section 2.4. The VISA-BORDER column compare images described in section 2.2 with those of section 2.3. The BORDER column compares images described in section 2.3. The WILD columns compare images described in section 2.5.

	Algorithm	FALSE NON-MATCH RATE (FNMR)										LESS CONSTRAINED, NON-COOP.					
		CONSTRAINED, COOPERATIVE								WILD							
		Name	VISAMC	VISA	MUGSHOT	MUGSHOT12+YRS	VISABORDER	BORDER	BORDER								
	FMR	0.0001	1E-06	1E-05	1E-05	1E-06	1E-06	1E-06	1E-05		0.0001						
221	mantra-000	0.0037	79	0.0052	78	0.0054	150	0.0056	108	0.0097	157	0.0181	142	0.0151	185	0.0350	223
222	maxvision-000	0.0078	185	0.0106	172	0.0110	247	0.0147	227	0.0368	288	1.0000	395	0.1545	323	0.0445	258
223	maxvision-001	0.0305	308	0.0528	314	0.1028	338	0.1921	341	0.0650	315	0.3001	301	0.1553	325	0.0539	276
224	megvii-003	0.0064	154	0.0094	151	0.0136	267	0.0260	277	0.0050	63	0.0080	36	0.0059	28	0.0288	115
225	megvii-004	0.0020	27	0.0033	31	0.0028	41	0.0035	43	0.0037	28	0.0074	25	0.0068	49	0.0283	88
226	meituan-000	0.0197	288	0.0424	305	0.0078	199	0.0074	146	0.0103	166	0.0193	151	0.0164	196	0.1063	317
227	meiya-001	0.0171	277	0.0275	281	0.0159	284	0.0261	280	0.0311	281	0.2250	293	0.0245	246	0.0363	233
228	mendaxiatech-000	0.0027	46	0.0036	36	0.0029	45	0.0036	46	0.0031	14	0.0057	8	0.0051	11	0.0275	23
229	microfocus-001	0.4482	381	0.5524	379	0.7256	384	0.8416	383	0.7301	369	0.6926	329	0.5180	355	0.2567	358
230	microfocus-002	0.3605	371	0.5057	374	0.5783	373	0.7223	372	0.5909	363	0.5963	322	0.4160	351	0.1582	332
231	minivision-000	0.0033	59	0.0048	67	0.0038	95	0.0049	87	0.0055	76	0.0094	58	0.0079	73	0.0273	12
232	mobai-000	0.0360	316	0.0439	307	0.0372	316	0.0700	317	0.0367	287	0.0939	262	0.0795	306	0.2640	360
233	mobai-001	0.0199	290	0.0219	252	0.0047	129	0.0061	122	0.0093	149	0.0174	135	0.0138	168	0.1045	316
234	mobbl-001	0.3208	366	0.4375	369	0.5680	372	0.7193	371	0.6282	365	0.5783	321	0.3984	349	0.1866	341
235	mobbl-002	0.9914	403	0.9970	401	0.9355	392	-	1.0000	394	1.0000	385	0.9999	392	0.9921	393	
236	mobipintech-000	0.0090	200	0.0149	211	0.0039	107	0.0057	109	0.0115	180	0.0465	231	0.0182	212	0.0315	185
237	moreedian-000	0.3874	373	0.4912	373	0.9988	396	-	0.9990	391	0.9999	380	0.9998	391	0.4788	376	
238	multimodality-000	0.0034	68	0.0047	64	0.0036	87	0.0044	73	0.0077	112	0.9976	373	0.4456	353	0.0287	113
239	mvision-001	0.0191	285	0.0233	259	0.0204	292	0.0356	295	0.0198	248	0.0337	210	0.0242	245	0.0431	253
240	nazhai-000	0.0040	89	0.0059	97	0.0036	83	0.0048	86	0.0057	81	0.0125	94	0.0083	83	0.0275	24
241	neosystems-002	0.2905	365	0.4077	367	0.2028	353	0.3252	352	0.4088	359	0.5519	319	0.3331	343	0.4500	375
242	neosystems-003	0.2429	357	0.3349	358	0.1844	351	0.2999	351	0.5942	364	0.3936	307	0.2292	330	0.1404	327
243	netbridgeotech-001	0.4749	382	0.6599	387	0.4438	365	0.5676	365	0.4491	360	1.0000	383	0.9541	381	0.1098	321
244	netbridgeotech-002	0.0101	218	0.0166	226	0.0077	197	0.0127	204	0.0133	198	0.8215	342	0.0523	288	0.0351	225
245	neurotechnology-012	0.0051	115	0.0070	112	0.0038	92	0.0056	107	0.0066	100	0.0112	80	0.0075	64	0.0279	52
246	neurotechnology-013	0.0032	55	0.0045	62	0.0026	29	0.0036	44	0.0037	27	0.0068	20	0.0052	13	0.0278	41
247	nhn-002	0.0068	162	0.0096	157	0.0057	162	0.0087	173	0.0136	201	0.0253	180	0.0186	217	0.0302	163
248	nhn-003	0.0033	62	0.0048	68	0.0027	34	0.0038	52	0.0036	24	0.0198	153	0.0071	55	0.0285	107
249	nodeflux-002	0.0186	283	0.0340	289	0.0261	305	0.0451	302	0.0548	308	1.0000	389	1.0000	394	0.0299	157
250	notiontag-001	0.6846	395	0.8006	395	0.3955	362	0.5247	361	0.8669	381	0.8313	345	0.6362	363	0.2221	348
251	notiontag-002	0.0066	157	0.0089	144	0.0045	125	0.0061	123	0.0077	113	0.0137	98	0.0104	121	0.0299	156
252	nsensecorp-002	0.4277	378	0.5375	377	0.6734	376	0.7924	376	0.7194	367	0.6937	330	0.5617	357	0.5530	379
253	nsensecorp-003	0.0251	299	0.0295	284	0.0212	295	0.0305	287	0.0131	196	0.2139	291	0.0141	172	0.0872	309
254	ntechlab-011	0.0012	7	0.0019	6	0.0024	13	0.0028	25	0.0029	10	0.0055	6	0.0047	6	0.0288	120
255	ntechlab-012	0.0011	5	0.0016	3	0.0023	6	0.0030	28	0.0026	4	0.0050	3	0.0043	4	0.0280	63
256	omnigarde-001	0.0168	274	0.0260	275	0.0203	291	0.0402	298	0.0243	266	0.0327	205	0.0177	205	0.0288	117
257	omnigarde-002	0.0033	65	0.0046	63	0.0027	37	0.0039	56	0.0041	35	0.0076	28	0.0059	29	0.0278	43
258	omsecurity-000	0.2573	361	0.3835	365	0.3590	360	0.4903	360	0.3956	358	0.5003	314	0.2595	333	0.2400	352
259	openface-001	0.1804	351	0.2921	356	0.2878	357	0.3906	357	0.2054	345	0.2338	296	0.1549	324	0.2445	353
260	oz-003	0.0095	209	0.0143	204	0.0054	151	0.0077	153	0.0096	155	0.0175	138	0.0118	144	0.0288	122
261	oz-004	0.0033	64	0.0049	71	0.0038	99	0.0055	102	0.0081	123	0.0163	129	0.0142	173	0.0329	201
262	papsav1923-001	0.0078	184	0.0130	196	0.0068	181	0.0105	187	0.0119	183	0.0221	167	0.0136	163	0.0293	141
263	papsav1923-002	0.0021	31	0.0034	32	0.0026	23	0.0030	30	0.0048	58	0.0093	54	0.0086	90	0.0312	181
264	paravision-008	0.0018	22	0.0025	19	0.0024	9	0.0025	8	0.0036	23	0.0070	23	0.0063	34	0.0279	49

Table 22: FNMR is the proportion of mated comparisons below a threshold set to achieve the FMR given in the header on the fourth row. FMR is the proportion of impostor comparisons at or above that threshold. The light grey values give rank over all algorithms in that column. The pink columns use only same-sex impostors; others are selected regardless of demographics. The exception, in the green column, uses “matched-covariates” i.e. impostors of the same sex, age group, and country of birth. The second pink column includes effects of extended ageing. Missing entries for border, visa, mugshot and wild images generally mean the algorithm did not run to completion. The VISA columns compare images described in section 2.1. The MUGSHOT columns compare images described in section 2.4. The VISA-BORDER column compare images described in section 2.2 with those of section 2.3. The BORDER column compares images described in section 2.3. The WILD columns compare images described in section 2.5.

Algorithm	FALSE NON-MATCH RATE (FNMR)															
	CONSTRAINED, COOPERATIVE															
	Name	VISAMC	VISA	MUGSHOT	MUGSHOT12+YRS	VISABORDER	BORDER	BORDER	LESS CONSTRAINED, NON-COOP.							
	FMR	0.0001	1E-06	1E-05	1E-05	1E-06	1E-06	1E-05	WILD							
265 paravision-010	0.0012	9	0.0021	10	0.0022	3	0.0021	4	0.0027	5	0.0055	7	0.0050	10	0.0288	123
266 pensees-001	0.0087	196	0.0133	198	0.0071	187	0.0122	198	0.0145	210	0.0252	179	0.0195	224	0.0283	84
267 pixelall-006	0.0032	57	0.0042	52	0.0032	64	0.0039	57	0.0063	95	0.9960	370	0.0723	302	0.0283	83
268 pixelall-007	0.0036	76	0.0049	72	0.0039	101	0.0044	72	0.0068	102	0.9873	363	0.0217	234	0.0285	106
269 psl-008	0.0026	42	0.0040	45	0.0024	12	0.0028	24	0.0041	36	0.0077	29	0.0055	20	0.0280	59
270 psl-009	0.0161	271	0.0294	283	0.0023	4	0.0025	6	0.0036	25	0.0065	17	0.0048	7	0.0482	267
271 ptakuratsatu-000	0.0060	145	0.0089	145	0.0070	184	0.0104	186	0.0096	156	0.0152	113	0.0100	111	0.0284	92
272 pxd-001	0.0488	324	0.0752	326	0.0586	328	0.1087	329	0.0946	327	0.1065	268	0.0625	294	0.1088	319
273 pyramid-000	0.0136	251	0.0233	260	0.0117	258	0.0192	255	0.0185	240	0.0322	204	0.0206	230	0.0304	166
274 qnap-000	0.0149	263	0.0228	257	0.0155	282	0.0267	281	0.0238	265	0.8329	346	0.0396	272	0.0324	193
275 qnap-001	0.0148	260	0.0215	250	0.0103	233	0.0162	238	0.0183	239	0.0301	196	0.0186	216	0.0360	232
276 quantasoft-003	0.0081	191	0.0113	185	0.0056	157	0.0076	151	0.0091	142	0.0161	124	0.0107	129	0.0414	249
277 rankone-011	0.0049	107	0.0075	123	0.0038	91	0.0048	85	0.0060	91	0.0143	103	0.0080	76	0.0359	231
278 rankone-012	0.0043	96	0.0058	92	0.0031	63	0.0038	51	0.0047	55	0.0081	38	0.0065	38	0.0358	230
279 realnetworks-005	0.0070	164	0.0093	149	0.0063	171	0.0089	175	0.0092	144	0.0161	125	0.0104	122	0.0289	129
280 realnetworks-006	0.0040	87	0.0056	88	0.8657	390	-		0.0059	86	0.0112	78	0.0085	88	0.1790	340
281 regula-000	0.0184	282	0.0376	298	0.0103	234	0.0185	250	0.0120	184	0.9983	374	0.0231	240	0.0273	15
282 regula-001	0.0072	174	0.0107	176	0.0102	231	0.0179	248	0.0123	189	0.0333	209	0.0174	203	0.0295	144
283 remarkai-001	0.0144	257	0.0256	273	0.0102	230	0.0159	235	0.0162	221	0.0582	240	0.0185	214	0.0308	175
284 remarkai-003	0.0047	105	0.0063	102	0.0033	73	0.0049	88	0.0054	73	0.0100	66	0.0072	57	0.0275	26
285 rendip-000	0.0055	131	0.0077	125	0.0048	132	0.0060	121	0.0080	119	0.0142	102	0.0110	131	0.0433	255
286 revealmedia-005	0.0050	111	0.0074	122	0.0050	138	0.0068	137	0.0075	110	0.0124	92	0.0104	125	0.3960	369
287 revealmedia-006	0.0040	90	0.0067	108	0.0041	114	0.0056	105	0.0056	77	0.0085	45	0.0068	47	0.0278	42
288 rokid-000	0.0093	206	0.0145	207	0.0073	192	0.0102	184	0.0164	223	0.0280	191	0.0214	233	0.0857	308
289 rokid-001	0.0105	222	0.0162	221	0.0094	228	0.0163	240	0.0181	235	0.0276	190	0.0165	198	0.0325	196
290 s1-003	0.0051	113	0.0073	117	0.0044	121	0.0063	127	0.0052	69	0.0096	62	0.0070	52	0.1321	325
291 s1-004	0.0053	123	0.0080	133	0.0038	93	0.0059	119	0.0057	80	0.0103	68	0.0073	60	0.0281	68
292 saffe-001	0.4339	379	0.5261	375	0.7539	386	0.8736	387	0.7977	373	0.9810	359	0.7435	371	0.3887	368
293 saffe-002	0.0119	236	0.0206	245	0.0107	244	0.0177	246	0.0244	267	0.9998	379	0.2785	338	0.0308	174
294 samsungsds-000	0.0046	101	0.0069	111	0.0132	264	0.0081	161	0.0099	161	0.0179	141	0.0162	194	0.1874	342
295 samtech-001	0.0197	289	0.0365	296	0.0146	277	0.0241	273	0.0238	264	0.0394	224	0.0251	247	0.0337	206
296 scanovate-002	0.0175	281	0.0355	294	0.0146	275	0.0286	285	0.0269	272	0.0301	195	0.0178	208	0.0301	162
297 scanovate-003	0.0054	125	0.0080	134	0.0054	148	0.0072	144	0.0312	282	0.0599	242	0.0568	290	0.0283	82
298 securifai-003	0.4086	375	0.7577	394	0.7233	382	0.8070	379	0.7787	371	1.0000	390	0.9988	390	0.8326	388
299 securifai-004	0.0136	250	0.0192	241	0.0064	173	0.0099	183	0.0115	179	0.0272	186	0.0127	155	0.0347	215
300 sensetime-005	0.0019	24	0.0029	25	0.0022	2	0.0021	3	0.0023	2	0.0044	2	0.0039	2	0.0273	13
301 sensetime-006	0.0014	14	0.0024	17	0.0021	1	0.0020	1	0.0021	1	0.0040	1	0.0036	1	0.0272	10
302 sertis-000	0.0118	234	0.0208	247	0.0080	202	0.0127	203	0.0110	176	0.0176	139	0.0114	138	0.0285	104
303 sertis-002	0.0049	108	0.0061	98	0.0039	106	0.0061	126	0.0055	75	0.0099	65	0.0070	53	0.0281	67
304 seventhsense-000	0.0067	161	0.0099	165	0.0045	123	0.0065	133	0.0093	146	0.0169	132	0.0124	151	0.0275	25
305 seventhsense-001	0.0034	71	0.0047	66	0.0025	21	0.0031	31	0.0029	9	0.0338	211	0.0109	130	0.0279	46
306 shaman-000	0.9297	400	0.9774	399	0.9990	397	-		0.9999	392	1.0000	386	0.9999	393	0.9575	391
307 shaman-001	0.3346	368	0.4616	370	0.2368	354	0.3723	356	0.3574	354	0.3527	304	0.2304	331	0.1498	331
308 shu-002	-	0.0079	131	0.0146	276	0.0308	288	1.0000	393	0.0183	144	0.0115	139	0.0284	93	

Table 23: FNMR is the proportion of mated comparisons below a threshold set to achieve the FMR given in the header on the fourth row. FMR is the proportion of impostor comparisons at or above that threshold. The light grey values give rank over all algorithms in that column. The pink columns use only same-sex impostors; others are selected regardless of demographics. The exception, in the green column, uses “matched-covariates” i.e. impostors of the same sex, age group, and country of birth. The second pink column includes effects of extended ageing. Missing entries for border, visa, mugshot and wild images generally mean the algorithm did not run to completion. The VISA columns compare images described in section 2.1. The MUGSHOT columns compare images described in section 2.4. The VISA-BORDER column compare images described in section 2.2 with those of section 2.3. The BORDER column compares images described in section 2.3. The WILD columns compare images described in section 2.5.

	Algorithm	FALSE NON-MATCH RATE (FNMR)										LESS CONSTRAINED, NON-COOP.					
		CONSTRAINED, COOPERATIVE								WILD							
		Name	VISAMC	VISA	MUGSHOT	MUGSHOT12+YRS	VISA BORDER	BORDER	BORDER								
	FMR	0.0001	1E-06	1E-05	1E-05	1E-06	1E-06	1E-06	1E-05		0.0001						
309	shu-003	0.0028	48	0.0041	51	0.0050	136	0.0088	174	0.0081	124	0.0133	97	0.0094	105	0.0283	89
310	siat-002	0.0091	201	0.0126	195	0.0109	246	0.0190	254	0.0276	274	0.0516	236	0.0464	282	0.0520	274
311	siat-005	0.0021	29	0.0038	39	0.0059	164	0.0049	89	0.0742	318	0.9623	357	0.6801	367	0.0279	48
312	sjtu-003	0.0017	21	0.0033	30	0.0030	52	0.0037	49	0.0058	82	0.0104	69	0.0081	78	0.0284	97
313	sjtu-004	0.0014	13	0.0025	18	0.0027	32	0.0028	26	0.0046	51	0.0086	47	0.0073	59	0.0272	8
314	sktelecom-000	0.0038	83	0.0054	83	0.0031	54	0.0051	96	0.0042	37	0.3418	303	0.0061	32	0.0293	142
315	smartengines-000	0.6240	394	0.7562	393	0.9552	393	0.9784	391	0.9515	388	0.9288	355	0.8200	374	0.8037	387
316	smilart-002	0.2440	358	0.3532	360	-	-	-	3785	355	0.4145	311	0.2611	335	-	-	-
317	smilart-003	0.6944	396	0.8836	396	0.0695	333	0.1193	333	0.0894	325	0.1221	274	0.0737	303	0.1190	323
318	sodec-000	0.0033	66	0.0044	60	0.0040	110	0.0053	100	0.0054	74	0.0096	61	0.0080	74	0.0274	18
319	sqisoft-001	0.1220	346	0.2088	346	0.1978	352	0.3386	353	0.2111	347	0.2798	300	0.1474	322	0.0519	273
320	sqisoft-002	0.0082	192	0.0124	190	0.0051	140	0.0086	171	0.0102	164	0.0183	145	0.0122	149	0.0287	114
321	staku-000	0.0139	254	0.0208	246	0.0104	235	0.0145	226	0.0156	214	0.8063	341	0.1408	321	0.0332	204
322	starhybrid-001	0.0108	224	0.0138	200	0.0081	205	0.0113	192	0.0152	213	0.0265	184	0.0189	218	0.0350	224
323	sukshi-000	0.5409	389	0.6612	388	0.4556	367	0.6567	369	0.9296	387	0.8898	347	0.7384	370	0.6892	382
324	suprema-001	0.0041	94	0.0053	81	0.0038	96	0.0047	81	0.0060	90	0.0111	76	0.0095	108	0.0382	237
325	suprema-002	0.0030	52	0.0041	50	0.0034	78	0.0040	60	0.0045	47	0.0085	44	0.0072	58	0.0295	145
326	supremaid-001	0.0053	124	0.0073	120	0.0045	124	0.0066	134	0.0099	162	0.0186	147	0.0148	181	0.0352	226
327	synesis-006	0.0070	166	0.0096	156	0.0107	242	0.0166	242	-	0.0128	96	0.0089	95	0.0292	139	
328	synesis-007	0.0050	112	0.0073	121	0.0062	170	0.0076	150	-	0.0105	70	0.0080	77	0.0288	116	
329	synology-000	0.0149	261	0.0238	265	0.0148	278	0.0261	278	0.0221	253	0.0331	206	0.0209	231	0.0330	202
330	synology-002	0.0104	221	0.0153	216	0.0107	243	0.0184	249	0.0189	243	0.2032	288	0.0180	209	0.0312	179
331	sztu-000	0.0092	204	0.0139	202	0.0091	222	0.0201	261	0.0136	200	0.0685	250	0.0118	145	0.0270	3
332	sztu-001	0.0031	53	0.0043	57	0.0025	19	0.0028	22	0.0051	65	0.0113	82	0.0089	96	0.0275	21
333	t4isb-000	0.0058	134	0.0087	141	0.0041	115	0.0064	131	0.0083	127	0.0157	119	0.0103	119	0.0282	75
334	tech5-004	0.0123	241	0.0234	262	0.0086	216	0.0162	237	0.0065	99	0.0112	79	0.0082	81	0.0281	72
335	tech5-005	0.0054	126	0.0072	114	0.0069	182	0.0122	197	0.0060	89	0.0094	57	0.0066	41	0.0349	221
336	techsign-000	0.0325	310	0.0511	311	0.0435	319	0.0710	318	0.0746	319	0.1104	272	0.0841	308	0.0639	289
337	tevian-007	0.0019	25	0.0027	22	0.0032	68	0.0041	62	0.0045	48	0.0086	46	0.0078	70	0.0310	178
338	tevian-008	0.0012	8	0.0017	4	0.0033	70	0.0042	67	0.0042	39	0.0081	37	0.0068	48	0.0290	132
339	tiger-005	0.0624	330	0.2450	350	0.0292	310	0.0556	310	0.0430	297	1.0000	381	0.9964	388	0.0278	39
340	tiger-006	0.0066	158	0.0101	167	0.0050	139	0.0075	149	0.0089	138	0.0158	121	0.0117	142	0.0290	138
341	tinkoff-001	0.0145	259	0.0244	266	0.0318	312	0.0636	316	0.0236	262	1.0000	397	0.0339	260	0.0563	282
342	tongyi-005	0.0073	176	0.0146	208	0.0187	288	0.0421	301	0.0161	219	0.0215	163	0.0149	183	0.0399	241
343	toppanidage-000	0.0021	28	0.0033	29	0.0026	24	0.0028	20	0.0039	32	0.0075	26	0.0068	46	0.0376	235
344	toshiba-004	0.0030	51	0.0042	55	0.0025	18	0.0027	17	0.0034	19	0.0063	13	0.0053	17	0.0278	38
345	toshiba-005	0.0023	35	0.0037	37	0.0024	11	0.0026	13	0.0072	108	0.0141	99	0.0130	158	0.0281	70
346	trueface-002	0.0060	146	0.0096	158	0.0048	131	0.0061	124	0.0112	178	0.0198	154	0.0155	190	0.0793	303
347	trueface-003	0.0070	167	0.0094	154	0.0053	146	0.0081	163	0.0122	185	0.0217	166	0.0159	193	0.0785	302
348	tuputech-000	0.3218	367	0.3696	363	-	-	-	0.3237	350	0.4304	312	0.2973	341	0.9415	390	
349	turingtechchip-001	0.0330	312	0.0540	315	0.0458	320	0.1007	326	0.4715	361	0.9286	354	0.8448	377	0.4035	370
350	twface-000	0.0051	114	0.0072	116	0.0041	113	0.0058	112	0.0071	105	0.0153	114	0.0100	110	0.0276	29
351	twface-001	0.0036	73	0.0051	76	0.0031	61	0.0038	50	0.0049	59	0.0091	52	0.0075	65	0.0277	33
352	ulsee-001	0.0151	265	0.0246	268	0.0113	254	0.0185	252	0.0187	242	0.6766	327	0.0181	211	0.0316	186

Table 24: FNMR is the proportion of mated comparisons below a threshold set to achieve the FMR given in the header on the fourth row. FMR is the proportion of impostor comparisons at or above that threshold. The light grey values give rank over all algorithms in that column. The pink columns use only same-sex impostors; others are selected regardless of demographics. The exception, in the green column, uses “matched-covariates” i.e. impostors of the same sex, age group, and country of birth. The second pink column includes effects of extended ageing. Missing entries for border, visa, mugshot and wild images generally mean the algorithm did not run to completion. The VISA columns compare images described in section 2.1. The MUGSHOT columns compare images described in section 2.4. The VISA-BORDER column compare images described in section 2.2 with those of section 2.3. The BORDER column compares images described in section 2.3. The WILD columns compare images described in section 2.5.

Algorithm	FALSE NON-MATCH RATE (FNMR)								LESS CONSTRAINED, NON-COOP.	
	CONSTRAINED, COOPERATIVE									
	Name	VISAMC	VISA	MUGSHOT	MUGSHOT12+YRS	VISABORDER	BORDER	BORDER		
FMR	0.0001	1E-06	1E-05	1E-05	1E-06	1E-06	1E-06	1E-05	0.0001	
353 ultinous-000	0.2343	356	0.3484	359	-	-	-	-	-	
354 ultinous-001	0.2485	359	0.4003	366	-	-	-	-	-	
355 uluface-002	0.0081	189	0.0123	187	0.0071	186	0.0095	181	0.0107	
356 uluface-003	0.0100	217	0.0150	214	0.0079	200	0.0128	206	-	
357 unissey-001	0.0095	207	0.0160	220	0.0134	266	0.0150	230	0.0147	
358 upc-001	0.0234	295	0.0519	312	0.0291	309	0.0490	308	0.0294	
359 vcog-002	0.7522	398	0.9033	397	-	-	-	-	-	
360 vd-002	0.0429	320	0.0704	322	0.0569	327	0.0844	322	0.0801	
361 vd-003	0.0199	291	0.0222	256	0.0115	257	0.0130	209	0.0138	
362 veridas-006	0.0098	212	0.0167	229	0.0079	201	0.0127	202	0.0127	
363 veridas-007	0.0063	151	0.0083	137	0.0044	120	0.0058	114	0.0080	
364 verigram-000	0.0032	54	0.0043	56	0.0031	55	0.0034	37	0.0093	
365 verigram-001	0.0032	58	0.0044	58	0.0027	33	0.0032	34	0.0030	
366 verihubs-inteligensia-000	0.0070	165	0.0098	160	0.0048	133	0.0076	152	0.0092	
367 via-000	0.0216	293	0.0365	297	0.0177	286	0.0287	286	0.0296	
368 via-001	0.0149	262	0.0229	258	0.0114	256	0.0177	247	0.0183	
369 videmo-000	0.0298	307	0.0423	303	0.0155	283	0.0260	276	0.0246	
370 videmo-001	0.0295	305	0.0417	301	0.0164	285	0.0261	279	0.0355	
371 videonetcs-001	0.5483	390	0.6446	385	0.7517	385	0.8607	384	0.8664	
372 videonetcs-002	0.4274	376	0.5329	376	0.6081	374	0.7438	374	0.7775	
373 viettelhightech-000	0.0117	232	0.0166	225	0.0110	248	0.0198	260	0.0167	
374 vigilantsolutions-010	0.0109	225	0.0164	223	0.0074	193	0.0095	180	0.0209	
375 vigilantsolutions-011	0.0124	243	0.0176	233	0.0073	189	0.0095	179	0.0196	
376 vinai-000	0.0081	190	0.0124	189	0.0045	122	0.0072	143	0.0089	
377 vinbigdata-001	0.2576	362	0.2763	353	0.1404	344	0.1988	343	0.1407	
378 vion-000	0.0419	318	0.0590	318	0.0422	318	0.0478	305	0.0581	
379 visage-000	0.0933	339	0.1441	339	0.1316	342	0.2416	346	0.1395	
380 visionbox-001	0.0159	270	0.0270	279	0.0111	250	0.0173	245	0.0190	
381 visionbox-002	0.0058	133	0.0079	129	0.0060	166	0.0074	145	0.0084	
382 visionlabs-010	0.0017	19	0.0024	16	0.0026	26	0.0030	29	0.0033	
383 visionlabs-011	0.0012	10	0.0022	12	0.0024	16	0.0026	14	0.0028	
384 visteam-002	0.1564	350	0.2789	354	0.1581	349	0.2567	349	0.1776	
385 visteam-003	0.0804	337	0.2166	347	0.0613	332	0.1204	334	0.0963	
386 vnpt-002	0.0351	315	0.0424	304	0.0220	297	0.0316	290	0.0471	
387 vnpt-003	0.0117	231	0.0138	201	0.0040	111	0.0058	117	0.0087	
388 vocord-009	0.0022	32	0.0029	26	0.0036	84	0.0046	78	0.0052	
389 vocord-010	0.0024	38	0.0031	27	0.0036	85	0.0049	91	0.0025	
390 vts-000	0.0103	219	0.0174	231	0.0080	203	0.0129	208	0.0250	
391 wicket-000	0.0018	23	0.0028	23	0.0024	14	0.0027	15	0.0031	
392 winsense-001	0.0062	149	0.0099	164	0.0092	224	0.0210	262	0.0093	
393 winsense-002	0.0050	110	0.0073	119	0.0038	94	0.0059	118	0.0064	
394 wuhantianyu-001	0.0163	272	0.0262	277	0.0281	308	0.0569	313	0.0316	
395 x-laboratory-000	0.0071	168	0.0106	171	0.0123	261	0.0138	218	0.0419	
396 x-laboratory-001	0.0059	141	0.0110	179	0.0054	149	0.0078	156	0.0094	

Table 25: FNMR is the proportion of mated comparisons below a threshold set to achieve the FMR given in the header on the fourth row. FMR is the proportion of impostor comparisons at or above that threshold. The light grey values give rank over all algorithms in that column. The pink columns use only same-sex impostors; others are selected regardless of demographics. The exception, in the green column, uses “matched-covariates” i.e. impostors of the same sex, age group, and country of birth. The second pink column includes effects of extended ageing. Missing entries for border, visa, mugshot and wild images generally mean the algorithm did not run to completion. The VISA columns compare images described in section 2.1. The MUGSHOT columns compare images described in section 2.4. The VISA-BORDER column compare images described in section 2.2 with those of section 2.3. The BORDER column compares images described in section 2.3. The WILD columns compare images described in section 2.5.

Algorithm	Name	FALSE NON-MATCH RATE (FNMR)								LESS CONSTRAINED, NON-COOP.							
		CONSTRAINED, COOPERATIVE															
		VISAMC	VISA	MUGSHOT	MUGSHOT12+YRS	VISABORDER	BORDER	BORDER	WILD								
FMR	0.0001	1E-06	1E-05	1E-05	1E-06	1E-06	1E-06	1E-05	0.0001								
397	xforwardai-001	0.0021	30	0.0034	33	0.0027	36	0.0028	21	0.0046	54	0.0088	49	0.0079	72	0.0281	71
398	xforwardai-002	0.0016	18	0.0023	13	0.0026	28	0.0025	7	0.0040	34	0.0081	39	0.0074	61	0.0282	73
399	xm-000	0.0015	15	0.0026	21	0.0031	59	0.0038	54	0.0058	83	0.0105	71	0.0082	82	0.0282	76
400	yisheng-004	0.1988	353	0.3329	357	0.1147	340	0.1849	339	0.2044	344	-	-	-	-	0.0908	310
401	yitu-003	0.0015	16	0.0026	20	0.0066	179	0.0085	168	0.0064	98	0.0114	83	0.0103	120	0.0325	197
402	yoonik-002	0.0052	120	0.0062	100	0.0029	46	0.0034	39	0.0615	313	0.1279	277	0.1166	315	0.0549	279
403	yoonik-003	0.0034	67	0.0047	65	0.0032	66	0.0037	47	0.0816	323	0.2033	289	0.1601	326	0.0699	297
404	ytu-000	0.0057	132	0.0087	139	0.0121	259	0.0238	272	0.0047	56	0.0078	34	0.0059	27	0.0286	109
405	yuan-003	0.0078	183	0.0111	180	0.0062	169	0.0091	176	0.0106	169	0.0511	234	0.0123	150	0.0320	191
406	yuan-004	0.0058	140	0.0078	128	0.0039	104	0.0055	104	0.0234	259	0.0442	227	0.0353	263	0.0299	158

Table 26: FNMR is the proportion of mated comparisons below a threshold set to achieve the FMR given in the header on the fourth row. FMR is the proportion of impostor comparisons at or above that threshold. The light grey values give rank over all algorithms in that column. The pink columns use only same-sex impostors; others are selected regardless of demographics. The exception, in the green column, uses “matched-covariates” i.e. impostors of the same sex, age group, and country of birth. The second pink column includes effects of extended ageing. Missing entries for border, visa, mugshot and wild images generally mean the algorithm did not run to completion. The VISA columns compare images described in section 2.1. The MUGSHOT columns compare images described in section 2.4. The VISA-BORDER column compare images described in section 2.2 with those of section 2.3. The BORDER column compares images described in section 2.3. The WILD columns compare images described in section 2.5.

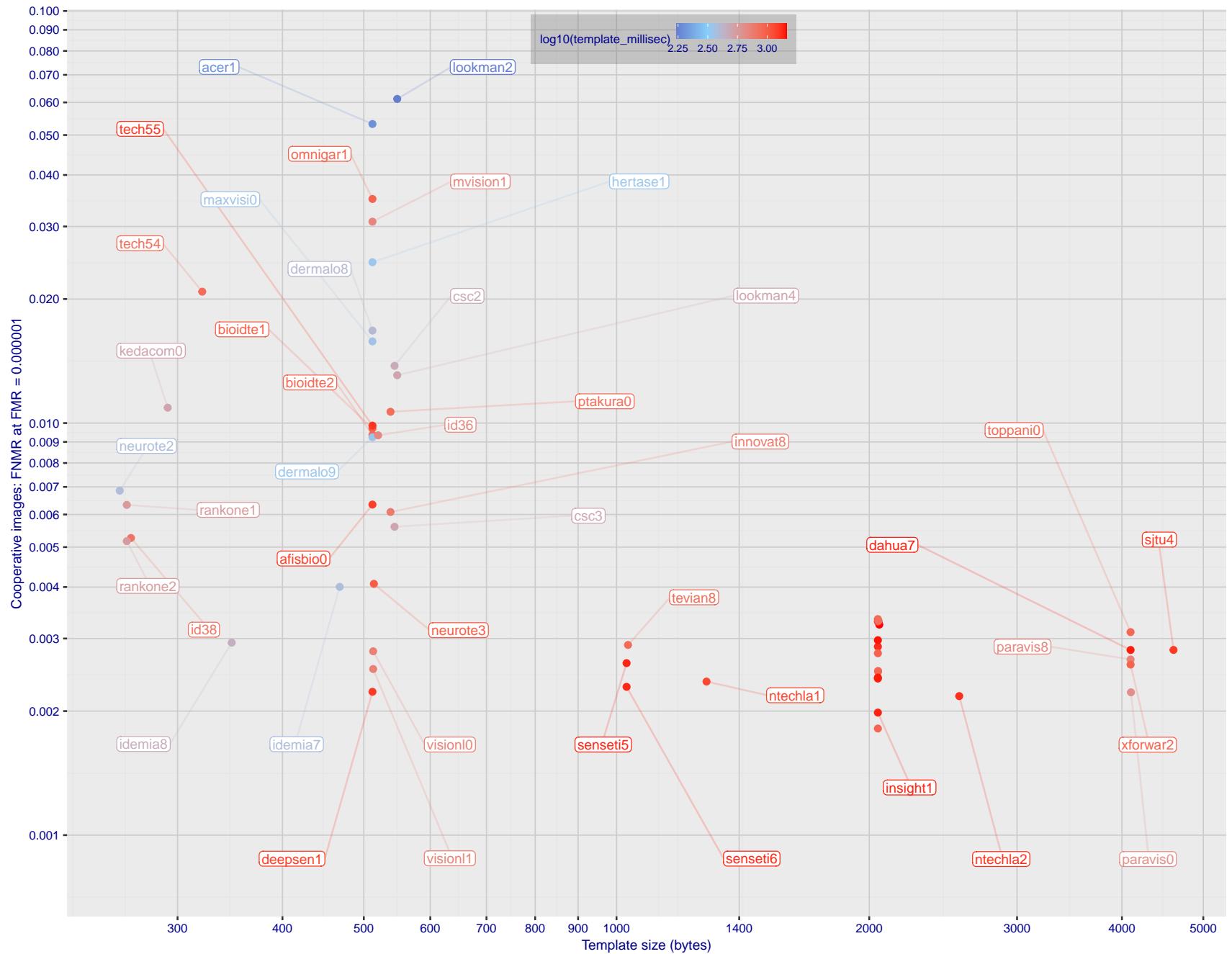


Figure 1: The points show false non-match rates (FNMR) versus the size of the encoded template. FNMR is the geometric mean of FNMR values for visa and mugshot images (from Figs. 60 and 81) at the false match rate (FMR) given in the y-axis label. The color of the points encodes template generation time - which spans at least one order of magnitude. Durations are measured on a single core of a c. 2016 Intel Xeon CPU E5-2630 v4 running at 2.20GHz. Algorithms with poor FNMR are omitted.

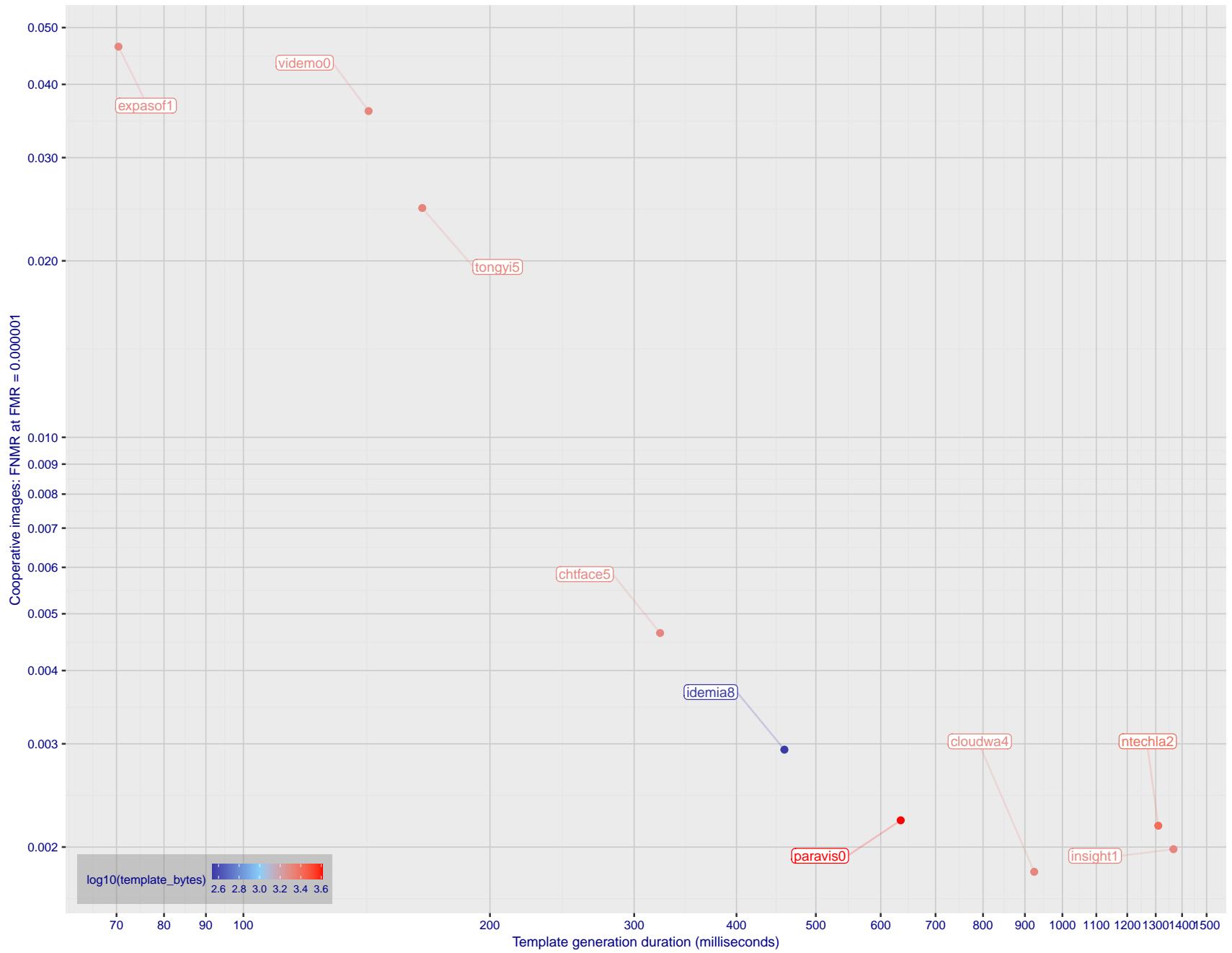


Figure 2: The points show false non-match rates (FNMR) versus the duration of the template generation operation. FNMR is the geometric mean of FNMR values for visa and mugshot images (from Figs. 60 and 81) at a false match rate (FMR) given in the y-axis label. Template generation time is a median estimated over 640 x 480 pixel portraits. It is measured on a single core of a c. 2016 Intel Xeon CPU E5-2630 v4 running at 2.20GHz. The color of the points encodes template size - which span two orders of magnitude. Algorithms with poor FNMR are omitted.

1 Metrics

1.1 Core accuracy

Given a vector of N genuine scores, u , the false non-match rate (FNMR) is computed as the proportion below some threshold, T:

$$\text{FNMR}(T) = 1 - \frac{1}{N} \sum_{i=1}^N H(u_i - T) \quad (1)$$

where $H(x)$ is the unit step function, and $H(0)$ taken to be 1.

Similarly, given a vector of N impostor scores, v , the false match rate (FMR) is computed as the proportion above T:

$$\text{FMR}(T) = \frac{1}{N} \sum_{i=1}^N H(v_i - T) \quad (2)$$

The threshold, T, can take on any value. We typically generate a set of thresholds from quantiles of the observed impostor scores, v , as follows. Given some interesting false match rate range, $[\text{FMR}_L, \text{FMR}_U]$, we form a vector of K thresholds corresponding to FMR measurements evenly spaced on a logarithmic scale

$$T_k = Q_v(1 - \text{FMR}_k) \quad (3)$$

where Q is the quantile function, and FMR_k comes from

$$\log_{10} \text{FMR}_k = \log_{10} \text{FMR}_L + \frac{k}{K} [\log_{10} \text{FMR}_U - \log_{10} \text{FMR}_L] \quad (4)$$

Error tradeoff characteristics are plots of FNMR(T) vs. FMR(T). These are plotted with $\text{FMR}_U \rightarrow 1$ and FMR_L as low as is sustained by the number of impostor comparisons, N. This is somewhat higher than the “rule of three” limit $3/N$ because samples are not independent, due to re-use of images.

1.2 Multi-template scoring methodology

There are some scenarios when one or more people exist and are detected in an image, and some of the proposed test images include $K > 1$ persons for some images and situations where the subject of interest may or may not be the foreground face (largest face in the image). The NIST FRVT 1:1 API supports this by allowing generation of multiple templates representing each person detected in an image. When this occurs, NIST will match all templates generated from the enrollment image with all templates generated from the verification image and use the **maximum** similarity score across all template comparisons. This scoring approach will be used in our calculation of FMR and FNMR (this applies to both genuine and imposter comparisons).

2 Datasets

2.1 Visa images

- ▷ The number of images is on the order of 10^5 .
- ▷ The number of subjects is on the order of 10^5 .
- ▷ The number of subjects with two images is on the order of 10^4 .
- ▷ The images have geometry in reasonable conformance with the ISO/IEC 19794-5 Full Frontal image type. Pose is generally excellent.
- ▷ The images are of size 252x300 pixels. The mean interocular distance (IOD) is 69 pixels.
- ▷ The images are of subjects from greater than 100 countries, with significant imbalance due to visa issuance patterns.
- ▷ The images are of subjects of all ages, including children, again with imbalance due to visa issuance demand.
- ▷ Many of the images are live capture. A substantial number of the images are photographs of paper photographs.
- ▷ When these images are input to the algorithm, they are labelled as being of type "ISO" - see Table 4 of the FRVT API.

2.2 Application images

- ▷ The number of images is on the order of 10^6 .
- ▷ The number of subjects is on the order of 10^6 .
- ▷ The number of subjects with two images is on the order of 10^6 .
- ▷ The images have geometry in good conformance with the ISO/IEC 19794-5 Full Frontal image type. Pose is generally excellent.
- ▷ The images are of size 300x300 pixels. The mean interocular distance (IOD) is 61 pixels.
- ▷ The images are of subjects from greater than 100 countries, with significant imbalance due to population and immigration patterns.
- ▷ The images are of subjects of adults with imbalance due to population and immigration patterns and demand.
- ▷ All of the images are live capture.
- ▷ When these images are input to the algorithm, they are labelled as being of type "ISO" - see Table 4 of the FRVT API.

2.3 Border crossing images

- ▷ The number of images is on the order of 10^6 .
- ▷ The number of subjects is on the order of 10^6 .
- ▷ The number of subjects with two images is on the order of 10^6 .
- ▷ The images are taken with a camera oriented by an attendant toward a cooperating subject. This is done under time constraints so there are roll, pitch and yaw angle variations. Also background illumination is sometimes strong, so the face is under-exposed. There is some perspective distortion due to close range images. Some faces are partially cropped.
- ▷ The images are of subjects from greater than 100 countries, with significant imbalance due to population and immigration patterns.
- ▷ The images are of subjects of adults with imbalance due to population and immigration patterns and demand.

- ▷ The images have mean IOD of 38 pixels.
- ▷ The images are all live capture.
- ▷ When these images are input to the algorithm, they are labelled as being of type "WILD" - see Table 4 of the FRVT API.

2.4 Mugshot images

- ▷ The number of images is on the order of 10^6 .
- ▷ The number of subjects is on the order of 10^6 .
- ▷ The number of subjects with two images is on the order of 10^6 .
- ▷ The images have geometry in reasonable conformance with the ISO/IEC 19794-5 Full Frontal image type.
- ▷ The images are of variable sizes. The median IOD is 105 pixels. The mean IOD is 113 pixels. The 1-st, 5-th, 10-th, 25-th, 75-th, 90-th and 99-th percentiles are 34, 58, 70, 87, 121, 161 and 297 pixels.
- ▷ The images are of subjects from the United States.
- ▷ The images are of adults.
- ▷ The images are all live capture.
- ▷ When these images are input to the algorithm, they are labelled as being of type "mugshot" - see Table 4 of the FRVT API.

2.5 Wild images

- ▷ The number of images is on the order of 10^5 .
- ▷ The number of subjects is on the order of 10^3 .
- ▷ The number of subjects with two images on the order of 10^3 .
- ▷ The images include many photojournalism-style images. Images are given to the algorithm using a variable but generally tight crop of the head. Resolution varies very widely. The images are very unconstrained, with wide yaw and pitch pose variation. Faces can be occluded, including hair and hands.
- ▷ The images are of adults.
- ▷ All of the images are live capture, none are scanned.
- ▷ When these images are input to the algorithm, they are labelled as being of type "WILD" - see Table 4 of the FRVT API.

3 Results

3.1 Test goals

- ▷ To state absolute accuracy for different kinds of images, including those with and without subject cooperation.
- ▷ To state comparative accuracy, across algorithms.

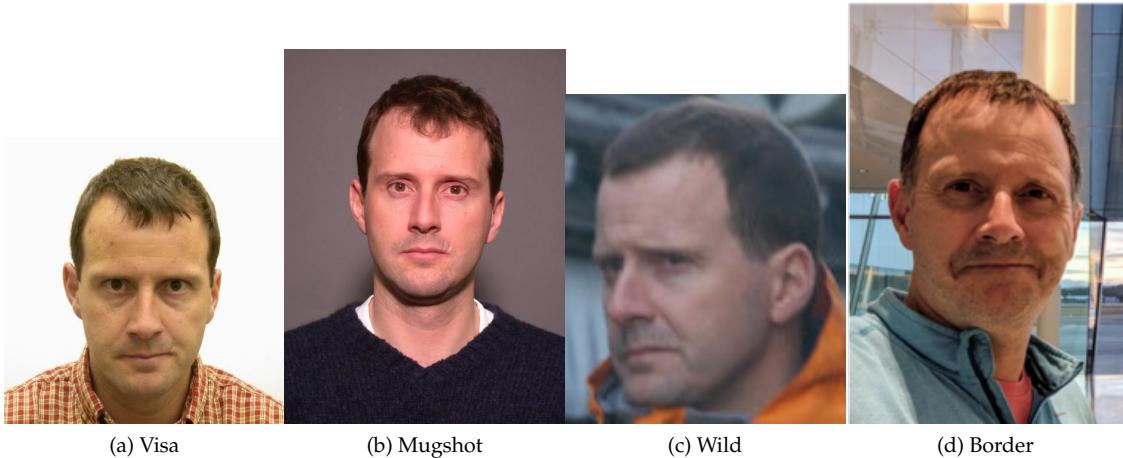


Figure 3: The figure gives simulated samples of image types used in this report.

3.2 Test design

Method: For visa images:

- ▷ The comparisons are of visa photos against visa photos.
 - ▷ The number of genuine comparisons is on the order of 10^4 .
 - ▷ The number of impostor comparisons is on the order of 10^{10} .
 - ▷ The comparisons are fully zero-effort, meaning impostors are paired without attention to sex, age or other covariates. However, later analysis is conducted on subsets.
 - ▷ The number of persons is on the order of 10^5 .
 - ▷ The number of images used to make 1 template is 1.
 - ▷ The number of templates used to make each comparison score is two corresponding to simple one-to-one verification.

Method: For mugshot images:

- ▷ The comparisons are of mugshot photos against mugshot photos.
 - ▷ The number of genuine comparisons is on the order of 10^6 .
 - ▷ The number of impostor comparisons is on the order of 10^8 .
 - ▷ The impostors are paired by sex, but not by age or other covariates.
 - ▷ The number of persons is on the order of 10^6 .
 - ▷ The number of images used to make 1 template is 1.
 - ▷ The number of templates used to make each comparison score is two corresponding to simple one-to-one verification.

Method: For visa-border comparisons:

- ▷ The comparisons are of visa-like frontals against border crossing webcam photos.
 - ▷ The number of genuine comparisons is on the order of 10^6 .
 - ▷ The number of impostor comparisons is on the order of 10^8 .

- ▷ The impostors are paired by sex, but not by age or other covariates.
- ▷ The number of persons is on the order of 10^6 .
- ▷ The number of images used to make 1 template is 1.
- ▷ The number of templates used to make each comparison score is two corresponding to simple one-to-one verification.

Method: For border-border comparisons:

- ▷ The comparisons are of border crossing webcam photos.
- ▷ The number of genuine comparisons is on the order of 10^6 .
- ▷ The number of impostor comparisons is on the order of 10^8 .
- ▷ The impostors are paired by sex, but not by age or other covariates.
- ▷ The number of persons is on the order of 10^6 .
- ▷ The number of images used to make 1 template is 1.
- ▷ The number of templates used to make each comparison score is two corresponding to simple one-to-one verification.

Method: For wild images:

- ▷ The comparisons are of wild photos against wild photos.
- ▷ The number of genuine comparisons is on the order of 10^6 .
- ▷ The number of impostor comparisons is on the order of 10^7 .
- ▷ The comparisons are fully zero-effort, meaning impostors are paired without attention to sex, age or other covariates.
- ▷ The number of persons is on the order of 10^4 .
- ▷ The number of images used to make 1 template is 1.
- ▷ The number of templates used to make each comparison score is two corresponding to simple one-to-one verification.

Method: For child exploitation images:

- ▷ The comparisons are of unconstrained child exploitation photos against others of the same type.
- ▷ The number of genuine comparisons is on the order of 10^4 .
- ▷ The number of impostor comparisons is on the order of 10^7 .
- ▷ The comparisons are fully zero-effort, meaning impostors are paired without attention to sex, age or other covariates.
- ▷ The number of persons is on the order of 10^3 .
- ▷ The number of images used to make 1 template is 1.
- ▷ The number of templates used to make each comparison score is two corresponding to simple one-to-one verification.
- ▷ We produce two performance statements. First, is a DET as used for visa and mugshot images. The second is a cumulative match characteristic (CMC) summarizing a simulated one-to-many search process. This is done as follows.
 - We regard M enrollment templates as items in a gallery.

- These M templates come from $M > N$ individuals, because multiple images of a subject are present in the gallery under separate identifiers.
- We regard the verification templates as search templates.
- For each search we compute the rank of the highest scoring mate.
- This process should properly be conducted with a 1:N algorithm, such as those tested in NIST IR 8009. We use the 1:1 algorithms in a simulated 1:N mode here to a) better reflect what a child exploitation analyst does, and b) to show algorithm efficacy is better than that revealed in the verification DETs.

3.3 Failure to enroll

Name	Algorithm	Failure to Enrol Rate ¹							
		APPLICATION		BORDER		CHILD-EXPLOIT		MUGSHOT	
		SEC. 2.2	SEC. 2.3	SEC. ??	SEC. 2.4	SEC. 2.1	SEC. 2.5		
1	20face-000	0.0000	200	0.0008	205	-	142	0.0000	122
2	20face-001	0.0000	258	0.0008	206	-	239	0.0000	120
3	3divi-006	0.0000	224	0.0007	180	-	385	0.0001	213
4	3divi-007	0.0000	231	0.0007	181	-	339	0.0001	212
5	acer-001	0.0000	188	0.0011	251	-	180	0.0001	190
6	acer-002	0.0000	325	0.0008	200	-	208	0.0003	280
7	acisw-003	0.0000	48	0.0000	11	-	127	0.0000	79
8	acisw-007	0.0000	71	0.0000	25	-	77	0.0000	59
9	adera-002	0.0000	307	0.0034	322	-	149	0.0003	288
10	adera-003	0.0000	308	0.0034	323	-	308	0.0003	287
11	advance-002	0.0000	223	0.0013	271	-	380	0.0000	173
12	advance-003	0.0000	294	0.0012	260	-	187	0.0001	231
13	afisbiometrics-000	0.0000	184	0.0008	193	-	205	0.0000	125
14	aifirst-001	0.0000	39	0.0000	8	0.0000	7	0.0000	76
15	aigen-001	0.0000	43	0.0000	9	-	133	0.0000	73
16	aigen-002	0.0000	143	0.0000	61	-	290	0.0000	17
17	ailabs-001	0.0000	175	0.0090	360	-	226	0.0007	337
18	aimall-002	0.0000	313	0.0043	336	-	278	0.0012	352
19	aimall-003	0.0000	288	0.0012	265	-	107	0.0004	302
20	aiunionface-000	0.0000	74	0.0000	18	-	63	0.0000	67
21	aize-001	0.0001	352	0.0040	331	-	87	0.0026	371
22	aize-002	0.0000	30	0.0014	274	-	166	0.0005	323
23	ajou-001	0.0000	174	0.0020	294	-	225	0.0001	218
24	alchera-002	0.0000	235	0.0008	211	-	335	0.0001	237
25	alchera-003	0.0001	363	0.0013	269	-	233	0.0002	266
26	alfabeto-001	0.0005	372	0.0650	389	-	258	0.0024	366
27	alice-000	0.0000	13	0.0006	157	-	199	0.0000	137
28	alleyes-000	0.0000	252	0.0010	234	-	276	0.0002	245
29	allgovision-000	0.0007	375	0.0062	353	-	372	0.0026	370
30	alphaface-001	0.0000	240	0.0012	257	-	320	0.0000	176
31	alphaface-002	0.0000	243	0.0012	256	-	302	0.0000	175
32	amplifiedgroup-001	0.0114	389	0.1023	392	-	250	0.0189	390
33	androvideo-000	0.0000	85	0.0000	21	-	51	0.0000	71
34	anke-004	0.0000	178	0.0011	248	0.0944	28	0.0001	222
35	anke-005	0.0000	180	0.0012	258	0.1228	30	0.0001	234
36	antheus-000	0.0000	102	0.0000	78	0.0000	20	0.0000	43
37	antheus-001	0.0000	171	0.0000	66	-	234	0.0000	12
38	anyvision-004	0.0000	299	0.0017	284	0.1660	33	0.0001	233
39	anyvision-005	0.0000	197	0.0013	266	-	154	0.0000	150
40	armatura-001	0.0000	316	0.0021	299	-	371	0.0005	318
41	asusaics-000	0.0000	165	0.0000	64	-	248	0.0000	6
42	asusaics-001	0.0000	154	0.0000	71	-	265	0.0000	2
43	authenmetric-003	0.0000	112	0.0000	81	-	358	0.0000	53
44	authenmetric-004	0.0000	111	0.0000	82	-	369	0.0000	49
45	aware-005	0.0000	276	0.0020	293	-	387	0.0001	244
46	aware-006	0.0000	239	0.0009	219	-	319	0.0000	153
47	awiros-001	0.0039	380	0.0369	384	-	80	0.0386	391
48	awiros-002	0.0000	329	0.0038	329	-	361	0.0007	336
49	ayftech-001	0.0002	365	0.0046	341	-	138	0.0043	381
50	ayonix-000	0.0053	383	0.0341	381	0.0000	19	0.0113	388
51	beethedata-000	0.0005	370	0.0042	335	-	108	0.0002	254
52	beyneai-000	0.0000	34	0.0000	44	-	158	0.0000	96
53	biocube-001	0.0006	373	0.0391	385	-	141	0.0015	357
54	boidtechswiss-001	0.0000	222	0.0007	175	-	381	0.0000	138
55	boidtechswiss-002	0.0000	254	0.0007	178	-	279	0.0000	144
56	bm-001	0.0000	144	0.0000	54	0.0000	14	0.0000	111
57	boetech-001	0.0087	387	0.0272	374	-	391	0.0032	377
58	boetech-002	0.0087	386	0.0272	373	-	188	0.0032	378

Table 27: FTE is the proportion of failed template generation attempts. Failures can occur because the software throws an exception, or because the software electively refuses to process the input image. This would typically occur if a face is not detected. FTE is measured as the number of function calls that give EITHER a non-zero error code OR that give a “small” template. This is defined as one whose size is less than 0.3 times the median template size for that algorithm. This second rule is needed because some algorithms incorrectly fail to return a non-zero error code when template generation fails.

A hyphen “-” indicates the dataset was not produced.¹ The effects of FTE are included in the accuracy results of this report by regarding any template comparison involving a failed template to produce a low similarity score. Thus higher FTE results in higher FNMR and lower FMR.

	Algorithm	Failure to Enrol Rate ¹											
		APPLICATION	BORDER	CHILD-EXPLOIT	MUGSHOT	VISA	WILD	SEC. 2.2	SEC. 2.3	SEC. ??	SEC. 2.4	SEC. 2.1	SEC. 2.5
59	bressee-001	0.0000	209	0.0010	240	-	118	0.0002	253	0.0003	158	0.0003	128
60	bressee-002	0.0000	301	0.0020	297	-	110	0.0008	338	0.0004	210	0.0031	291
61	camvi-002	0.0000	57	0.0000	4	0.0000	5	0.0000	83	0.0000	108	0.0000	73
62	camvi-004	0.0000	52	0.0000	109	0.0000	6	0.0000	82	0.0000	105	0.0000	70
63	canon-002	0.0000	123	0.0000	104	-	340	0.0000	25	0.0000	5	0.0000	29
64	canon-003	0.0000	230	0.0008	194	-	337	0.0000	172	0.0004	232	0.0003	159
65	ceiec-003	0.0000	81	0.0013	272	-	58	0.0001	197	0.0004	252	0.0004	172
66	ceiec-004	0.0000	109	0.0008	204	-	367	0.0000	147	0.0004	193	0.0004	201
67	chosun-001	0.0000	26	0.0000	47	-	178	0.0000	89	0.0000	53	0.0000	64
68	chosun-002	0.0000	92	0.0000	92	-	392	0.0000	39	0.0000	19	0.0000	14
69	chiface-003	0.0000	300	0.0018	287	-	152	0.0001	201	0.0006	330	0.0010	257
70	chiface-004	0.0000	96	0.0017	282	-	393	0.0000	162	0.0004	256	0.0020	283
71	clearviewai-000	0.0000	213	0.0003	133	-	94	0.0000	164	0.0003	143	0.0003	129
72	closeli-001	0.0000	32	0.0000	50	-	168	0.0000	91	0.0000	55	0.0001	115
73	cloudmatrix-000	0.0000	281	0.0012	261	-	277	0.0001	191	0.0004	182	0.0004	191
74	cloudmatrix-001	-	401	-	401	-	365	-	397	-	399	-	393
75	cloudwalk-hr-003	0.0000	225	0.0008	207	-	374	0.0001	200	0.0004	187	0.0113	324
76	cloudwalk-hr-004	0.0000	211	0.0011	254	-	99	0.0004	304	0.0003	169	0.0129	327
77	cloudwalk-mt-003	0.0000	241	0.0007	170	-	309	0.0002	261	0.0004	261	0.0004	175
78	cloudwalk-mt-004	0.0000	234	0.0009	212	-	344	0.0002	268	0.0004	274	0.0004	186
79	clova-000	0.0000	319	0.0022	300	-	253	0.0006	330	0.0005	294	0.0019	280
80	cogent-005	0.0000	133	0.0000	98	-	318	0.0000	29	0.0000	11	0.0000	24
81	cogent-006	0.0000	106	0.0000	74	-	377	0.0000	45	0.0000	22	0.0000	3
82	cognitec-003	0.0001	346	0.0194	369	-	251	0.0003	294	0.0005	302	0.0039	295
83	cognitec-004	0.0001	347	0.0037	328	-	143	0.0003	295	0.0005	305	0.0035	292
84	cor-001	0.0000	260	0.0006	161	-	235	0.0002	274	0.0004	222	0.0004	212
85	coretech-000	0.0000	50	0.0000	1	-	121	0.0000	80	0.0000	106	0.0000	71
86	corsight-001	0.0000	257	0.0006	166	-	254	0.0001	240	0.0004	209	0.0004	192
87	corsight-002	0.0000	236	0.0005	155	-	316	0.0001	223	0.0004	212	0.0003	158
88	csc-002	0.0015	377	0.0033	319	-	162	0.0006	332	0.0006	337	0.0968	376
89	csc-003	0.0015	378	0.0033	318	-	76	0.0006	331	0.0006	338	0.0968	377
90	ctbcbank-000	0.0001	349	0.0051	346	0.3285	40	0.0011	350	0.0019	371	0.0868	371
91	ctbcbank-001	0.0000	328	0.0036	327	-	389	0.0005	320	0.0010	345	0.0844	368
92	cubox-001	0.0000	35	0.0000	42	-	160	0.0000	95	0.0000	59	0.0000	62
93	cubox-002	0.0000	278	0.0006	164	-	366	0.0002	275	0.0005	319	0.0016	276
94	cudocommunication-001	0.0000	28	0.0000	48	-	175	0.0000	87	0.0000	51	0.0000	94
95	cuhkee-001	0.0000	172	0.0011	253	-	228	0.0000	124	0.0004	214	0.1278	384
96	cybercore-000	0.0000	227	0.0073	357	-	355	0.0001	209	0.0005	300	0.0383	357
97	cybercore-001	0.0000	311	0.0001	120	-	332	0.0002	248	0.0002	121	0.0018	279
98	cyberextruder-001	0.0029	379	0.0293	375	0.5338	46	0.0024	364	0.0029	384	0.0597	364
99	cyberextruder-002	0.0013	376	0.0840	391	0.2672	39	0.0027	372	0.0028	381	0.0335	354
100	cyberlink-007	0.0000	131	0.0003	127	-	324	0.0000	116	0.0003	156	0.0001	101
101	cyberlink-008	0.0000	161	0.0004	145	-	246	0.0000	115	0.0003	157	0.0002	125
102	dahua-006	0.0000	93	0.0000	107	-	396	0.0000	168	0.0003	166	0.0000	17
103	dahua-007	0.0000	18	0.0000	106	-	194	0.0000	171	0.0003	168	0.0000	50
104	daon-000	0.0000	333	0.0028	310	-	301	0.0014	356	0.0015	366	0.0030	290
105	decatur-000	0.0000	277	0.0020	292	-	383	0.0004	310	0.0005	292	0.0236	342
106	decatur-001	0.0000	253	0.0009	226	-	280	0.0001	202	0.0004	205	0.0004	204
107	deepglint-003	0.0000	247	0.0004	144	-	291	0.0002	267	0.0004	198	0.0003	144
108	deepglint-004	0.0000	242	0.0005	149	-	314	0.0002	271	0.0004	192	0.0003	147
109	deepsea-001	0.0000	103	0.0000	77	0.0000	18	0.0000	48	0.0000	24	0.0000	1
110	deepsense-000	0.0000	37	0.0006	167	-	150	0.0000	132	0.0004	174	0.0003	151
111	dermalog-008	0.0000	324	0.0031	315	-	289	0.0006	325	0.0003	132	0.0002	117
112	dermalog-009	0.0000	323	0.0031	316	-	287	0.0006	326	0.0003	133	0.0002	116
113	didiglobalface-001	0.0000	208	0.0012	255	0.2175	35	0.0000	177	0.0004	260	0.0004	178
114	digitdata-000	0.0000	207	0.0023	301	-	114	0.0004	313	0.0006	333	0.0006	232
115	digitalbarriers-002	0.0001	355	0.0045	338	-	274	0.0028	374	0.0027	378	0.0071	311
116	dps-000	0.0000	156	0.0000	69	-	268	0.0000	1	0.0000	32	0.0000	47

Table 28: FTE is the proportion of failed template generation attempts. Failures can occur because the software throws an exception, or because the software electively refuses to process the input image. This would typically occur if a face is not detected. FTE is measured as the number of function calls that give EITHER a non-zero error code OR that give a “small” template. This is defined as one whose size is less than 0.3 times the median template size for that algorithm. This second rule is needed because some algorithms incorrectly fail to return a non-zero error code when template generation fails.

A hyphen “-” indicates the dataset was not produced.¹ The effects of FTE are included in the accuracy results of this report by regarding any template comparison involving a failed template to produce a low similarity score. Thus higher FTE results in higher FNMR and lower FMR.

	Algorithm	Failure to Enrol Rate ¹											
		APPLICATION	BORDER	CHILD-EXPLOIT	MUGSHOT	VISA	WILD	SEC. 2.2	SEC. 2.3	SEC. ??	SEC. 2.4	SEC. 2.1	SEC. 2.5
117	dsk-000	0.0000	167	0.0000	62	0.0000	12	0.0000	10	0.0000	37	0.0000	40
118	einetworks-000	0.0000	327	0.0017	283	-	224	0.0002	264	0.0005	314	0.0008	252
119	ekin-002	0.0000	91	0.0000	111	-	400	0.0000	117	0.0000	112	0.0019	281
120	enface-000	0.0000	4	0.0012	264	-	217	0.0000	159	0.0004	218	0.0004	194
121	enface-001	0.0000	51	0.0012	263	-	120	0.0000	140	0.0004	215	0.0004	180
122	eocortex-000	0.0095	388	0.0062	388	-	273	0.0094	387	0.0059	388	0.1405	388
123	ercacat-001	0.0000	29	0.0005	150	-	169	0.0000	158	0.0003	159	0.0002	120
124	euronovate-001	0.0255	393	0.0102	362	-	207	0.0021	361	0.0004	286	0.2451	390
125	expasoft-001	0.0000	27	0.0000	46	-	177	0.0000	88	0.0000	52	0.0000	65
126	expasoft-002	0.0000	3	0.0000	37	-	218	0.0000	100	0.0000	63	0.0000	55
127	f8-001	0.0003	366	0.0059	352	0.2026	34	0.0035	379	0.0030	385	0.0087	318
128	f8-002	-	394	-	396	-	192	-	404	-	402	-	400
129	faceonlive-001	0.0000	338	0.0029	313	-	294	0.0013	354	0.0011	352	0.0160	333
130	facesoft-000	0.0000	147	0.0000	53	0.0000	15	0.0000	18	0.0000	47	0.0000	31
131	facetag-000	0.0000	12	0.0000	34	-	200	0.0000	105	0.0000	74	0.0000	51
132	facetag-002	0.0000	116	0.0000	103	-	351	0.0000	22	0.0000	3	0.0000	28
133	facex-001	0.0001	361	0.0360	382	-	98	0.0047	384	0.0027	380	0.1109	380
134	facex-002	0.0001	362	0.0360	383	-	384	0.0047	383	0.0027	379	0.1109	379
135	farfaces-001	0.0000	326	0.0007	177	-	259	0.0003	290	0.0003	150	0.0006	240
136	fiberhome-nanjing-003	0.0000	83	0.0004	141	-	59	0.0000	68	0.0003	137	0.0001	104
137	fiberhome-nanjing-004	0.0000	164	0.0004	142	-	245	0.0000	7	0.0003	136	0.0001	102
138	fincore-000	0.0000	251	0.0008	209	-	282	0.0001	184	0.0004	251	0.0006	233
139	fujitsulab-002	0.0000	54	0.0009	217	-	112	0.0001	230	0.0003	138	0.0003	135
140	fujitsulab-003	0.0000	122	0.0008	198	-	349	0.0001	221	0.0001	118	0.0003	130
141	geo-002	0.0000	248	0.0015	275	-	293	0.0001	181	0.0004	271	0.0017	278
142	geo-004	0.0000	217	0.0005	154	-	57	0.0001	214	0.0004	202	0.0009	256
143	glory-003	0.0000	285	0.0027	307	-	171	0.0004	303	0.0005	297	0.0244	345
144	glory-004	0.0000	269	0.0020	296	-	119	0.0001	227	0.0004	270	0.0167	334
145	gorilla-007	0.0000	185	0.0009	229	-	195	0.0001	206	0.0004	247	0.0004	184
146	gorilla-008	0.0000	229	0.0009	230	-	338	0.0001	203	0.0004	248	0.0004	183
147	graymatics-001	0.0000	40	0.0010	231	-	136	0.0001	241	0.0004	207	0.0006	237
148	griaule-000	0.0000	334	0.0026	305	-	326	0.0004	312	0.0010	346	0.0023	284
149	hertasecurity-000	0.0133	390	0.0077	359	-	222	0.0025	369	0.0243	394	0.0171	336
150	hertasecurity-001	0.0000	46	0.0000	112	-	132	0.0000	129	0.0001	114	0.0002	127
151	hik-001	0.0000	53	0.0000	114	-	106	0.0000	81	0.0000	104	0.0000	69
152	hisign-001	0.0000	1	0.0000	39	-	223	0.0000	98	0.0000	65	0.0000	57
153	hyperverge-001	0.0000	343	0.0072	355	-	292	0.0015	359	0.0014	365	0.0042	296
154	hyperverge-002	0.0000	24	0.0008	197	-	181	0.0002	276	0.0004	206	0.0004	205
155	hzailu-001	0.0000	317	0.0016	278	-	260	0.0003	297	0.0005	317	0.0075	313
156	icm-002	0.0000	128	0.0001	117	-	327	0.0000	27	0.0000	110	0.0000	95
157	icm-003	0.0000	136	0.0001	118	-	313	0.0000	31	0.0000	111	0.0000	96
158	icthtc-000	0.0001	360	0.0047	344	-	229	0.0028	375	0.0029	382	0.0086	317
159	id3-006	0.0000	293	0.0009	228	-	243	0.0004	306	0.0005	313	0.0008	250
160	id3-008	0.0000	38	0.0006	165	-	148	0.0001	239	0.0004	177	0.0003	132
161	idemia-007	0.0000	145	0.0004	147	-	285	0.0000	127	0.0003	160	0.0003	141
162	idemia-008	0.0000	47	0.0004	146	-	126	0.0000	130	0.0003	162	0.0003	142
163	iit-002	0.0000	332	0.0021	298	-	172	0.0009	346	0.0005	324	0.0443	359
164	iit-003	0.0000	206	0.0008	208	-	115	0.0000	149	0.0004	184	0.0069	310
165	imagus-002	0.0000	287	0.0018	285	-	123	0.0000	157	0.0004	242	0.0296	349
166	imagus-004	0.0000	31	0.0000	51	-	165	0.0000	92	0.0000	56	0.0000	67
167	imagus-005	-	400	-	403	-	403	-	394	-	398	-	396
168	imperial-000	0.0000	68	0.0000	26	-	85	0.0000	57	0.0000	81	0.0000	91
169	imperial-002	0.0000	44	0.0000	5	0.0000	8	0.0000	72	0.0000	96	0.0000	76
170	incode-009	0.0000	280	0.0009	221	-	331	0.0002	256	0.0004	196	0.0007	246
171	incode-010	0.0000	264	0.0009	220	-	189	0.0002	259	0.0004	200	0.0007	247
172	inneflabs-000	0.0000	228	0.0024	302	-	352	0.0003	291	0.0005	310	0.0004	190
173	innovativetechnologyltd-001	0.0001	359	0.0050	345	-	105	0.0024	367	0.0025	377	0.0055	303
174	innovativetechnologyltd-002	0.0000	290	0.0046	340	-	330	0.0057	386	0.0005	311	0.0247	347

Table 29: FTE is the proportion of failed template generation attempts. Failures can occur because the software throws an exception, or because the software electively refuses to process the input image. This would typically occur if a face is not detected. FTE is measured as the number of function calls that give EITHER a non-zero error code OR that give a "small" template. This is defined as one whose size is less than 0.3 times the median template size for that algorithm. This second rule is needed because some algorithms incorrectly fail to return a non-zero error code when template generation fails.

A hyphen “-” indicates the dataset was not produced. ¹The effects of FTE are included in the accuracy results of this report by regarding any template comparison involving a failed template to produce a low similarity score. Thus higher FTE results in higher FNMR and lower FMR.

Algorithm	Failure to Enrol Rate ¹							
	Name	APPLICATION	BORDER	CHILD-EXPLOIT	MUGSHOT	VISA	WILD	
Name	SEC. 2.2	SEC. 2.3	SEC. ??	SEC. 2.4	SEC. 2.1	SEC. 2.5		
175 innovatrics-007	0.0000	232	0.0007	188	-	341	0.0001	182
176 innovatrics-008	0.0000	194	0.0009	223	-	161	0.0000	155
177 insightface-001	0.0000	20	0.0000	35	-	191	0.0000	109
178 insightface-002	0.0000	117	0.0000	102	-	353	0.0000	21
179 intellicloudai-001	0.0000	70	0.0000	27	-	82	0.0000	56
180 intellicloudai-002	0.0000	78	0.0008	201	-	66	0.0000	148
181 intellifusion-001	0.0000	191	0.0005	151	0.0949	29	0.0001	199
182 intellifusion-002	0.0000	69	0.0000	110	-	86	0.0000	112
183 intellivision-001	0.0042	381	0.0296	376	0.5495	47	0.0048	385
184 intellivision-002	0.0000	344	0.0046	339	-	197	0.0012	351
185 intellivision-003	-	398	-	393	-	68	-	400
186 intelresearch-004	0.0000	250	0.0006	160	-	288	0.0000	133
187 intelresearch-005	0.0000	196	0.0006	159	-	151	0.0000	136
188 intsysmsu-001	0.0000	150	0.0010	238	-	271	0.0001	216
189 intsysmsu-002	0.0000	21	0.0010	237	-	184	0.0001	219
190 ionetworks-000	0.0000	129	0.0016	280	-	328	0.0004	300
191 iqface-000	0.0000	153	0.0000	55	0.0000	13	0.0000	19
192 iqface-003	0.0000	330	0.0076	358	-	325	0.0006	327
193 irex-000	0.0000	298	0.0009	227	-	373	0.0000	163
194 isap-001	0.0000	95	0.0000	91	-	394	0.0000	37
195 isap-002	0.0000	49	0.0000	10	-	128	0.0000	78
196 isityou-000	0.0068	385	0.0316	379	0.4714	43	0.0023	363
197 isystems-001	0.0000	337	0.0035	325	0.1421	32	0.0010	347
198 isystems-002	0.0000	336	0.0035	324	0.1421	31	0.0010	348
199 itmo-007	0.0000	84	0.0009	216	-	61	0.0003	298
200 itmo-008	0.0000	9	0.0135	366	-	210	0.0024	368
201 ivacognitive-001	0.0000	275	0.0011	250	-	54	0.0001	192
202 iws-000	0.0005	371	0.0650	390	-	346	0.0024	365
203 kakao-005	0.0000	135	0.0000	108	-	311	0.0000	33
204 kakao-007	0.0000	130	0.0007	169	-	323	0.0001	210
205 kakaopay-001	0.0000	273	0.0013	270	-	75	0.0001	196
206 kasikornlabs-000	-	404	-	399	-	286	-	392
207 kedacom-000	0.0000	75	0.0000	17	0.0000	2	0.0000	65
208 kiwitech-000	0.0000	218	0.0009	213	-	49	0.0004	308
209 kneron-003	0.0239	391	0.0306	377	0.4883	45	0.0044	382
210 kneron-005	0.0000	339	0.0226	370	-	256	0.0006	324
211 knowutech-000	0.0000	259	0.0008	195	-	237	0.0000	151
212 kookmin-002	0.0000	134	0.0000	97	-	310	0.0000	34
213 kuke3d-001	0.0000	152	0.0000	56	-	269	0.0000	20
214 lebentech-000	-	396	-	398	-	153	-	402
215 lemalabs-001	0.0000	89	0.0005	153	-	402	0.0002	262
216 line-000	0.0000	41	0.0000	6	-	135	0.0000	75
217 line-001	0.0000	108	0.0000	83	-	368	0.0000	50
218 lookman-002	0.0000	42	0.0000	7	-	134	0.0000	74
219 lookman-004	0.0000	168	0.0000	63	0.0000	11	0.0000	9
220 luxand-000	0.0000	139	0.0000	60	-	296	0.0000	16
221 mantra-000	0.0001	348	0.0041	334	-	89	0.0003	289
222 maxvision-000	0.0000	73	0.0000	105	-	62	0.0000	66
223 megvii-003	0.0000	183	0.0010	245	-	215	0.0002	272
224 megvii-004	0.0000	219	0.0010	236	-	56	0.0002	257
225 meituan-000	0.0000	158	0.0001	119	-	257	0.0000	126
226 meiya-001	0.0000	335	0.0028	311	-	307	0.0004	311
227 mendaxiatech-000	0.0000	186	0.0010	232	-	190	0.0002	273
228 microfocus-001	0.0001	358	0.0053	349	0.0791	27	0.0008	340
229 microfocus-002	0.0001	357	0.0053	348	0.0791	26	0.0008	341
230 minivision-000	0.0000	140	0.0000	58	-	300	0.0000	14
231 mobai-000	0.0000	302	0.0114	364	-	73	0.0003	293
232 mobai-001	0.0000	265	0.0040	330	-	186	0.0001	224

Table 30: FTE is the proportion of failed template generation attempts. Failures can occur because the software throws an exception, or because the software electively refuses to process the input image. This would typically occur if a face is not detected. FTE is measured as the number of function calls that give EITHER a non-zero error code OR that give a “small” template. This is defined as one whose size is less than 0.3 times the median template size for that algorithm. This second rule is needed because some algorithms incorrectly fail to return a non-zero error code when template generation fails.

A hyphen “-” indicates the dataset was not produced.¹ The effects of FTE are included in the accuracy results of this report by regarding any template comparison involving a failed template to produce a low similarity score. Thus higher FTE results in higher FNMR and lower FMR.

	Algorithm Name	Failure to Enrol Rate ¹											
		APPLICATION	BORDER	CHILD-EXPLOIT	MUGSHOT	VISA	WILD	SEC. 2.2	SEC. 2.3	SEC. ??	SEC. 2.4	SEC. 2.1	SEC. 2.5
233	mobbl-001	0.0000	331	0.0052	347	-	72	0.0002	250	0.0005	316	0.0181	338
234	mobbl-002	0.0000	340	0.0029	314	-	261	0.0002	265	0.0009	344	0.0026	288
235	mobiptimech-000	0.0000	163	0.0000	65	-	244	0.0000	8	0.0000	39	0.0000	41
236	moreedian-000	0.0000	221	0.0009	214	-	397	0.0004	307	0.0005	295	0.0004	207
237	multimodality-000	0.0000	127	0.0000	93	-	322	0.0000	28	0.0000	6	0.0000	18
238	mvision-001	0.0000	72	0.0000	19	-	74	0.0000	60	0.0000	91	0.0000	85
239	nazhiai-000	0.0000	76	0.0000	16	-	65	0.0000	63	0.0000	89	0.0000	80
240	neosystems-002	0.0000	17	0.0000	30	-	193	0.0000	108	0.0000	71	0.0000	49
241	neosystems-003	0.0000	15	0.0000	32	-	203	0.0000	103	0.0000	72	0.0000	53
242	netbridgetech-001	0.0000	23	0.0000	49	-	183	0.0000	86	0.0000	54	0.0000	66
243	netbridgetech-002	0.0000	105	0.0000	73	-	378	0.0000	46	0.0000	23	0.0000	2
244	neurotechnology-012	0.0000	320	0.0010	247	-	156	0.0001	232	0.0004	228	0.0005	222
245	neurotechnology-013	0.0000	118	0.0008	210	-	356	0.0000	121	0.0001	115	0.0004	188
246	nhn-001	0.0000	199	0.0019	289	-	147	0.0001	205	0.0004	281	0.0020	282
247	nhn-002	0.0000	10	0.0004	148	-	209	0.0000	146	0.0003	142	0.0003	133
248	nhn-003	-	403	-	404	-	354	-	393	-	397	-	397
249	nodeflux-002	0.0000	181	0.0261	372	-	212	0.0008	339	0.0005	312	0.0008	253
250	notiontag-001	0.0000	6	0.0000	41	-	211	0.0027	373	0.0000	69	0.0132	329
251	notiontag-002	0.0000	141	0.0000	57	-	299	0.0000	15	0.0000	44	0.0000	36
252	nsensecorp-002	0.0000	216	0.0009	215	-	71	0.0003	281	0.0011	351	0.0178	337
253	nsensecorp-003	0.0000	148	0.0000	116	-	281	0.0000	134	0.0007	342	0.0150	331
254	ntechlab-011	0.0000	146	0.0003	129	-	284	0.0000	165	0.0004	172	0.0003	153
255	ntechlab-012	0.0000	56	0.0003	128	-	100	0.0000	169	0.0004	175	0.0003	155
256	null-020	-	397	-	395	-	84	-	398	-	403	-	404
257	omnigarde-001	0.0000	198	0.0008	192	-	155	0.0000	142	0.0004	227	0.0003	164
258	omnigarde-002	0.0000	212	0.0008	191	-	103	0.0000	141	0.0004	231	0.0003	166
259	omsecurity-000	0.0000	55	0.0000	3	-	104	0.0000	84	0.0000	109	0.1160	381
260	openface-001	0.0000	309	0.0104	363	-	379	0.0004	305	0.0006	336	0.0856	370
261	oz-003	0.0000	63	0.0002	122	-	91	0.0000	118	0.0003	130	0.0002	119
262	oz-004	0.0000	318	0.0003	131	-	262	0.0000	119	0.0002	120	0.0006	229
263	papsav1923-001	0.0000	187	0.0007	179	-	185	0.0001	215	0.0002	127	0.0005	216
264	papsav1923-002	0.0000	202	0.0018	288	-	130	0.0000	156	0.0004	243	0.0004	189
265	paravision-008	0.0000	170	0.0010	235	-	236	0.0001	207	0.0004	176	0.0003	160
266	paravision-010	0.0000	58	0.0010	233	-	101	0.0001	208	0.0004	179	0.0003	165
267	pensees-001	0.0000	192	0.0000	52	-	170	0.0000	90	0.0000	57	0.0000	68
268	pixelall-006	0.0000	155	0.0000	70	-	266	0.0000	3	0.0000	34	0.0000	46
269	pixelall-007	0.0000	115	0.0000	79	-	362	0.0000	51	0.0000	26	0.0000	7
270	psl-008	0.0000	204	0.0003	130	-	129	0.0000	123	0.0003	155	0.0002	126
271	psl-009	0.0000	245	0.0004	140	-	297	0.0000	110	0.0004	171	0.0003	146
272	ptakuratsatu-000	0.0000	176	0.0007	187	-	227	0.0001	183	0.0003	152	0.0003	145
273	pxl-001	0.0000	345	0.0044	337	-	124	0.0005	317	0.0022	375	0.0323	351
274	pyramid-000	0.0001	354	0.0041	333	-	202	0.0005	316	0.0007	341	0.0015	275
275	qnap-000	0.0000	138	0.0007	189	-	303	0.0002	255	0.0002	119	0.0003	131
276	qnap-001	0.0000	237	0.0000	113	-	315	0.0000	161	0.0001	116	0.0001	112
277	quantasoft-003	0.0000	304	0.0015	276	-	336	0.0005	315	0.0006	334	0.0088	319
278	rankone-011	0.0000	77	0.0000	15	-	67	0.0000	64	0.0000	90	0.0000	79
279	rankone-012	0.0000	11	0.0000	33	-	201	0.0000	106	0.0000	75	0.0000	52
280	realnetworks-005	0.0000	201	0.0002	125	-	140	0.0000	113	0.0002	129	0.0003	140
281	realnetworks-006	0.0000	179	0.0002	126	-	219	0.0000	114	0.0002	128	0.0003	139
282	regula-000	0.0000	33	0.0000	45	-	164	0.0000	93	0.0000	61	0.0000	63
283	regula-001	0.0000	86	0.0000	20	-	53	0.0000	70	0.0000	93	0.0000	86
284	remarkai-001	0.0000	90	0.0000	84	-	401	0.0000	36	0.0000	12	0.0000	99
285	remarkai-003	0.0000	244	0.0007	176	-	306	0.0000	160	0.0004	188	0.0004	193
286	rendip-000	0.0000	286	0.0016	279	-	157	0.0002	258	0.0004	285	0.0013	273
287	revealmedia-005	0.0000	296	0.0007	183	-	50	0.0009	345	0.0004	289	0.0076	314
288	revealmedia-006	0.0000	110	0.0009	224	-	370	0.0001	220	0.0004	250	0.0004	211
289	rokid-000	0.0000	114	0.0072	356	-	364	0.0001	211	0.0005	307	0.0354	355
290	rokid-001	0.0000	8	0.0013	268	-	206	0.0000	102	0.0000	67	0.0007	244

Table 31: FTE is the proportion of failed template generation attempts. Failures can occur because the software throws an exception, or because the software electively refuses to process the input image. This would typically occur if a face is not detected. FTE is measured as the number of function calls that give EITHER a non-zero error code OR that give a “small” template. This is defined as one whose size is less than 0.3 times the median template size for that algorithm. This second rule is needed because some algorithms incorrectly fail to return a non-zero error code when template generation fails.

A hyphen “-” indicates the dataset was not produced.¹ The effects of FTE are included in the accuracy results of this report by regarding any template comparison involving a failed template to produce a low similarity score. Thus higher FTE results in higher FNMR and lower FMR.

	Algorithm	Failure to Enrol Rate ¹							
		Name	APPLICATION	BORDER	CHILD-EXPLOIT	MUGSHOT	VISA	WILD	
	Name	SEC. 2.2	SEC. 2.3	SEC. ??	SEC. 2.4	SEC. 2.1	SEC. 2.5		
291	s1-003	0.0000	59	0.0002	124	-	102	0.0007	334
292	s1-004	0.0000	62	0.0000	115	-	97	0.0000	178
293	saffe-001	0.0000	98	0.0000	87	0.0000	21	0.0000	41
294	saffe-002	0.0000	60	0.0000	2	-	96	0.0000	85
295	samsungsds-000	0.0000	291	0.0055	351	-	329	0.0038	380
296	samtech-001	0.0001	353	0.0032	317	-	137	0.0004	309
297	scanovate-002	0.0000	262	0.0018	286	-	213	0.0000	179
298	scanovate-003	0.0000	266	0.0233	371	-	145	0.0006	328
299	securifai-003	0.0000	19	0.0000	29	-	198	0.0000	107
300	securifai-004	0.0000	94	0.0000	90	-	395	0.0000	38
301	sensetime-005	0.0000	125	0.0004	139	-	343	0.0000	145
302	sensetime-006	0.0000	166	0.0004	138	-	242	0.0000	143
303	sertis-000	0.0000	61	0.0007	182	-	95	0.0000	180
304	sertis-002	0.0000	101	0.0007	173	-	382	0.0000	174
305	seventhsense-000	0.0000	189	0.0006	168	-	182	0.0001	186
306	shaman-000	0.0000	2	0.0000	38	0.0000	10	0.0000	97
307	shaman-001	0.0000	120	0.0000	101	0.0000	17	0.0000	23
308	shu-002	0.0000	268	0.0010	241	-	117	0.0005	314
309	shu-003	0.0000	16	0.0007	171	-	196	0.0001	189
310	siat-002	0.0000	249	0.0012	262	0.0616	25	0.0000	154
311	siat-005	0.0000	132	0.0000	99	-	317	0.0000	30
312	sjtu-003	0.0000	88	0.0005	156	-	399	0.0000	167
313	sjtu-004	0.0000	97	0.0000	89	-	386	0.0000	42
314	sktelecom-000	0.0000	173	0.0008	203	-	230	0.0000	170
315	smartengines-000	0.0066	384	0.0150	367	-	334	0.0022	362
316	smilart-002	0.0000	341	0.0036	326	0.2422	38	-	395
317	smilart-003	0.0003	367	0.0100	361	-	304	0.0014	355
318	sodec-000	0.0000	113	0.0000	80	-	360	0.0000	52
319	sqisoft-001	0.0000	66	0.0003	135	-	88	0.0000	128
320	sqisoft-002	0.0000	159	0.0003	134	-	255	0.0000	131
321	stachu-000	0.0000	87	0.0000	85	-	404	0.0000	35
322	starhybrid-001	0.0001	356	0.0033	321	0.2340	37	0.0009	344
323	sukshi-000	0.0000	5	0.0000	36	-	221	0.0000	99
324	suprema-001	0.0000	292	0.0027	306	-	272	0.0003	283
325	suprema-002	0.0000	274	0.0010	243	-	60	0.0002	251
326	supremaid-001	0.0000	233	0.0020	295	-	345	0.0001	217
327	synesis-006	0.0000	151	0.0003	136	-	270	0.0000	166
328	synesis-007	0.0000	238	0.0013	267	-	321	0.0002	269
329	synology-000	0.0000	99	0.0000	86	-	390	0.0000	40
330	synology-002	0.0000	126	0.0000	94	-	333	0.0000	26
331	sztu-000	0.0000	79	0.0000	13	-	69	0.0000	62
332	sztu-001	0.0000	36	0.0000	43	-	159	0.0000	94
333	t4isb-000	0.0000	137	0.0000	95	-	312	0.0000	32
334	tech5-004	0.0000	256	0.0008	196	-	264	0.0003	284
335	tech5-005	0.0000	203	0.0007	190	-	125	0.0000	139
336	techsign-000	0.0007	374	0.0334	380	-	347	0.0020	360
337	tevian-007	0.0000	177	0.0015	277	-	232	0.0002	263
338	tevian-008	0.0000	190	0.0006	158	-	174	0.0000	135
339	tiger-005	0.0000	210	0.0009	225	-	113	0.0001	204
340	tiger-006	0.0000	270	0.0011	252	-	111	0.0001	238
341	tinkoff-001	0.0000	279	0.0008	202	-	359	0.0001	229
342	tongyi-005	0.0000	80	0.0000	14	0.0000	3	0.0000	61
343	toppanidgate-000	0.0000	195	0.0008	199	-	163	0.0004	301
344	toshiba-004	0.0000	64	0.0000	23	-	93	0.0000	55
345	toshiba-005	0.0000	255	0.0004	143	-	267	0.0001	235
346	trueface-002	0.0000	271	0.0046	342	-	109	0.0003	279
347	trueface-003	0.0000	267	0.0046	343	-	144	0.0003	278
348	tuputech-000	0.0003	368	0.0116	365	-	81	-	399

Table 32: FTE is the proportion of failed template generation attempts. Failures can occur because the software throws an exception, or because the software electively refuses to process the input image. This would typically occur if a face is not detected. FTE is measured as the number of function calls that give EITHER a non-zero error code OR that give a “small” template. This is defined as one whose size is less than 0.3 times the median template size for that algorithm. This second rule is needed because some algorithms incorrectly fail to return a non-zero error code when template generation fails.

A hyphen “-” indicates the dataset was not produced.¹ The effects of FTE are included in the accuracy results of this report by regarding any template comparison involving a failed template to produce a low similarity score. Thus higher FTE results in higher FNMR and lower FMR.

Algorithm	Name	Failure to Enrol Rate ¹							
		APPLICATION	BORDER	CHILD-EXPLOIT	MUGSHOT	VISA	WILD		
		SEC. 2.2	SEC. 2.3	SEC. ??	SEC. 2.4	SEC. 2.1	SEC. 2.5		
349	turingtechvip-001	0.0001	350	0.0007	184	-	139	0.0007	333
350	twface-000	0.0000	119	0.0000	100	-	348	0.0000	24
351	twface-001	0.0000	7	0.0000	40	-	216	0.0000	101
352	ulsee-001	0.0000	107	0.0000	76	-	375	0.0000	44
353	ultinous-000	-	402	-	402	0.0007	23	-	396
354	ultinous-001	-	399	-	394	0.0007	22	-	401
355	uluface-002	0.0000	67	0.0000	28	0.0000	4	0.0000	58
356	uluface-003	0.0000	25	0.0001	121	-	176	0.0002	247
357	unissey-001	0.0000	157	0.0000	68	-	263	0.0000	4
358	upc-001	0.0000	315	0.0003	132	0.0450	24	0.0003	282
359	vcog-002	-	395	-	397	0.2209	36	-	403
360	vd-002	0.0000	160	0.0000	72	-	252	0.0000	5
361	vd-003	0.0001	351	0.0041	332	-	231	0.0030	376
362	veridas-006	0.0000	312	0.0026	303	-	305	0.0001	226
363	veridas-007	0.0000	314	0.0026	304	-	249	0.0001	225
364	verigram-000	0.0000	289	0.0068	354	-	83	0.0003	299
365	verihubs-inteligensia-000	0.0000	205	0.0029	312	-	116	0.0001	193
366	via-000	0.0000	14	0.0000	31	0.0000	9	0.0000	104
367	via-001	0.0000	65	0.0000	24	-	90	0.0000	54
368	videmo-000	0.0000	272	0.0019	290	-	92	0.0003	292
369	videmo-001	0.0000	303	0.0170	368	-	52	0.0010	349
370	videonetics-001	0.0004	369	0.0309	378	0.4799	44	0.0015	358
371	videonetics-002	0.0000	283	0.0459	387	0.4598	42	0.0006	329
372	viettelhightech-000	0.0000	321	0.0019	291	-	146	0.0007	335
373	vigilantsolutions-010	0.0000	305	0.0028	308	-	283	0.0001	195
374	vigilantsolutions-011	0.0000	306	0.0028	309	-	238	0.0001	194
375	vinai-000	0.0000	142	0.0000	59	-	298	0.0000	13
376	vinbigdata-001	0.0000	169	0.0000	67	-	240	0.0000	11
377	vion-000	0.0050	382	0.0392	386	0.6388	48	0.0130	389
378	visage-000	0.0000	322	0.0054	350	-	64	0.0009	343
379	visionbox-001	0.0000	342	0.0033	320	-	79	0.0005	322
380	visionbox-002	0.0000	121	0.0017	281	-	350	0.0000	152
381	visionlabs-010	0.0000	295	0.0009	218	-	122	0.0001	236
382	visionlabs-011	0.0000	124	0.0006	163	-	342	0.0001	198
383	visteam-002	0.0000	297	0.0014	273	-	55	0.0002	252
384	visteam-003	0.0000	193	0.0010	242	-	167	0.0001	188
385	vnpt-002	0.0000	220	0.0002	123	-	398	0.0003	296
386	vnpt-003	0.0000	162	0.0004	137	-	247	0.0002	246
387	vocord-009	0.0000	214	0.0006	162	-	78	0.0001	242
388	vocord-010	0.0000	263	0.0005	152	-	204	0.0002	260
389	vts-000	0.0000	284	0.0011	249	-	173	0.0001	243
390	winsense-001	0.0000	82	0.0000	22	0.0000	1	0.0000	69
391	winsense-002	0.0000	45	0.0000	12	-	131	0.0000	77
392	wuhantianyu-001	0.0000	149	0.0007	174	-	275	0.0001	185
393	x-laboratory-000	0.0247	392	0.0000	96	0.0000	16	0.0005	321
394	x-laboratory-001	0.0000	215	0.0012	259	-	70	0.0001	228
395	xforwardai-001	0.0000	226	0.0007	186	-	363	0.0003	285
396	xforwardai-002	0.0000	182	0.0007	185	-	214	0.0003	286
397	xm-000	0.0000	22	0.0007	172	-	179	0.0001	187
398	yisheng-004	0.0002	364	-	400	0.4279	41	0.0013	353
399	yitu-003	0.0000	100	0.0000	88	-	388	0.0009	342
400	yoonik-002	0.0000	282	0.0010	239	-	241	0.0003	277
401	yoonik-003	0.0000	261	0.0009	222	-	220	0.0002	249
402	ytu-000	0.0000	246	0.0010	246	-	295	0.0002	270
403	yuan-003	0.0000	310	0.0010	244	-	357	0.0005	319
404	yuan-004	0.0000	104	0.0000	75	-	376	0.0000	47

Table 33: FTE is the proportion of failed template generation attempts. Failures can occur because the software throws an exception, or because the software electively refuses to process the input image. This would typically occur if a face is not detected. FTE is measured as the number of function calls that give EITHER a non-zero error code OR that give a “small” template. This is defined as one whose size is less than 0.3 times the median template size for that algorithm. This second rule is needed because some algorithms incorrectly fail to return a non-zero error code when template generation fails.

A hyphen “-” indicates the dataset was not produced. ¹The effects of FTE are included in the accuracy results of this report by regarding any template comparison involving a failed template to produce a low similarity score. Thus higher FTE results in higher FNMR and lower FMR.

3.4 Recognition accuracy

Core algorithm accuracy is stated via:

▷ **Cooperative subjects**

- The summary table of Figure 26;
- The visa image DETs of Figure 60;
- The mugshot DETs of Figure 81;
- The mugshot ageing profiles of Figure 294;
- The human-difficult pairs of Figure 19

▷ **Non-cooperative subjects**

- The photojournalism DET of Figure 98

Figure 235 shows dependence of false match rate on algorithm score threshold. This allows a deployer to set a threshold to target a particular false match rate appropriate to the security objectives of the application.

Figure 194 likewise shows FMR(T) but for mugshots, and specially four subsets of the population.

Note that in both the mugshot and visa sets false match rates vary with the ethnicity, age, and sex, of the enrollee and impostor. For example figure 118 summarizes FMR for impostors paired from four groups black females, black males, white females, white males.

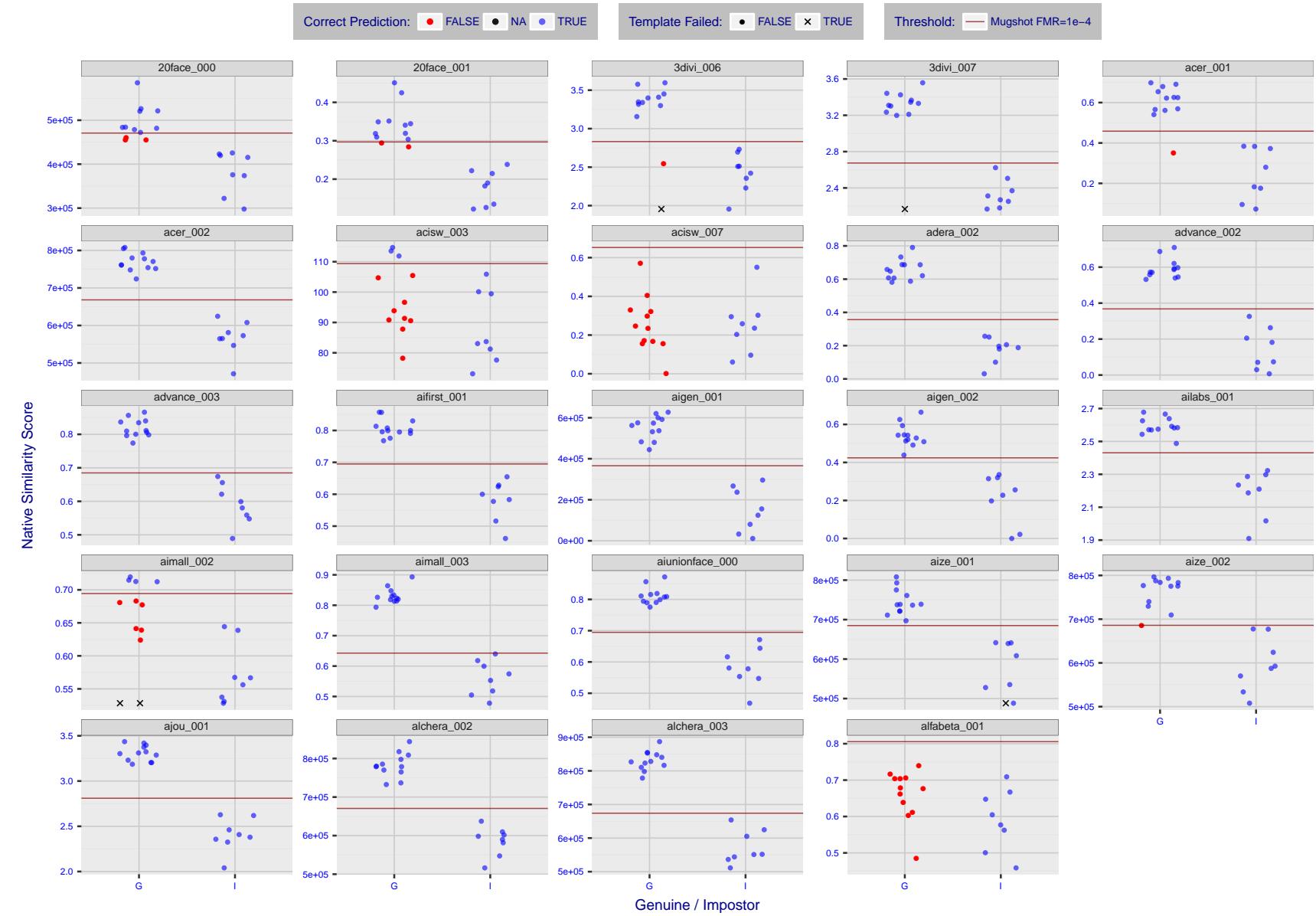


Figure 4: The figure shows algorithms' similarity scores for 12 genuine and 8 impostor image pairs used in the May 2018 paper Face recognition accuracy of forensic examiners, superrecognizers, and face recognition algorithms (Phillips et al. [1]). The threshold (red horizontal line) is a value calibrated to give $FMR = 0.0001$ on mugshot images. Points above the threshold correspond to pairs predicted to be genuine, and points below the threshold correspond to pairs predicted to be impostors. The figure shows whether the predicted class (genuine or impostor) matches the real class. Blue denotes a correct prediction, and red denotes incorrect. An "X" represents face detection failure in either of the images in the pair. Note that the sample size ($n=20$) is small, and the figure may change substantially if larger or different sets are used. The images can be downloaded from the [Supplemental Information](#) page provided with that publication.

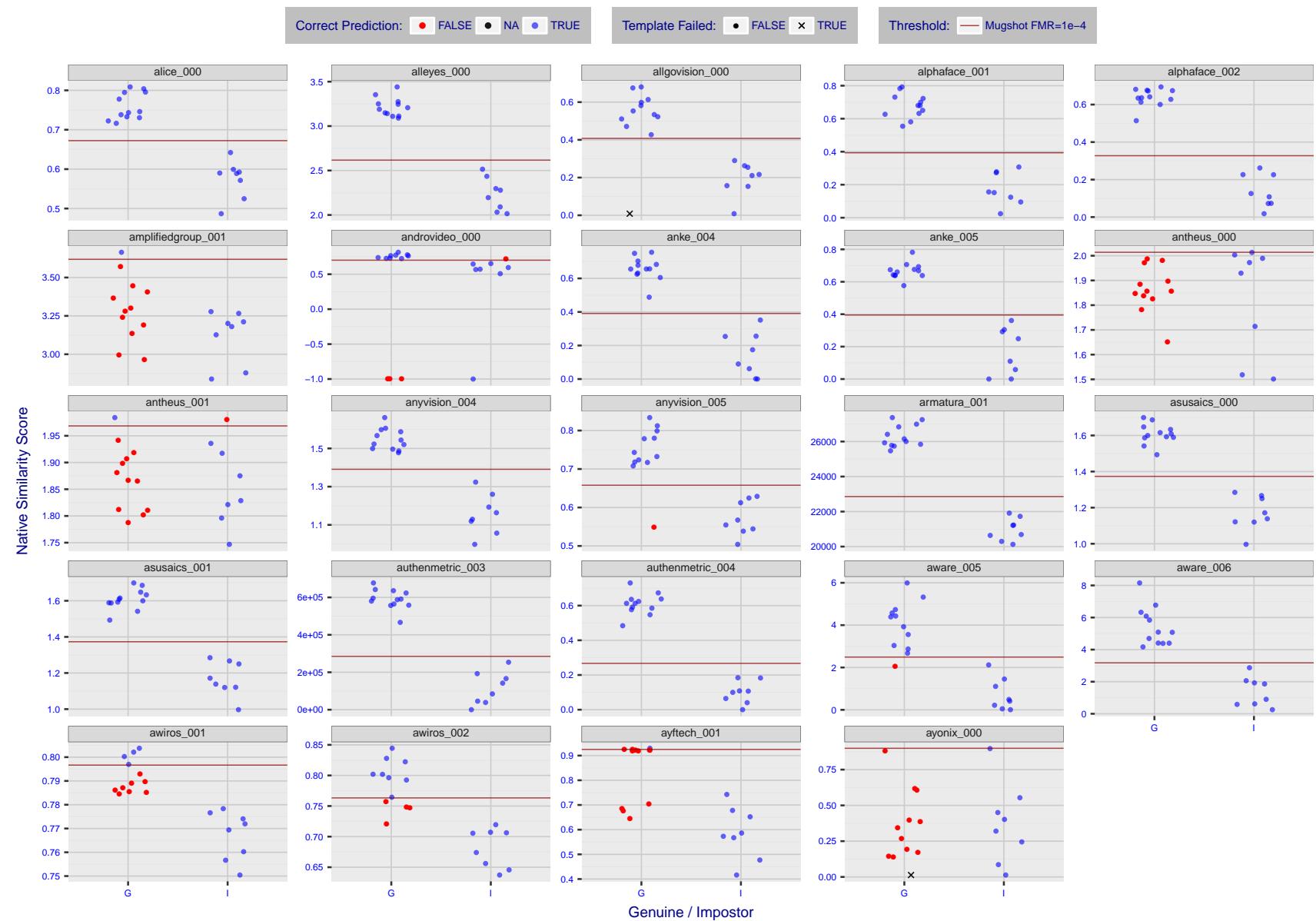


Figure 5: The figure shows algorithms' similarity scores for 12 genuine and 8 impostor image pairs used in the May 2018 paper Face recognition accuracy of forensic examiners, superrecognizers, and face recognition algorithms (Phillips et al. [1]). The threshold (red horizontal line) is a value calibrated to give $FMR = 0.0001$ on mugshot images. Points above the threshold correspond to pairs predicted to be genuine, and points below the threshold correspond to pairs predicted to be impostors. The figure shows whether the predicted class (genuine or impostor) matches the real class. Blue denotes a correct prediction, and red denotes incorrect. An "X" represents face detection failure in either of the images in the pair. Note that the sample size ($n=20$) is small, and the figure may change substantially if larger or different sets are used. The images can be downloaded from the [Supplemental Information](#) page provided with that publication.

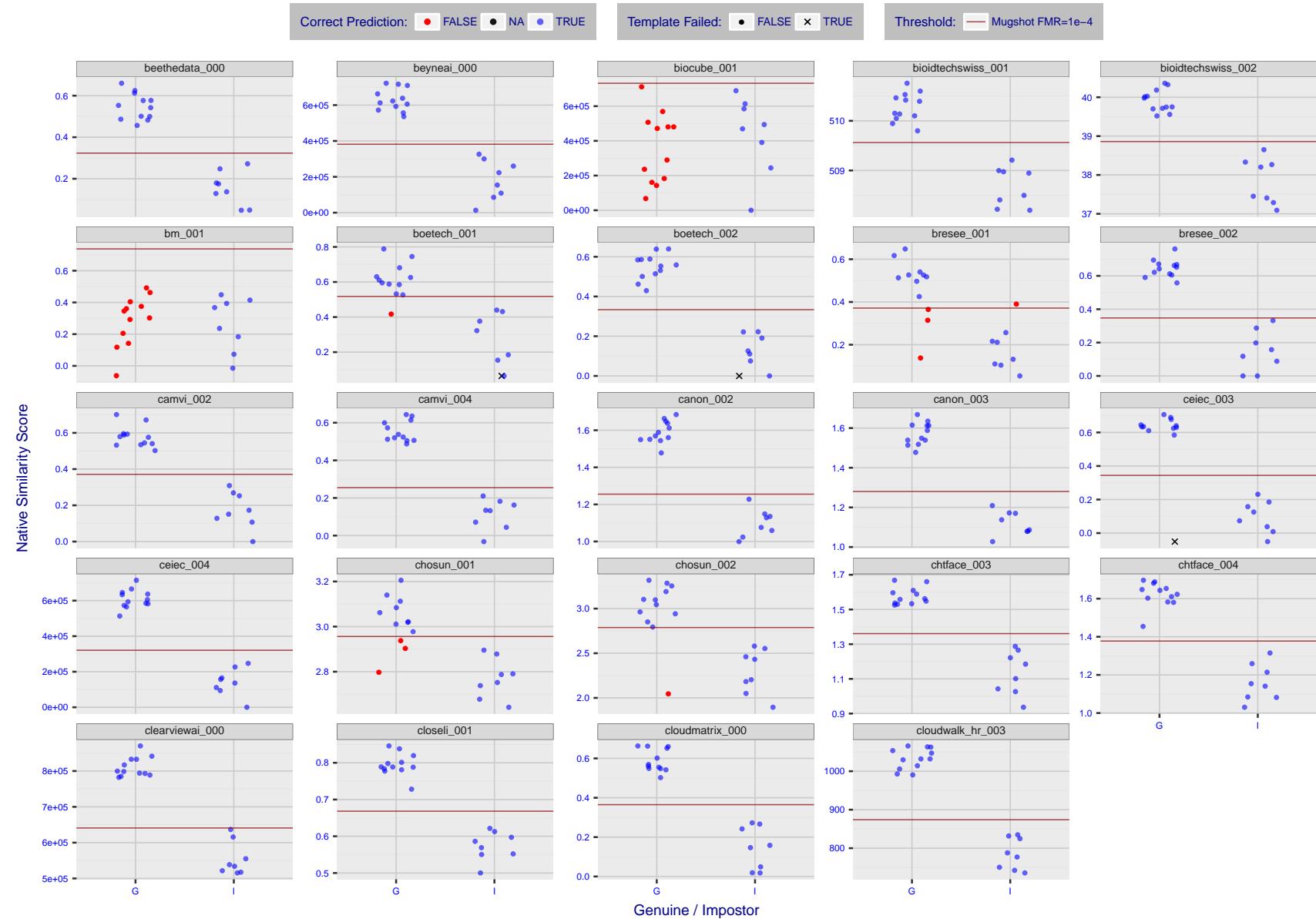


Figure 6: The figure shows algorithms' similarity scores for 12 genuine and 8 impostor image pairs used in the May 2018 paper Face recognition accuracy of forensic examiners, superrecognizers, and face recognition algorithms (Phillips et al. [1]). The threshold (red horizontal line) is a value calibrated to give $FMR = 0.0001$ on mugshot images. Points above the threshold correspond to pairs predicted to be genuine, and points below the threshold correspond to pairs predicted to be impostors. The figure shows whether the predicted class (genuine or impostor) matches the real class. Blue denotes a correct prediction, and red denotes incorrect. An "X" represents face detection failure in either of the images in the pair. Note that the sample size ($n=20$) is small, and the figure may change substantially if larger or different sets are used. The images can be downloaded from the [Supplemental Information](#) page provided with that publication.

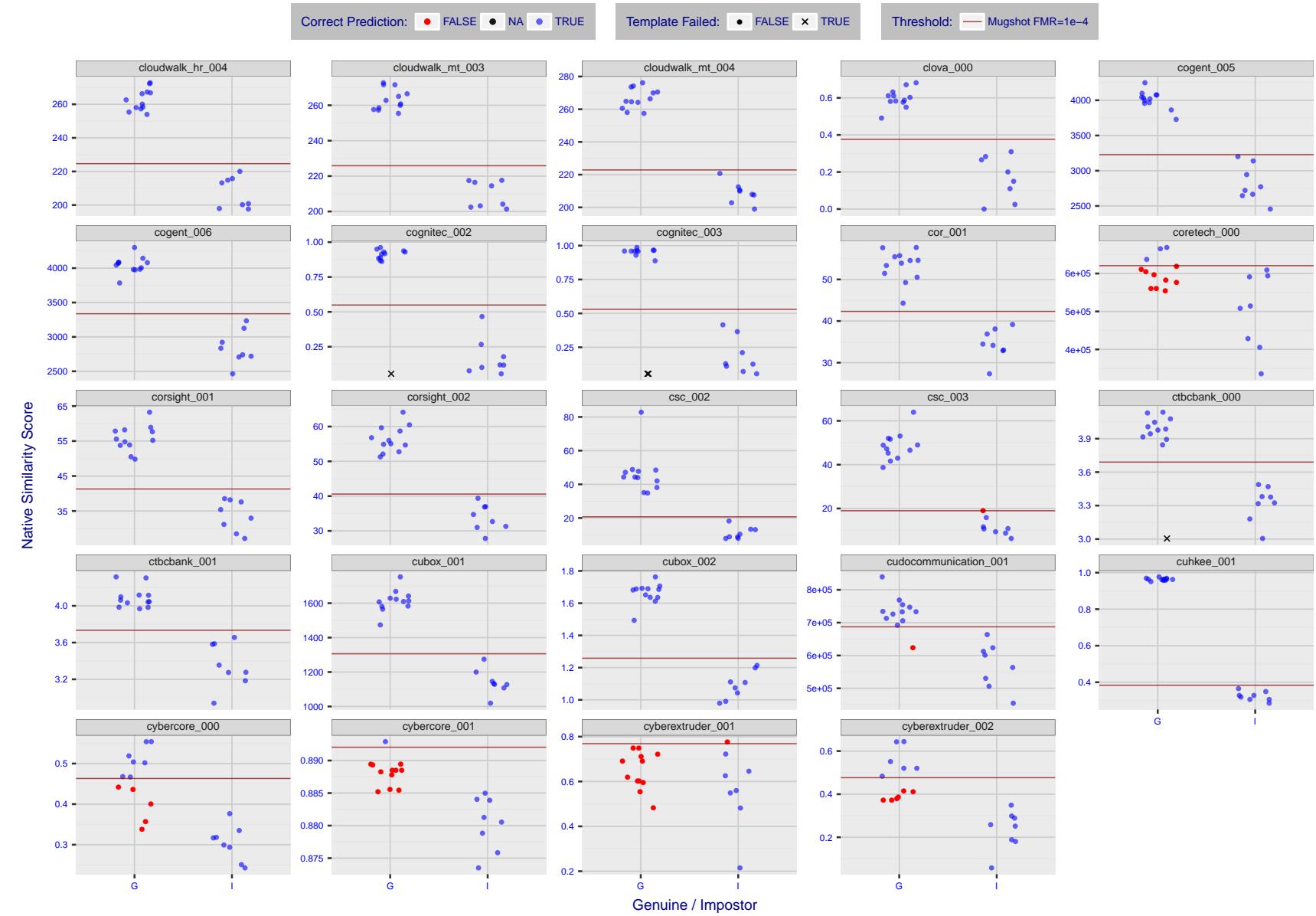


Figure 7: The figure shows algorithms' similarity scores for 12 genuine and 8 impostor image pairs used in the May 2018 paper Face recognition accuracy of forensic examiners, superrecognizers, and face recognition algorithms (Phillips et al. [1]). The threshold (red horizontal line) is a value calibrated to give $FMR = 0.0001$ on mugshot images. Points above the threshold correspond to pairs predicted to be genuine, and points below the threshold correspond to pairs predicted to be impostors. The figure shows whether the predicted class (genuine or impostor) matches the real class. Blue denotes a correct prediction, and red denotes incorrect. An "X" represents face detection failure in either of the images in the pair. Note that the sample size ($n=20$) is small, and the figure may change substantially if larger or different sets are used. The images can be downloaded from the [Supplemental Information](#) page provided with that publication.

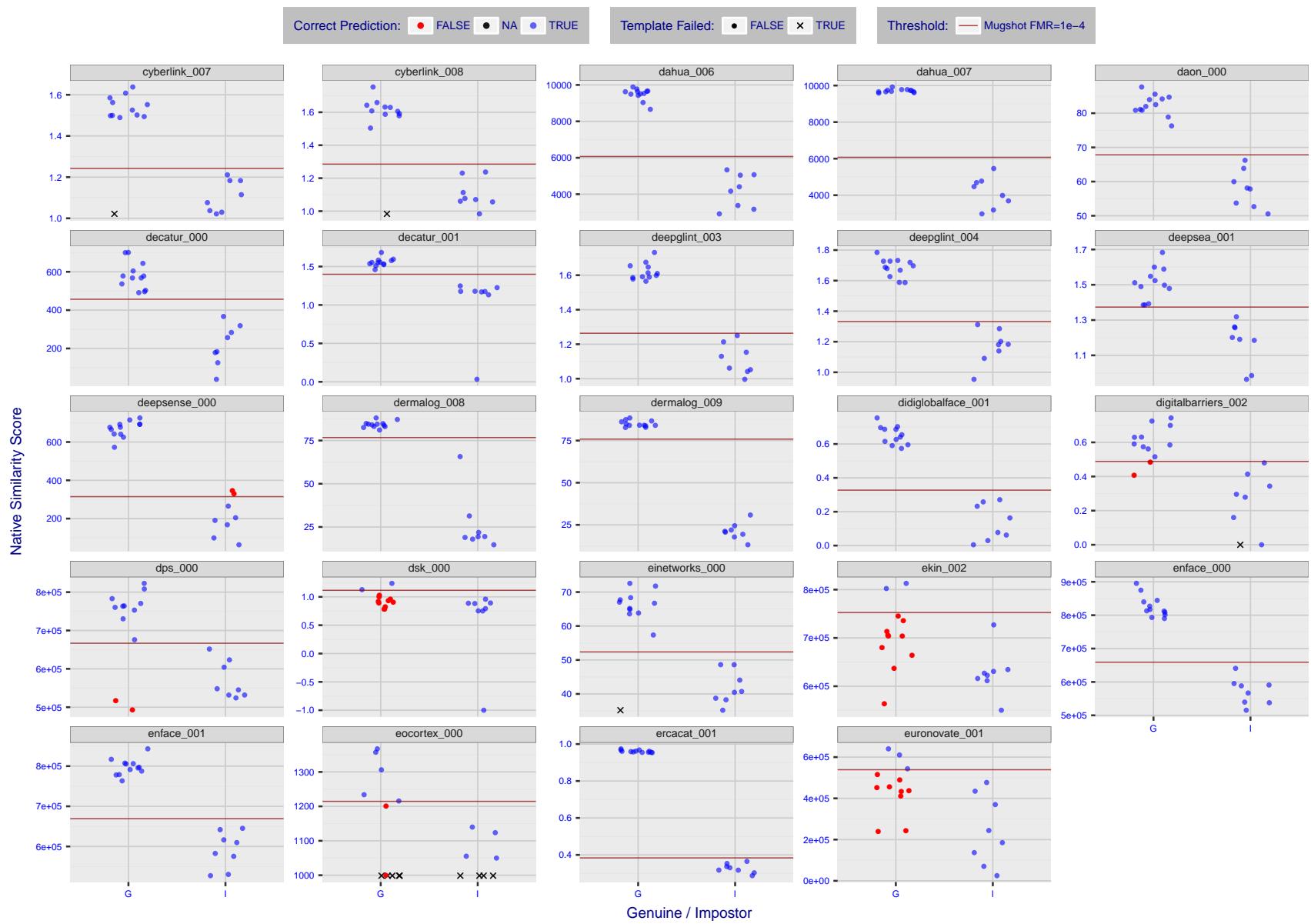


Figure 8: The figure shows algorithms' similarity scores for 12 genuine and 8 impostor image pairs used in the May 2018 paper Face recognition accuracy of forensic examiners, superrecognizers, and face recognition algorithms (Phillips et al. [1]). The threshold (red horizontal line) is a value calibrated to give $FMR = 0.0001$ on mugshot images. Points above the threshold correspond to pairs predicted to be genuine, and points below the threshold correspond to pairs predicted to be impostors. The figure shows whether the predicted class (genuine or impostor) matches the real class. Blue denotes a correct prediction, and red denotes incorrect. An "X" represents face detection failure in either of the images in the pair. Note that the sample size ($n=20$) is small, and the figure may change substantially if larger or different sets are used. The images can be downloaded from the [Supplemental Information](#) page provided with that publication.

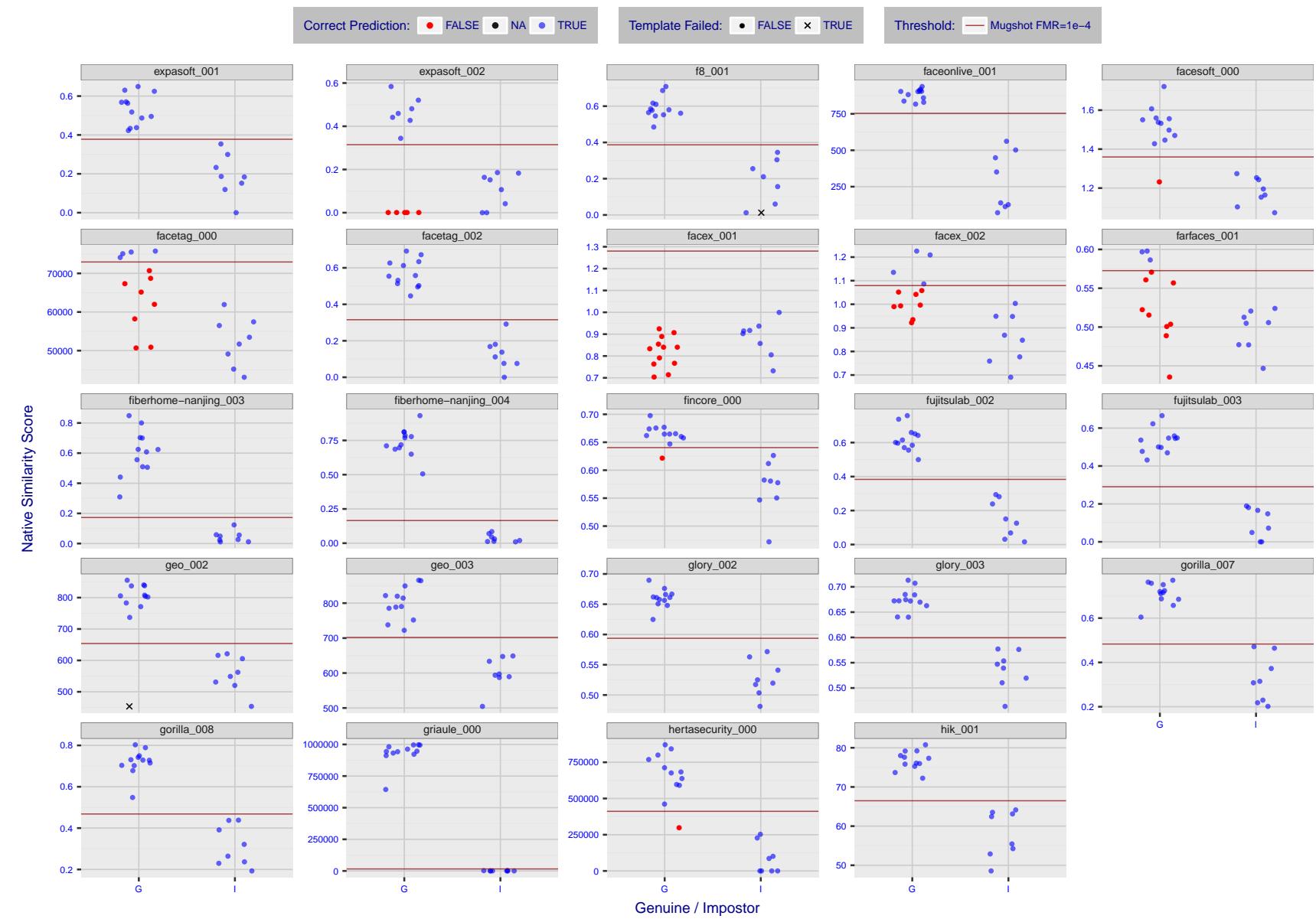


Figure 9: The figure shows algorithms' similarity scores for 12 genuine and 8 impostor image pairs used in the May 2018 paper Face recognition accuracy of forensic examiners, superrecognizers, and face recognition algorithms (Phillips et al. [1]). The threshold (red horizontal line) is a value calibrated to give $FMR = 0.0001$ on mugshot images. Points above the threshold correspond to pairs predicted to be genuine, and points below the threshold correspond to pairs predicted to be impostors. The figure shows whether the predicted class (genuine or impostor) matches the real class. Blue denotes a correct prediction, and red denotes incorrect. An "X" represents face detection failure in either of the images in the pair. Note that the sample size ($n=20$) is small, and the figure may change substantially if larger or different sets are used. The images can be downloaded from the [Supplemental Information](#) page provided with that publication.

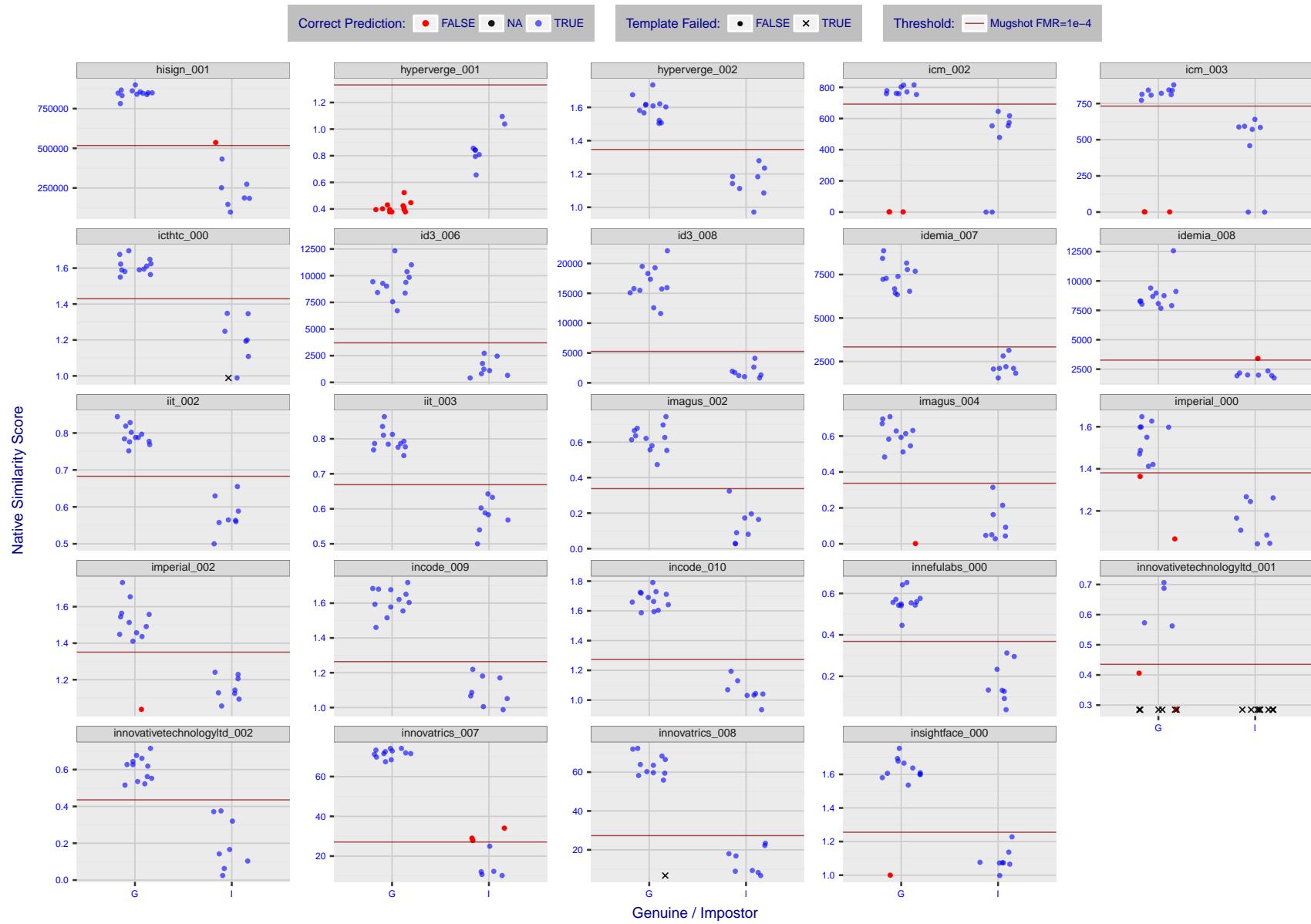


Figure 10: The figure shows algorithms' similarity scores for 12 genuine and 8 impostor image pairs used in the May 2018 paper [Face recognition accuracy of forensic examiners, superrecognizers, and face recognition algorithms](#) (Phillips et al. [1]). The threshold (red horizontal line) is a value calibrated to give $FMR = 0.0001$ on mugshot images. Points above the threshold correspond to pairs predicted to be genuine, and points below the threshold correspond to pairs predicted to be impostors. The figure shows whether the predicted class (genuine or impostor) matches the real class. Blue denotes a correct prediction, and red denotes incorrect. An "X" represents face detection failure in either of the images in the pair. Note that the sample size ($n=20$) is small, and the figure may change substantially if larger or different sets are used. The images can be downloaded from the [Supplemental Information](#) page provided with that publication.

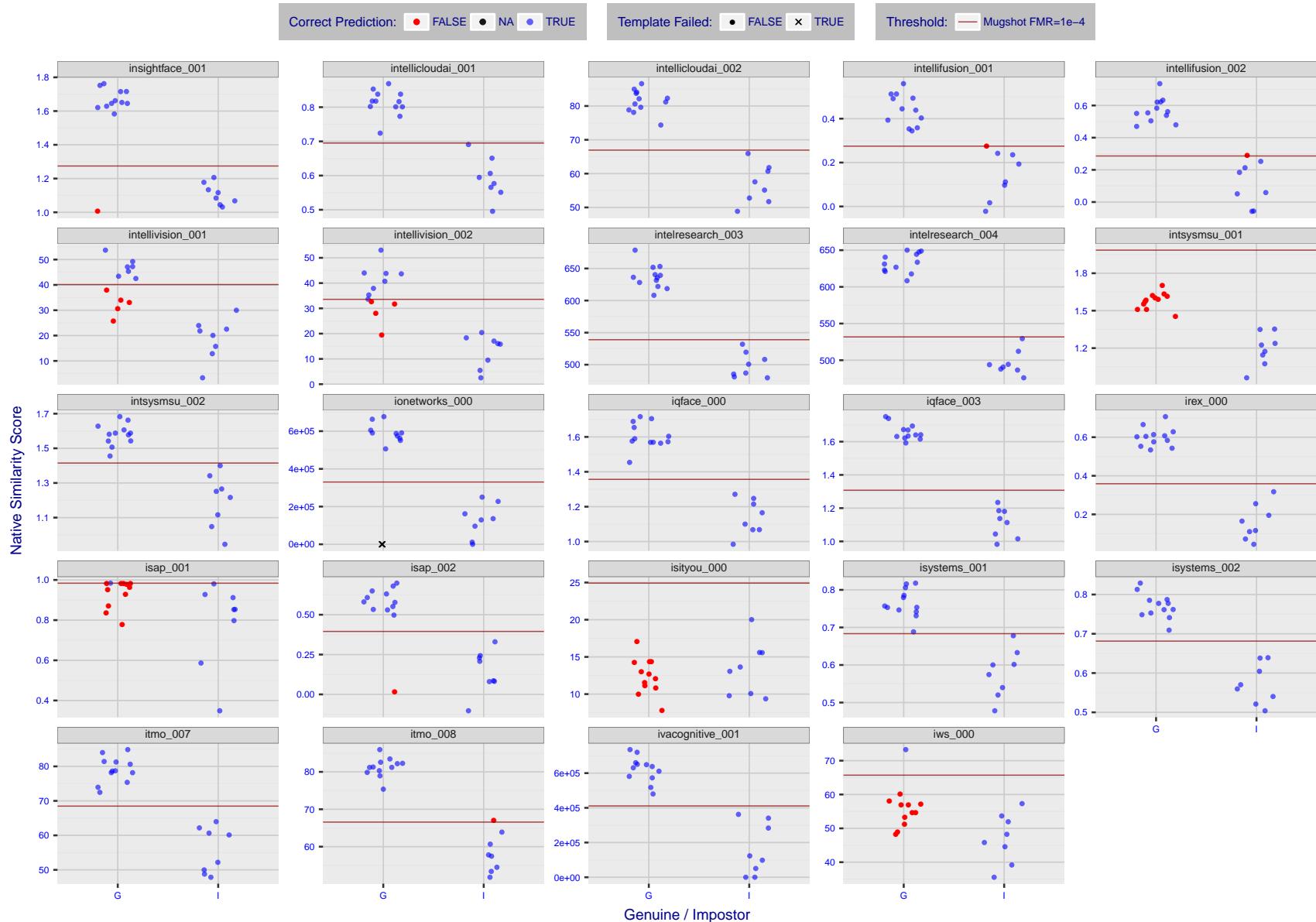


Figure 11: The figure shows algorithms' similarity scores for 12 genuine and 8 impostor image pairs used in the May 2018 paper Face recognition accuracy of forensic examiners, superrecognizers, and face recognition algorithms (Phillips et al. [1]). The threshold (red horizontal line) is a value calibrated to give $FMR = 0.0001$ on mugshot images. Points above the threshold correspond to pairs predicted to be genuine, and points below the threshold correspond to pairs predicted to be impostors. The figure shows whether the predicted class (genuine or impostor) matches the real class. Blue denotes a correct prediction, and red denotes incorrect. An "X" represents face detection failure in either of the images in the pair. Note that the sample size ($n=20$) is small, and the figure may change substantially if larger or different sets are used. The images can be downloaded from the [Supplemental Information](#) page provided with that publication.

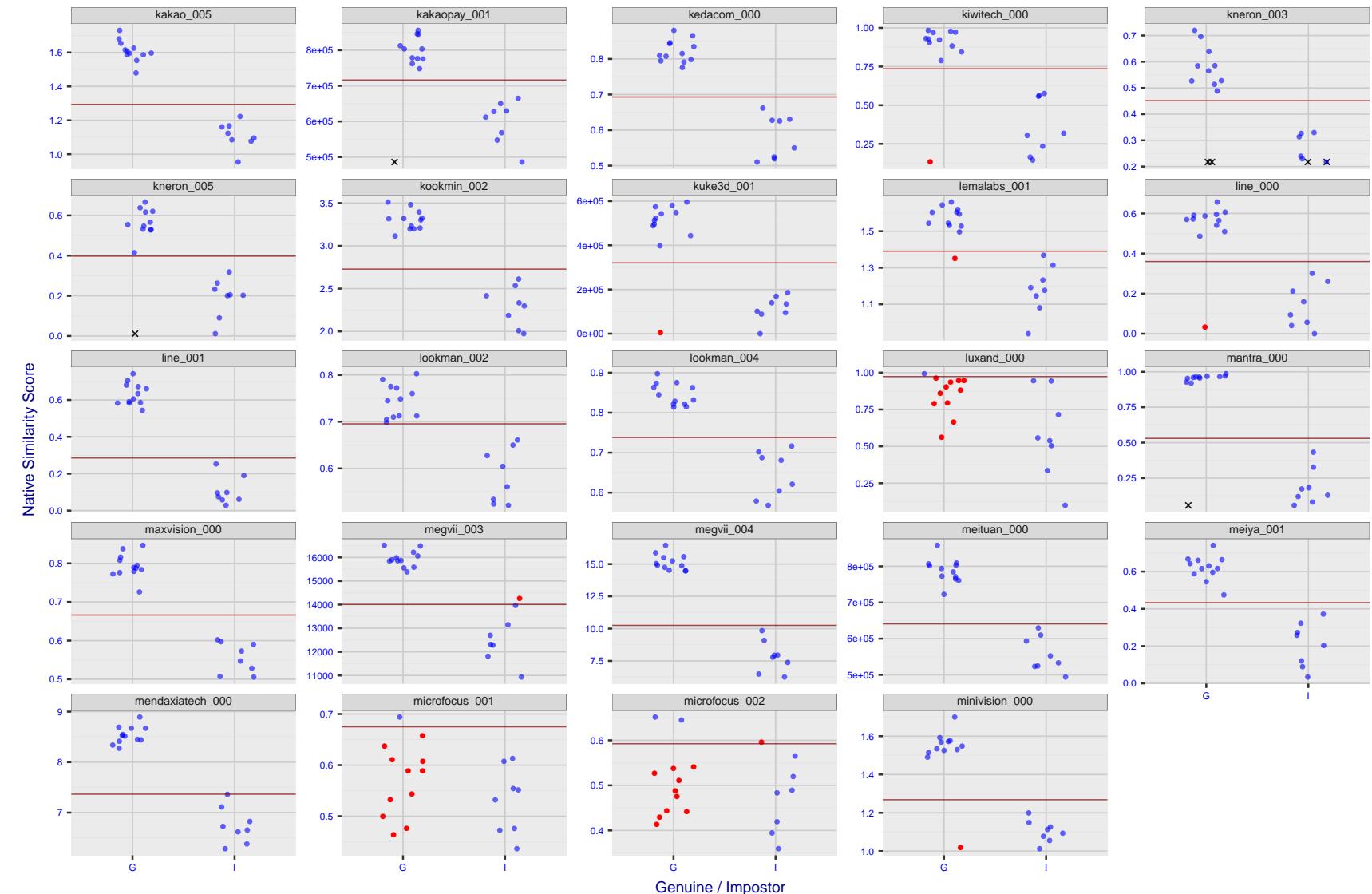


Figure 12: The figure shows algorithms' similarity scores for 12 genuine and 8 impostor image pairs used in the May 2018 paper Face recognition accuracy of forensic examiners, superrecognizers, and face recognition algorithms (Phillips et al. [1]). The threshold (red horizontal line) is a value calibrated to give $FMR = 0.0001$ on mugshot images. Points above the threshold correspond to pairs predicted to be genuine, and points below the threshold correspond to pairs predicted to be impostors. The figure shows whether the predicted class (genuine or impostor) matches the real class. Blue denotes a correct prediction, and red denotes incorrect. An "X" represents face detection failure in either of the images in the pair. Note that the sample size ($n=20$) is small, and the figure may change substantially if larger or different sets are used. The images can be downloaded from the [Supplemental Information](#) page provided with that publication.

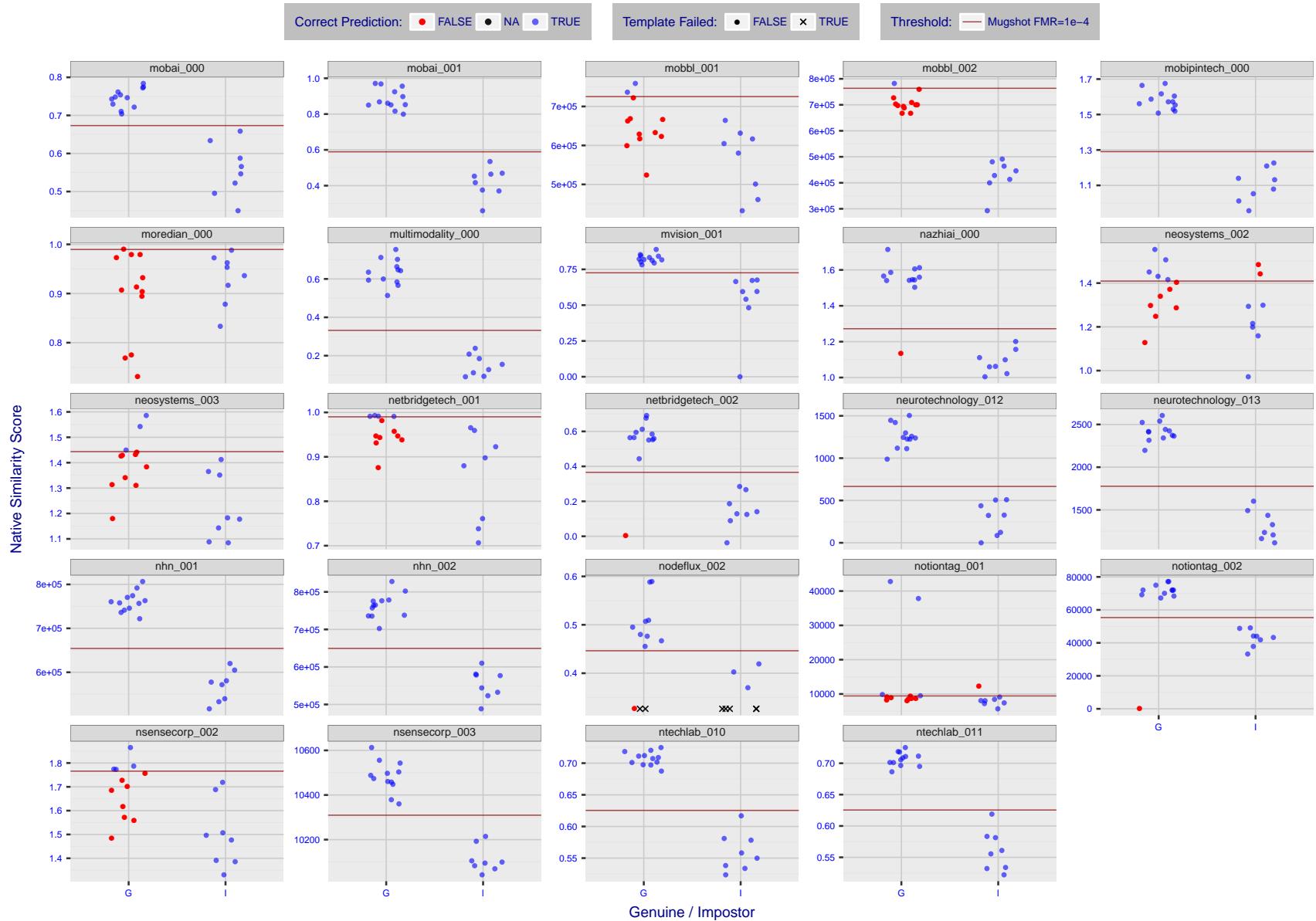


Figure 13: The figure shows algorithms' similarity scores for 12 genuine and 8 impostor image pairs used in the May 2018 paper Face recognition accuracy of forensic examiners, superrecognizers, and face recognition algorithms (Phillips et al. [1]). The threshold (red horizontal line) is a value calibrated to give $FMR = 0.0001$ on mugshot images. Points above the threshold correspond to pairs predicted to be genuine, and points below the threshold correspond to pairs predicted to be impostors. The figure shows whether the predicted class (genuine or impostor) matches the real class. Blue denotes a correct prediction, and red denotes incorrect. An "X" represents face detection failure in either of the images in the pair. Note that the sample size ($n=20$) is small, and the figure may change substantially if larger or different sets are used. The images can be downloaded from the [Supplemental Information](#) page provided with that publication.

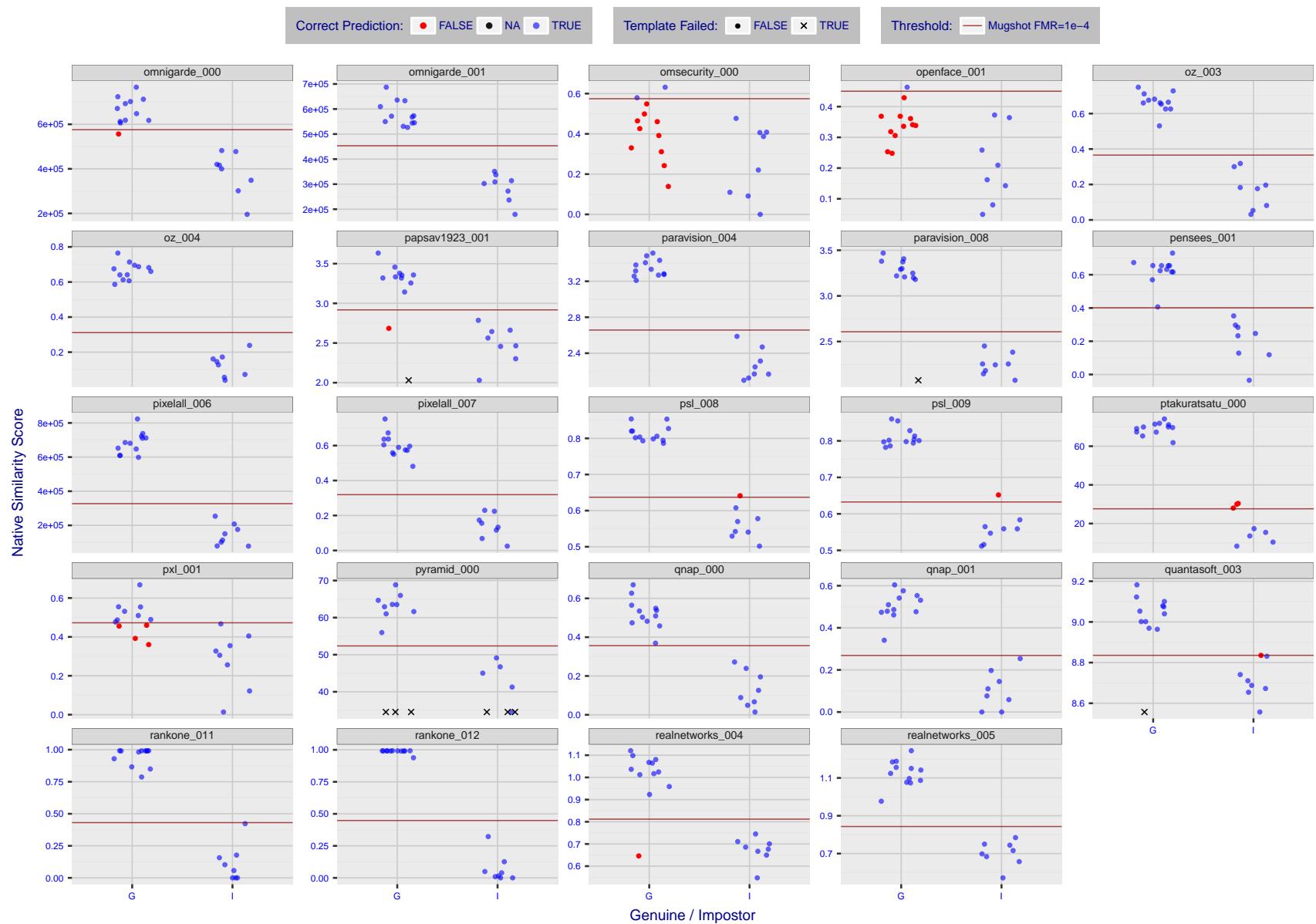


Figure 14: The figure shows algorithms' similarity scores for 12 genuine and 8 impostor image pairs used in the May 2018 paper Face recognition accuracy of forensic examiners, superrecognizers, and face recognition algorithms (Phillips et al. [1]). The threshold (red horizontal line) is a value calibrated to give $FMR = 0.0001$ on mugshot images. Points above the threshold correspond to pairs predicted to be genuine, and points below the threshold correspond to pairs predicted to be impostors. The figure shows whether the predicted class (genuine or impostor) matches the real class. Blue denotes a correct prediction, and red denotes incorrect. An "X" represents face detection failure in either of the images in the pair. Note that the sample size ($n=20$) is small, and the figure may change substantially if larger or different sets are used. The images can be downloaded from the [Supplemental Information](#) page provided with that publication.

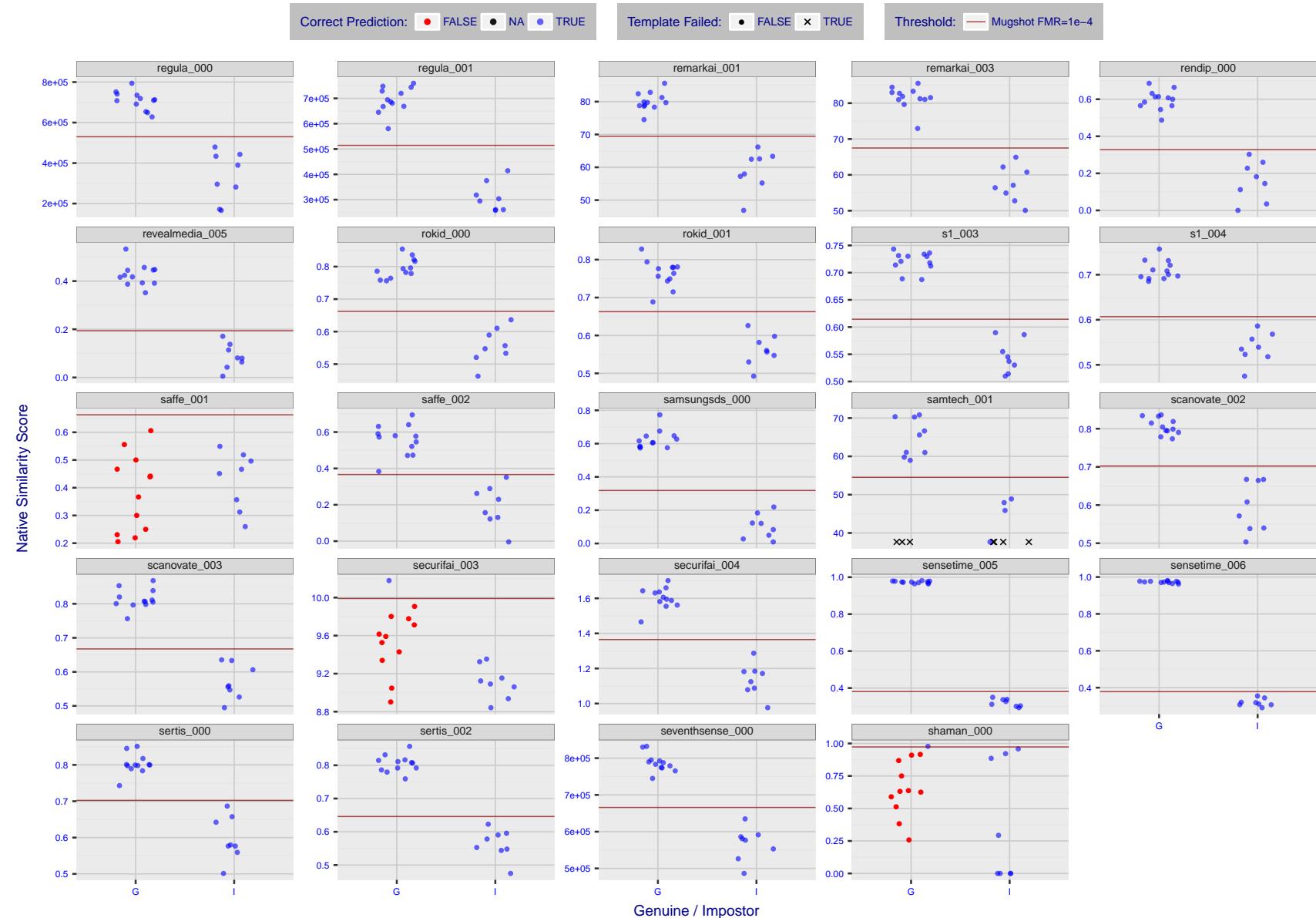


Figure 15: The figure shows algorithms' similarity scores for 12 genuine and 8 impostor image pairs used in the May 2018 paper Face recognition accuracy of forensic examiners, superrecognizers, and face recognition algorithms (Phillips et al. [1]). The threshold (red horizontal line) is a value calibrated to give $FMR = 0.0001$ on mugshot images. Points above the threshold correspond to pairs predicted to be genuine, and points below the threshold correspond to pairs predicted to be impostors. The figure shows whether the predicted class (genuine or impostor) matches the real class. Blue denotes a correct prediction, and red denotes incorrect. An "X" represents face detection failure in either of the images in the pair. Note that the sample size ($n=20$) is small, and the figure may change substantially if larger or different sets are used. The images can be downloaded from the [Supplemental Information](#) page provided with that publication.

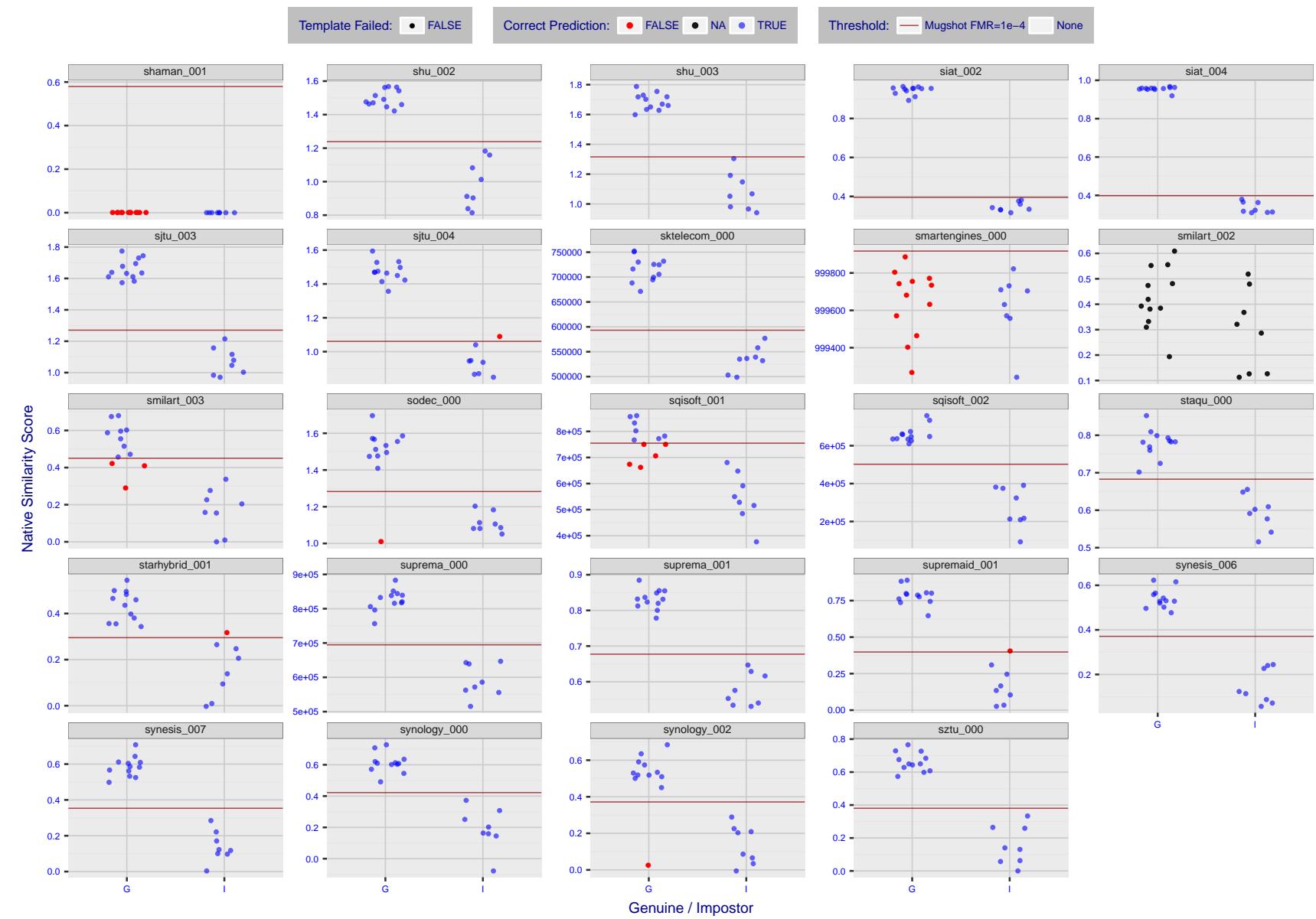


Figure 16: The figure shows algorithms' similarity scores for 12 genuine and 8 impostor image pairs used in the May 2018 paper Face recognition accuracy of forensic examiners, superrecognizers, and face recognition algorithms (Phillips et al. [1]). The threshold (red horizontal line) is a value calibrated to give $FMR = 0.0001$ on mugshot images. Points above the threshold correspond to pairs predicted to be genuine, and points below the threshold correspond to pairs predicted to be impostors. The figure shows whether the predicted class (genuine or impostor) matches the real class. Blue denotes a correct prediction, and red denotes incorrect. An "X" represents face detection failure in either of the images in the pair. Note that the sample size ($n=20$) is small, and the figure may change substantially if larger or different sets are used. The images can be downloaded from the [Supplemental Information](#) page provided with that publication.

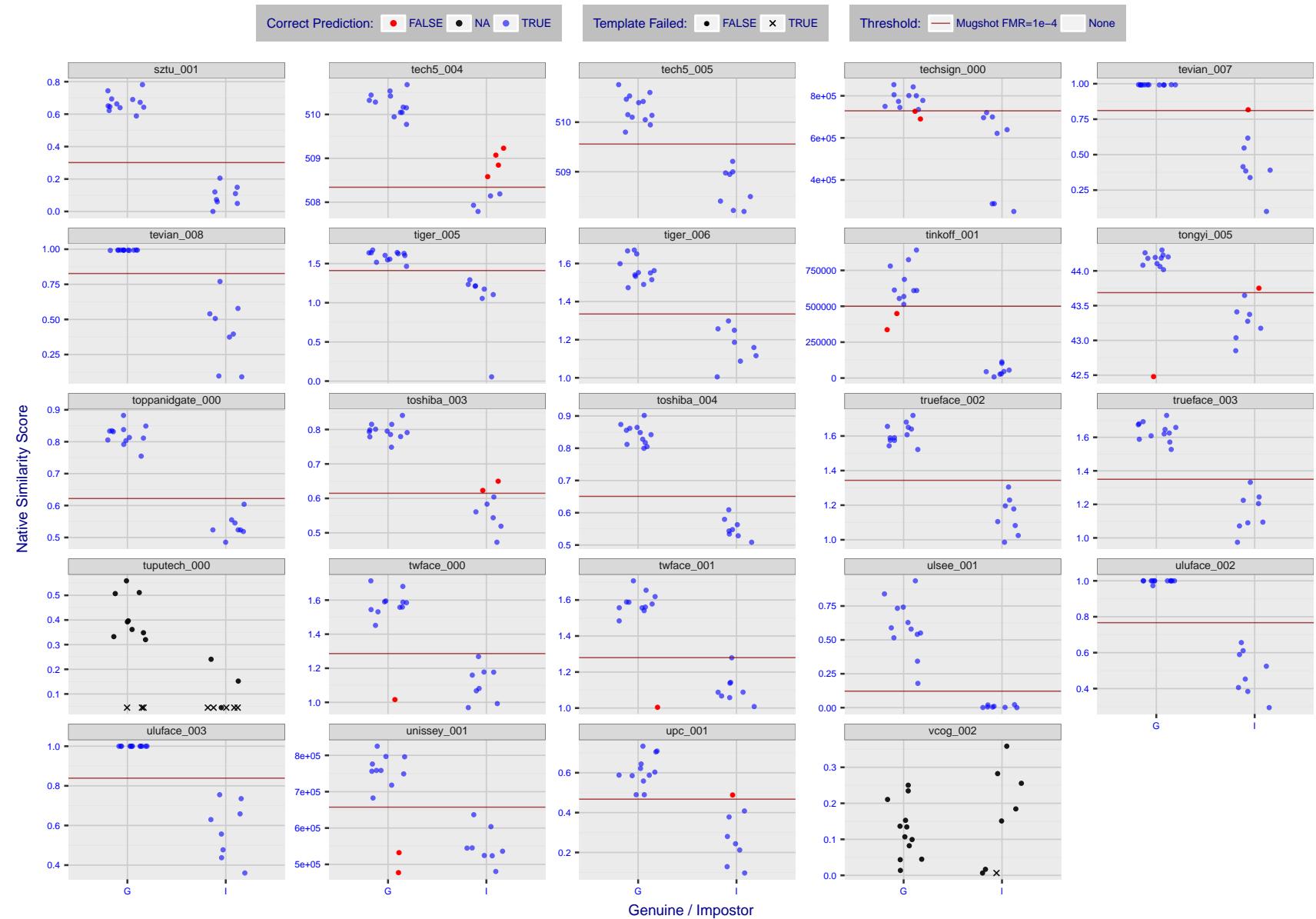


Figure 17: The figure shows algorithms' similarity scores for 12 genuine and 8 impostor image pairs used in the May 2018 paper Face recognition accuracy of forensic examiners, superrecognizers, and face recognition algorithms (Phillips et al. [1]). The threshold (red horizontal line) is a value calibrated to give $FMR = 0.0001$ on mugshot images. Points above the threshold correspond to pairs predicted to be genuine, and points below the threshold correspond to pairs predicted to be impostors. The figure shows whether the predicted class (genuine or impostor) matches the real class. Blue denotes a correct prediction, and red denotes incorrect. An "X" represents face detection failure in either of the images in the pair. Note that the sample size ($n=20$) is small, and the figure may change substantially if larger or different sets are used. The images can be downloaded from the [Supplemental Information](#) page provided with that publication.



Figure 18: The figure shows algorithms' similarity scores for 12 genuine and 8 impostor image pairs used in the May 2018 paper Face recognition accuracy of forensic examiners, superrecognizers, and face recognition algorithms (Phillips et al. [1]). The threshold (red horizontal line) is a value calibrated to give FMR = 0.0001 on mugshot images. Points above the threshold correspond to pairs predicted to be genuine, and points below the threshold correspond to pairs predicted to be impostors. The figure shows whether the predicted class (genuine or impostor) matches the real class. Blue denotes a correct prediction, and red denotes incorrect. An "X" represents face detection failure in either of the images in the pair. Note that the sample size ($n=20$) is small, and the figure may change substantially if larger or different sets are used. The images can be downloaded from the [Supplemental Information](#) page provided with that publication.

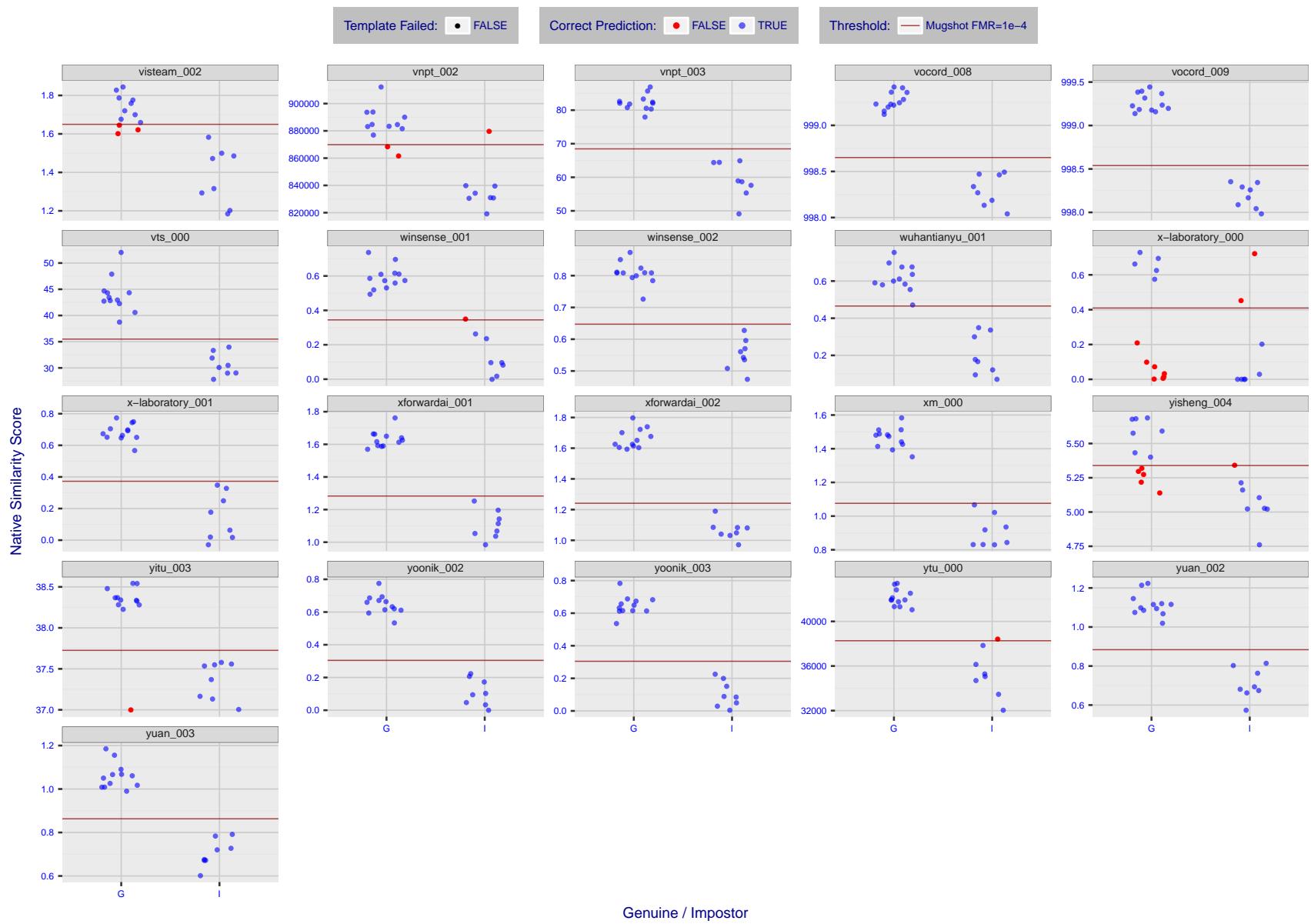


Figure 19: The figure shows algorithms' similarity scores for 12 genuine and 8 impostor image pairs used in the May 2018 paper Face recognition accuracy of forensic examiners, superrecognizers, and face recognition algorithms (Phillips et al. [1]). The threshold (red horizontal line) is a value calibrated to give $FMR = 0.0001$ on mugshot images. Points above the threshold correspond to pairs predicted to be genuine, and points below the threshold correspond to pairs predicted to be impostors. The figure shows whether the predicted class (genuine or impostor) matches the real class. Blue denotes a correct prediction, and red denotes incorrect. An "X" represents face detection failure in either of the images in the pair. Note that the sample size ($n=20$) is small, and the figure may change substantially if larger or different sets are used. The images can be downloaded from the [Supplemental Information](#) page provided with that publication.

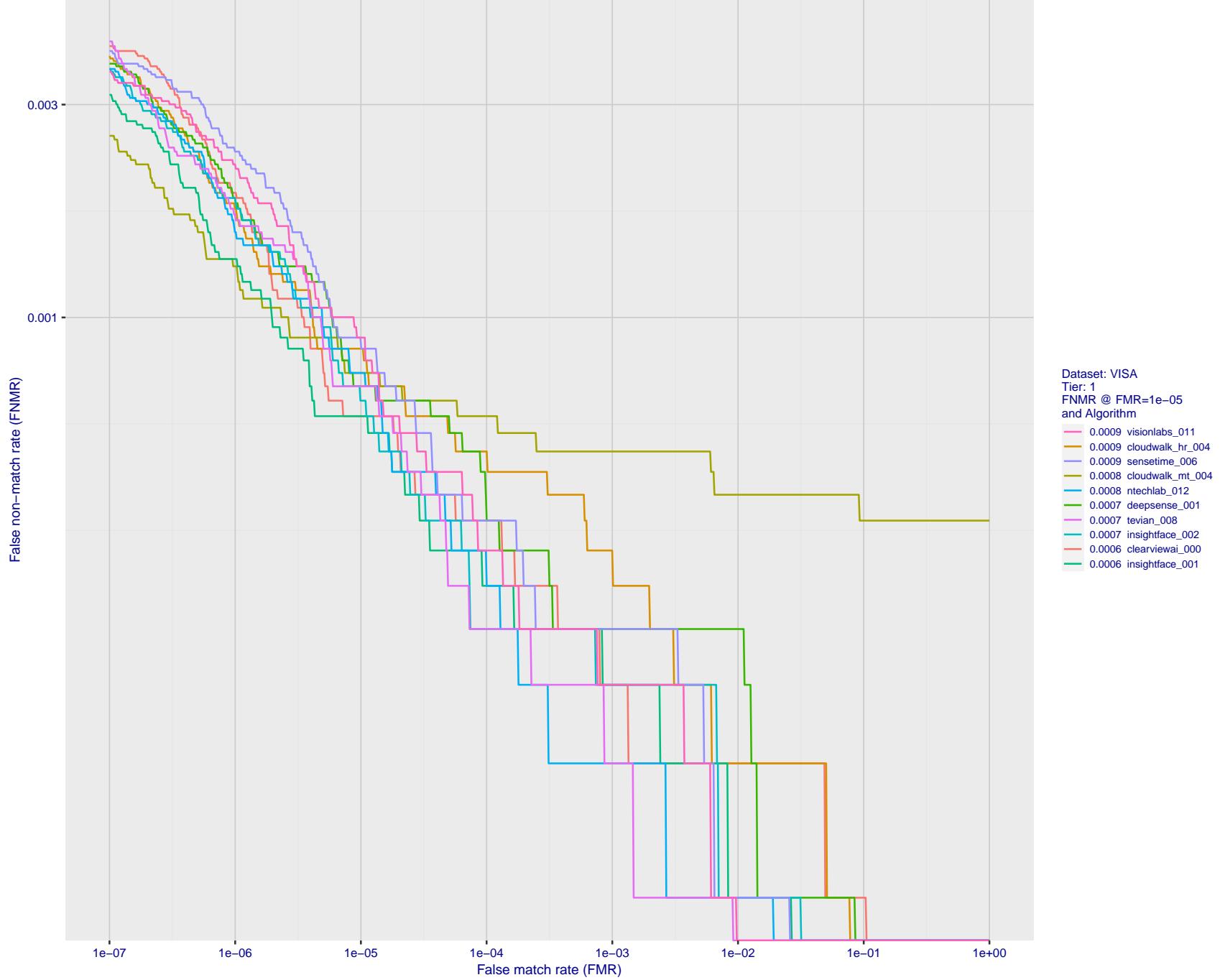


Figure 20: For the visa images, detection error tradeoff (DET) characteristics showing false non-match rate vs. false match rate plotted parametrically on threshold, T . The scales are logarithmic in order to show many decades of FMR.

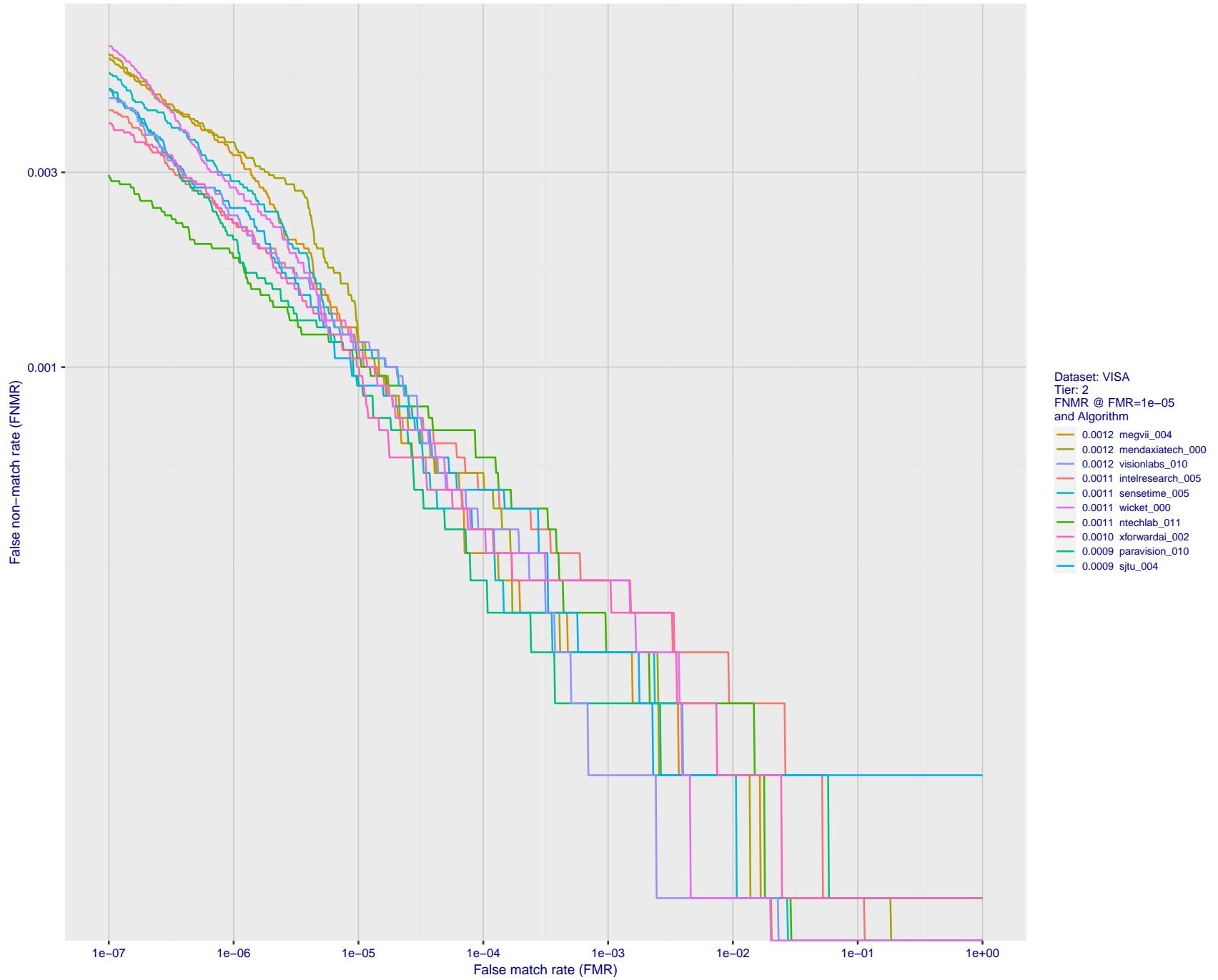


Figure 21: For the visa images, detection error tradeoff (DET) characteristics showing false non-match rate vs. false match rate plotted parametrically on threshold, T . The scales are logarithmic in order to show many decades of FMR.

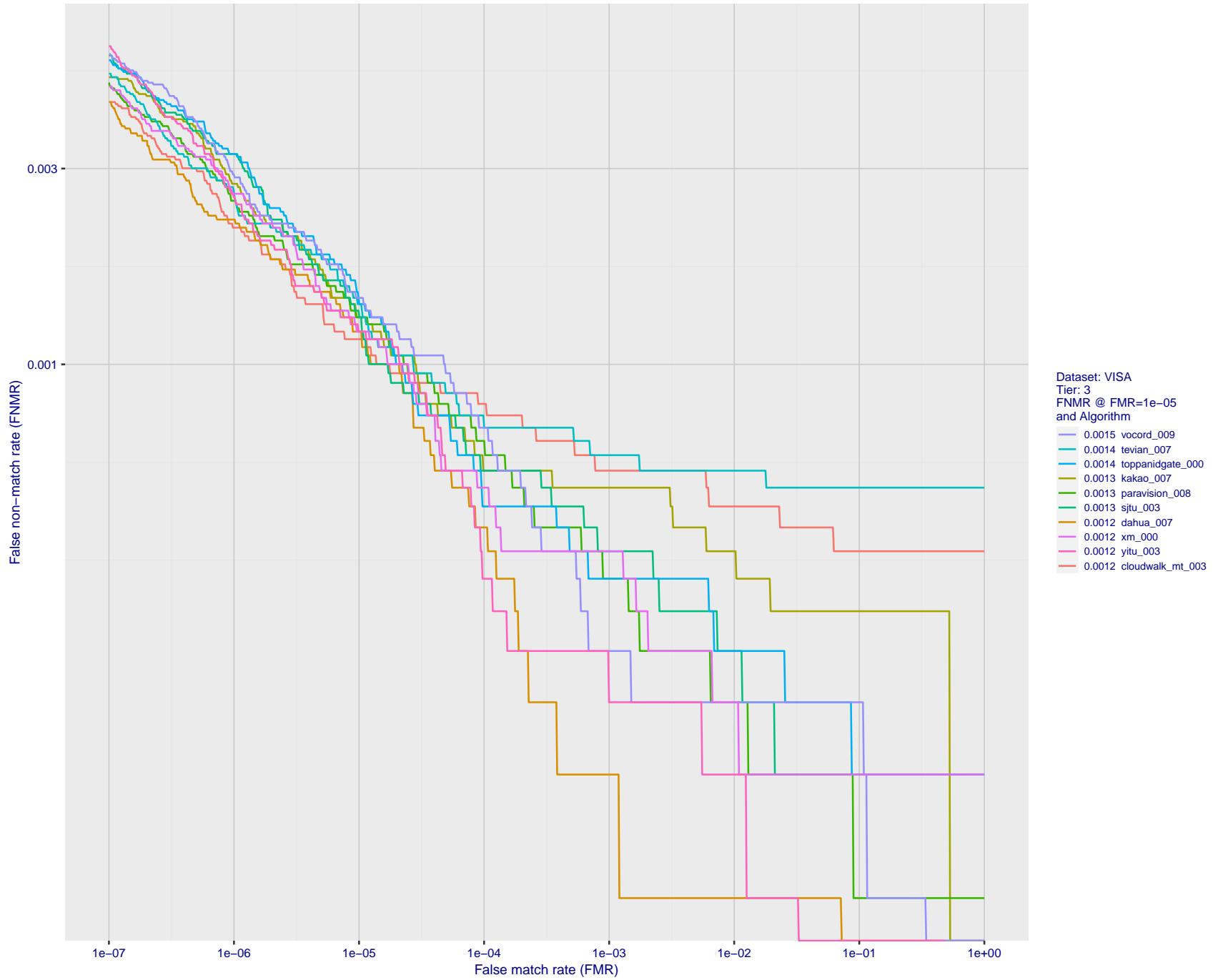


Figure 22: For the visa images, detection error tradeoff (DET) characteristics showing false non-match rate vs. false match rate plotted parametrically on threshold, T . The scales are logarithmic in order to show many decades of FMR.

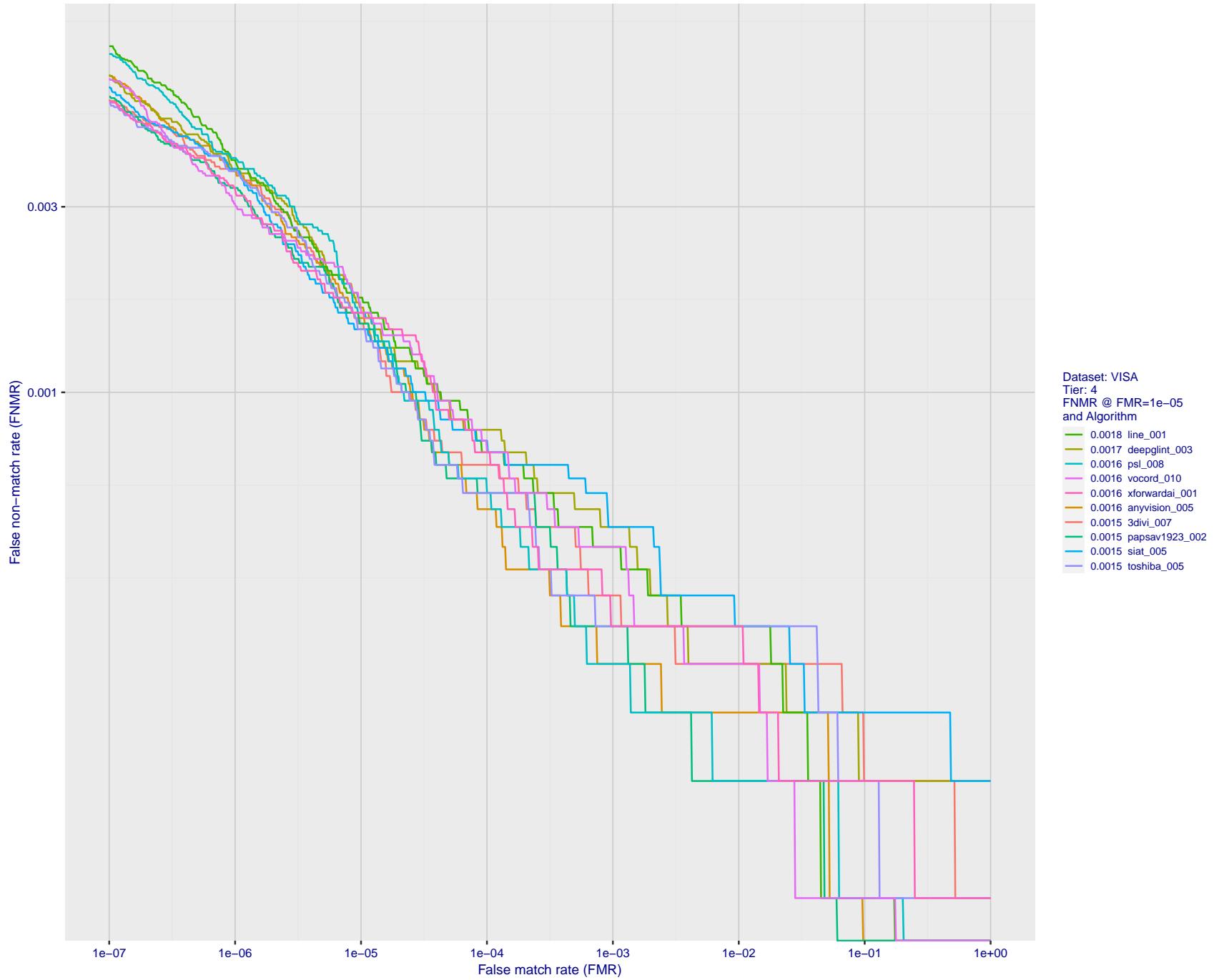


Figure 23: For the visa images, detection error tradeoff (DET) characteristics showing false non-match rate vs. false match rate plotted parametrically on threshold, T . The scales are logarithmic in order to show many decades of FMR.

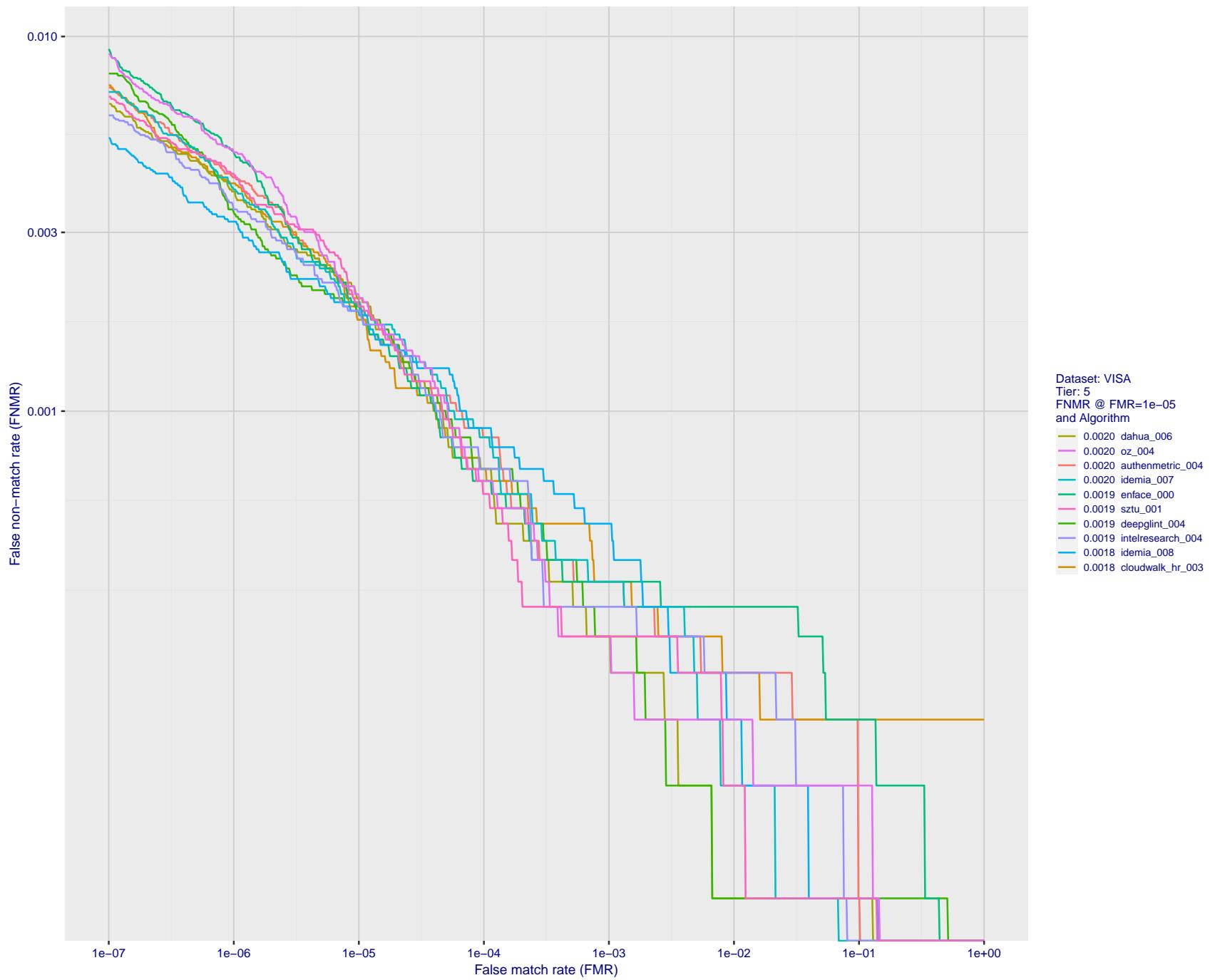


Figure 24: For the visa images, detection error tradeoff (DET) characteristics showing false non-match rate vs. false match rate plotted parametrically on threshold, T . The scales are logarithmic in order to show many decades of FMR.

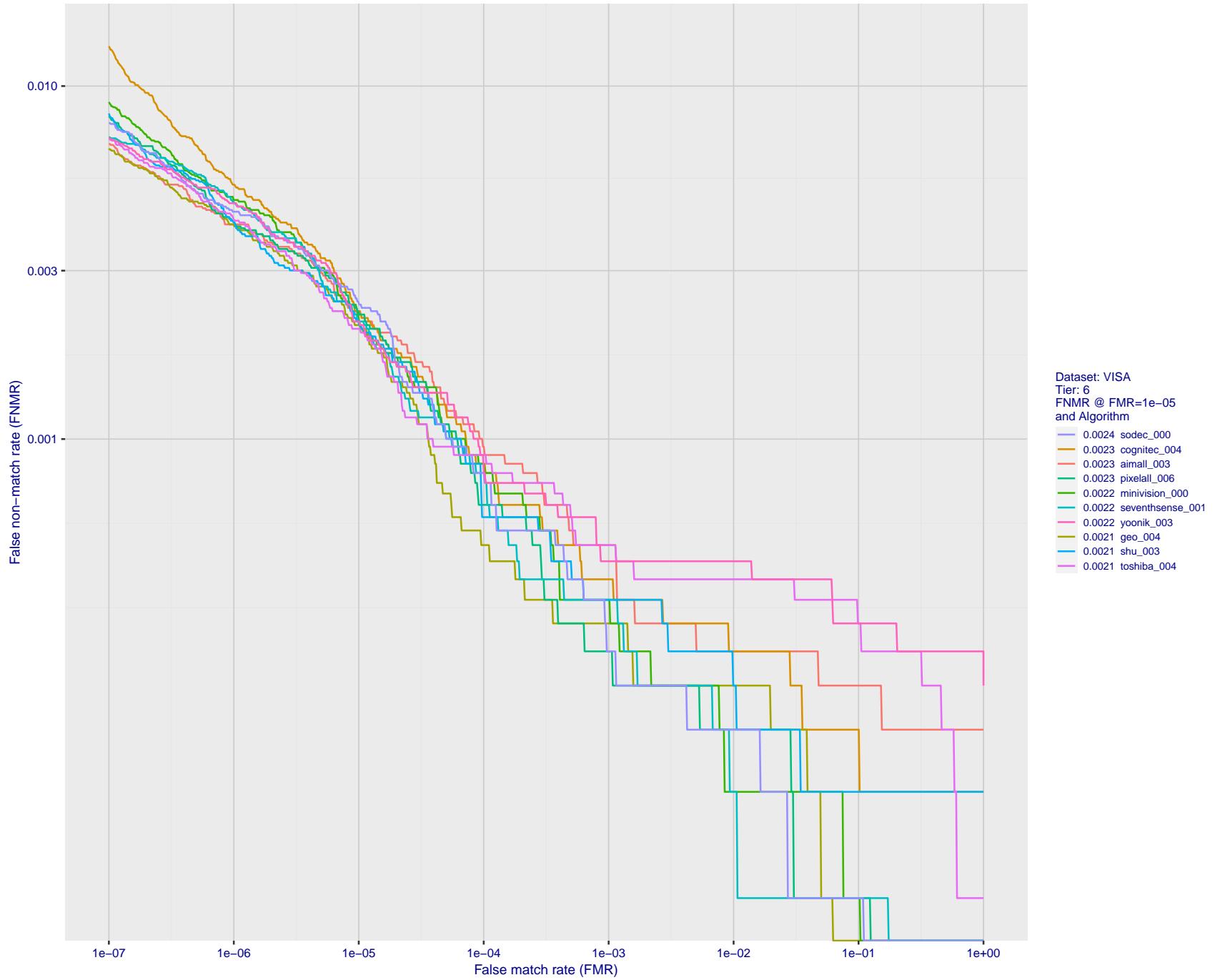


Figure 25: For the visa images, detection error tradeoff (DET) characteristics showing false non-match rate vs. false match rate plotted parametrically on threshold, T . The scales are logarithmic in order to show many decades of FMR.

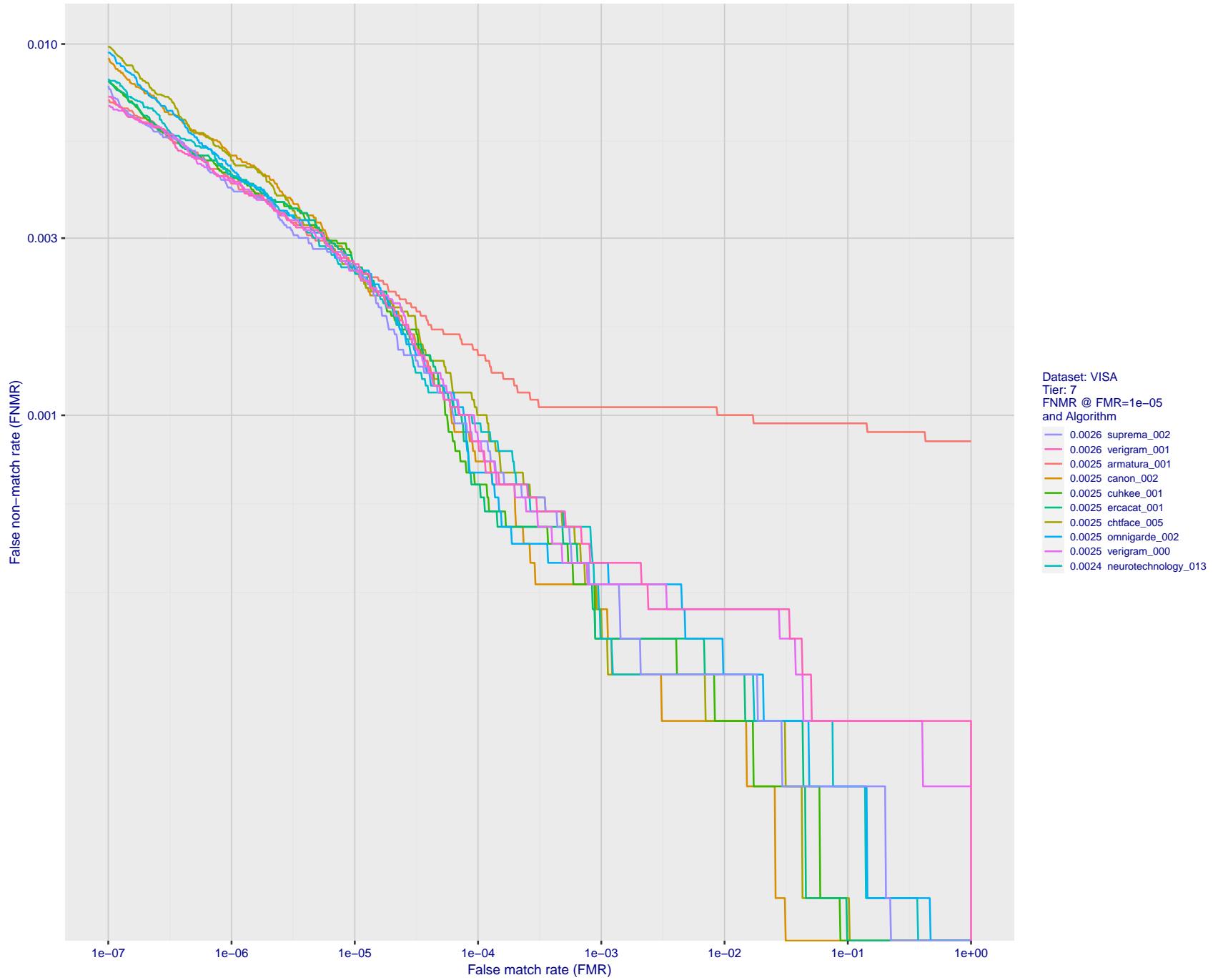


Figure 26: For the visa images, detection error tradeoff (DET) characteristics showing false non-match rate vs. false match rate plotted parametrically on threshold, T . The scales are logarithmic in order to show many decades of FMR.

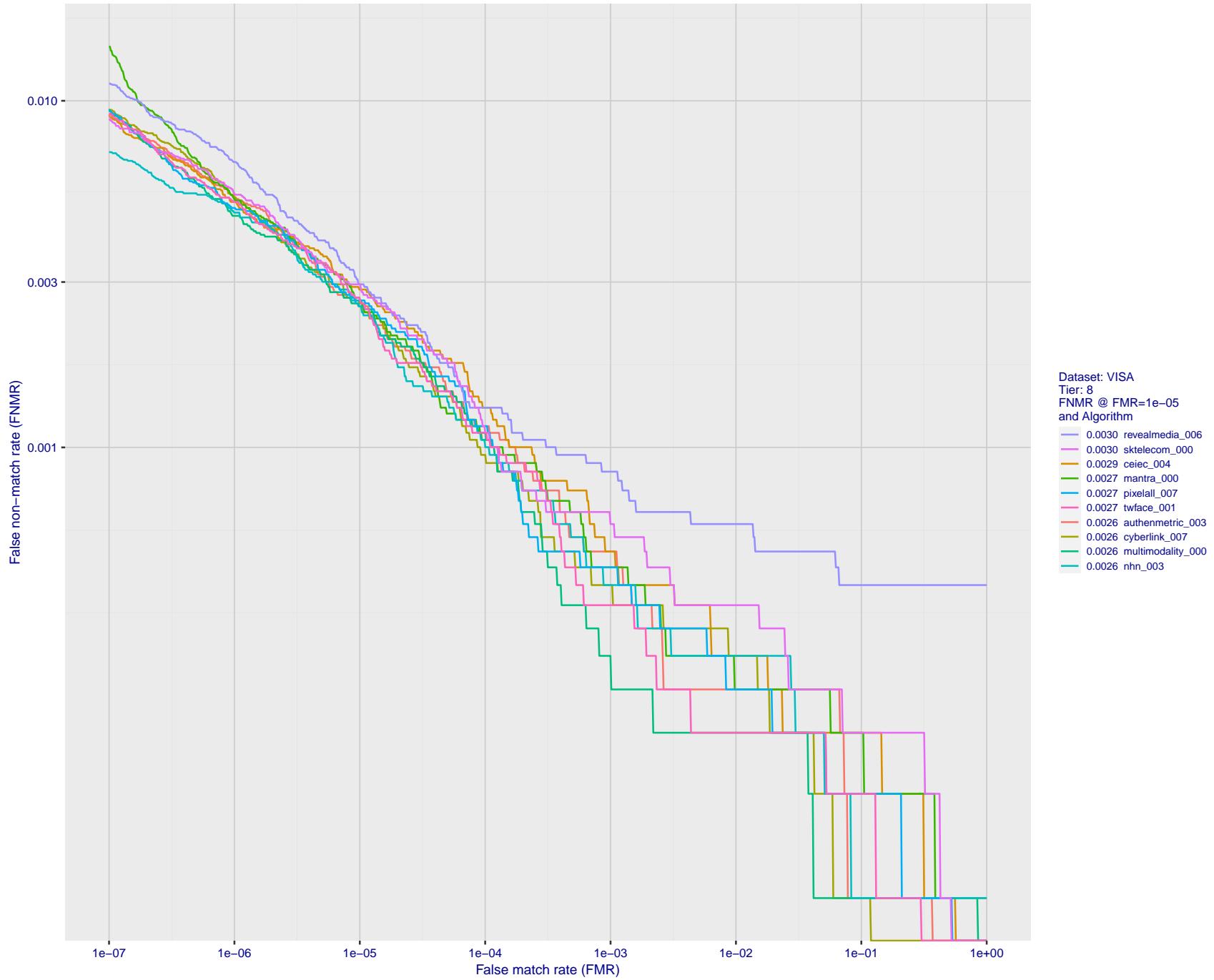


Figure 27: For the visa images, detection error tradeoff (DET) characteristics showing false non-match rate vs. false match rate plotted parametrically on threshold, T . The scales are logarithmic in order to show many decades of FMR.

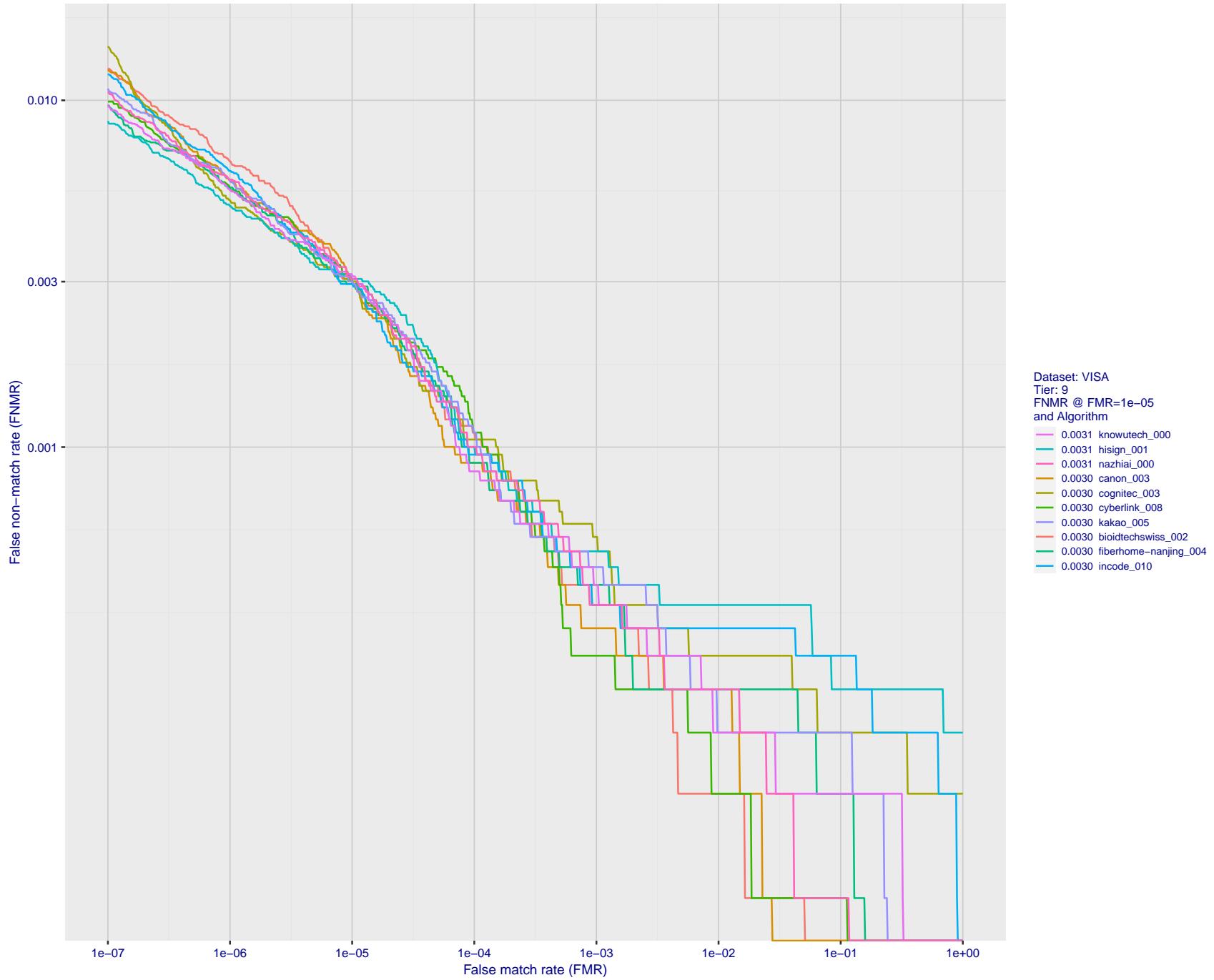


Figure 28: For the visa images, detection error tradeoff (DET) characteristics showing false non-match rate vs. false match rate plotted parametrically on threshold, T . The scales are logarithmic in order to show many decades of FMR.

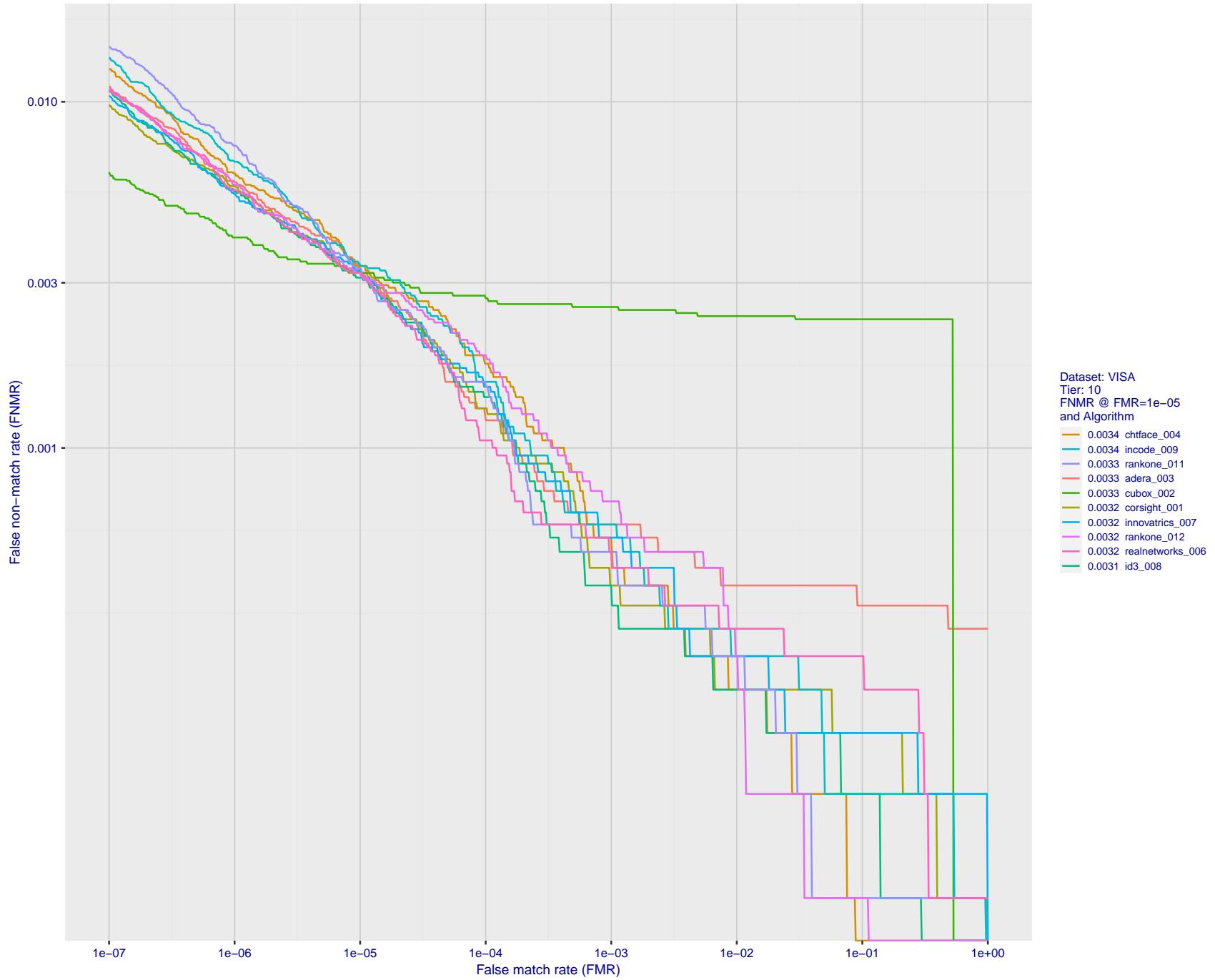


Figure 29: For the visa images, detection error tradeoff (DET) characteristics showing false non-match rate vs. false match rate plotted parametrically on threshold, T . The scales are logarithmic in order to show many decades of FMR.

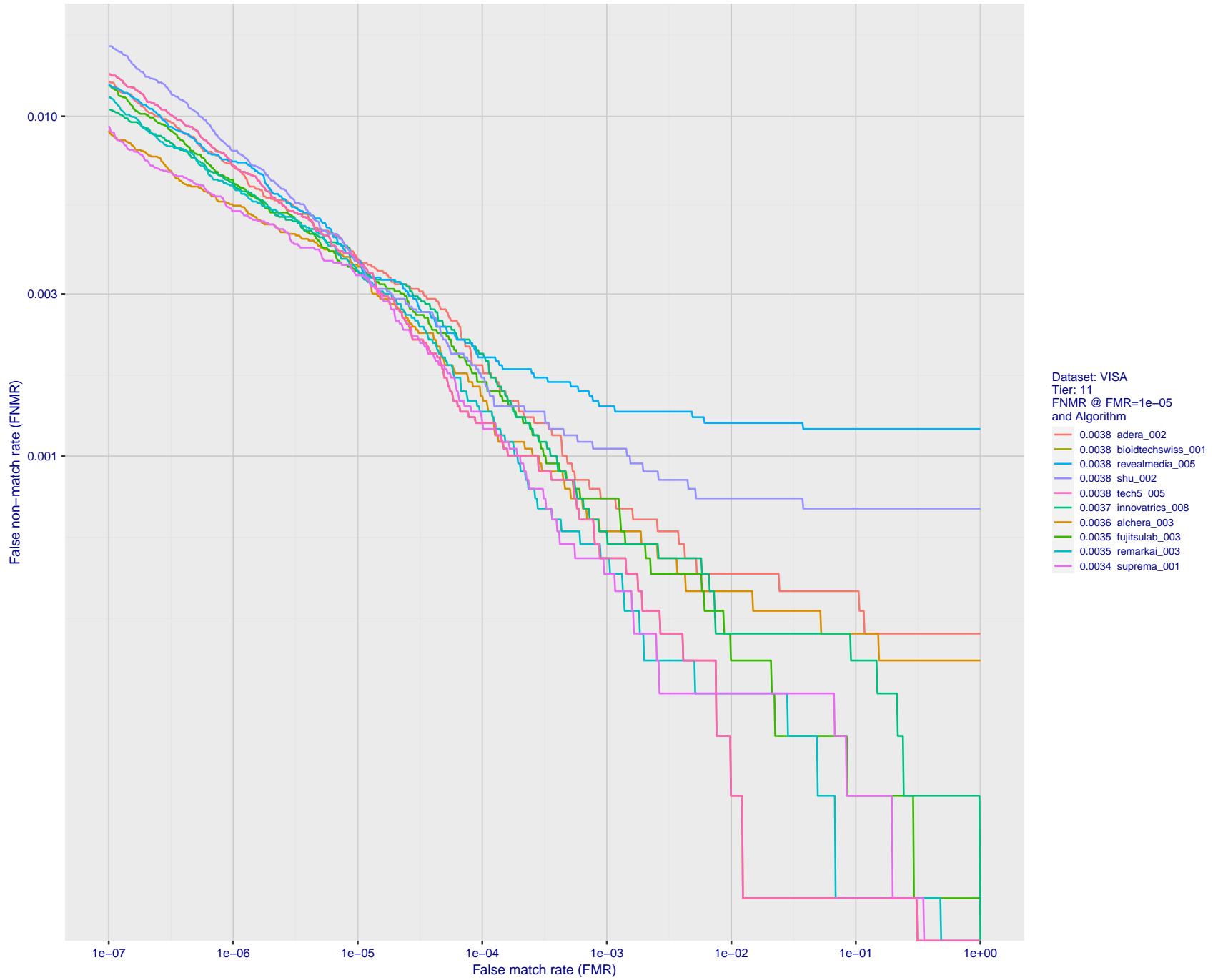


Figure 30: For the visa images, detection error tradeoff (DET) characteristics showing false non-match rate vs. false match rate plotted parametrically on threshold, T . The scales are logarithmic in order to show many decades of FMR.

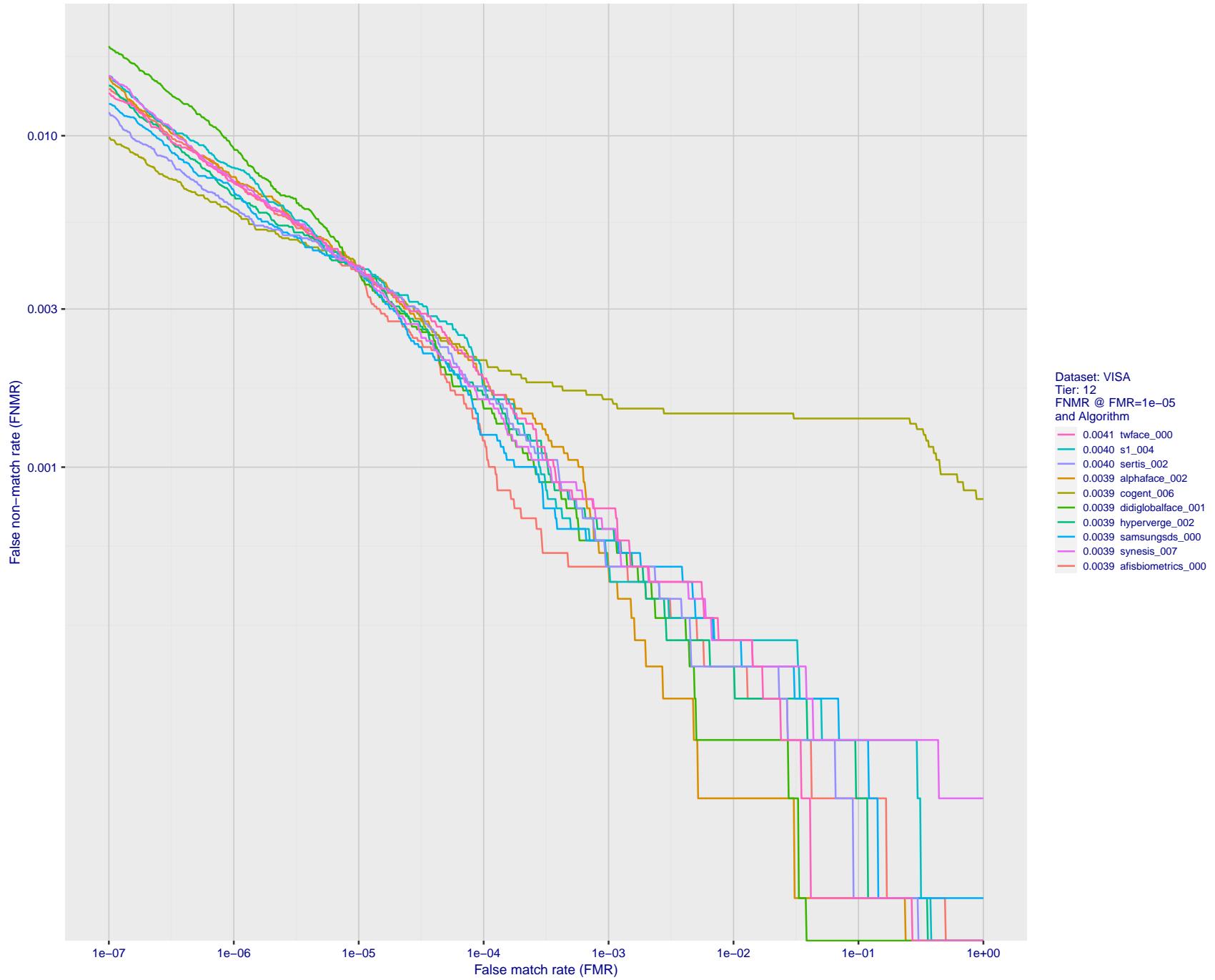


Figure 31: For the visa images, detection error tradeoff (DET) characteristics showing false non-match rate vs. false match rate plotted parametrically on threshold, T . The scales are logarithmic in order to show many decades of FMR.

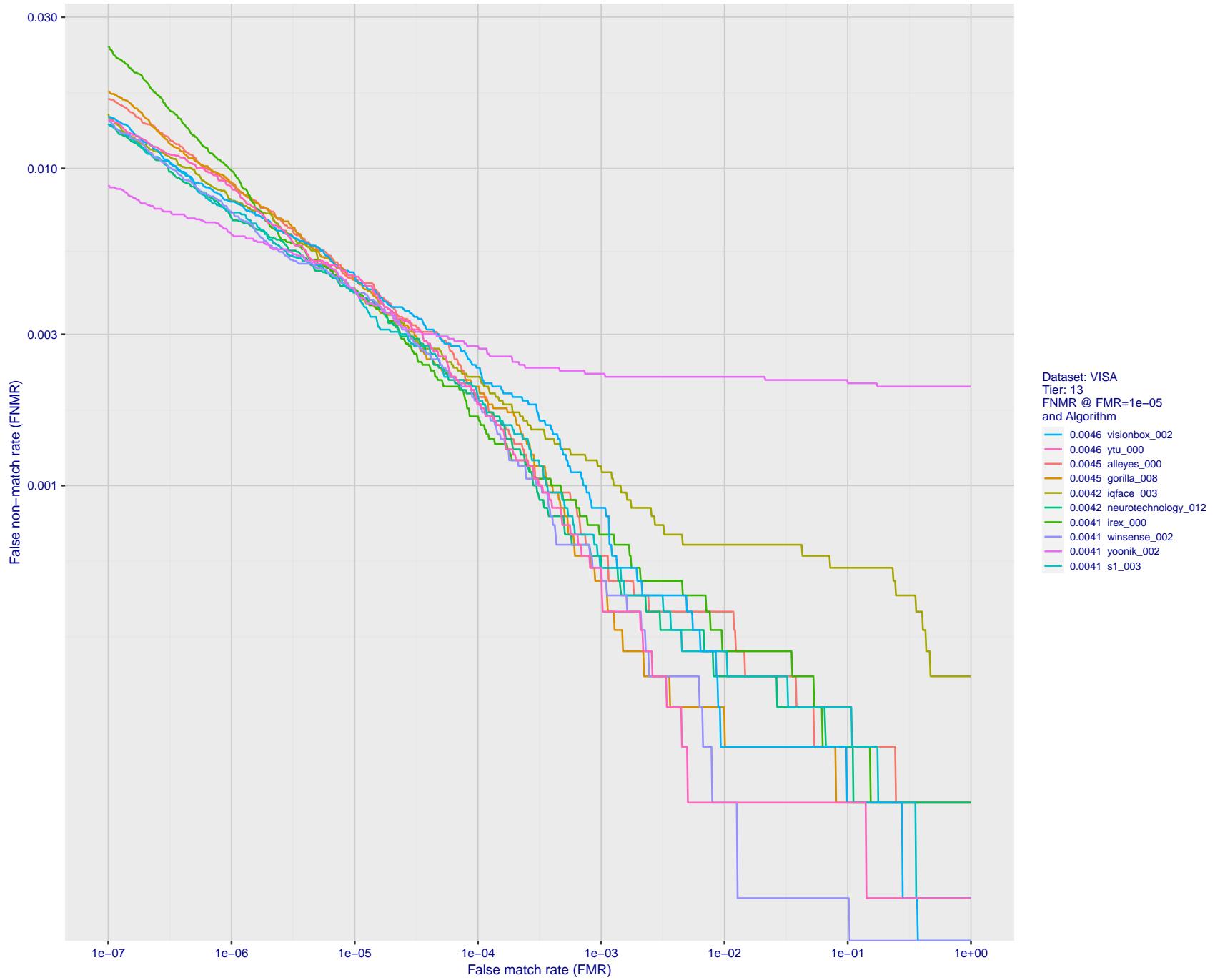


Figure 32: For the visa images, detection error tradeoff (DET) characteristics showing false non-match rate vs. false match rate plotted parametrically on threshold, T . The scales are logarithmic in order to show many decades of FMR.

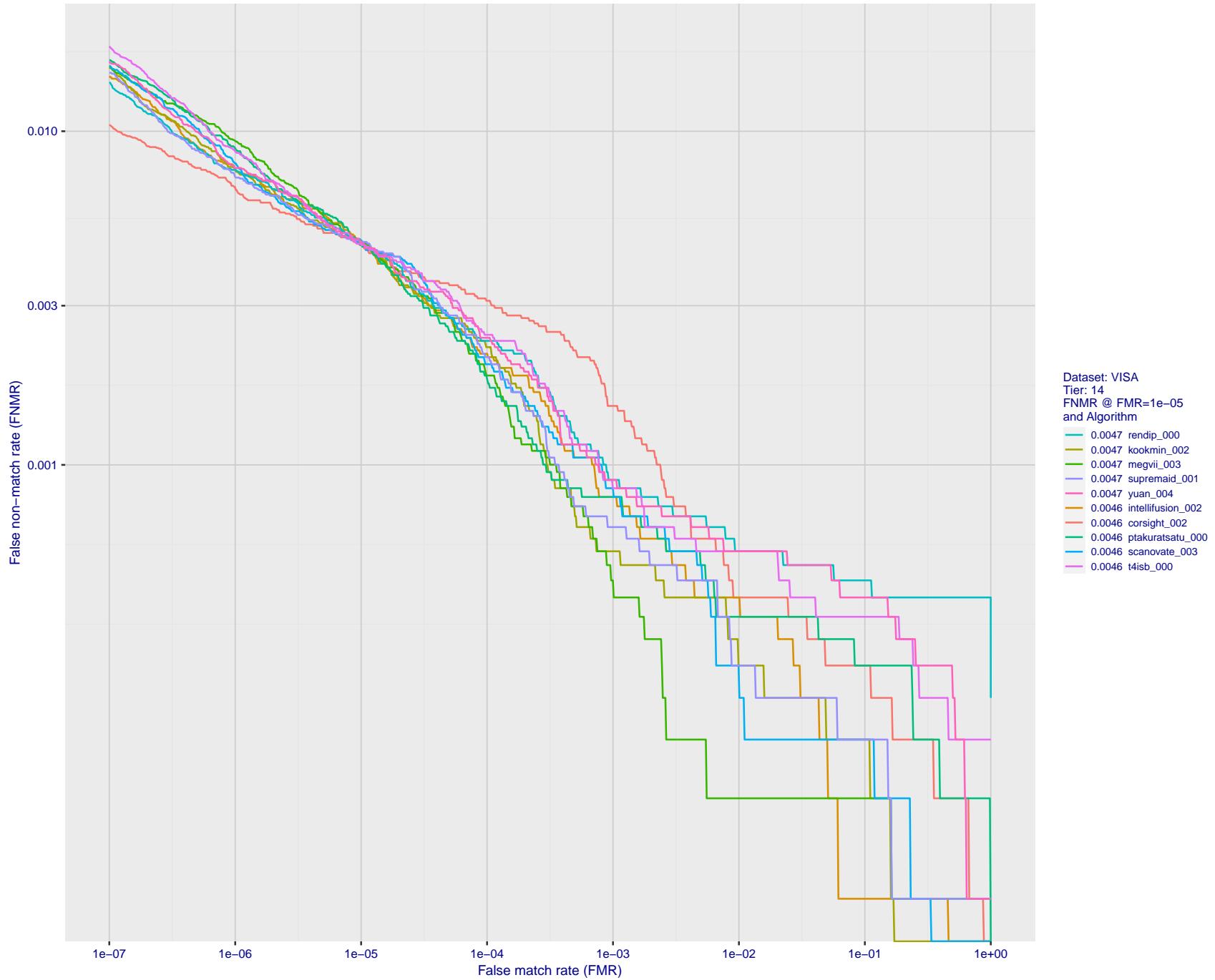


Figure 33: For the visa images, detection error tradeoff (DET) characteristics showing false non-match rate vs. false match rate plotted parametrically on threshold, T . The scales are logarithmic in order to show many decades of FMR.

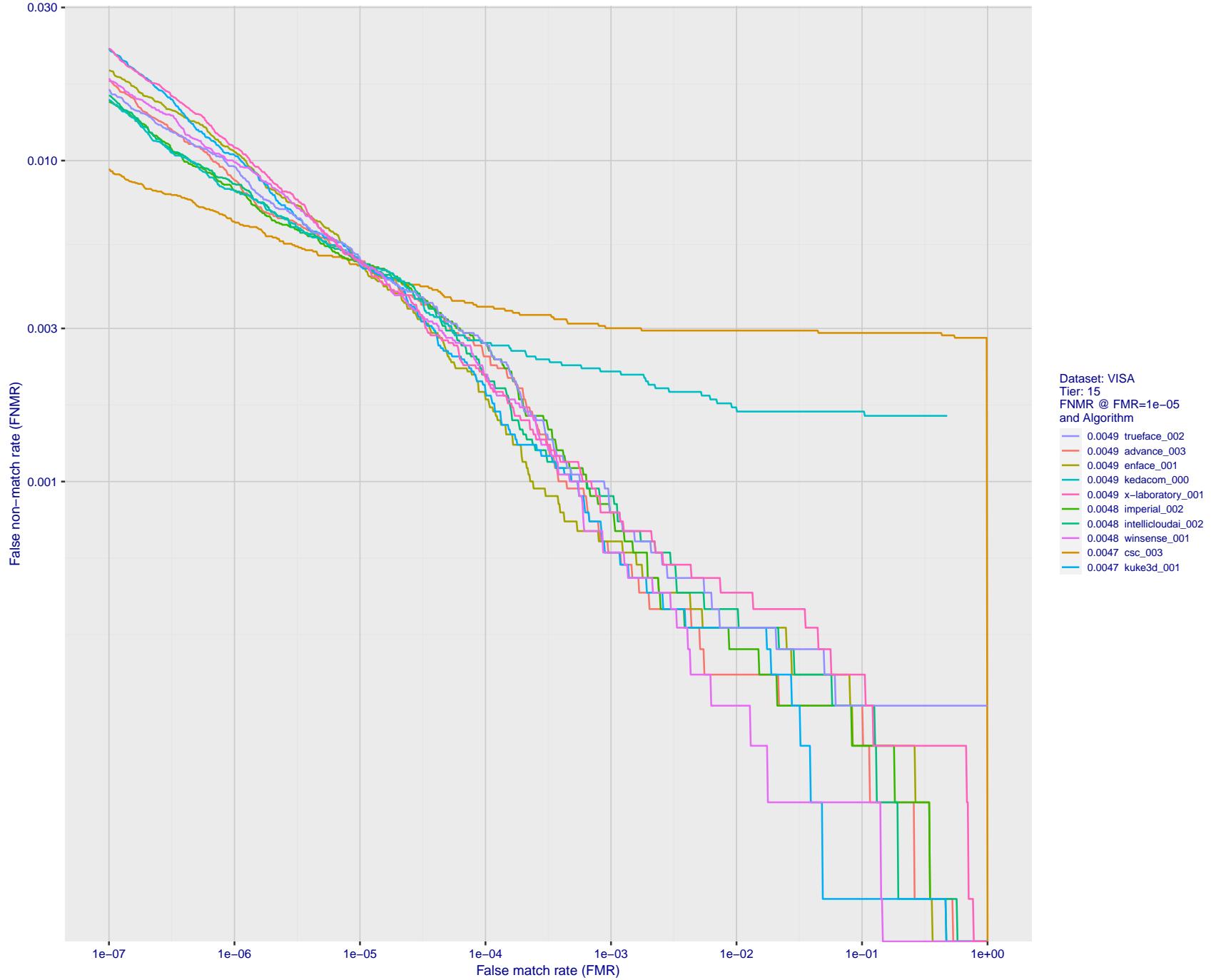


Figure 34: For the visa images, detection error tradeoff (DET) characteristics showing false non-match rate vs. false match rate plotted parametrically on threshold, T . The scales are logarithmic in order to show many decades of FMR.

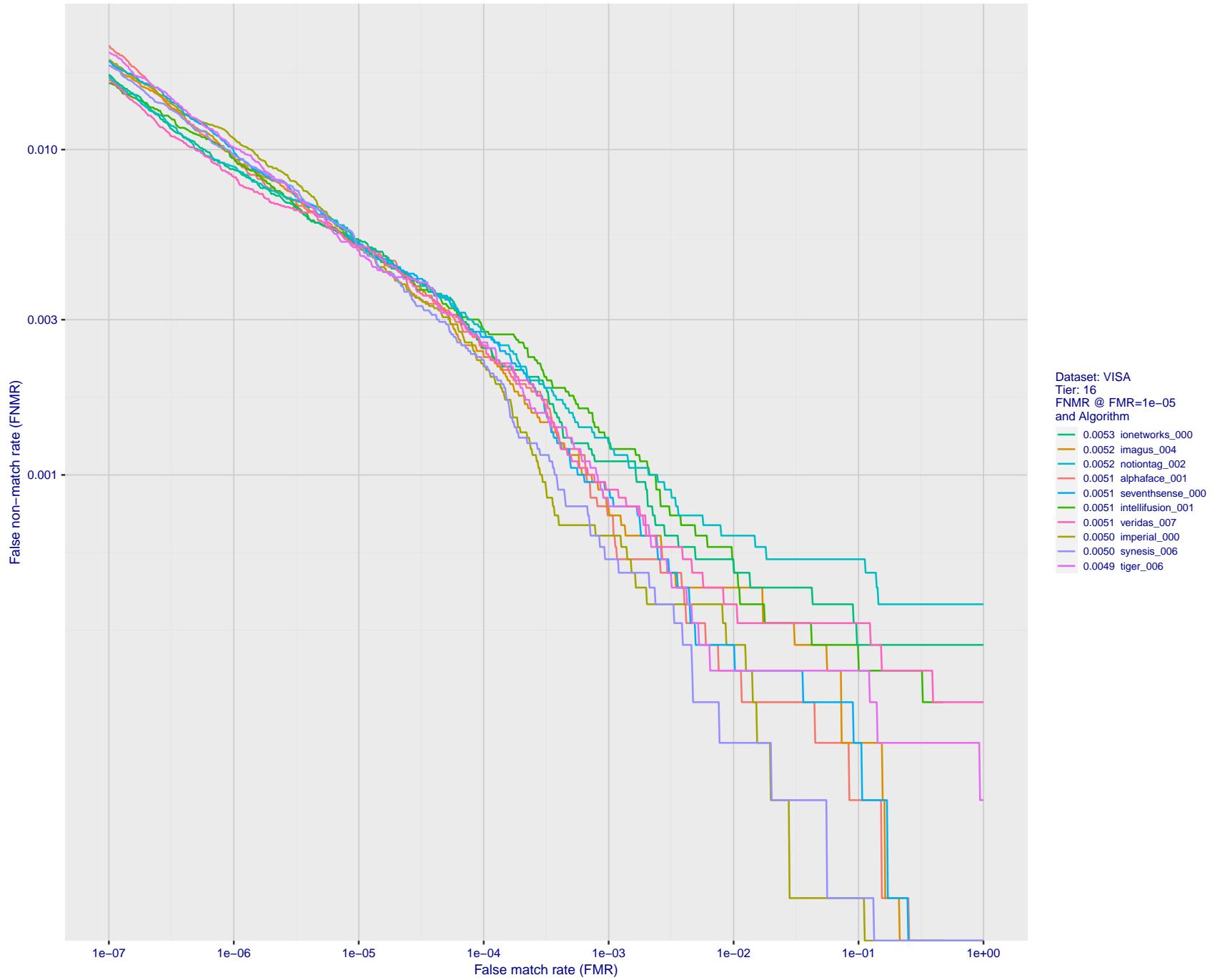


Figure 35: For the visa images, detection error tradeoff (DET) characteristics showing false non-match rate vs. false match rate plotted parametrically on threshold, T . The scales are logarithmic in order to show many decades of FMR.

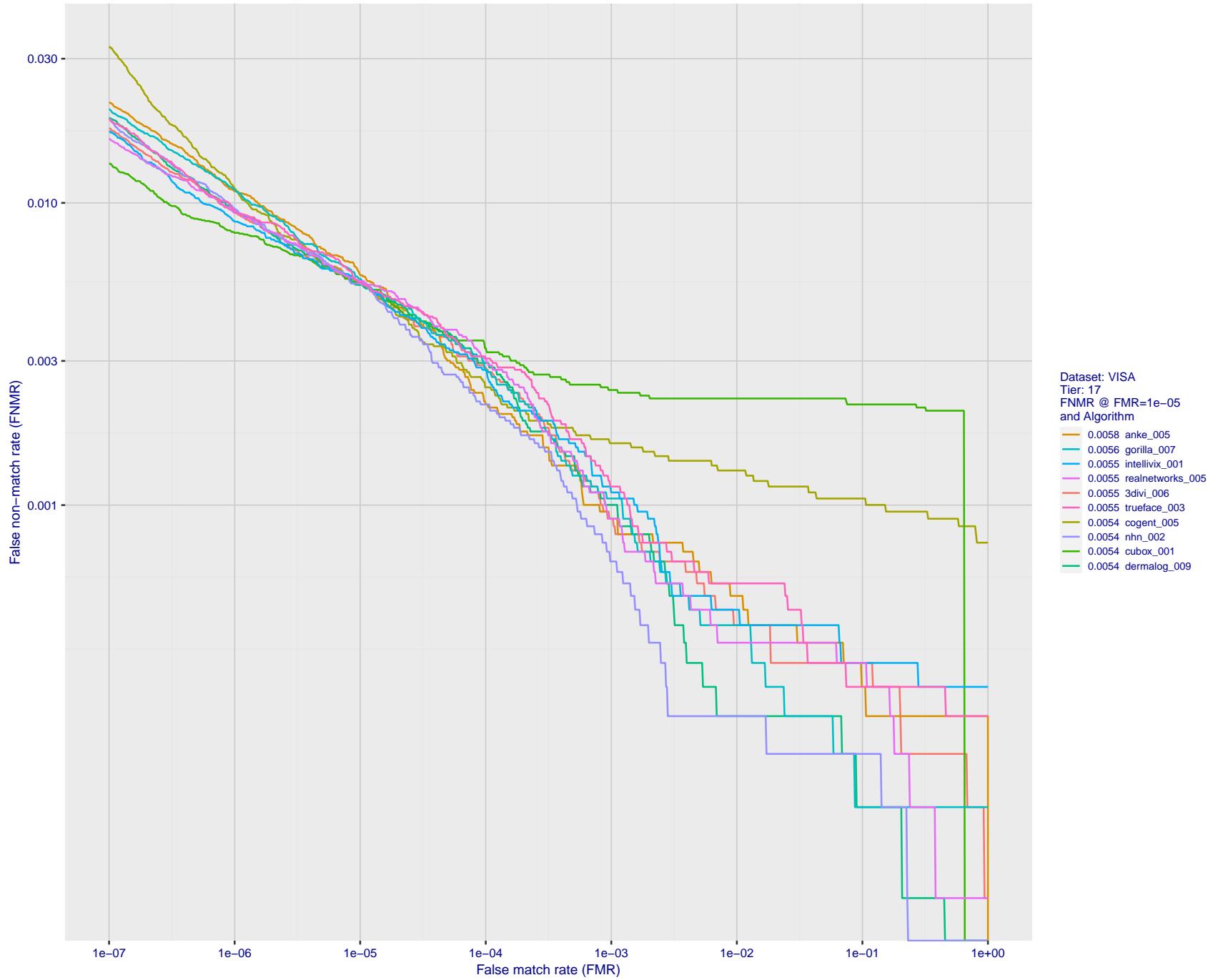


Figure 36: For the visa images, detection error tradeoff (DET) characteristics showing false non-match rate vs. false match rate plotted parametrically on threshold, T . The scales are logarithmic in order to show many decades of FMR.

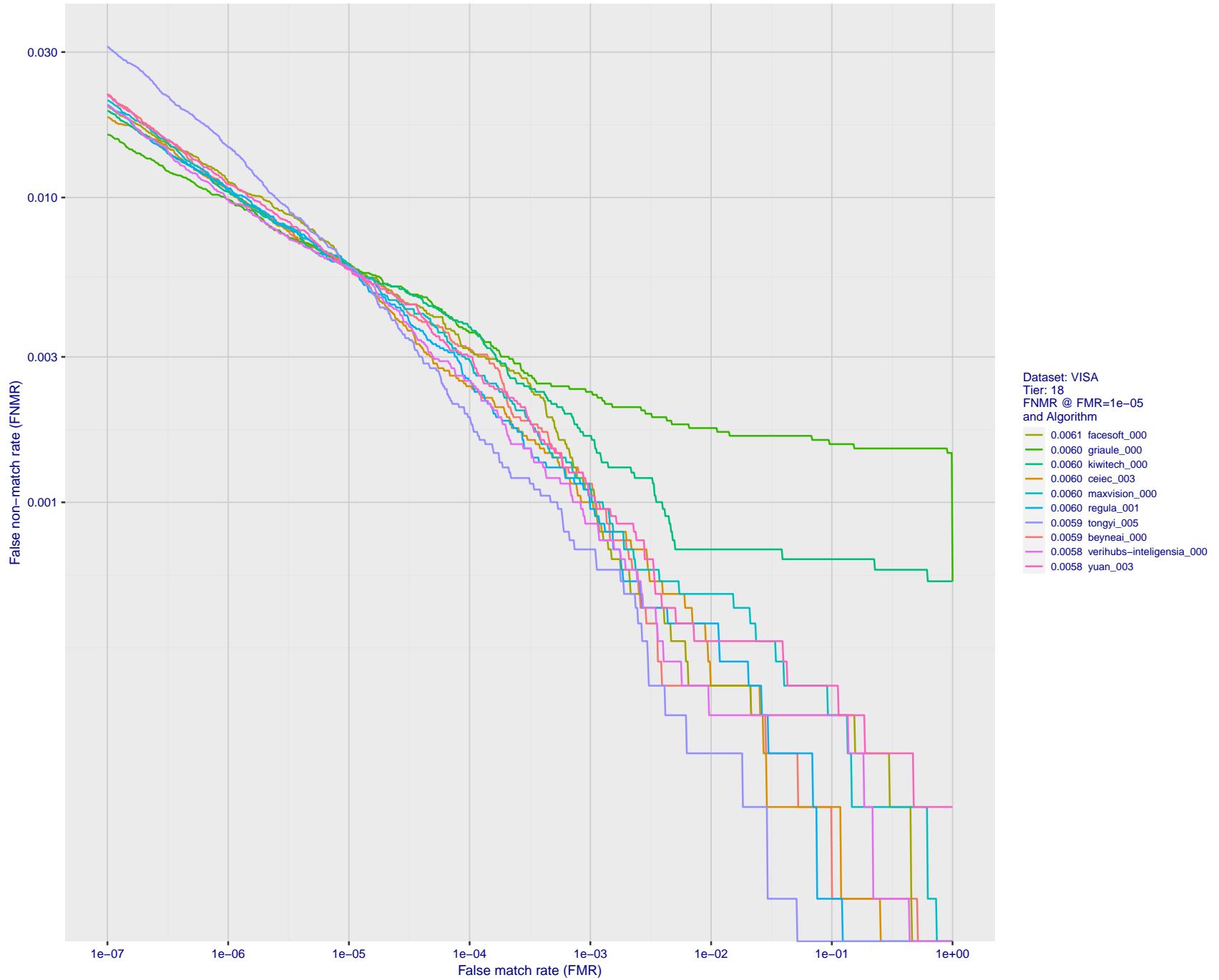


Figure 37: For the visa images, detection error tradeoff (DET) characteristics showing false non-match rate vs. false match rate plotted parametrically on threshold, T . The scales are logarithmic in order to show many decades of FMR.

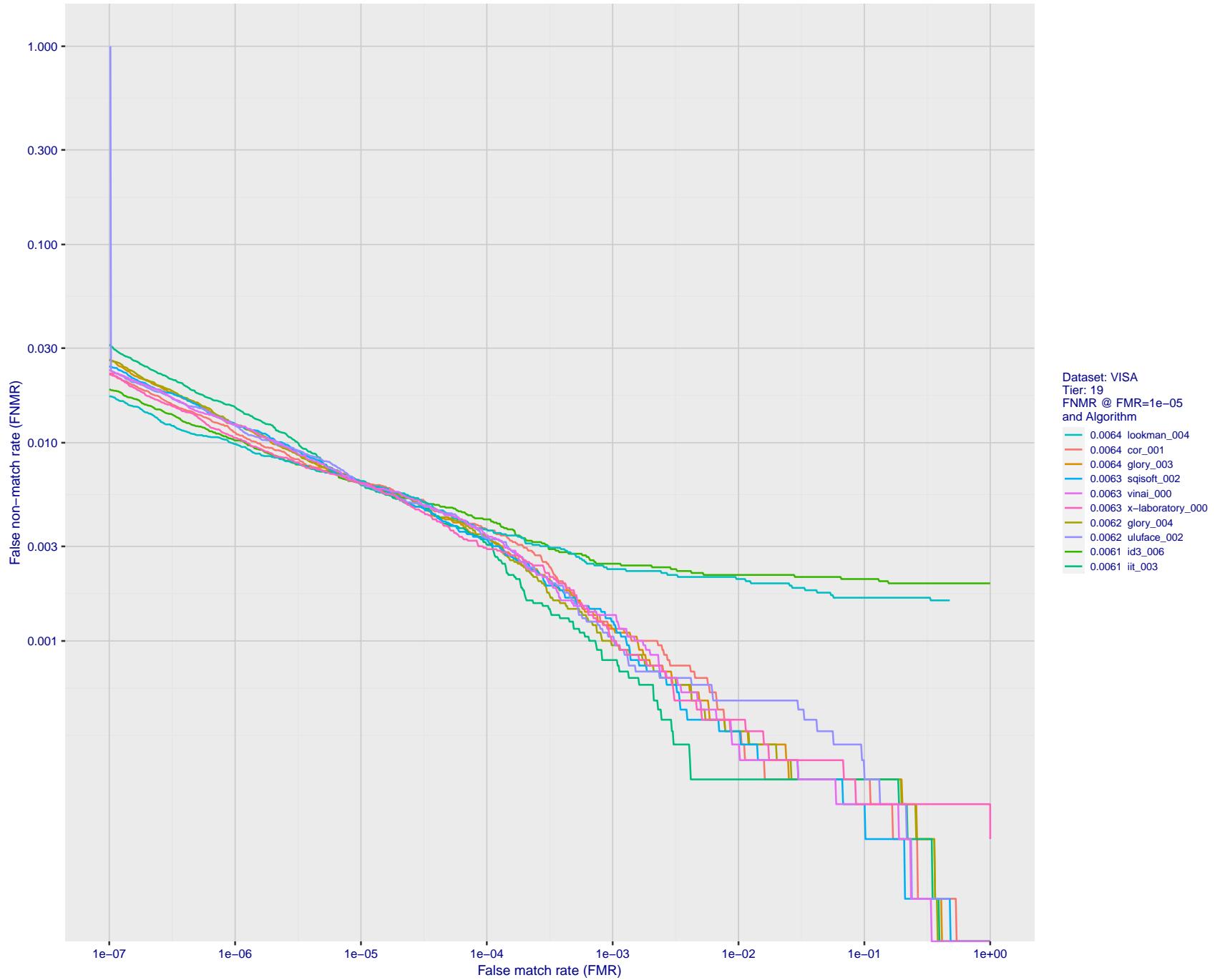


Figure 38: For the visa images, detection error tradeoff (DET) characteristics showing false non-match rate vs. false match rate plotted parametrically on threshold, T . The scales are logarithmic in order to show many decades of FMR.

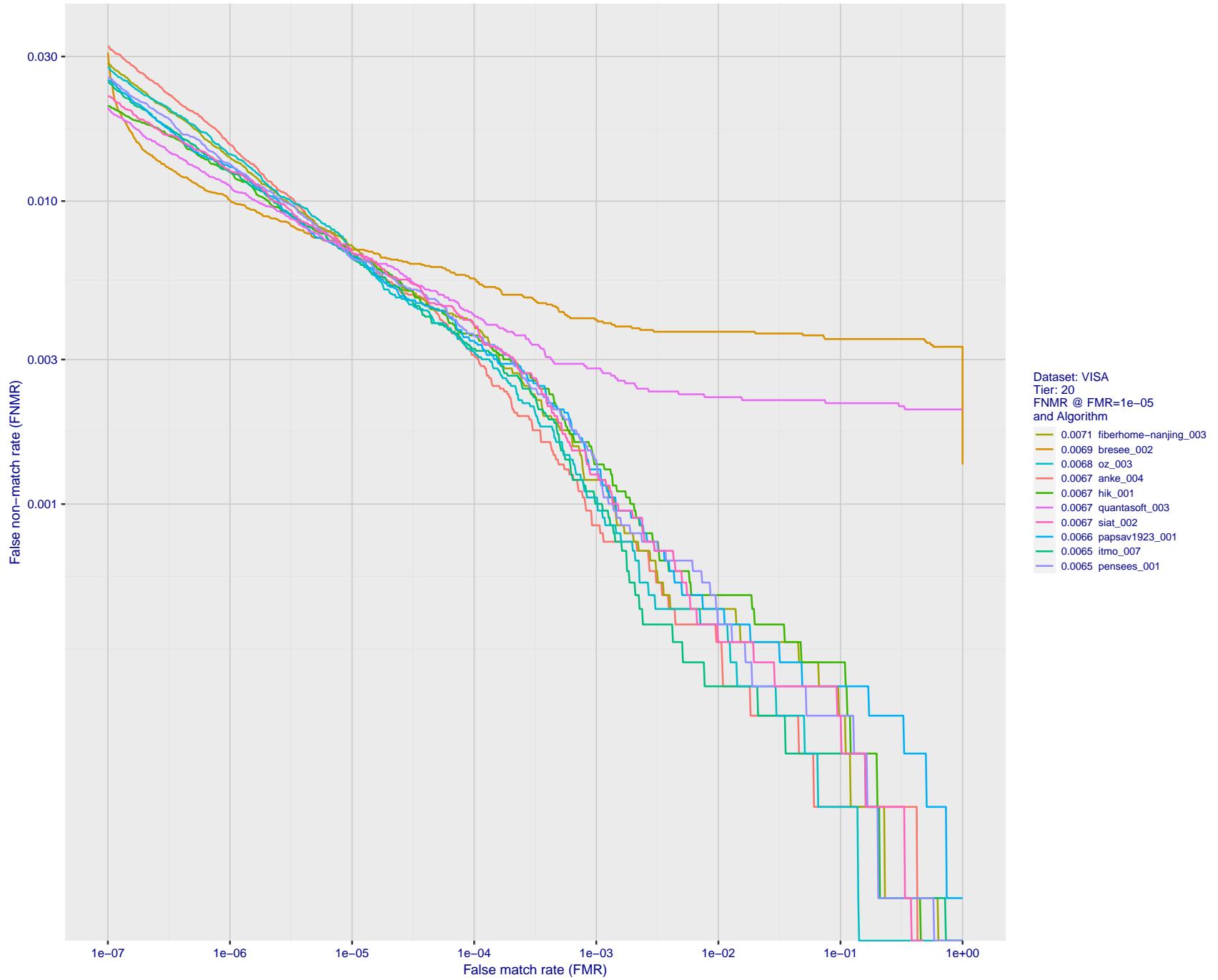


Figure 39: For the visa images, detection error tradeoff (DET) characteristics showing false non-match rate vs. false match rate plotted parametrically on threshold, T . The scales are logarithmic in order to show many decades of FMR.

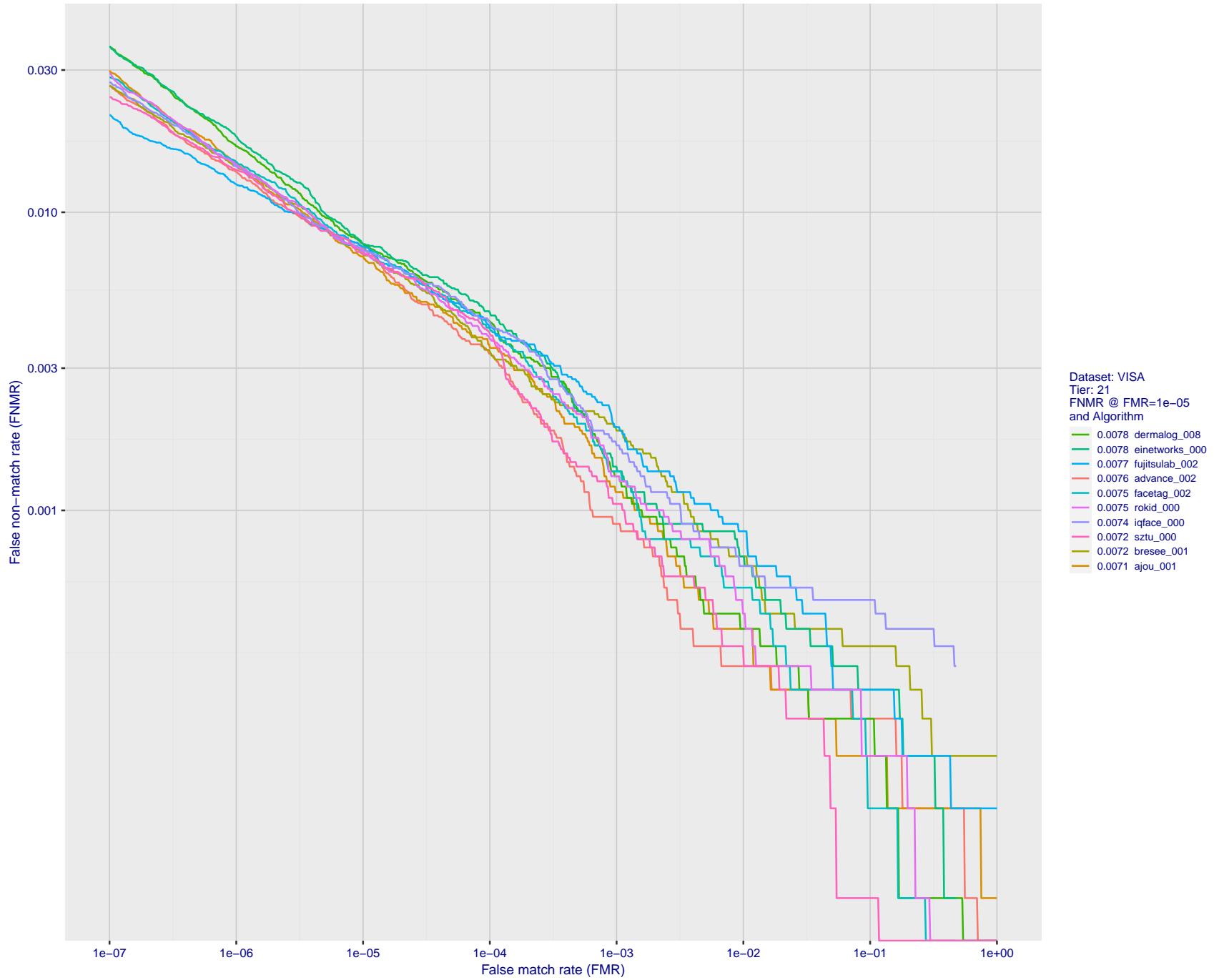


Figure 40: For the visa images, detection error tradeoff (DET) characteristics showing false non-match rate vs. false match rate plotted parametrically on threshold, T . The scales are logarithmic in order to show many decades of FMR.

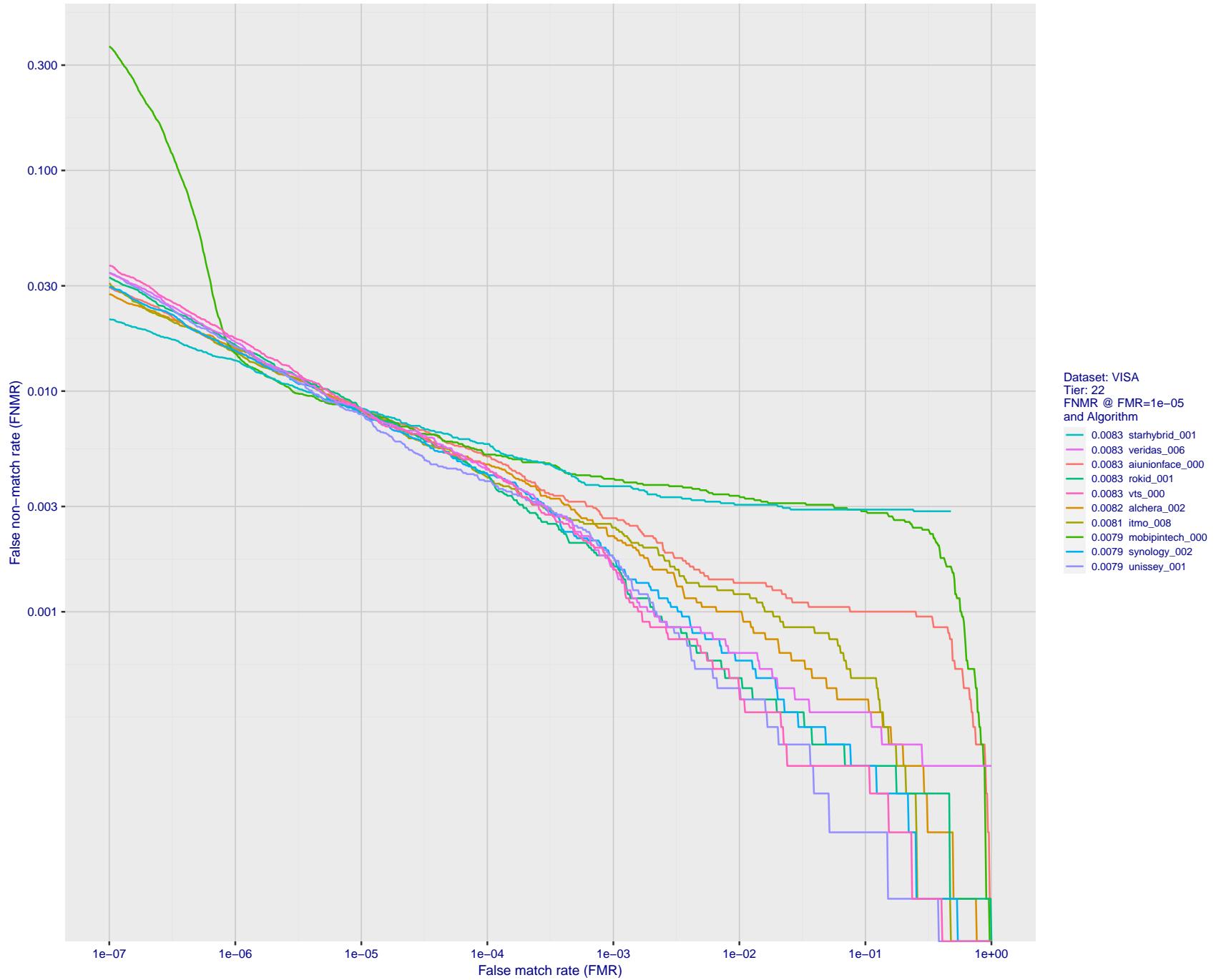


Figure 41: For the visa images, detection error tradeoff (DET) characteristics showing false non-match rate vs. false match rate plotted parametrically on threshold, T . The scales are logarithmic in order to show many decades of FMR.

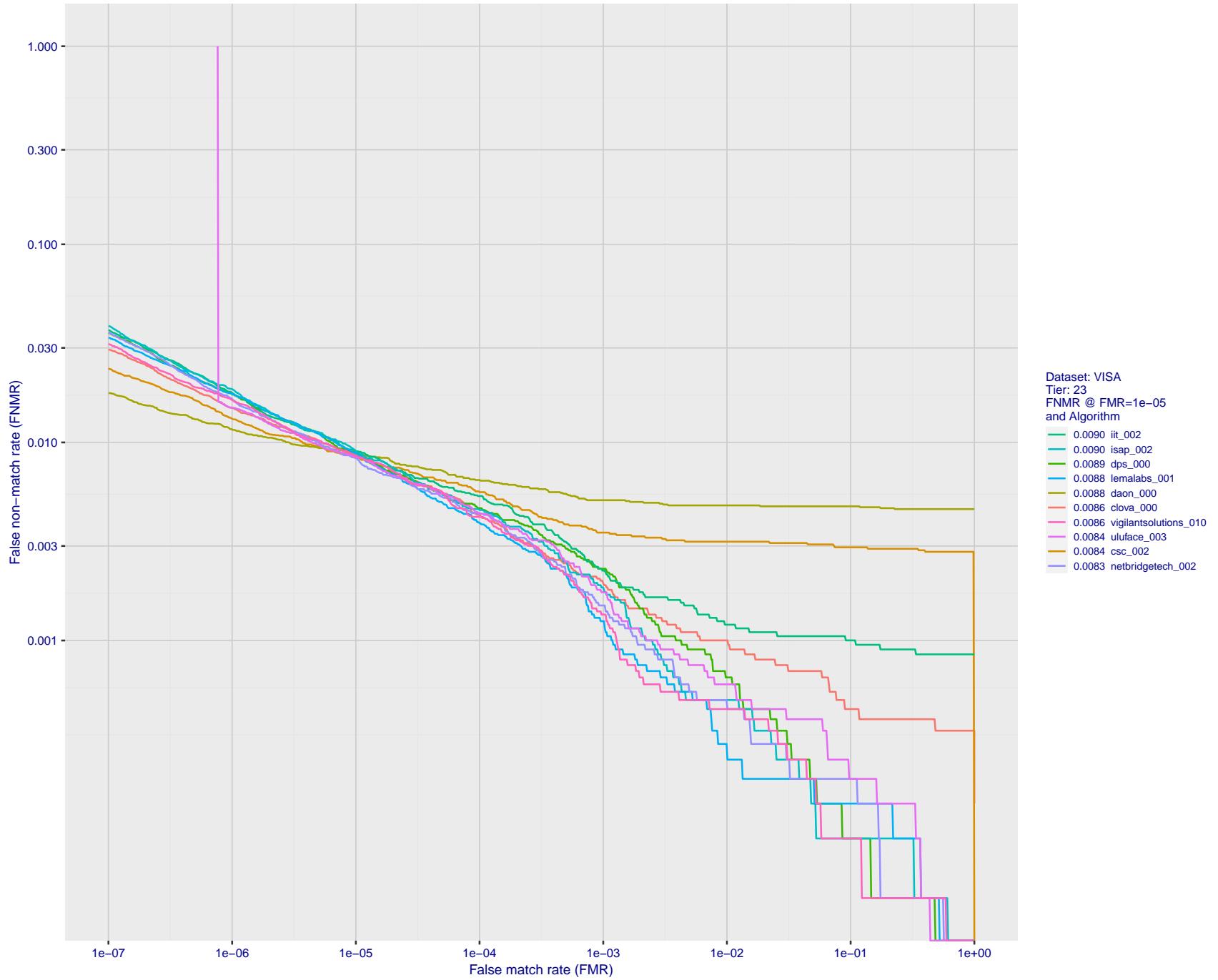


Figure 42: For the visa images, detection error tradeoff (DET) characteristics showing false non-match rate vs. false match rate plotted parametrically on threshold, T . The scales are logarithmic in order to show many decades of FMR.

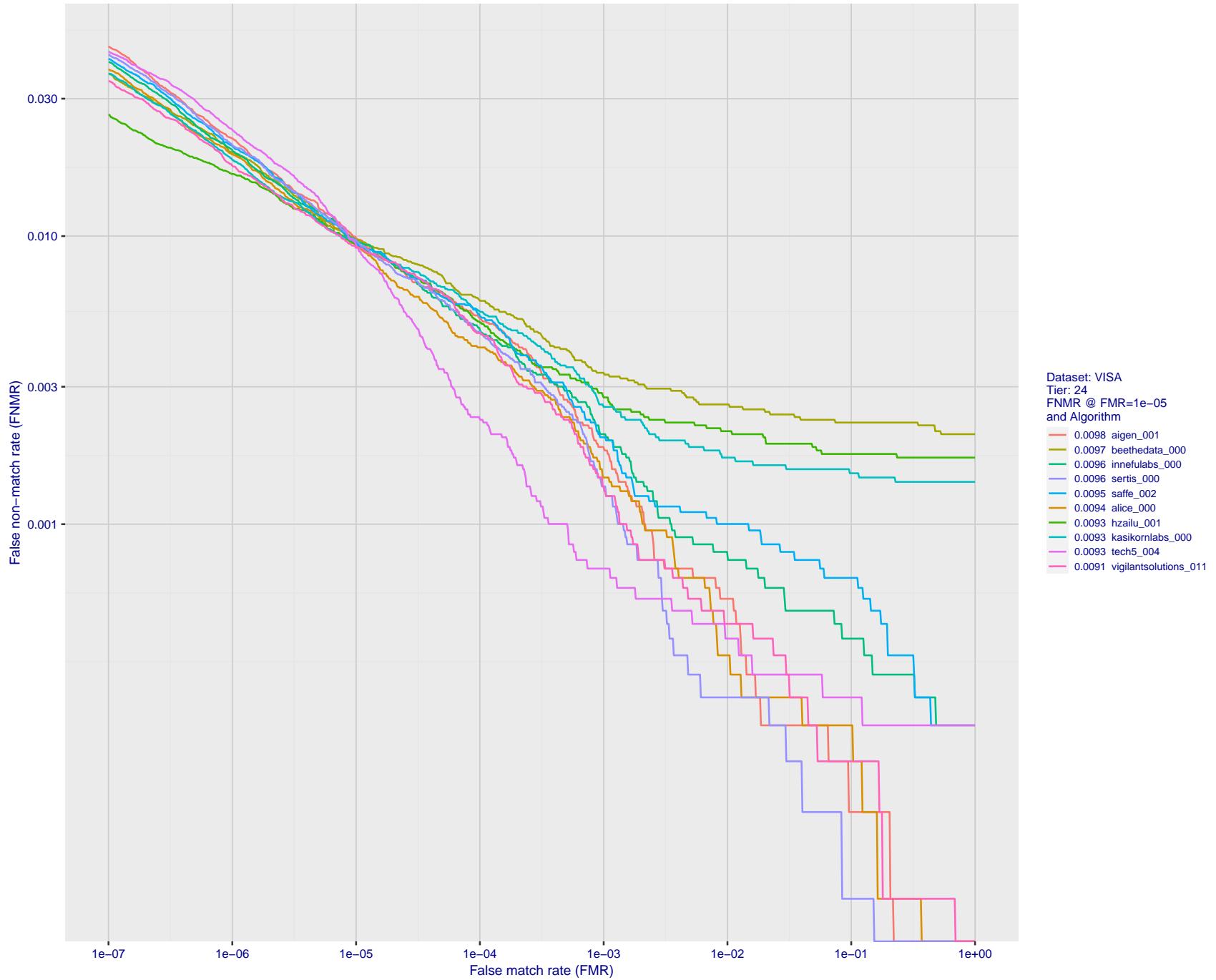


Figure 43: For the visa images, detection error tradeoff (DET) characteristics showing false non-match rate vs. false match rate plotted parametrically on threshold, T . The scales are logarithmic in order to show many decades of FMR.

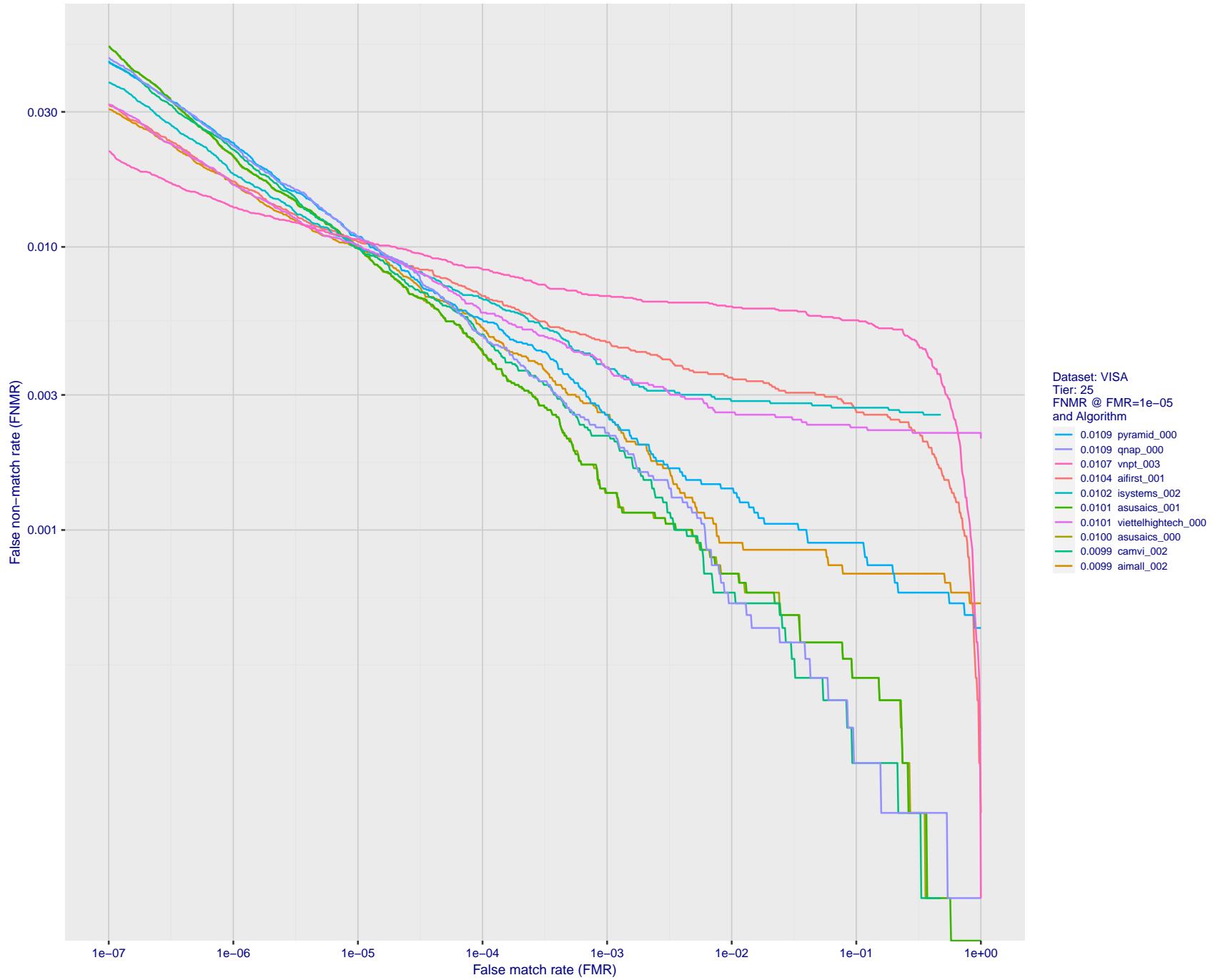


Figure 44: For the visa images, detection error tradeoff (DET) characteristics showing false non-match rate vs. false match rate plotted parametrically on threshold, T . The scales are logarithmic in order to show many decades of FMR.

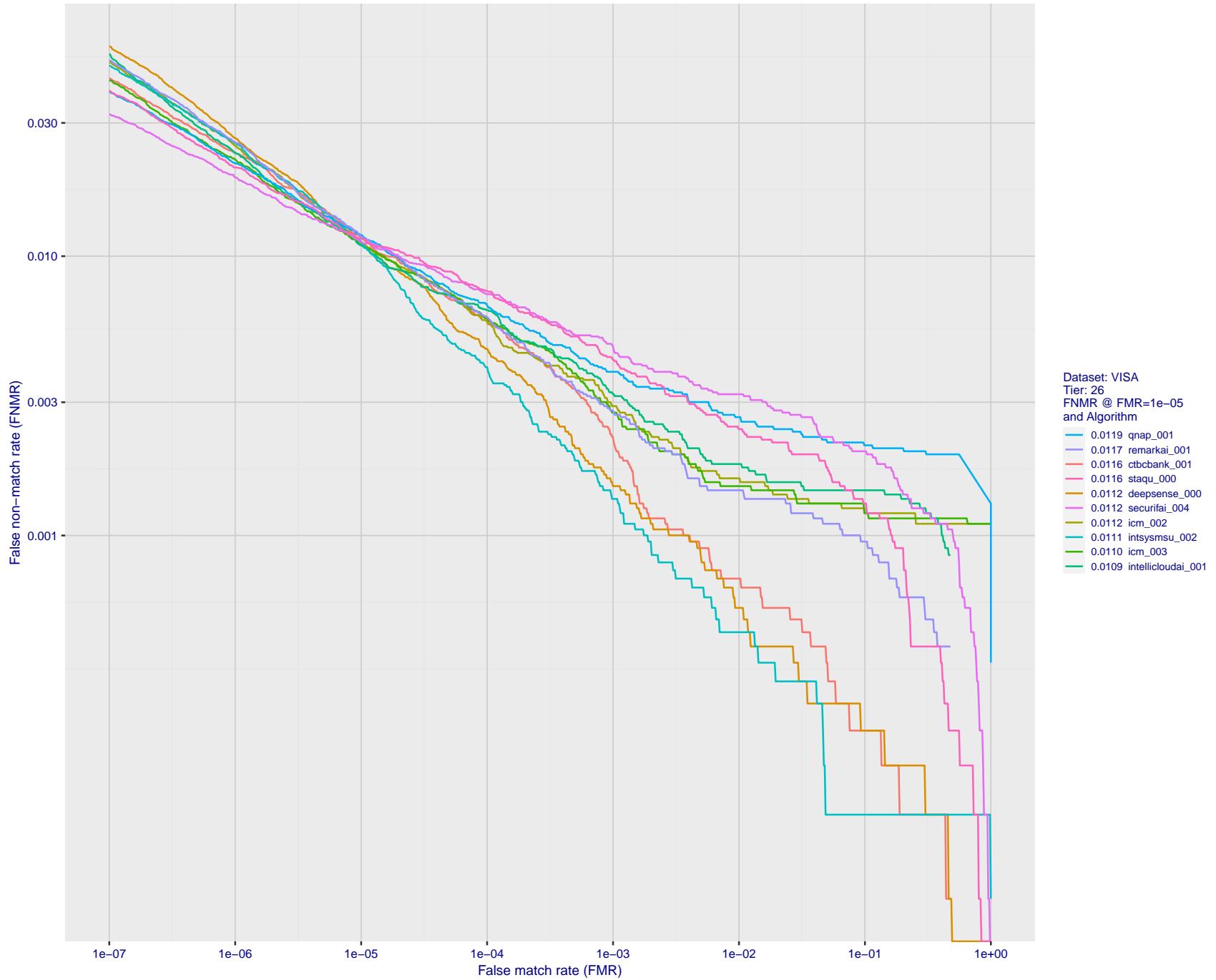


Figure 45: For the visa images, detection error tradeoff (DET) characteristics showing false non-match rate vs. false match rate plotted parametrically on threshold, T . The scales are logarithmic in order to show many decades of FMR.

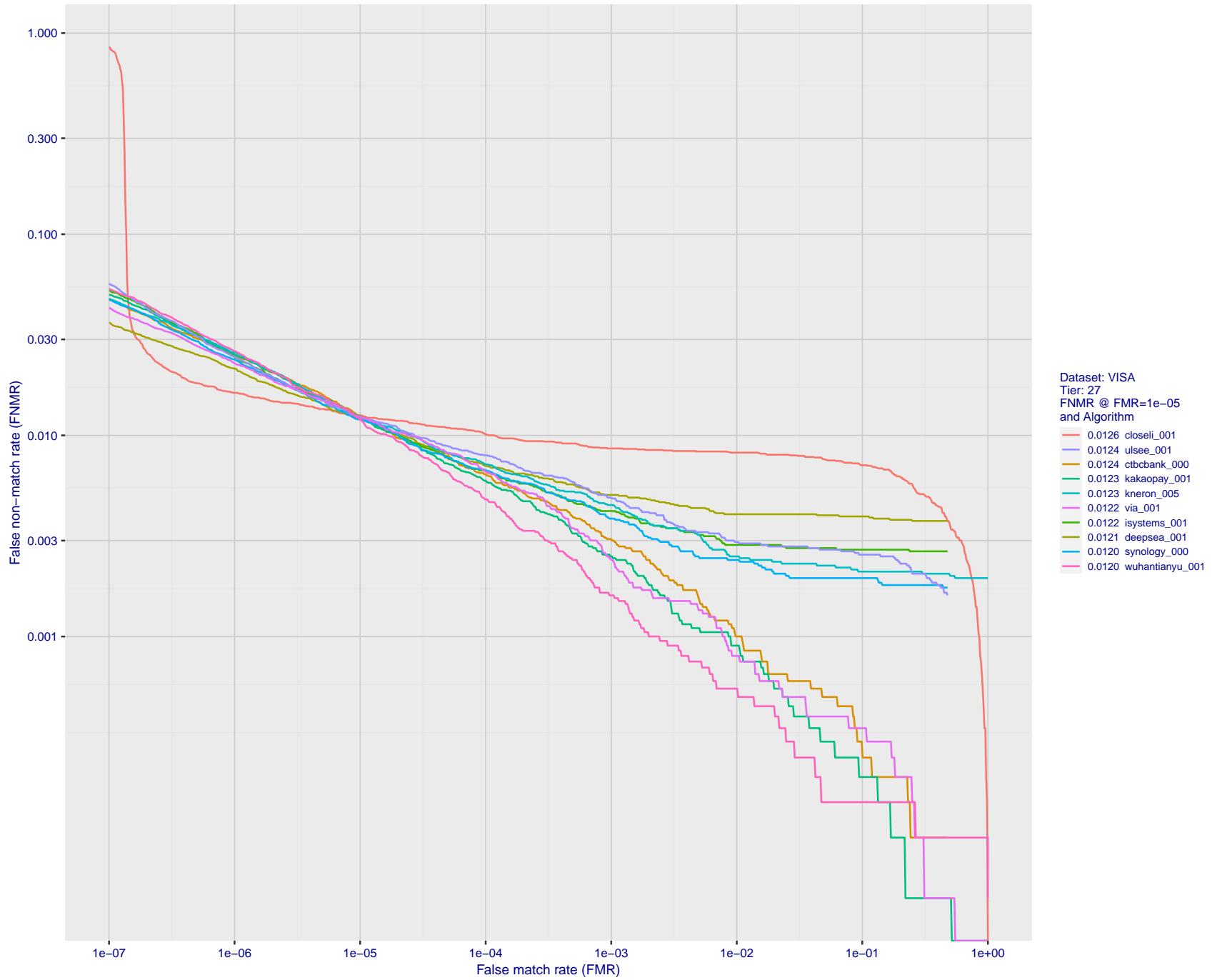


Figure 46: For the visa images, detection error tradeoff (DET) characteristics showing false non-match rate vs. false match rate plotted parametrically on threshold, T . The scales are logarithmic in order to show many decades of FMR.

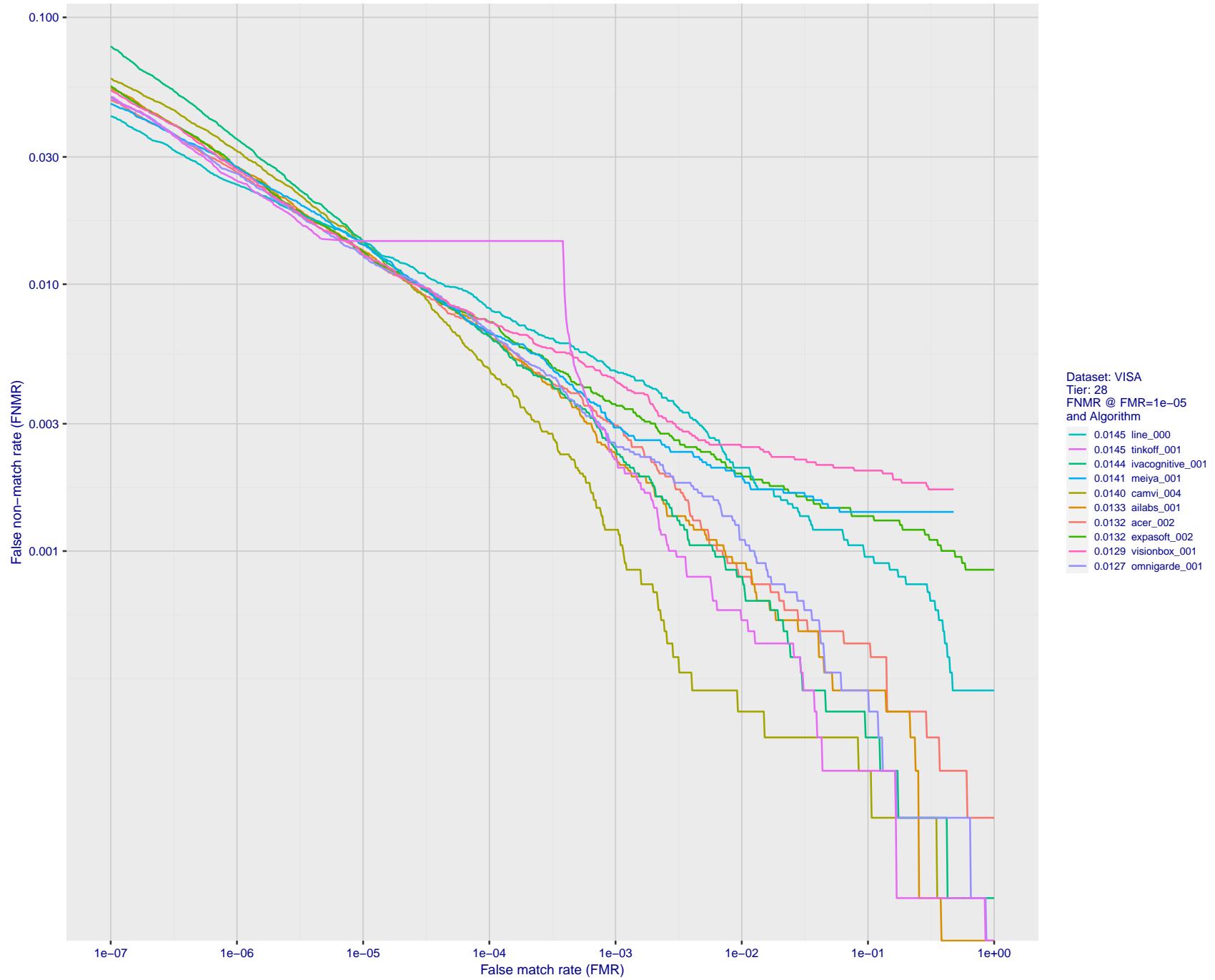


Figure 47: For the visa images, detection error tradeoff (DET) characteristics showing false non-match rate vs. false match rate plotted parametrically on threshold, T . The scales are logarithmic in order to show many decades of FMR.

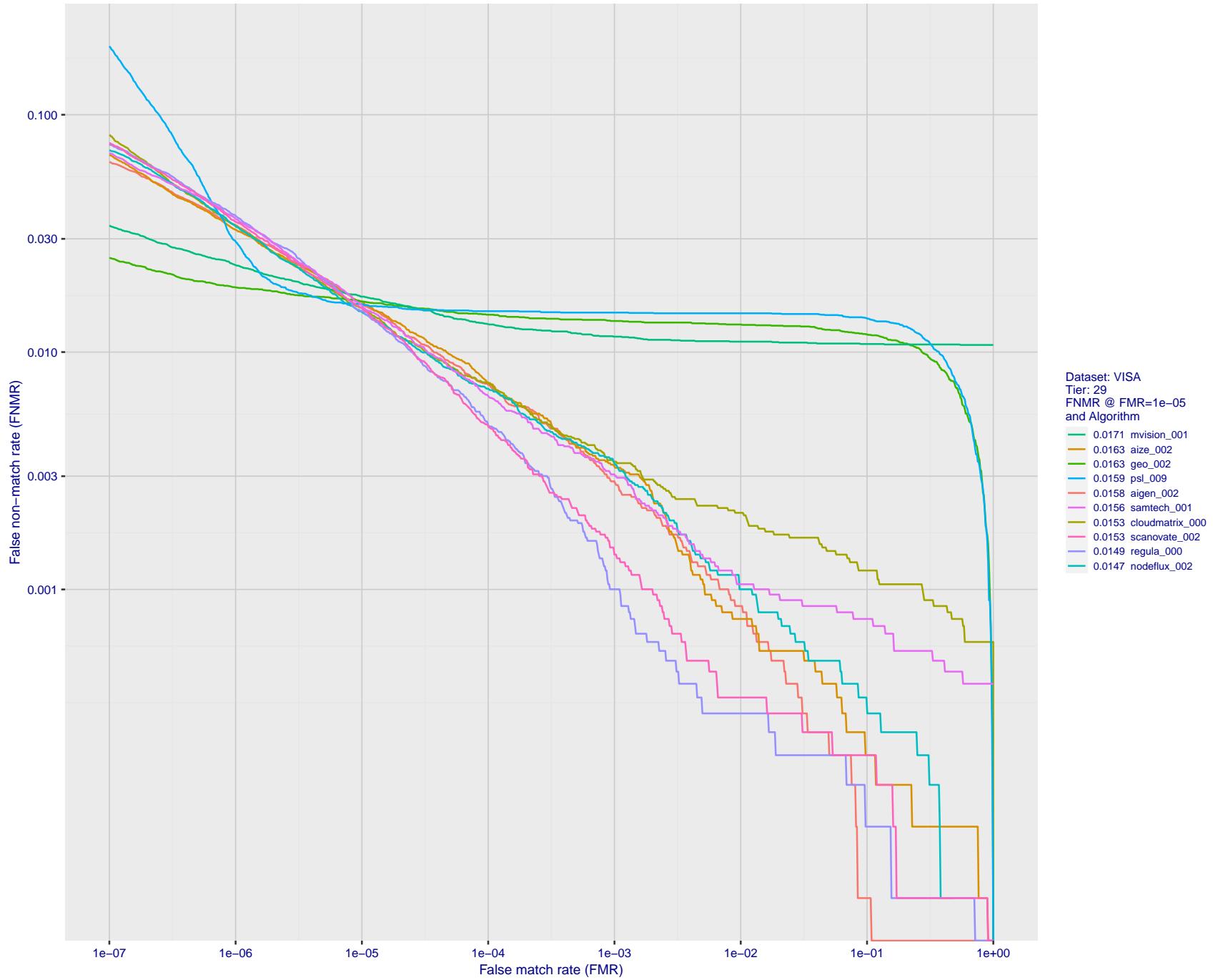


Figure 48: For the visa images, detection error tradeoff (DET) characteristics showing false non-match rate vs. false match rate plotted parametrically on threshold, T . The scales are logarithmic in order to show many decades of FMR.

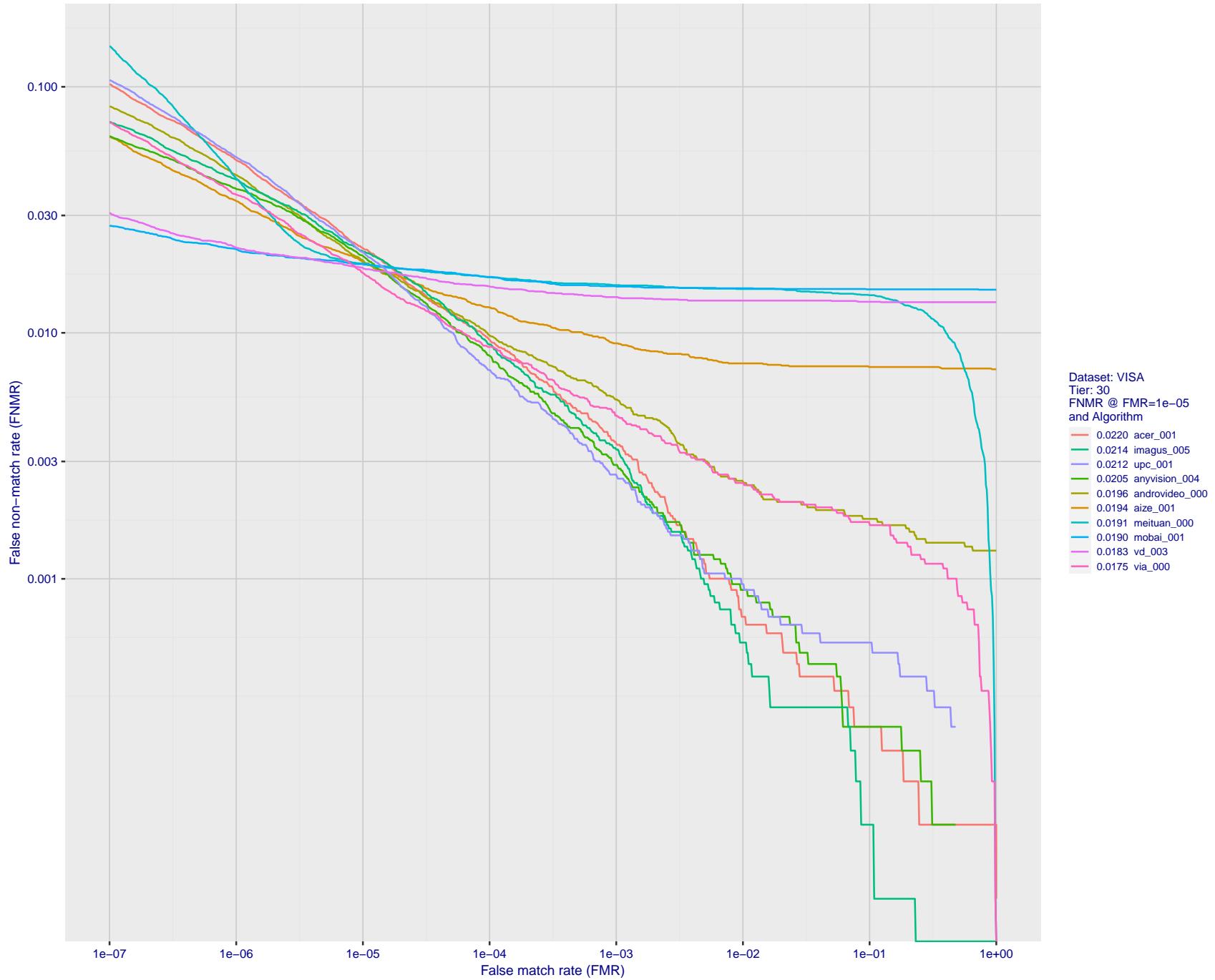


Figure 49: For the visa images, detection error tradeoff (DET) characteristics showing false non-match rate vs. false match rate plotted parametrically on threshold, T . The scales are logarithmic in order to show many decades of FMR.

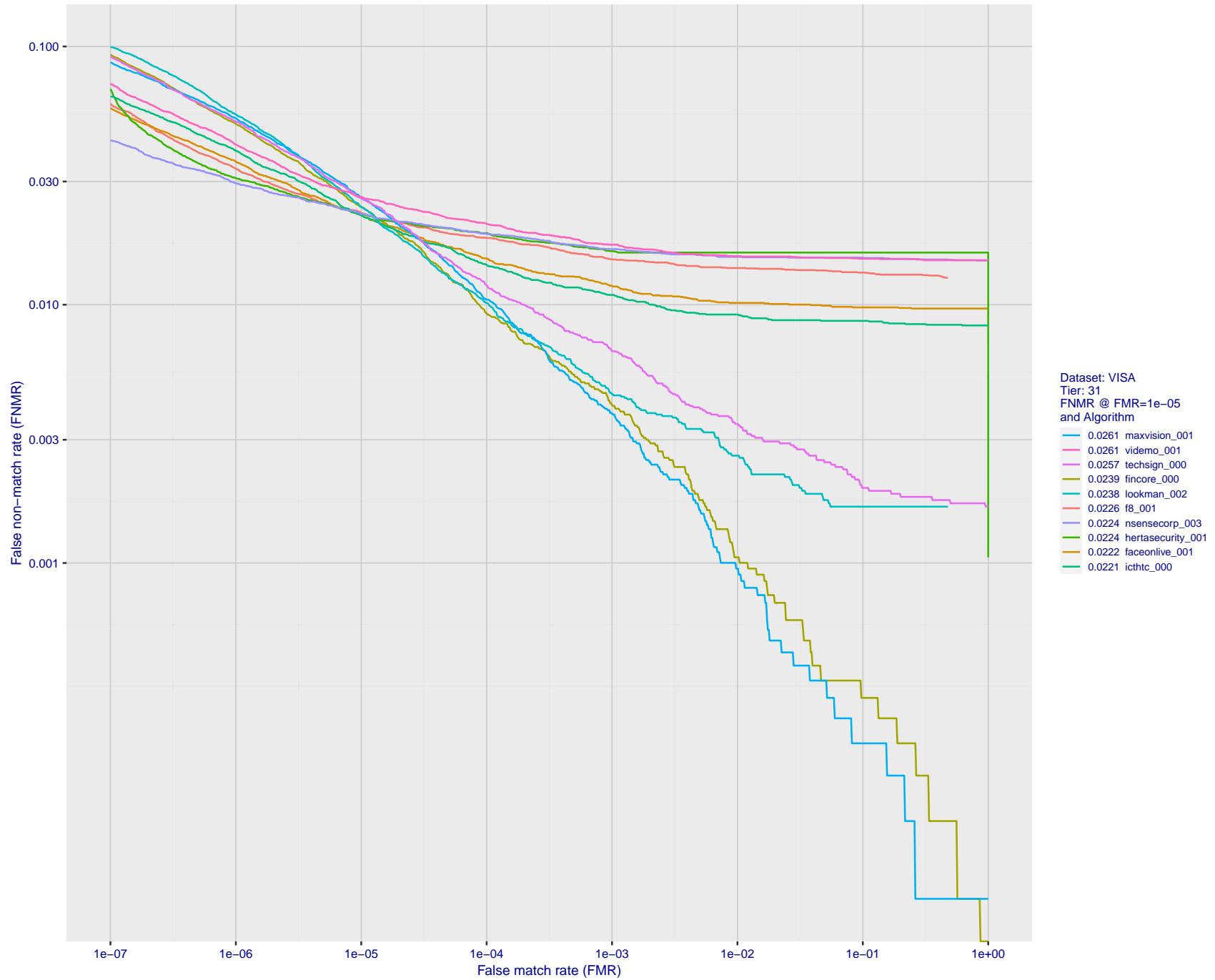


Figure 50: For the visa images, detection error tradeoff (DET) characteristics showing false non-match rate vs. false match rate plotted parametrically on threshold, T . The scales are logarithmic in order to show many decades of FMR.

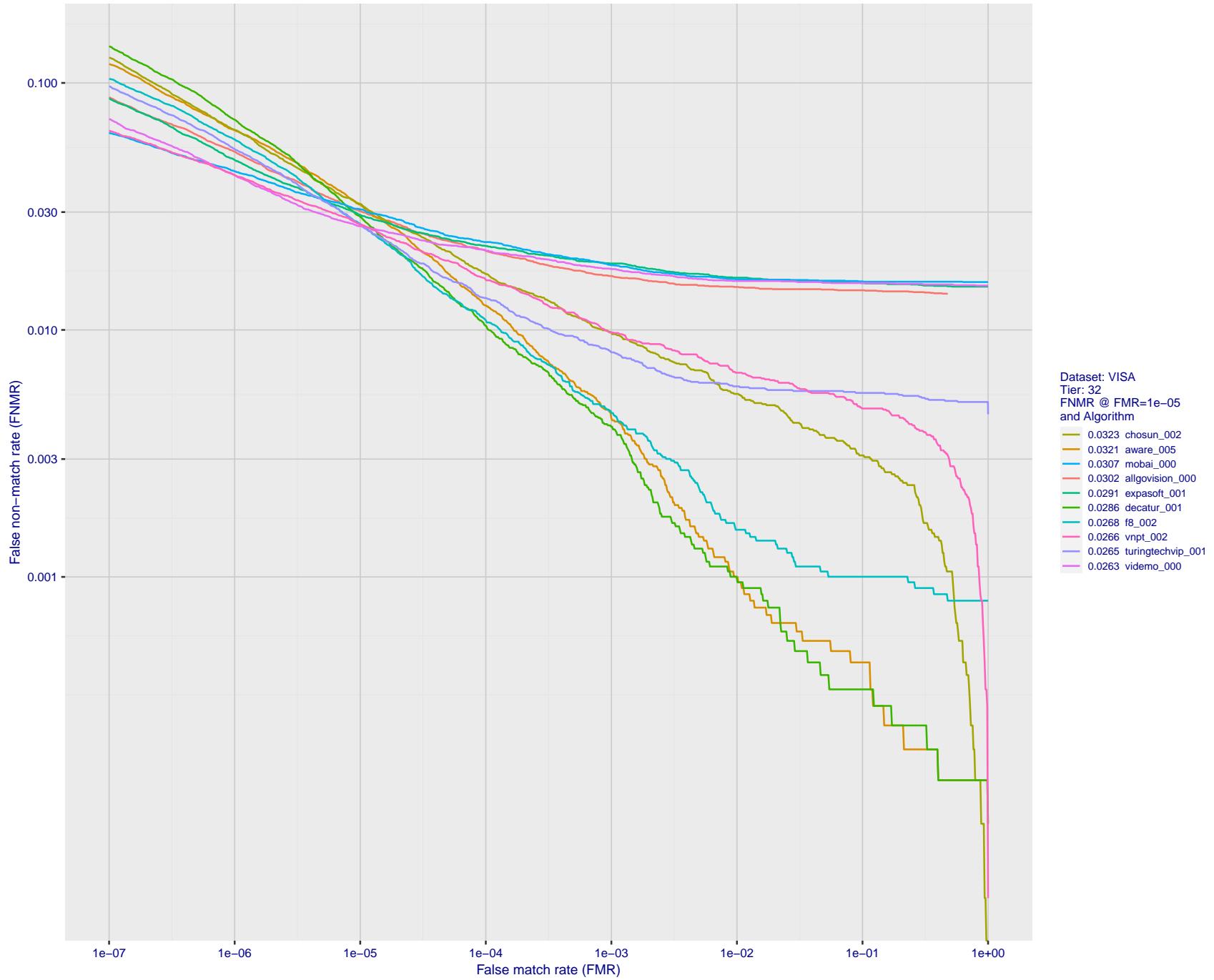


Figure 51: For the visa images, detection error tradeoff (DET) characteristics showing false non-match rate vs. false match rate plotted parametrically on threshold, T . The scales are logarithmic in order to show many decades of FMR.

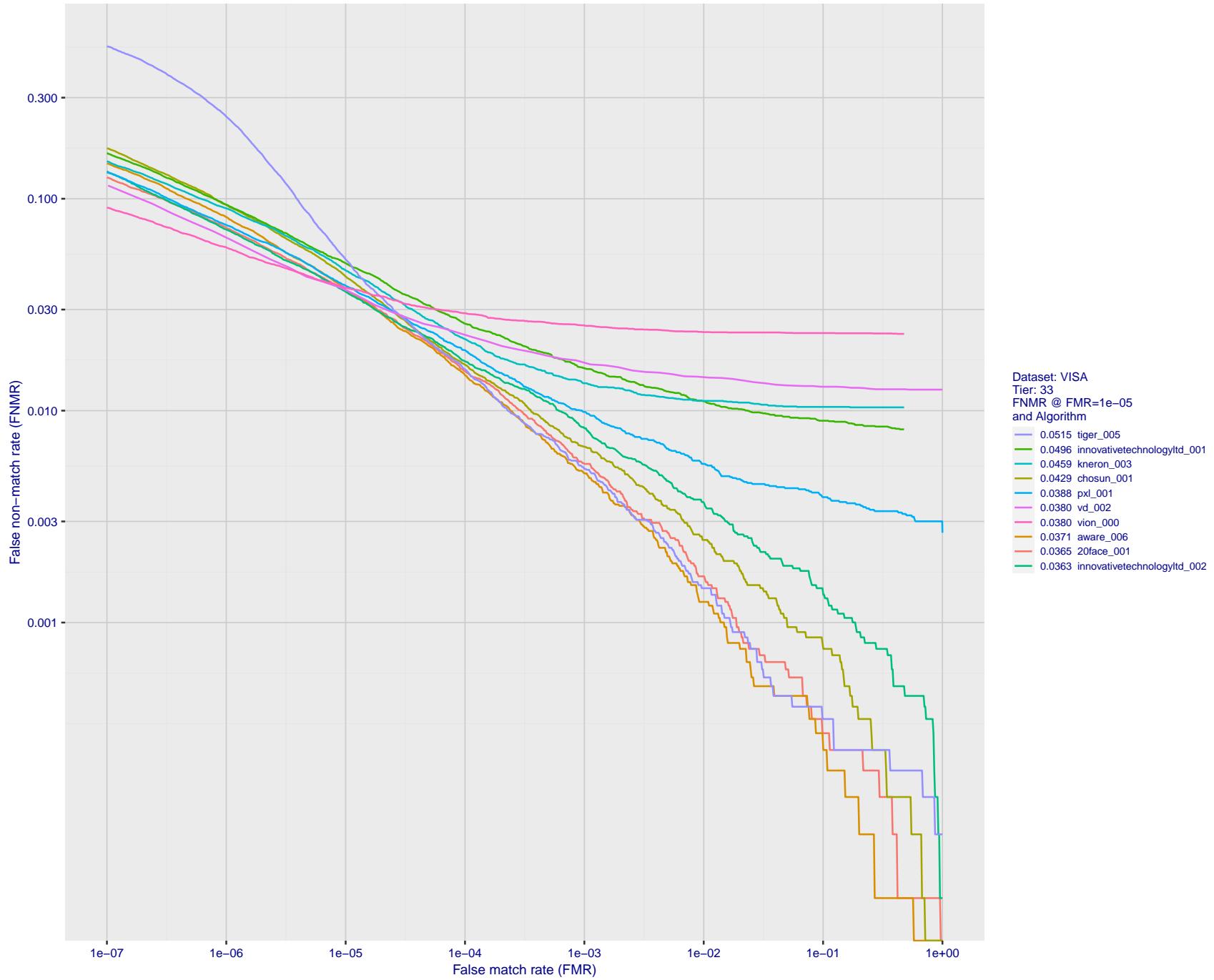


Figure 52: For the visa images, detection error tradeoff (DET) characteristics showing false non-match rate vs. false match rate plotted parametrically on threshold, T . The scales are logarithmic in order to show many decades of FMR.

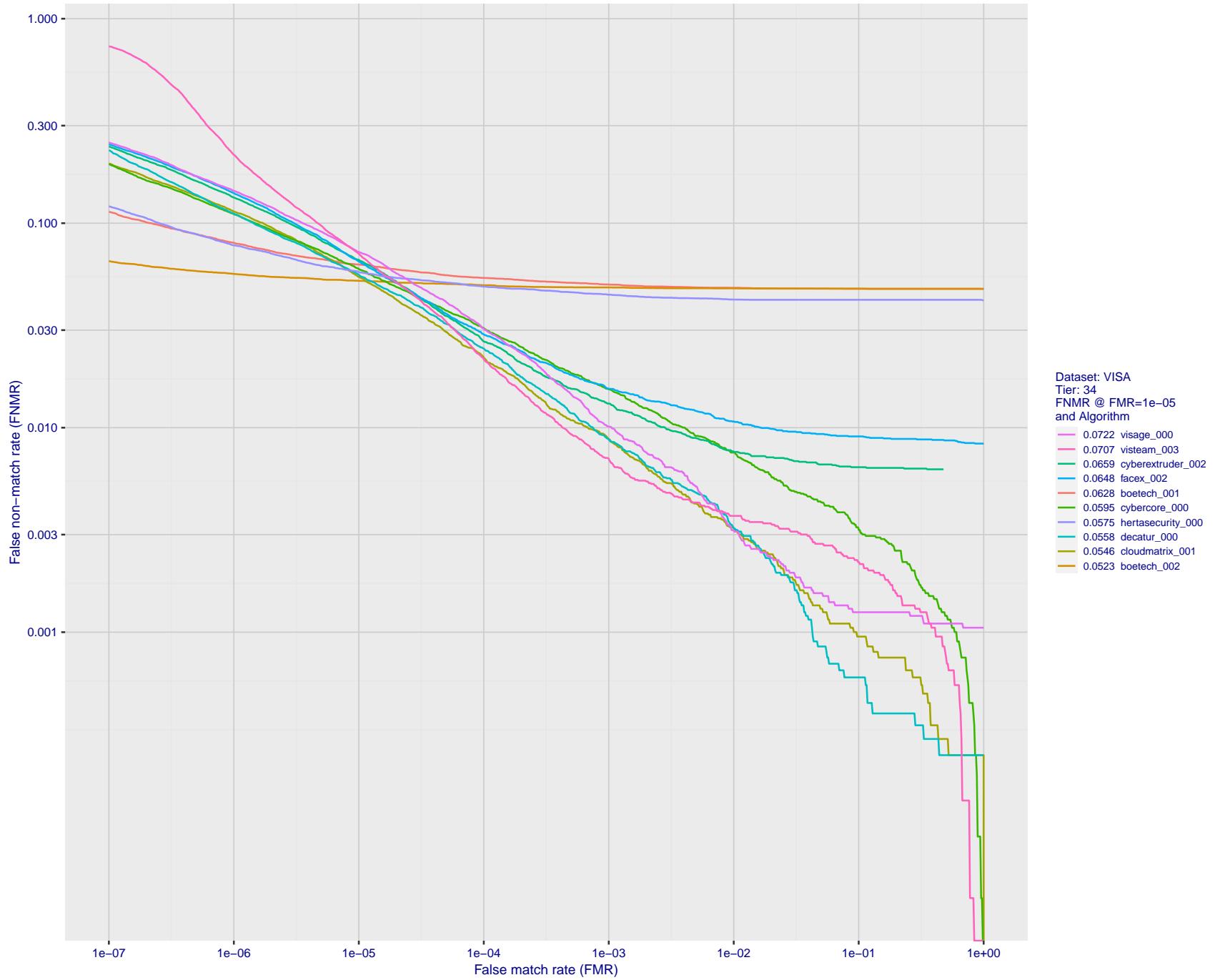


Figure 53: For the visa images, detection error tradeoff (DET) characteristics showing false non-match rate vs. false match rate plotted parametrically on threshold, T . The scales are logarithmic in order to show many decades of FMR.

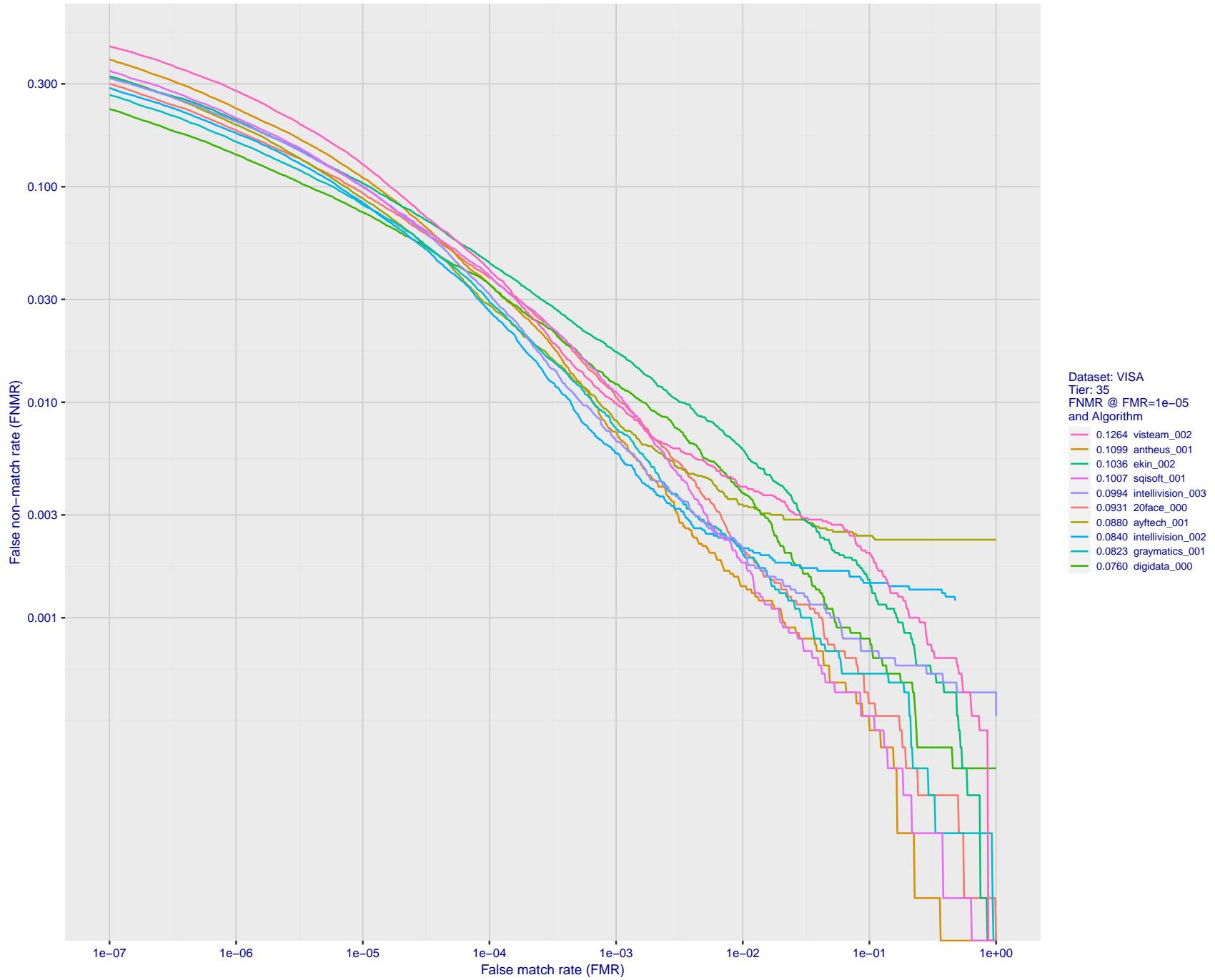


Figure 54: For the visa images, detection error tradeoff (DET) characteristics showing false non-match rate vs. false match rate plotted parametrically on threshold, T . The scales are logarithmic in order to show many decades of FMR.

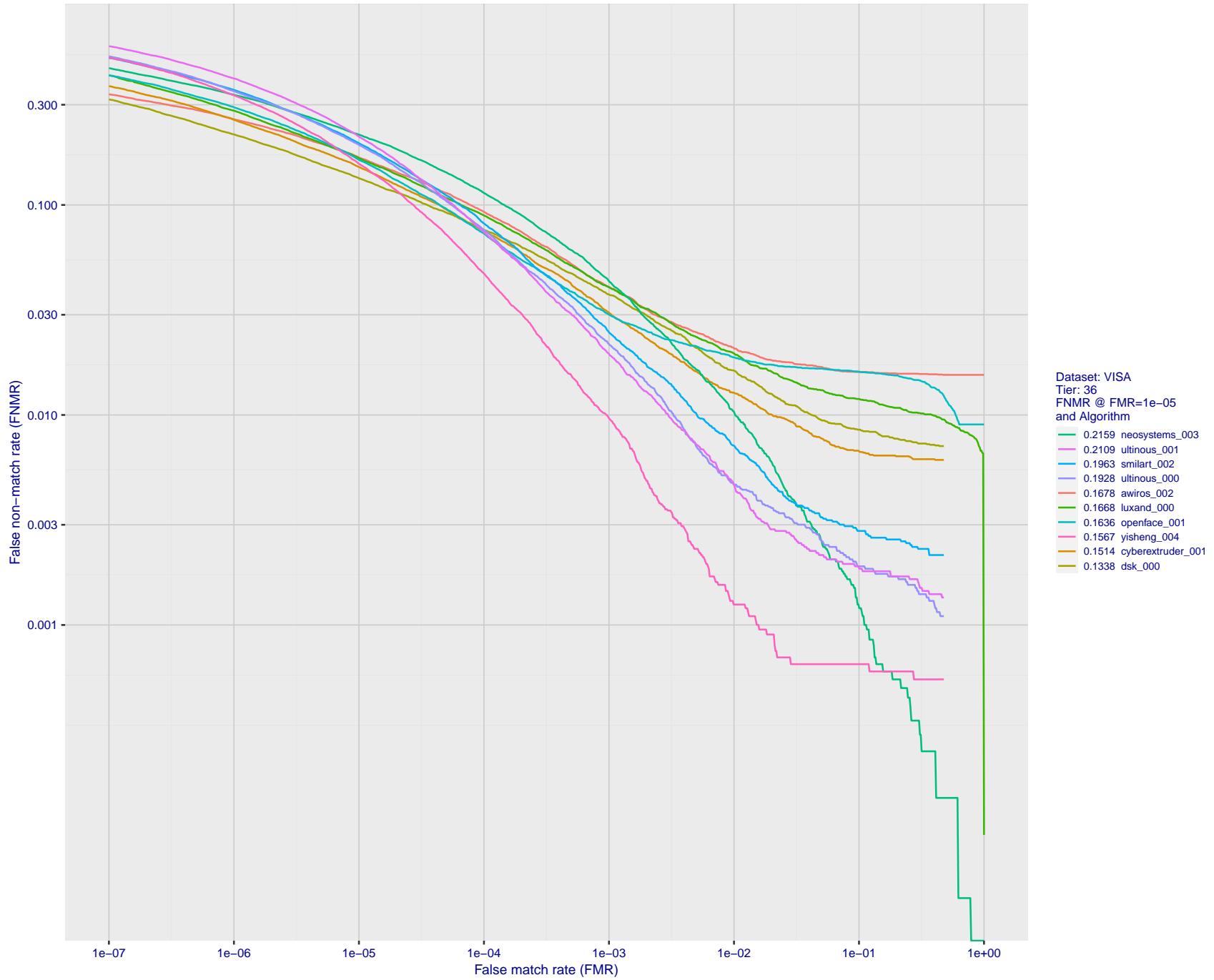


Figure 55: For the visa images, detection error tradeoff (DET) characteristics showing false non-match rate vs. false match rate plotted parametrically on threshold, T . The scales are logarithmic in order to show many decades of FMR.

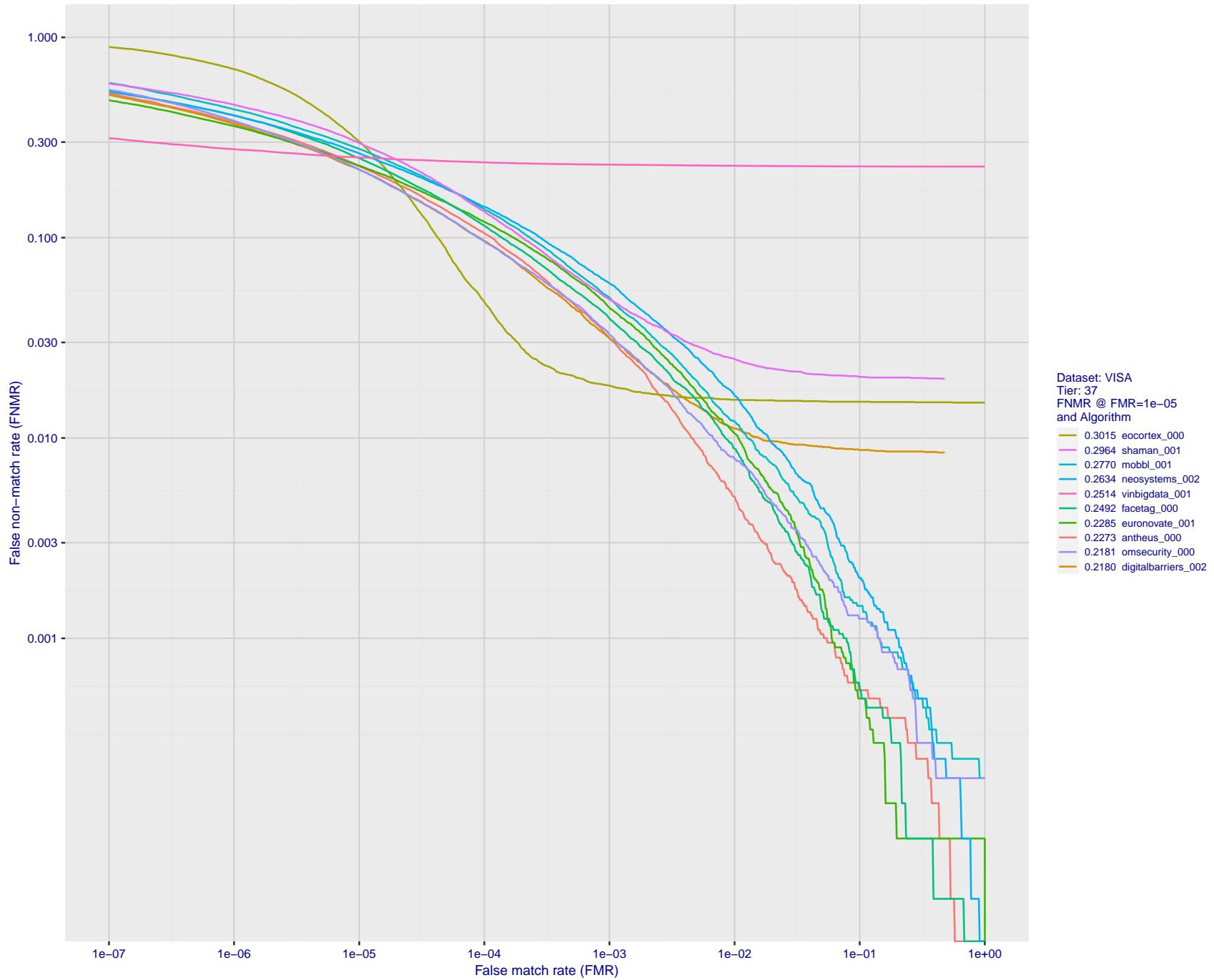


Figure 56: For the visa images, detection error tradeoff (DET) characteristics showing false non-match rate vs. false match rate plotted parametrically on threshold, T . The scales are logarithmic in order to show many decades of FMR.

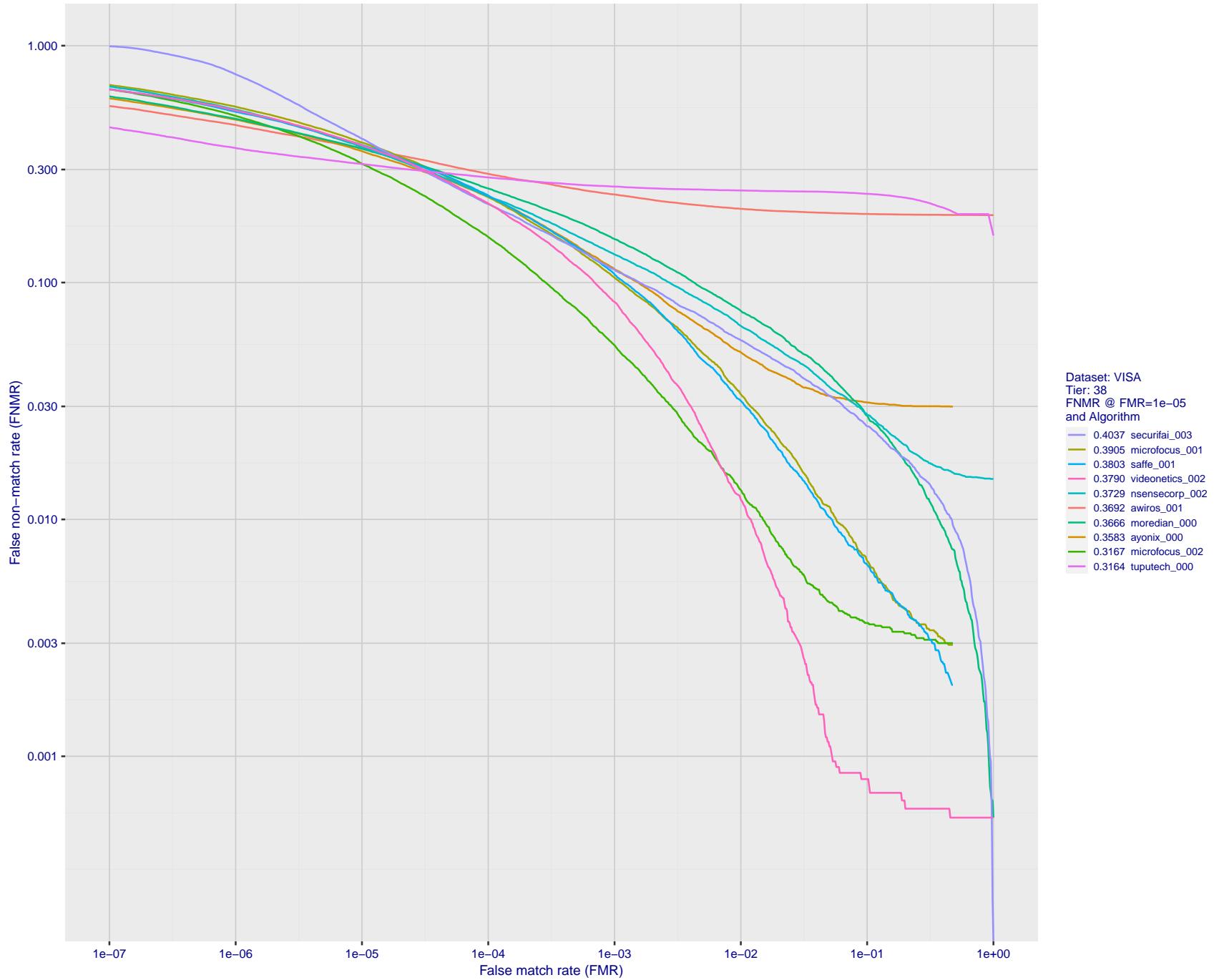


Figure 57: For the visa images, detection error tradeoff (DET) characteristics showing false non-match rate vs. false match rate plotted parametrically on threshold, T . The scales are logarithmic in order to show many decades of FMR.

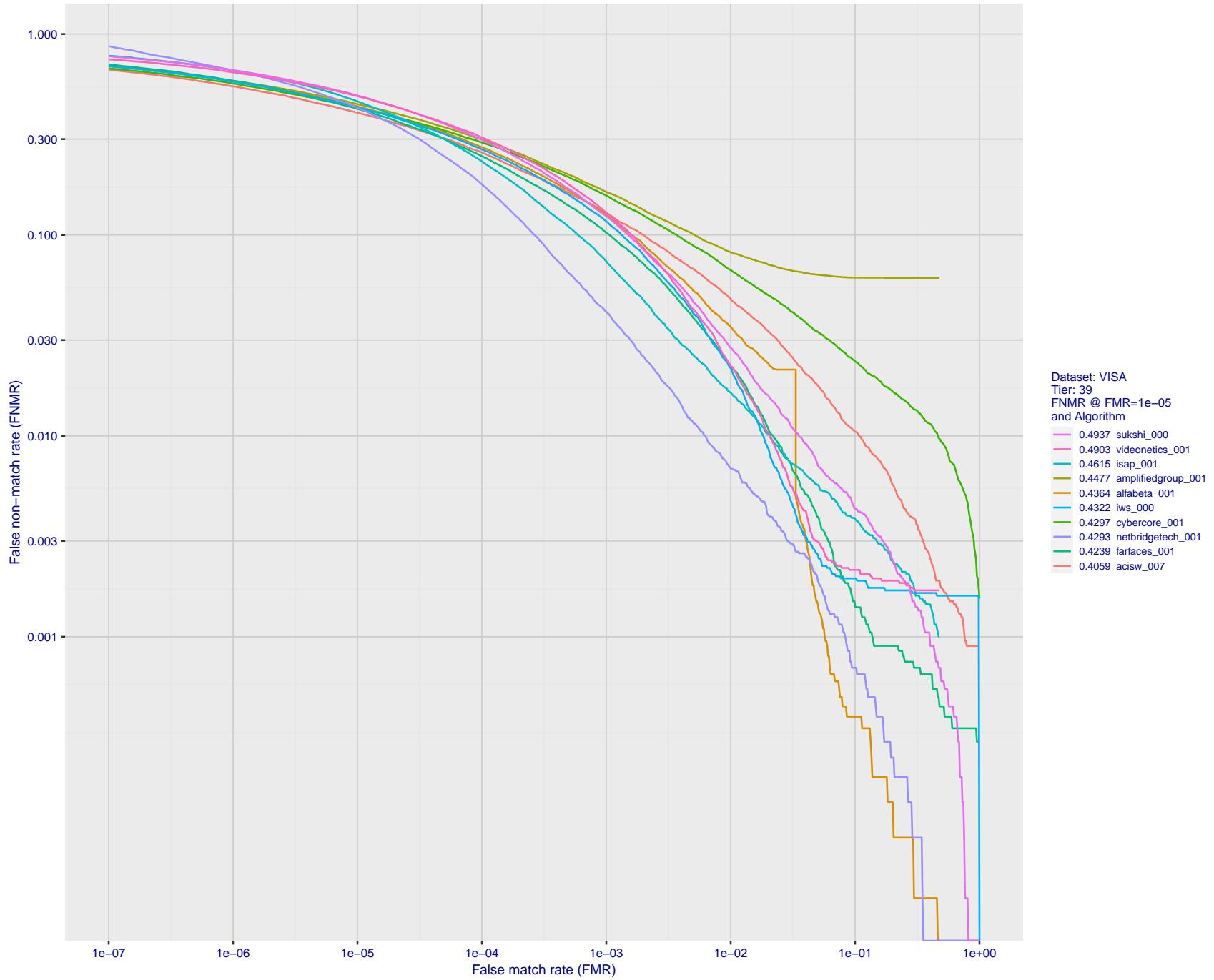


Figure 58: For the visa images, detection error tradeoff (DET) characteristics showing false non-match rate vs. false match rate plotted parametrically on threshold, T . The scales are logarithmic in order to show many decades of FMR.

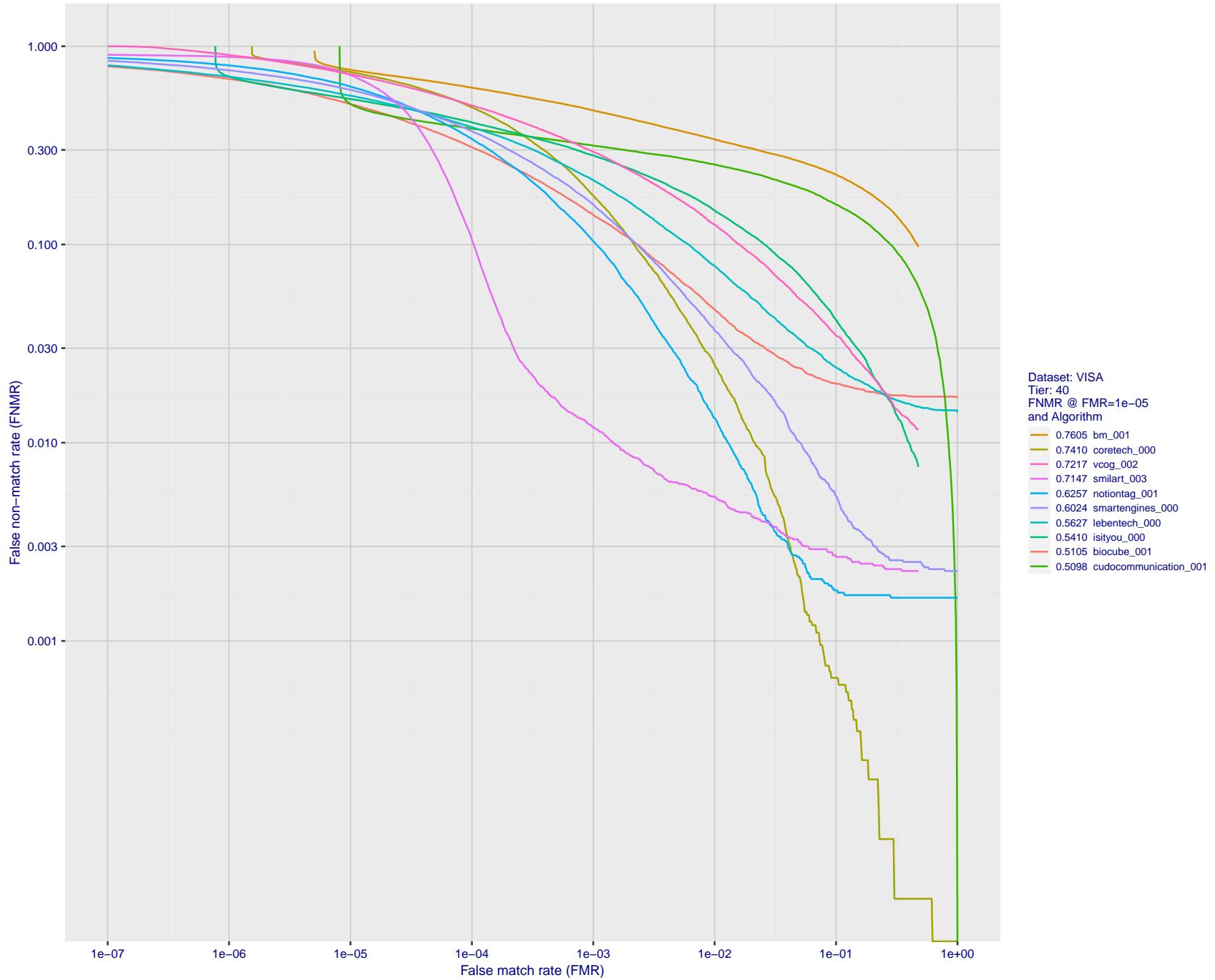


Figure 59: For the visa images, detection error tradeoff (DET) characteristics showing false non-match rate vs. false match rate plotted parametrically on threshold, T . The scales are logarithmic in order to show many decades of FMR.

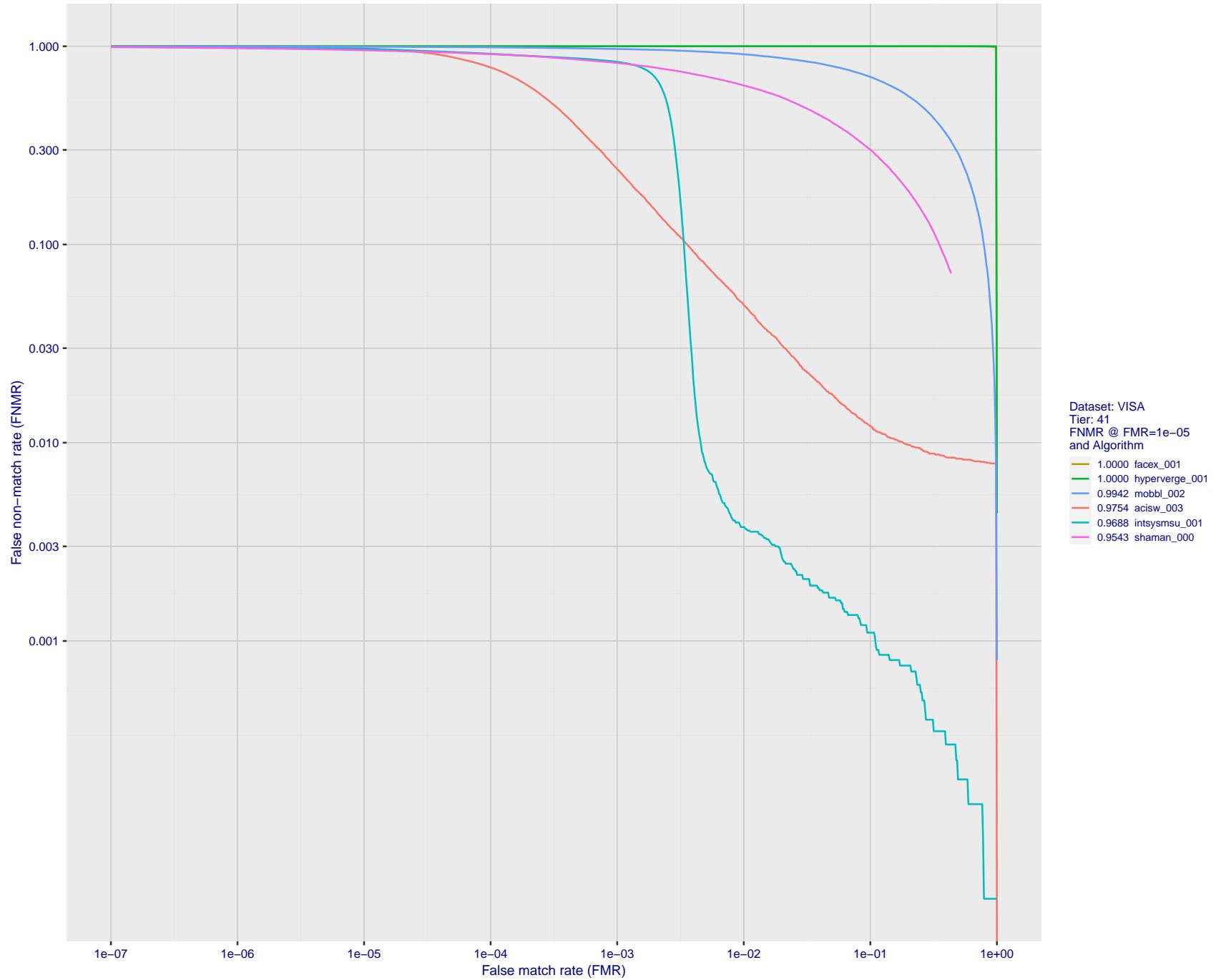


Figure 60: For the visa images, detection error tradeoff (DET) characteristics showing false non-match rate vs. false match rate plotted parametrically on threshold, T . The scales are logarithmic in order to show many decades of FMR.

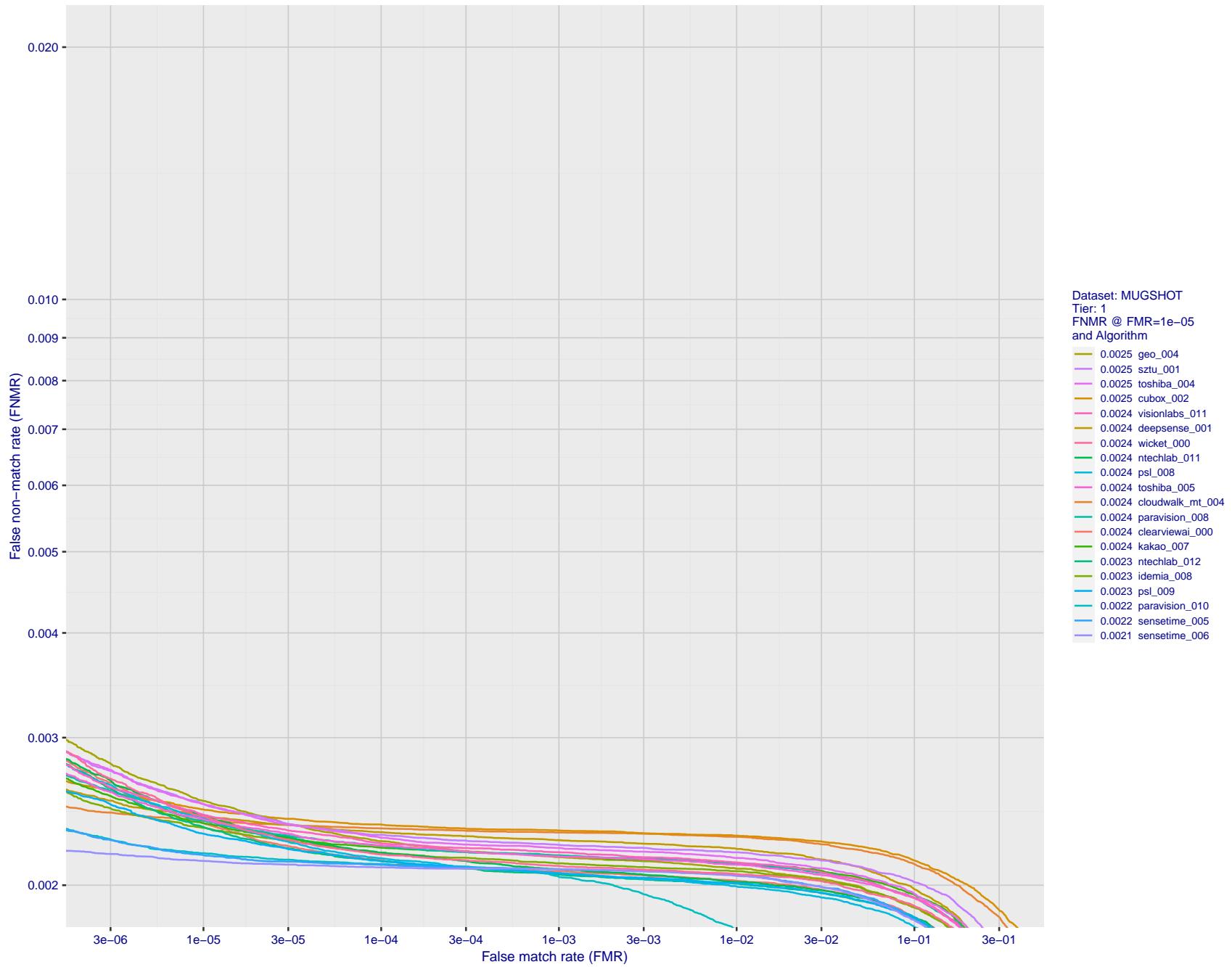


Figure 61: For the mugshot images, detection error tradeoff (DET) characteristics showing false non-match rate vs. false match rate plotted parametrically on threshold, T . The scales are logarithmic in order to show decades of FMR.

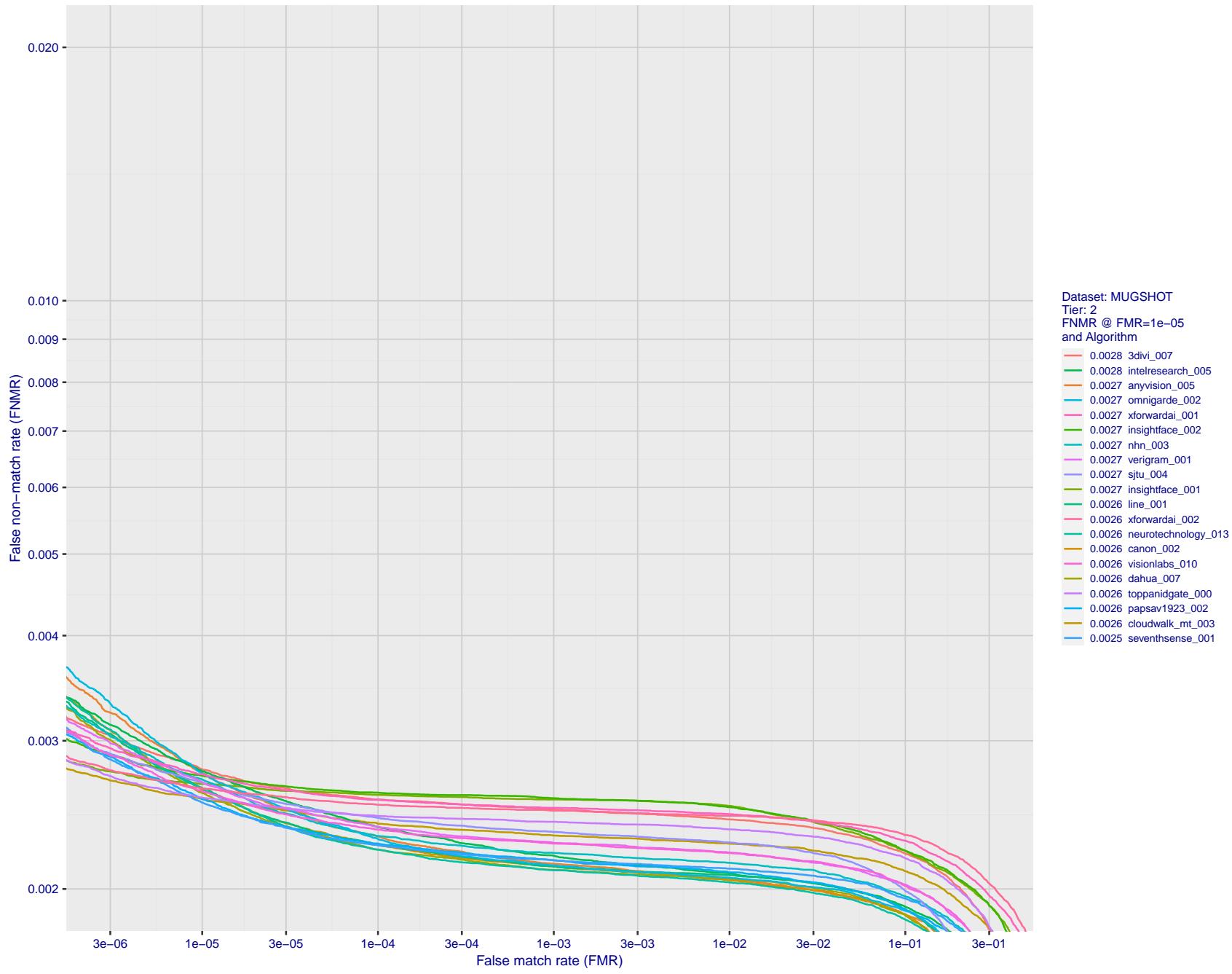


Figure 62: For the mugshot images, detection error tradeoff (DET) characteristics showing false non-match rate vs. false match rate plotted parametrically on threshold, T . The scales are logarithmic in order to show decades of FMR.

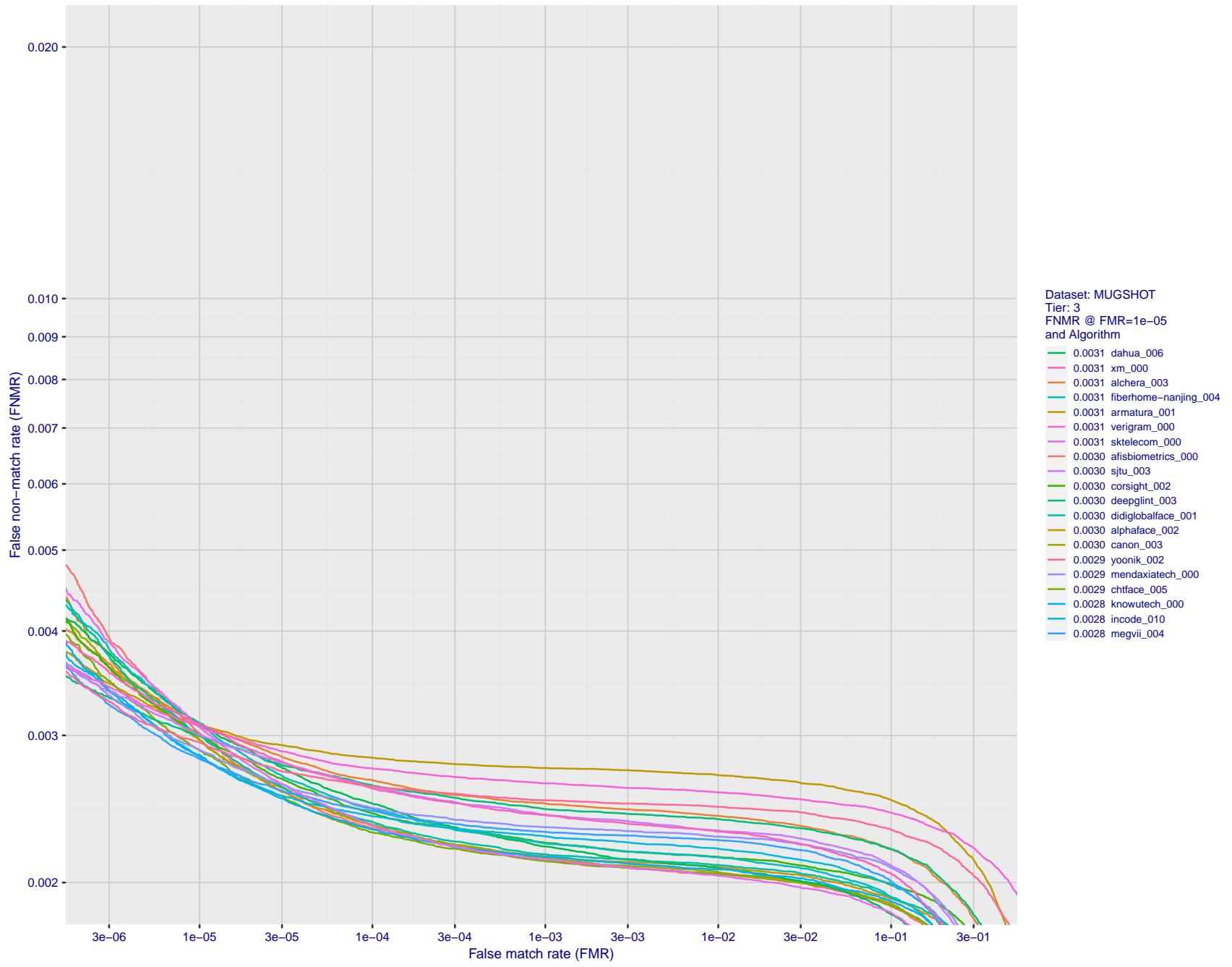


Figure 63: For the mugshot images, detection error tradeoff (DET) characteristics showing false non-match rate vs. false match rate plotted parametrically on threshold, T . The scales are logarithmic in order to show decades of FMR.

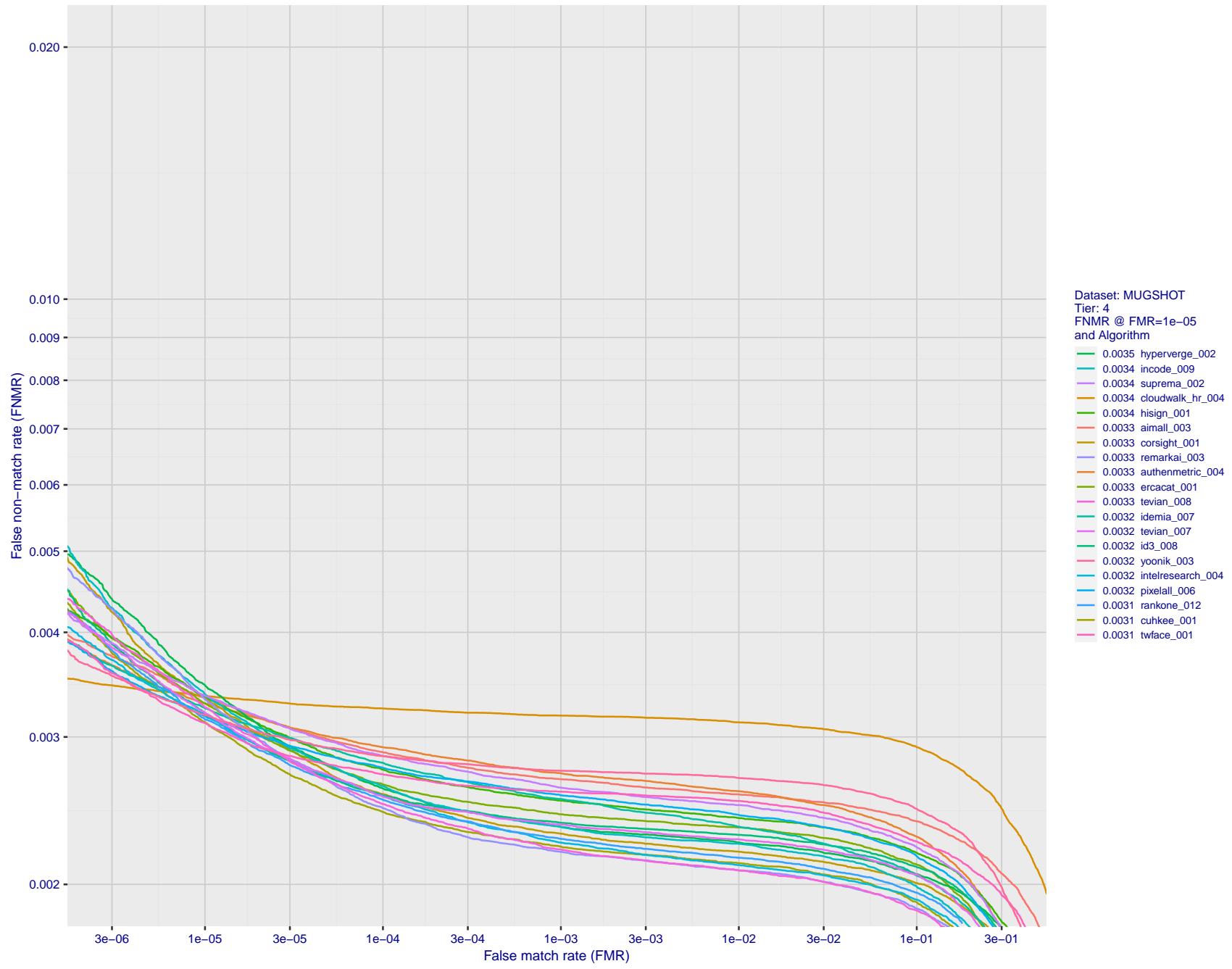


Figure 64: For the mugshot images, detection error tradeoff (DET) characteristics showing false non-match rate vs. false match rate plotted parametrically on threshold, T . The scales are logarithmic in order to show decades of FMR.

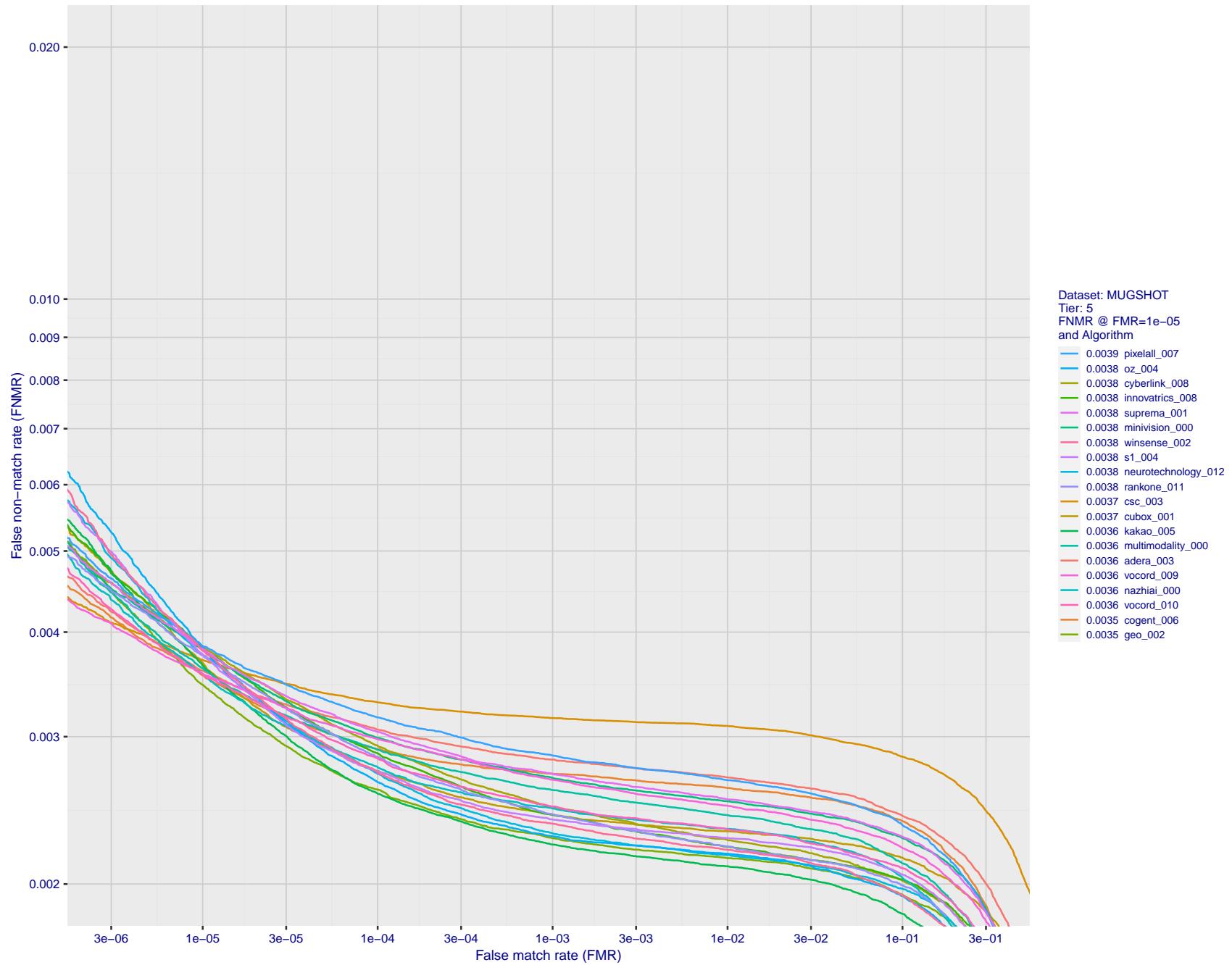


Figure 65: For the mugshot images, detection error tradeoff (DET) characteristics showing false non-match rate vs. false match rate plotted parametrically on threshold, T . The scales are logarithmic in order to show decades of FMR.

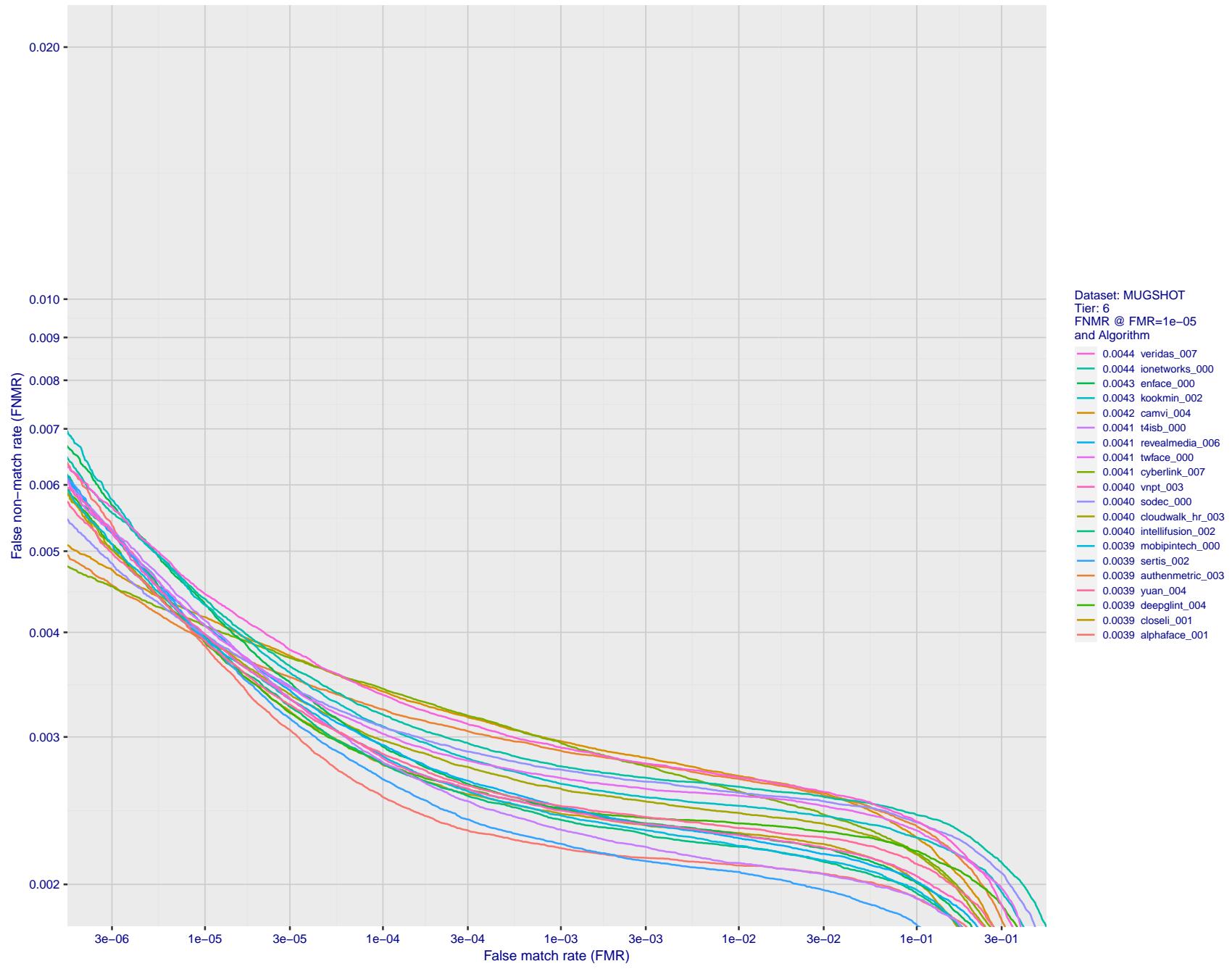


Figure 66: For the mugshot images, detection error tradeoff (DET) characteristics showing false non-match rate vs. false match rate plotted parametrically on threshold, T . The scales are logarithmic in order to show decades of FMR.

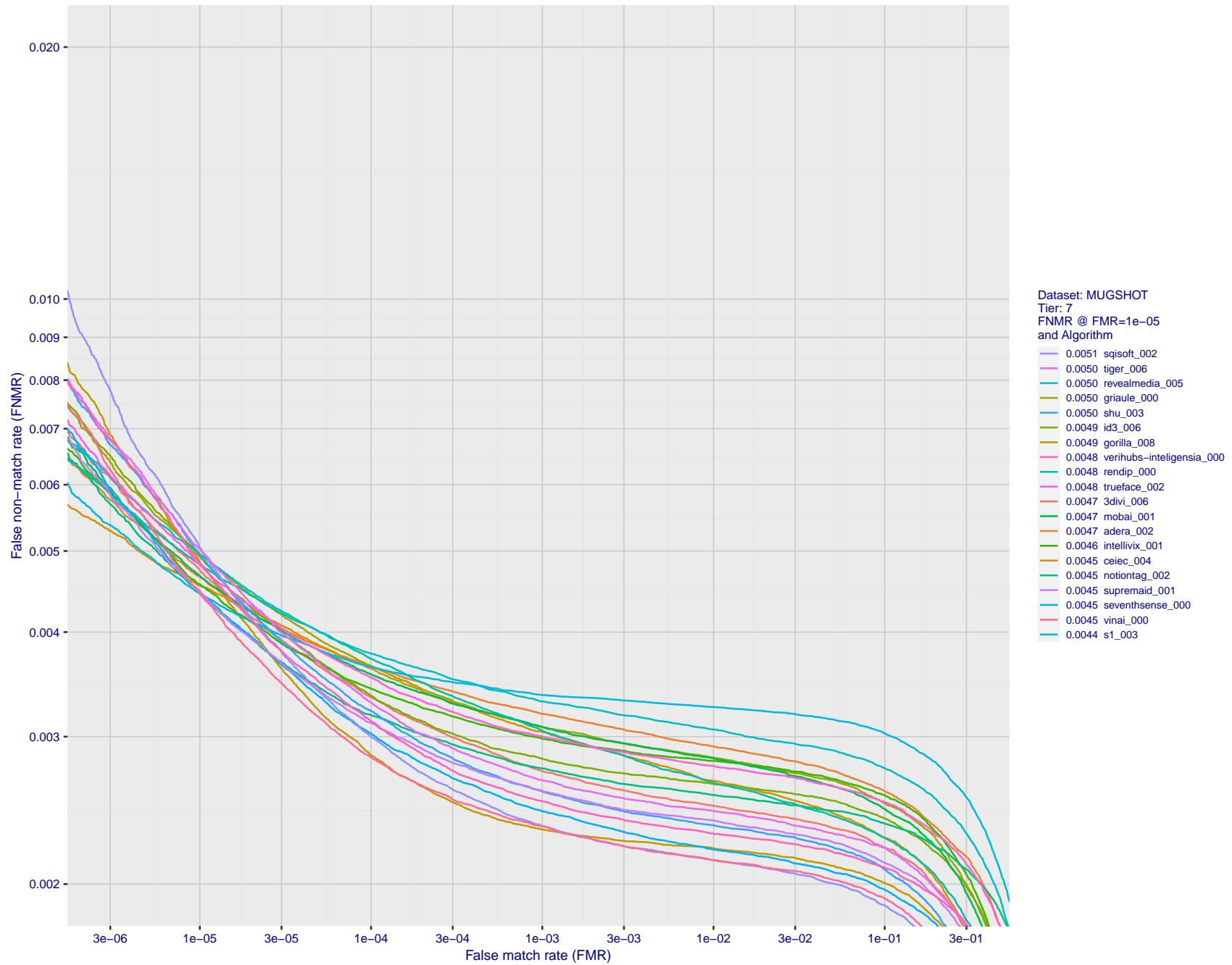


Figure 67: For the mugshot images, detection error tradeoff (DET) characteristics showing false non-match rate vs. false match rate plotted parametrically on threshold, T . The scales are logarithmic in order to show decades of FMR.

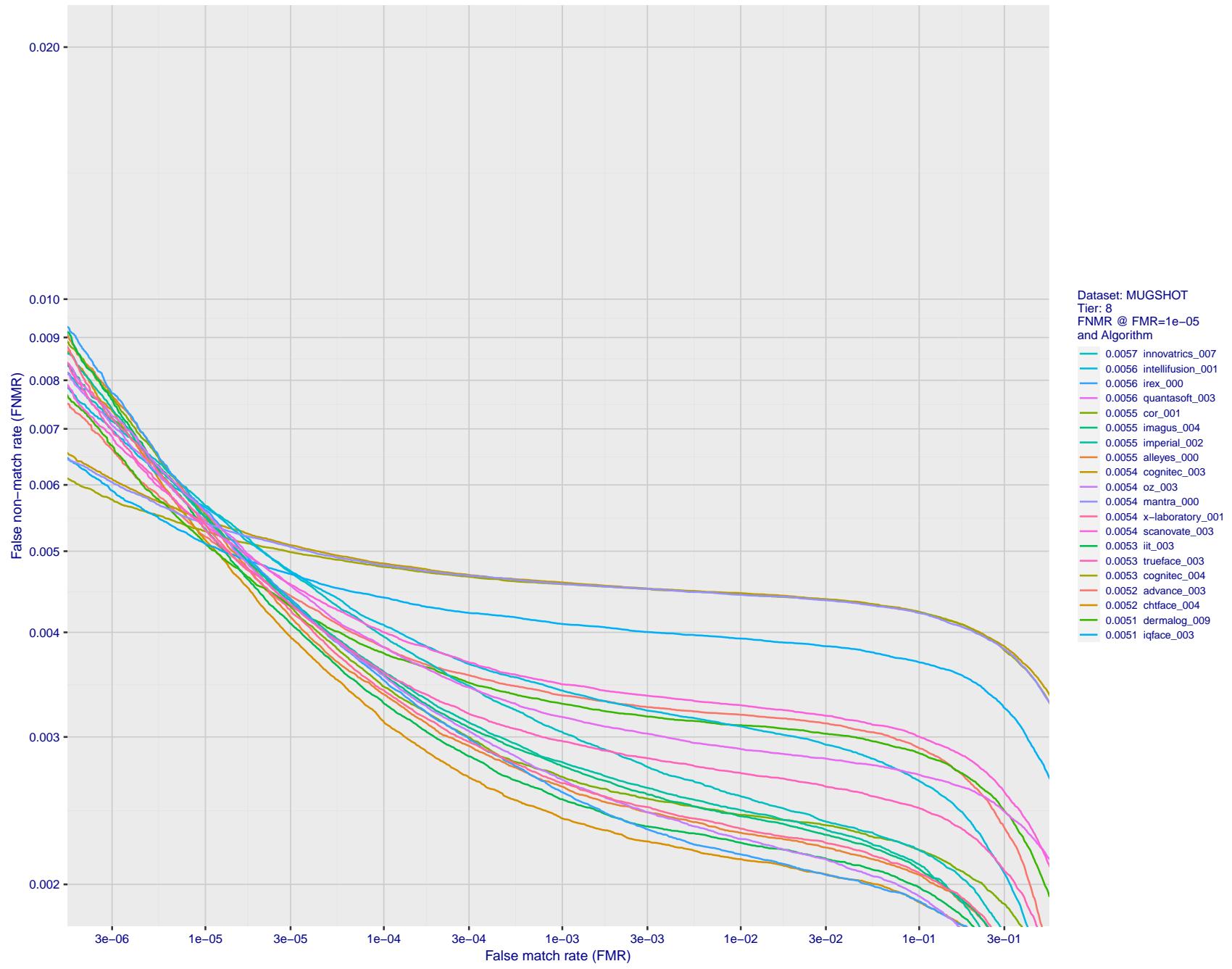


Figure 68: For the mugshot images, detection error tradeoff (DET) characteristics showing false non-match rate vs. false match rate plotted parametrically on threshold, T . The scales are logarithmic in order to show decades of FMR.

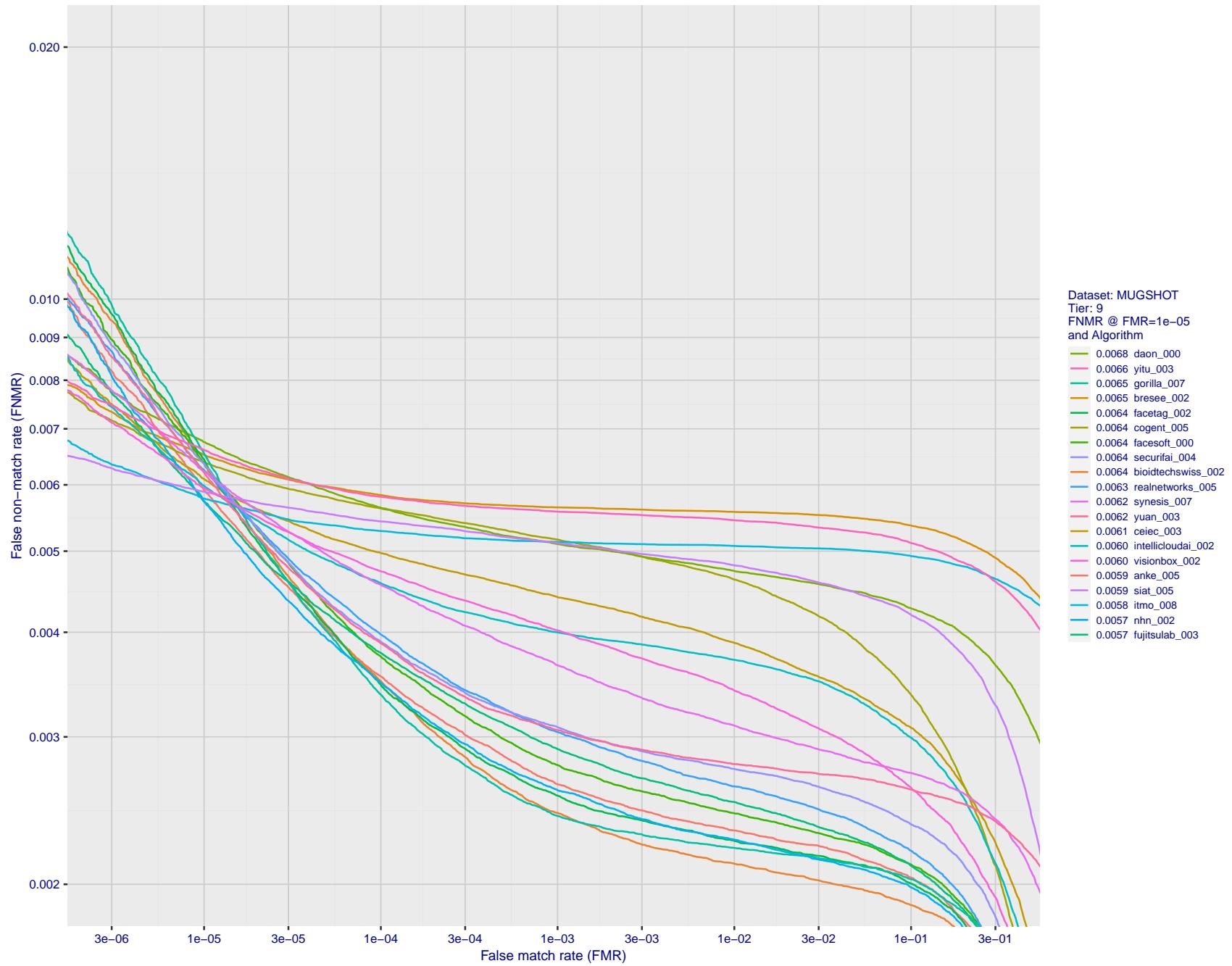


Figure 69: For the mugshot images, detection error tradeoff (DET) characteristics showing false non-match rate vs. false match rate plotted parametrically on threshold, T . The scales are logarithmic in order to show decades of FMR.

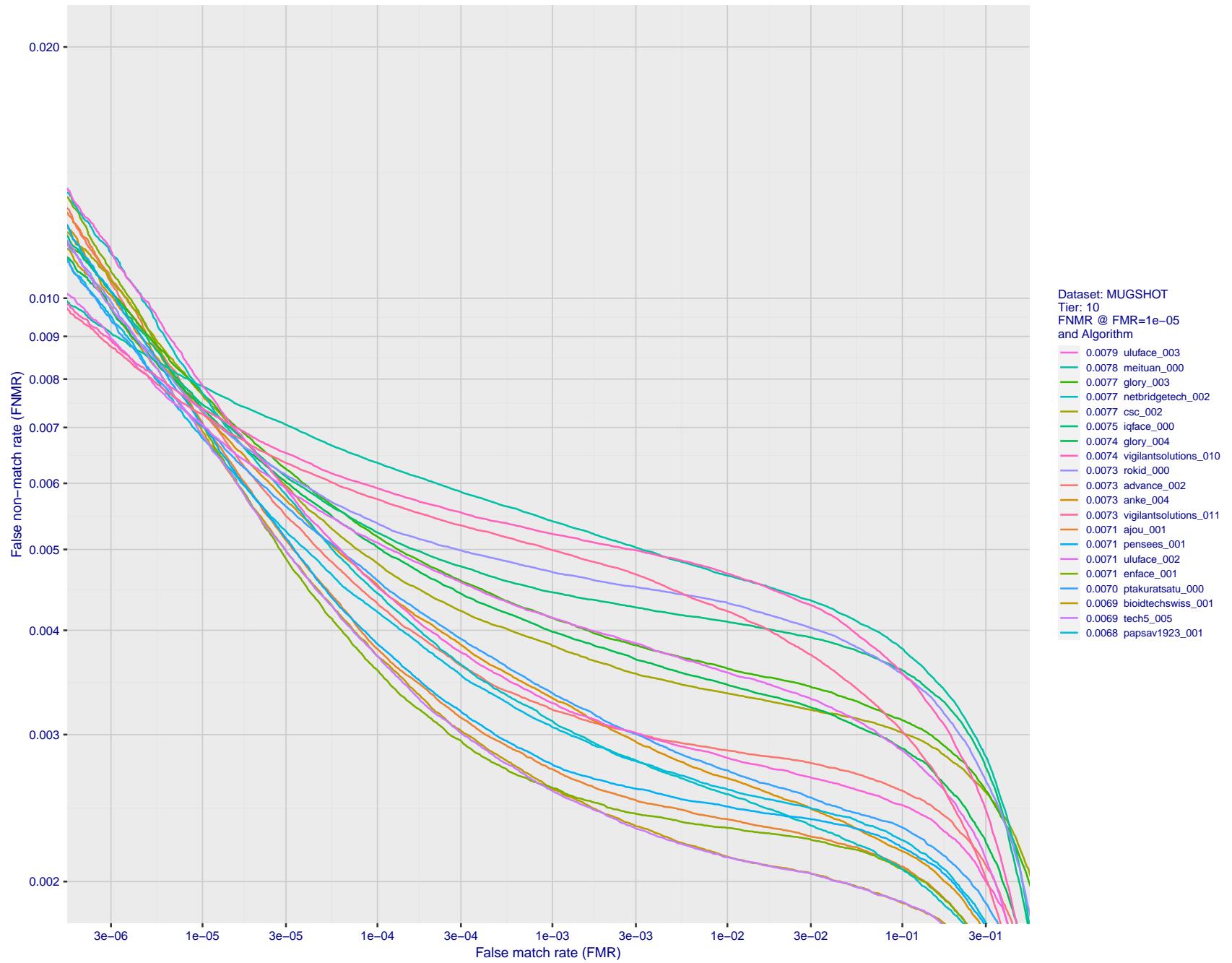


Figure 70: For the mugshot images, detection error tradeoff (DET) characteristics showing false non-match rate vs. false match rate plotted parametrically on threshold, T . The scales are logarithmic in order to show decades of FMR.

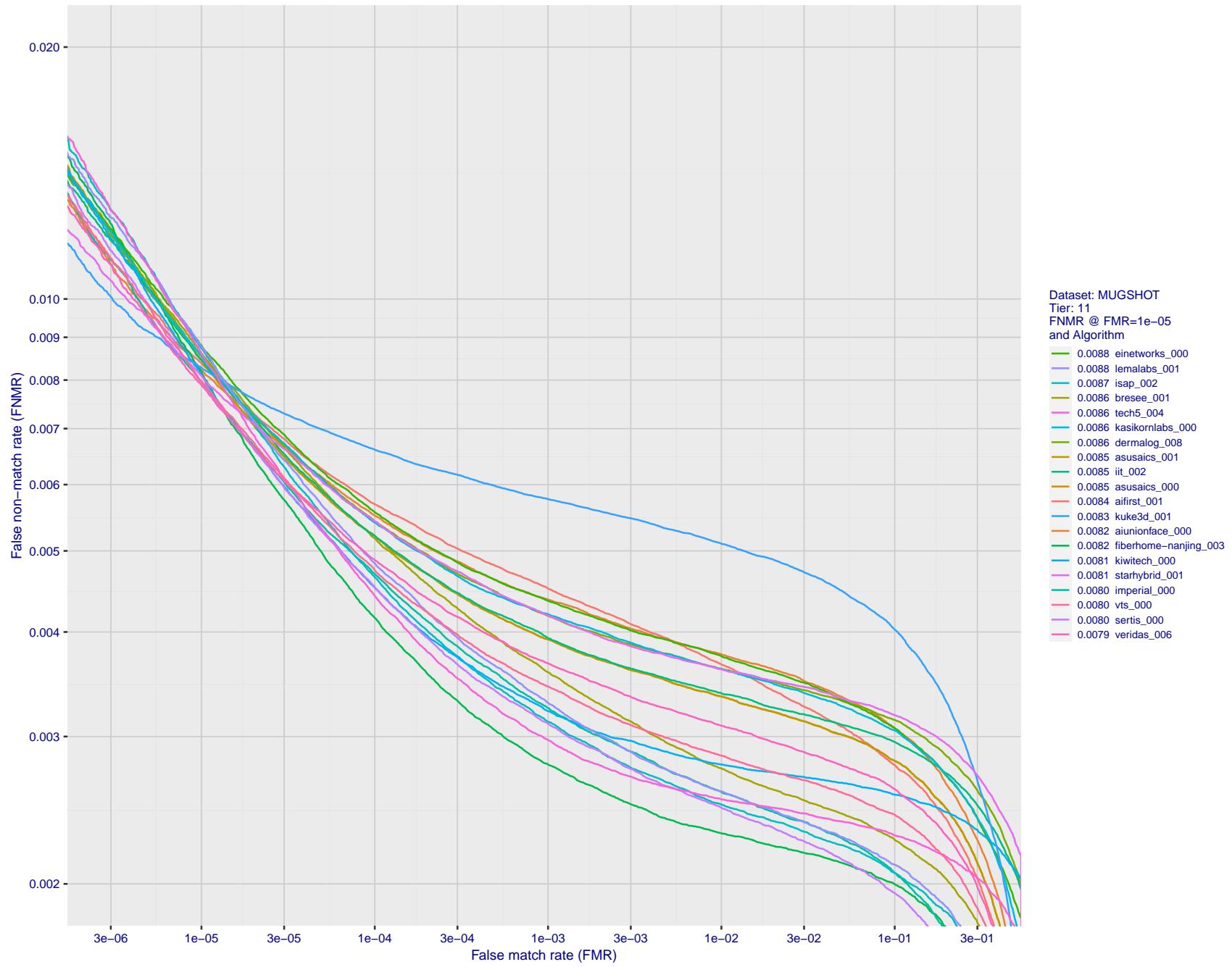


Figure 71: For the mugshot images, detection error tradeoff (DET) characteristics showing false non-match rate vs. false match rate plotted parametrically on threshold, T . The scales are logarithmic in order to show decades of FMR.

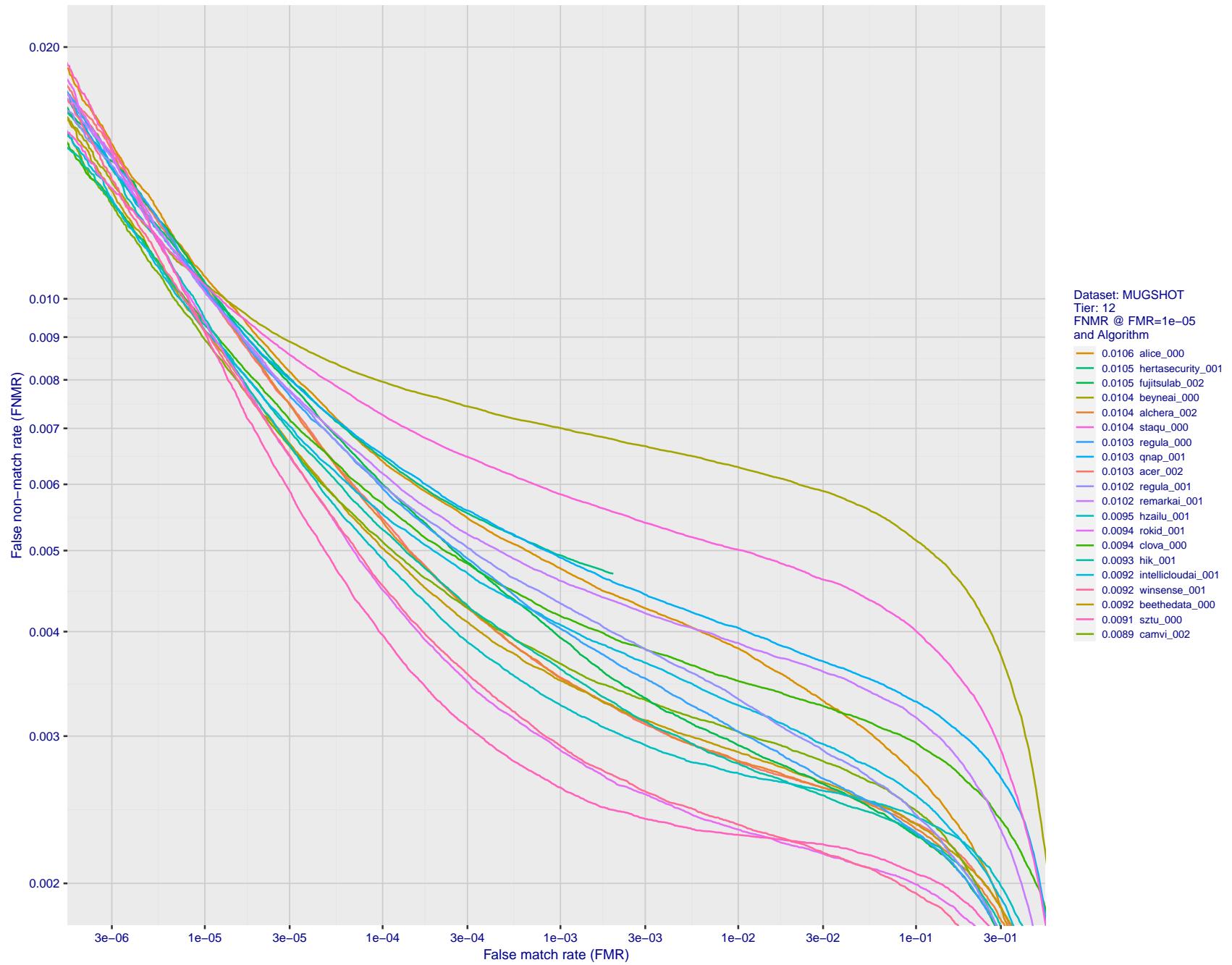


Figure 72: For the mugshot images, detection error tradeoff (DET) characteristics showing false non-match rate vs. false match rate plotted parametrically on threshold, T. The scales are logarithmic in order to show decades of FMR.

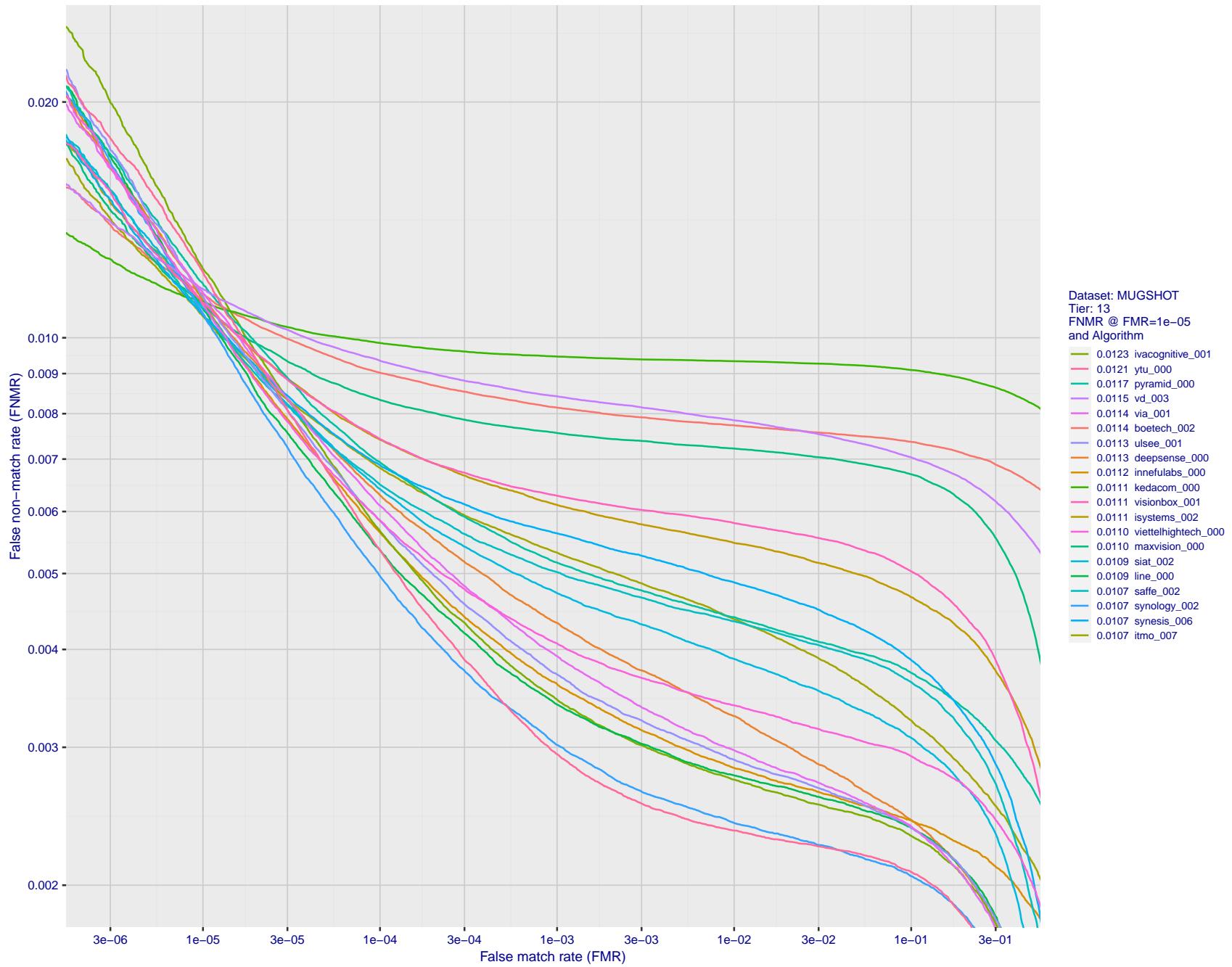


Figure 73: For the mugshot images, detection error tradeoff (DET) characteristics showing false non-match rate vs. false match rate plotted parametrically on threshold, T. The scales are logarithmic in order to show decades of FMR.

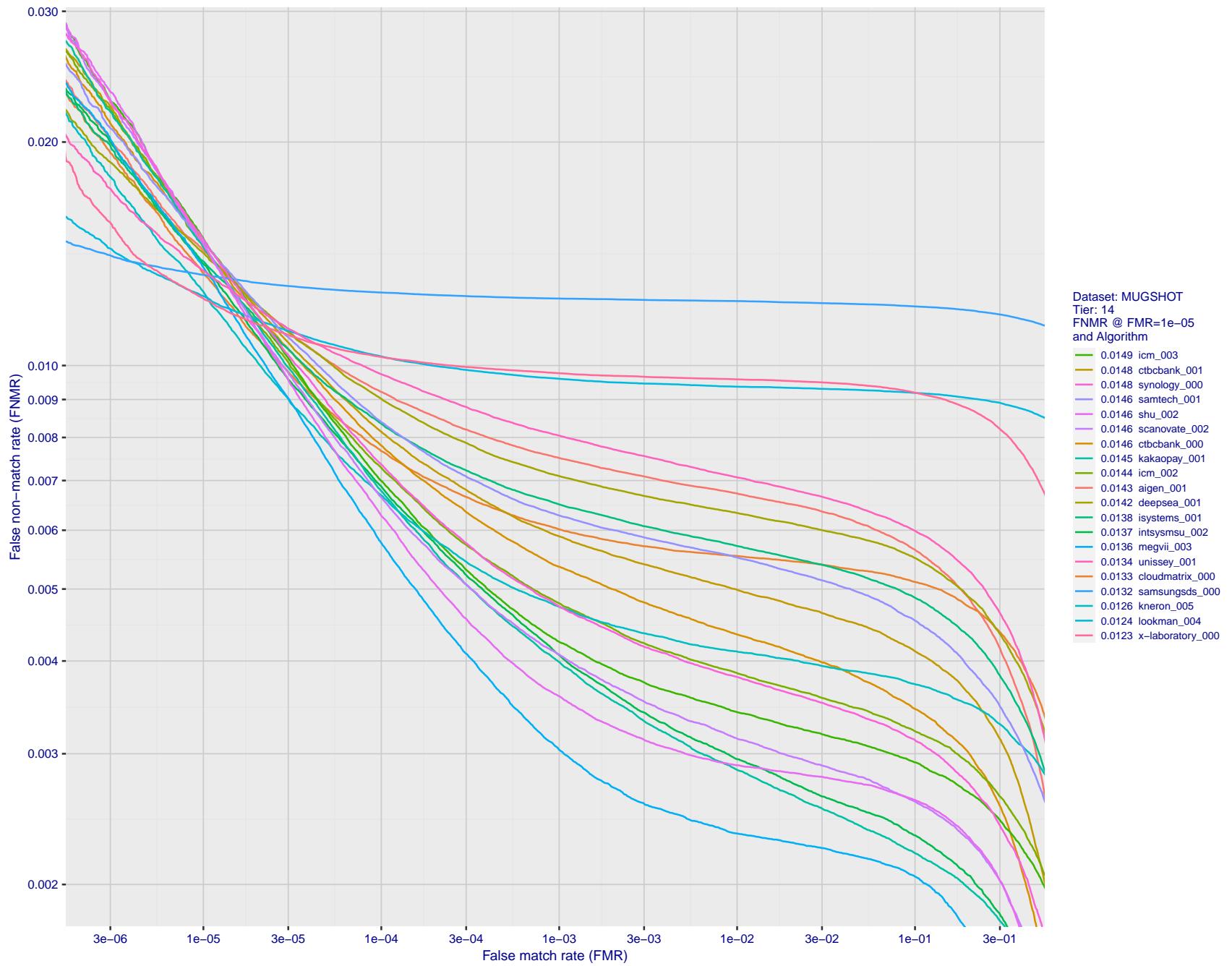


Figure 74: For the mugshot images, detection error tradeoff (DET) characteristics showing false non-match rate vs. false match rate plotted parametrically on threshold, T . The scales are logarithmic in order to show decades of FMR.

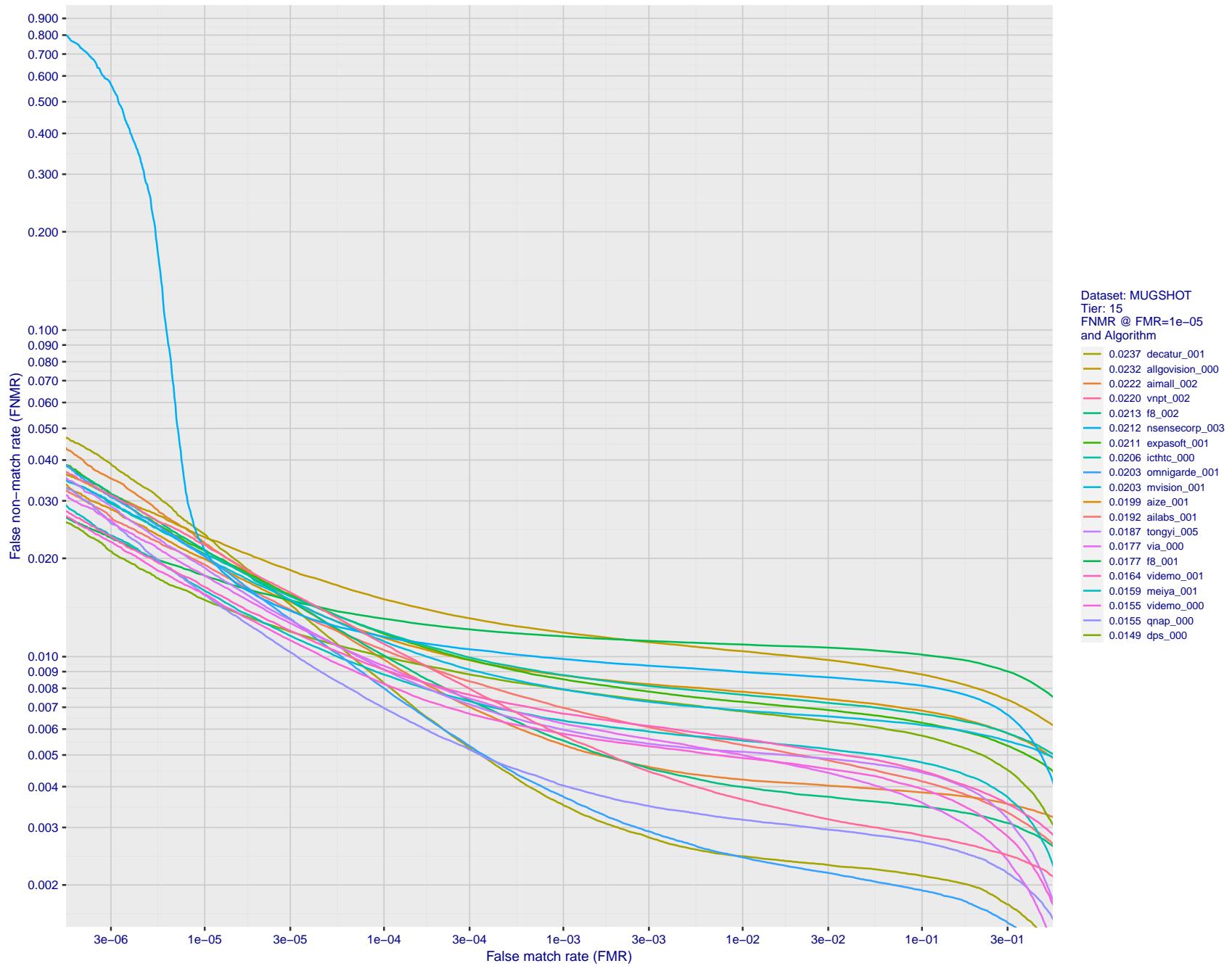


Figure 75: For the mugshot images, detection error tradeoff (DET) characteristics showing false non-match rate vs. false match rate plotted parametrically on threshold, T . The scales are logarithmic in order to show decades of FMR.

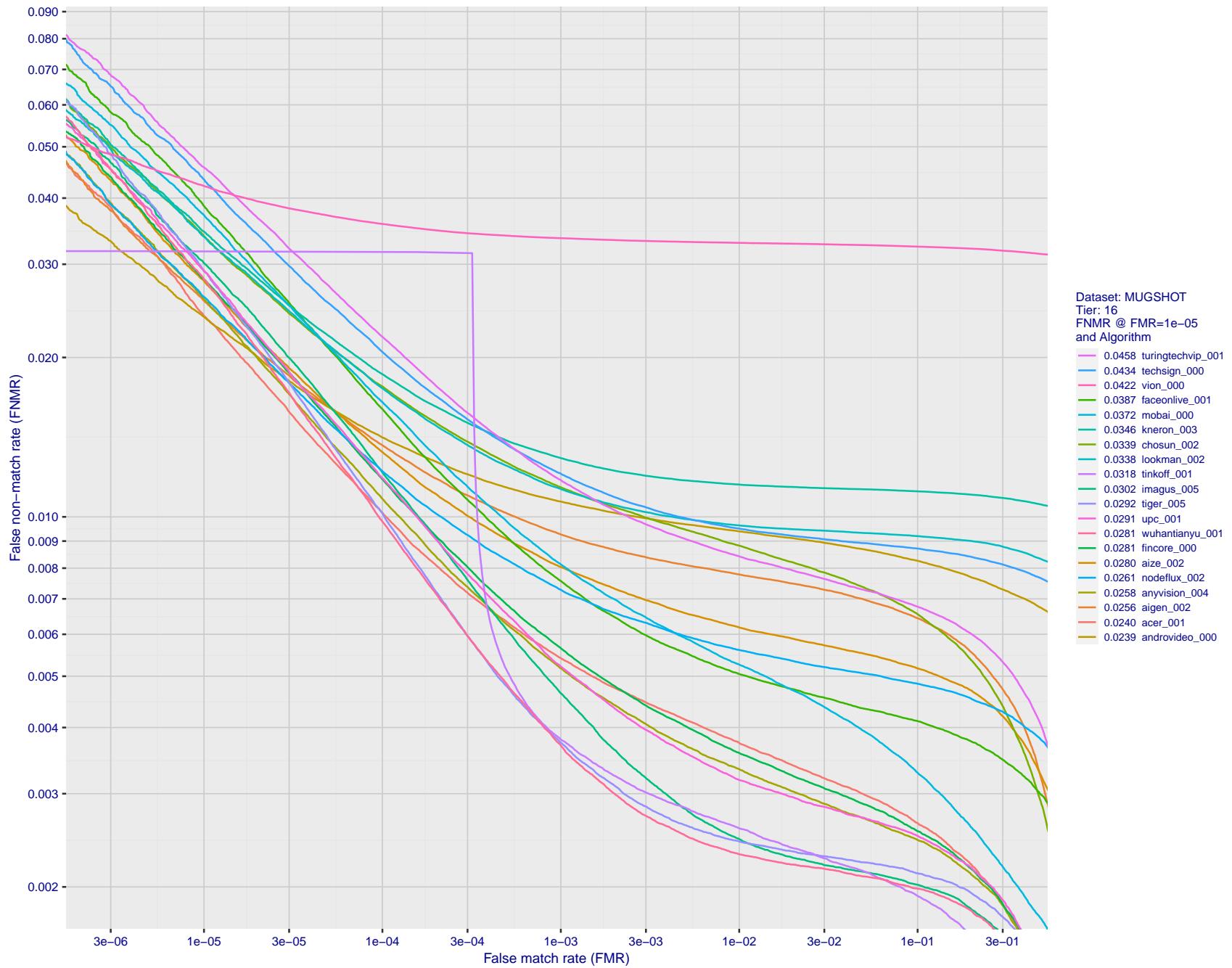


Figure 76: For the mugshot images, detection error tradeoff (DET) characteristics showing false non-match rate vs. false match rate plotted parametrically on threshold, T . The scales are logarithmic in order to show decades of FMR.

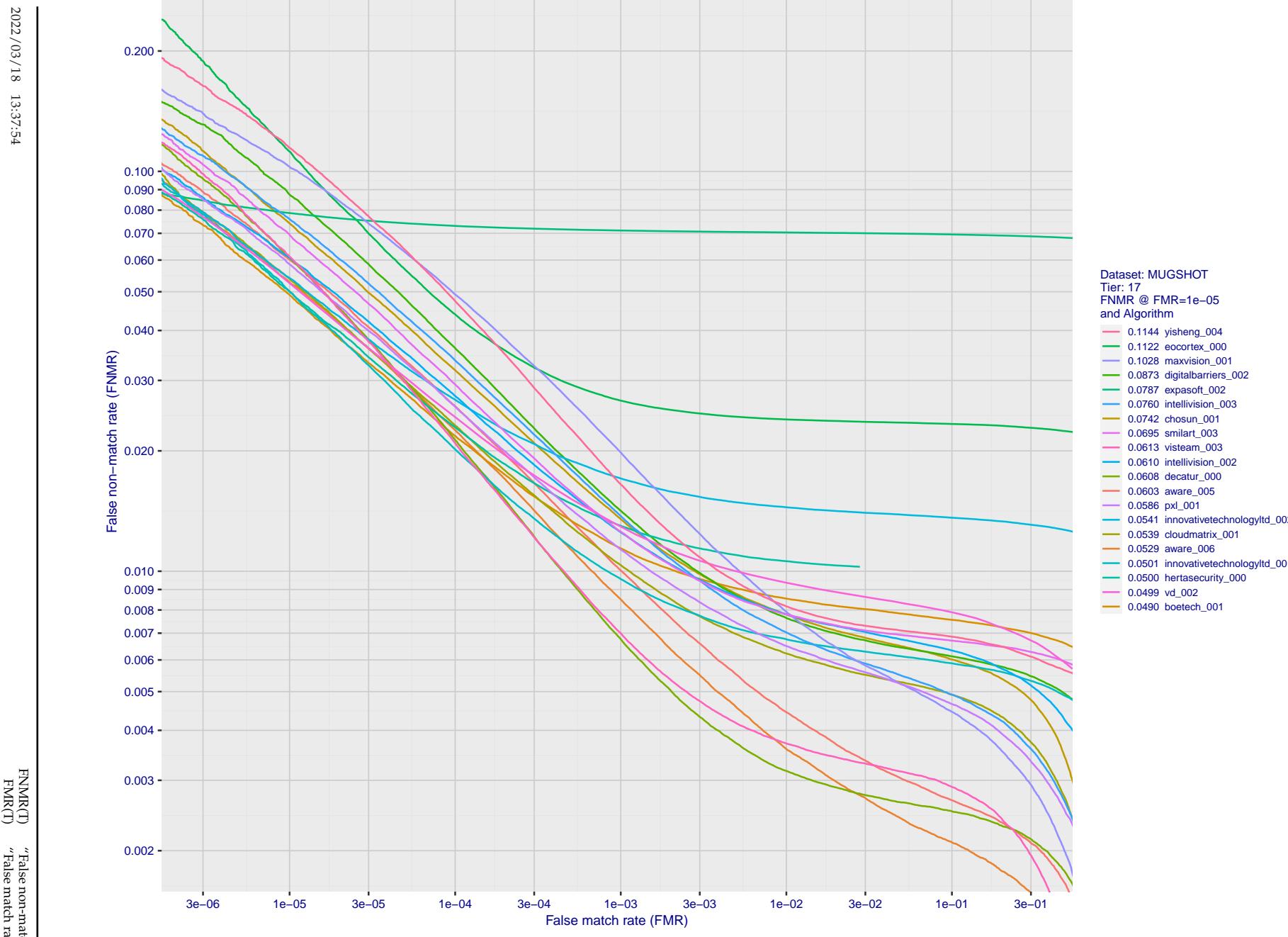


Figure 77: For the mugshot images, detection error tradeoff (DET) characteristics showing false non-match rate vs. false match rate plotted parametrically on threshold, T . The scales are logarithmic in order to show decades of FMR.

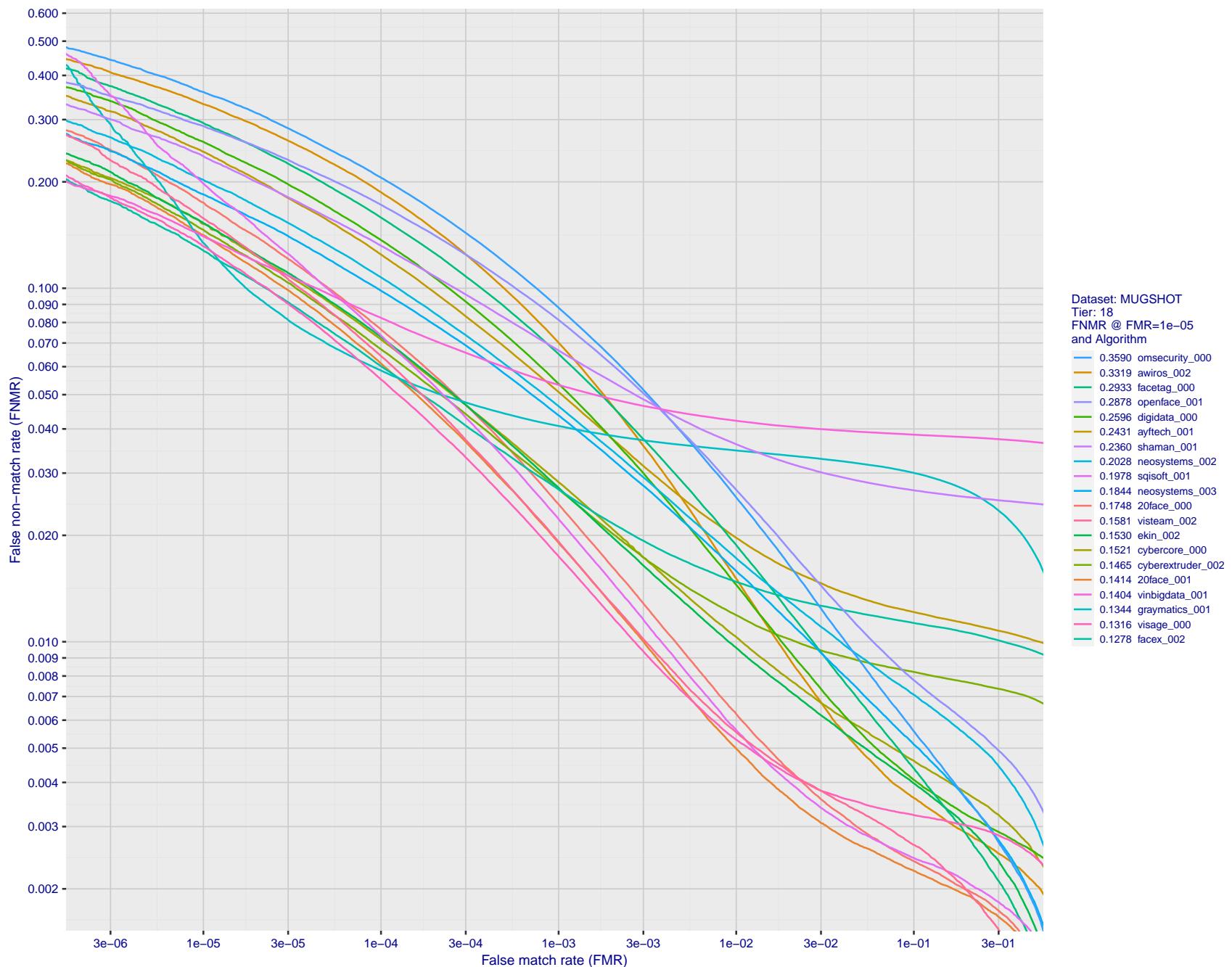


Figure 78: For the mugshot images, detection error tradeoff (DET) characteristics showing false non-match rate vs. false match rate plotted parametrically on threshold, T . The scales are logarithmic in order to show decades of FMR.

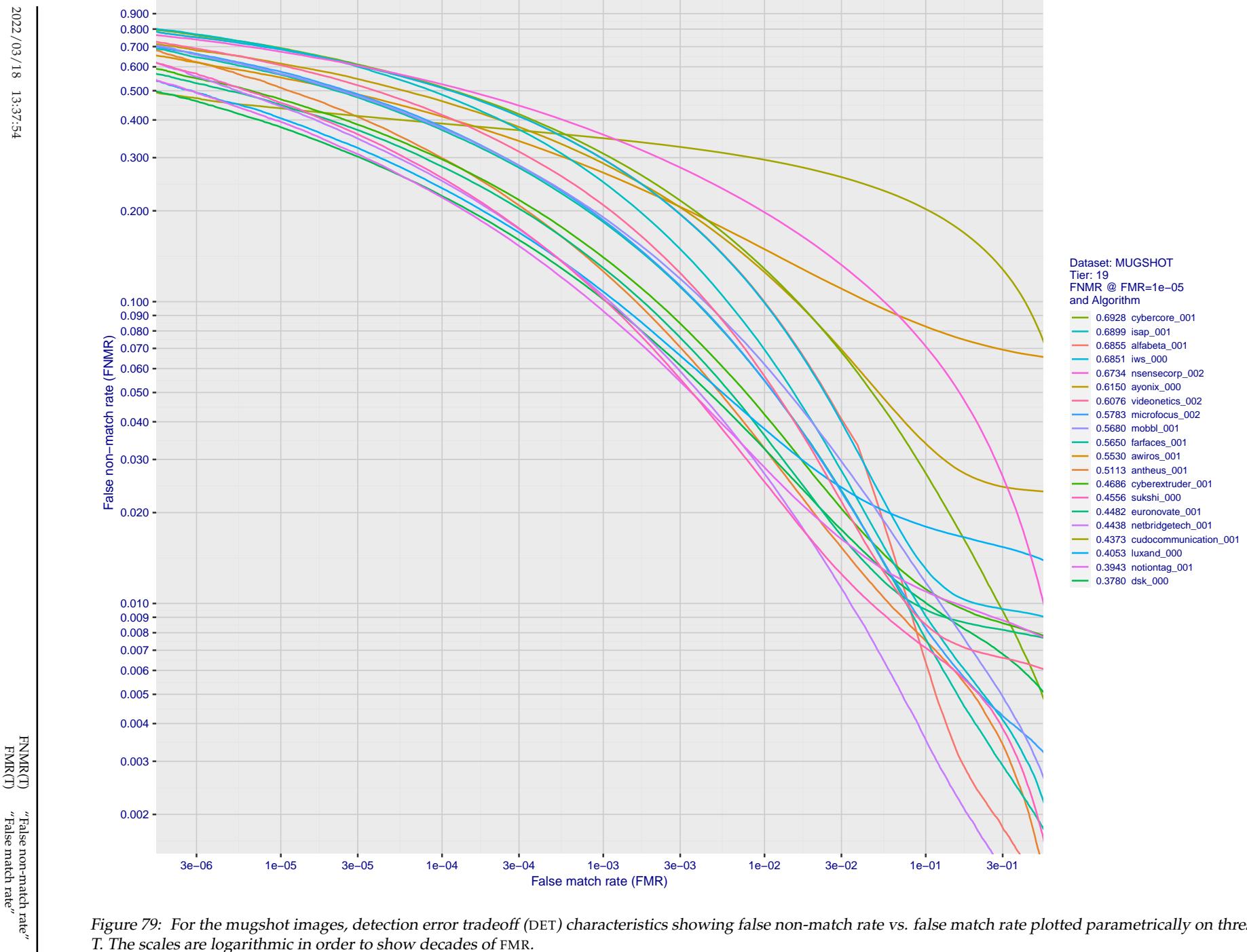


Figure 79: For the mugshot images, detection error tradeoff (DET) characteristics showing false non-match rate vs. false match rate plotted parametrically on threshold, T. The scales are logarithmic in order to show decades of FMR.

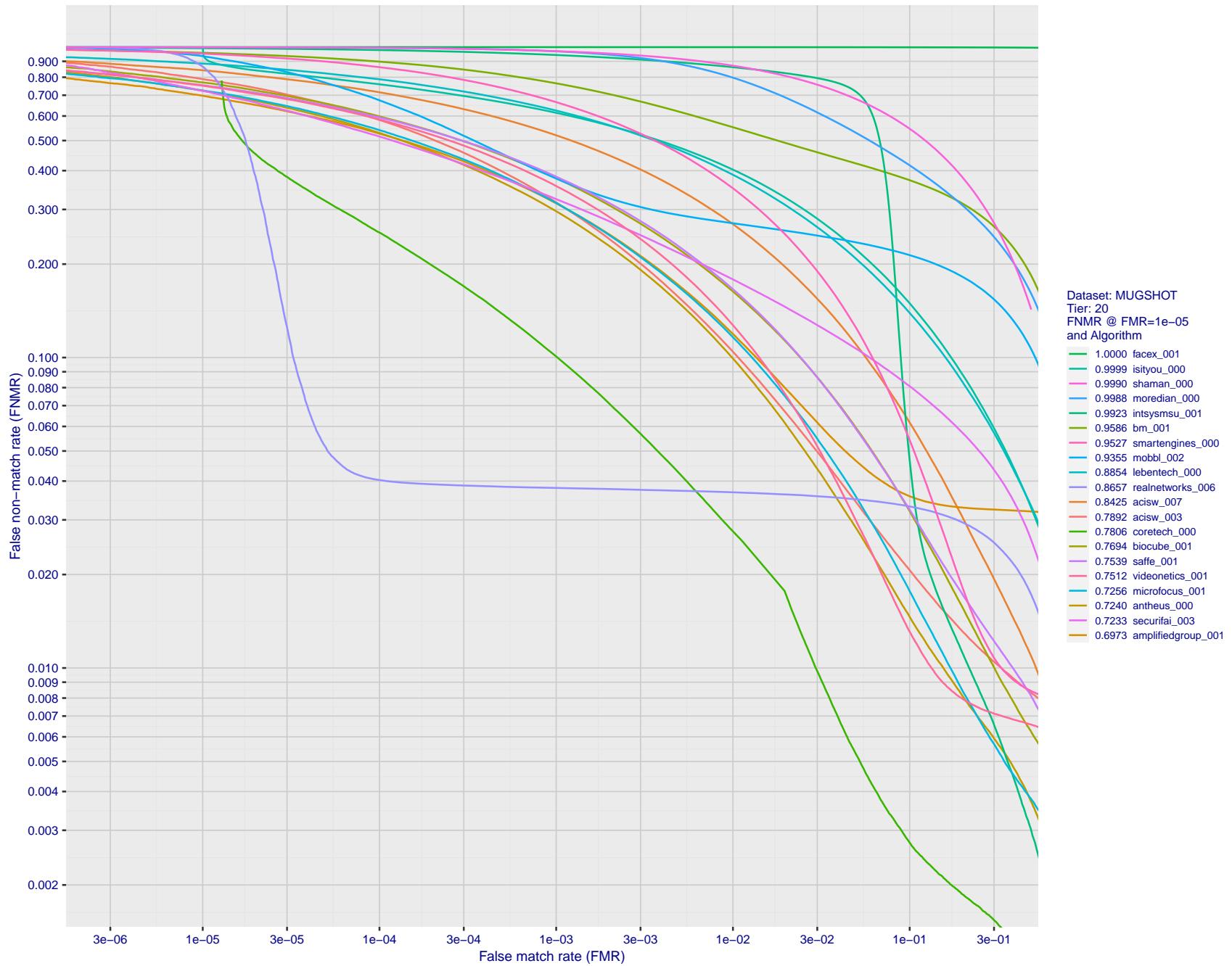


Figure 80: For the mugshot images, detection error tradeoff (DET) characteristics showing false non-match rate vs. false match rate plotted parametrically on threshold, T . The scales are logarithmic in order to show decades of FMR.

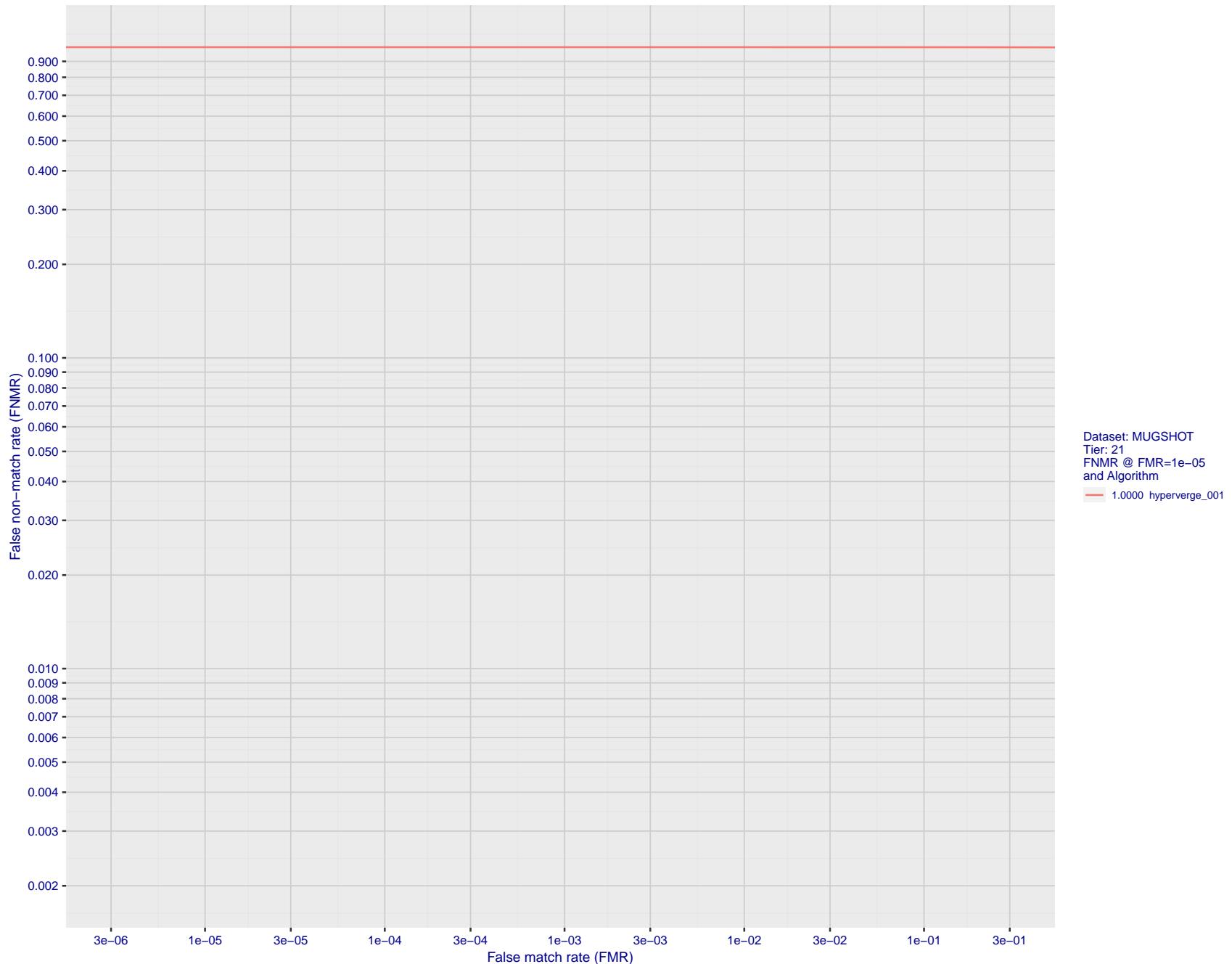


Figure 81: For the mugshot images, detection error tradeoff (DET) characteristics showing false non-match rate vs. false match rate plotted parametrically on threshold, T . The scales are logarithmic in order to show decades of FMR.

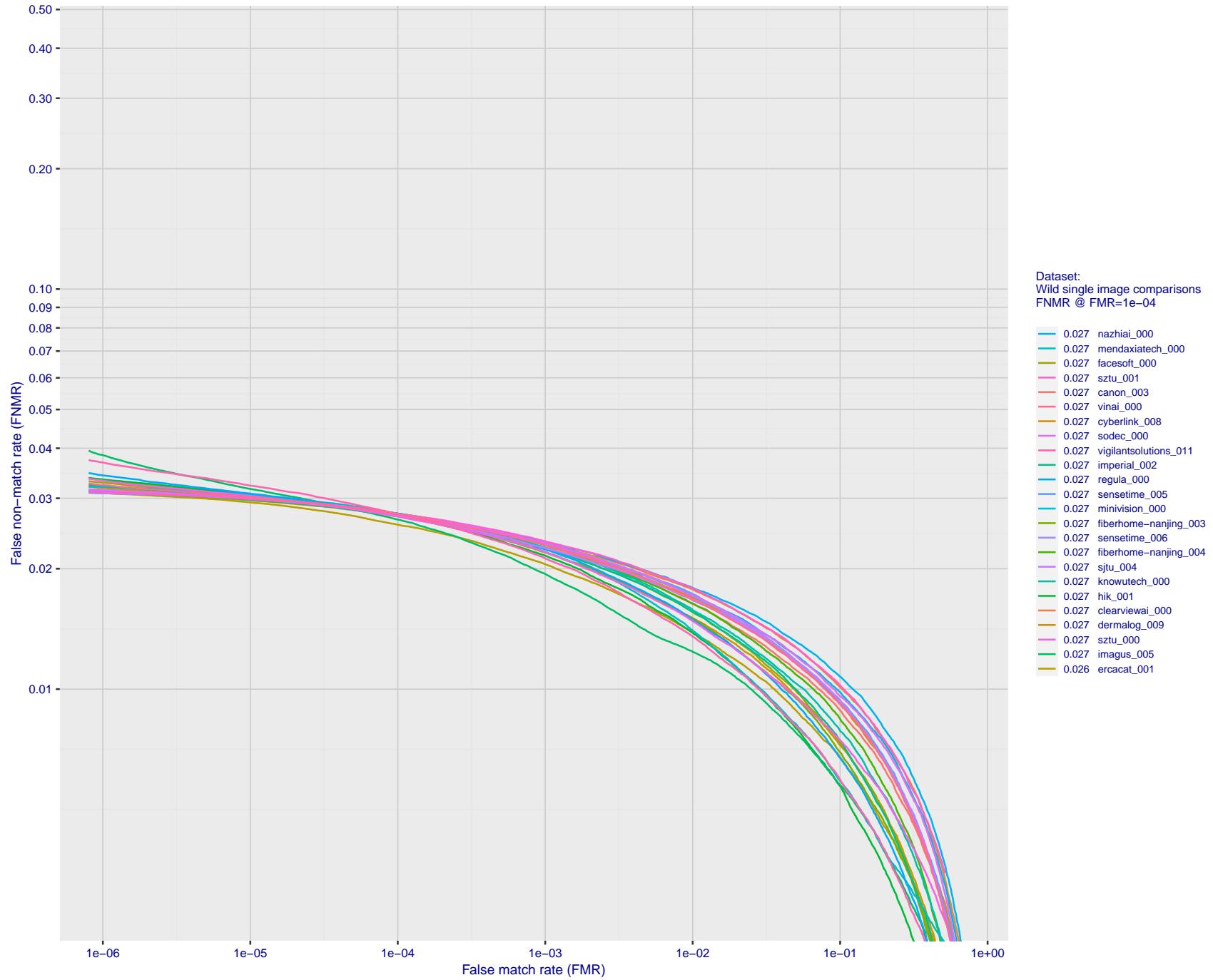


Figure 82: For the 2018 wild image comparisons, detection error tradeoff (DET) characteristics showing false non-match rate vs. false match rate plotted parametrically on threshold, T . The scales are logarithmic in order to show several decades of FMR.

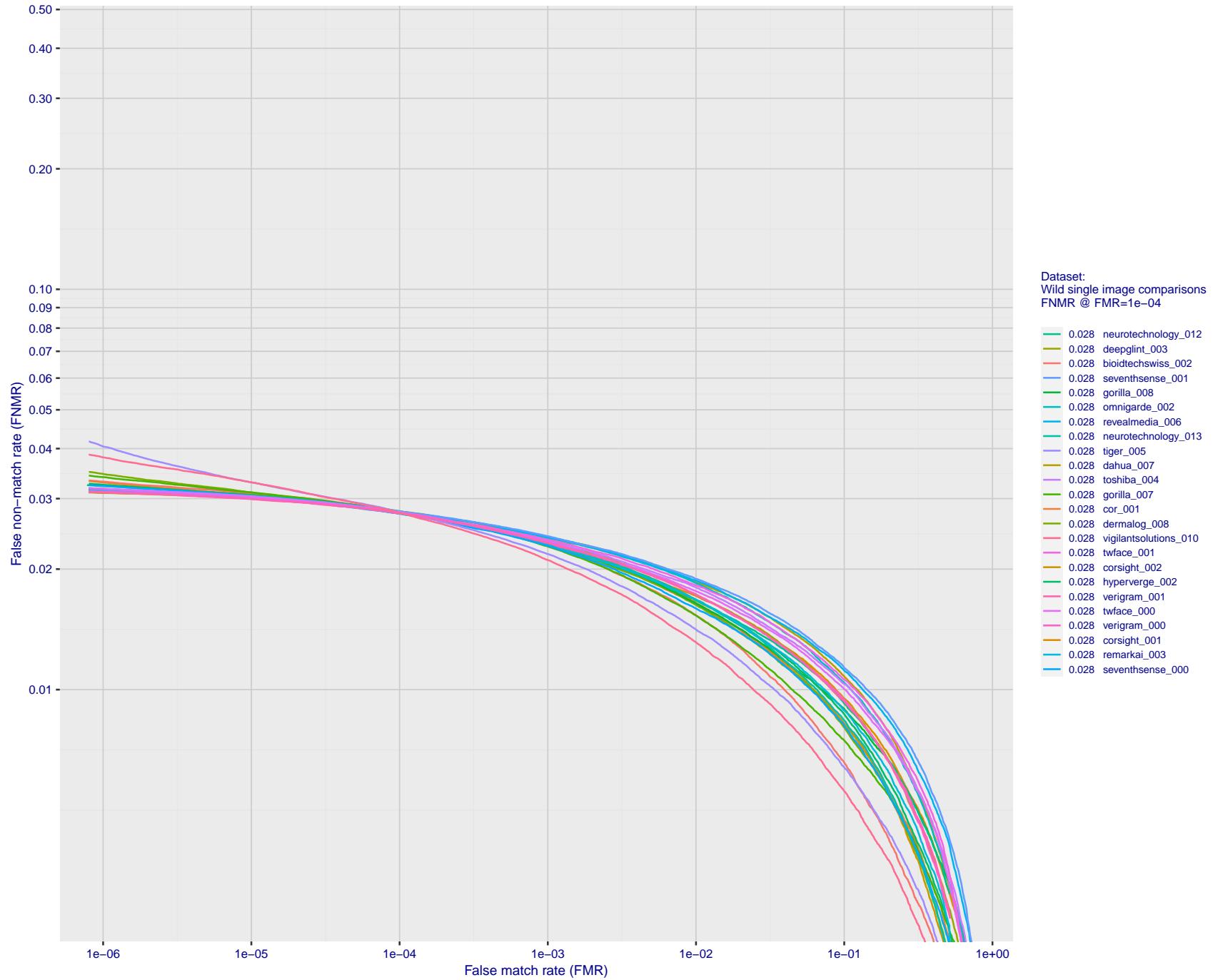


Figure 83: For the 2018 wild image comparisons, detection error tradeoff (DET) characteristics showing false non-match rate vs. false match rate plotted parametrically on threshold, T. The scales are logarithmic in order to show several decades of FMR.

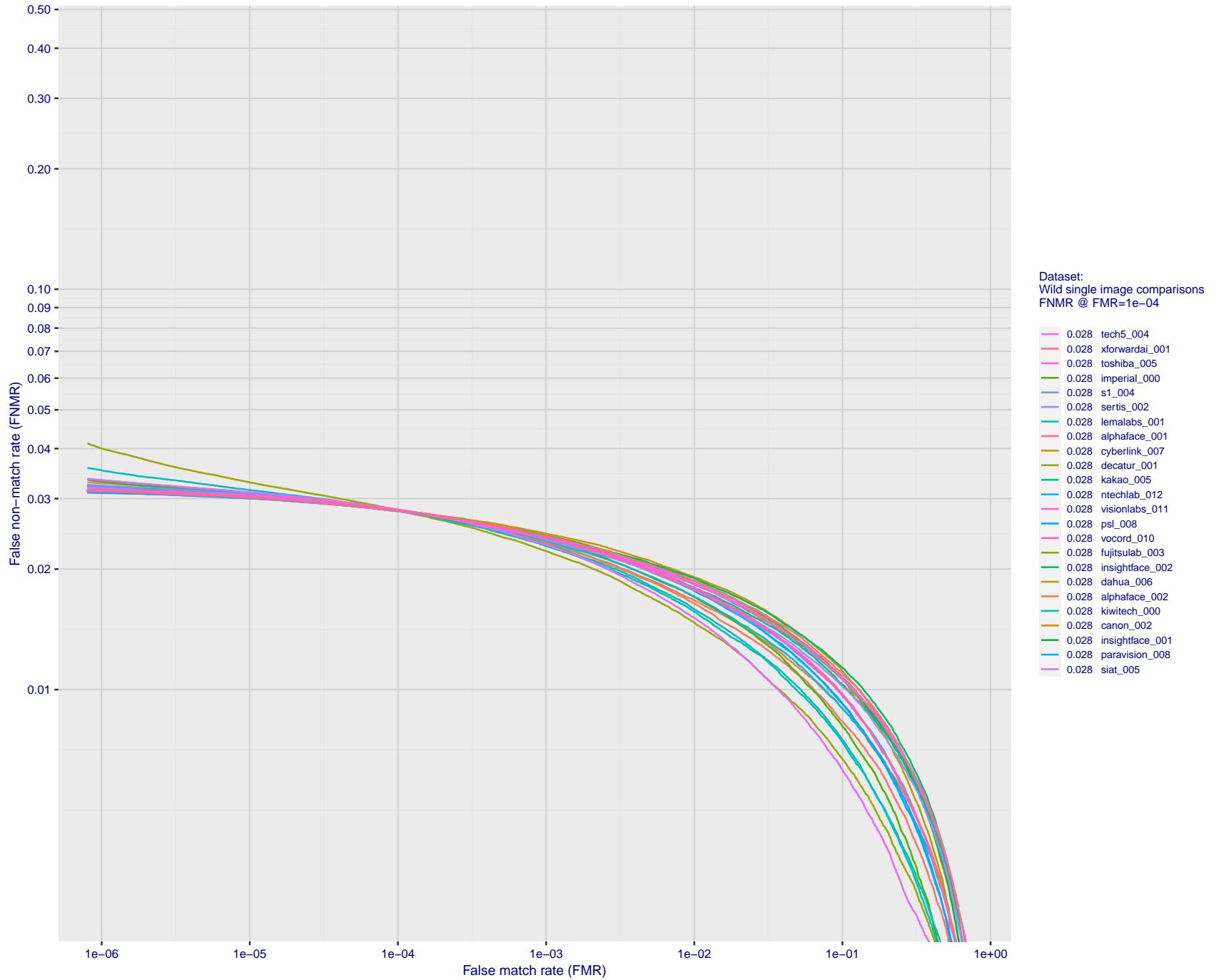


Figure 84: For the 2018 wild image comparisons, detection error tradeoff (DET) characteristics showing false non-match rate vs. false match rate plotted parametrically on threshold, T . The scales are logarithmic in order to show several decades of FMR.

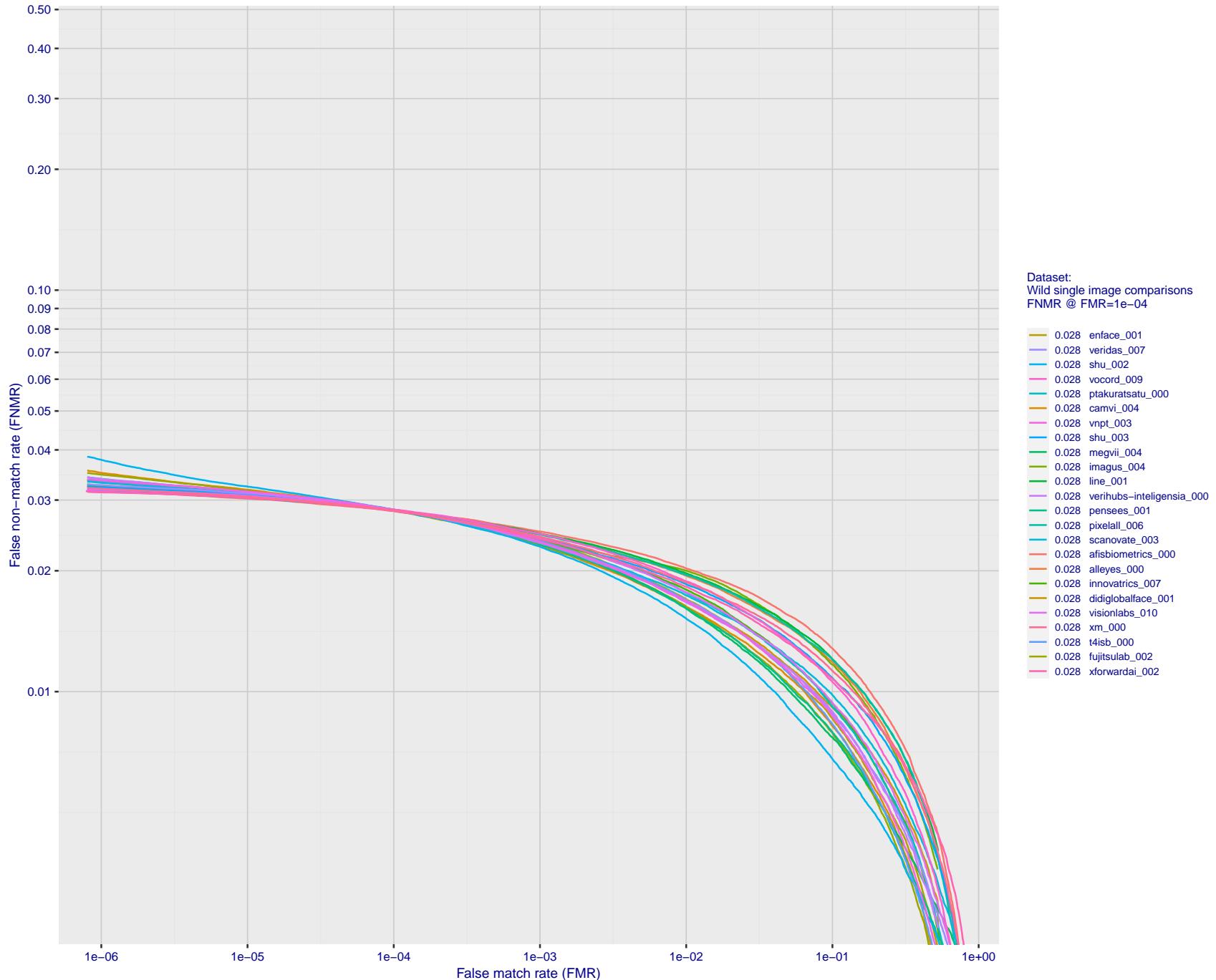


Figure 85: For the 2018 wild image comparisons, detection error tradeoff (DET) characteristics showing false non-match rate vs. false match rate plotted parametrically on threshold, T . The scales are logarithmic in order to show several decades of FMR.

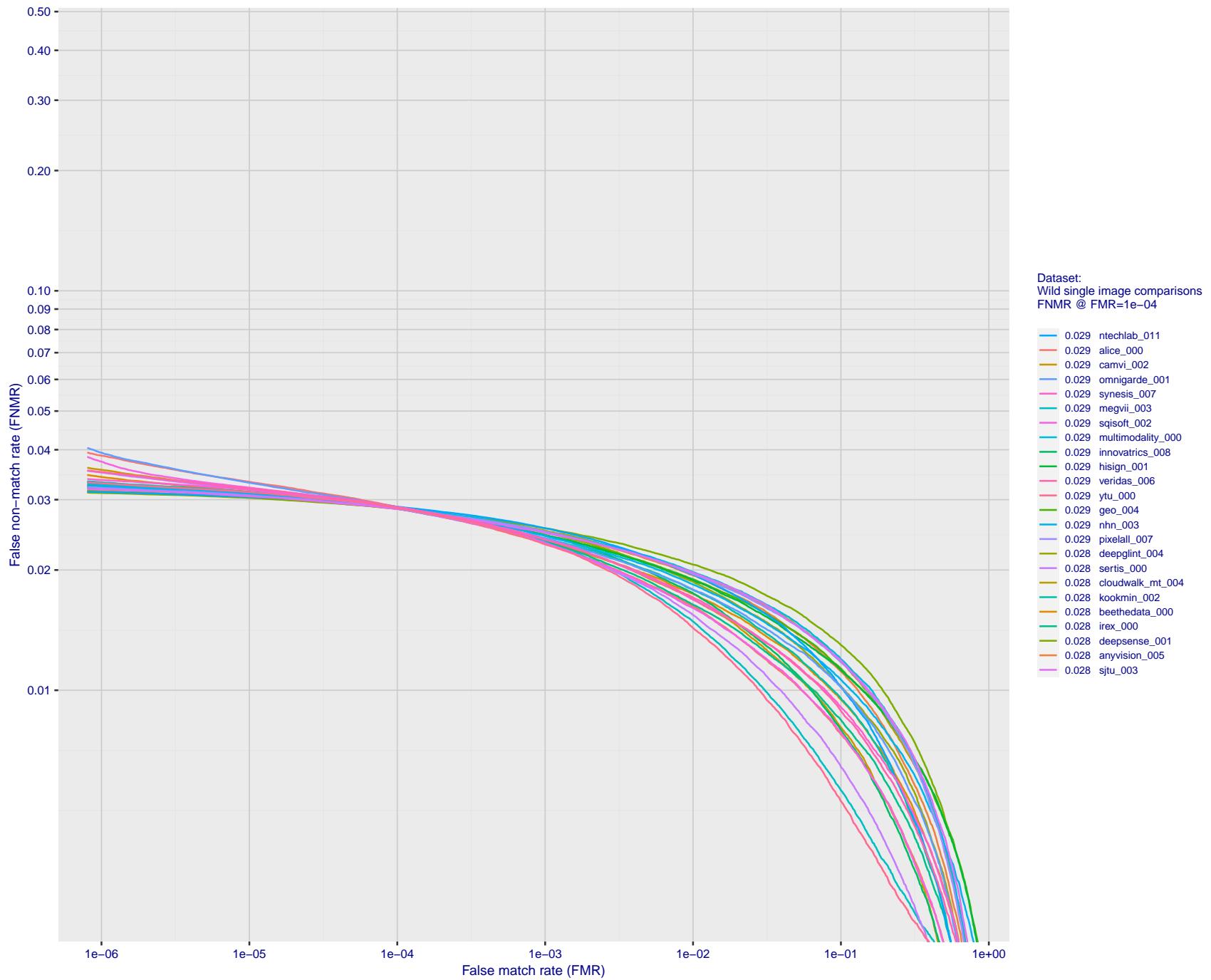


Figure 86: For the 2018 wild image comparisons, detection error tradeoff (DET) characteristics showing false non-match rate vs. false match rate plotted parametrically on threshold, T . The scales are logarithmic in order to show several decades of FMR.

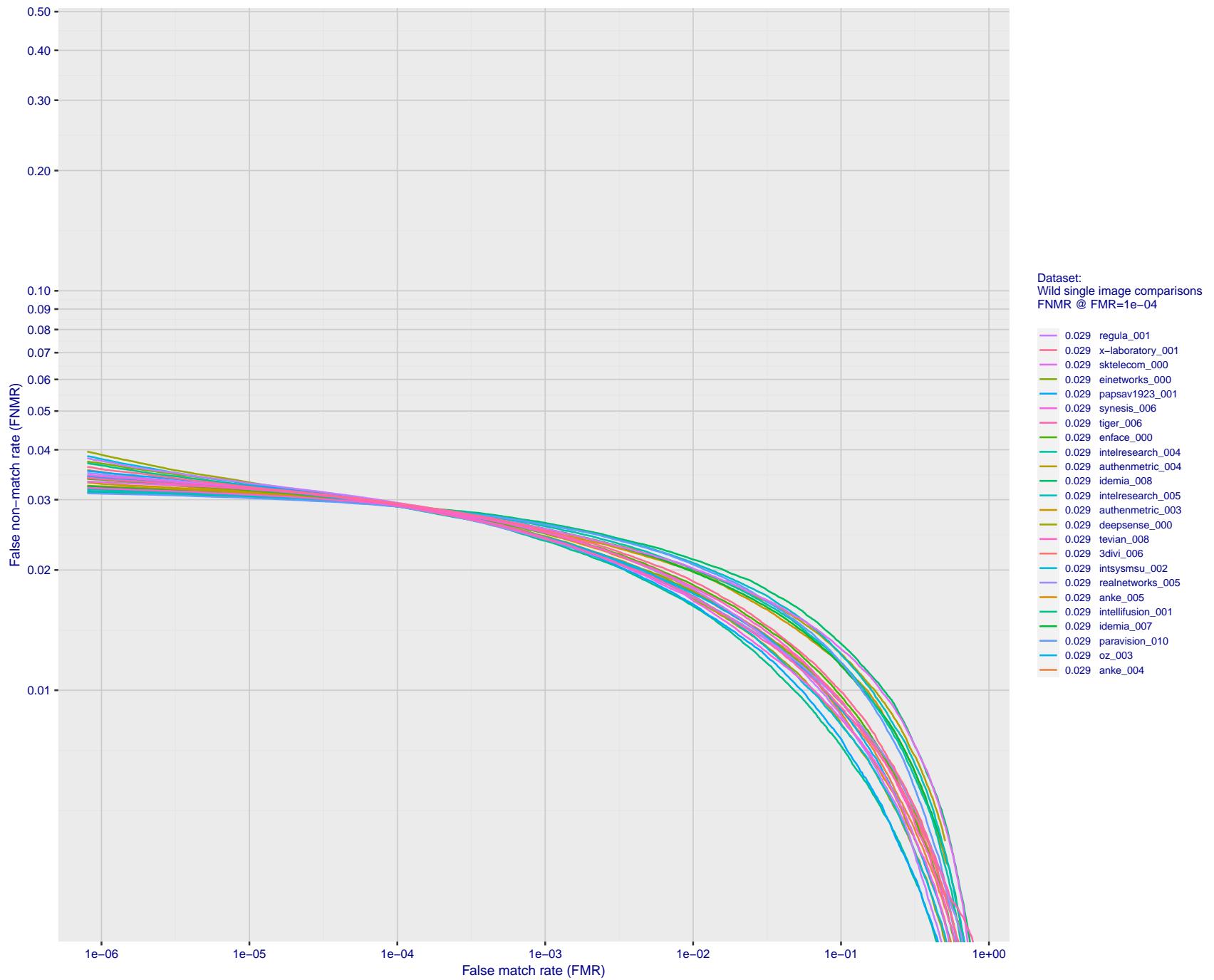


Figure 87: For the 2018 wild image comparisons, detection error tradeoff (DET) characteristics showing false non-match rate vs. false match rate plotted parametrically on threshold, T . The scales are logarithmic in order to show several decades of FMR.

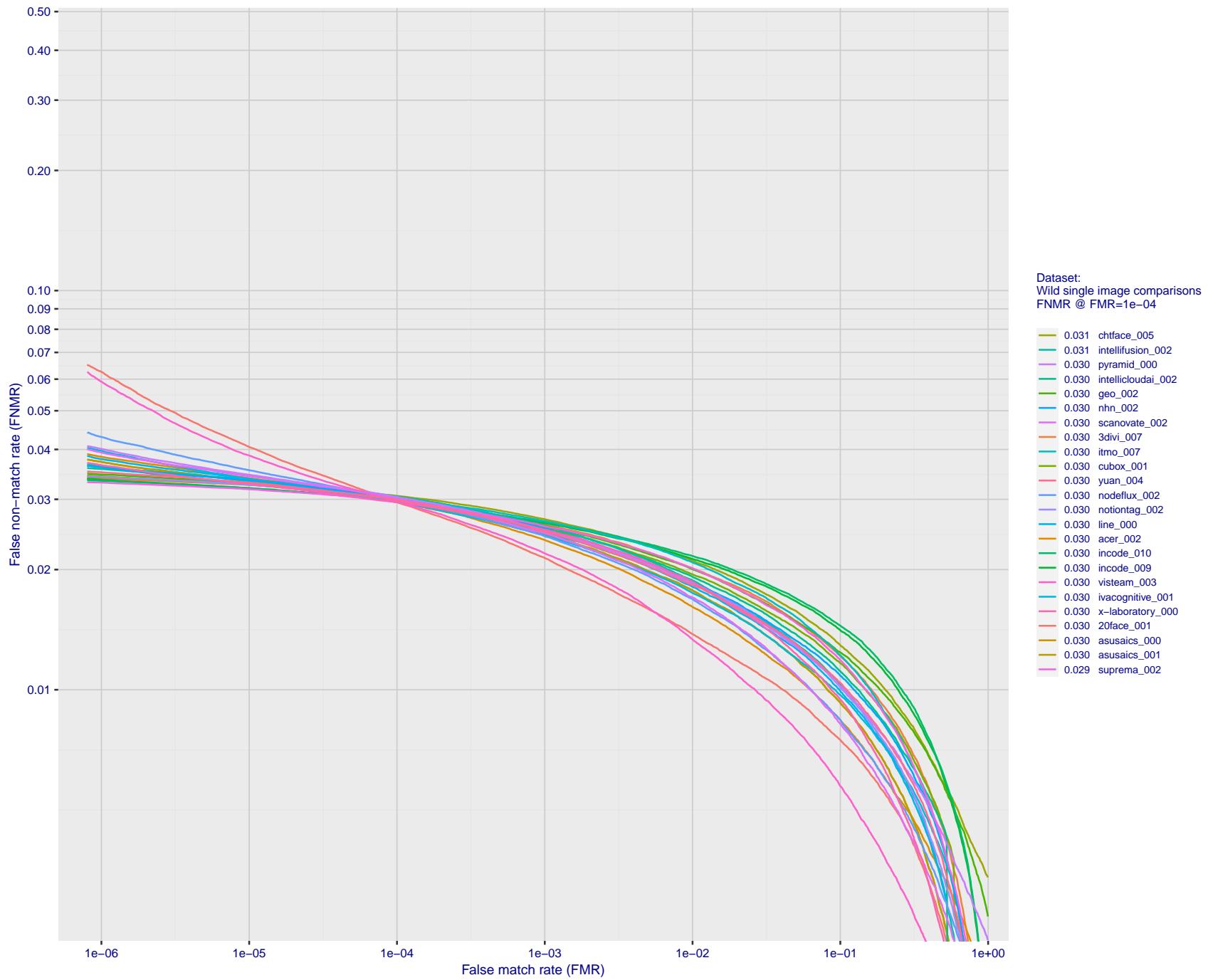


Figure 88: For the 2018 wild image comparisons, detection error tradeoff (DET) characteristics showing false non-match rate vs. false match rate plotted parametrically on threshold, T. The scales are logarithmic in order to show several decades of FMR.

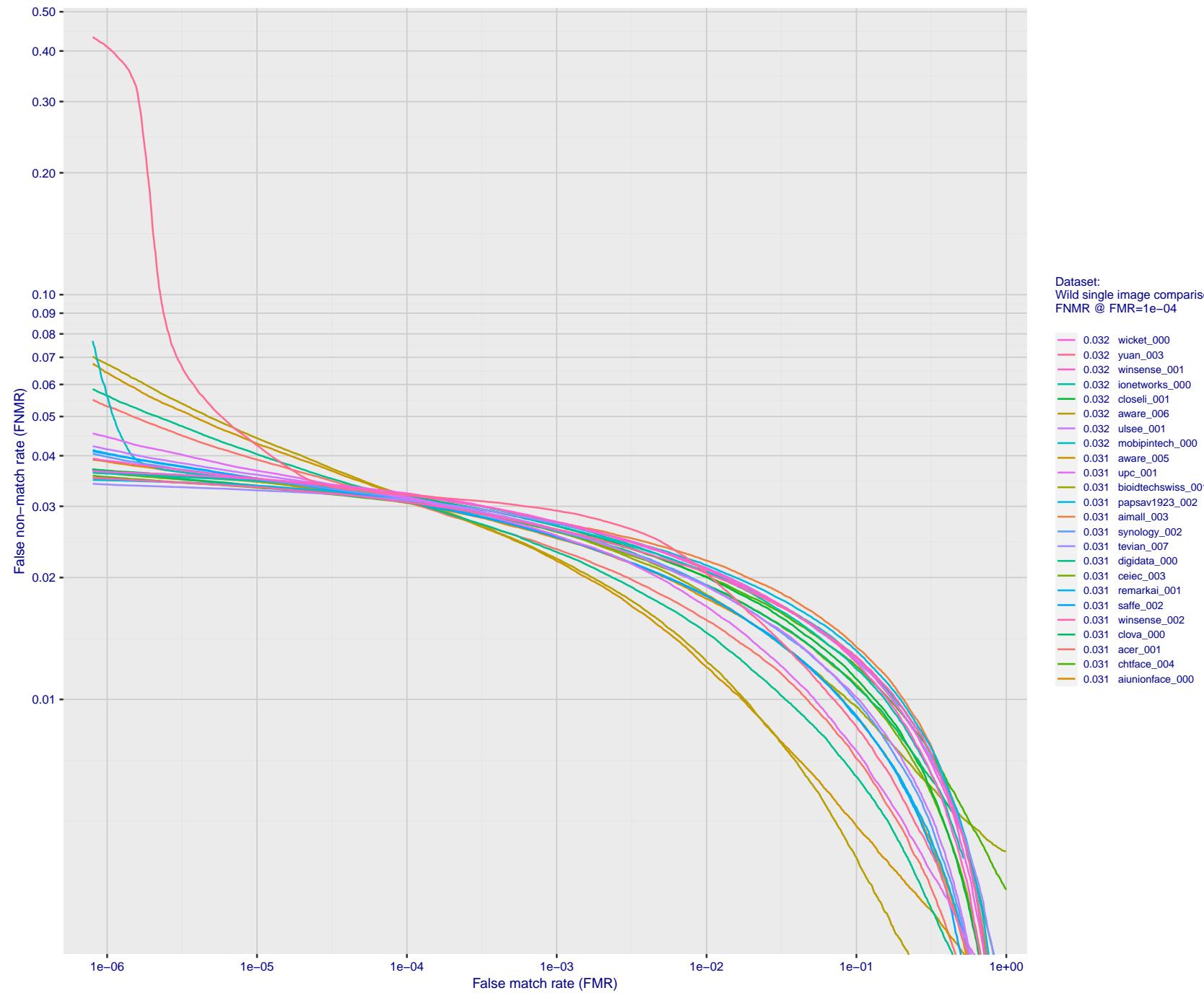


Figure 89: For the 2018 wild image comparisons, detection error tradeoff (DET) characteristics showing false non-match rate vs. false match rate plotted parametrically on threshold, T. The scales are logarithmic in order to show several decades of FMR.

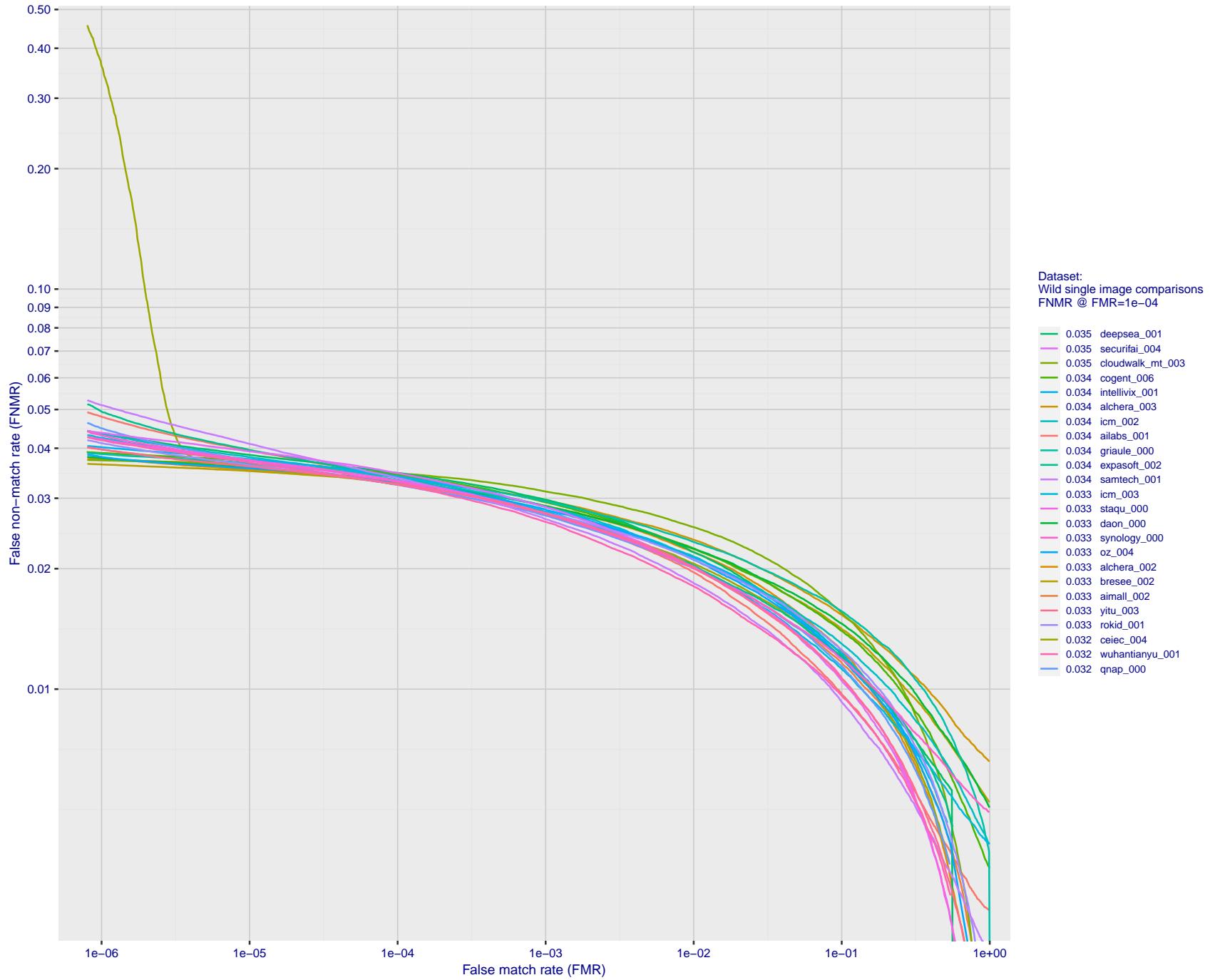


Figure 90: For the 2018 wild image comparisons, detection error tradeoff (DET) characteristics showing false non-match rate vs. false match rate plotted parametrically on threshold, T . The scales are logarithmic in order to show several decades of FMR.

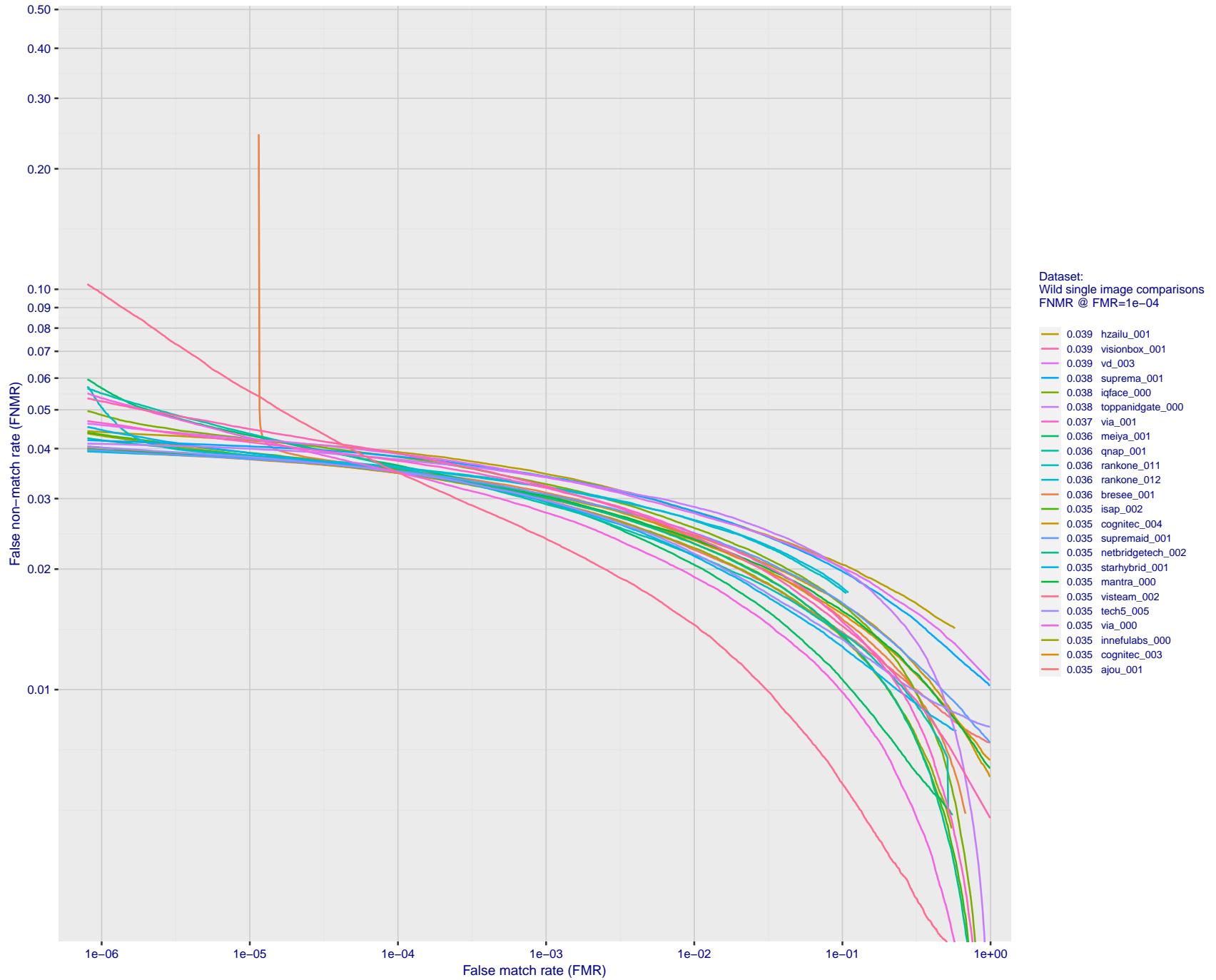


Figure 91: For the 2018 wild image comparisons, detection error tradeoff (DET) characteristics showing false non-match rate vs. false match rate plotted parametrically on threshold, T . The scales are logarithmic in order to show several decades of FMR.

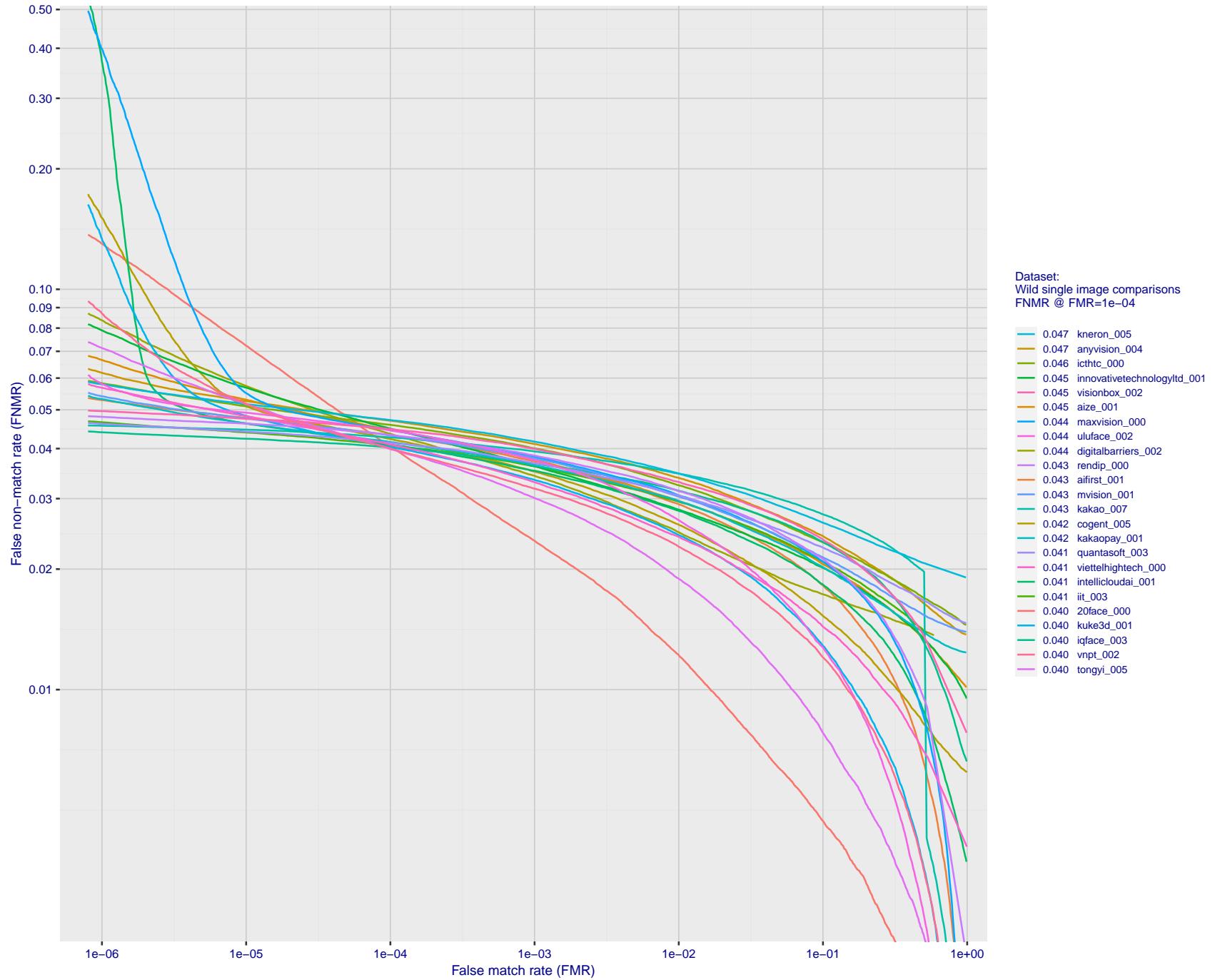


Figure 92: For the 2018 wild image comparisons, detection error tradeoff (DET) characteristics showing false non-match rate vs. false match rate plotted parametrically on threshold, T . The scales are logarithmic in order to show several decades of FMR.

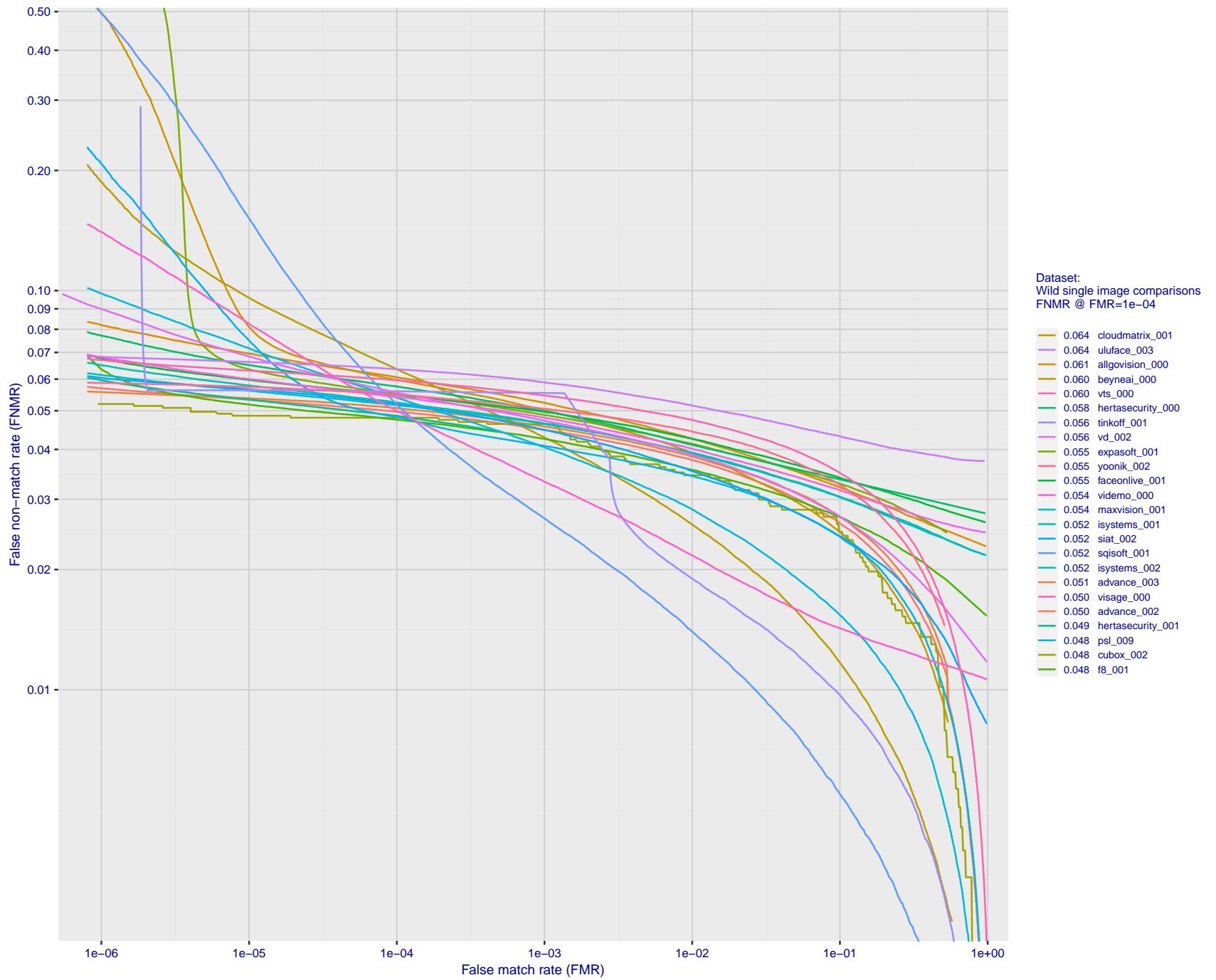


Figure 93: For the 2018 wild image comparisons, detection error tradeoff (DET) characteristics showing false non-match rate vs. false match rate plotted parametrically on threshold, T . The scales are logarithmic in order to show several decades of FMR.

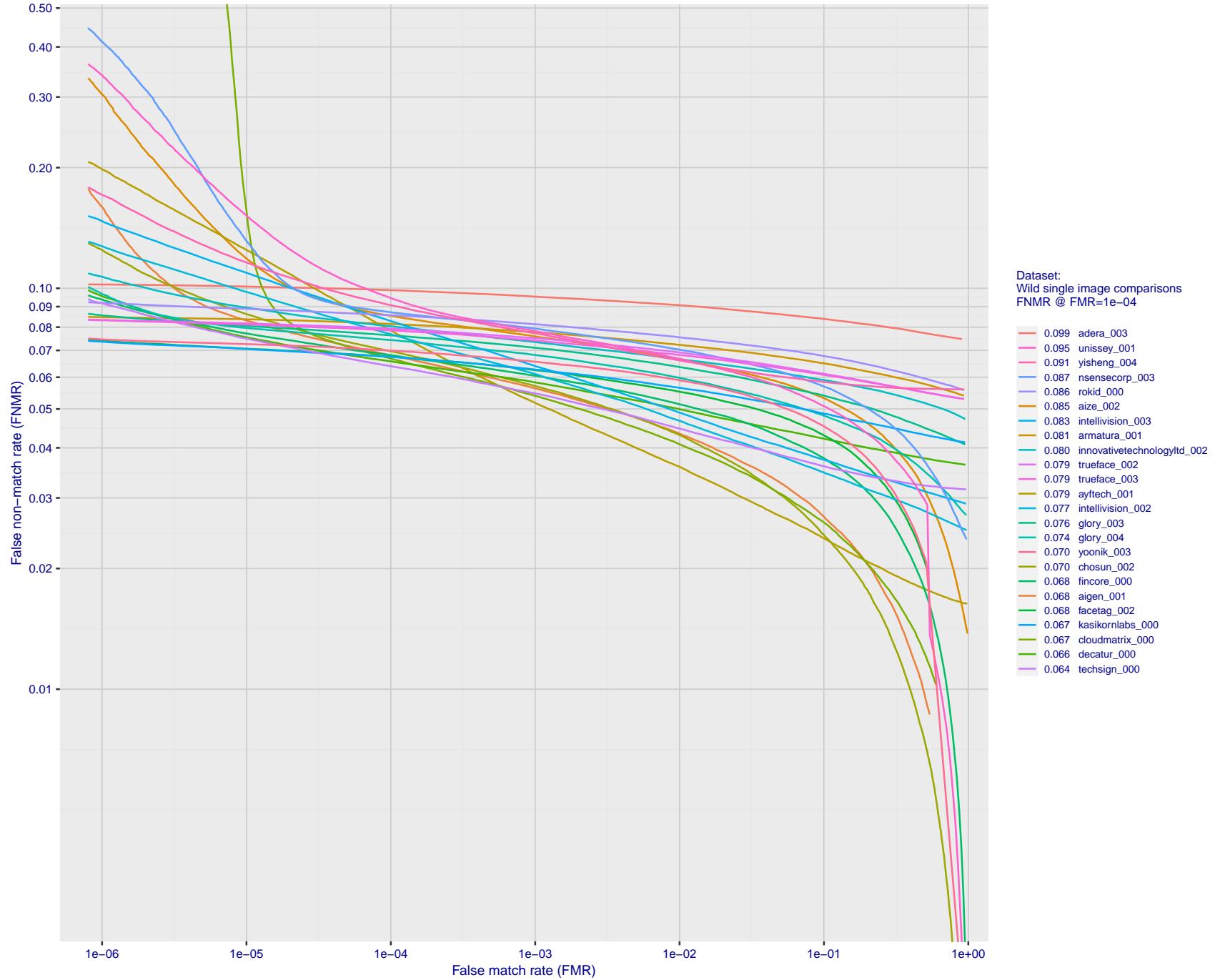


Figure 94: For the 2018 wild image comparisons, detection error tradeoff (DET) characteristics showing false non-match rate vs. false match rate plotted parametrically on threshold, T . The scales are logarithmic in order to show several decades of FMR.

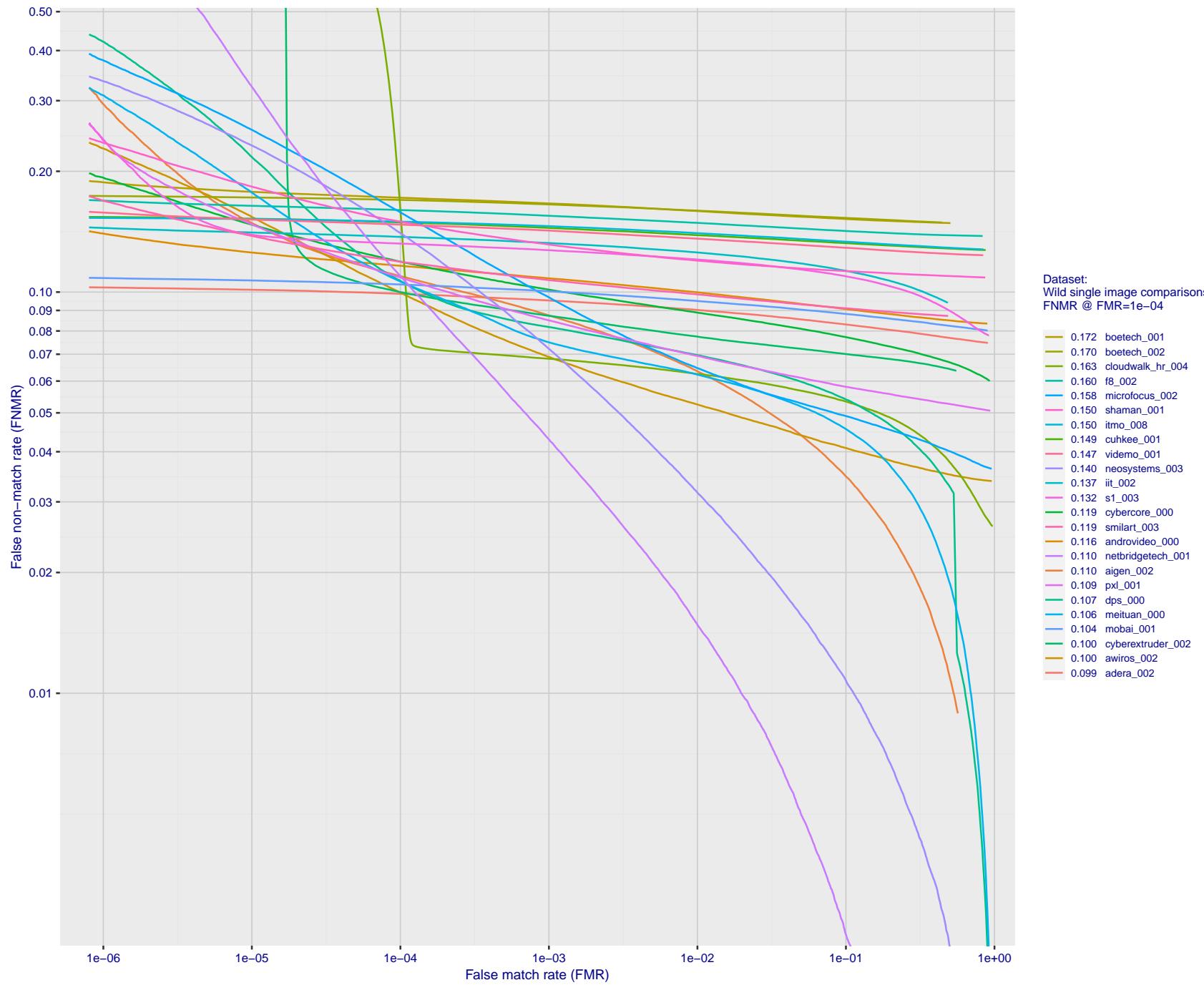


Figure 95: For the 2018 wild image comparisons, detection error tradeoff (DET) characteristics showing false non-match rate vs. false match rate plotted parametrically on threshold, T . The scales are logarithmic in order to show several decades of FMR.

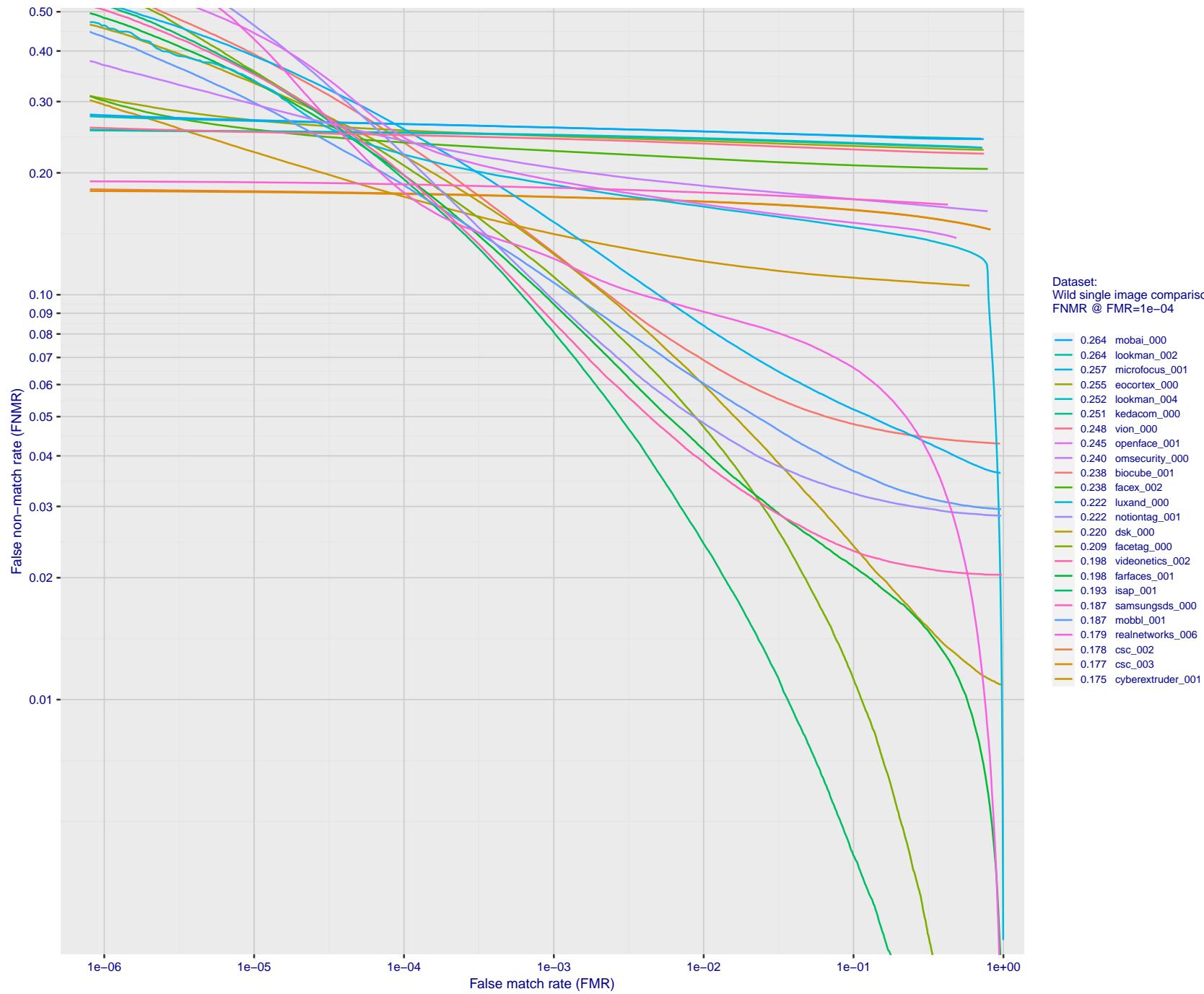


Figure 96: For the 2018 wild image comparisons, detection error tradeoff (DET) characteristics showing false non-match rate vs. false match rate plotted parametrically on threshold, T. The scales are logarithmic in order to show several decades of FMR.

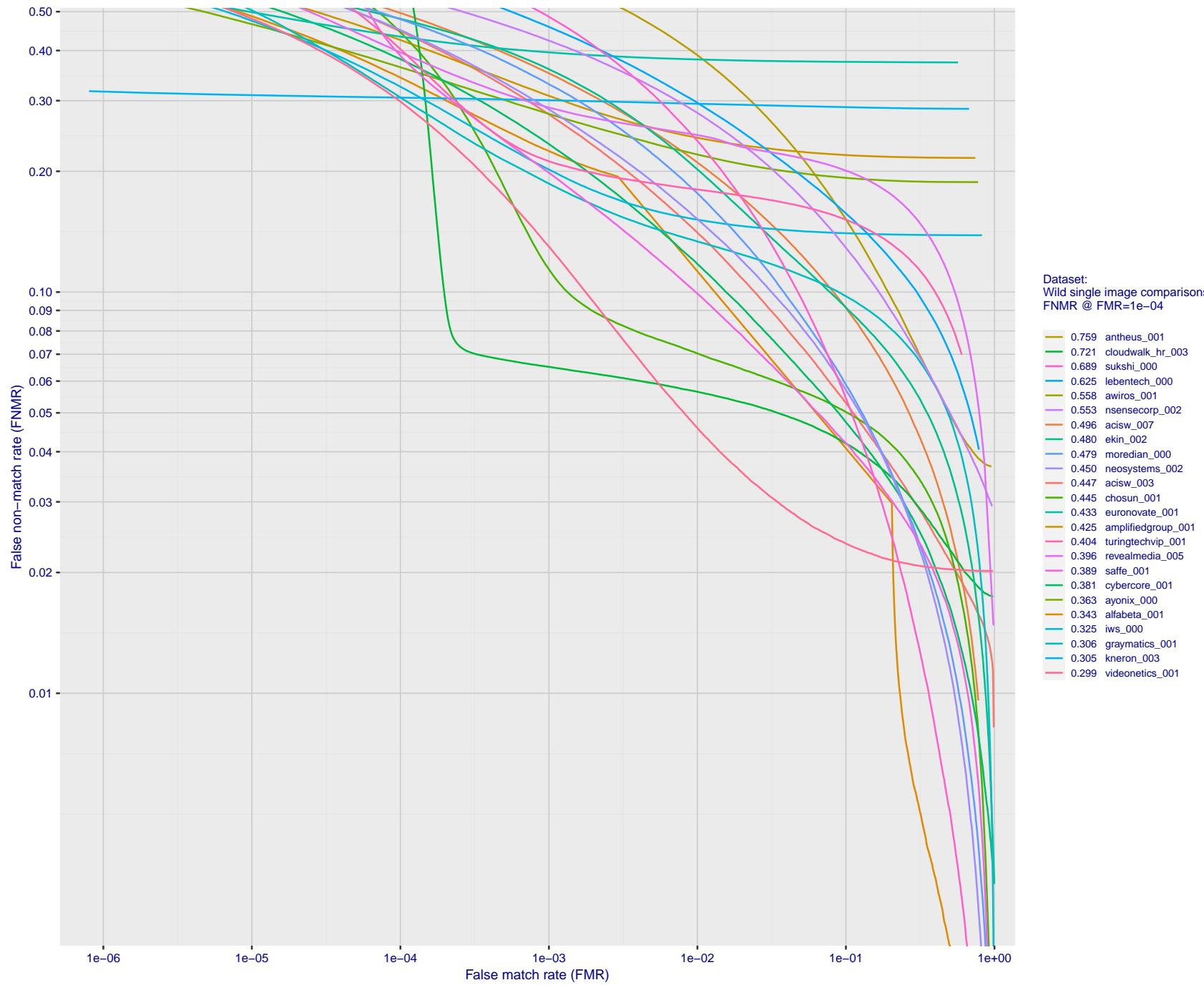


Figure 97: For the 2018 wild image comparisons, detection error tradeoff (DET) characteristics showing false non-match rate vs. false match rate plotted parametrically on threshold, T. The scales are logarithmic in order to show several decades of FMR.

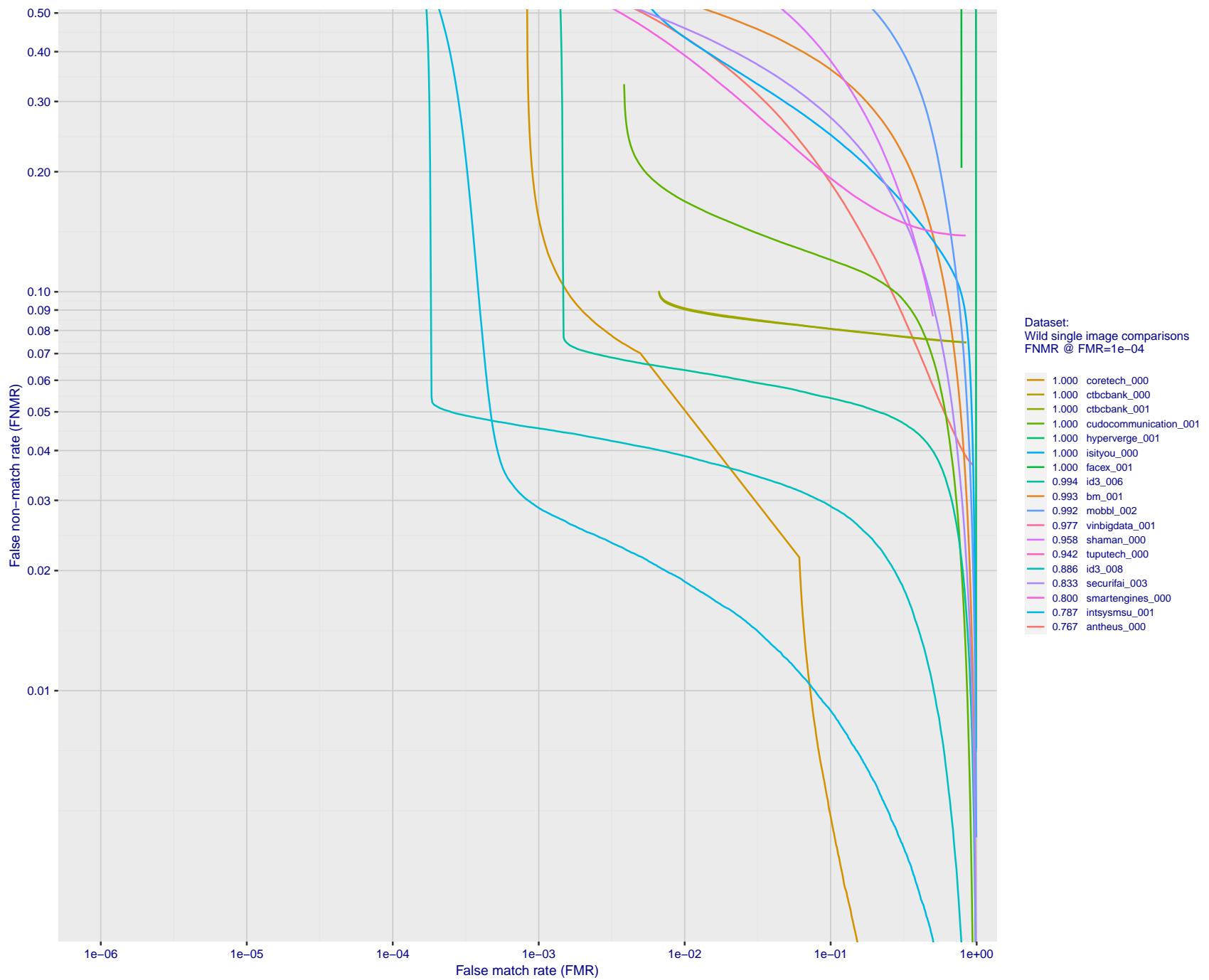


Figure 98: For the 2018 wild image comparisons, detection error tradeoff (DET) characteristics showing false non-match rate vs. false match rate plotted parametrically on threshold, T. The scales are logarithmic in order to show several decades of FMR.

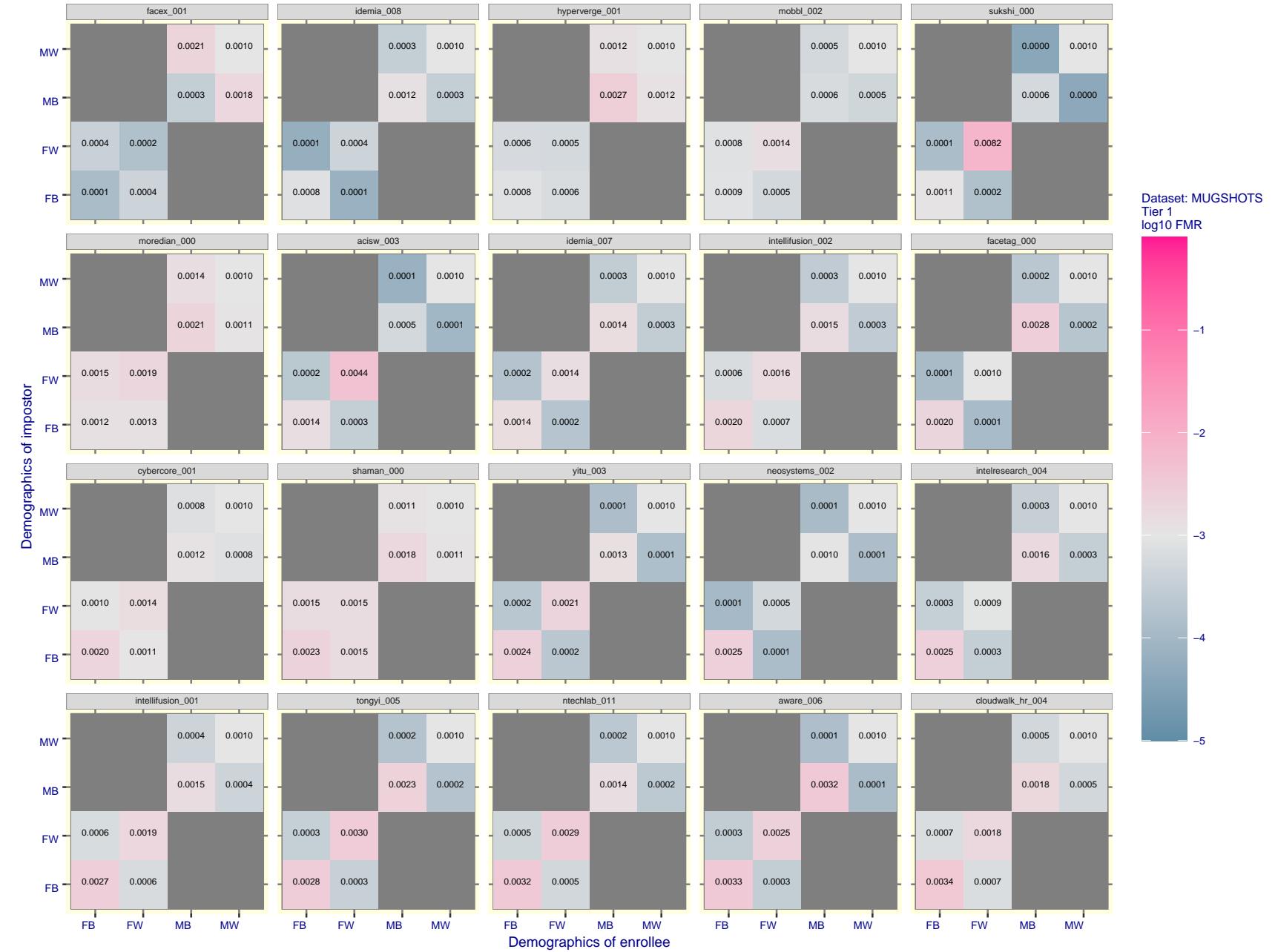


Figure 99: For the mugshot images, FMR for same-sex impostor pairs of images annotated with codes for black female, black male, white female, white male. The threshold is set for each algorithm to give FMR = 0.001 for white males which is the demographic that usually gives the lowest FMR. This means the top right box is the same color in all panels. The panels are sorted over multiple pages in order of FMR on black females, which is the demographic that usually gives the highest FMR.

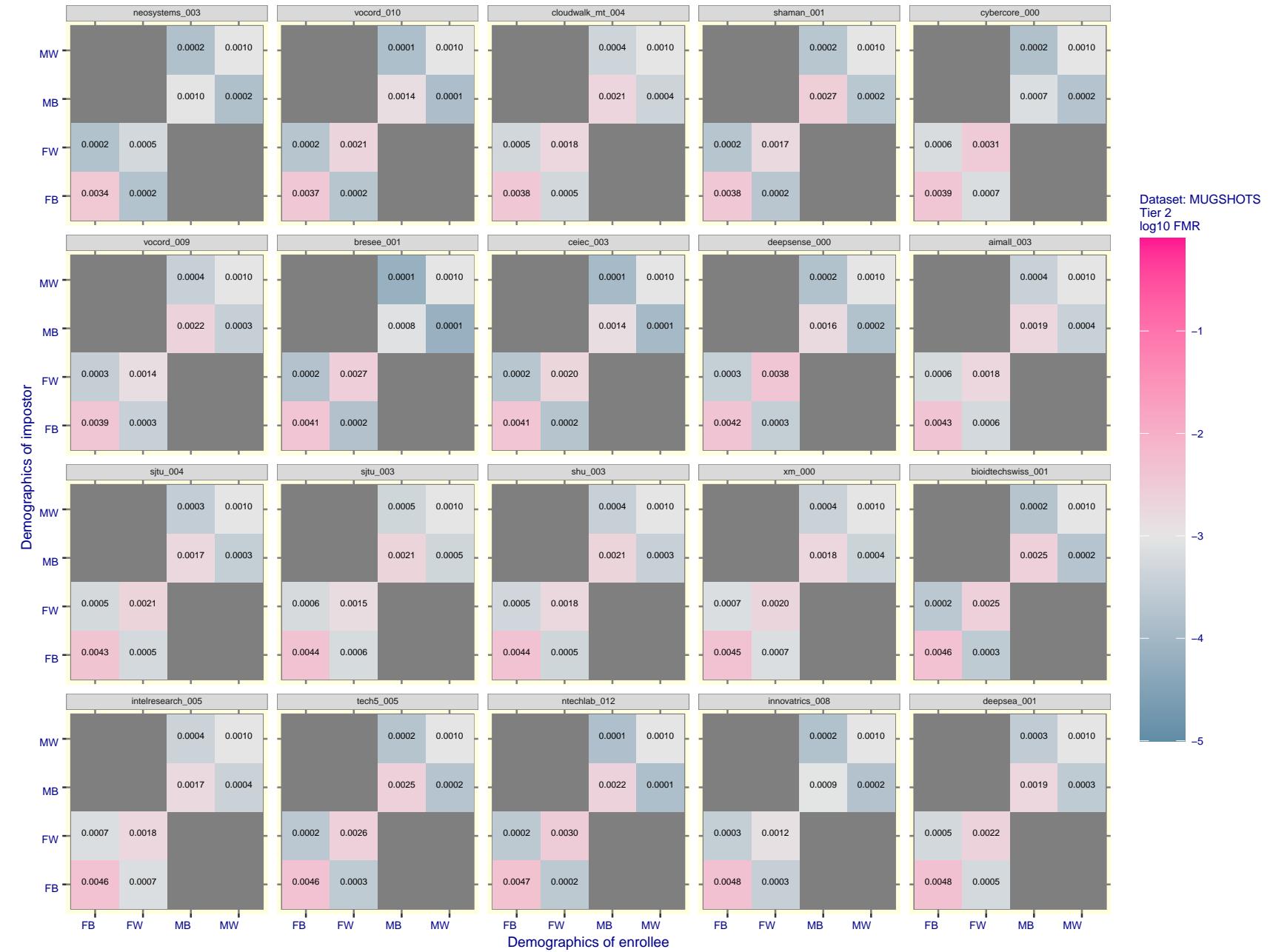


Figure 100: For the mugshot images, FMR for same-sex impostor pairs of images annotated with codes for black female, black male, white female, white male. The threshold is set for each algorithm to give FMR = 0.001 for white males which is the demographic that usually gives the lowest FMR. This means the top right box is the same color in all panels. The panels are sorted over multiple pages in order of FMR on black females, which is the demographic that usually gives the highest FMR.

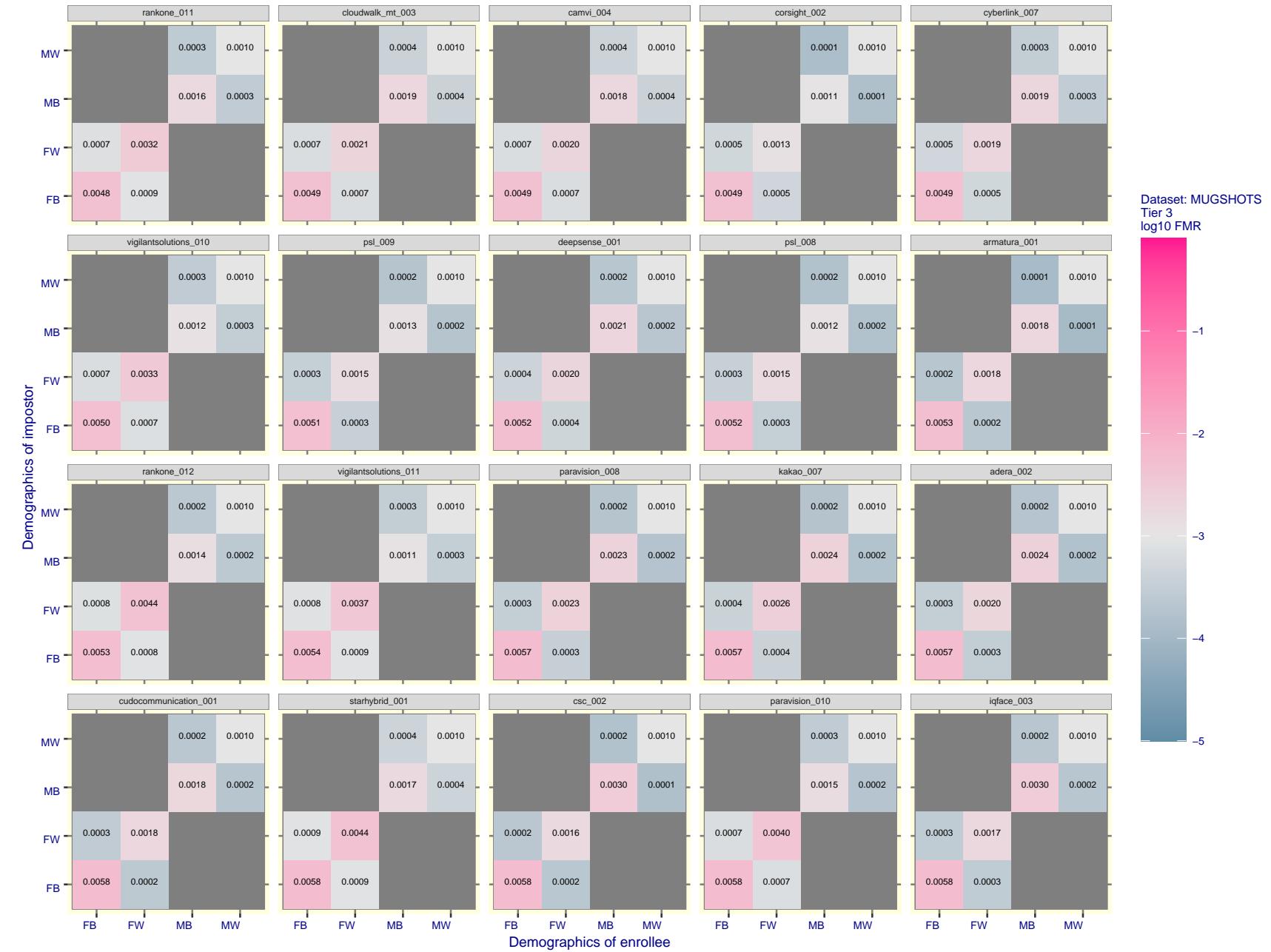


Figure 101: For the mugshot images, FMR for same-sex impostor pairs of images annotated with codes for black female, black male, white female, white male. The threshold is set for each algorithm to give FMR = 0.001 for white males which is the demographic that usually gives the lowest FMR. This means the top right box is the same color in all panels. The panels are sorted over multiple pages in order of FMR on black females, which is the demographic that usually gives the highest FMR.

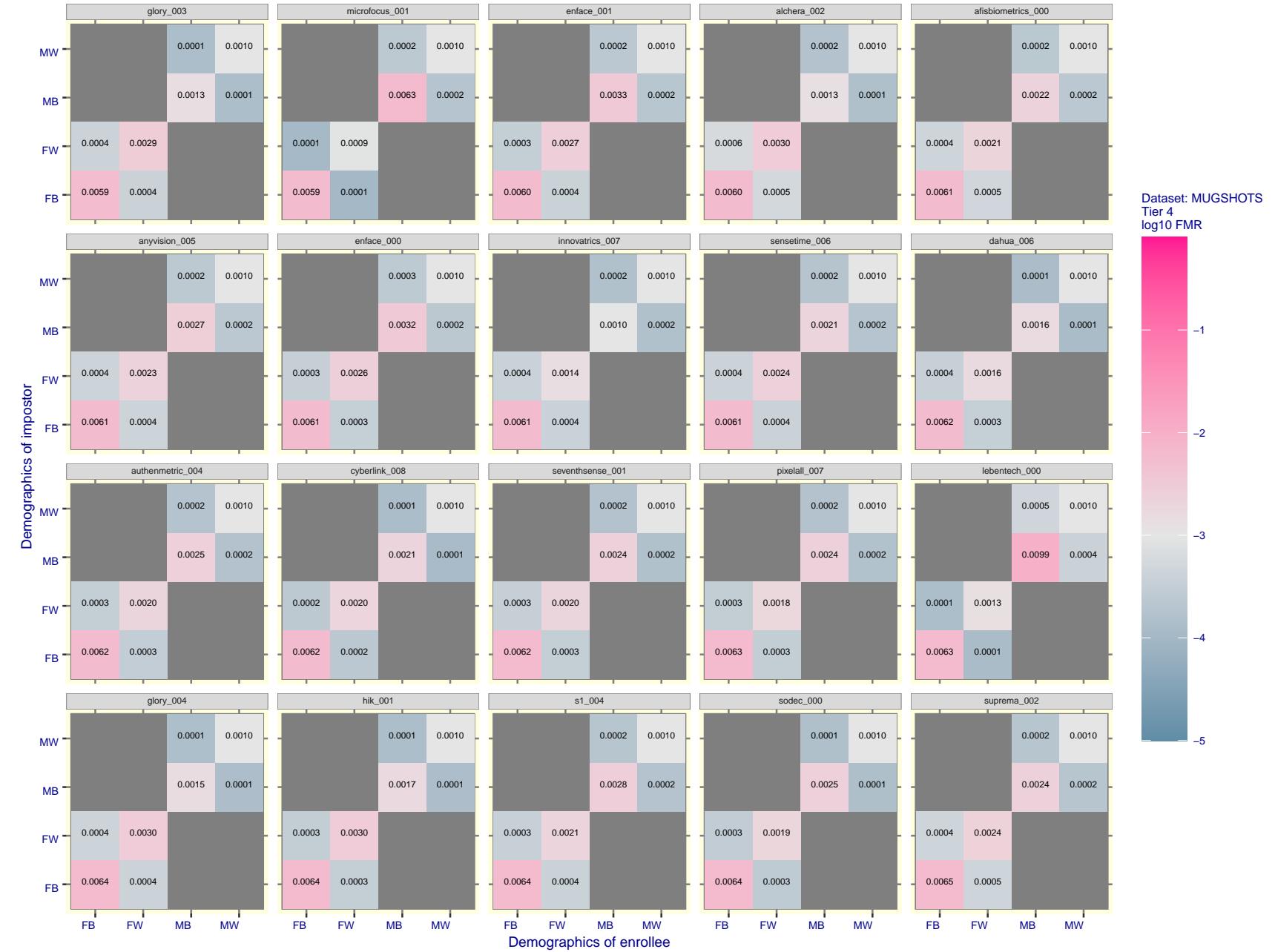


Figure 102: For the mugshot images, FMR for same-sex impostor pairs of images annotated with codes for black female, black male, white female, white male. The threshold is set for each algorithm to give $\text{FMR} = 0.001$ for white males which is the demographic that usually gives the lowest FMR. This means the top right box is the same color in all panels. The panels are sorted over multiple pages in order of FMR on black females, which is the demographic that usually gives the highest FMR.

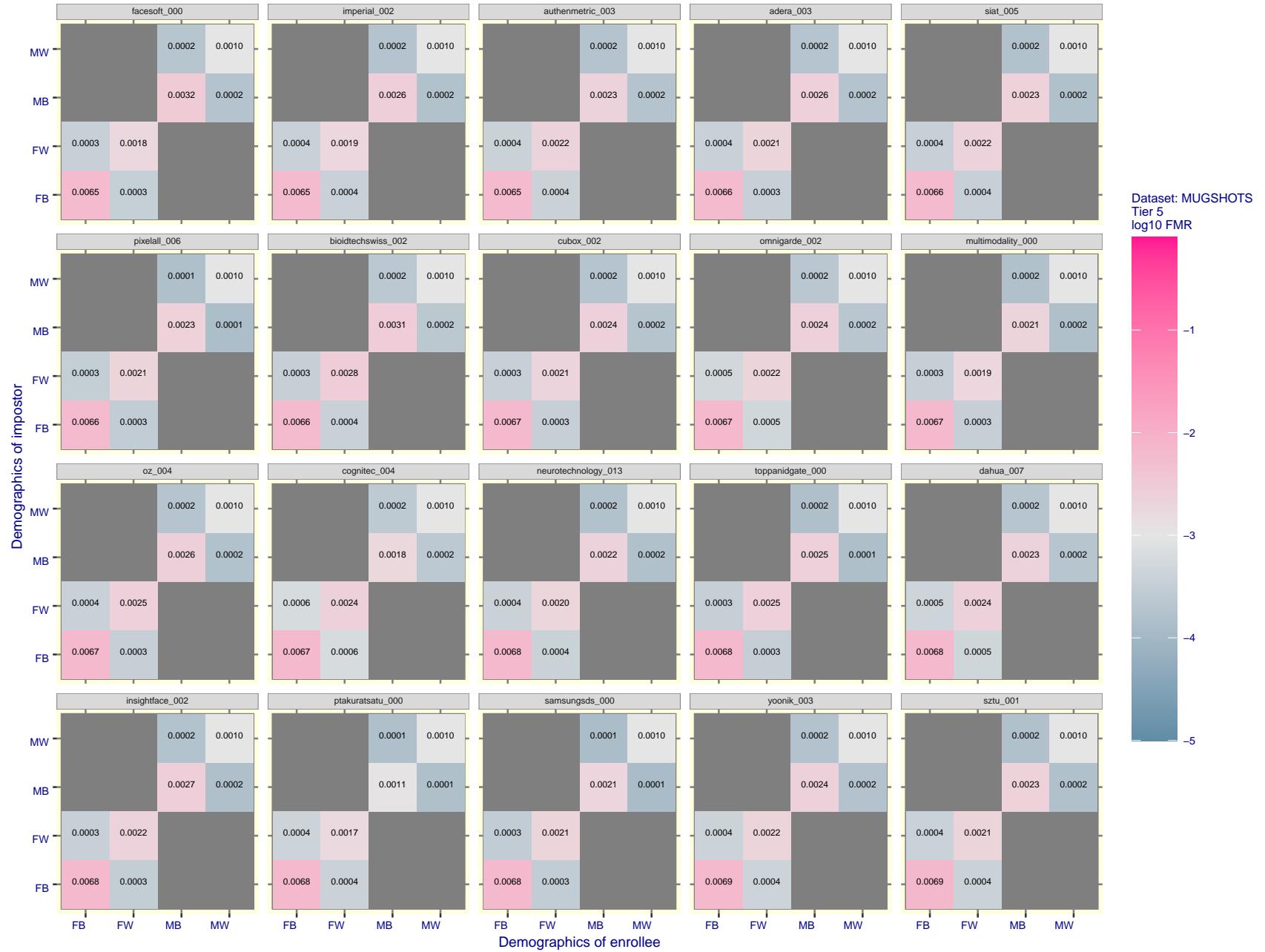


Figure 103: For the mugshot images, FMR for same-sex impostor pairs of images annotated with codes for black female, black male, white female, white male. The threshold is set for each algorithm to give FMR = 0.001 for white males which is the demographic that usually gives the lowest FMR. This means the top right box is the same color in all panels. The panels are sorted over multiple pages in order of FMR on black females, which is the demographic that usually gives the highest FMR.

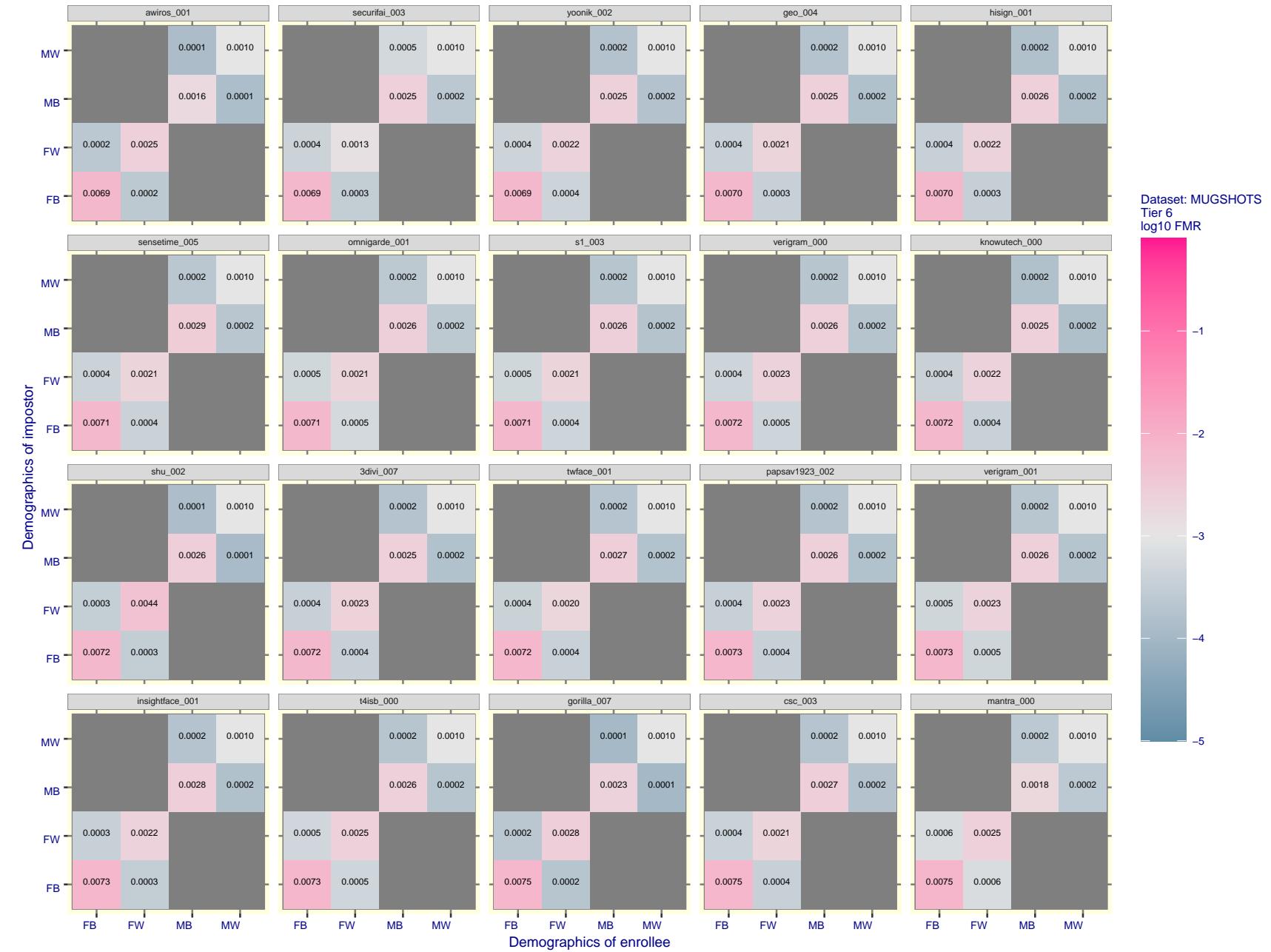


Figure 104: For the mugshot images, FMR for same-sex impostor pairs of images annotated with codes for black female, black male, white female, white male. The threshold is set for each algorithm to give FMR = 0.001 for white males which is the demographic that usually gives the lowest FMR. This means the top right box is the same color in all panels. The panels are sorted over multiple pages in order of FMR on black females, which is the demographic that usually gives the highest FMR.

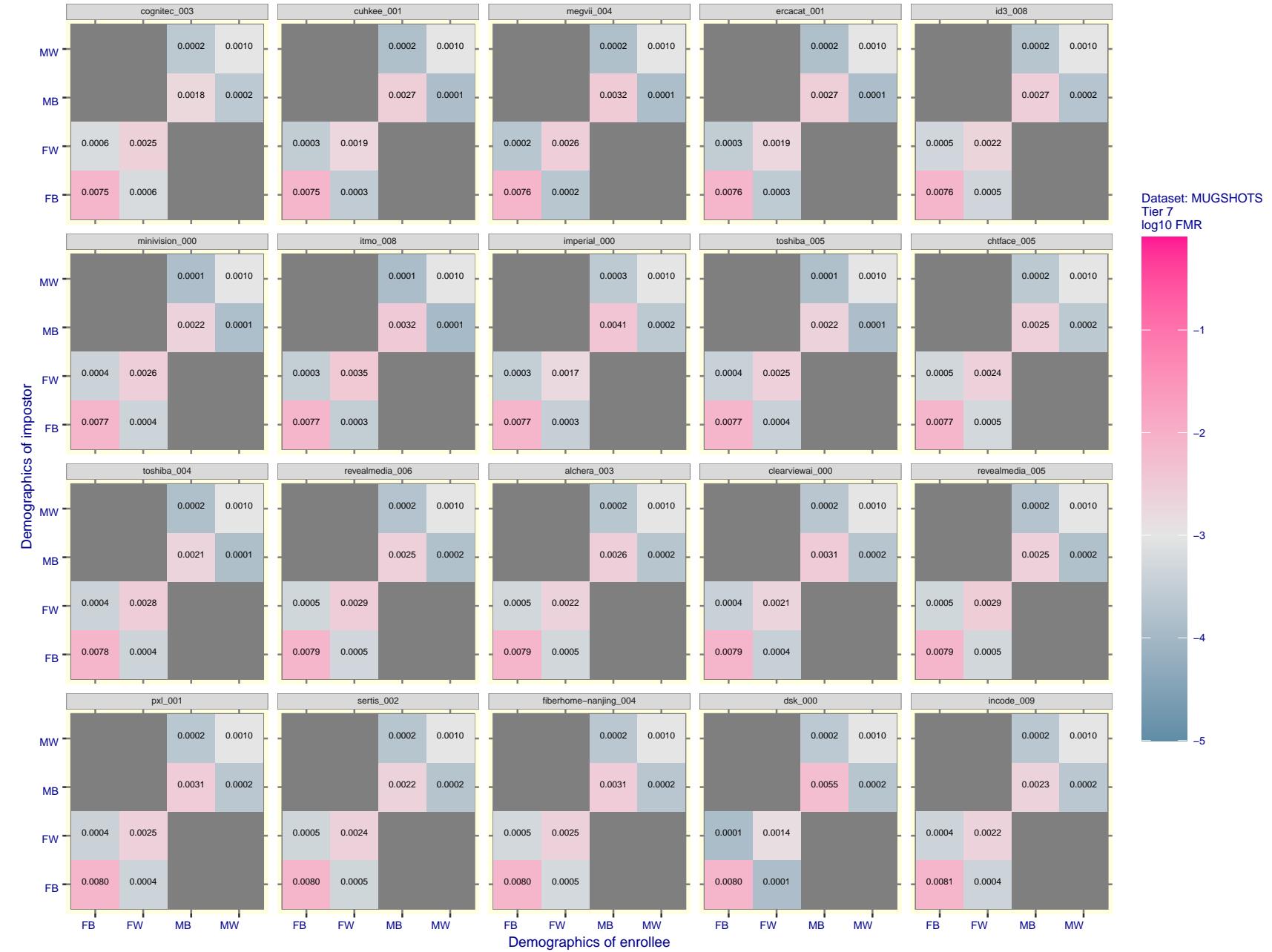


Figure 105: For the mugshot images, FMR for same-sex impostor pairs of images annotated with codes for black female, black male, white female, white male. The threshold is set for each algorithm to give $\text{FMR} = 0.001$ for white males which is the demographic that usually gives the lowest FMR. This means the top right box is the same color in all panels. The panels are sorted over multiple pages in order of FMR on black females, which is the demographic that usually gives the highest FMR.

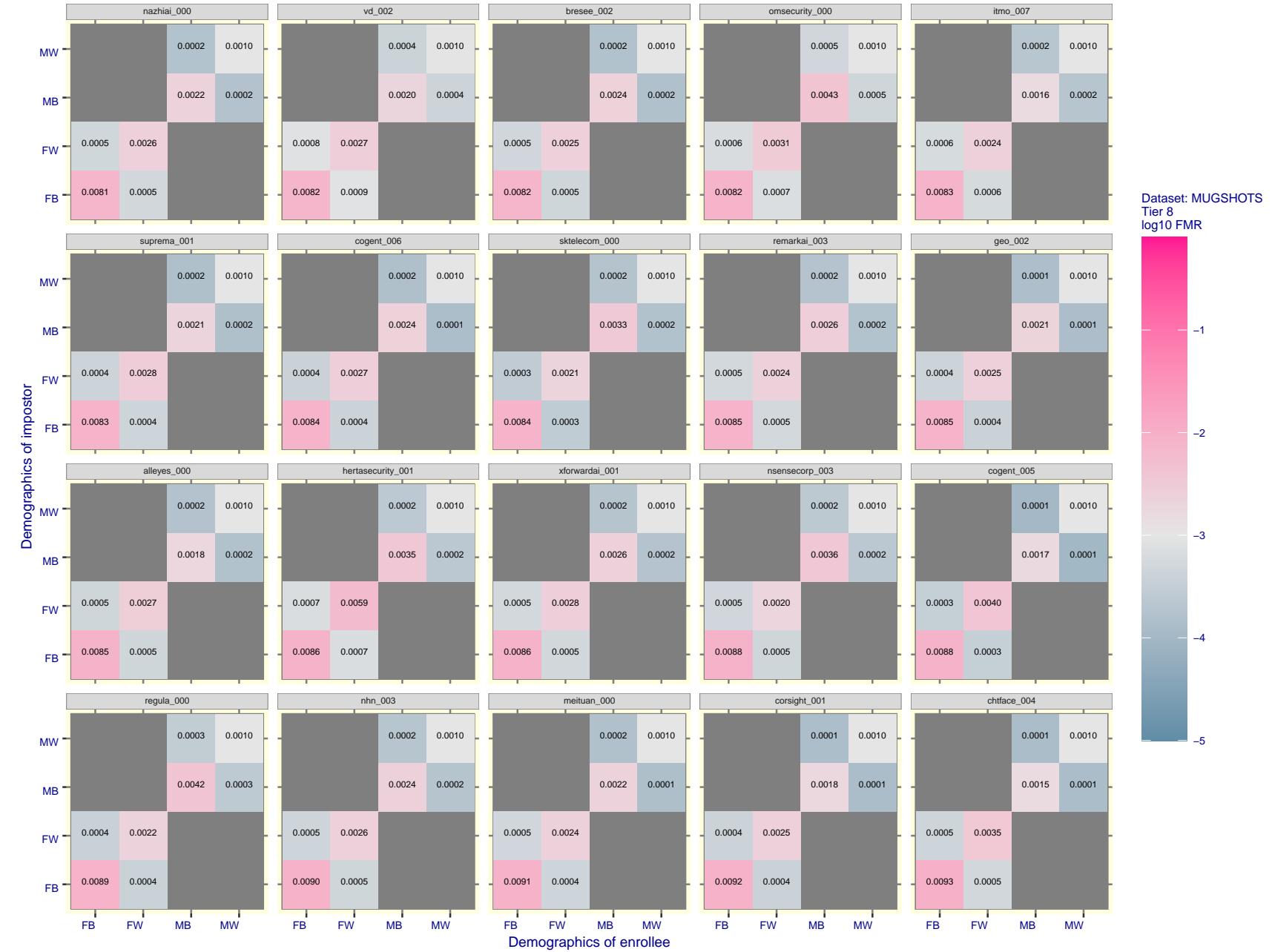


Figure 106: For the mugshot images, FMR for same-sex impostor pairs of images annotated with codes for black female, black male, white female, white male. The threshold is set for each algorithm to give $FMR = 0.001$ for white males which is the demographic that usually gives the lowest FMR. This means the top right box is the same color in all panels. The panels are sorted over multiple pages in order of FMR on black females, which is the demographic that usually gives the highest FMR.

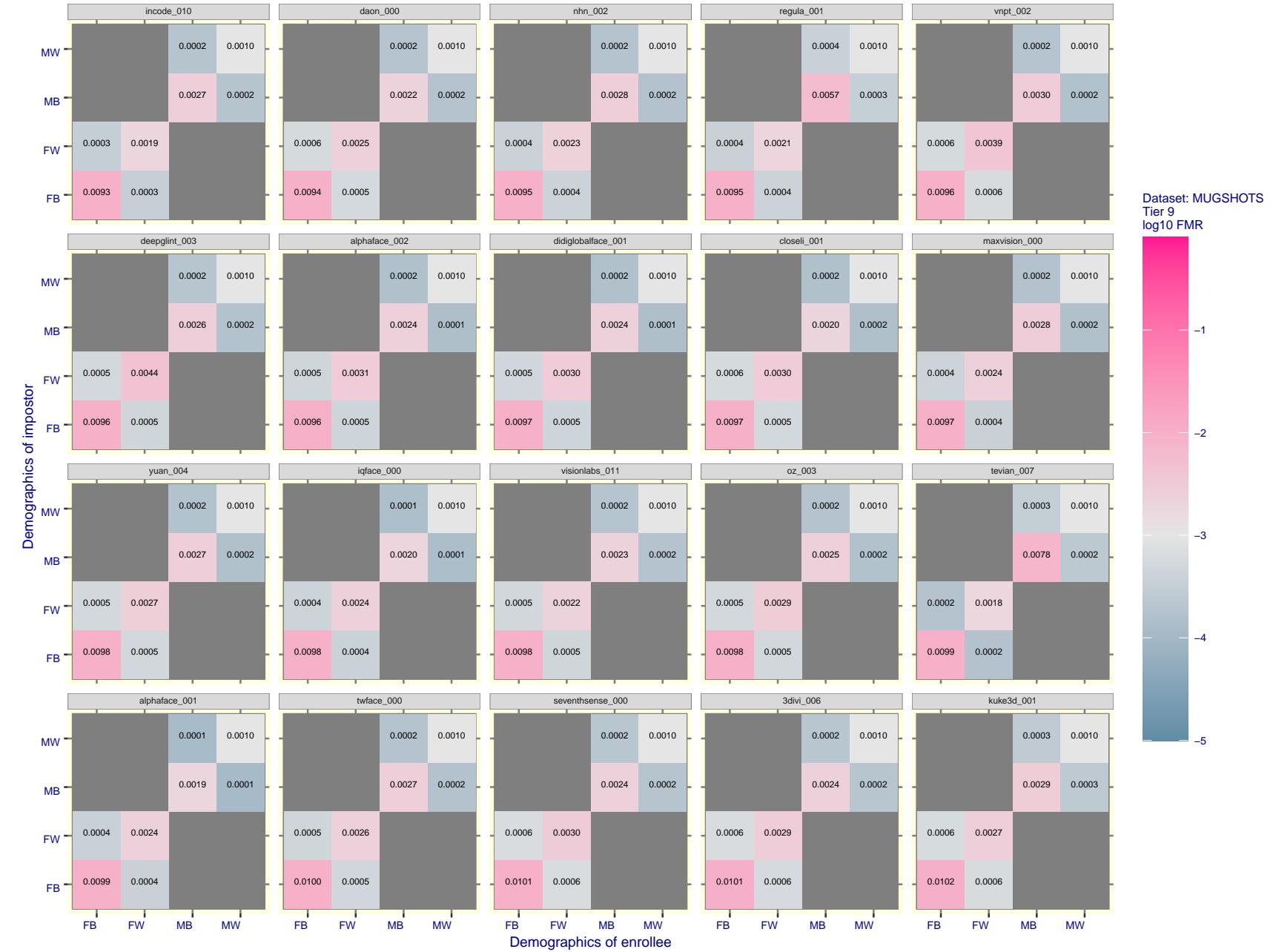


Figure 107: For the mugshot images, FMR for same-sex impostor pairs of images annotated with codes for black female, black male, white female, white male. The threshold is set for each algorithm to give FMR = 0.001 for white males which is the demographic that usually gives the lowest FMR. This means the top right box is the same color in all panels. The panels are sorted over multiple pages in order of FMR on black females, which is the demographic that usually gives the highest FMR.

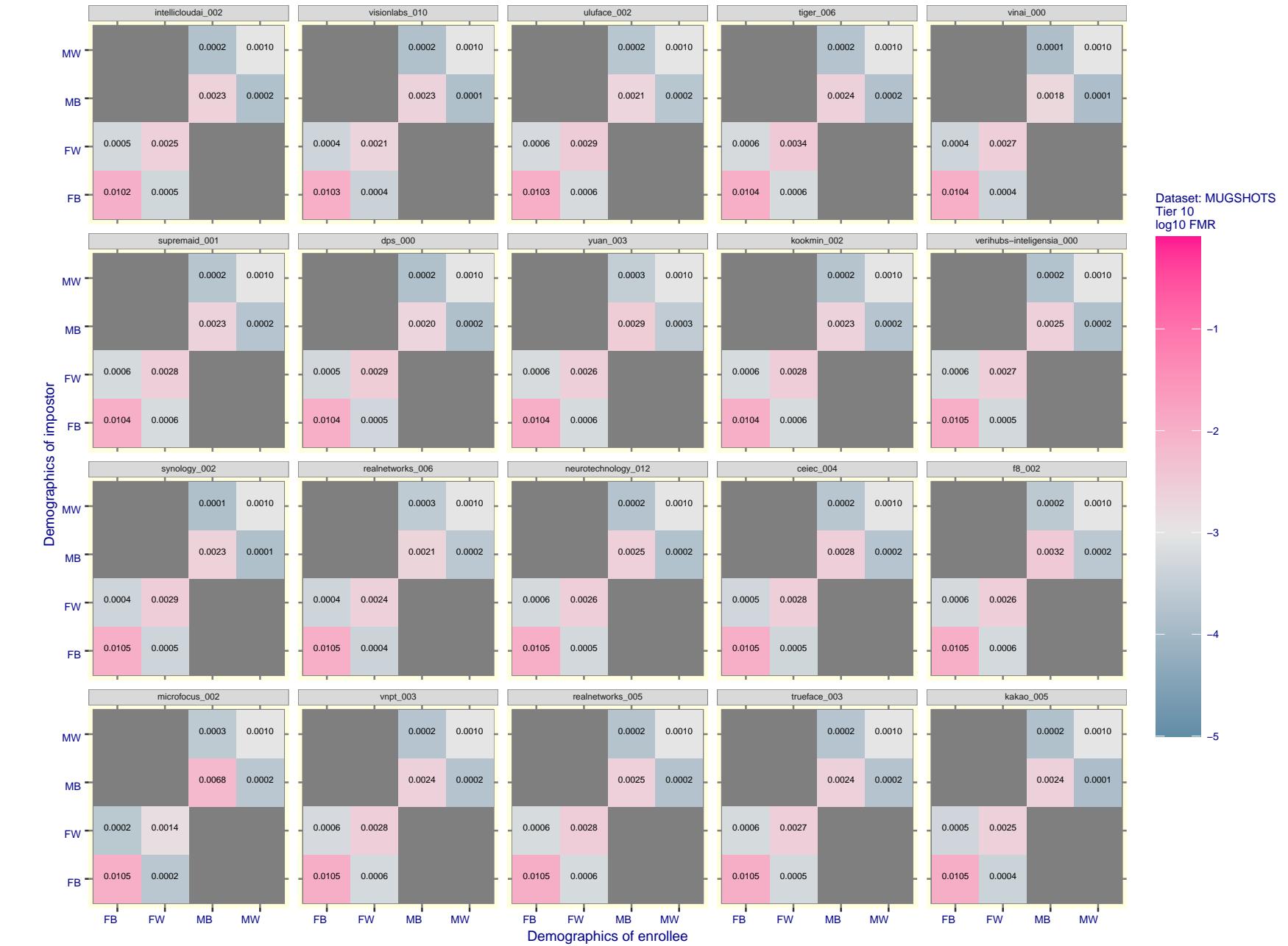


Figure 108: For the mugshot images, FMR for same-sex impostor pairs of images annotated with codes for black female, black male, white female, white male. The threshold is set for each algorithm to give $FMR = 0.001$ for white males which is the demographic that usually gives the lowest FMR. This means the top right box is the same color in all panels. The panels are sorted over multiple pages in order of FMR on black females, which is the demographic that usually gives the highest FMR.

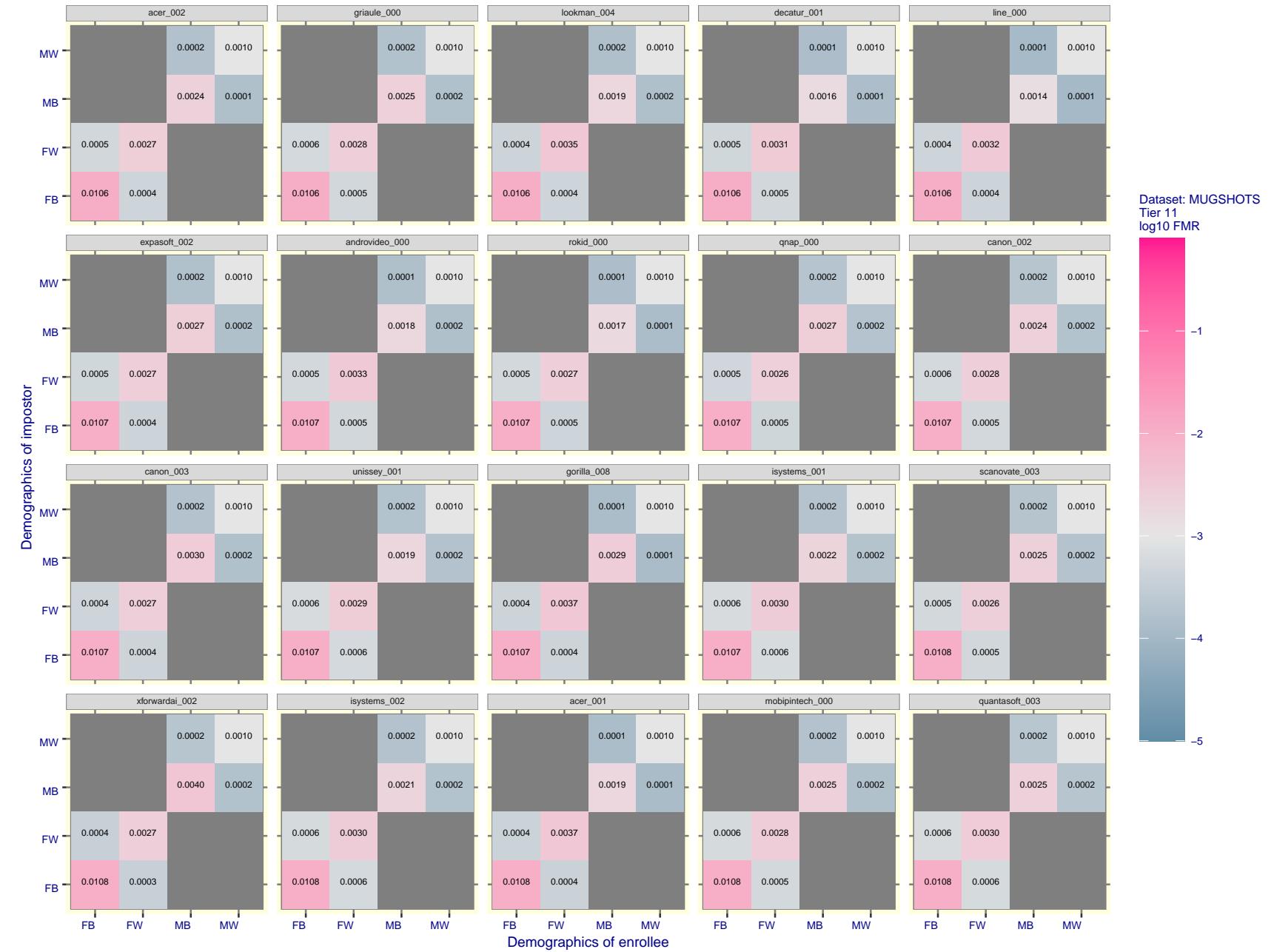


Figure 109: For the mugshot images, FMR for same-sex impostor pairs of images annotated with codes for black female, black male, white female, white male. The threshold is set for each algorithm to give FMR = 0.001 for white males which is the demographic that usually gives the lowest FMR. This means the top right box is the same color in all panels. The panels are sorted over multiple pages in order of FMR on black females, which is the demographic that usually gives the highest FMR.

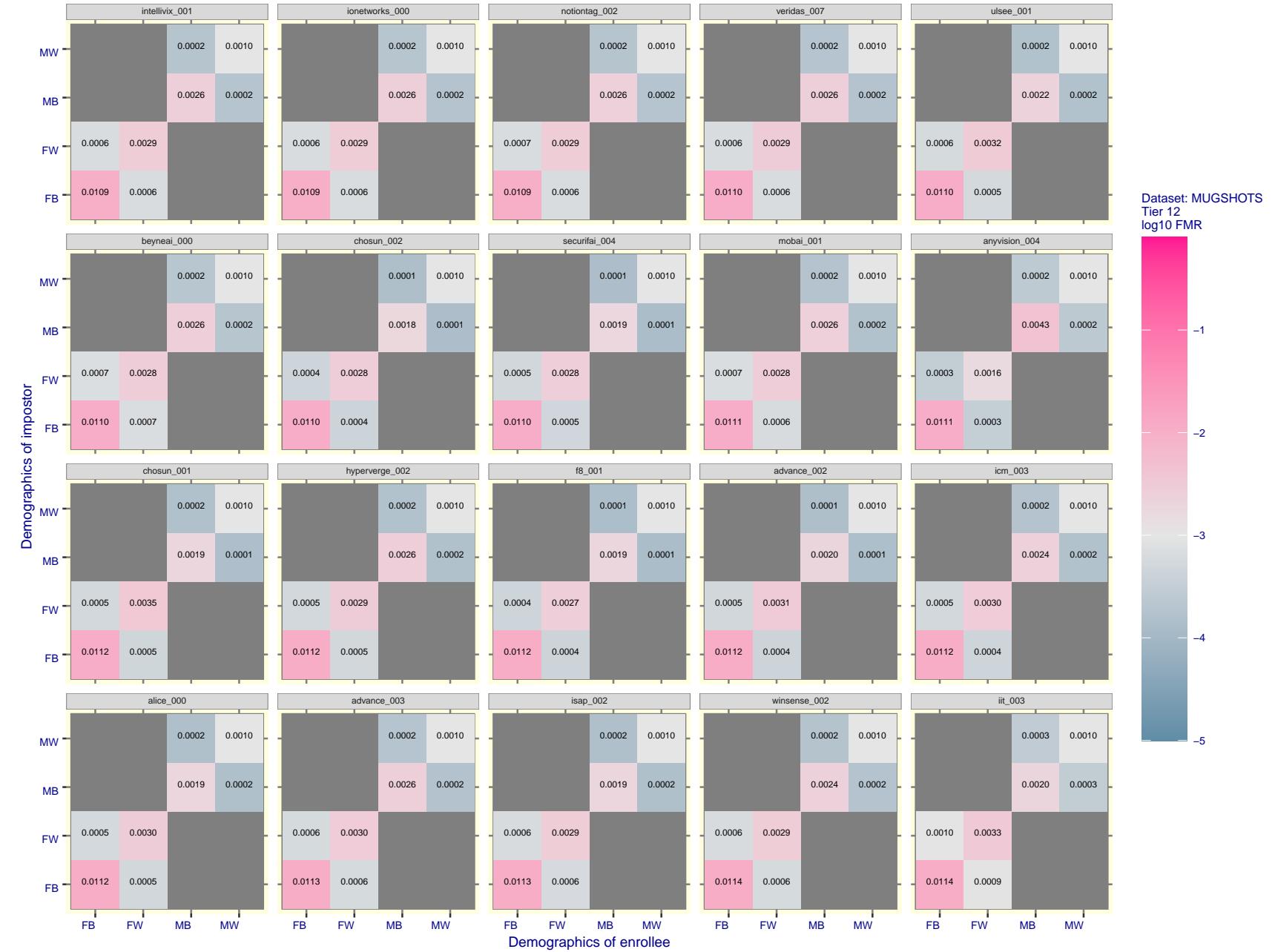


Figure 110: For the mugshot images, FMR for same-sex impostor pairs of images annotated with codes for black female, black male, white female, white male. The threshold is set for each algorithm to give $FMR = 0.001$ for white males which is the demographic that usually gives the lowest FMR. This means the top right box is the same color in all panels. The panels are sorted over multiple pages in order of FMR on black females, which is the demographic that usually gives the highest FMR.

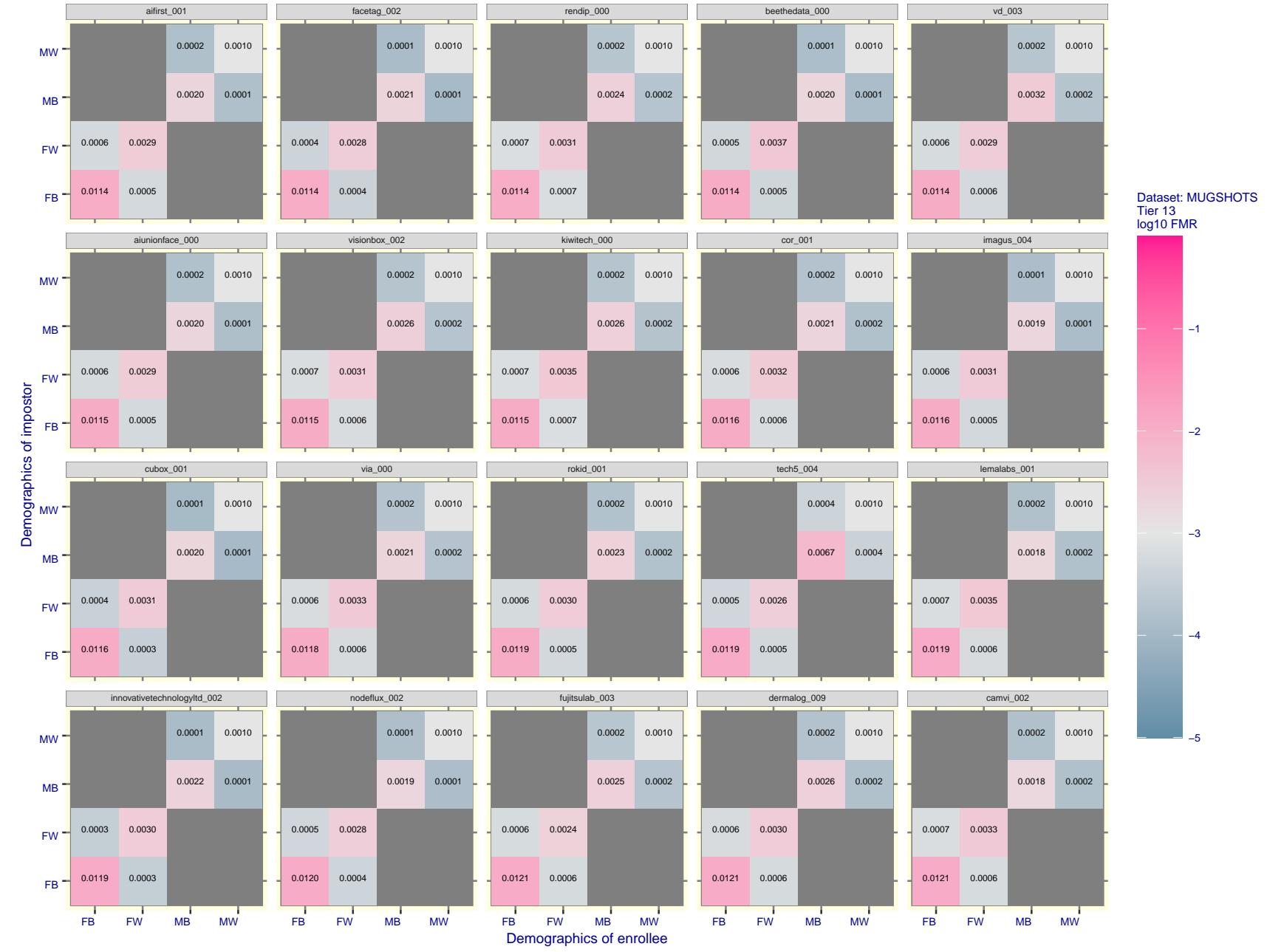


Figure 111: For the mugshot images, FMR for same-sex impostor pairs of images annotated with codes for black female, black male, white female, white male. The threshold is set for each algorithm to give $FMR = 0.001$ for white males which is the demographic that usually gives the lowest FMR. This means the top right box is the same color in all panels. The panels are sorted over multiple pages in order of FMR on black females, which is the demographic that usually gives the highest FMR.

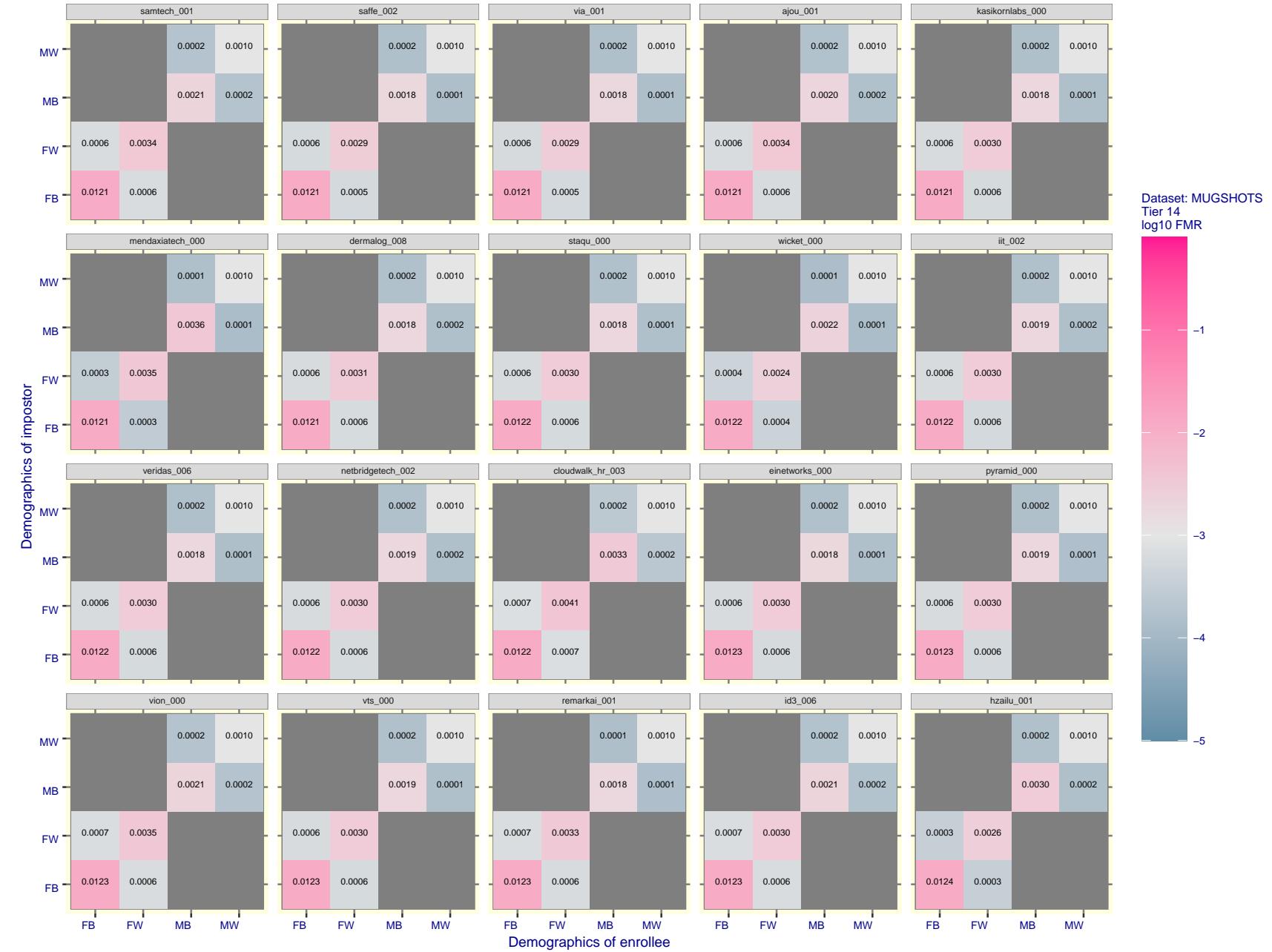


Figure 112: For the mugshot images, FMR for same-sex impostor pairs of images annotated with codes for black female, black male, white female, white male. The threshold is set for each algorithm to give $FMR = 0.001$ for white males which is the demographic that usually gives the lowest FMR. This means the top right box is the same color in all panels. The panels are sorted over multiple pages in order of FMR on black females, which is the demographic that usually gives the highest FMR.

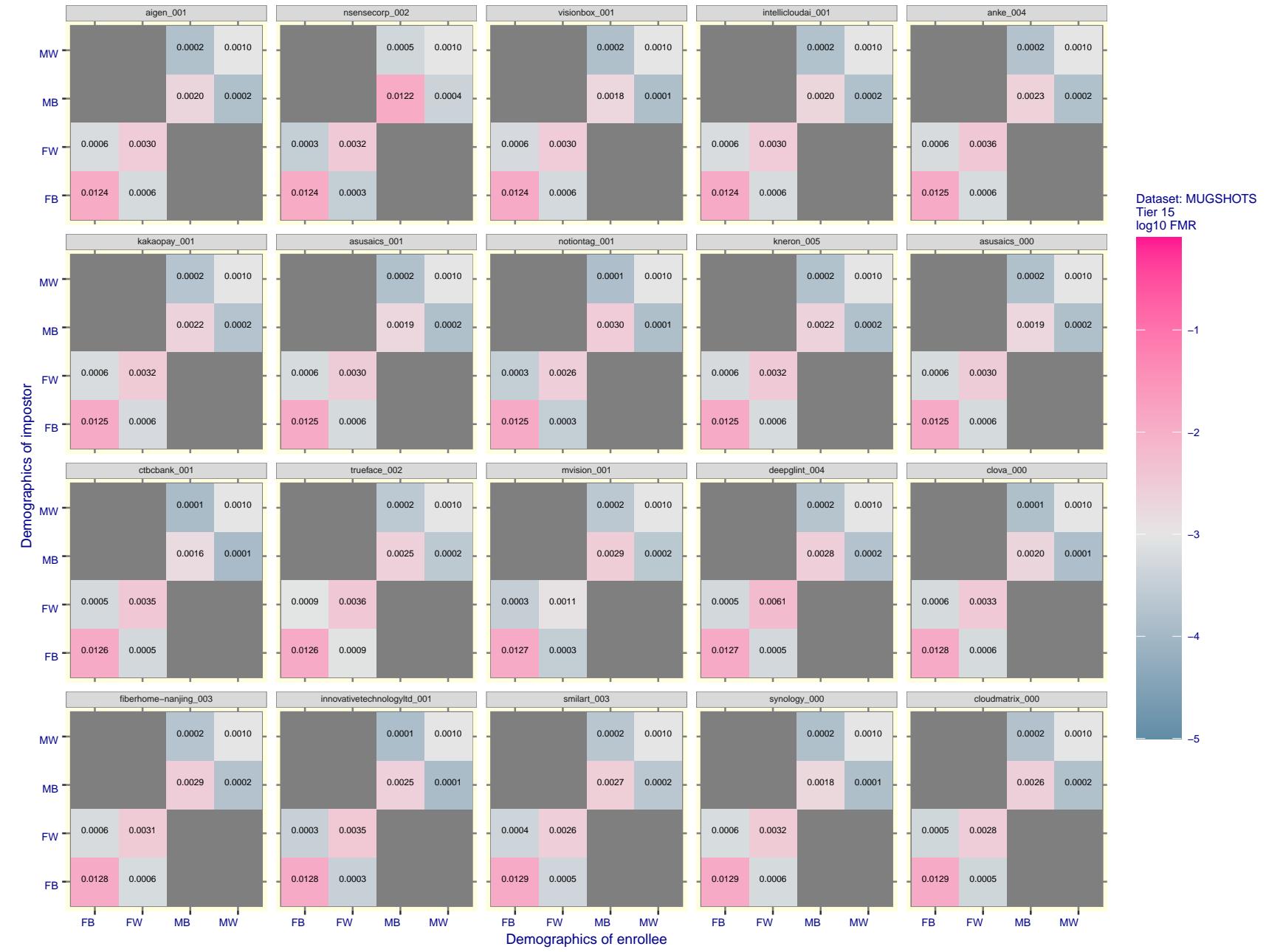


Figure 113: For the mugshot images, FMR for same-sex impostor pairs of images annotated with codes for black female, black male, white female, white male. The threshold is set for each algorithm to give FMR = 0.001 for white males which is the demographic that usually gives the lowest FMR. This means the top right box is the same color in all panels. The panels are sorted over multiple pages in order of FMR on black females, which is the demographic that usually gives the highest FMR.

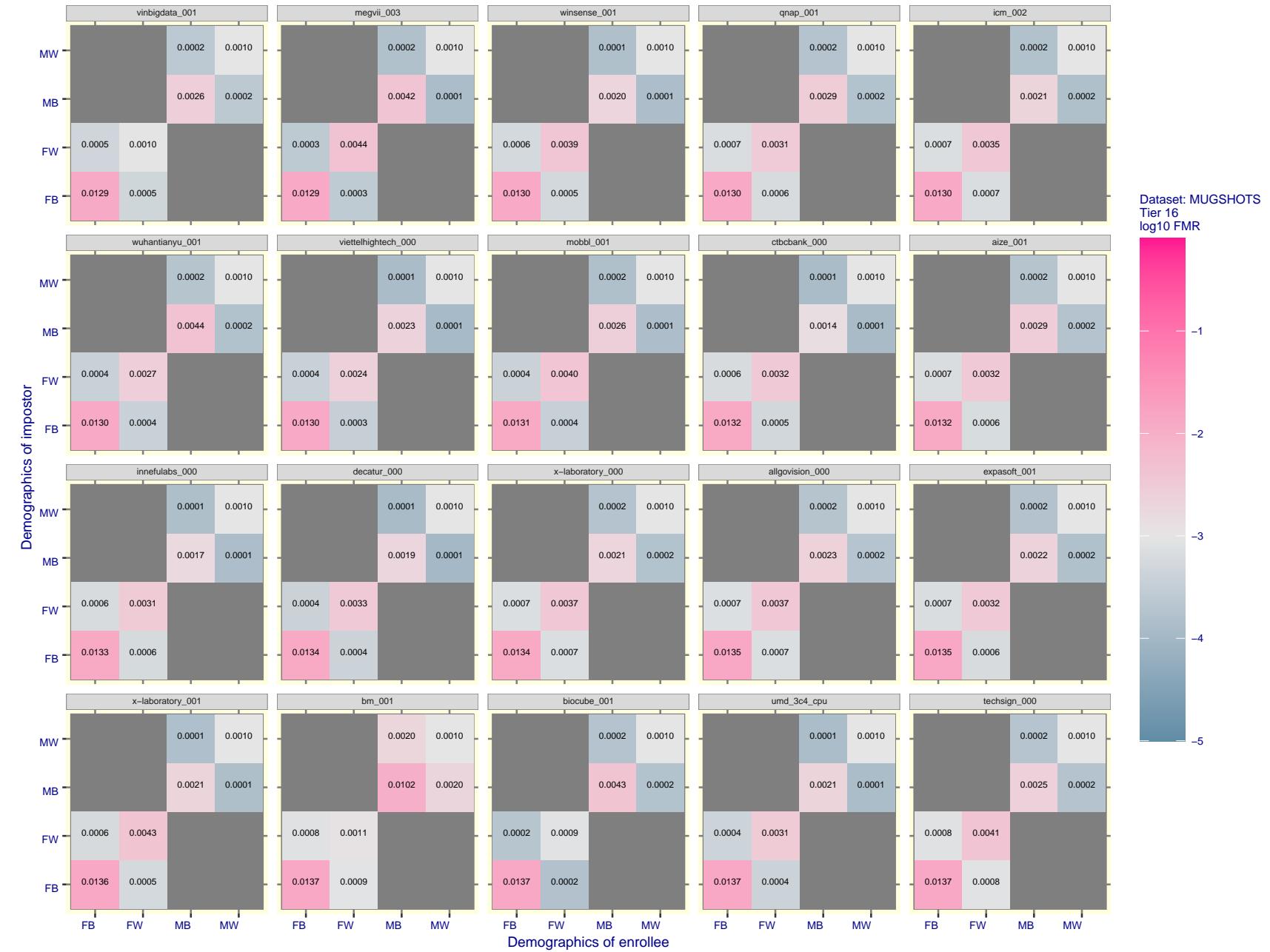


Figure 114: For the mugshot images, FMR for same-sex impostor pairs of images annotated with codes for black female, black male, white female, white male. The threshold is set for each algorithm to give $FMR = 0.001$ for white males which is the demographic that usually gives the lowest FMR. This means the top right box is the same color in all panels. The panels are sorted over multiple pages in order of FMR on black females, which is the demographic that usually gives the highest FMR.

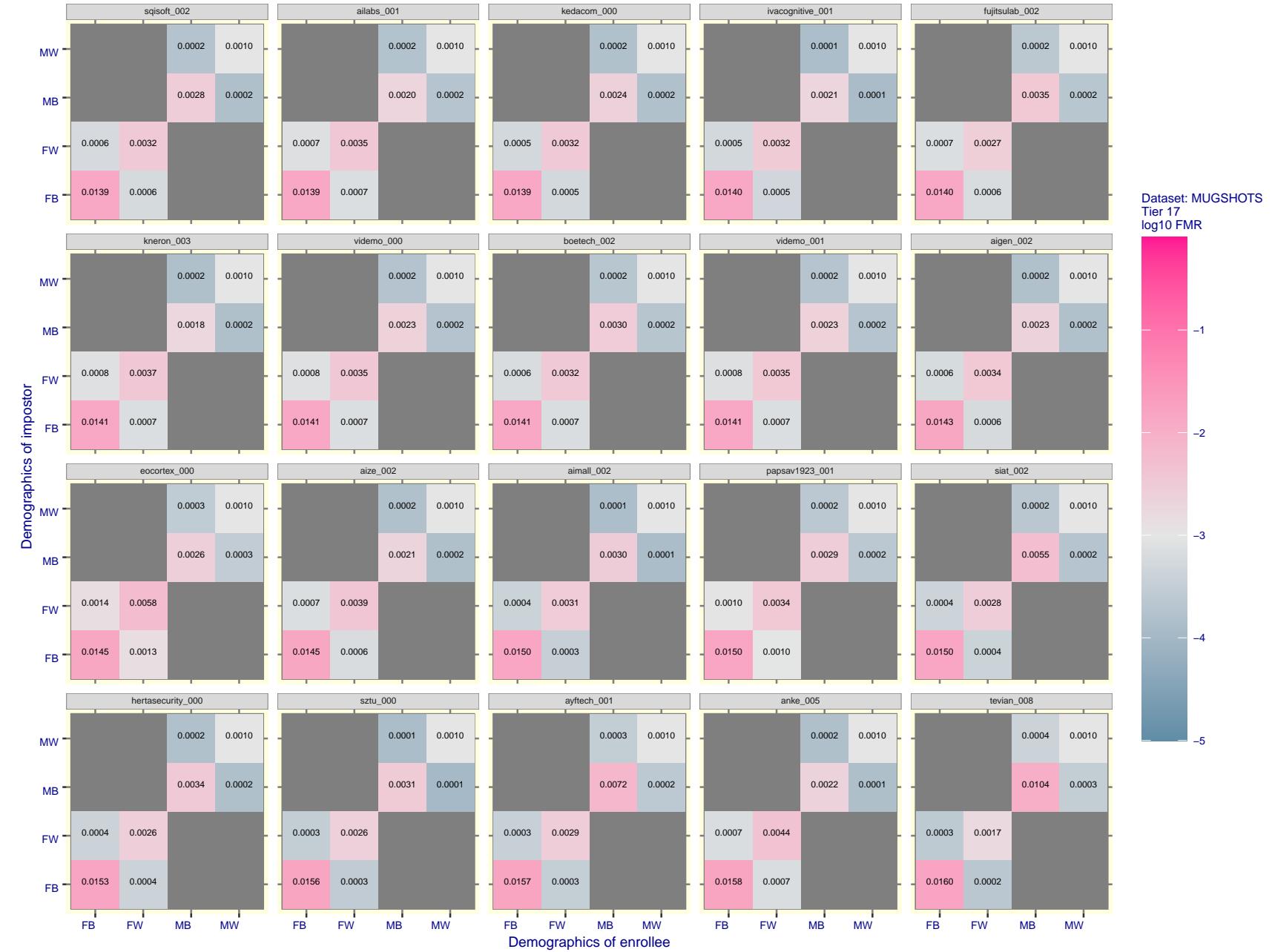


Figure 115: For the mugshot images, FMR for same-sex impostor pairs of images annotated with codes for black female, black male, white female, white male. The threshold is set for each algorithm to give FMR = 0.001 for white males which is the demographic that usually gives the lowest FMR. This means the top right box is the same color in all panels. The panels are sorted over multiple pages in order of FMR on black females, which is the demographic that usually gives the highest FMR.

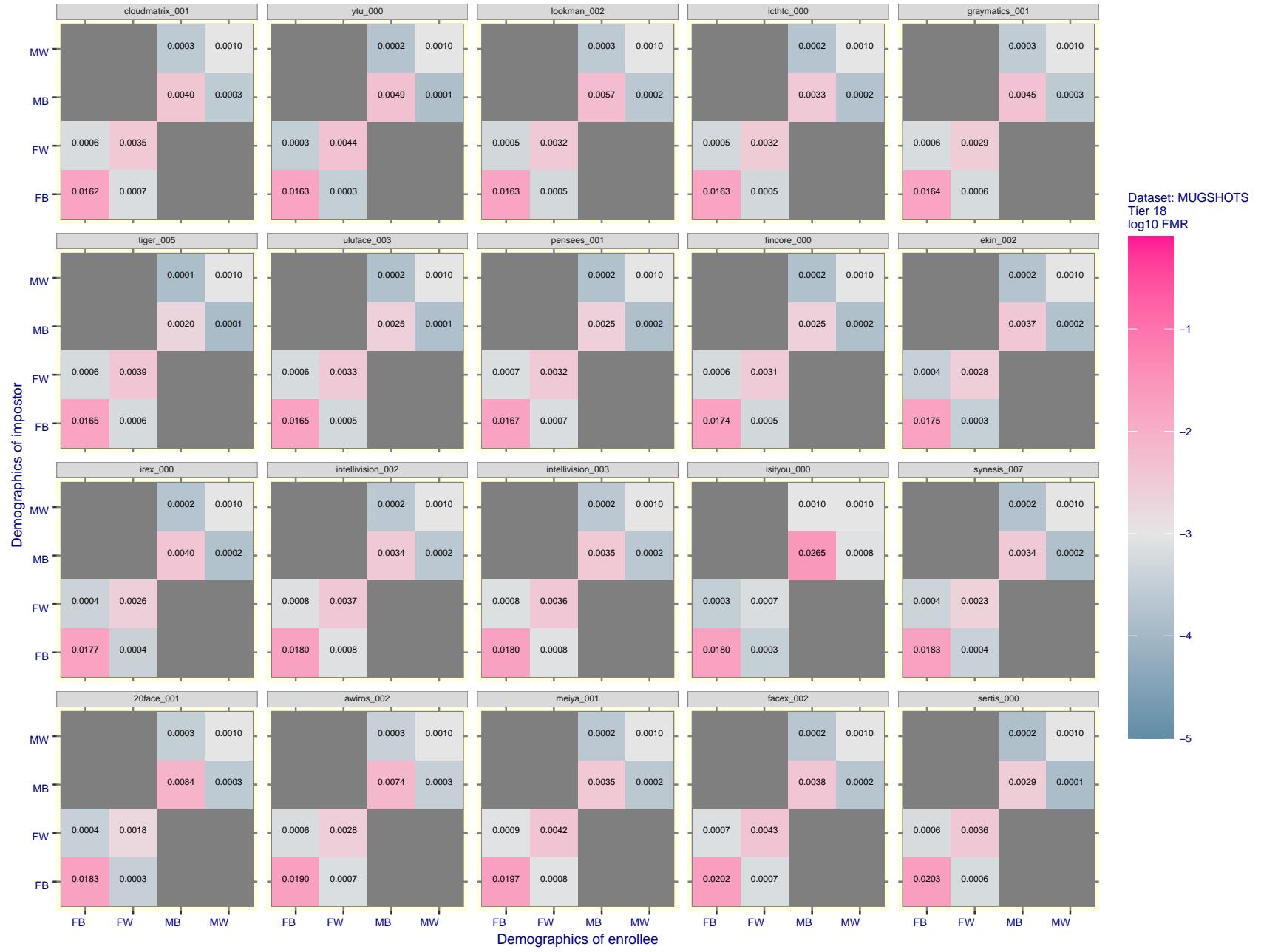


Figure 116: For the mugshot images, FMR for same-sex impostor pairs of images annotated with codes for black female, black male, white female, white male. The threshold is set for each algorithm to give $FMR = 0.001$ for white males which is the demographic that usually gives the lowest FMR. This means the top right box is the same color in all panels. The panels are sorted over multiple pages in order of FMR on black females, which is the demographic that usually gives the highest FMR.

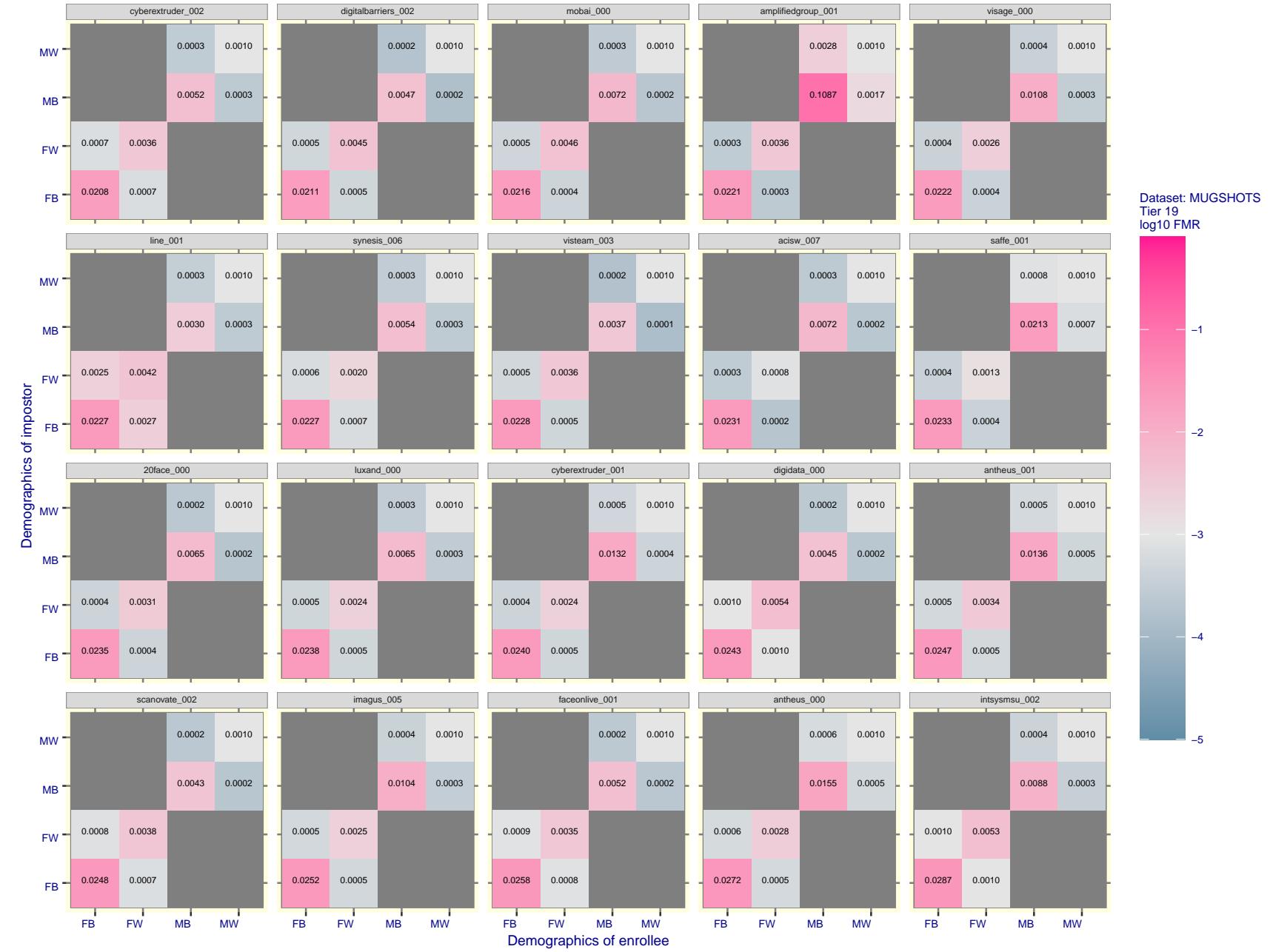


Figure 117: For the mugshot images, FMR for same-sex impostor pairs of images annotated with codes for black female, black male, white female, white male. The threshold is set for each algorithm to give FMR = 0.001 for white males which is the demographic that usually gives the lowest FMR. This means the top right box is the same color in all panels. The panels are sorted over multiple pages in order of FMR on black females, which is the demographic that usually gives the highest FMR.

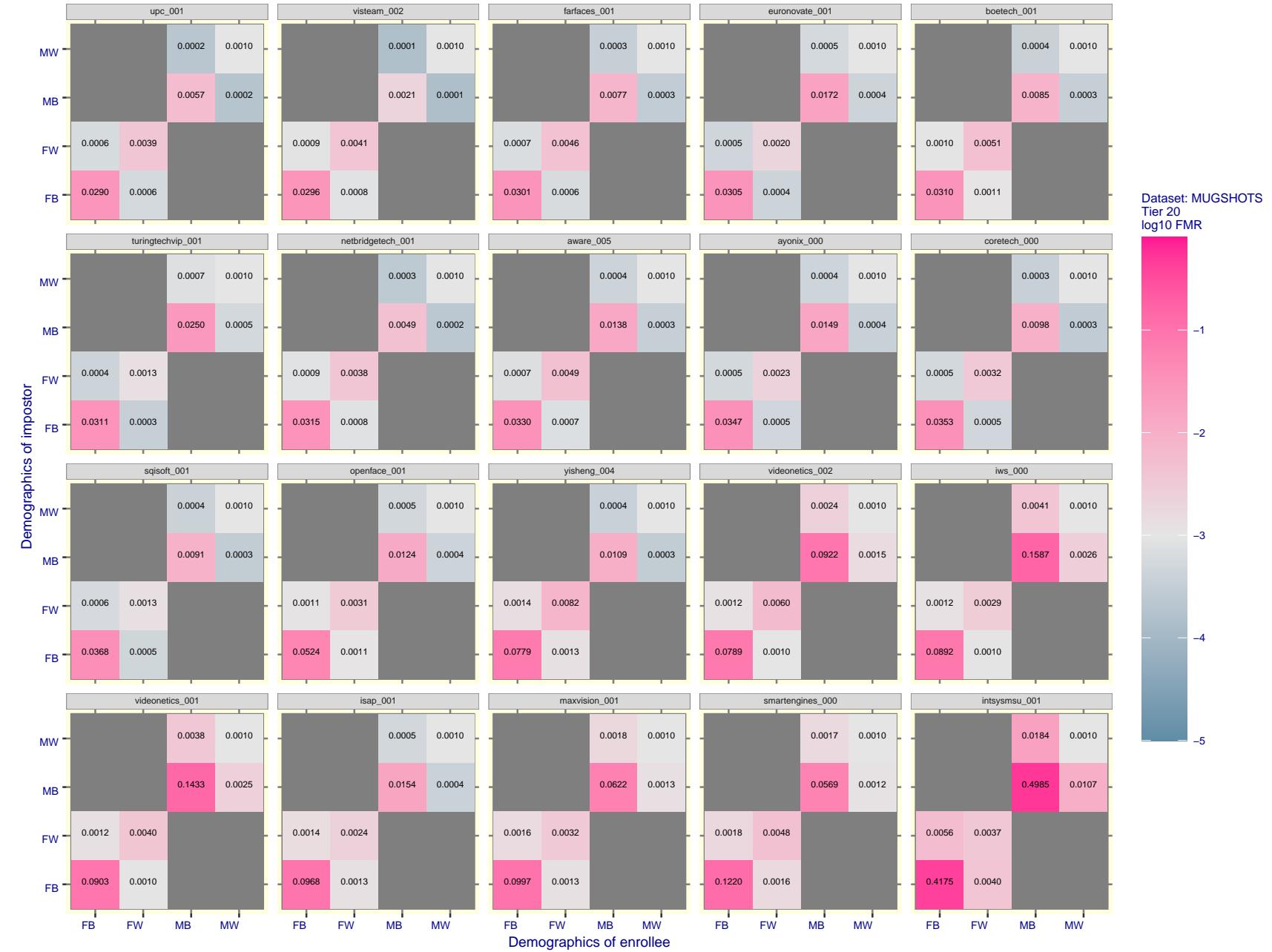


Figure 118: For the mugshot images, FMR for same-sex impostor pairs of images annotated with codes for black female, black male, white female, white male. The threshold is set for each algorithm to give $FMR = 0.001$ for white males which is the demographic that usually gives the lowest FMR. This means the top right box is the same color in all panels. The panels are sorted over multiple pages in order of FMR on black females, which is the demographic that usually gives the highest FMR.

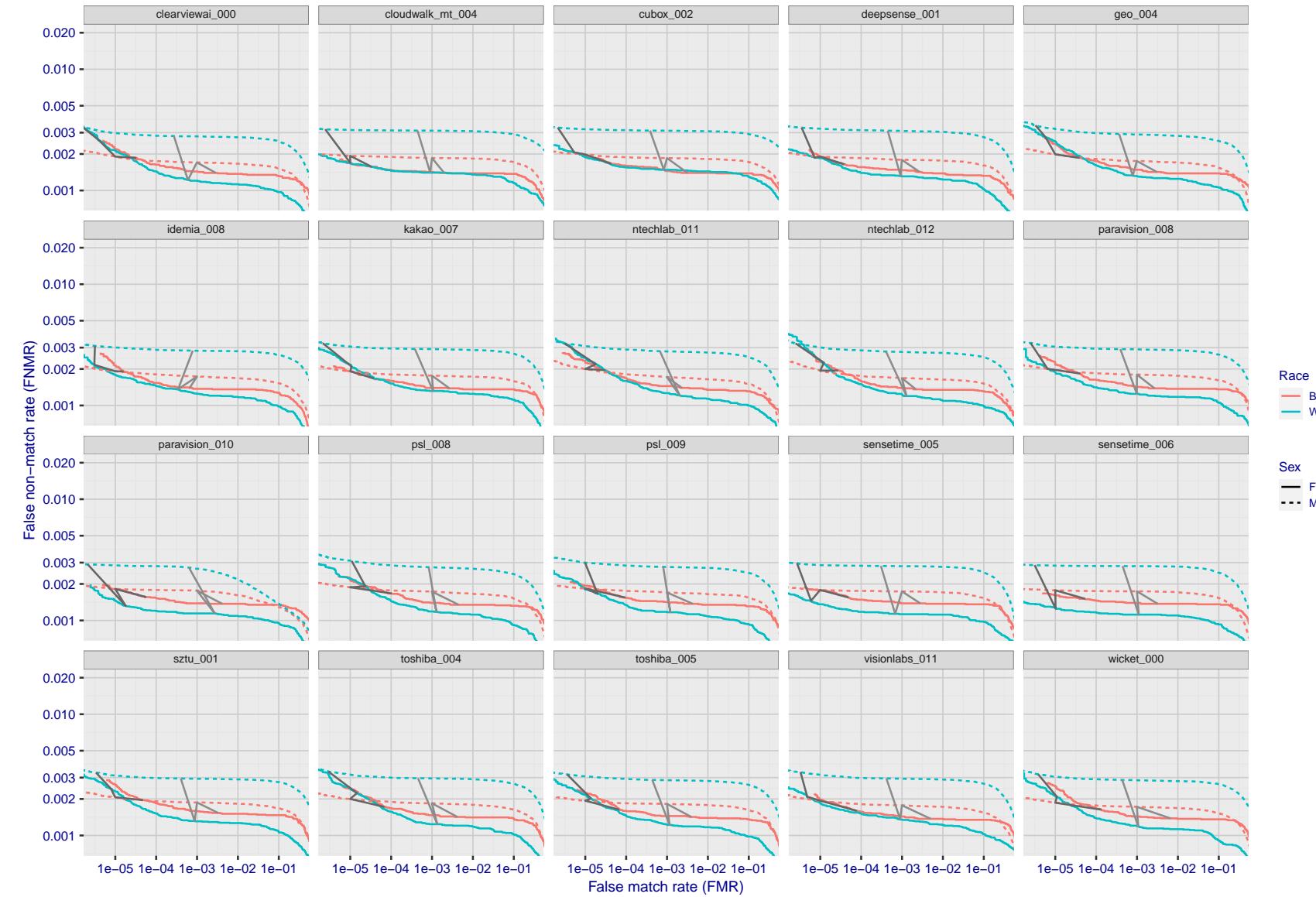


Figure 119: For the mugshot images, error tradeoff characteristics for white females, black females, black males and white males. The Z-shaped grey lines correspond to fixed thresholds, showing both FNMR and FMR vary at one T value. Note: Many of the plots will naively be read as saying women gives worse error rates than men because the solid traces lie above the dotted ones. However, this is misleading and incomplete: The grey lines show the traces reveal horizontal shifts. Thus for the cogent-003 algorithm FNMR for men is higher than for women at a fixed threshold but, at the same time, FMR is higher for women - see Figure 194. As access control systems almost always operate at a fixed threshold, the naive interpretation is incorrect.

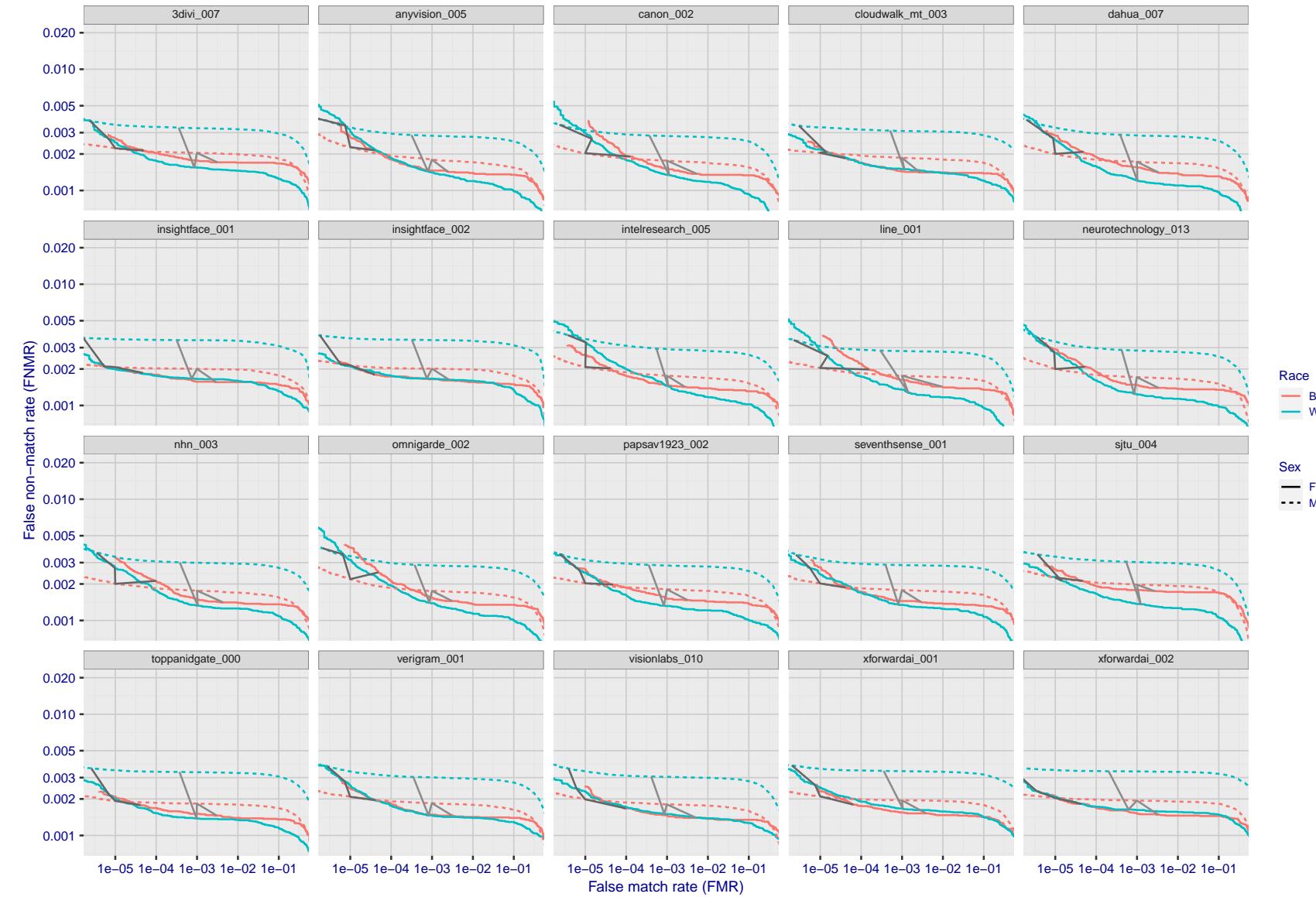


Figure 120: For the mugshot images, error tradeoff characteristics for white females, black females, black males and white males. The Z-shaped grey lines correspond to fixed thresholds, showing both FNMR and FMR vary at one T value. Note: Many of the plots will naively be read as saying women gives worse error rates than men because the solid traces lie above the dotted ones. However, this is misleading and incomplete: The grey lines show the traces reveal horizontal shifts. Thus for the cogent-003 algorithm FNMR for men is higher than for women at a fixed threshold but, at the same time, FMR is higher for women - see Figure 194. As access control systems almost always operate at a fixed threshold, the naive interpretation is incorrect.

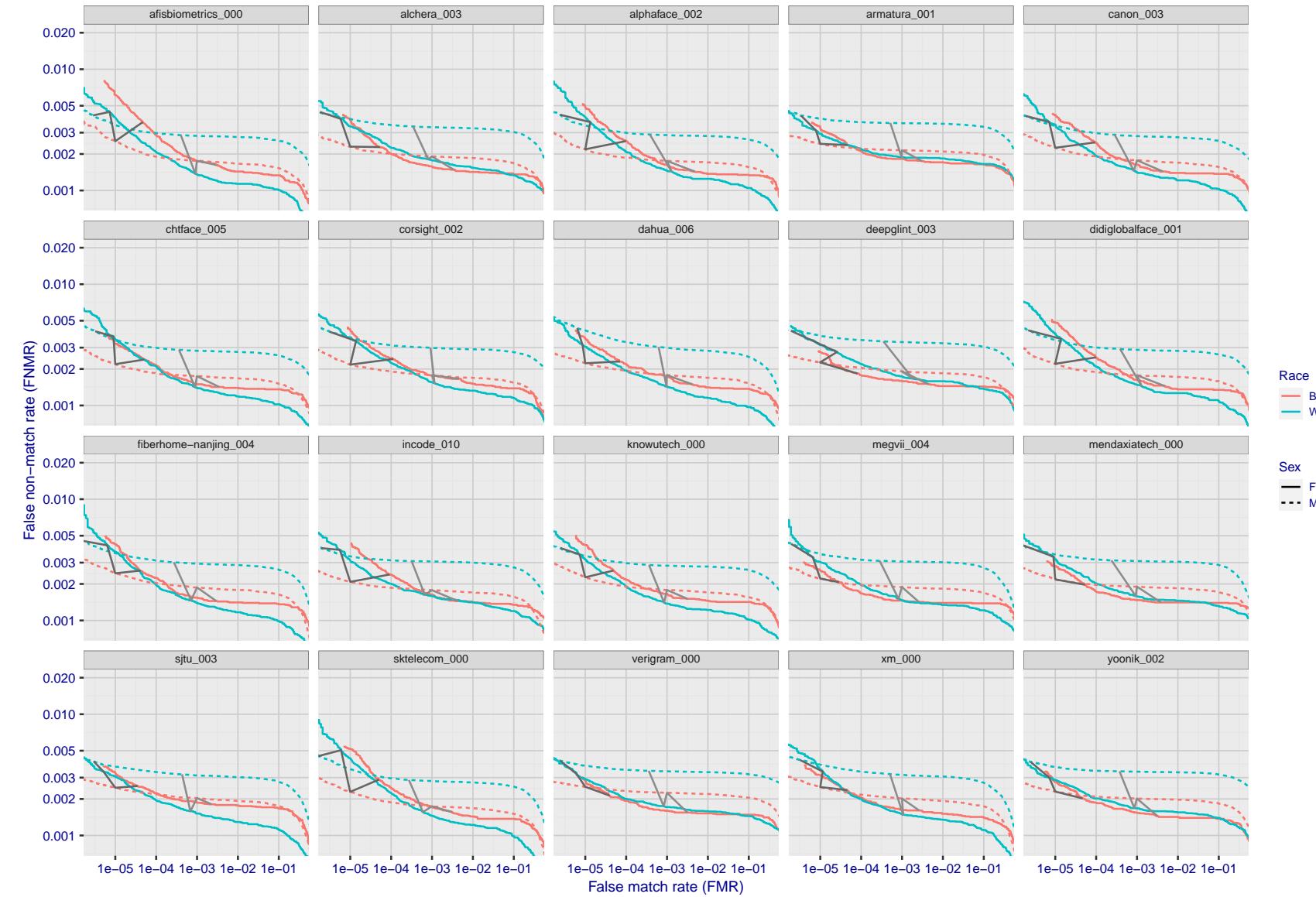


Figure 121: For the mugshot images, error tradeoff characteristics for white females, black females, black males and white males. The Z-shaped grey lines correspond to fixed thresholds, showing both FNMR and FMR vary at one T value. Note: Many of the plots will naively be read as saying women gives worse error rates than men because the solid traces lie above the dotted ones. However, this is misleading and incomplete: The grey lines show the traces reveal horizontal shifts. Thus for the cogent-003 algorithm FNMR for men is higher than for women at a fixed threshold but, at the same time, FMR is higher for women - see Figure 194. As access control systems almost always operate at a fixed threshold, the naive interpretation is incorrect.

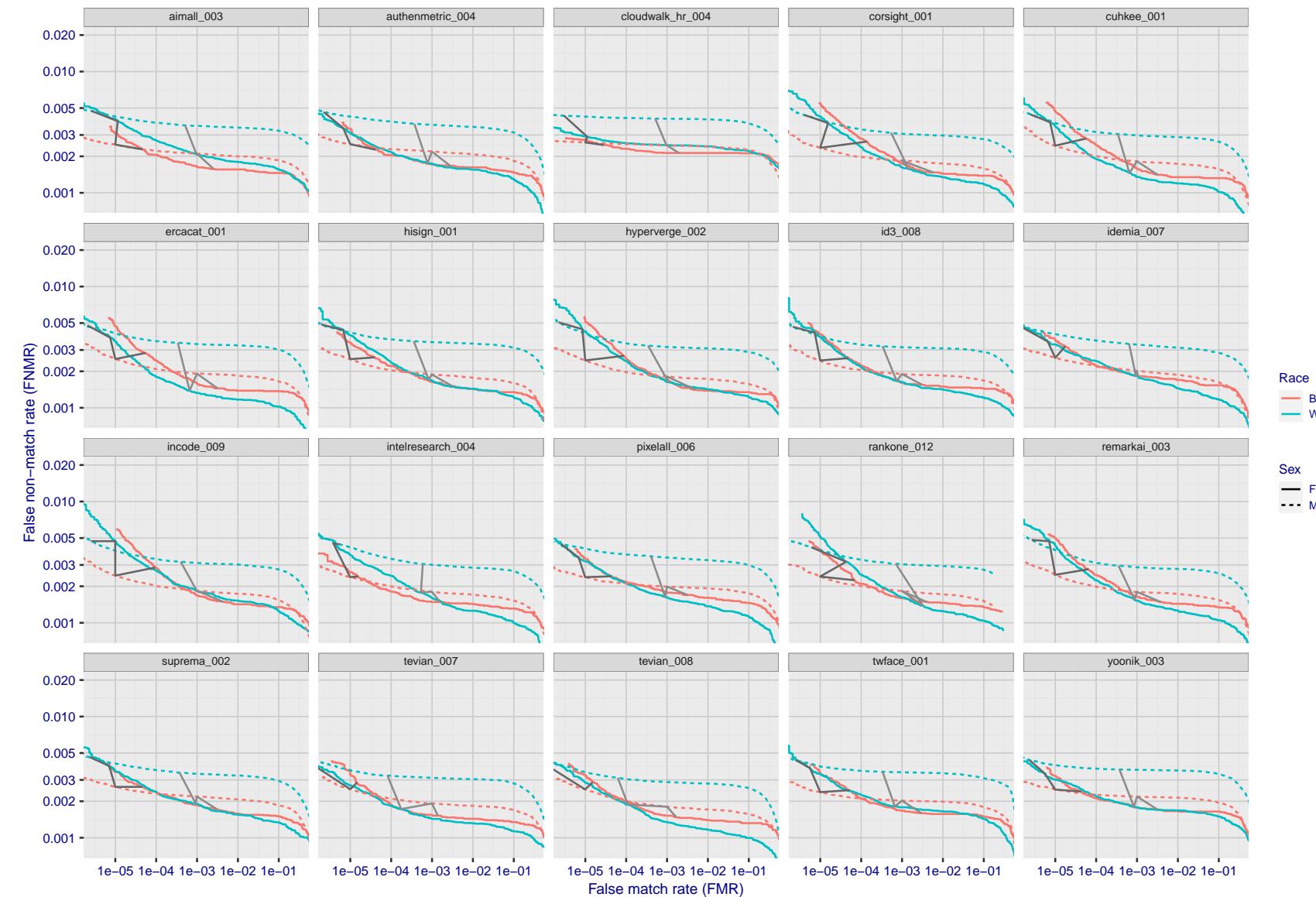


Figure 122: For the mugshot images, error tradeoff characteristics for white females, black females, black males and white males. The Z-shaped grey lines correspond to fixed thresholds, showing both FNMR and FMR vary at one T value. Note: Many of the plots will naively be read as saying women gives worse error rates than men because the solid traces lie above the dotted ones. However, this is misleading and incomplete: The grey lines show the traces reveal horizontal shifts. Thus for the cogent-003 algorithm FNMR for men is higher than for women at a fixed threshold but, at the same time, FMR is higher for women - see Figure 194. As access control systems almost always operate at a fixed threshold, the naive interpretation is incorrect.

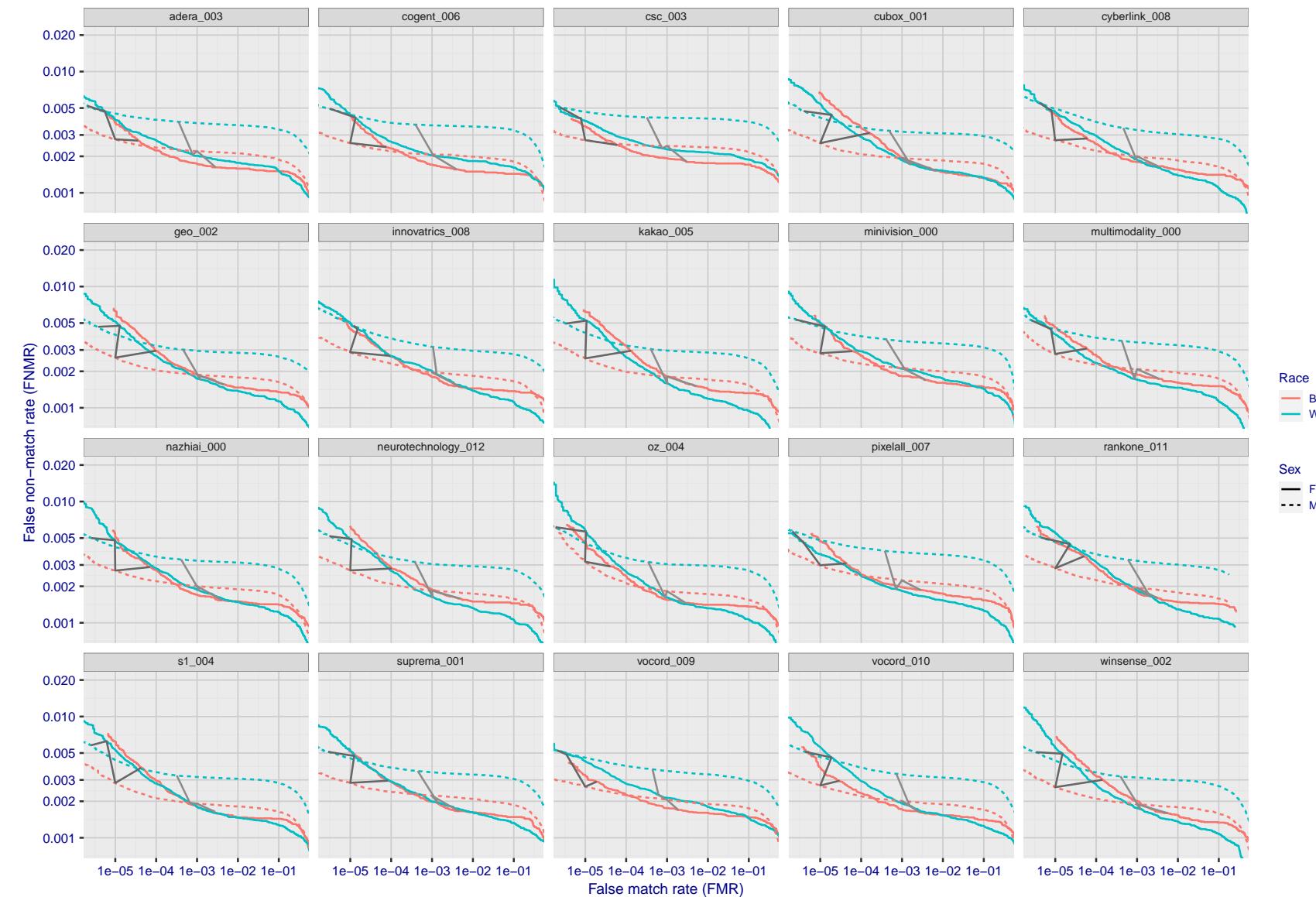


Figure 123: For the mugshot images, error tradeoff characteristics for white females, black females, black males and white males. The Z-shaped grey lines correspond to fixed thresholds, showing both FNMR and FMR vary at one T value. Note: Many of the plots will naively be read as saying women gives worse error rates than men because the solid traces lie above the dotted ones. However, this is misleading and incomplete: The grey lines show the traces reveal horizontal shifts. Thus for the cogent-003 algorithm FNMR for men is higher than for women at a fixed threshold but, at the same time, FMR is higher for women - see Figure 194. As access control systems almost always operate at a fixed threshold, the naive interpretation is incorrect.

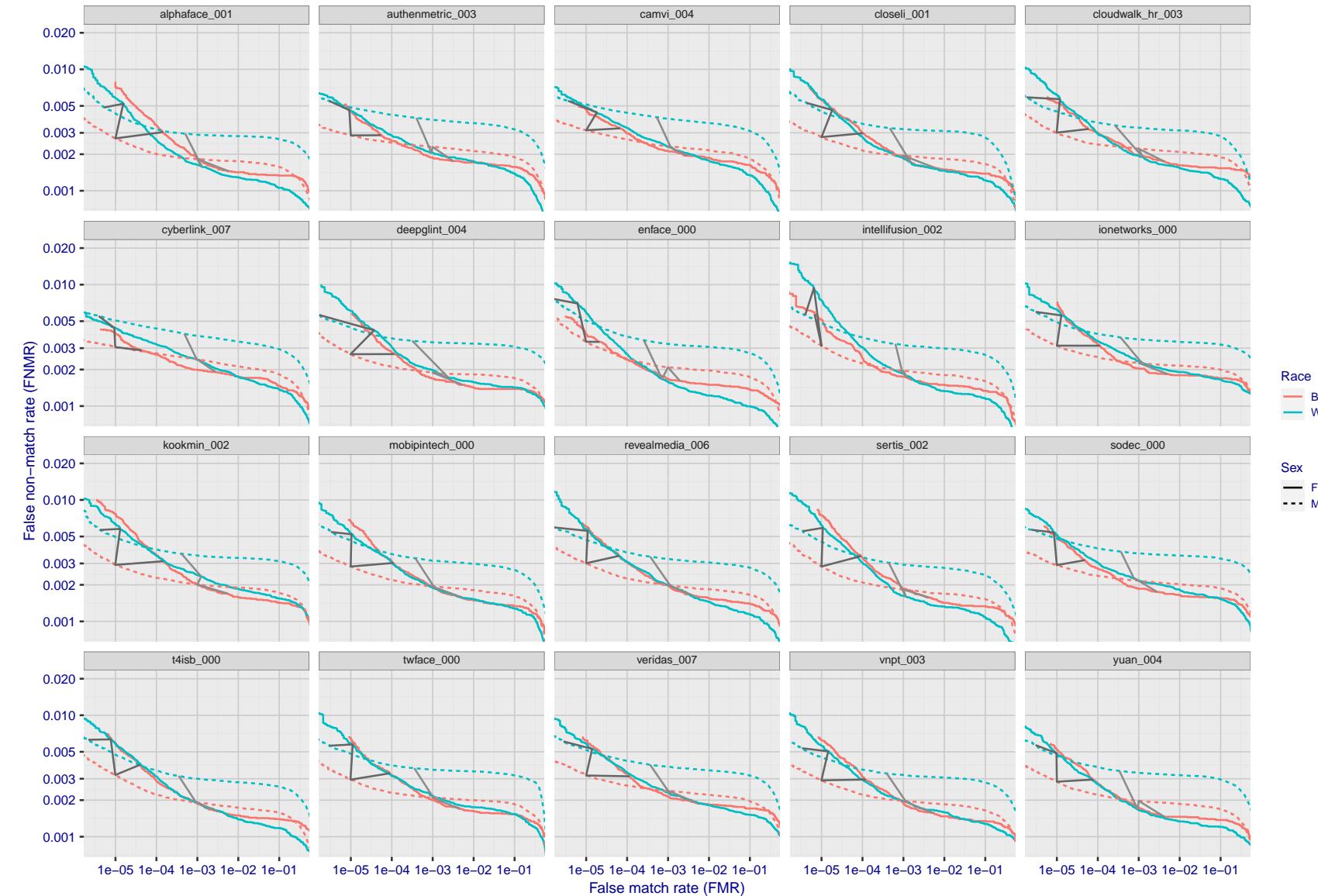


Figure 124: For the mugshot images, error tradeoff characteristics for white females, black females, black males and white males. The Z-shaped grey lines correspond to fixed thresholds, showing both FNMR and FMR vary at one T value. Note: Many of the plots will naively be read as saying women gives worse error rates than men because the solid traces lie above the dotted ones. However, this is misleading and incomplete: The grey lines show the traces reveal horizontal shifts. Thus for the cogent-003 algorithm FNMR for men is higher than for women at a fixed threshold but, at the same time, FMR is higher for women - see Figure 194. As access control systems almost always operate at a fixed threshold, the naive interpretation is incorrect.

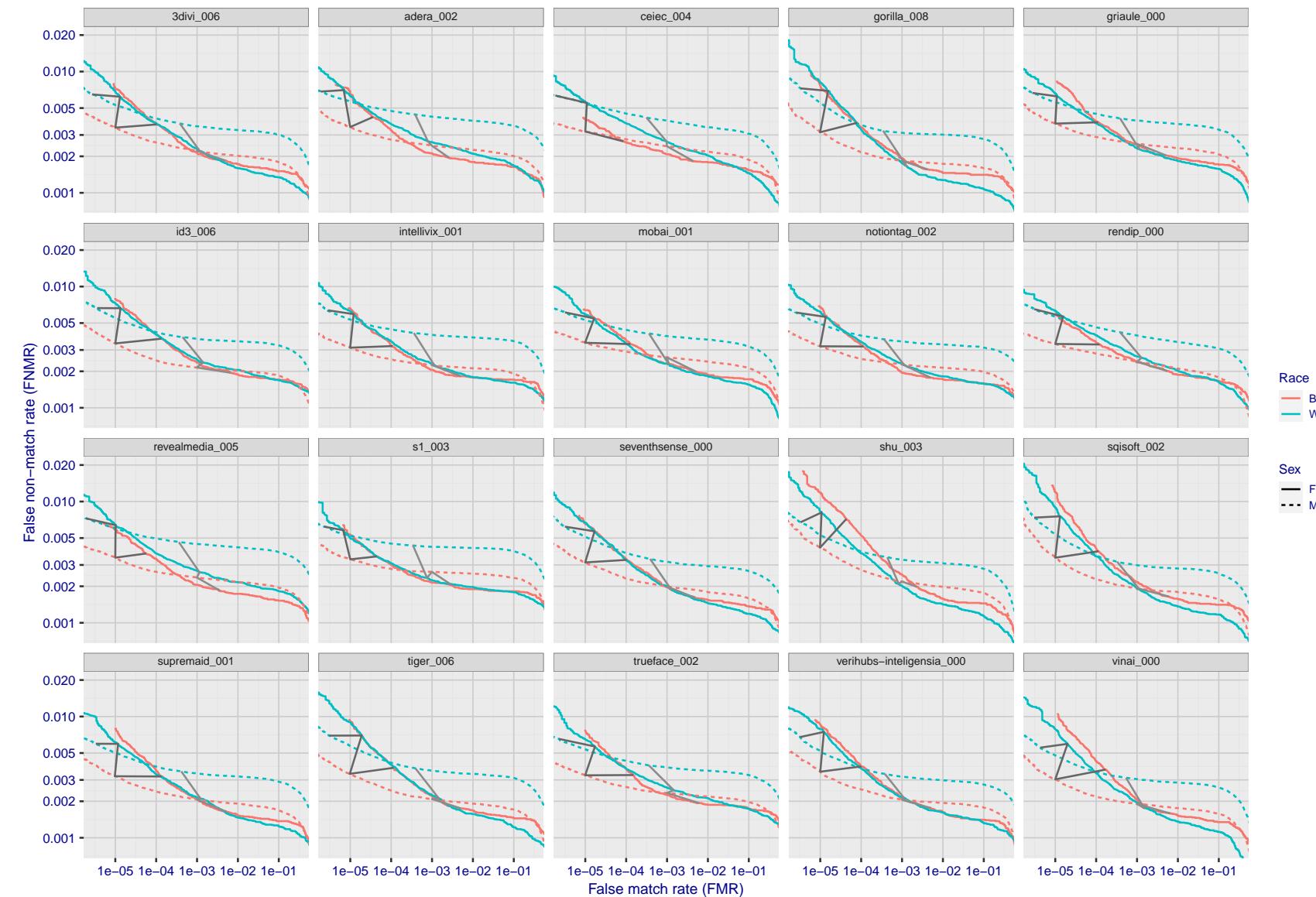


Figure 125: For the mugshot images, error tradeoff characteristics for white females, black females, black males and white males. The Z-shaped grey lines correspond to fixed thresholds, showing both FNMR and FMR vary at one T value. Note: Many of the plots will naively be read as saying women gives worse error rates than men because the solid traces lie above the dotted ones. However, this is misleading and incomplete: The grey lines show the traces reveal horizontal shifts. Thus for the cogent-003 algorithm FNMR for men is higher than for women at a fixed threshold but, at the same time, FMR is higher for women - see Figure 194. As access control systems almost always operate at a fixed threshold, the naive interpretation is incorrect.

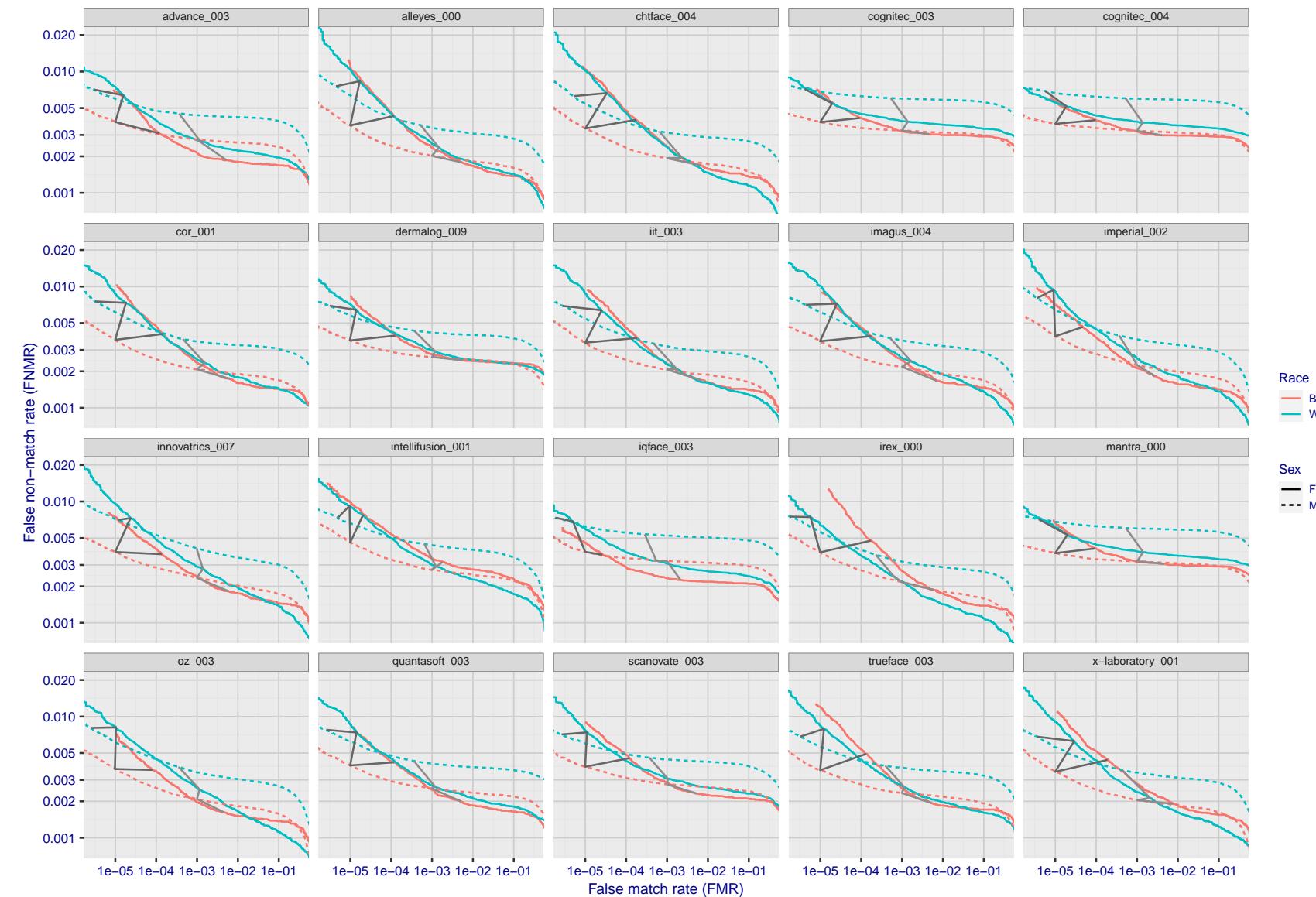


Figure 126: For the mugshot images, error tradeoff characteristics for white females, black females, black males and white males. The Z-shaped grey lines correspond to fixed thresholds, showing both FNMR and FMR vary at one T value. Note: Many of the plots will naively be read as saying women gives worse error rates than men because the solid traces lie above the dotted ones. However, this is misleading and incomplete: The grey lines show the traces reveal horizontal shifts. Thus for the cogent-003 algorithm FNMR for men is higher than for women at a fixed threshold but, at the same time, FMR is higher for women - see Figure 194. As access control systems almost always operate at a fixed threshold, the naive interpretation is incorrect.

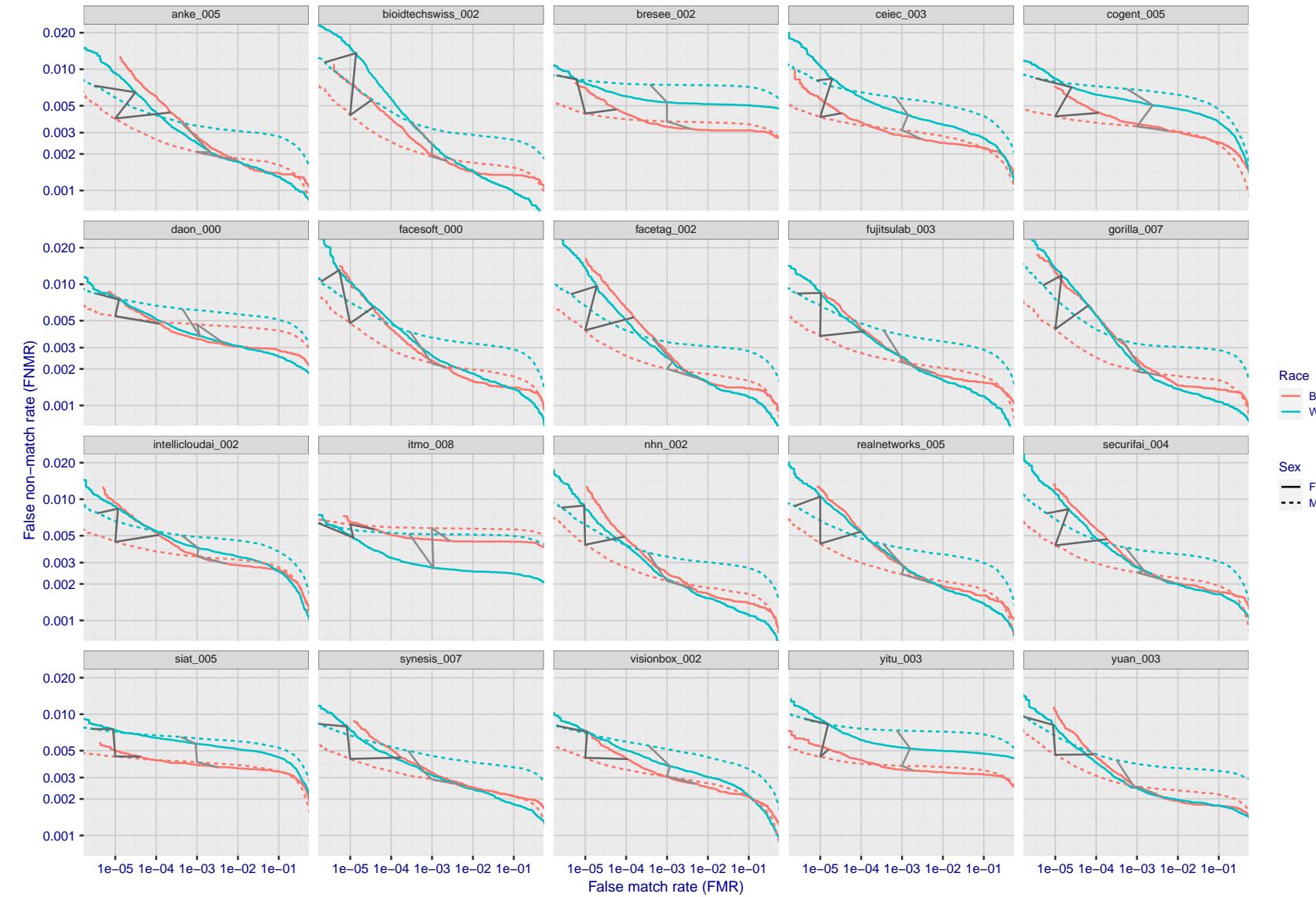


Figure 127: For the mugshot images, error tradeoff characteristics for white females, black females, black males and white males. The Z-shaped grey lines correspond to fixed thresholds, showing both FNMR and FMR vary at one T value. Note: Many of the plots will naively be read as saying women gives worse error rates than men because the solid traces lie above the dotted ones. However, this is misleading and incomplete: The grey lines show the traces reveal horizontal shifts. Thus for the cogent-003 algorithm FNMR for men is higher than for women at a fixed threshold but, at the same time, FMR is higher for women - see Figure 194. As access control systems almost always operate at a fixed threshold, the naive interpretation is incorrect.

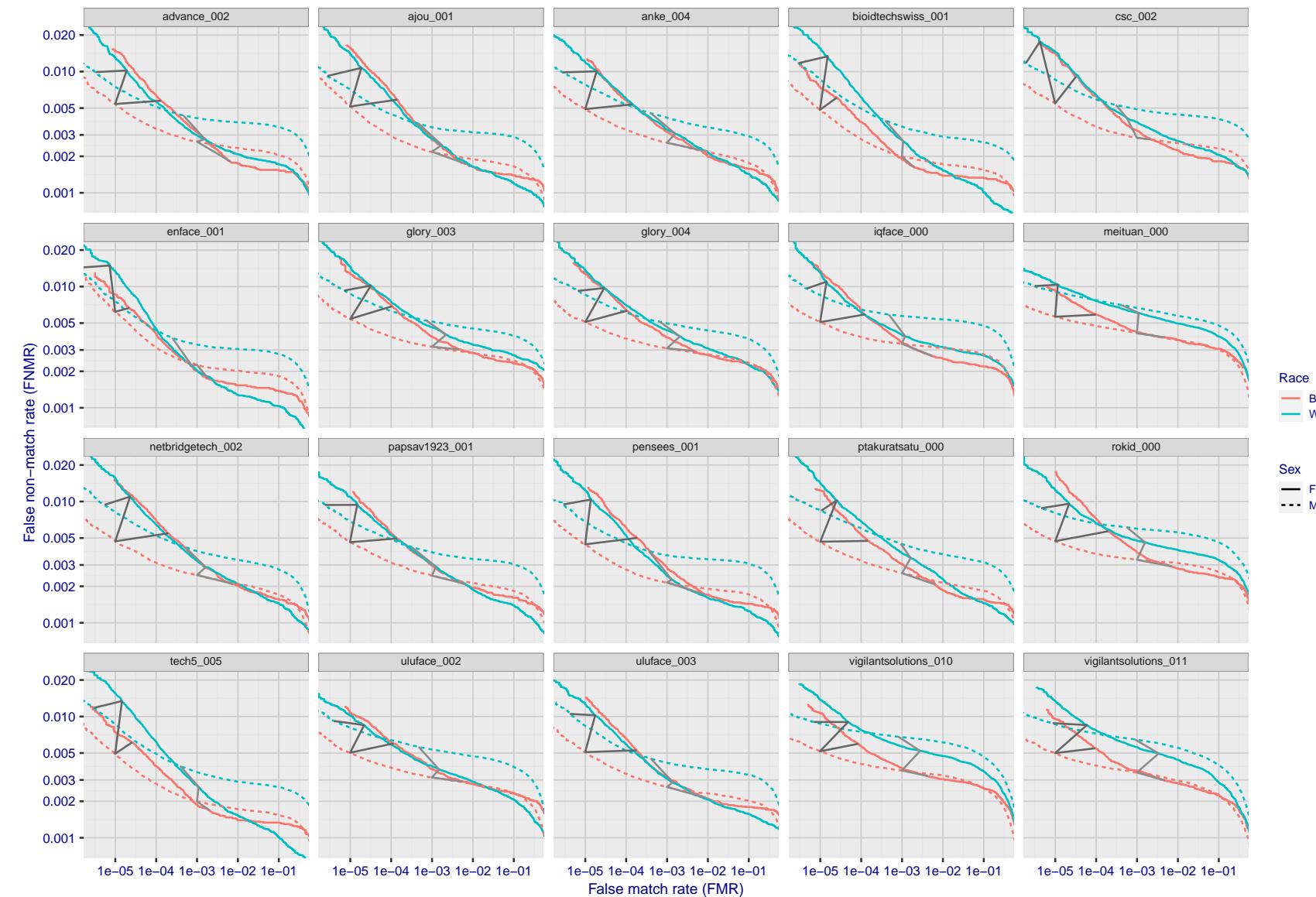


Figure 128: For the mugshot images, error tradeoff characteristics for white females, black females, black males and white males. The Z-shaped grey lines correspond to fixed thresholds, showing both FNMR and FMR vary at one T value. Note: Many of the plots will naively be read as saying women gives worse error rates than men because the solid traces lie above the dotted ones. However, this is misleading and incomplete: The grey lines show the traces reveal horizontal shifts. Thus for the cogent-003 algorithm FNMR for men is higher than for women at a fixed threshold but, at the same time, FMR is higher for women - see Figure 194. As access control systems almost always operate at a fixed threshold, the naive interpretation is incorrect.

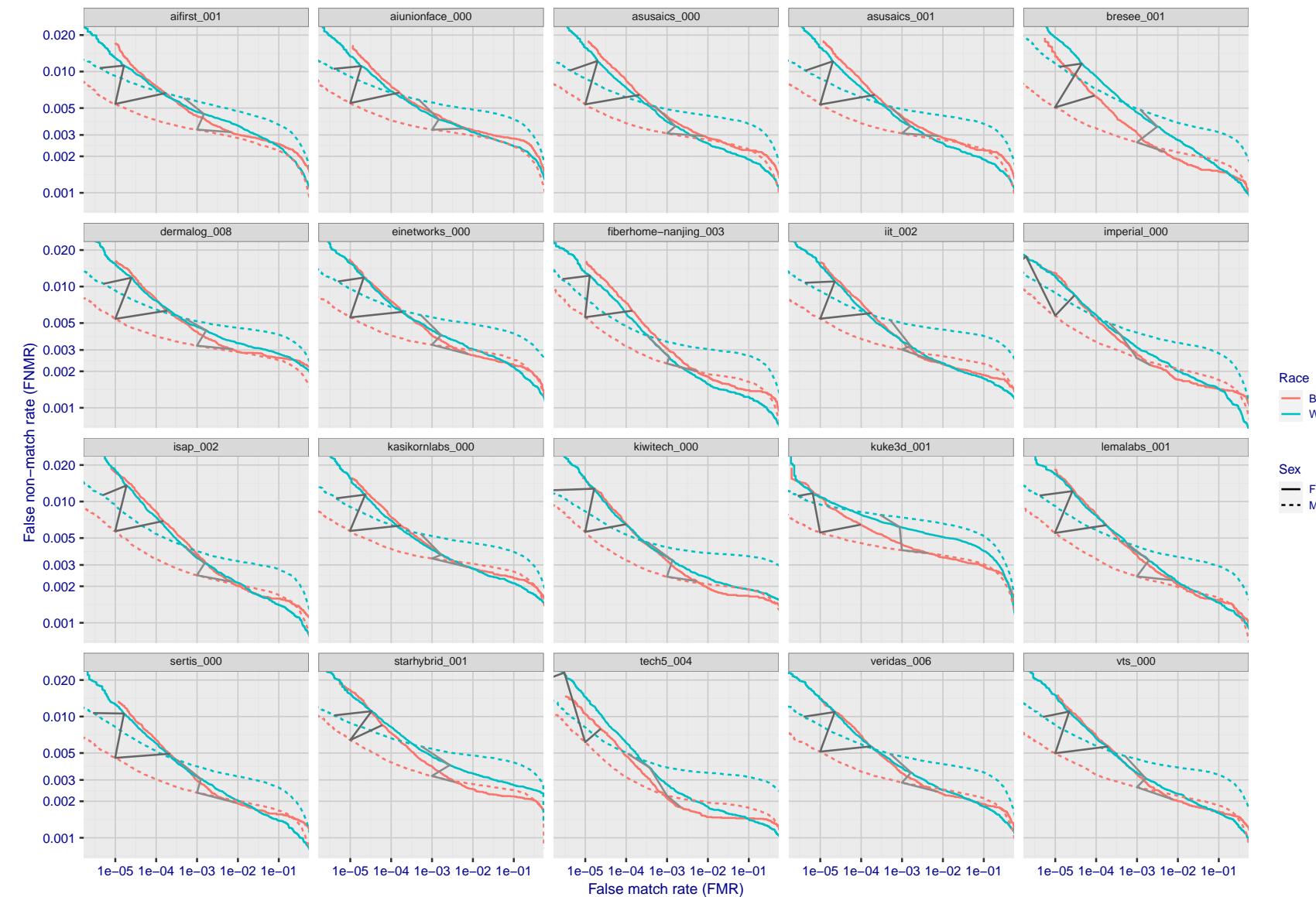


Figure 129: For the mugshot images, error tradeoff characteristics for white females, black females, black males and white males. The Z-shaped grey lines correspond to fixed thresholds, showing both FNMR and FMR vary at one T value. Note: Many of the plots will naively be read as saying women gives worse error rates than men because the solid traces lie above the dotted ones. However, this is misleading and incomplete: The grey lines show the traces reveal horizontal shifts. Thus for the cogent-003 algorithm FNMR for men is higher than for women at a fixed threshold but, at the same time, FMR is higher for women - see Figure 194. As access control systems almost always operate at a fixed threshold, the naive interpretation is incorrect.

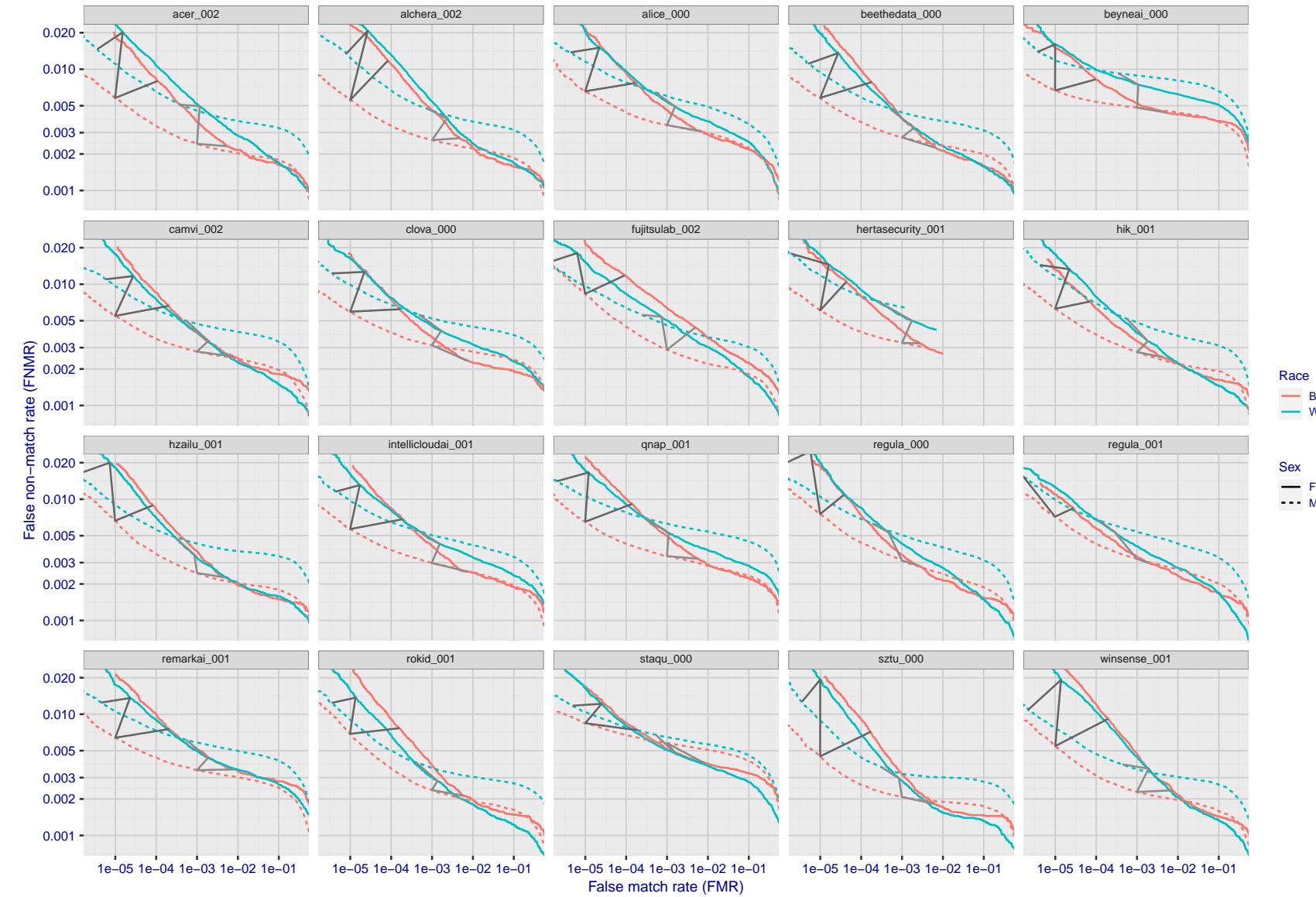


Figure 130: For the mugshot images, error tradeoff characteristics for white females, black females, black males and white males. The Z-shaped grey lines correspond to fixed thresholds, showing both FNMR and FMR vary at one T value. Note: Many of the plots will naively be read as saying women gives worse error rates than men because the solid traces lie above the dotted ones. However, this is misleading and incomplete: The grey lines show the traces reveal horizontal shifts. Thus for the cogent-003 algorithm FNMR for men is higher than for women at a fixed threshold but, at the same time, FMR is higher for women - see Figure 194. As access control systems almost always operate at a fixed threshold, the naive interpretation is incorrect.

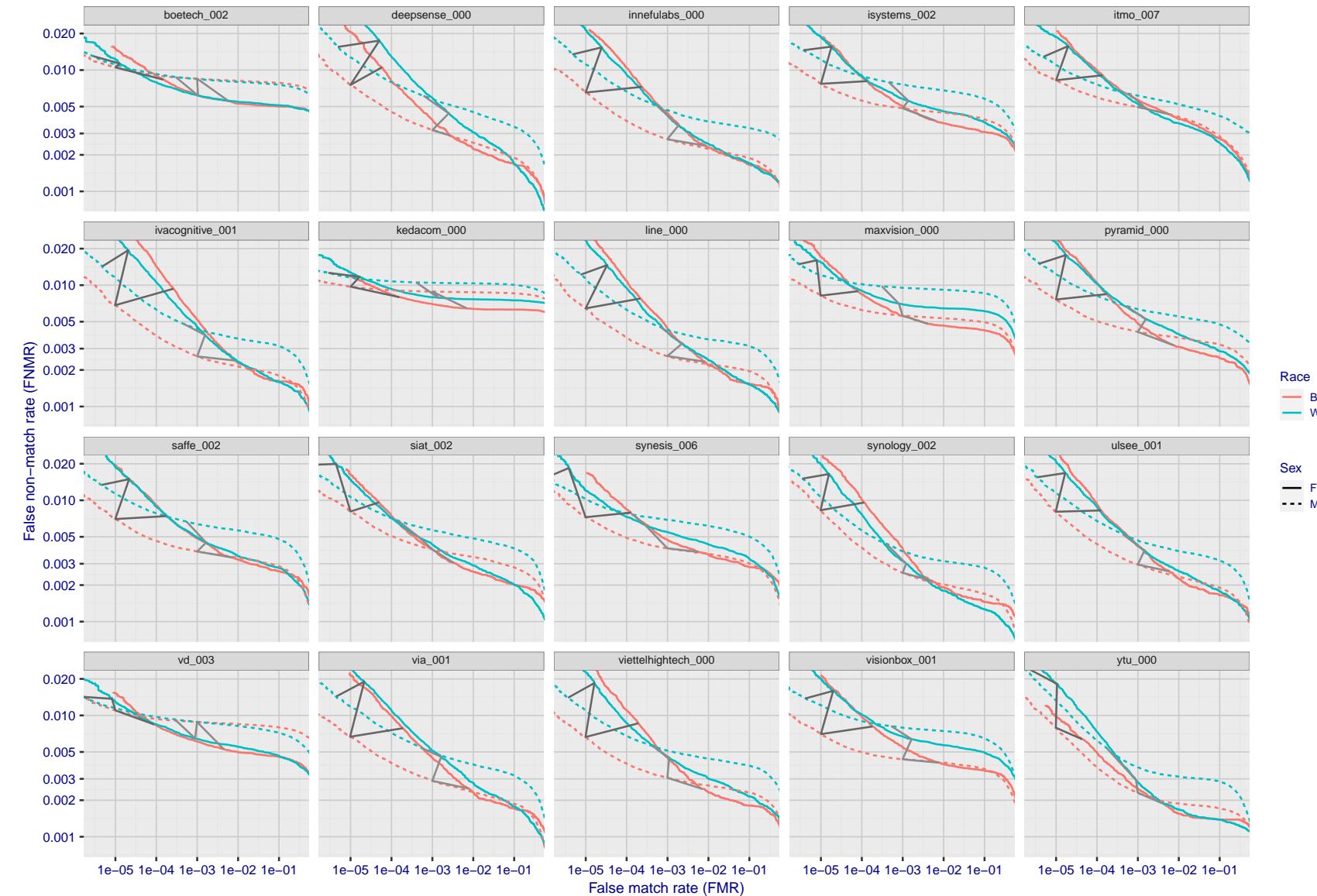


Figure 131: For the mugshot images, error tradeoff characteristics for white females, black females, black males and white males. The Z-shaped grey lines correspond to fixed thresholds, showing both FNMR and FMR vary at one T value. Note: Many of the plots will naively be read as saying women gives worse error rates than men because the solid traces lie above the dotted ones. However, this is misleading and incomplete: The grey lines show the traces reveal horizontal shifts. Thus for the cogent-003 algorithm FNMR for men is higher than for women at a fixed threshold but, at the same time, FMR is higher for women - see Figure 194. As access control systems almost always operate at a fixed threshold, the naive interpretation is incorrect.

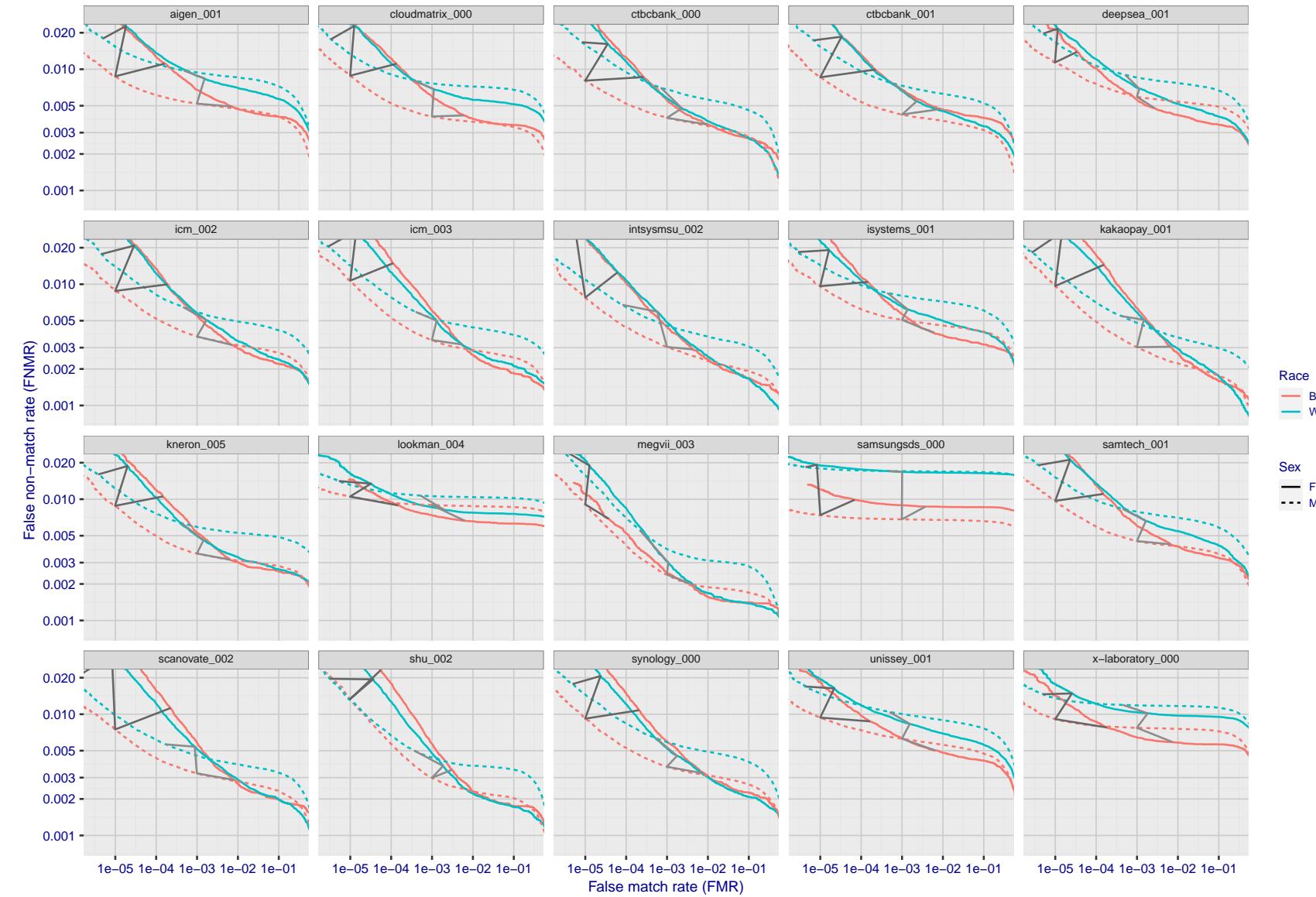


Figure 132: For the mugshot images, error tradeoff characteristics for white females, black females, black males and white males. The Z-shaped grey lines correspond to fixed thresholds, showing both FNMR and FMR vary at one T value. Note: Many of the plots will naively be read as saying women gives worse error rates than men because the solid traces lie above the dotted ones. However, this is misleading and incomplete: The grey lines show the traces reveal horizontal shifts. Thus for the cogent-003 algorithm FNMR for men is higher than for women at a fixed threshold but, at the same time, FMR is higher for women - see Figure 194. As access control systems almost always operate at a fixed threshold, the naive interpretation is incorrect.

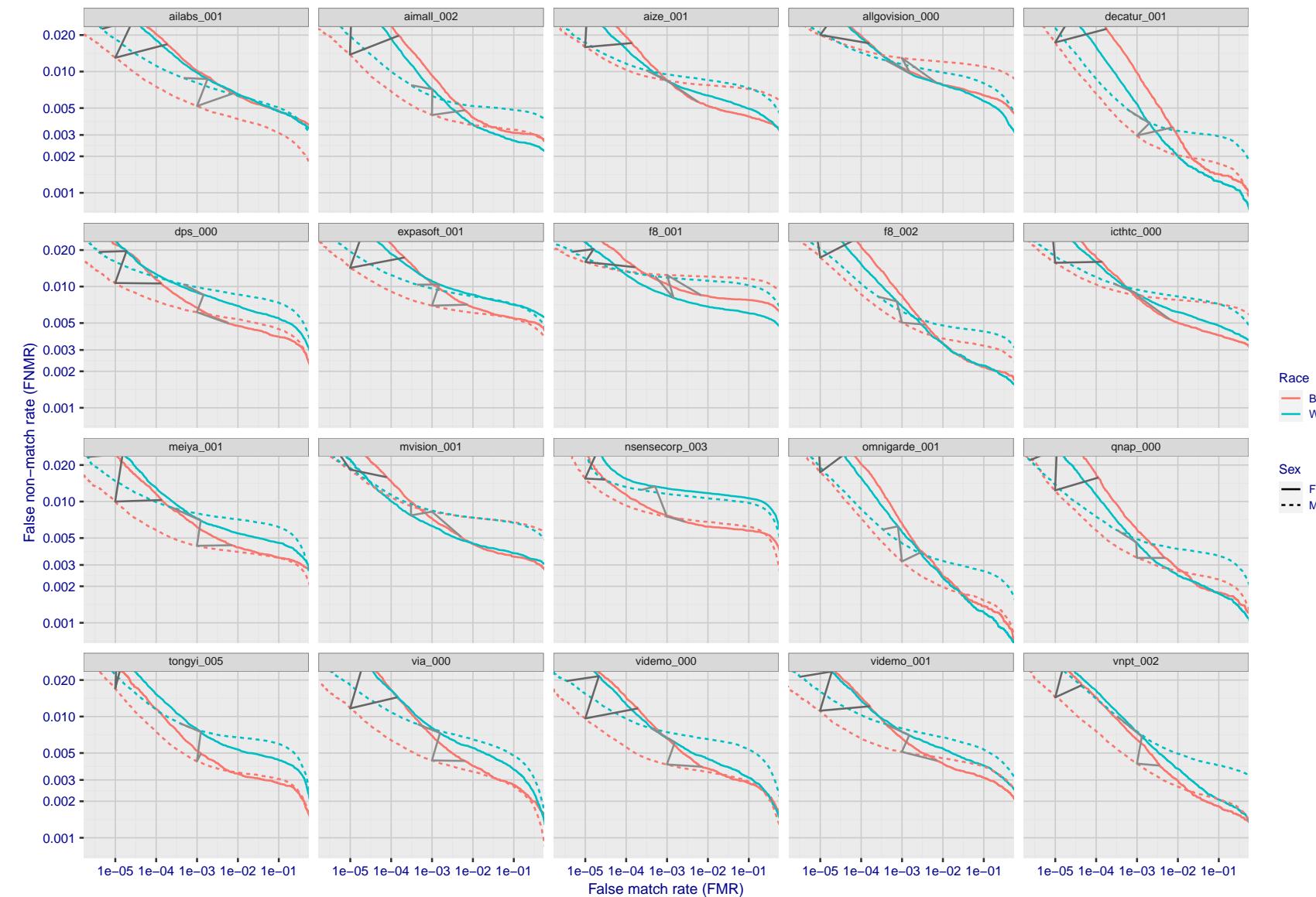


Figure 133: For the mugshot images, error tradeoff characteristics for white females, black females, black males and white males. The Z-shaped grey lines correspond to fixed thresholds, showing both FNMR and FMR vary at one T value. Note: Many of the plots will naively be read as saying women gives worse error rates than men because the solid traces lie above the dotted ones. However, this is misleading and incomplete: The grey lines show the traces reveal horizontal shifts. Thus for the cogent-003 algorithm FNMR for men is higher than for women at a fixed threshold but, at the same time, FMR is higher for women - see Figure 194. As access control systems almost always operate at a fixed threshold, the naive interpretation is incorrect.

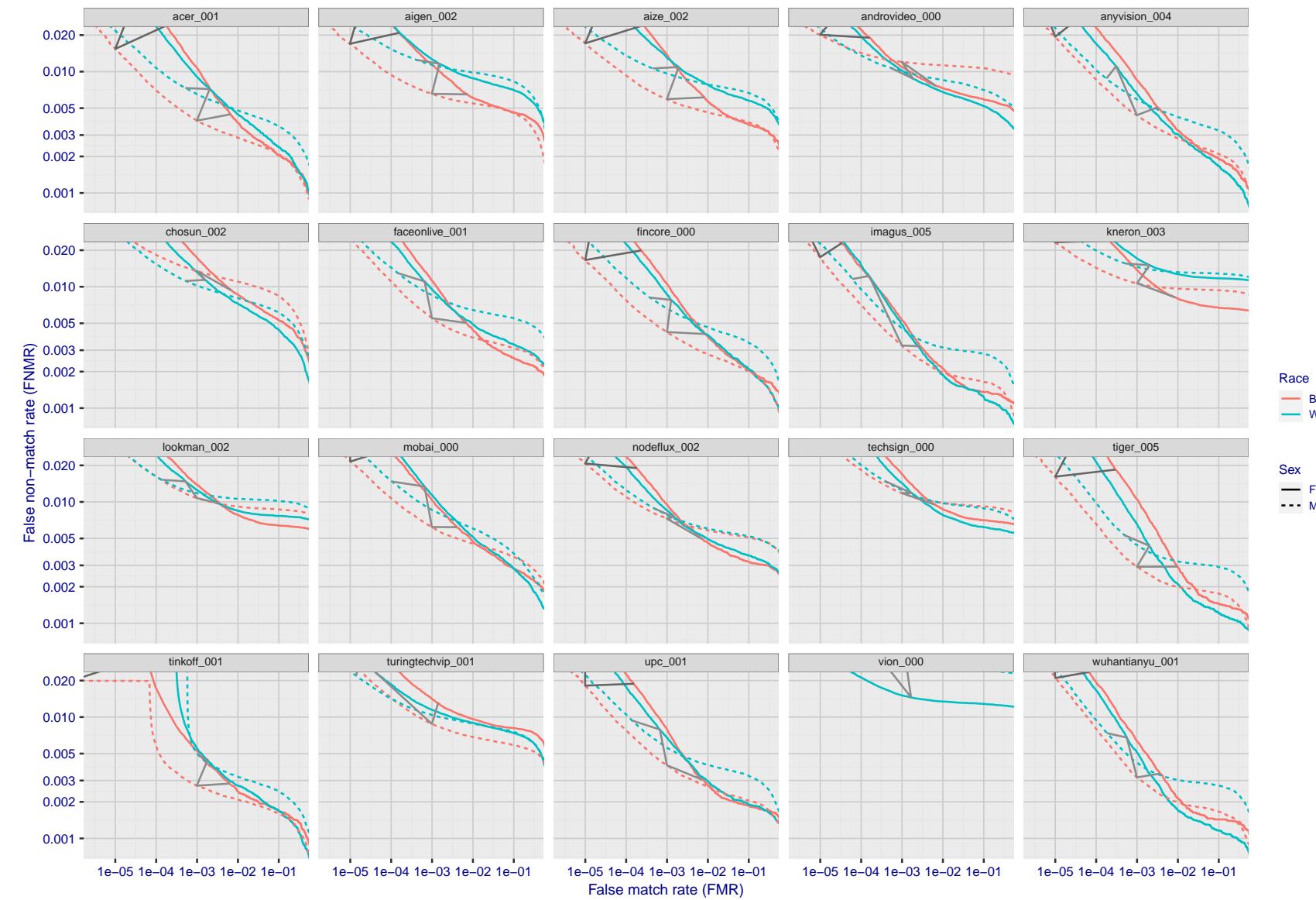


Figure 134: For the mugshot images, error tradeoff characteristics for white females, black females, black males and white males. The Z-shaped grey lines correspond to fixed thresholds, showing both FNMR and FMR vary at one T value. Note: Many of the plots will naively be read as saying women gives worse error rates than men because the solid traces lie above the dotted ones. However, this is misleading and incomplete: The grey lines show the traces reveal horizontal shifts. Thus for the cogent-003 algorithm FNMR for men is higher than for women at a fixed threshold but, at the same time, FMR is higher for women - see Figure 194. As access control systems almost always operate at a fixed threshold, the naive interpretation is incorrect.

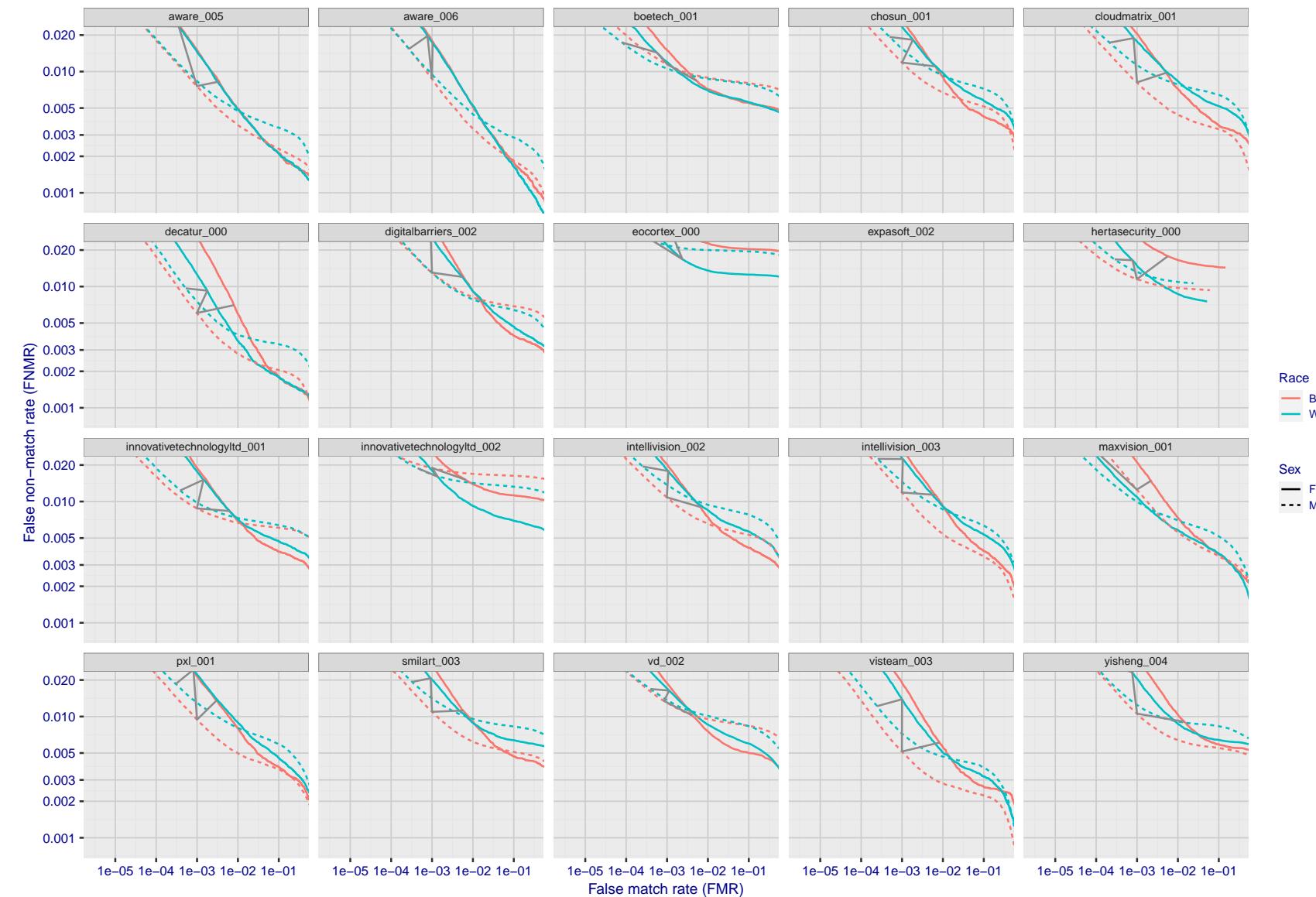


Figure 135: For the mugshot images, error tradeoff characteristics for white females, black females, black males and white males. The Z-shaped grey lines correspond to fixed thresholds, showing both FNMR and FMR vary at one T value. Note: Many of the plots will naively be read as saying women gives worse error rates than men because the solid traces lie above the dotted ones. However, this is misleading and incomplete: The grey lines show the traces reveal horizontal shifts. Thus for the cogent-003 algorithm FNMR for men is higher than for women at a fixed threshold but, at the same time, FMR is higher for women - see Figure 194. As access control systems almost always operate at a fixed threshold, the naive interpretation is incorrect.

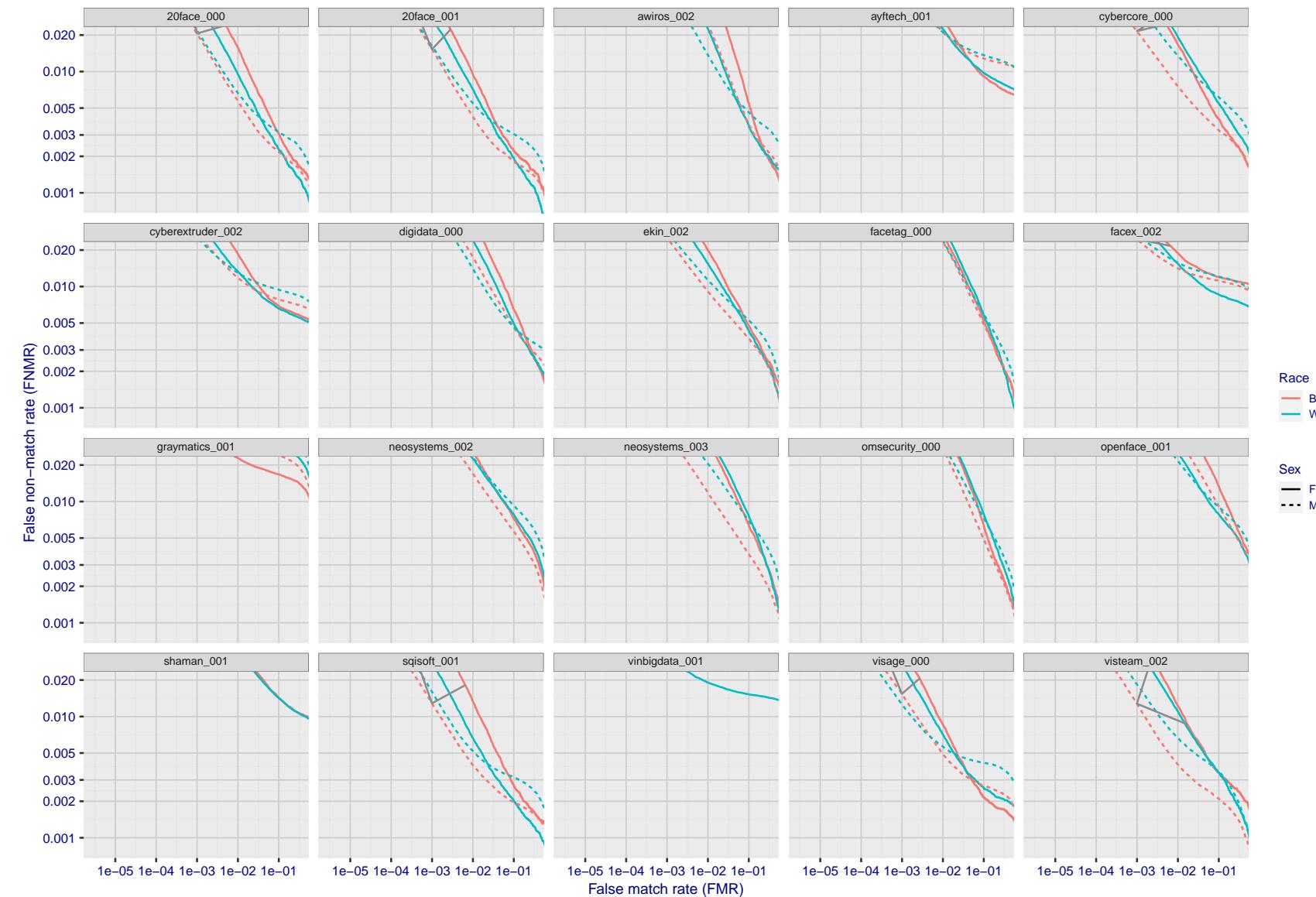


Figure 136: For the mugshot images, error tradeoff characteristics for white females, black females, black males and white males. The Z-shaped grey lines correspond to fixed thresholds, showing both FNMR and FMR vary at one T value. Note: Many of the plots will naively be read as saying women gives worse error rates than men because the solid traces lie above the dotted ones. However, this is misleading and incomplete: The grey lines show the traces reveal horizontal shifts. Thus for the cogent-003 algorithm FNMR for men is higher than for women at a fixed threshold but, at the same time, FMR is higher for women - see Figure 194. As access control systems almost always operate at a fixed threshold, the naive interpretation is incorrect.

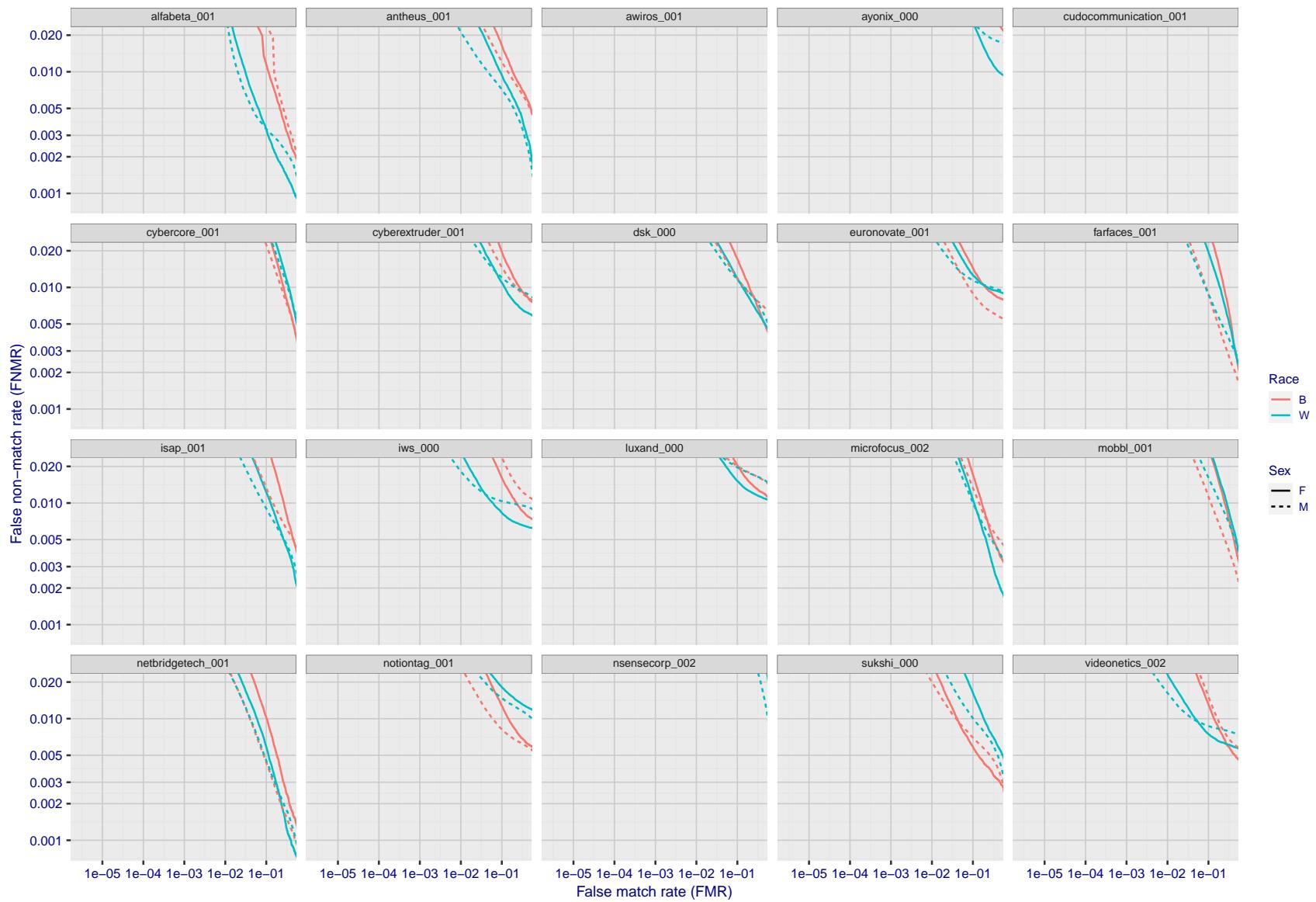


Figure 137: For the mugshot images, error tradeoff characteristics for white females, black females, black males and white males. The Z-shaped grey lines correspond to fixed thresholds, showing both FNMR and FMR vary at one T value. Note: Many of the plots will naively be read as saying women gives worse error rates than men because the solid traces lie above the dotted ones. However, this is misleading and incomplete: The grey lines show the traces reveal horizontal shifts. Thus for the cogent-003 algorithm FNMR for men is higher than for women at a fixed threshold but, at the same time, FMR is higher for women - see Figure 194. As access control systems almost always operate at a fixed threshold, the naive interpretation is incorrect.

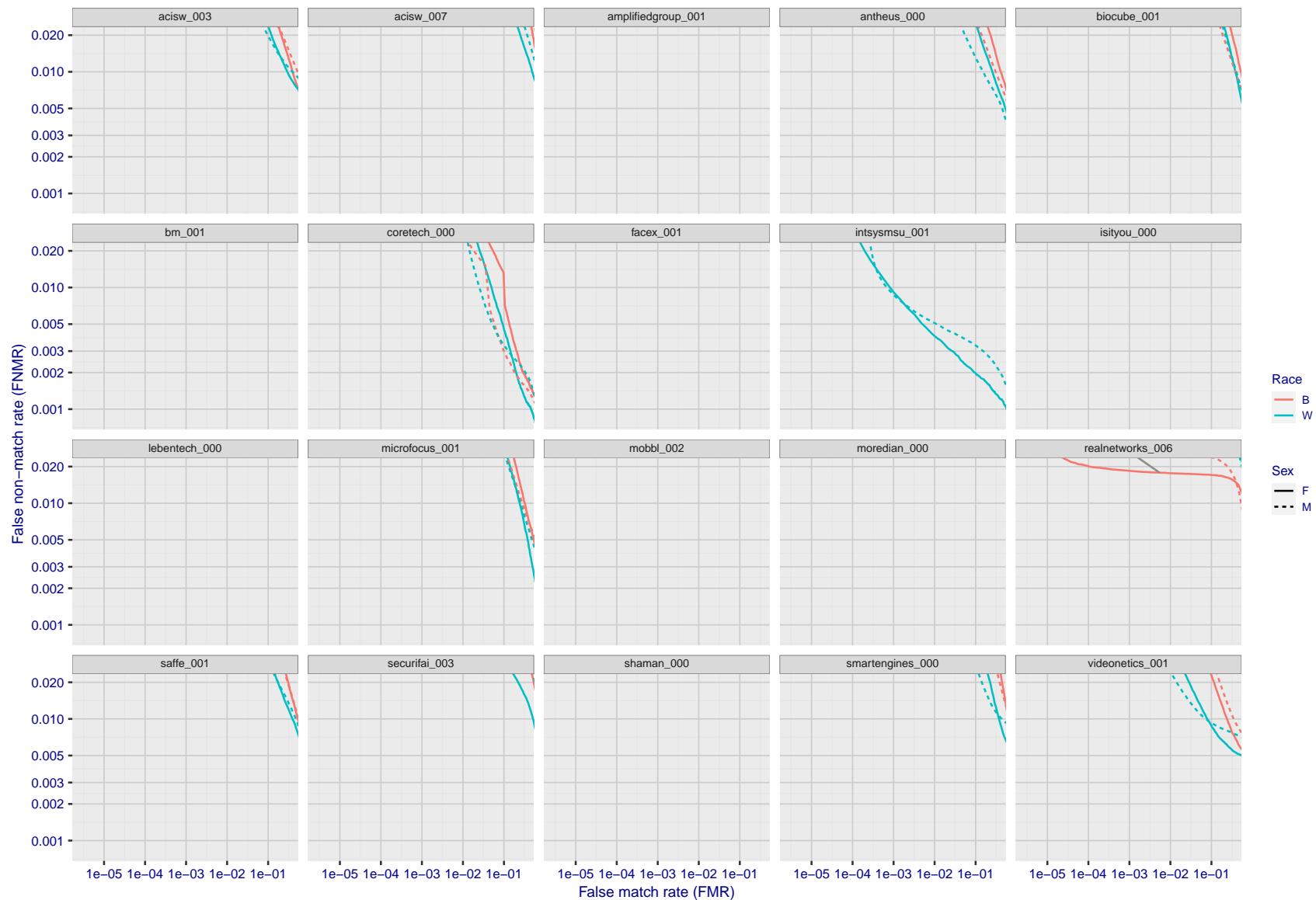


Figure 138: For the mugshot images, error tradeoff characteristics for white females, black females, black males and white males. The Z-shaped grey lines correspond to fixed thresholds, showing both FNMR and FMR vary at one T value. Note: Many of the plots will naively be read as saying women gives worse error rates than men because the solid traces lie above the dotted ones. However, this is misleading and incomplete: The grey lines show the traces reveal horizontal shifts. Thus for the cogent-003 algorithm FNMR for men is higher than for women at a fixed threshold but, at the same time, FMR is higher for women - see Figure 194. As access control systems almost always operate at a fixed threshold, the naive interpretation is incorrect.

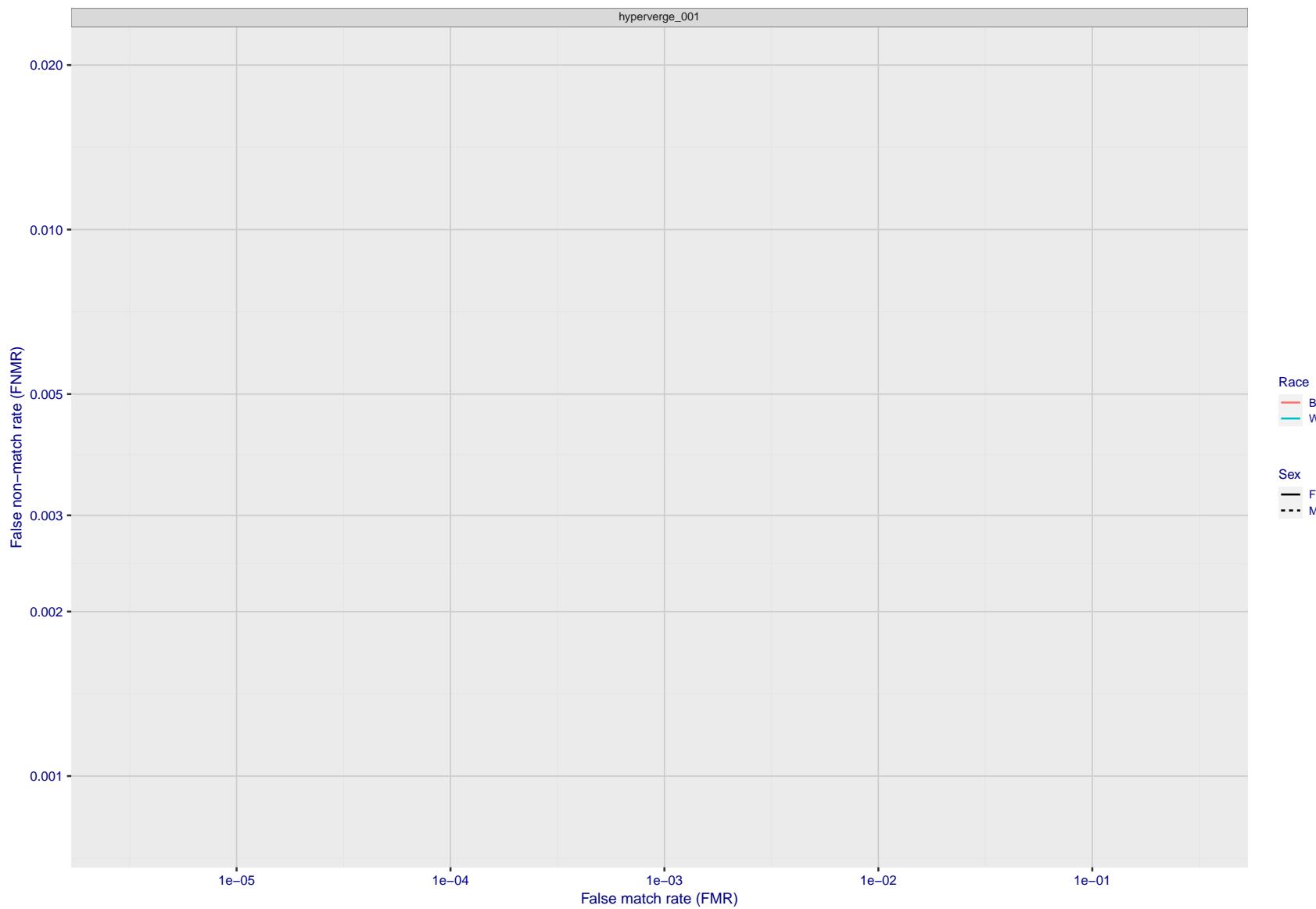


Figure 139: For the mugshot images, error tradeoff characteristics for white females, black females, black males and white males. The Z-shaped grey lines correspond to fixed thresholds, showing both FNMR and FMR vary at one T value. Note: Many of the plots will naively be read as saying women gives worse error rates than men because the solid traces lie above the dotted ones. However, this is misleading and incomplete: The grey lines show the traces reveal horizontal shifts. Thus for the cogent-003 algorithm FNMR for men is higher than for women at a fixed threshold but, at the same time, FMR is higher for women - see Figure 194. As access control systems almost always operate at a fixed threshold, the naive interpretation is incorrect.

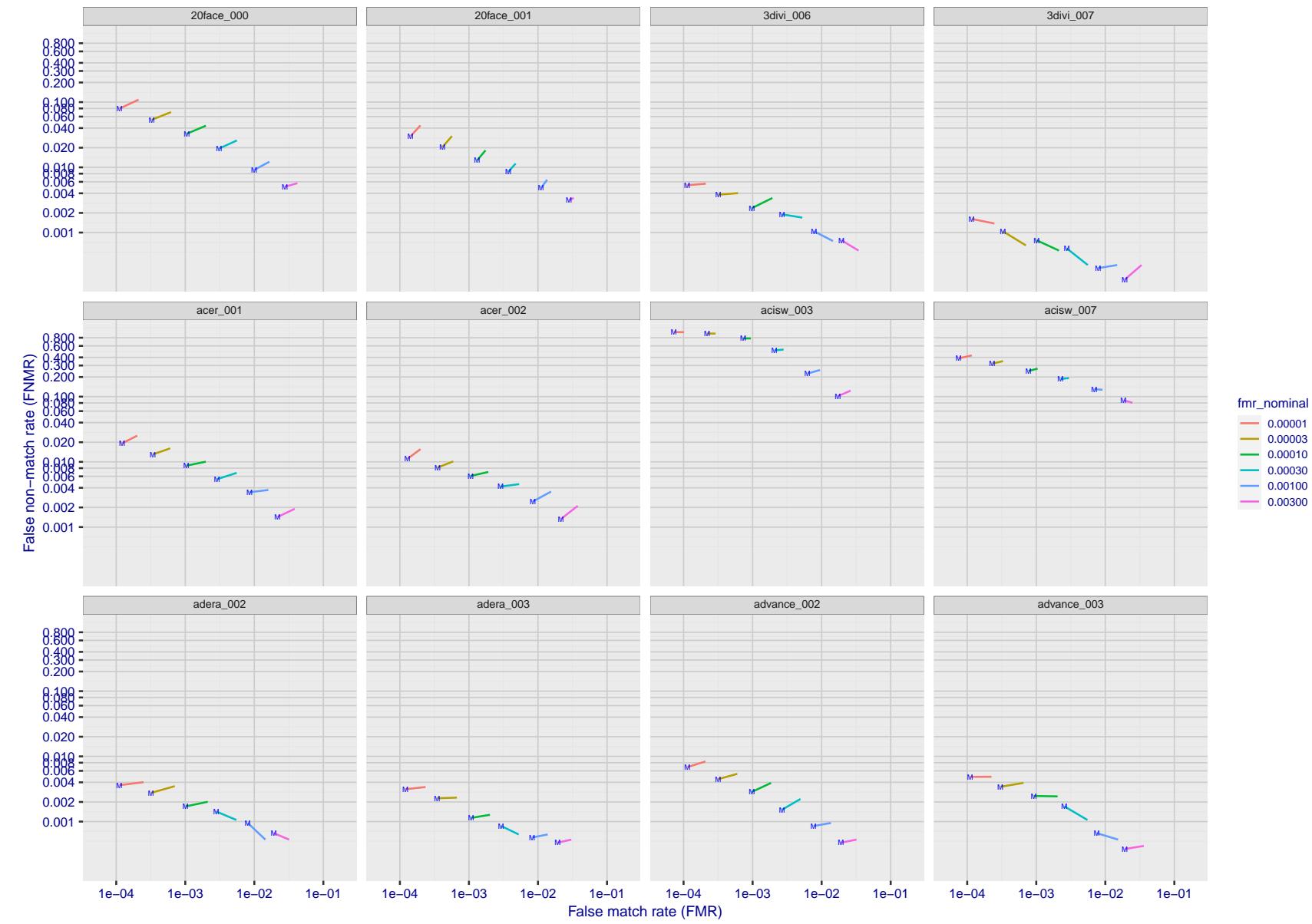


Figure 140: For the visa images, FNMR and FMR at six operating points along the DET characteristic. At each point a line is drawn between $(FMR, FNMR)_{MALE}$ and $(FMR, FNMR)_{FEMALE}$ showing how which sex has lower FMR and/or FNMR. The "M" label denotes male, the other end of the line corresponds to female. The six operating thresholds are selected to give the nominal false match rates given in the legend, and are computed over all impostor pairs regardless of age, sex, and place of birth. The plotted FMR values are broadly an order of magnitude larger than the nominal rates because FMR is computed over demographically-matched impostor pairs i.e individuals of the same sex, from the same geographic region (see section 3.6.1), and the same age group (see section 3.6.2).

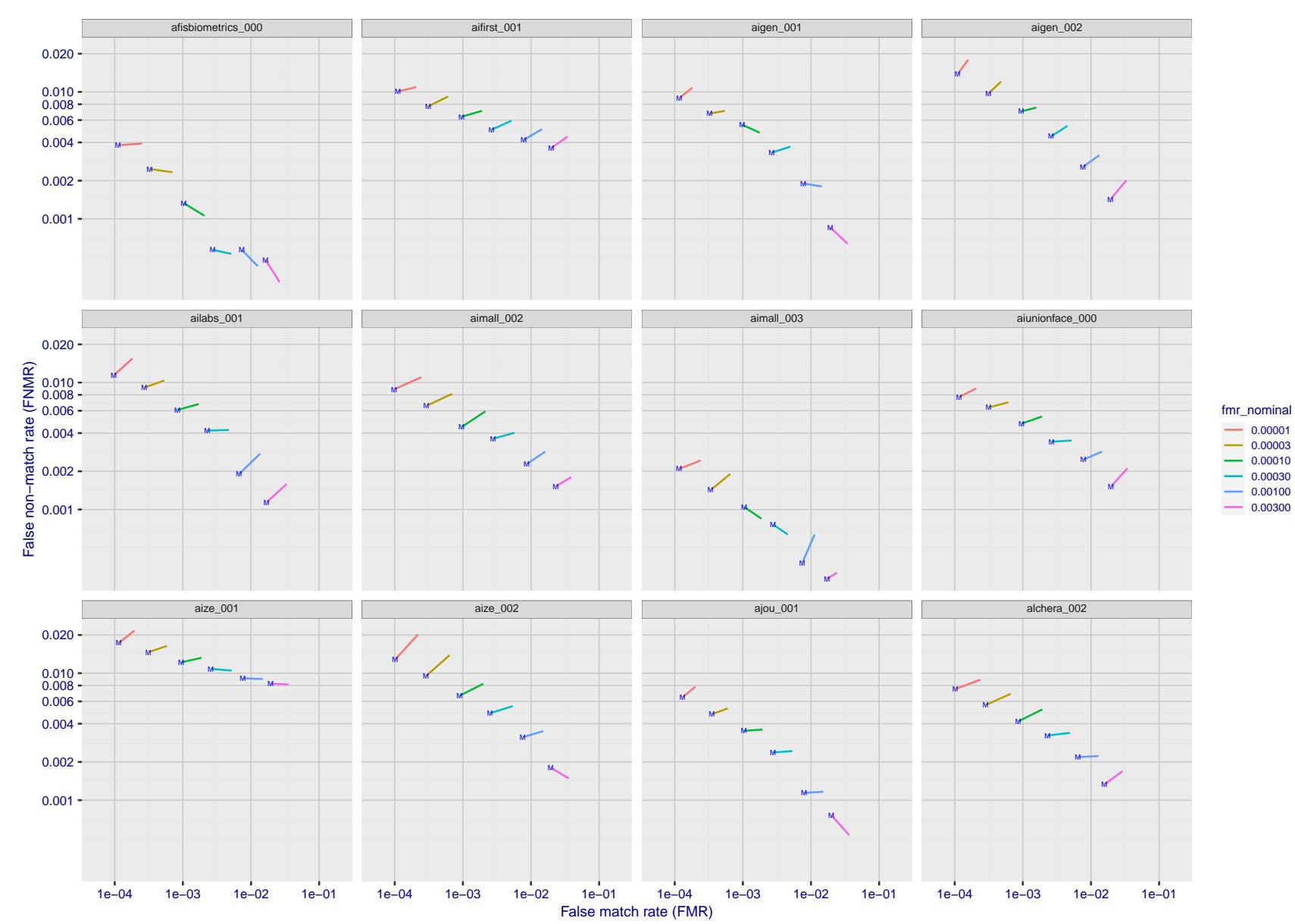


Figure 141: For the visa images, FNMR and FMR at six operating points along the DET characteristic. At each point a line is drawn between $(FMR, FNMR)_{MALE}$ and $(FMR, FNMR)_{FEMALE}$ showing how which sex has lower FMR and/or FNMR. The "M" label denotes male, the other end of the line corresponds to female. The six operating thresholds are selected to give the nominal false match rates given in the legend, and are computed over all impostor pairs regardless of age, sex, and place of birth. The plotted FMR values are broadly an order of magnitude larger than the nominal rates because FMR is computed over demographically-matched impostor pairs i.e individuals of the same sex, from the same geographic region (see section 3.6.1), and the same age group (see section 3.6.2).

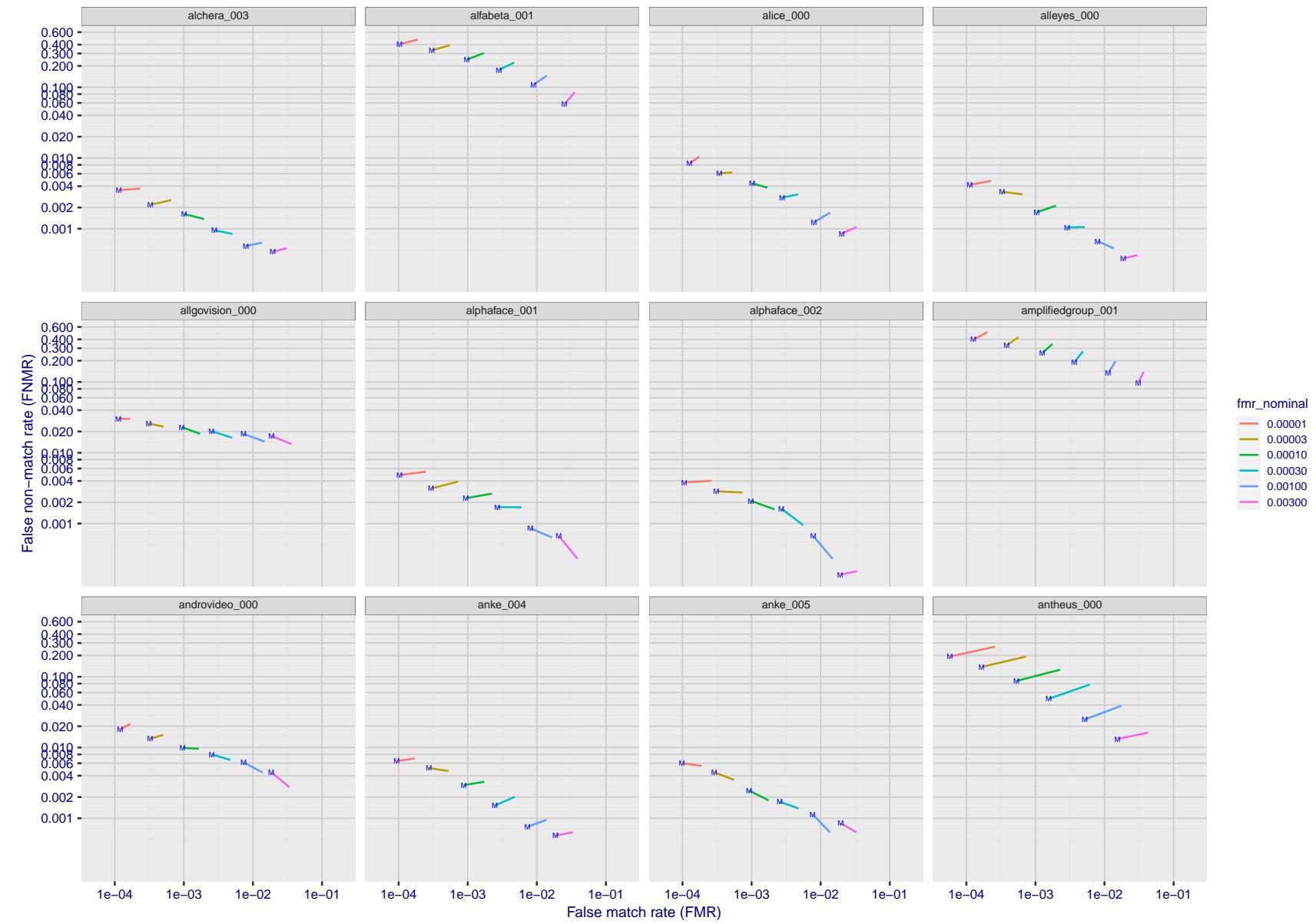


Figure 142: For the visa images, FNMR and FMR at six operating points along the DET characteristic. At each point a line is drawn between $(FMR, FNMR)_{MALE}$ and $(FMR, FNMR)_{FEMALE}$ showing how which sex has lower FMR and/or FNMR. The "M" label denotes male, the other end of the line corresponds to female. The six operating thresholds are selected to give the nominal false match rates given in the legend, and are computed over all impostor pairs regardless of age, sex, and place of birth. The plotted FMR values are broadly an order of magnitude larger than the nominal rates because FMR is computed over demographically-matched impostor pairs i.e individuals of the same sex, from the same geographic region (see section 3.6.1), and the same age group (see section 3.6.2).

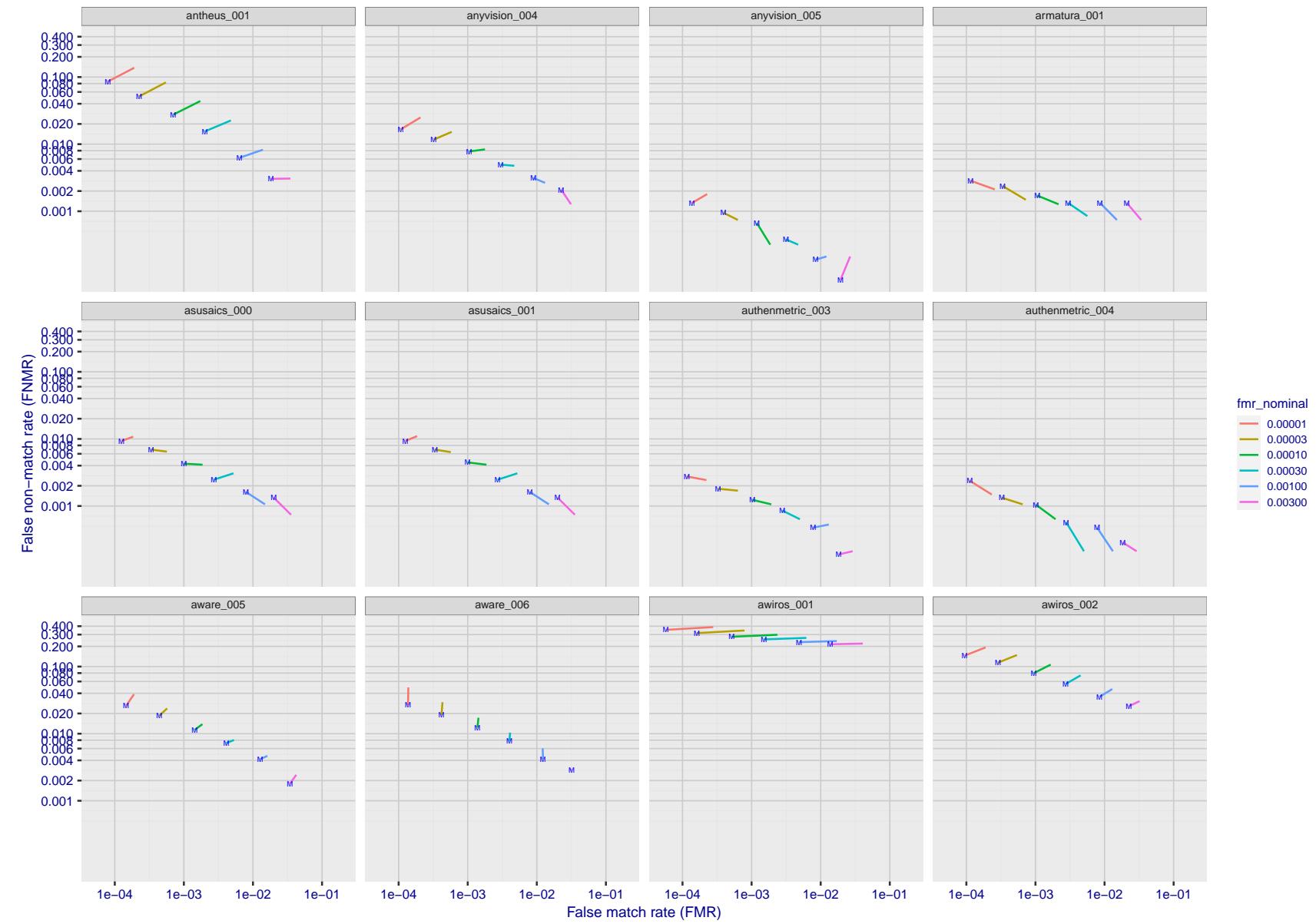


Figure 143: For the visa images, FNMR and FMR at six operating points along the DET characteristic. At each point a line is drawn between $(FMR, FNMR)_{MALE}$ and $(FMR, FNMR)_{FEMALE}$ showing how which sex has lower FMR and/or FNMR. The "M" label denotes male, the other end of the line corresponds to female. The six operating thresholds are selected to give the nominal false match rates given in the legend, and are computed over all impostor pairs regardless of age, sex, and place of birth. The plotted FMR values are broadly an order of magnitude larger than the nominal rates because FMR is computed over demographically-matched impostor pairs i.e individuals of the same sex, from the same geographic region (see section 3.6.1), and the same age group (see section 3.6.2).

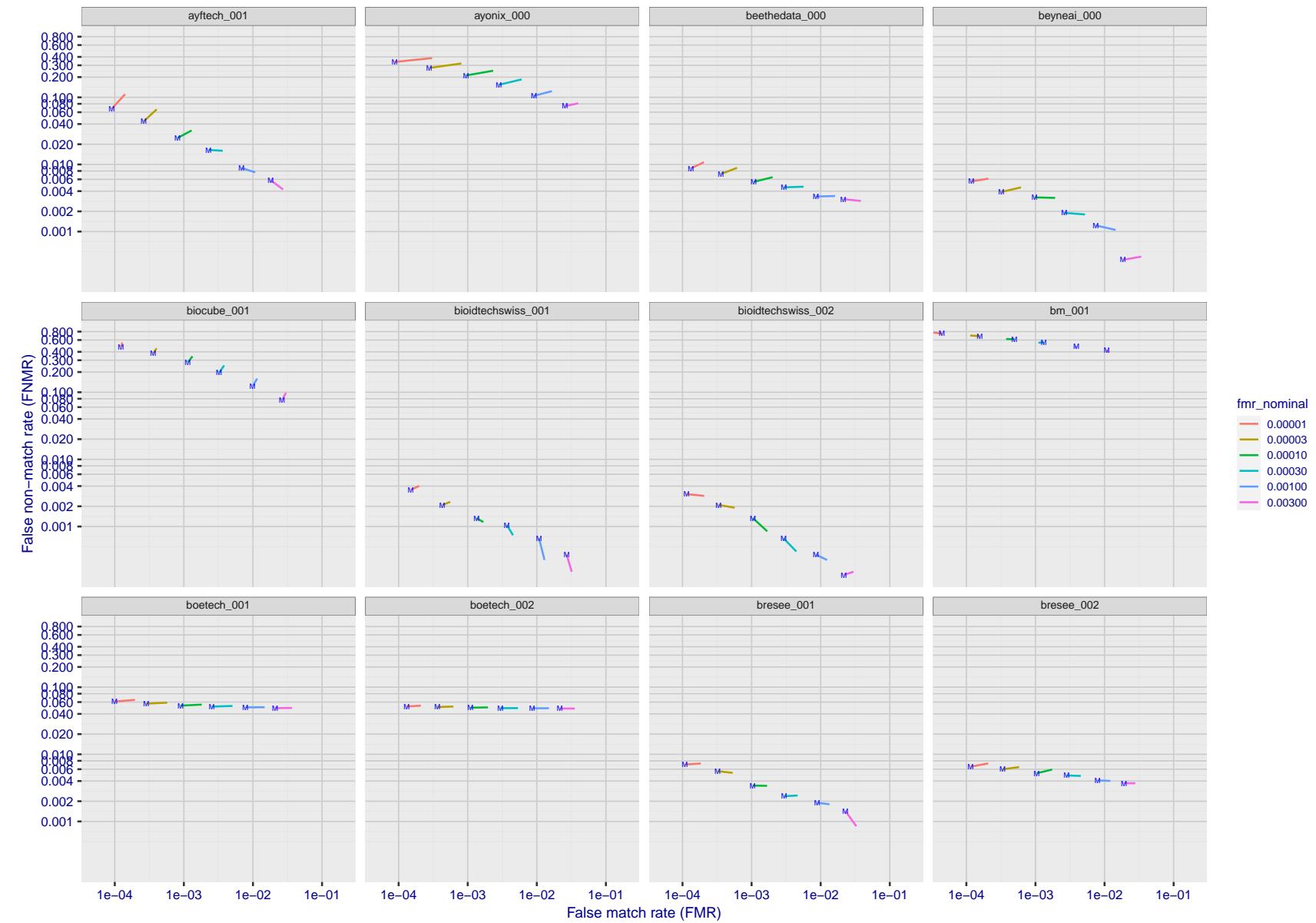


Figure 144: For the visa images, FNMR and FMR at six operating points along the DET characteristic. At each point a line is drawn between $(FMR, FNMR)_{MALE}$ and $(FMR, FNMR)_{FEMALE}$ showing how which sex has lower FMR and/or FNMR. The "M" label denotes male, the other end of the line corresponds to female. The six operating thresholds are selected to give the nominal false match rates given in the legend, and are computed over all impostor pairs regardless of age, sex, and place of birth. The plotted FMR values are broadly an order of magnitude larger than the nominal rates because FMR is computed over demographically-matched impostor pairs i.e individuals of the same sex, from the same geographic region (see section 3.6.1), and the same age group (see section 3.6.2).

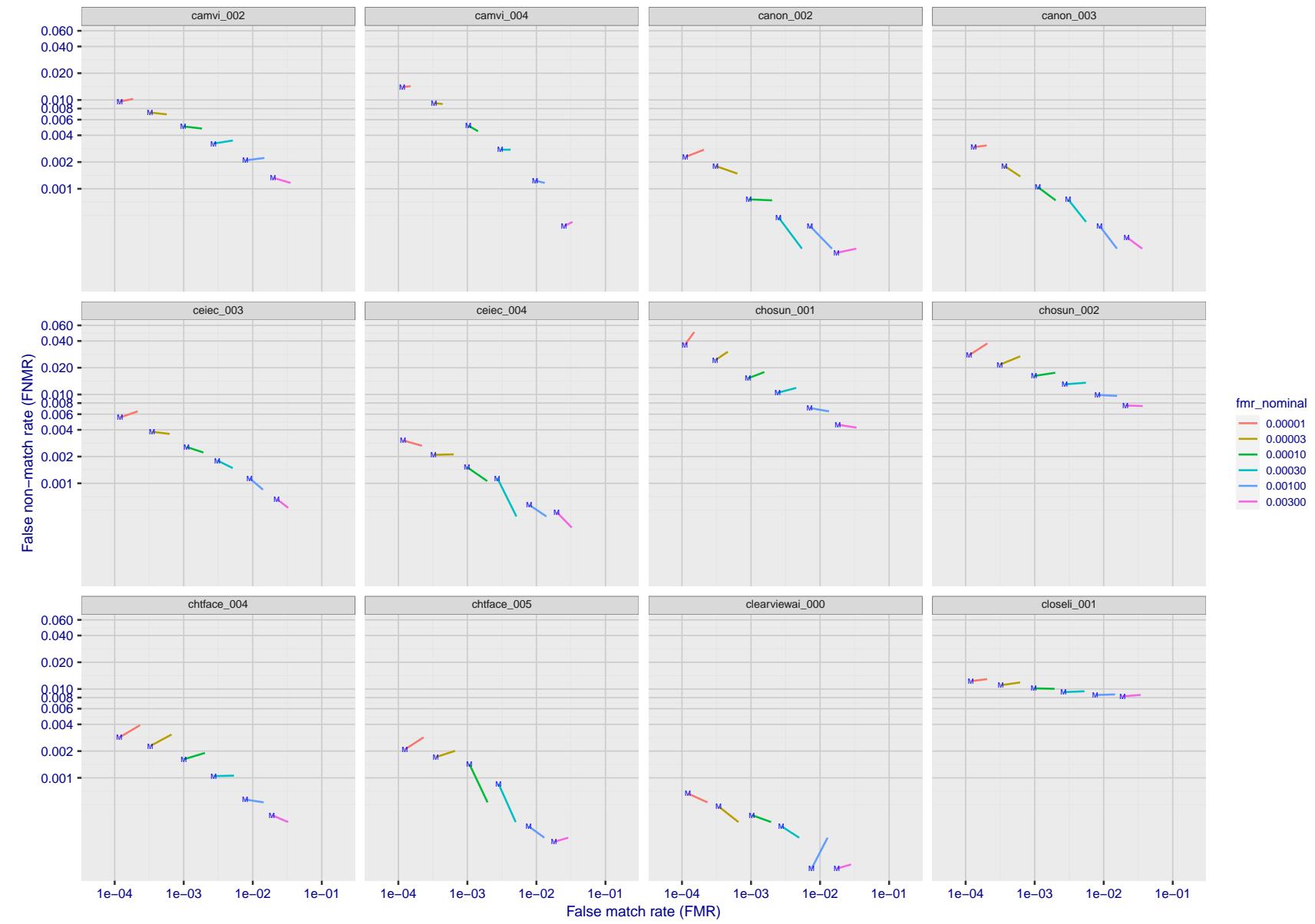


Figure 145: For the visa images, FNMR and FMR at six operating points along the DET characteristic. At each point a line is drawn between $(FMR, FNMR)_{MALE}$ and $(FMR, FNMR)_{FEMALE}$ showing how which sex has lower FMR and/or FNMR. The "M" label denotes male, the other end of the line corresponds to female. The six operating thresholds are selected to give the nominal false match rates given in the legend, and are computed over all impostor pairs regardless of age, sex, and place of birth. The plotted FMR values are broadly an order of magnitude larger than the nominal rates because FMR is computed over demographically-matched impostor pairs i.e individuals of the same sex, from the same geographic region (see section 3.6.1), and the same age group (see section 3.6.2).

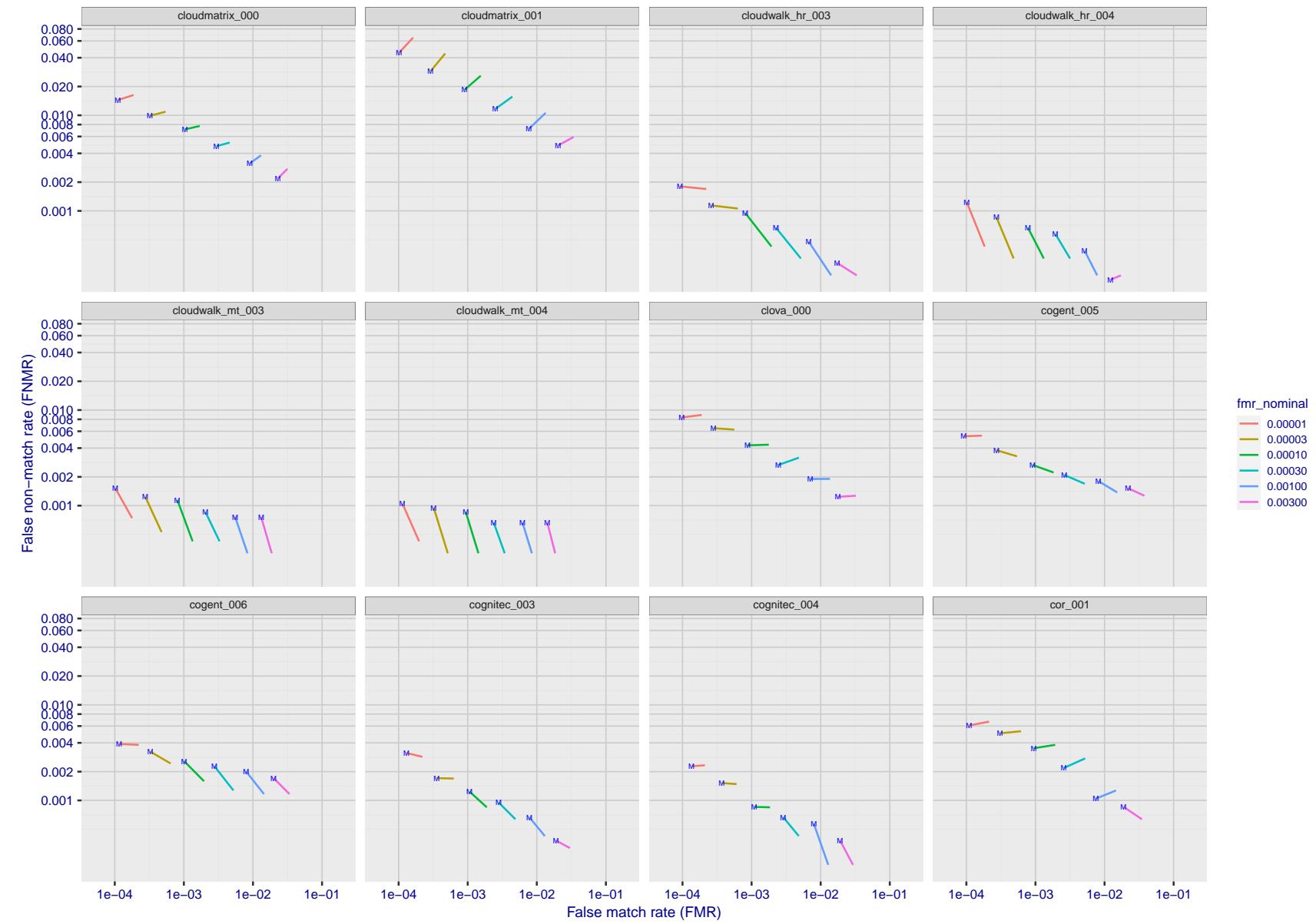


Figure 146: For the visa images, FNMR and FMR at six operating points along the DET characteristic. At each point a line is drawn between $(FMR, FNMR)_{MALE}$ and $(FMR, FNMR)_{FEMALE}$ showing how which sex has lower FMR and/or FNMR. The "M" label denotes male, the other end of the line corresponds to female. The six operating thresholds are selected to give the nominal false match rates given in the legend, and are computed over all impostor pairs regardless of age, sex, and place of birth. The plotted FMR values are broadly an order of magnitude larger than the nominal rates because FMR is computed over demographically-matched impostor pairs i.e individuals of the same sex, from the same geographic region (see section 3.6.1), and the same age group (see section 3.6.2).

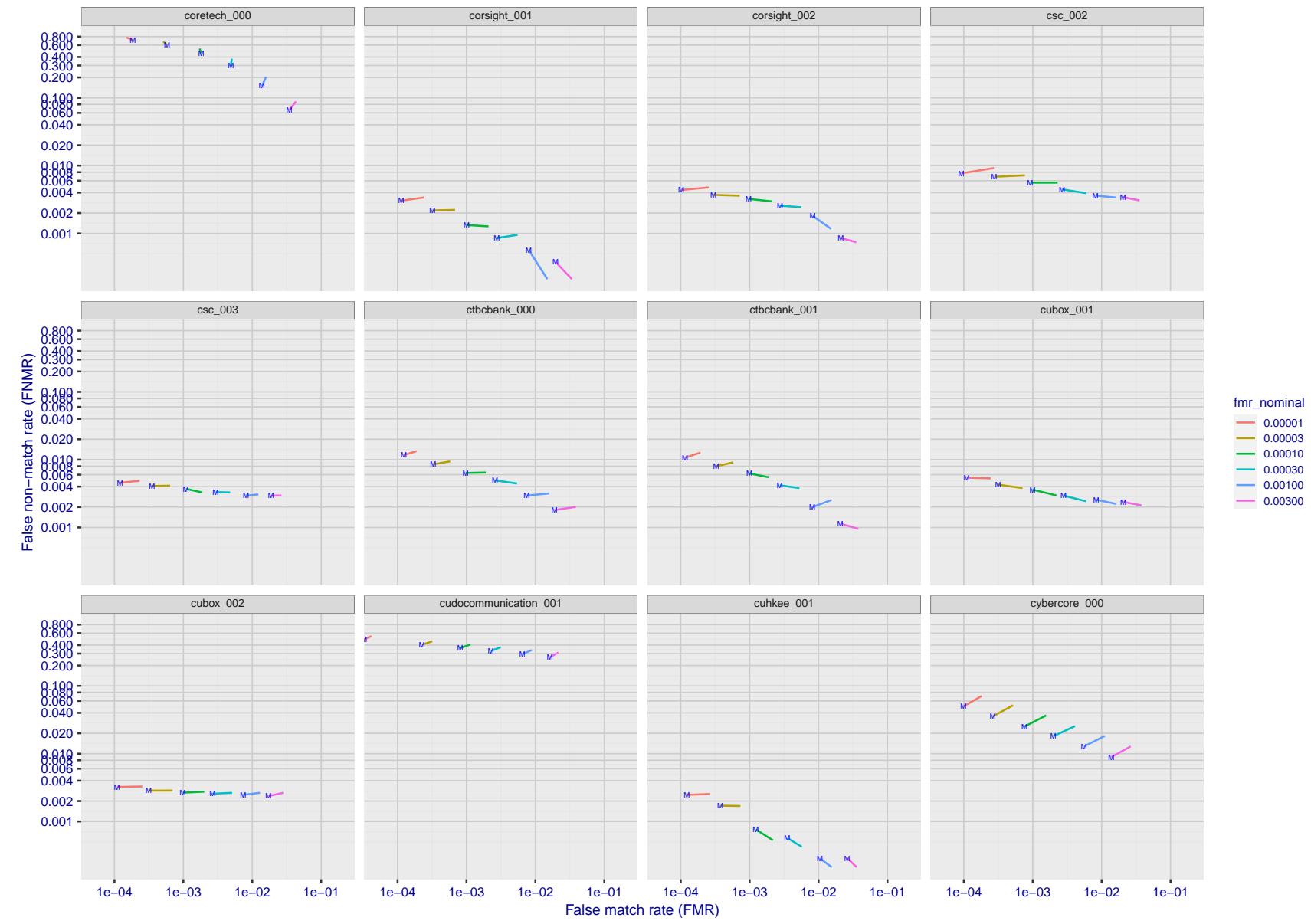


Figure 147: For the visa images, FNMR and FMR at six operating points along the DET characteristic. At each point a line is drawn between $(FMR, FNMR)_{MALE}$ and $(FMR, FNMR)_{FEMALE}$ showing how which sex has lower FMR and/or FNMR. The "M" label denotes male, the other end of the line corresponds to female. The six operating thresholds are selected to give the nominal false match rates given in the legend, and are computed over all impostor pairs regardless of age, sex, and place of birth. The plotted FMR values are broadly an order of magnitude larger than the nominal rates because FMR is computed over demographically-matched impostor pairs i.e individuals of the same sex, from the same geographic region (see section 3.6.1), and the same age group (see section 3.6.2).

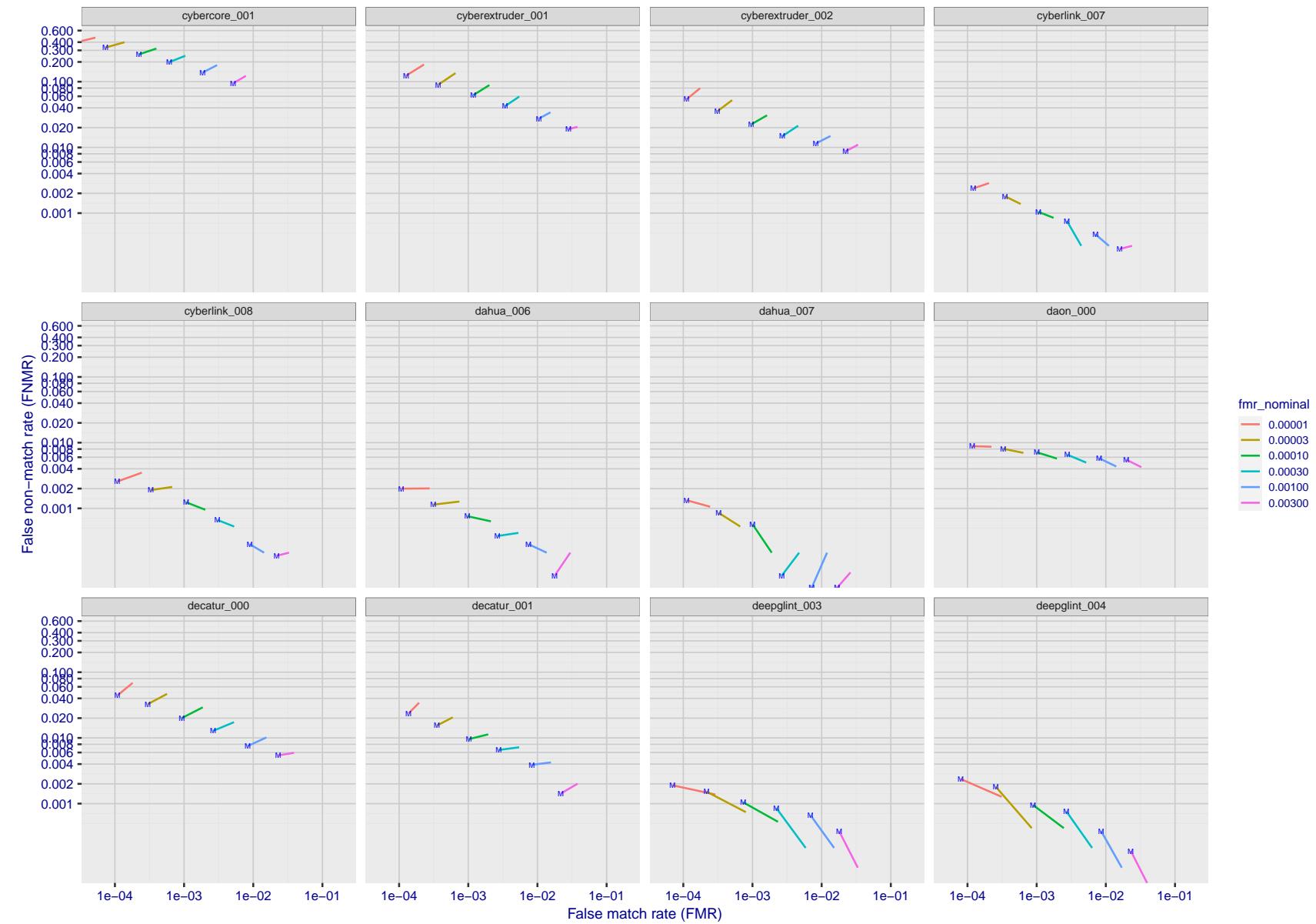


Figure 148: For the visa images, FNMR and FMR at six operating points along the DET characteristic. At each point a line is drawn between $(FMR, FNMR)_{MALE}$ and $(FMR, FNMR)_{FEMALE}$ showing how which sex has lower FMR and/or FNMR. The "M" label denotes male, the other end of the line corresponds to female. The six operating thresholds are selected to give the nominal false match rates given in the legend, and are computed over all impostor pairs regardless of age, sex, and place of birth. The plotted FMR values are broadly an order of magnitude larger than the nominal rates because FMR is computed over demographically-matched impostor pairs i.e individuals of the same sex, from the same geographic region (see section 3.6.1), and the same age group (see section 3.6.2).

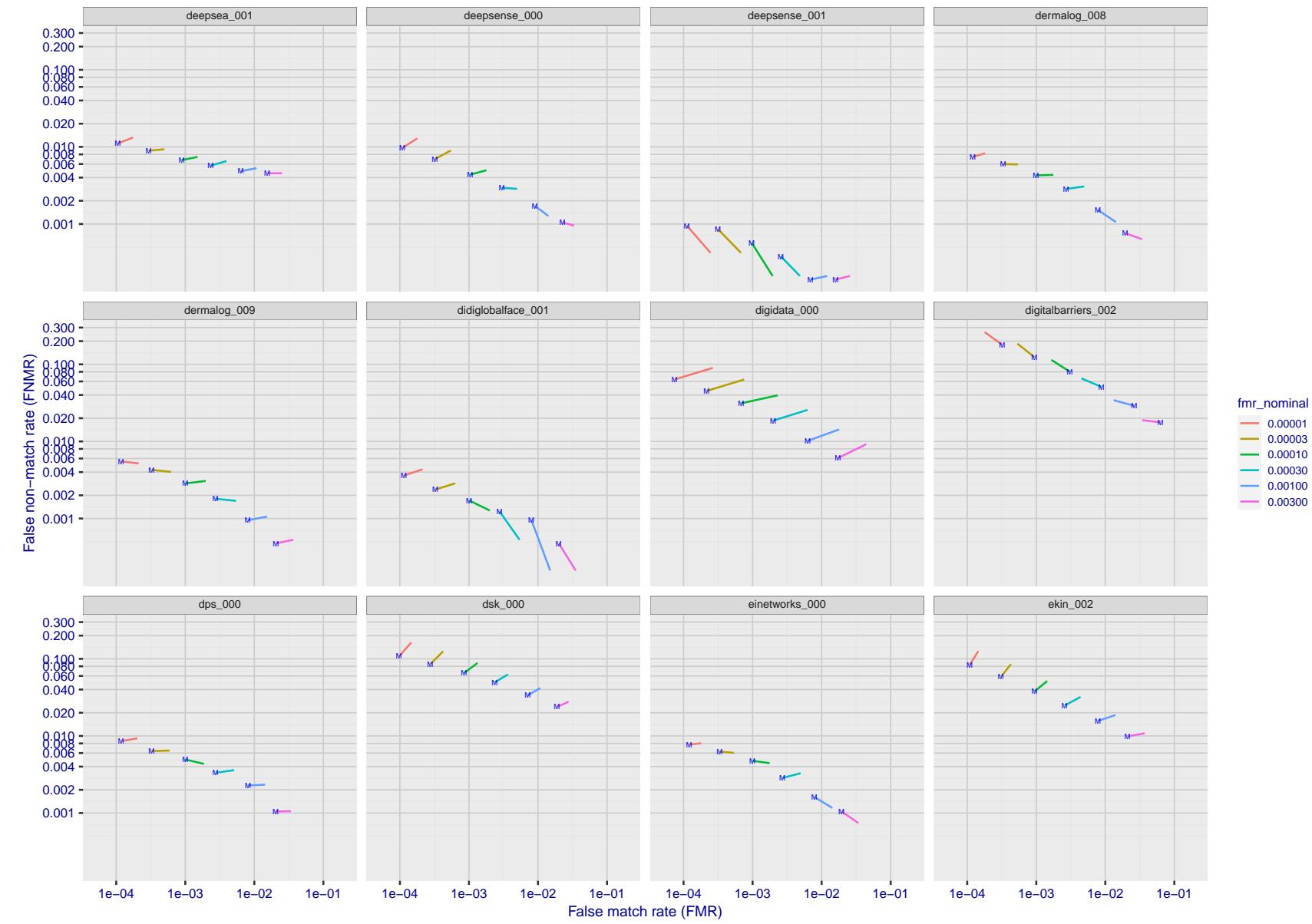


Figure 149: For the visa images, FNMR and FMR at six operating points along the DET characteristic. At each point a line is drawn between $(FMR, FNMR)_{MALE}$ and $(FMR, FNMR)_{FEMALE}$ showing how which sex has lower FMR and/or FNMR. The "M" label denotes male, the other end of the line corresponds to female. The six operating thresholds are selected to give the nominal false match rates given in the legend, and are computed over all impostor pairs regardless of age, sex, and place of birth. The plotted FMR values are broadly an order of magnitude larger than the nominal rates because FMR is computed over demographically-matched impostor pairs i.e individuals of the same sex, from the same geographic region (see section 3.6.1), and the same age group (see section 3.6.2).

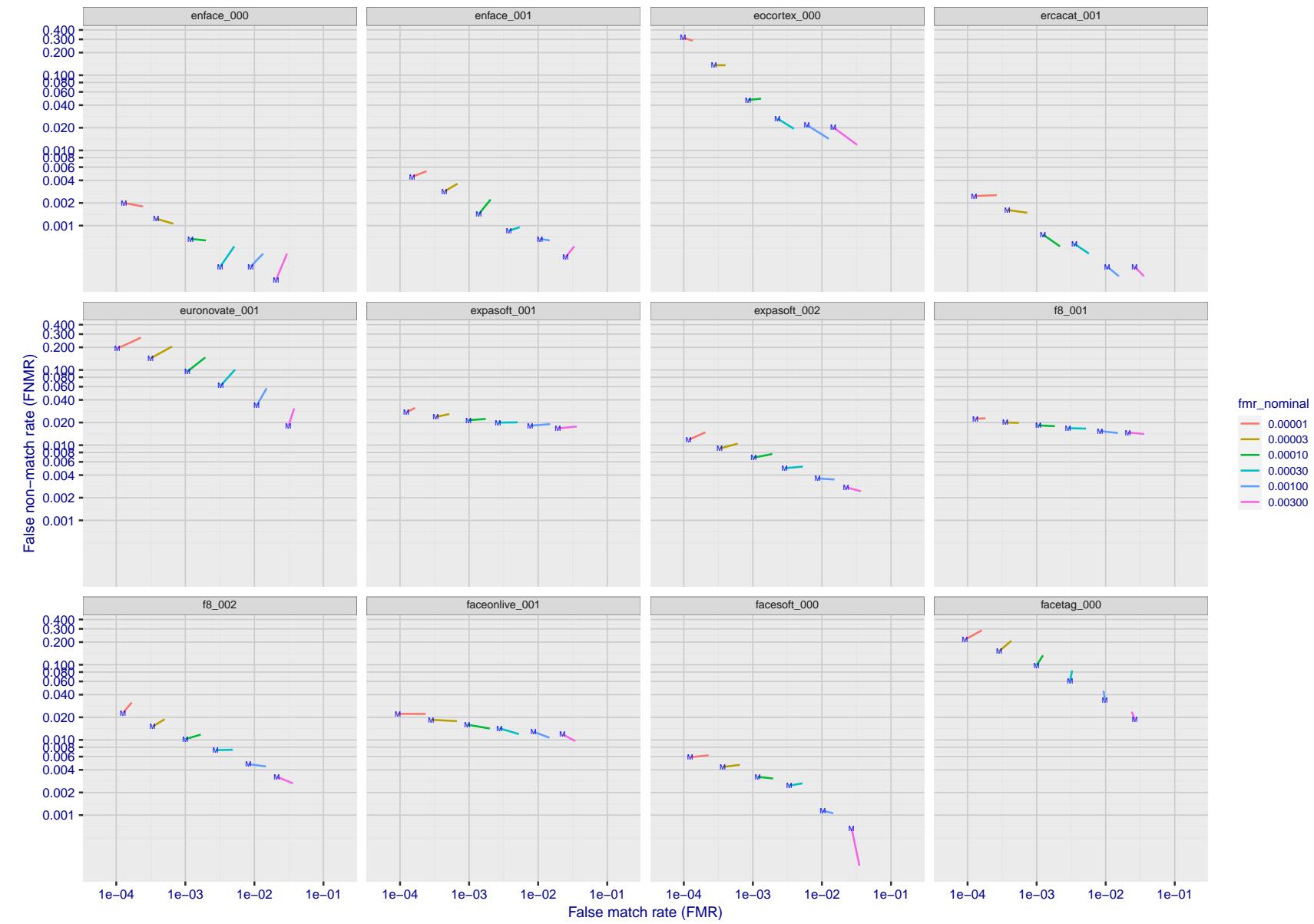


Figure 150: For the visa images, FNMR and FMR at six operating points along the DET characteristic. At each point a line is drawn between $(FMR, FNMR)_{MALE}$ and $(FMR, FNMR)_{FEMALE}$ showing how which sex has lower FMR and/or FNMR. The "M" label denotes male, the other end of the line corresponds to female. The six operating thresholds are selected to give the nominal false match rates given in the legend, and are computed over all impostor pairs regardless of age, sex, and place of birth. The plotted FMR values are broadly an order of magnitude larger than the nominal rates because FMR is computed over demographically-matched impostor pairs i.e individuals of the same sex, from the same geographic region (see section 3.6.1), and the same age group (see section 3.6.2).

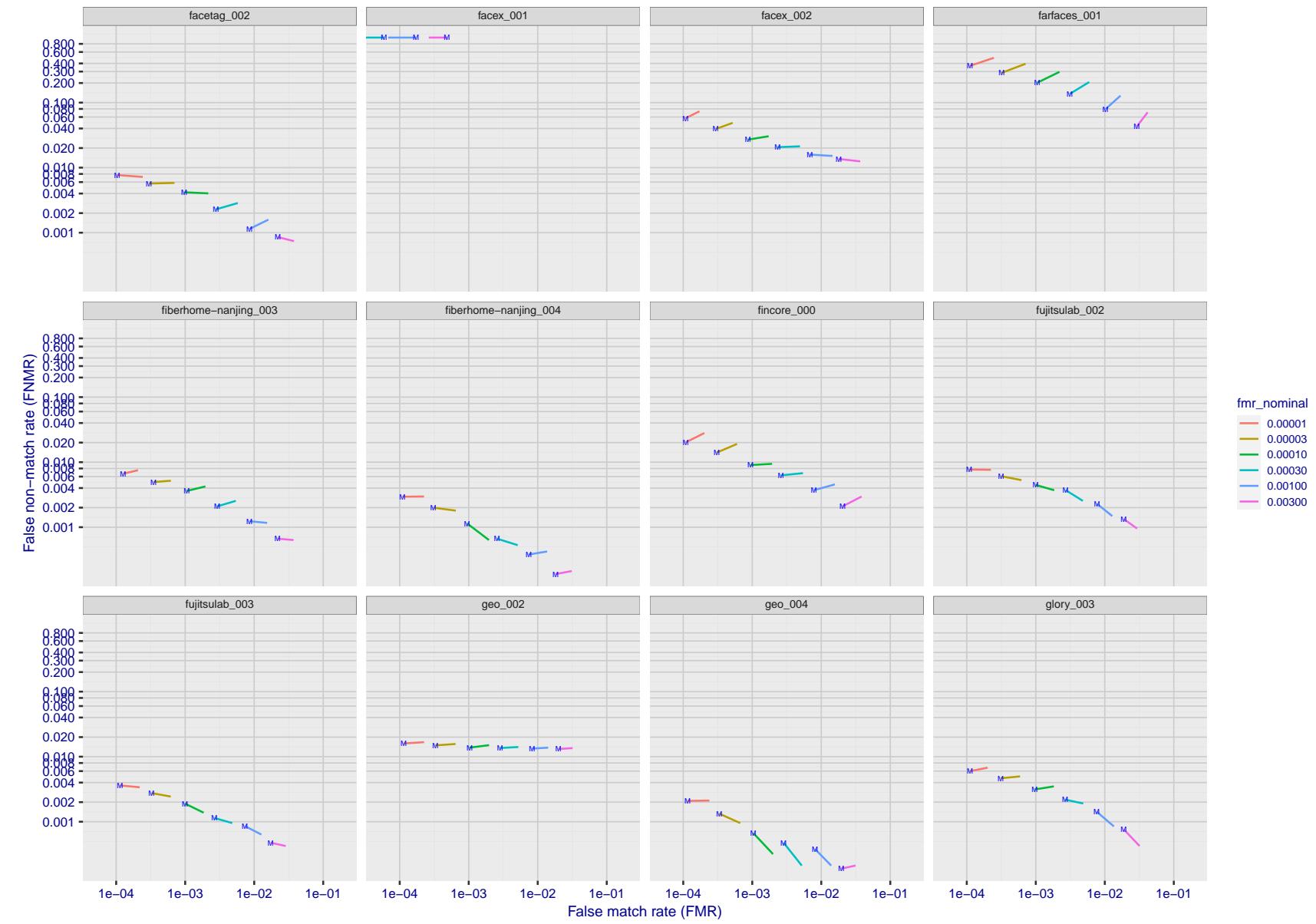


Figure 151: For the visa images, FNMR and FMR at six operating points along the DET characteristic. At each point a line is drawn between $(FMR, FNMR)_{MALE}$ and $(FMR, FNMR)_{FEMALE}$ showing how which sex has lower FMR and/or FNMR. The "M" label denotes male, the other end of the line corresponds to female. The six operating thresholds are selected to give the nominal false match rates given in the legend, and are computed over all impostor pairs regardless of age, sex, and place of birth. The plotted FMR values are broadly an order of magnitude larger than the nominal rates because FMR is computed over demographically-matched impostor pairs i.e individuals of the same sex, from the same geographic region (see section 3.6.1), and the same age group (see section 3.6.2).

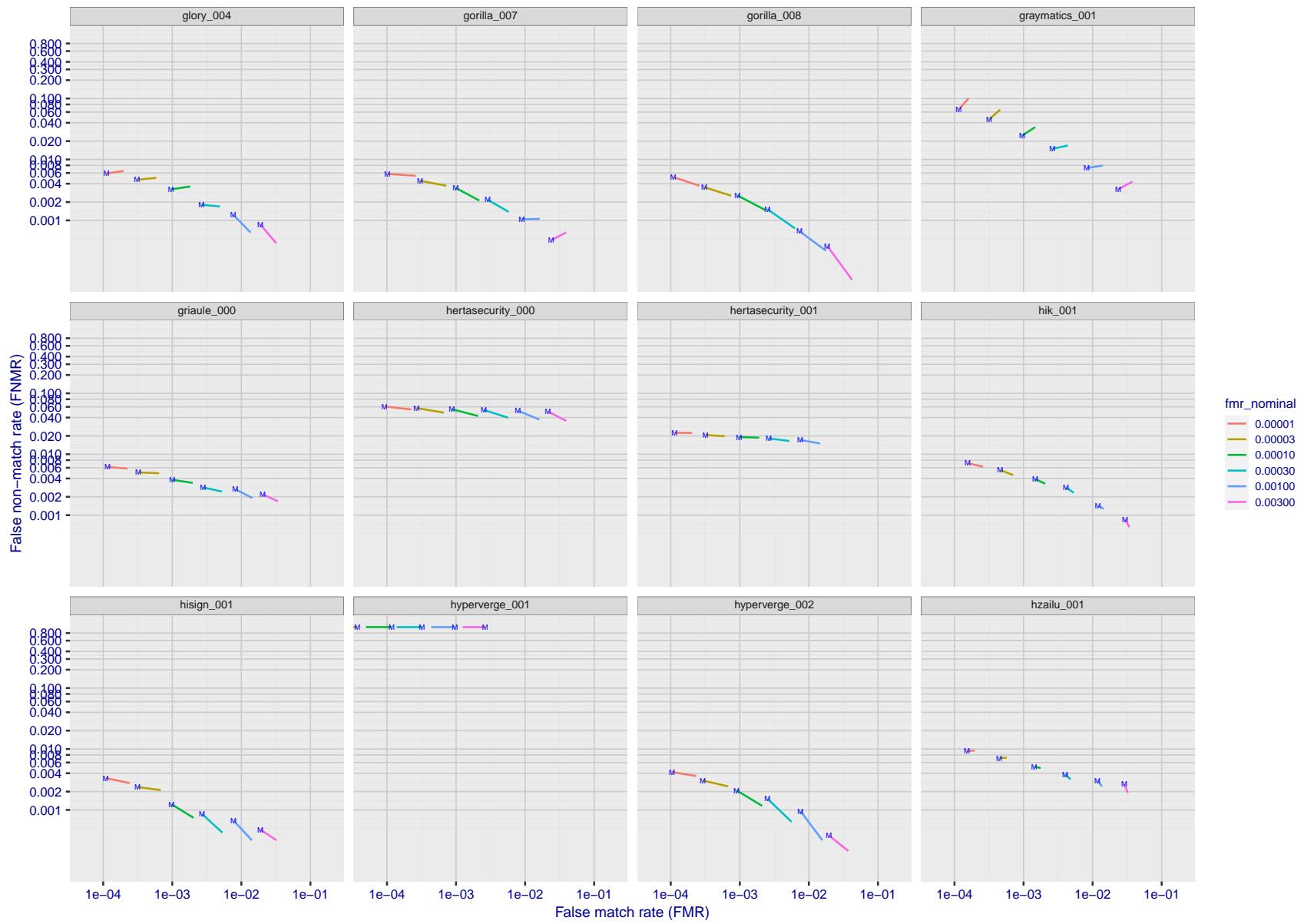


Figure 152: For the visa images, FNMR and FMR at six operating points along the DET characteristic. At each point a line is drawn between $(FMR, FNMR)_{MALE}$ and $(FMR, FNMR)_{FEMALE}$ showing how which sex has lower FMR and/or FNMR. The "M" label denotes male, the other end of the line corresponds to female. The six operating thresholds are selected to give the nominal false match rates given in the legend, and are computed over all impostor pairs regardless of age, sex, and place of birth. The plotted FMR values are broadly an order of magnitude larger than the nominal rates because FMR is computed over demographically-matched impostor pairs i.e individuals of the same sex, from the same geographic region (see section 3.6.1), and the same age group (see section 3.6.2).

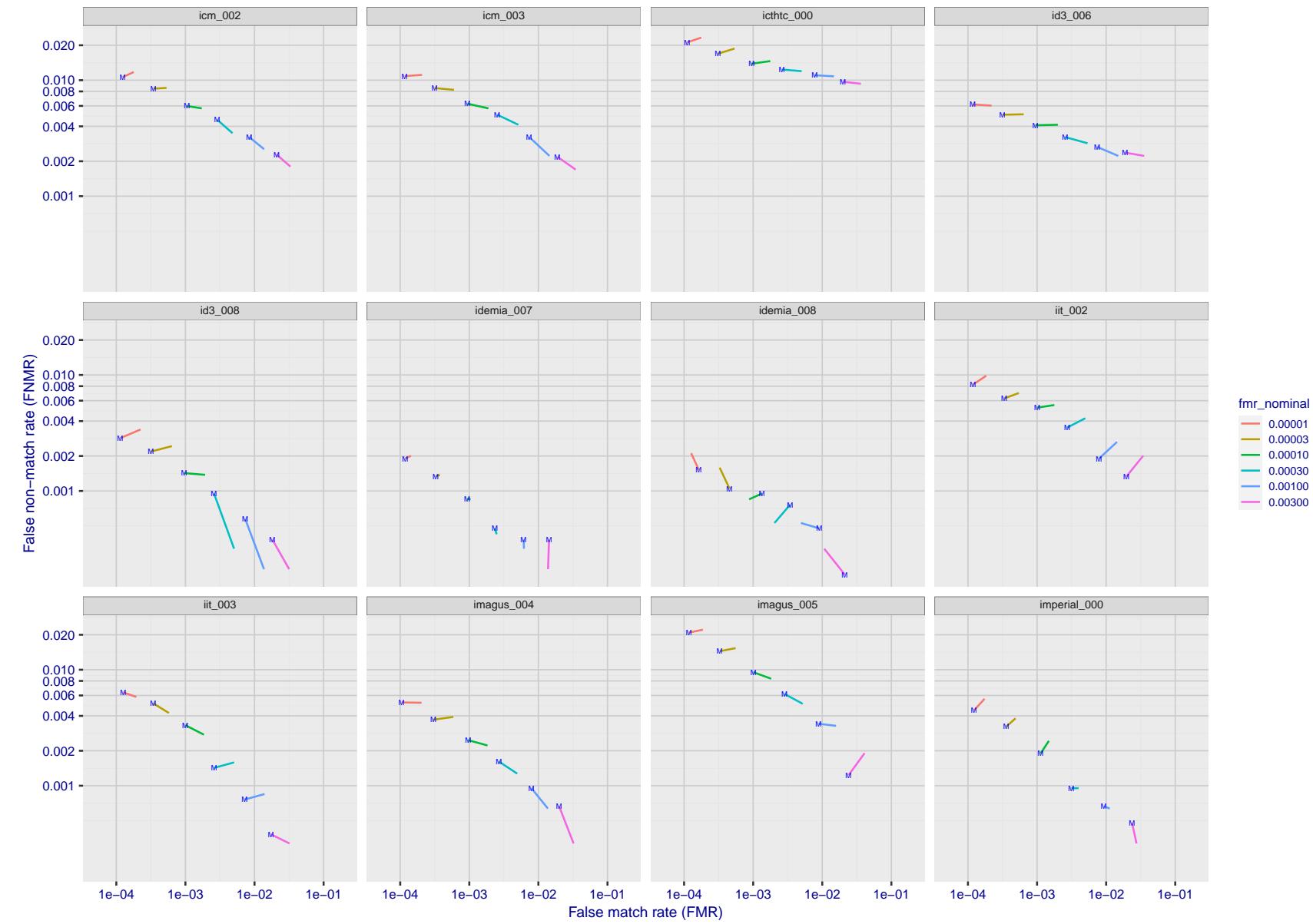


Figure 153: For the visa images, FNMR and FMR at six operating points along the DET characteristic. At each point a line is drawn between $(FMR, FNMR)_{MALE}$ and $(FMR, FNMR)_{FEMALE}$ showing how which sex has lower FMR and/or FNMR. The "M" label denotes male, the other end of the line corresponds to female. The six operating thresholds are selected to give the nominal false match rates given in the legend, and are computed over all impostor pairs regardless of age, sex, and place of birth. The plotted FMR values are broadly an order of magnitude larger than the nominal rates because FMR is computed over demographically-matched impostor pairs i.e individuals of the same sex, from the same geographic region (see section 3.6.1), and the same age group (see section 3.6.2).

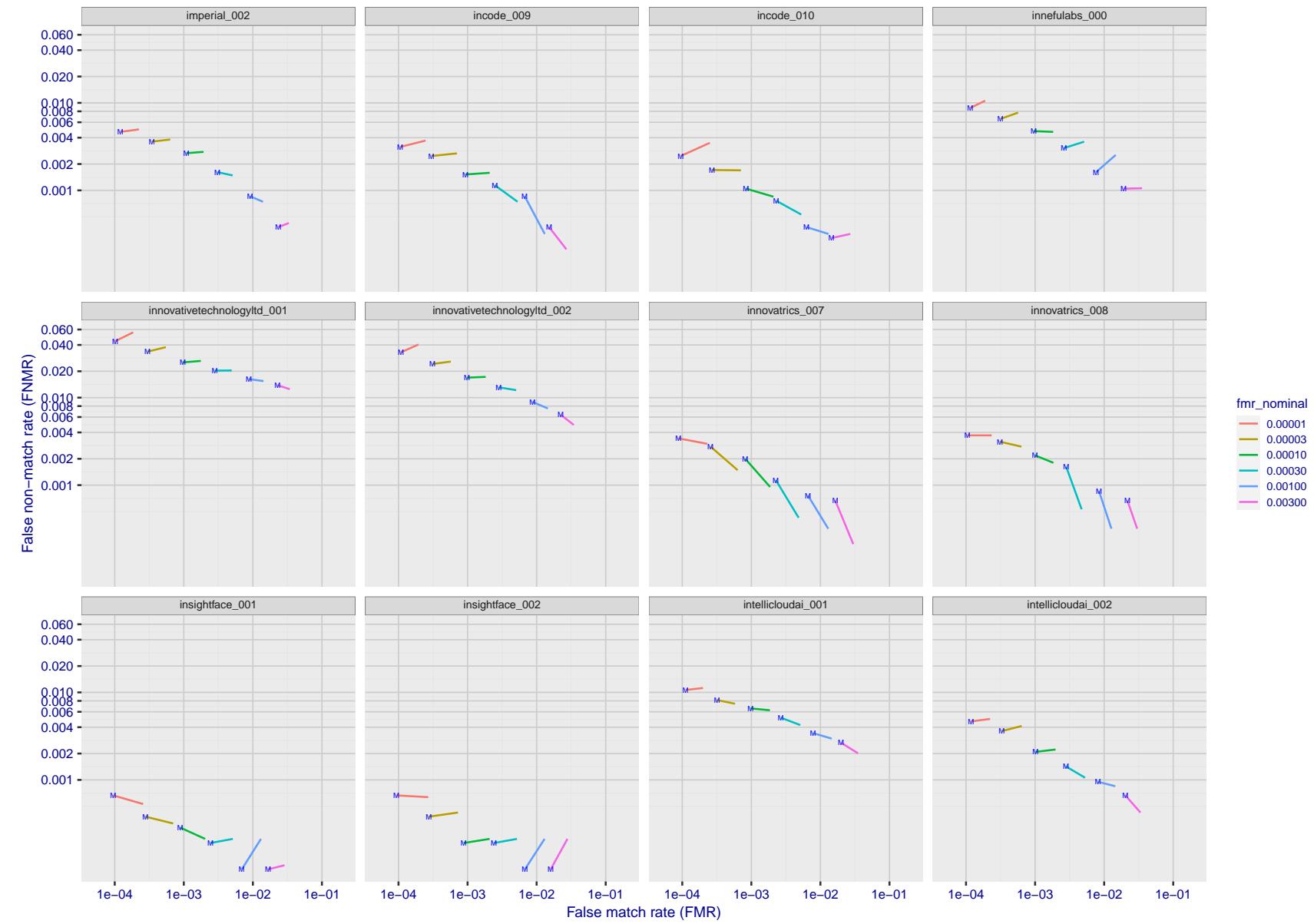


Figure 154: For the visa images, FNMR and FMR at six operating points along the DET characteristic. At each point a line is drawn between $(FMR, FNMR)_{MALE}$ and $(FMR, FNMR)_{FEMALE}$ showing how which sex has lower FMR and/or FNMR. The "M" label denotes male, the other end of the line corresponds to female. The six operating thresholds are selected to give the nominal false match rates given in the legend, and are computed over all impostor pairs regardless of age, sex, and place of birth. The plotted FMR values are broadly an order of magnitude larger than the nominal rates because FMR is computed over demographically-matched impostor pairs i.e individuals of the same sex, from the same geographic region (see section 3.6.1), and the same age group (see section 3.6.2).

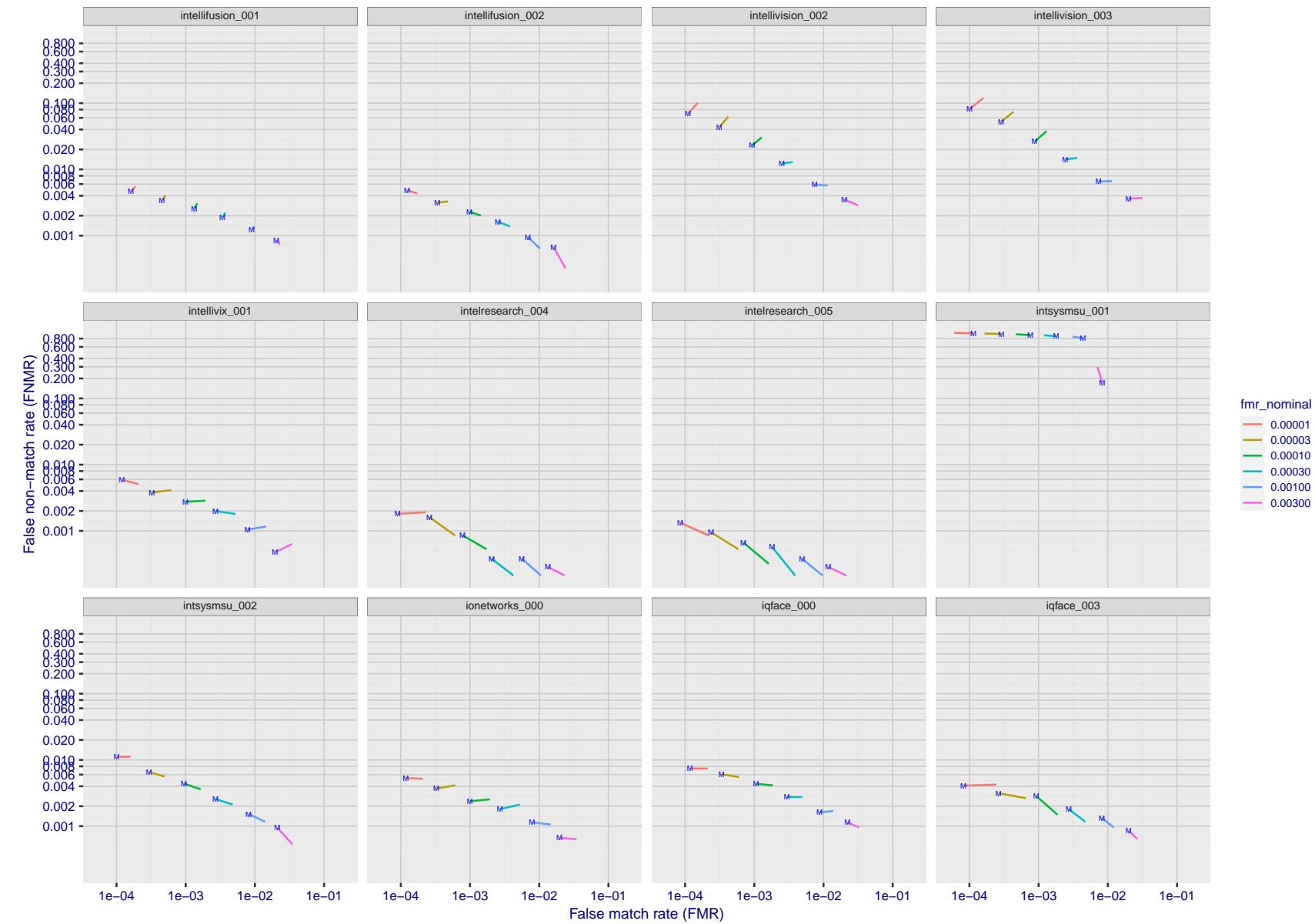


Figure 155: For the visa images, FNMR and FMR at six operating points along the DET characteristic. At each point a line is drawn between $(FMR, FNMR)_{MALE}$ and $(FMR, FNMR)_{FEMALE}$ showing how which sex has lower FMR and/or FNMR. The "M" label denotes male, the other end of the line corresponds to female. The six operating thresholds are selected to give the nominal false match rates given in the legend, and are computed over all impostor pairs regardless of age, sex, and place of birth. The plotted FMR values are broadly an order of magnitude larger than the nominal rates because FMR is computed over demographically-matched impostor pairs i.e individuals of the same sex, from the same geographic region (see section 3.6.1), and the same age group (see section 3.6.2).

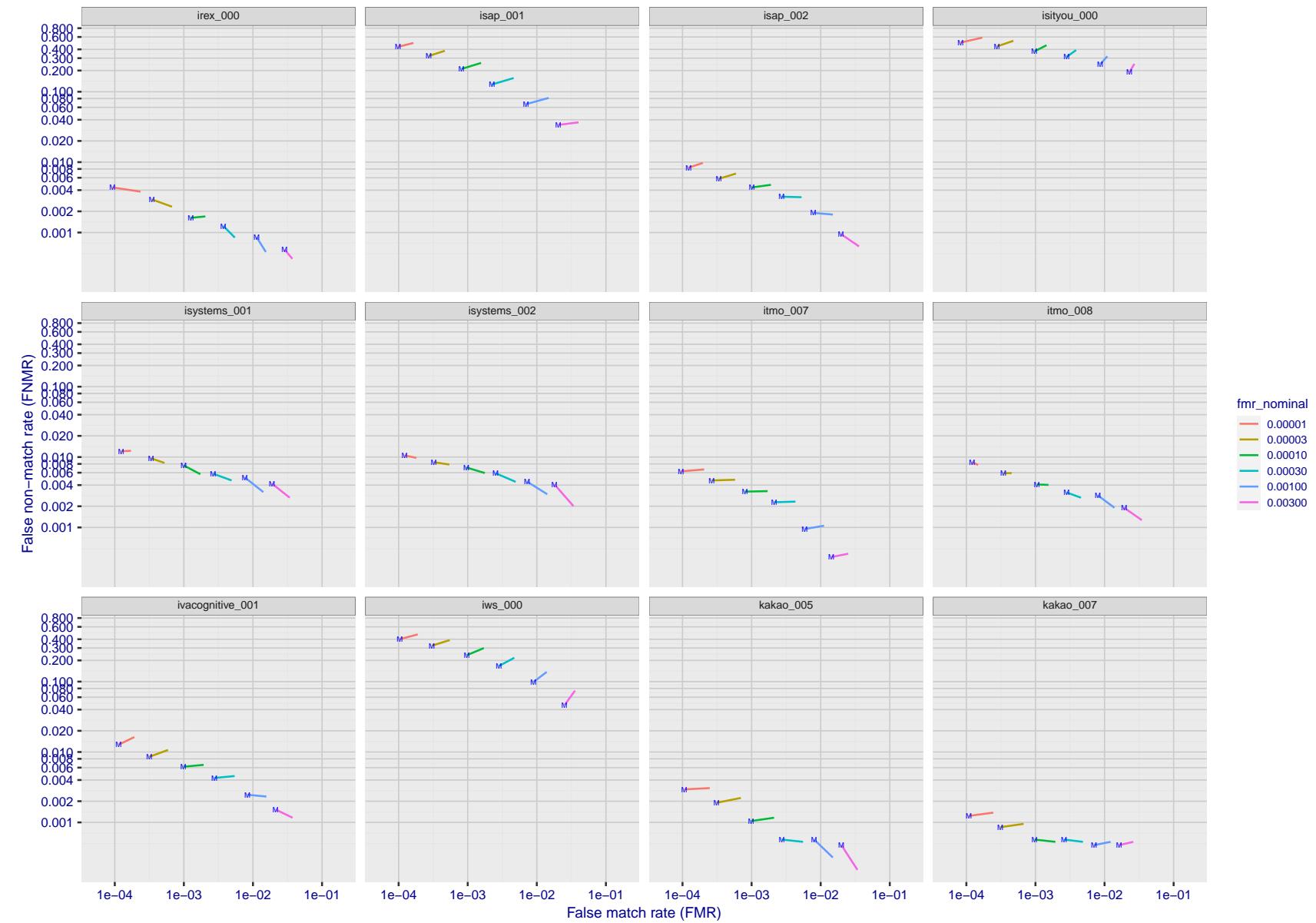


Figure 156: For the visa images, FNMR and FMR at six operating points along the DET characteristic. At each point a line is drawn between $(FMR, FNMR)_{MALE}$ and $(FMR, FNMR)_{FEMALE}$ showing how which sex has lower FMR and/or FNMR. The "M" label denotes male, the other end of the line corresponds to female. The six operating thresholds are selected to give the nominal false match rates given in the legend, and are computed over all impostor pairs regardless of age, sex, and place of birth. The plotted FMR values are broadly an order of magnitude larger than the nominal rates because FMR is computed over demographically-matched impostor pairs i.e individuals of the same sex, from the same geographic region (see section 3.6.1), and the same age group (see section 3.6.2).

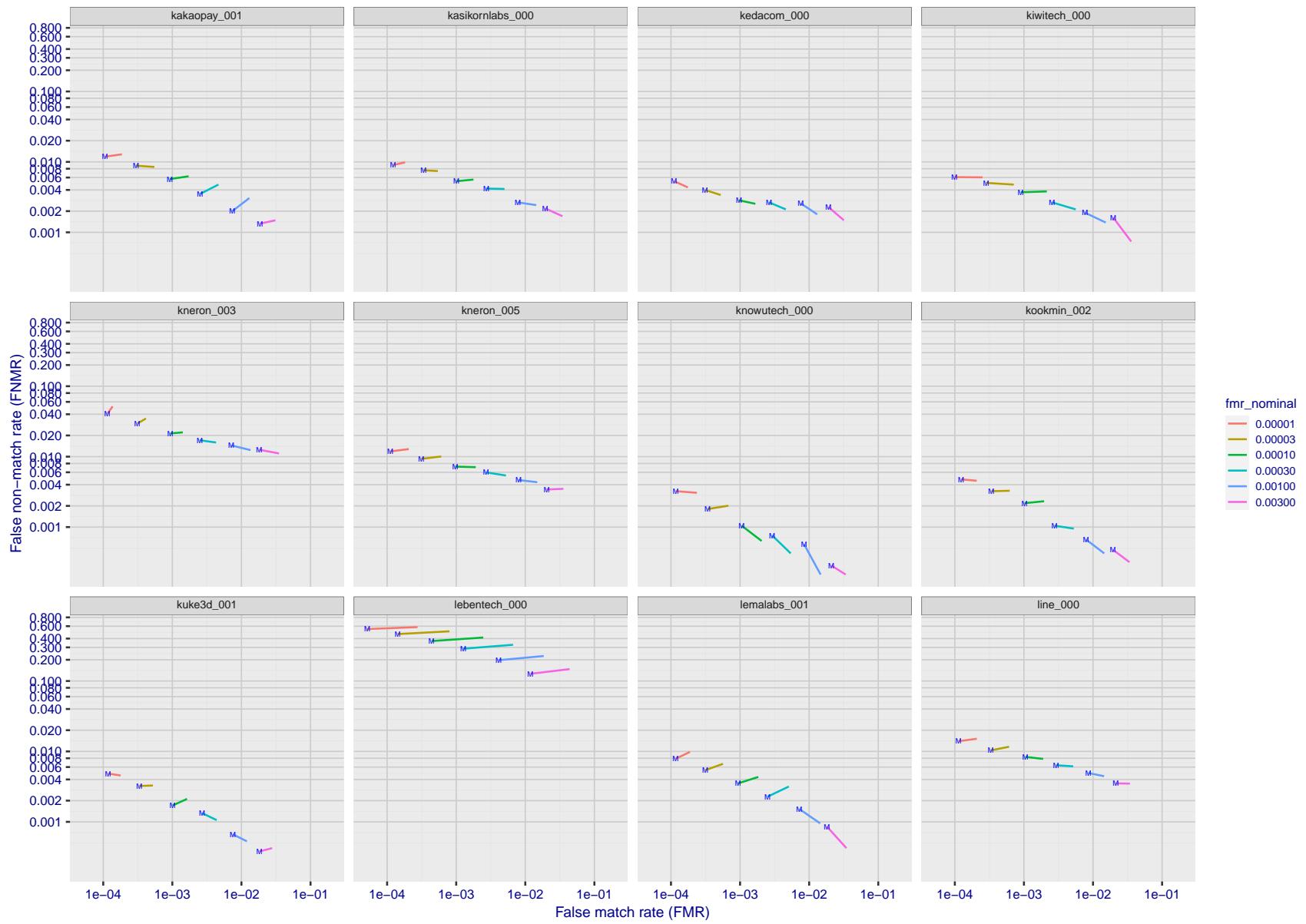


Figure 157: For the visa images, FNMR and FMR at six operating points along the DET characteristic. At each point a line is drawn between $(FMR, FNMR)_{MALE}$ and $(FMR, FNMR)_{FEMALE}$ showing how which sex has lower FMR and/or FNMR. The "M" label denotes male, the other end of the line corresponds to female. The six operating thresholds are selected to give the nominal false match rates given in the legend, and are computed over all impostor pairs regardless of age, sex, and place of birth. The plotted FMR values are broadly an order of magnitude larger than the nominal rates because FMR is computed over demographically-matched impostor pairs i.e individuals of the same sex, from the same geographic region (see section 3.6.1), and the same age group (see section 3.6.2).

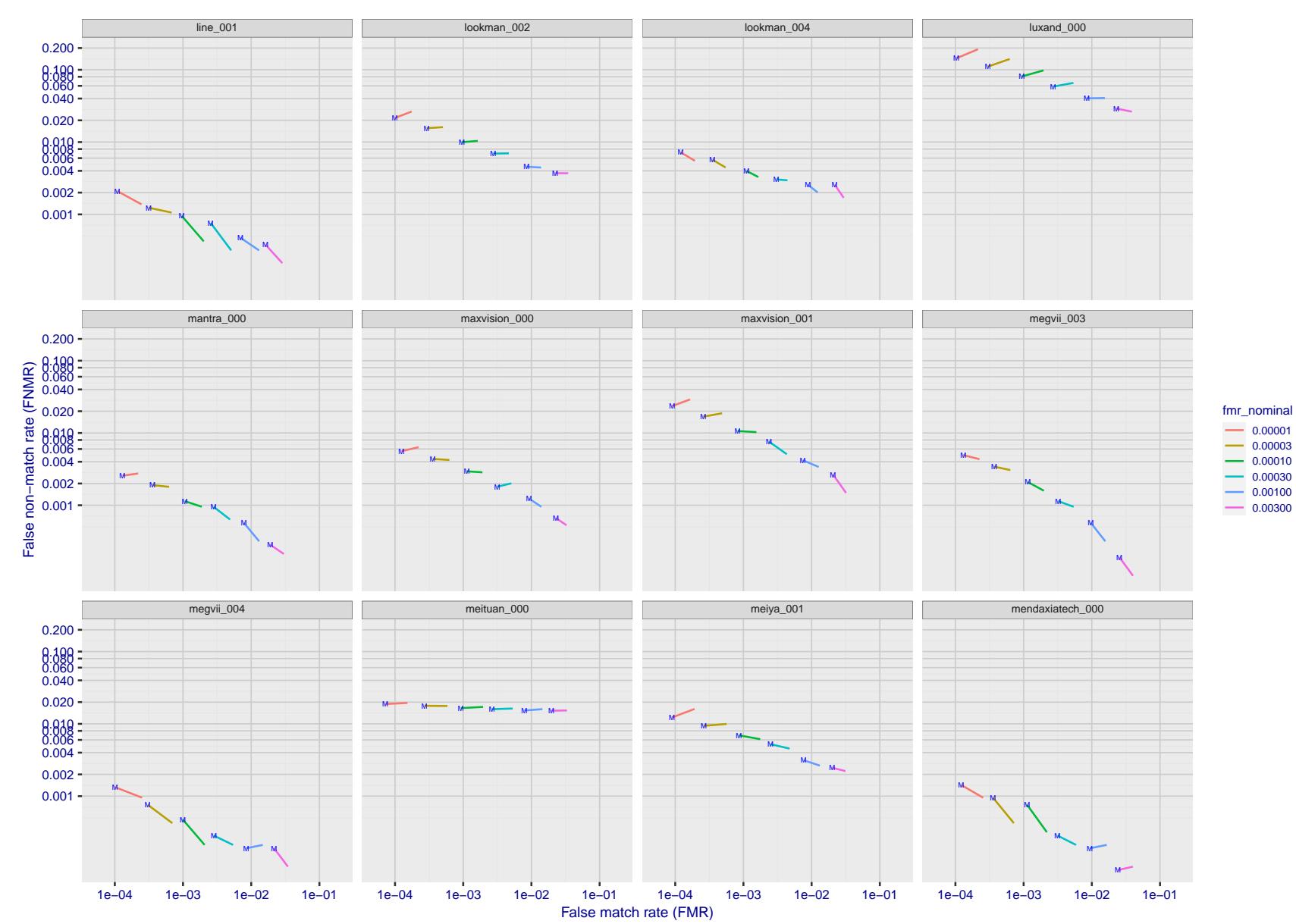


Figure 158: For the visa images, FNMR and FMR at six operating points along the DET characteristic. At each point a line is drawn between $(FMR, FNMR)_{MALE}$ and $(FMR, FNMR)_{FEMALE}$ showing how which sex has lower FMR and/or FNMR. The "M" label denotes male, the other end of the line corresponds to female. The six operating thresholds are selected to give the nominal false match rates given in the legend, and are computed over all impostor pairs regardless of age, sex, and place of birth. The plotted FMR values are broadly an order of magnitude larger than the nominal rates because FMR is computed over demographically-matched impostor pairs i.e individuals of the same sex, from the same geographic region (see section 3.6.1), and the same age group (see section 3.6.2).

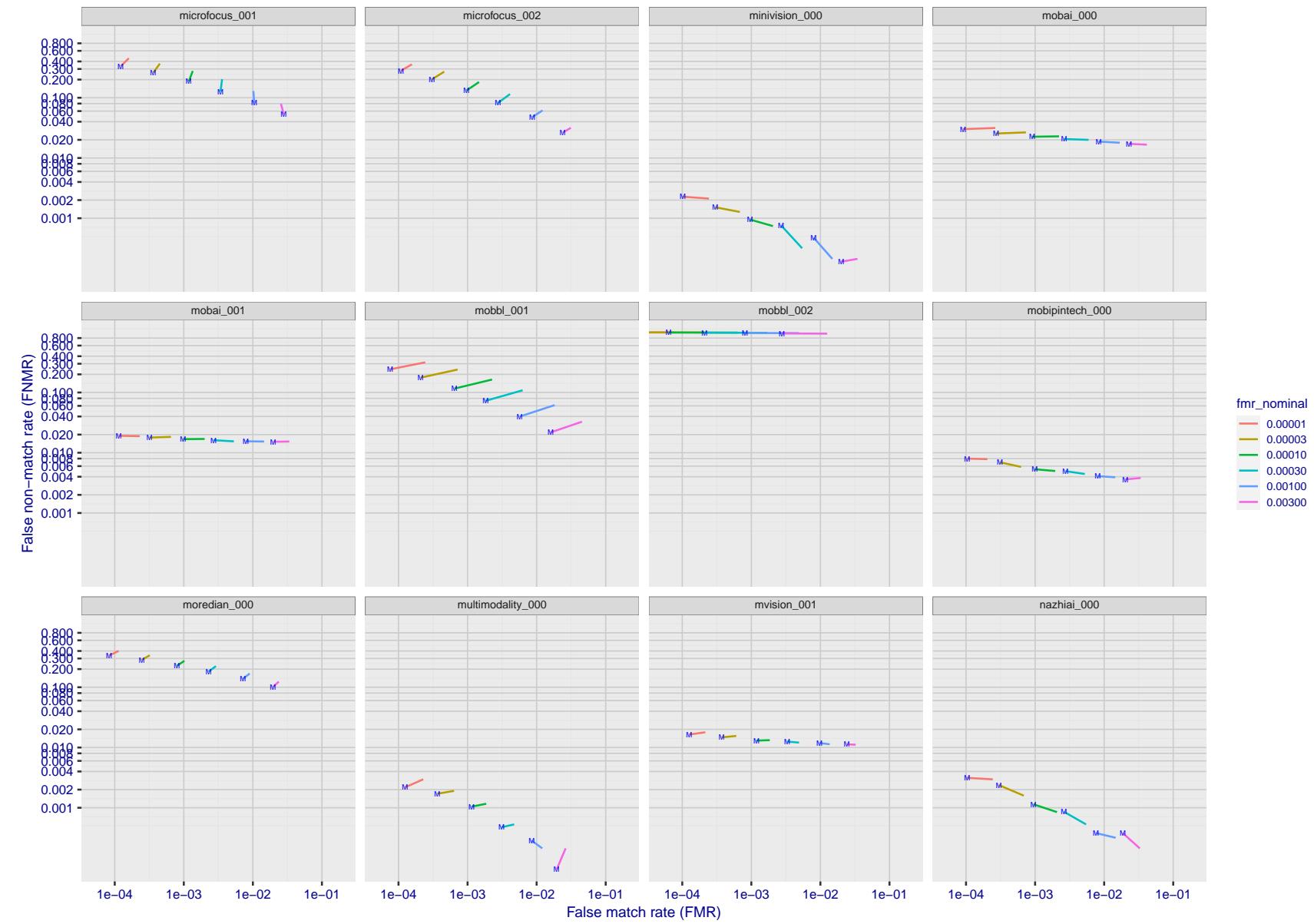


Figure 159: For the visa images, FNMR and FMR at six operating points along the DET characteristic. At each point a line is drawn between $(FMR, FNMR)_{MALE}$ and $(FMR, FNMR)_{FEMALE}$ showing how which sex has lower FMR and/or FNMR. The "M" label denotes male, the other end of the line corresponds to female. The six operating thresholds are selected to give the nominal false match rates given in the legend, and are computed over all impostor pairs regardless of age, sex, and place of birth. The plotted FMR values are broadly an order of magnitude larger than the nominal rates because FMR is computed over demographically-matched impostor pairs i.e individuals of the same sex, from the same geographic region (see section 3.6.1), and the same age group (see section 3.6.2).

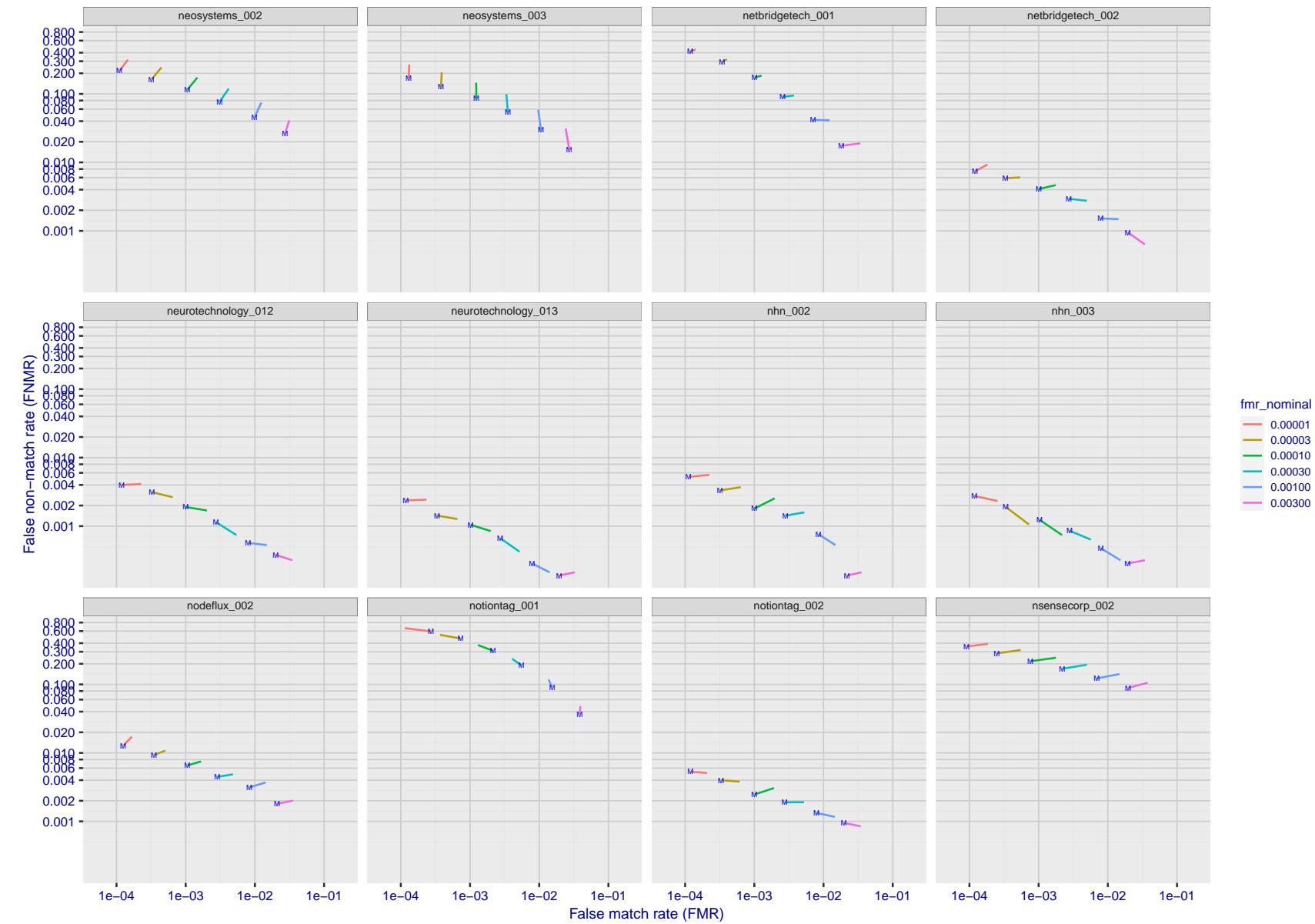


Figure 160: For the visa images, FNMR and FMR at six operating points along the DET characteristic. At each point a line is drawn between $(FMR, FNMR)_{MALE}$ and $(FMR, FNMR)_{FEMALE}$ showing how which sex has lower FMR and/or FNMR. The "M" label denotes male, the other end of the line corresponds to female. The six operating thresholds are selected to give the nominal false match rates given in the legend, and are computed over all impostor pairs regardless of age, sex, and place of birth. The plotted FMR values are broadly an order of magnitude larger than the nominal rates because FMR is computed over demographically-matched impostor pairs i.e individuals of the same sex, from the same geographic region (see section 3.6.1), and the same age group (see section 3.6.2).

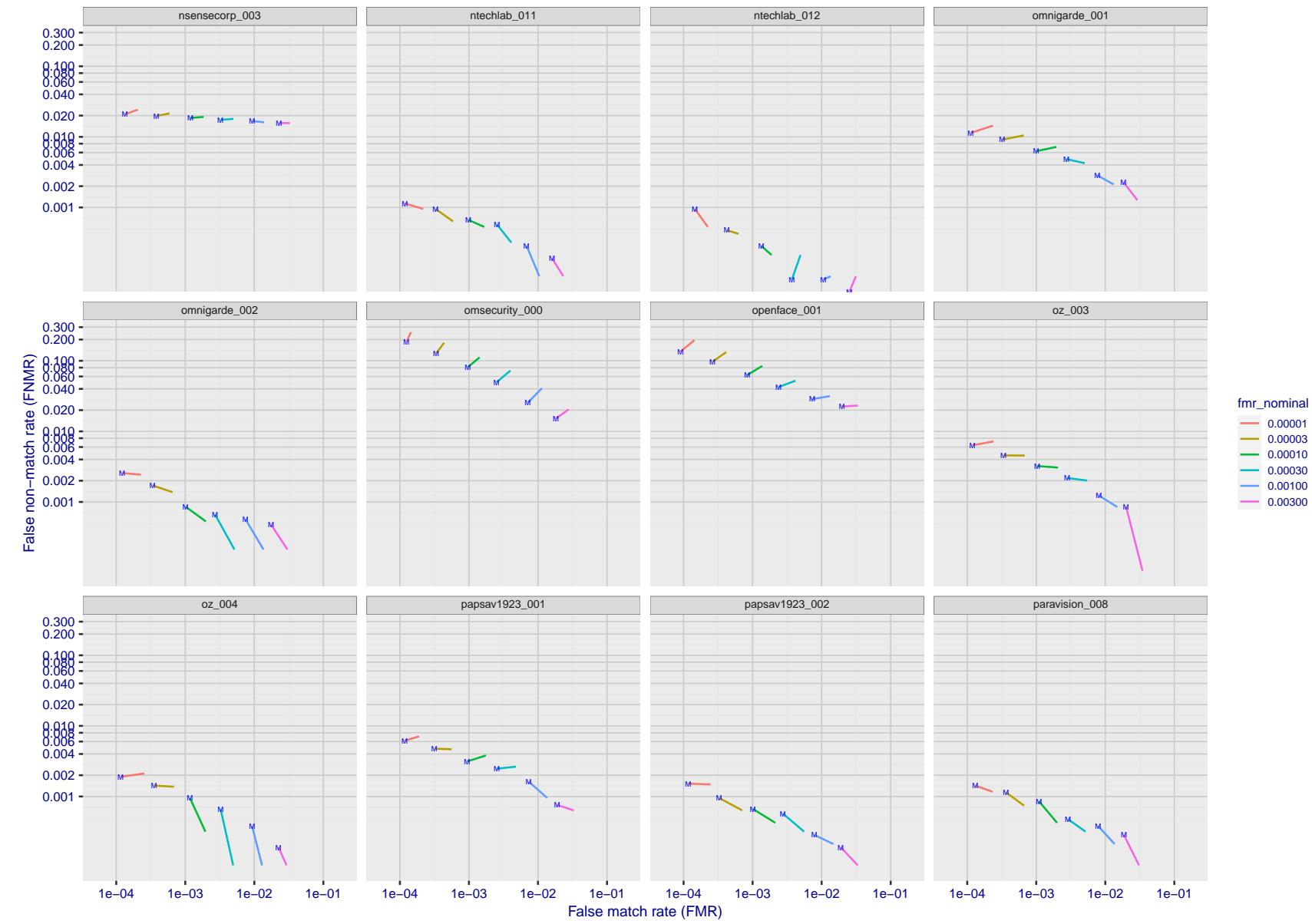


Figure 161: For the visa images, FNMR and FMR at six operating points along the DET characteristic. At each point a line is drawn between $(FMR, FNMR)_{MALE}$ and $(FMR, FNMR)_{FEMALE}$ showing how which sex has lower FMR and/or FNMR. The "M" label denotes male, the other end of the line corresponds to female. The six operating thresholds are selected to give the nominal false match rates given in the legend, and are computed over all impostor pairs regardless of age, sex, and place of birth. The plotted FMR values are broadly an order of magnitude larger than the nominal rates because FMR is computed over demographically-matched impostor pairs i.e individuals of the same sex, from the same geographic region (see section 3.6.1), and the same age group (see section 3.6.2).

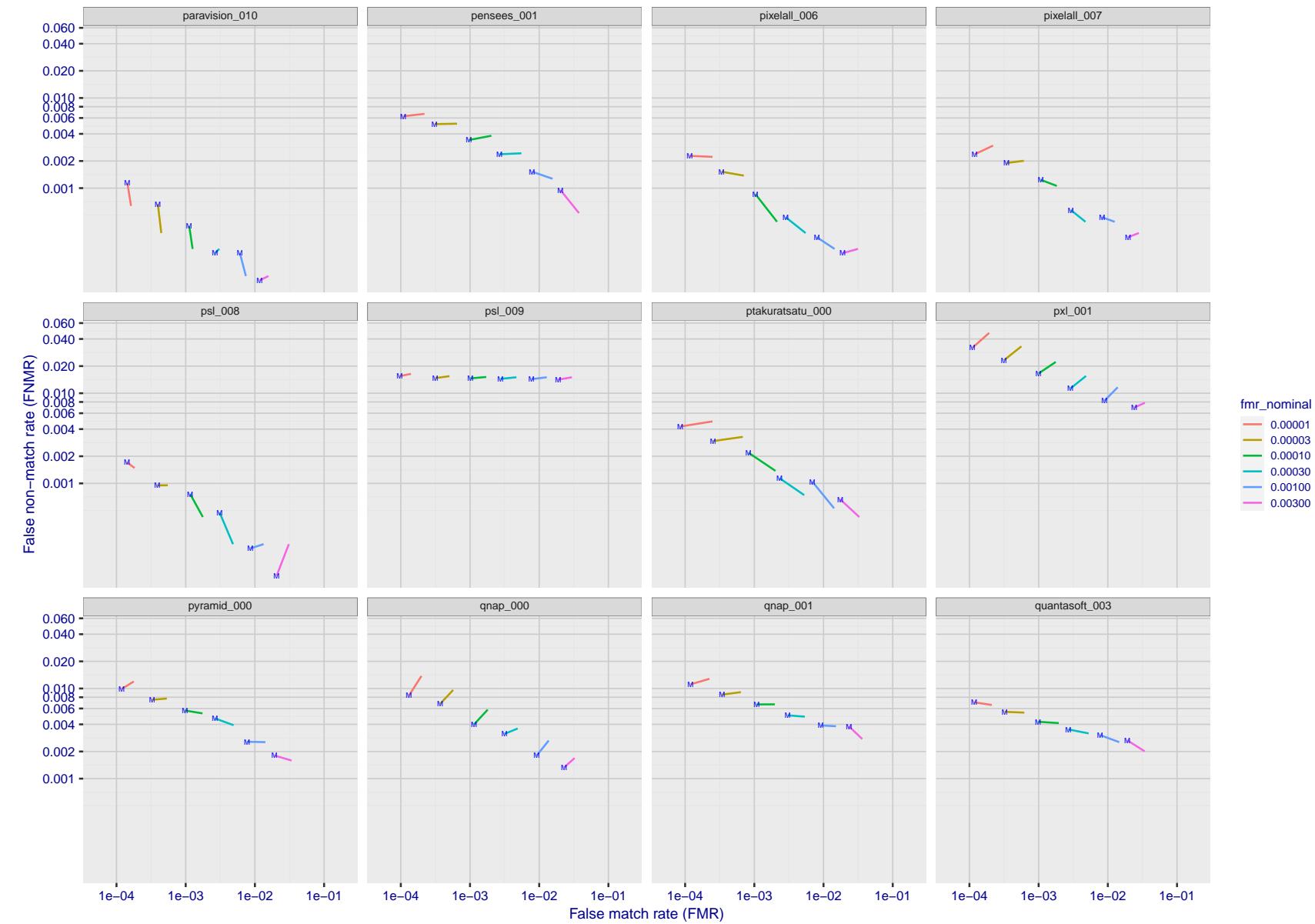


Figure 162: For the visa images, FNMR and FMR at six operating points along the DET characteristic. At each point a line is drawn between $(FMR, FNMR)_{MALE}$ and $(FMR, FNMR)_{FEMALE}$ showing how which sex has lower FMR and/or FNMR. The "M" label denotes male, the other end of the line corresponds to female. The six operating thresholds are selected to give the nominal false match rates given in the legend, and are computed over all impostor pairs regardless of age, sex, and place of birth. The plotted FMR values are broadly an order of magnitude larger than the nominal rates because FMR is computed over demographically-matched impostor pairs i.e individuals of the same sex, from the same geographic region (see section 3.6.1), and the same age group (see section 3.6.2).

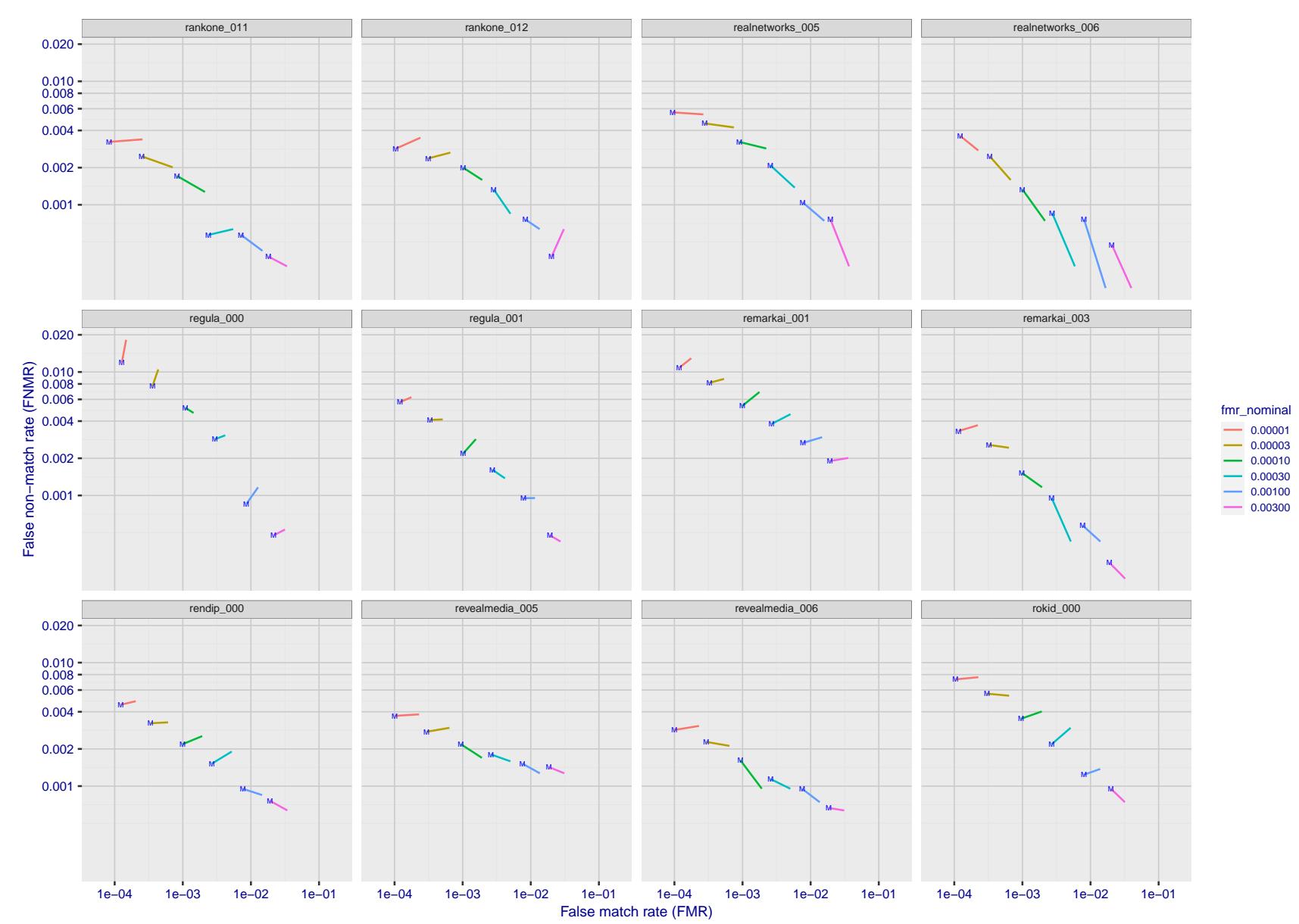


Figure 163: For the visa images, FNMR and FMR at six operating points along the DET characteristic. At each point a line is drawn between $(FMR, FNMR)_{MALE}$ and $(FMR, FNMR)_{FEMALE}$ showing how which sex has lower FMR and/or FNMR. The "M" label denotes male, the other end of the line corresponds to female. The six operating thresholds are selected to give the nominal false match rates given in the legend, and are computed over all impostor pairs regardless of age, sex, and place of birth. The plotted FMR values are broadly an order of magnitude larger than the nominal rates because FMR is computed over demographically-matched impostor pairs i.e individuals of the same sex, from the same geographic region (see section 3.6.1), and the same age group (see section 3.6.2).

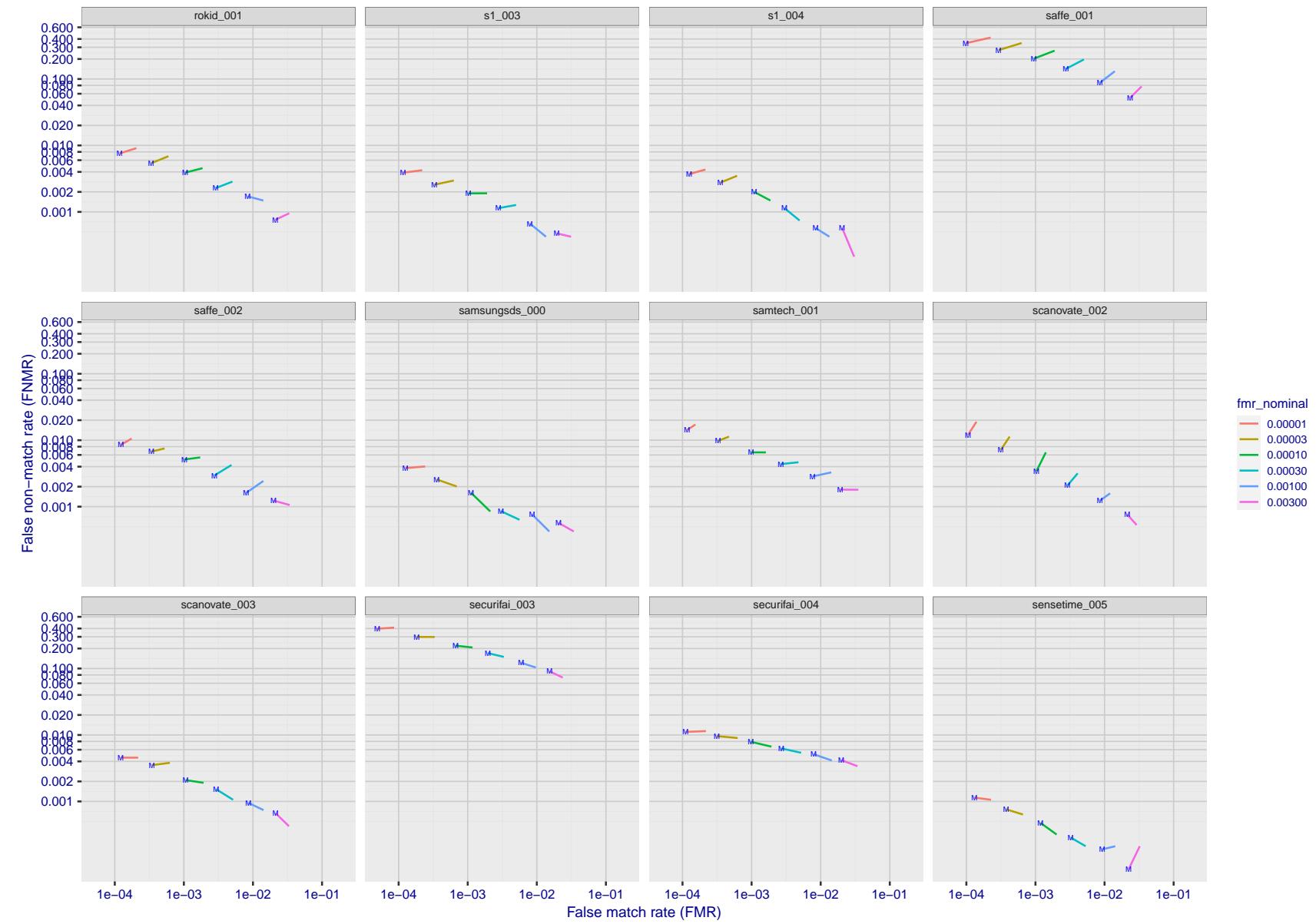


Figure 164: For the visa images, FNMR and FMR at six operating points along the DET characteristic. At each point a line is drawn between $(FMR, FNMR)_{MALE}$ and $(FMR, FNMR)_{FEMALE}$ showing how which sex has lower FMR and/or FNMR. The "M" label denotes male, the other end of the line corresponds to female. The six operating thresholds are selected to give the nominal false match rates given in the legend, and are computed over all impostor pairs regardless of age, sex, and place of birth. The plotted FMR values are broadly an order of magnitude larger than the nominal rates because FMR is computed over demographically-matched impostor pairs i.e individuals of the same sex, from the same geographic region (see section 3.6.1), and the same age group (see section 3.6.2).

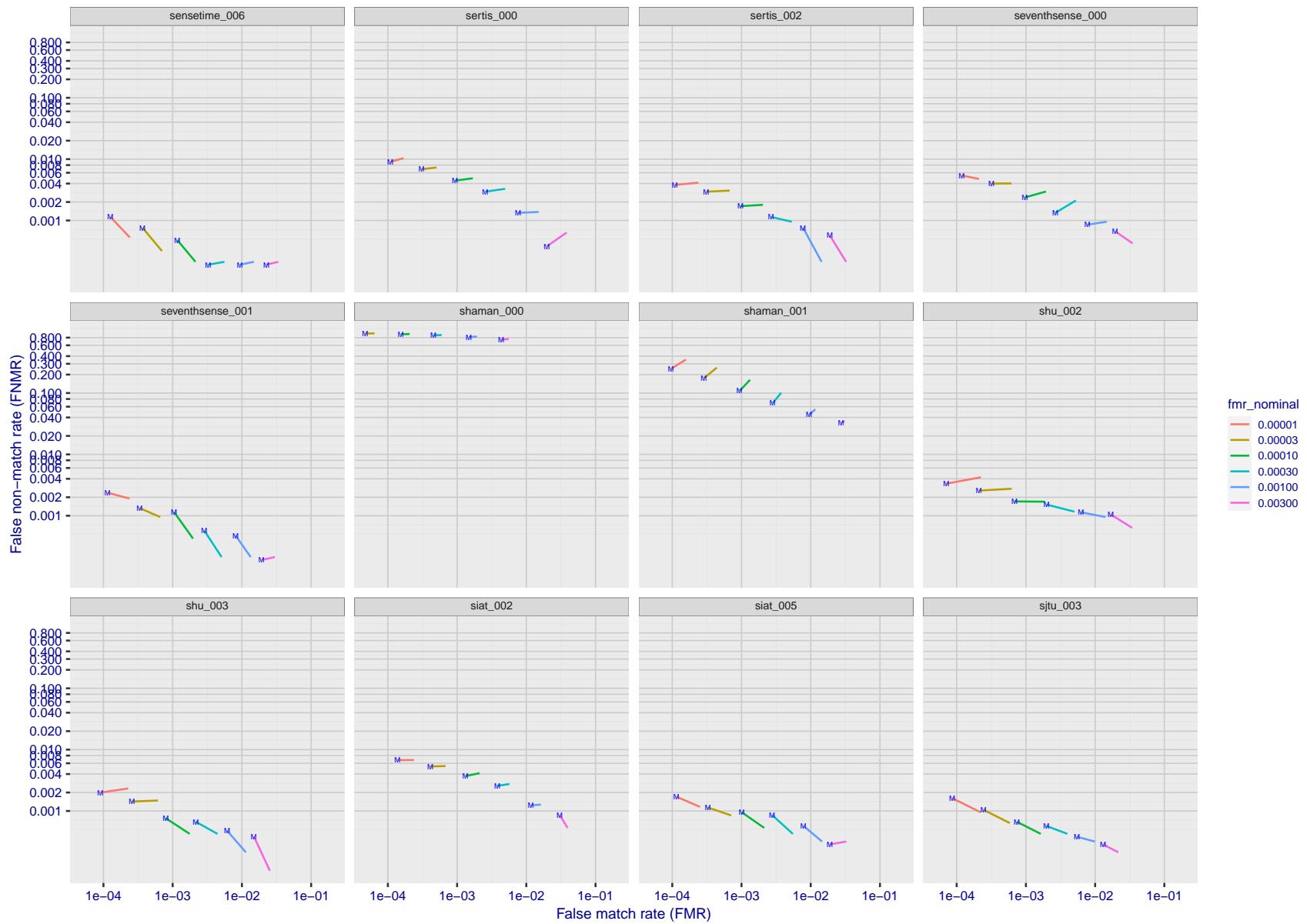


Figure 165: For the visa images, FNMR and FMR at six operating points along the DET characteristic. At each point a line is drawn between $(FMR, FNMR)_{MALE}$ and $(FMR, FNMR)_{FEMALE}$ showing how which sex has lower FMR and/or FNMR. The "M" label denotes male, the other end of the line corresponds to female. The six operating thresholds are selected to give the nominal false match rates given in the legend, and are computed over all impostor pairs regardless of age, sex, and place of birth. The plotted FMR values are broadly an order of magnitude larger than the nominal rates because FMR is computed over demographically-matched impostor pairs i.e individuals of the same sex, from the same geographic region (see section 3.6.1), and the same age group (see section 3.6.2).

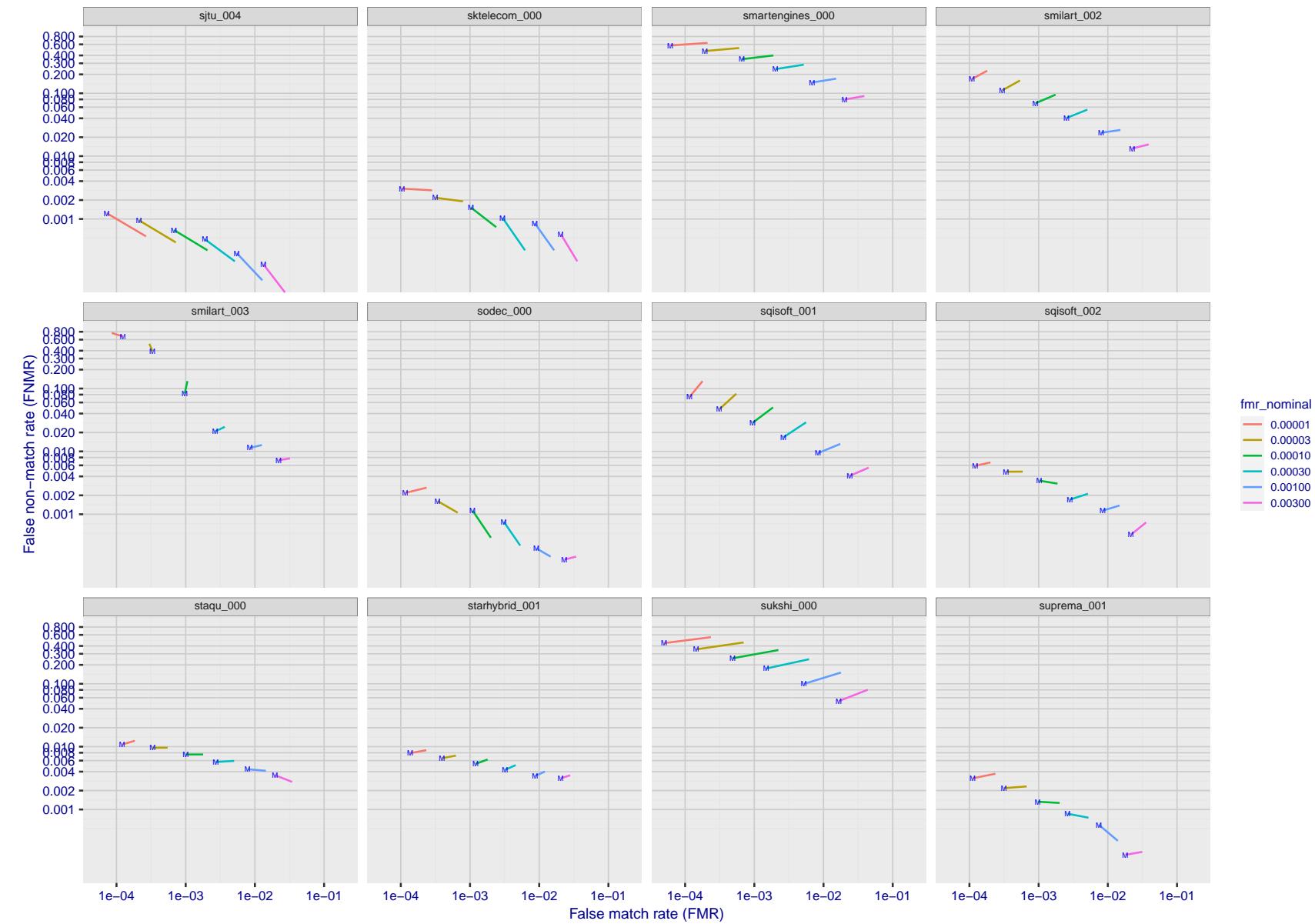


Figure 166: For the visa images, FNMR and FMR at six operating points along the DET characteristic. At each point a line is drawn between $(FMR, FNMR)_{MALE}$ and $(FMR, FNMR)_{FEMALE}$ showing how which sex has lower FMR and/or FNMR. The "M" label denotes male, the other end of the line corresponds to female. The six operating thresholds are selected to give the nominal false match rates given in the legend, and are computed over all impostor pairs regardless of age, sex, and place of birth. The plotted FMR values are broadly an order of magnitude larger than the nominal rates because FMR is computed over demographically-matched impostor pairs i.e individuals of the same sex, from the same geographic region (see section 3.6.1), and the same age group (see section 3.6.2).

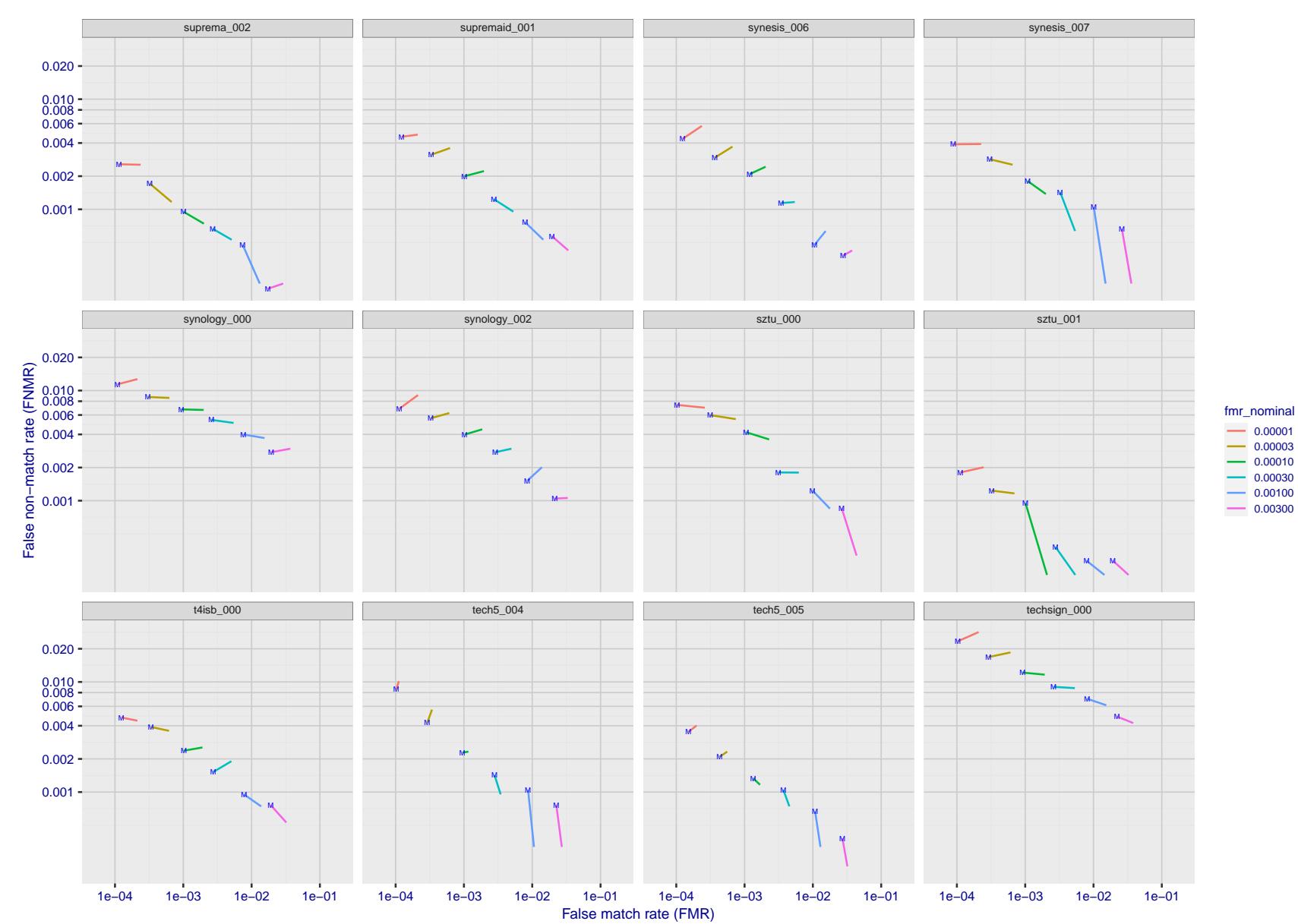


Figure 167: For the visa images, FNMR and FMR at six operating points along the DET characteristic. At each point a line is drawn between $(\text{FMR}, \text{FNMR})_{\text{MALE}}$ and $(\text{FMR}, \text{FNMR})_{\text{FEMALE}}$ showing how which sex has lower FMR and/or FNMR. The "M" label denotes male, the other end of the line corresponds to female. The six operating thresholds are selected to give the nominal false match rates given in the legend, and are computed over all impostor pairs regardless of age, sex, and place of birth. The plotted FMR values are broadly an order of magnitude larger than the nominal rates because FMR is computed over demographically-matched impostor pairs i.e individuals of the same sex, from the same geographic region (see section 3.6.1), and the same age group (see section 3.6.2).

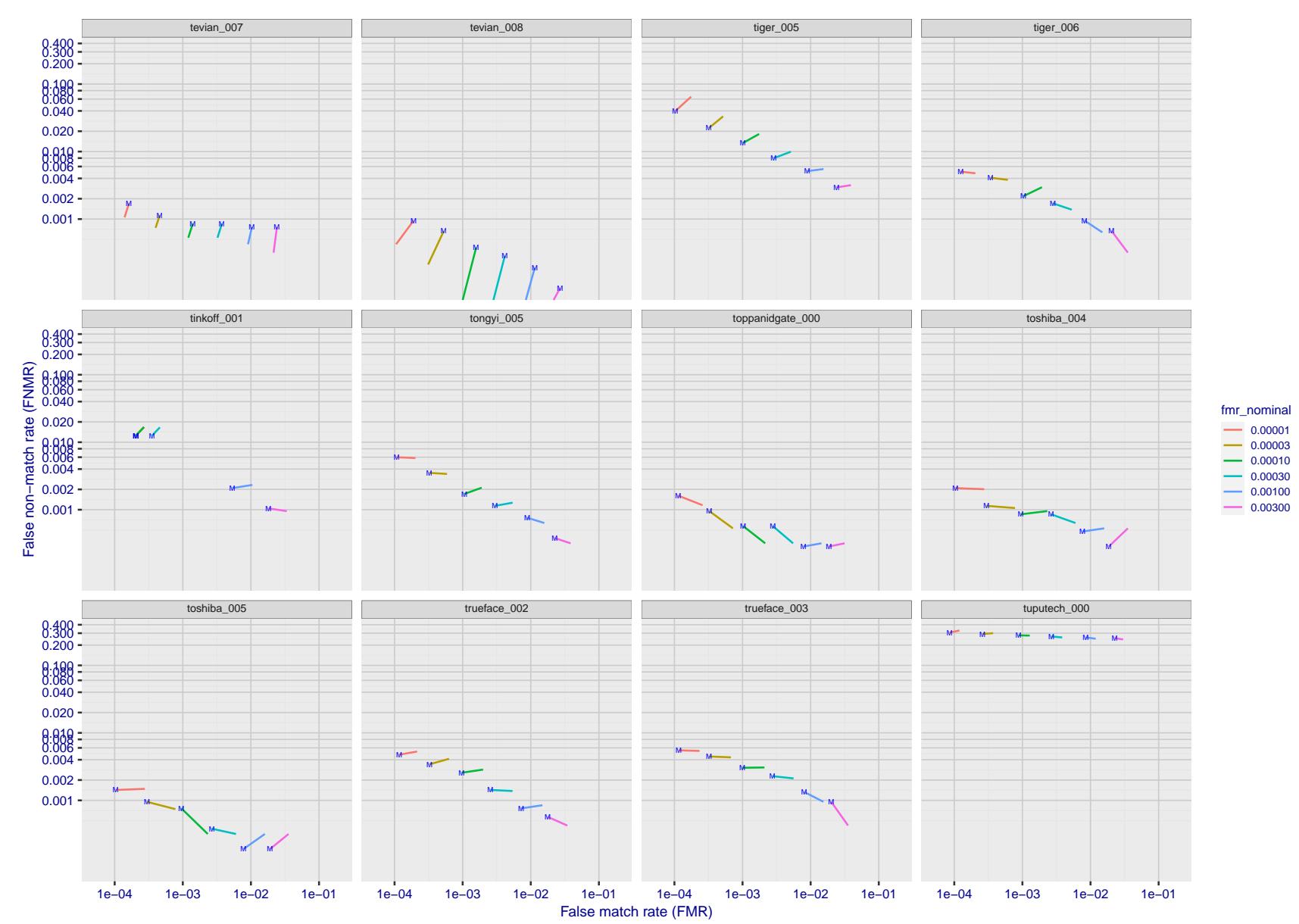


Figure 168: For the visa images, FNMR and FMR at six operating points along the DET characteristic. At each point a line is drawn between $(FMR, FNMR)_{MALE}$ and $(FMR, FNMR)_{FEMALE}$ showing how which sex has lower FMR and/or FNMR. The "M" label denotes male, the other end of the line corresponds to female. The six operating thresholds are selected to give the nominal false match rates given in the legend, and are computed over all impostor pairs regardless of age, sex, and place of birth. The plotted FMR values are broadly an order of magnitude larger than the nominal rates because FMR is computed over demographically-matched impostor pairs i.e individuals of the same sex, from the same geographic region (see section 3.6.1), and the same age group (see section 3.6.2).

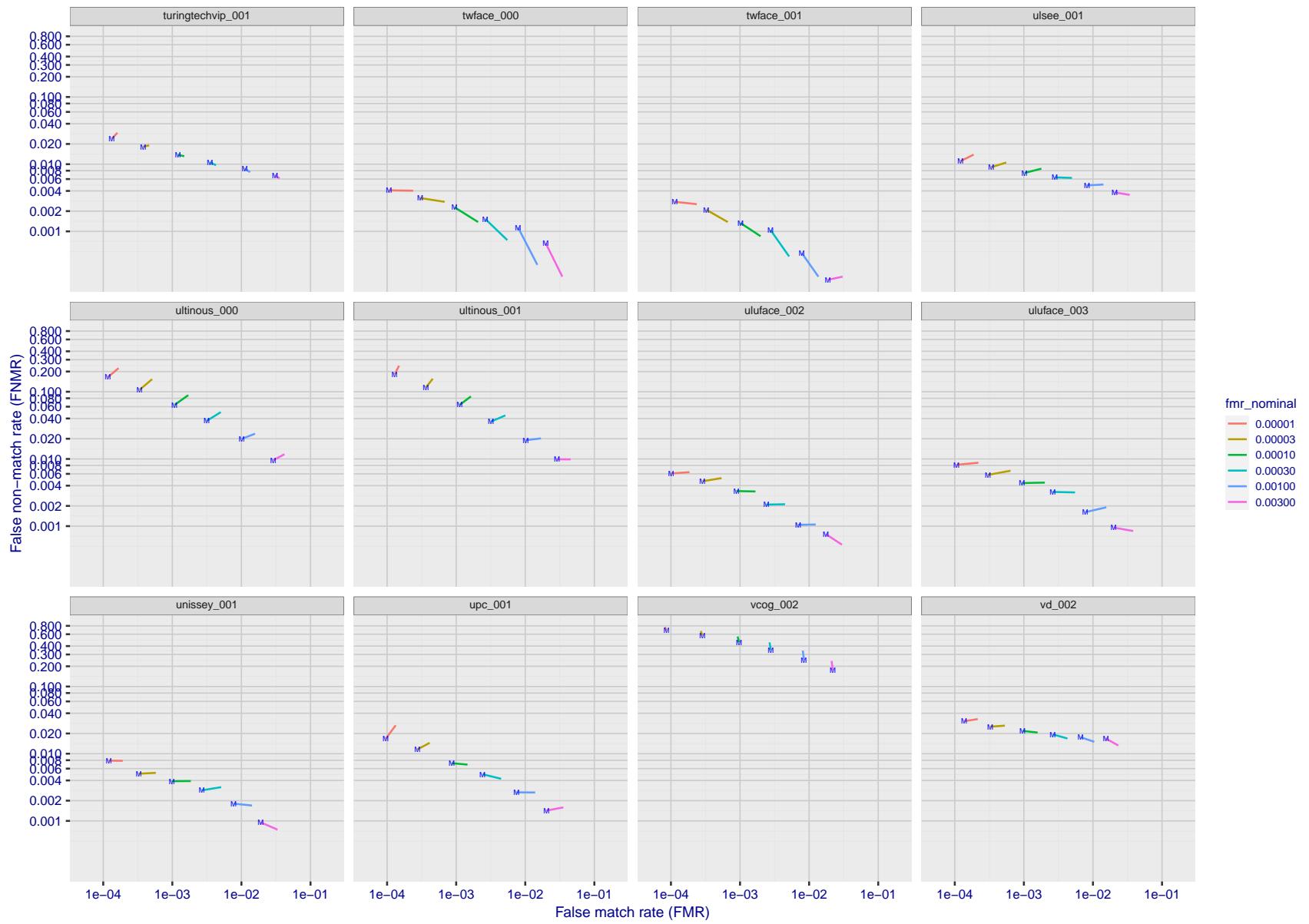


Figure 169: For the visa images, FNMR and FMR at six operating points along the DET characteristic. At each point a line is drawn between $(FMR, FNMR)_{MALE}$ and $(FMR, FNMR)_{FEMALE}$ showing how which sex has lower FMR and/or FNMR. The "M" label denotes male, the other end of the line corresponds to female. The six operating thresholds are selected to give the nominal false match rates given in the legend, and are computed over all impostor pairs regardless of age, sex, and place of birth. The plotted FMR values are broadly an order of magnitude larger than the nominal rates because FMR is computed over demographically-matched impostor pairs i.e individuals of the same sex, from the same geographic region (see section 3.6.1), and the same age group (see section 3.6.2).

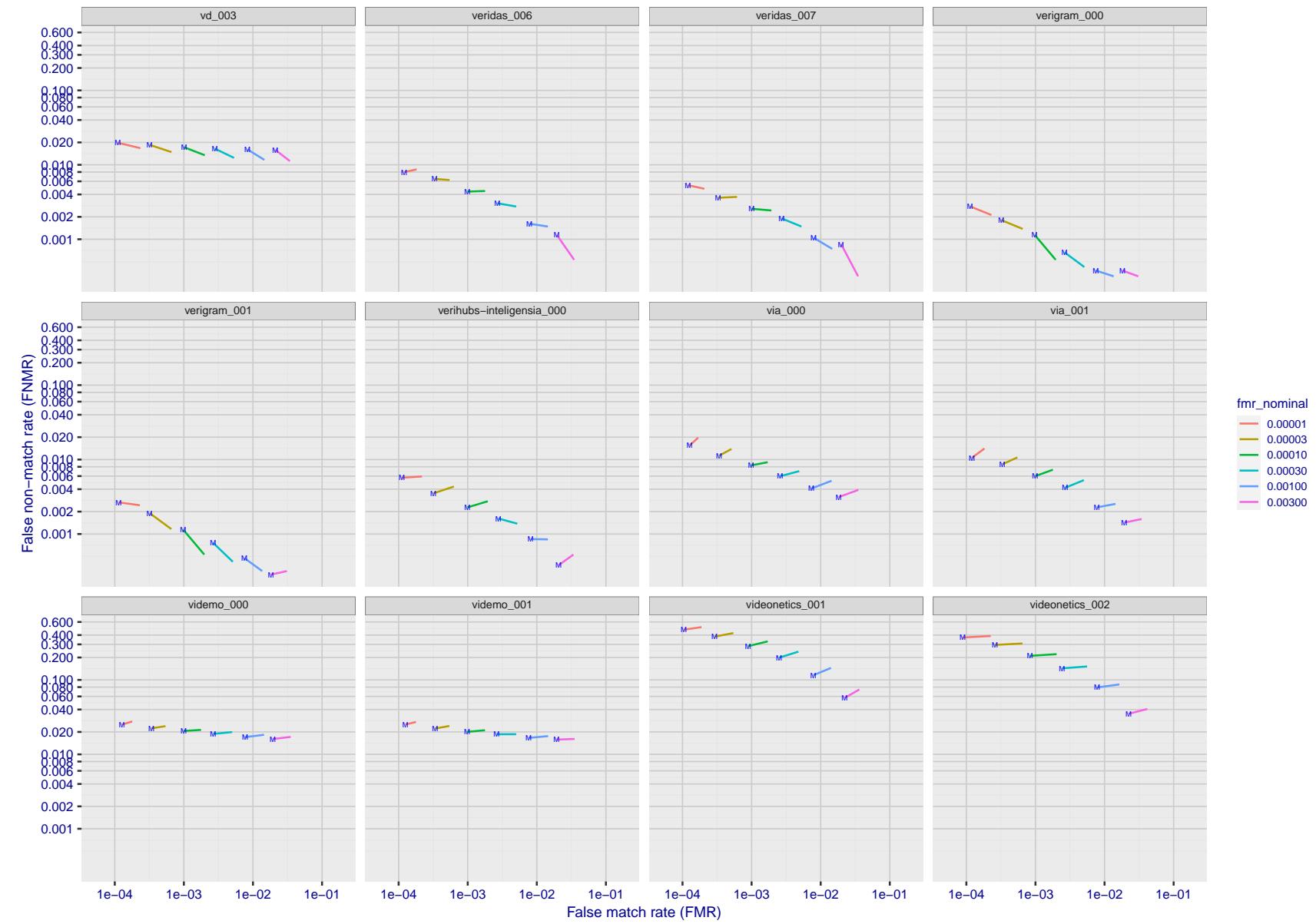


Figure 170: For the visa images, FNMR and FMR at six operating points along the DET characteristic. At each point a line is drawn between $(FMR, FNMR)_{MALE}$ and $(FMR, FNMR)_{FEMALE}$ showing how which sex has lower FMR and/or FNMR. The "M" label denotes male, the other end of the line corresponds to female. The six operating thresholds are selected to give the nominal false match rates given in the legend, and are computed over all impostor pairs regardless of age, sex, and place of birth. The plotted FMR values are broadly an order of magnitude larger than the nominal rates because FMR is computed over demographically-matched impostor pairs i.e individuals of the same sex, from the same geographic region (see section 3.6.1), and the same age group (see section 3.6.2).

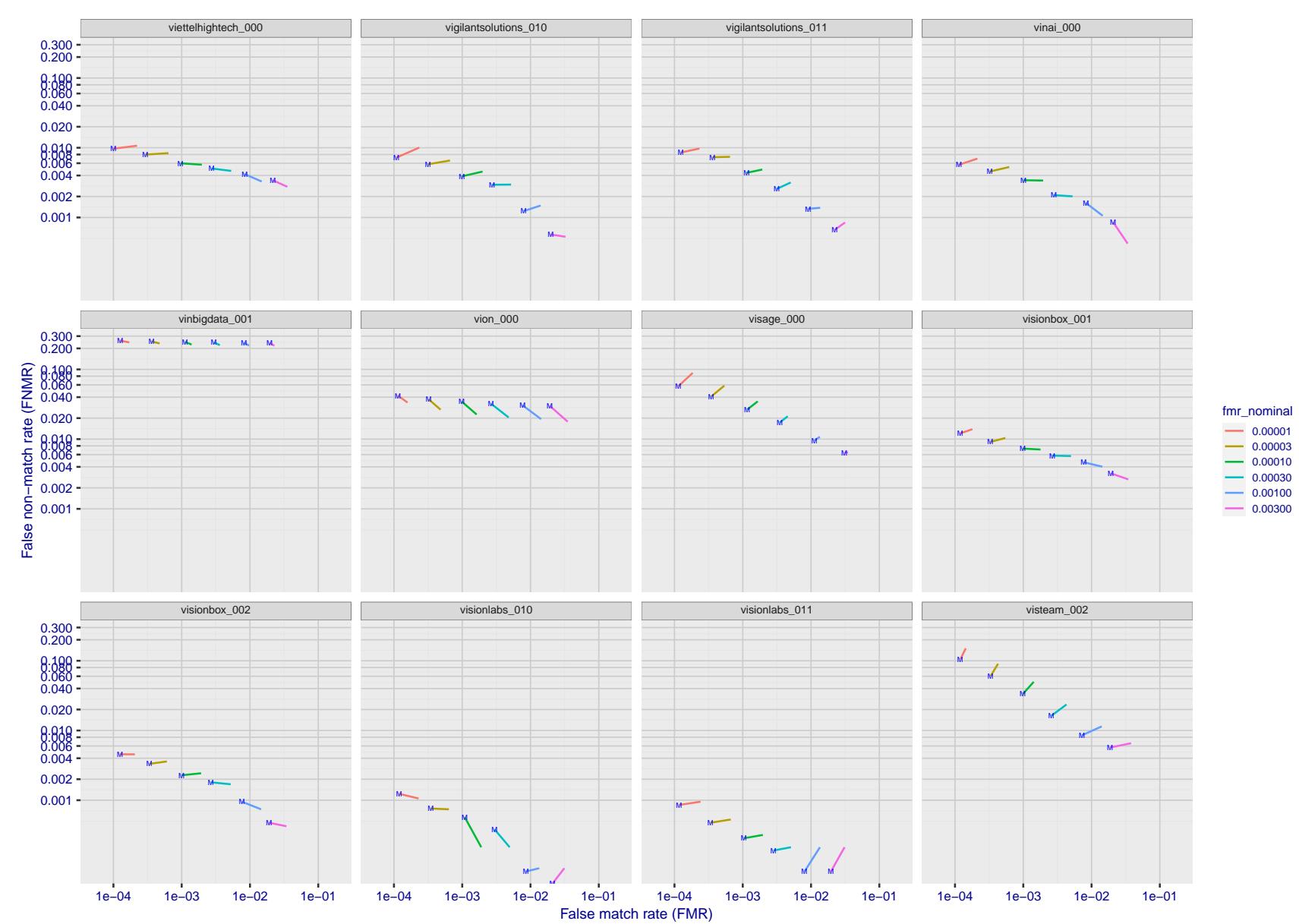


Figure 171: For the visa images, FNMR and FMR at six operating points along the DET characteristic. At each point a line is drawn between $(FMR, FNMR)_{MALE}$ and $(FMR, FNMR)_{FEMALE}$ showing how which sex has lower FMR and/or FNMR. The "M" label denotes male, the other end of the line corresponds to female. The six operating thresholds are selected to give the nominal false match rates given in the legend, and are computed over all impostor pairs regardless of age, sex, and place of birth. The plotted FMR values are broadly an order of magnitude larger than the nominal rates because FMR is computed over demographically-matched impostor pairs i.e individuals of the same sex, from the same geographic region (see section 3.6.1), and the same age group (see section 3.6.2).

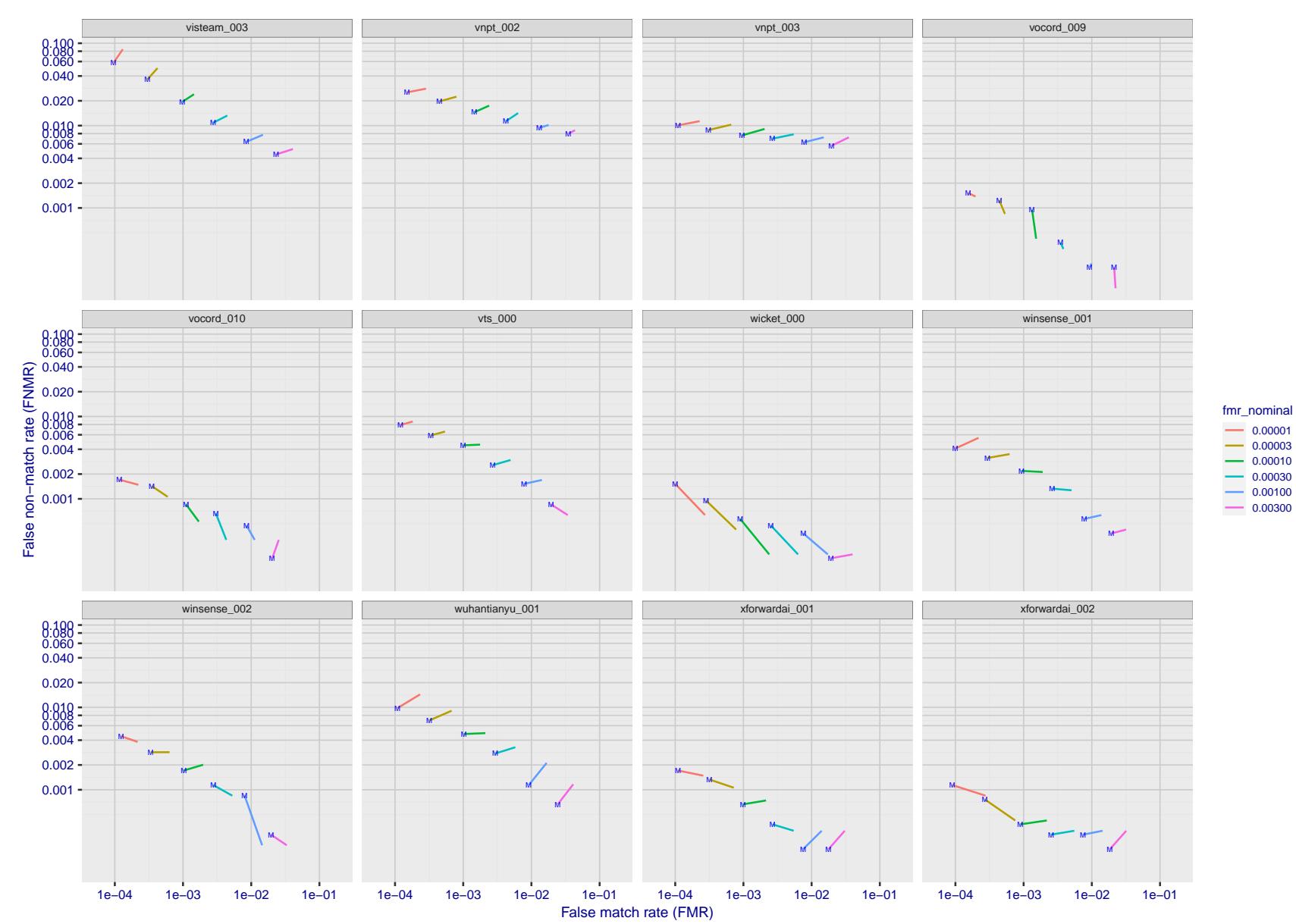


Figure 172: For the visa images, FNMR and FMR at six operating points along the DET characteristic. At each point a line is drawn between $(FMR, FNMR)_{MALE}$ and $(FMR, FNMR)_{FEMALE}$ showing how which sex has lower FMR and/or FNMR. The "M" label denotes male, the other end of the line corresponds to female. The six operating thresholds are selected to give the nominal false match rates given in the legend, and are computed over all impostor pairs regardless of age, sex, and place of birth. The plotted FMR values are broadly an order of magnitude larger than the nominal rates because FMR is computed over demographically-matched impostor pairs i.e individuals of the same sex, from the same geographic region (see section 3.6.1), and the same age group (see section 3.6.2).

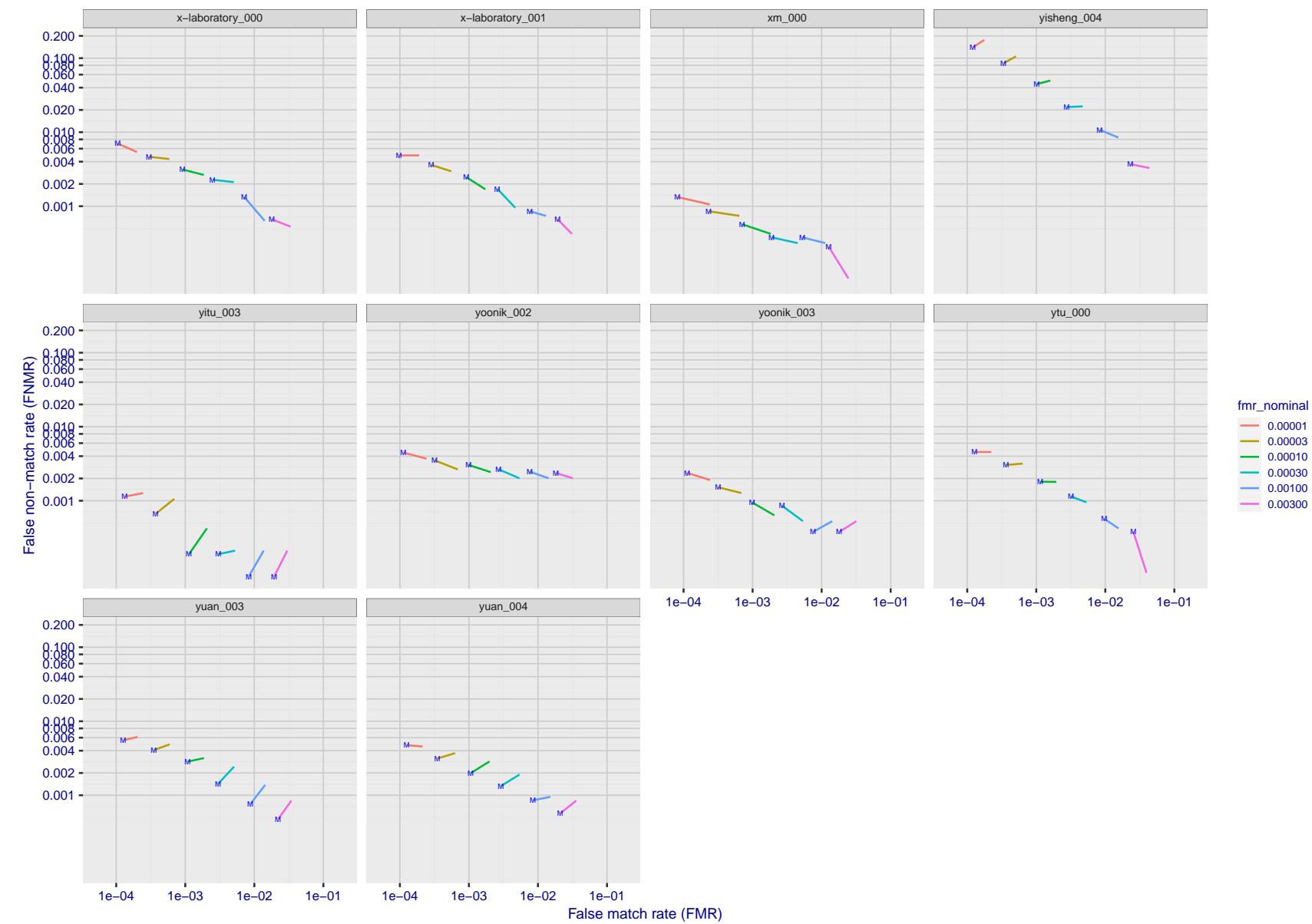


Figure 173: For the visa images, FNMR and FMR at six operating points along the DET characteristic. At each point a line is drawn between $(FMR, FNMR)_{MALE}$ and $(FMR, FNMR)_{FEMALE}$ showing how which sex has lower FMR and/or FNMR. The "M" label denotes male, the other end of the line corresponds to female. The six operating thresholds are selected to give the nominal false match rates given in the legend, and are computed over all impostor pairs regardless of age, sex, and place of birth. The plotted FMR values are broadly an order of magnitude larger than the nominal rates because FMR is computed over demographically-matched impostor pairs i.e individuals of the same sex, from the same geographic region (see section 3.6.1), and the same age group (see section 3.6.2).

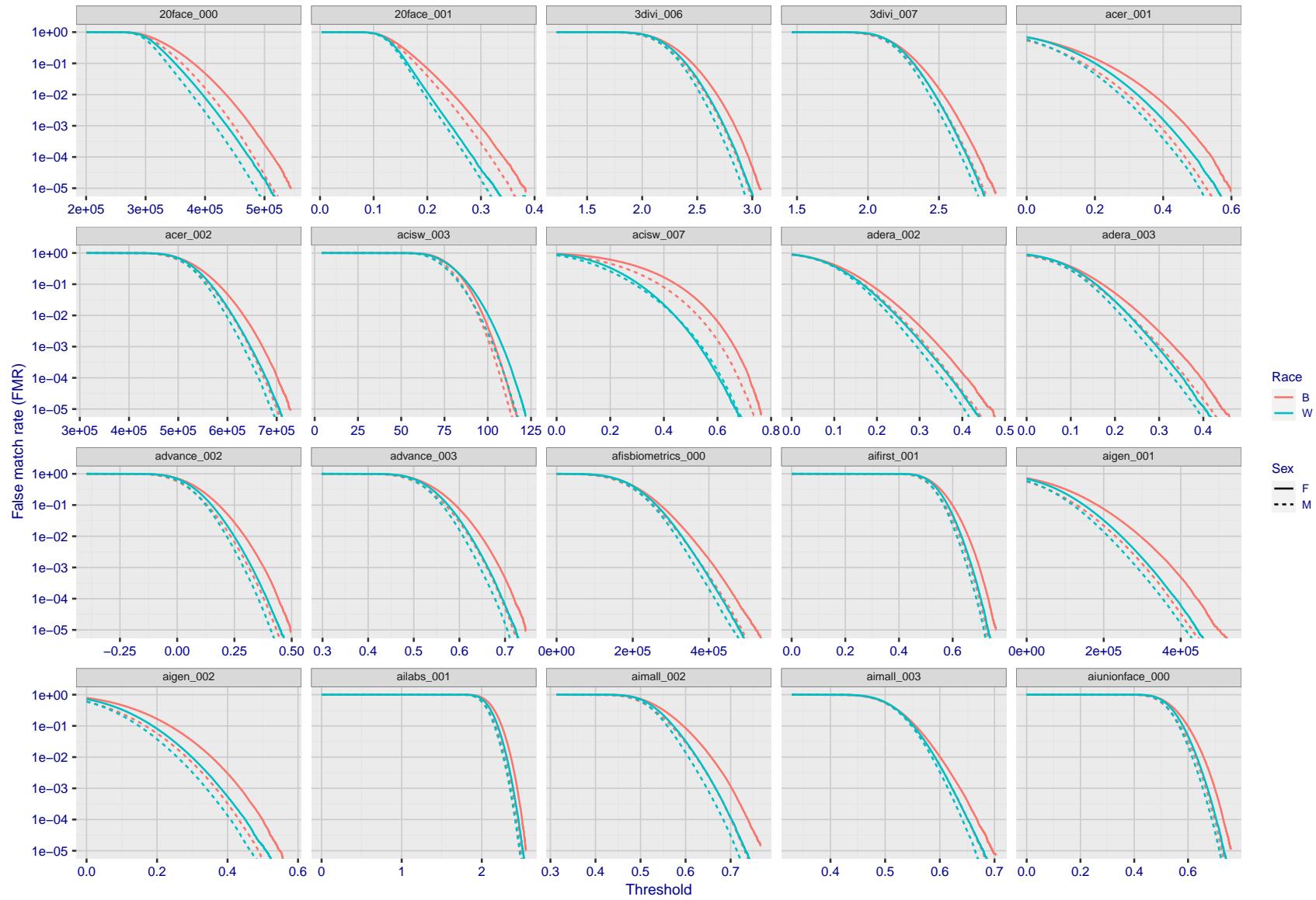


Figure 174: For the mugshot images, the false match calibration curves show false match rate vs. threshold. Separate curves appear for white females, black females, black males and white males.

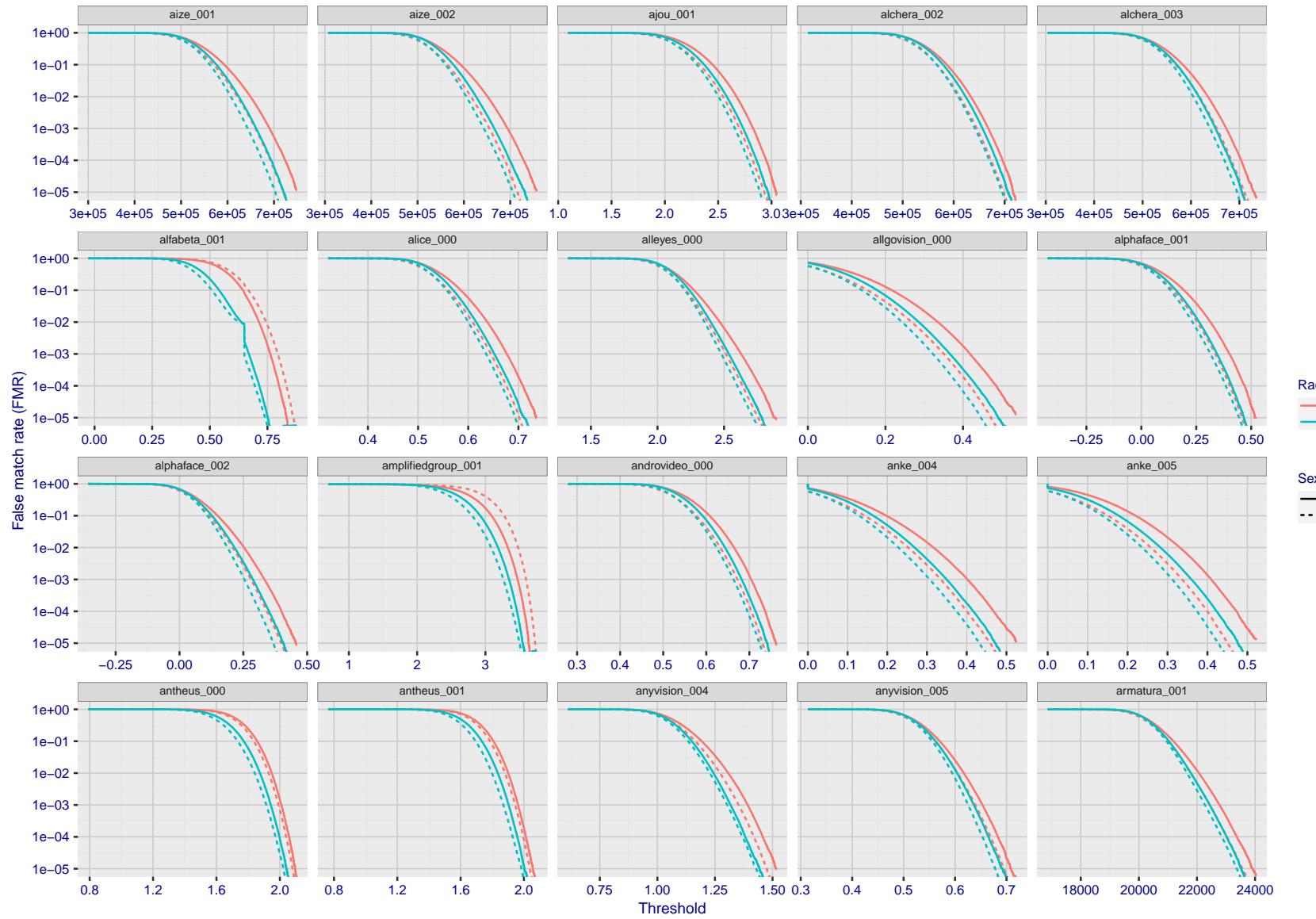


Figure 175: For the mugshot images, the false match calibration curves show false match rate vs. threshold. Separate curves appear for white females, black females, black males and white males.

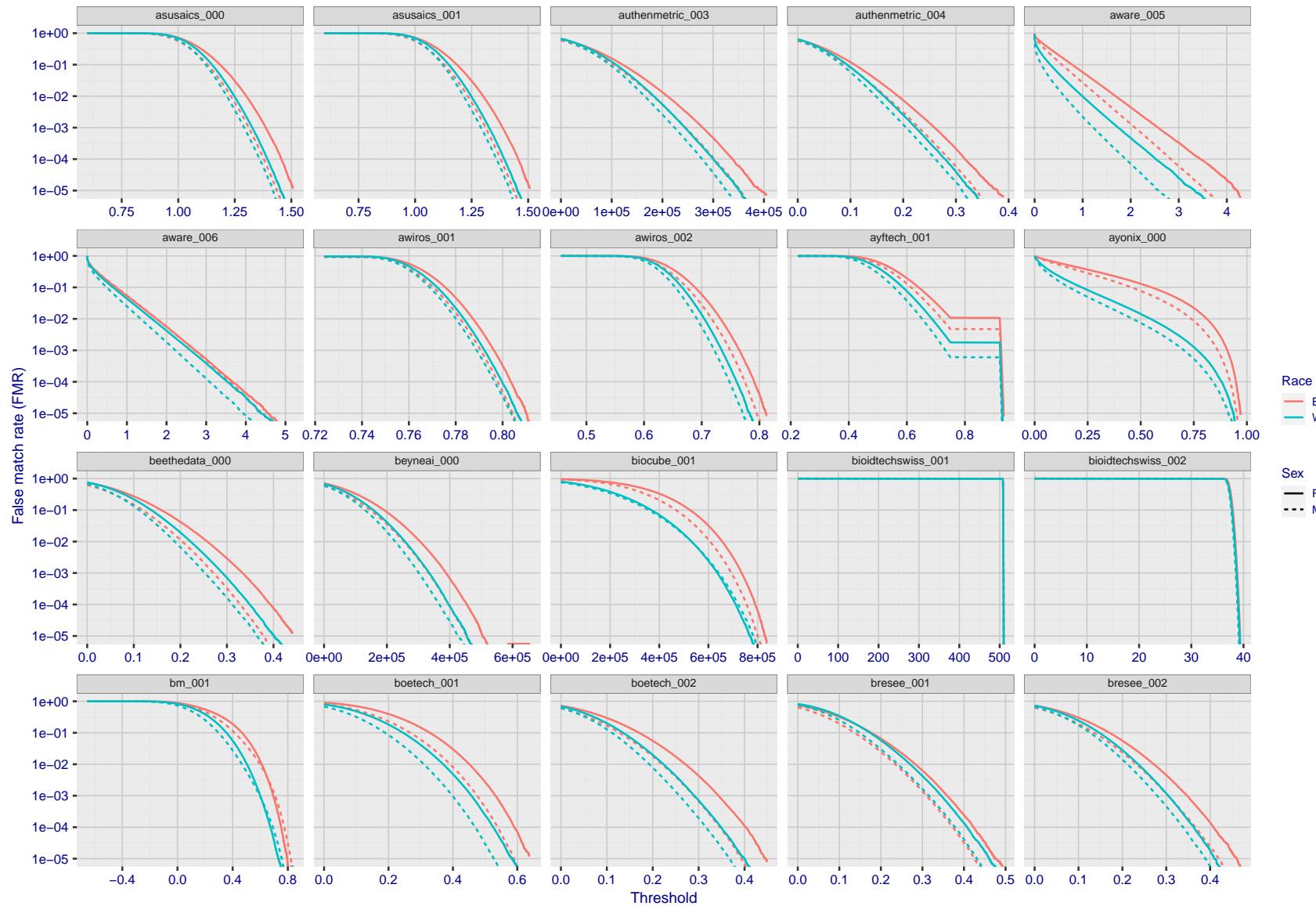


Figure 176: For the mugshot images, the false match calibration curves show false match rate vs. threshold. Separate curves appear for white females, black females, black males and white males.

2022/03/18 13:37:54

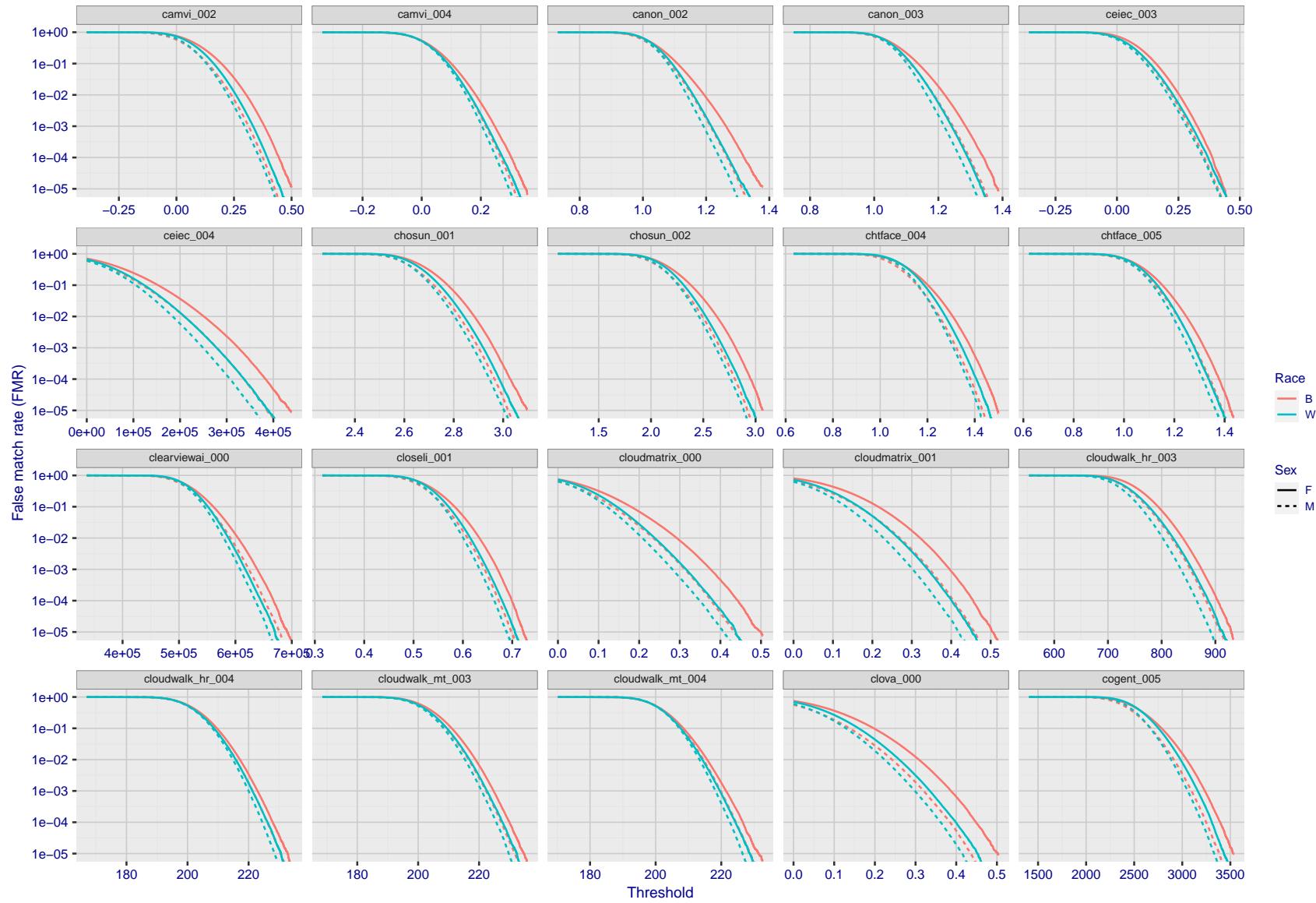


Figure 177: For the mugshot images, the false match calibration curves show false match rate vs. threshold. Separate curves appear for white females, black females, black males and white males.

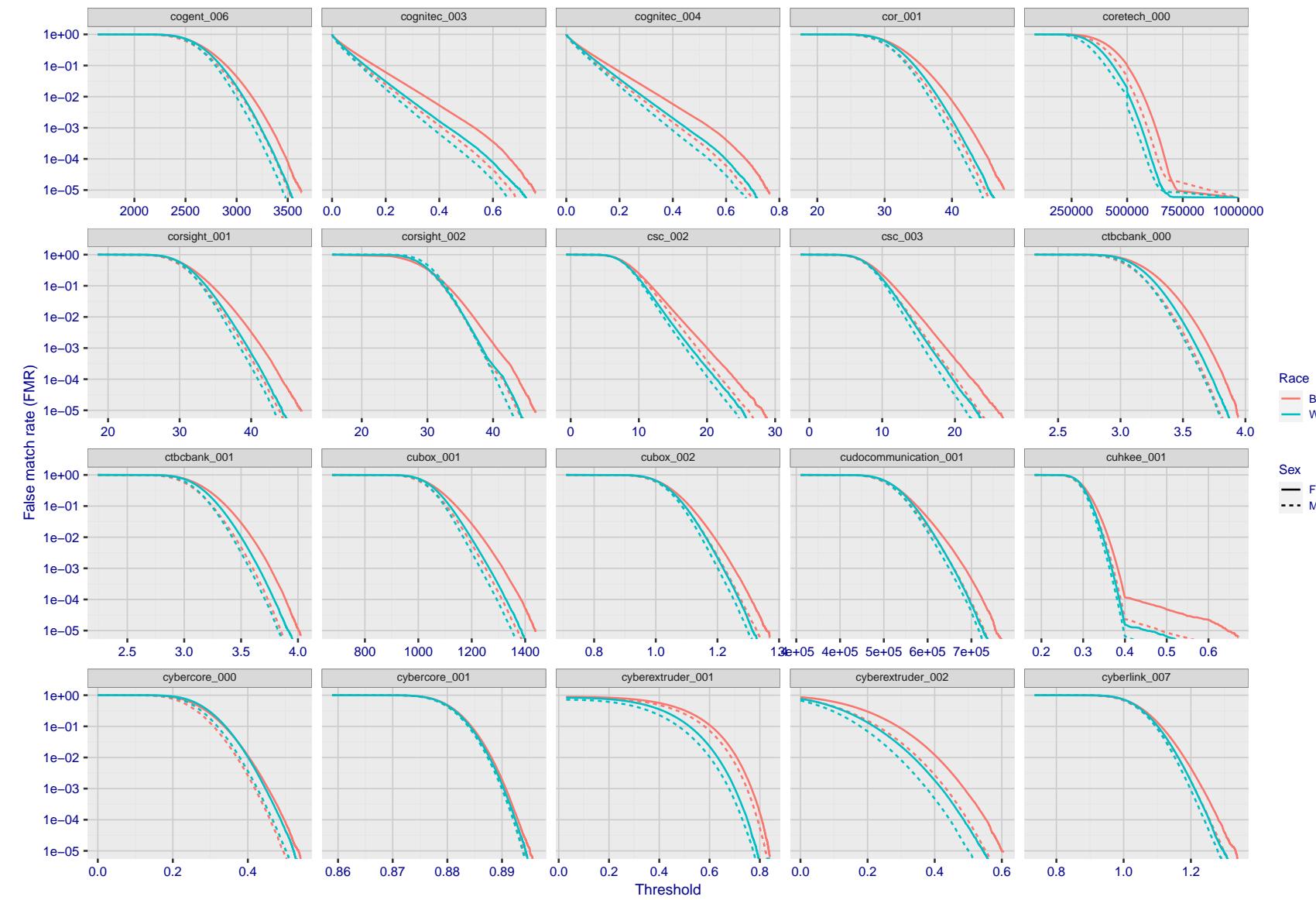
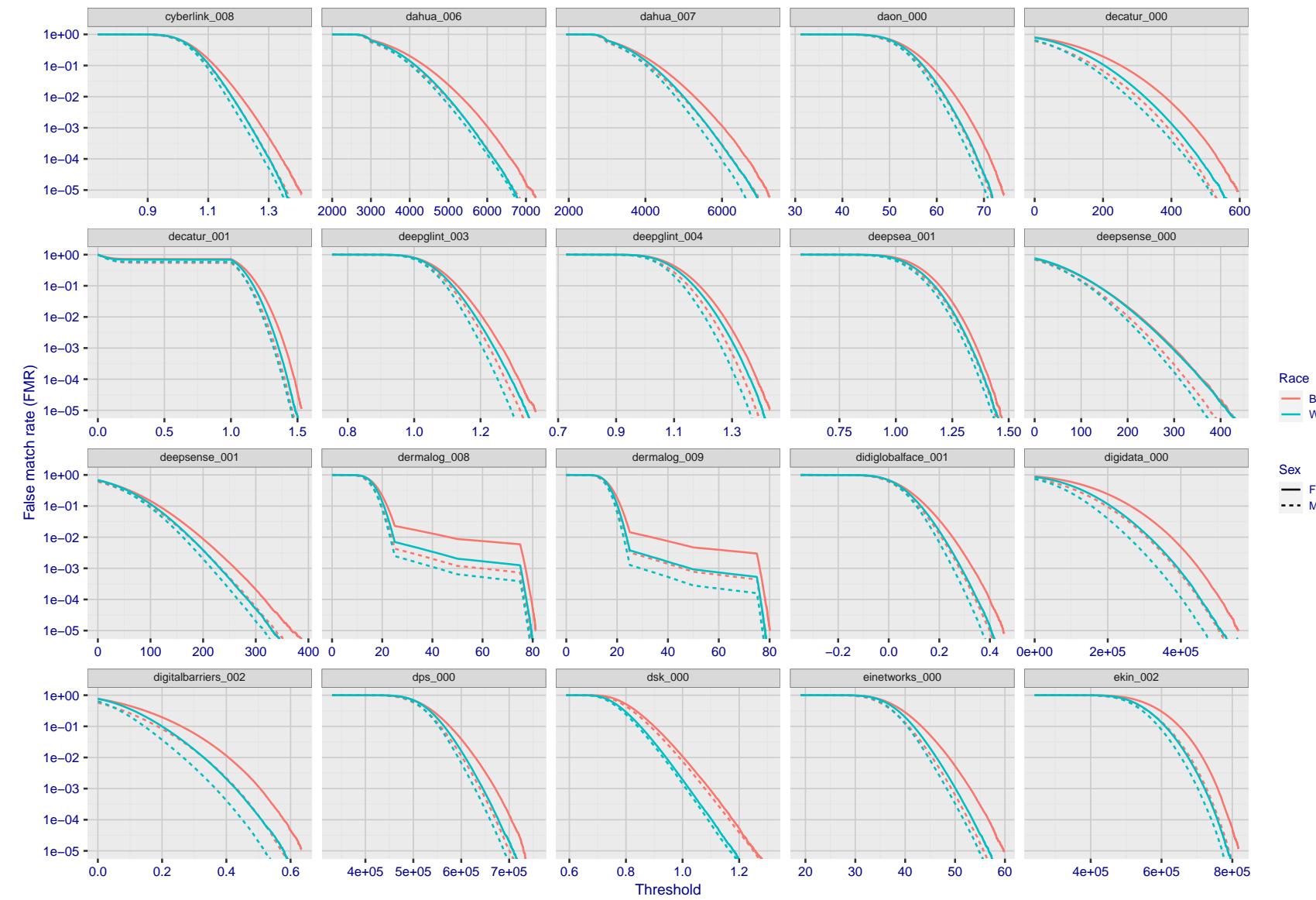


Figure 178: For the mugshot images, the false match calibration curves show false match rate vs. threshold. Separate curves appear for white females, black females, black males and white males.



FNMR(T)
"False non-match rate"
"False match rate"

Figure 179: For the mugshot images, the false match calibration curves show false match rate vs. threshold. Separate curves appear for white females, black females, black males and white males.

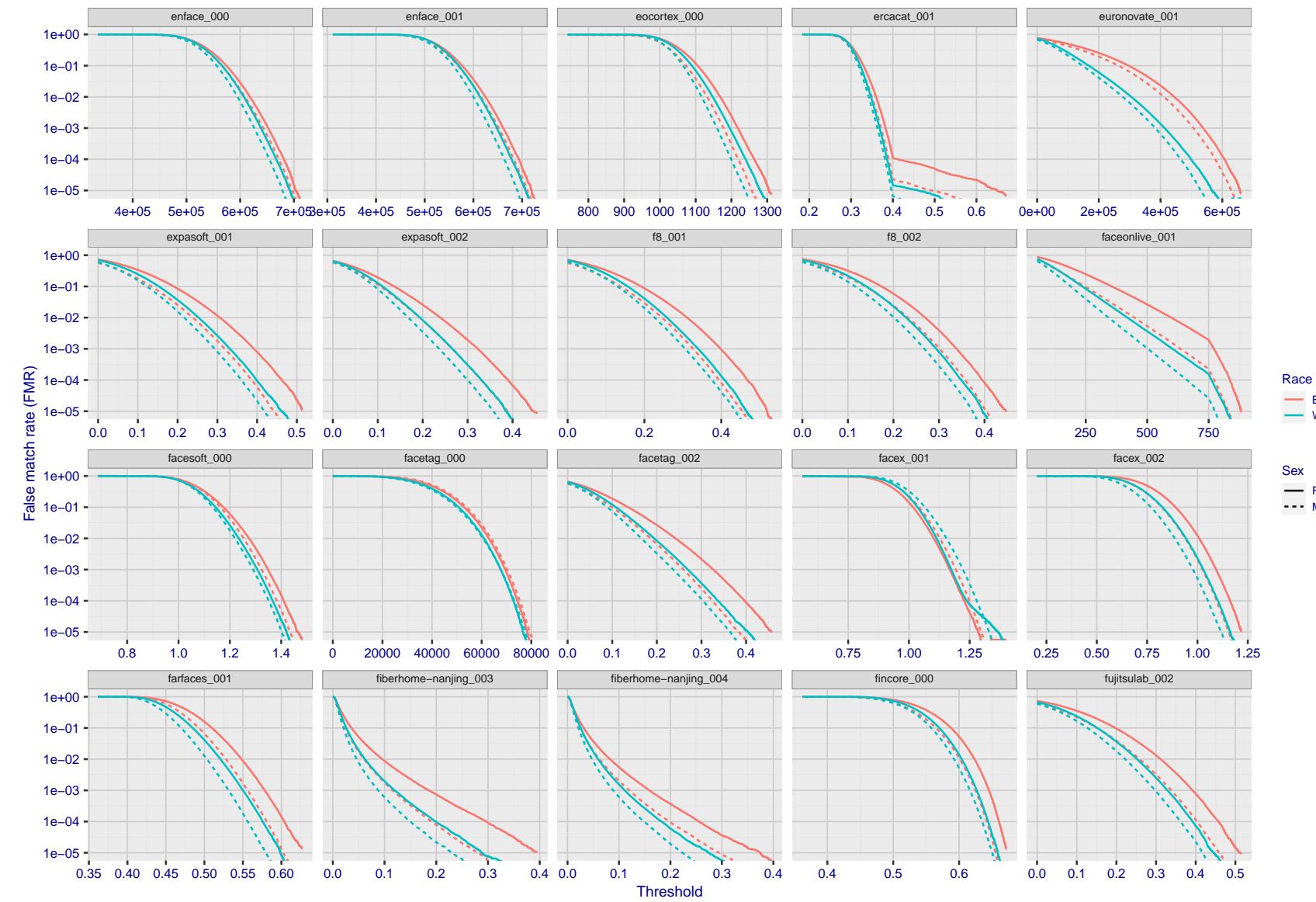


Figure 180: For the mugshot images, the false match calibration curves show false match rate vs. threshold. Separate curves appear for white females, black females, black males and white males.

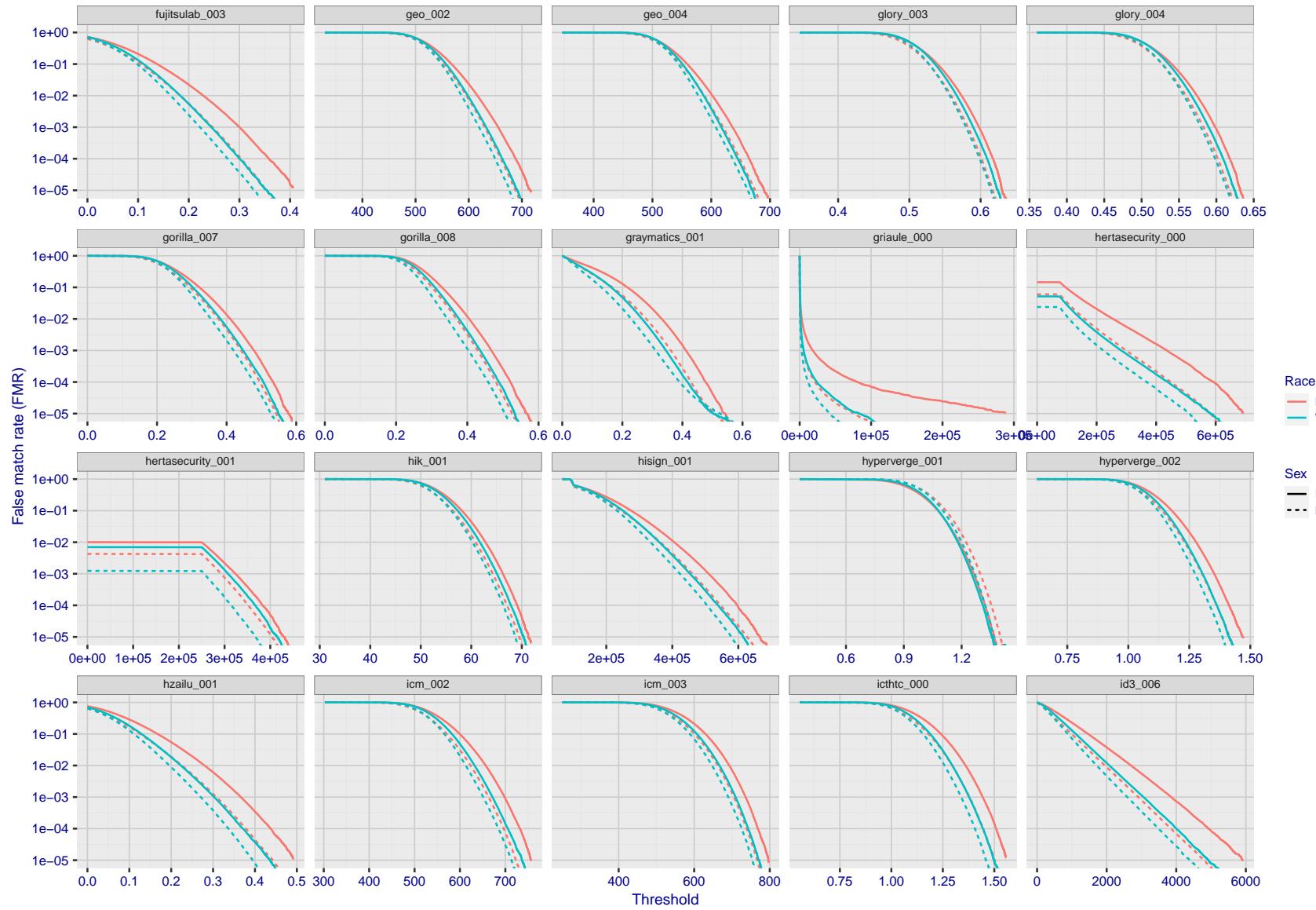


Figure 181: For the mugshot images, the false match calibration curves show false match rate vs. threshold. Separate curves appear for white females, black females, black males and white males.

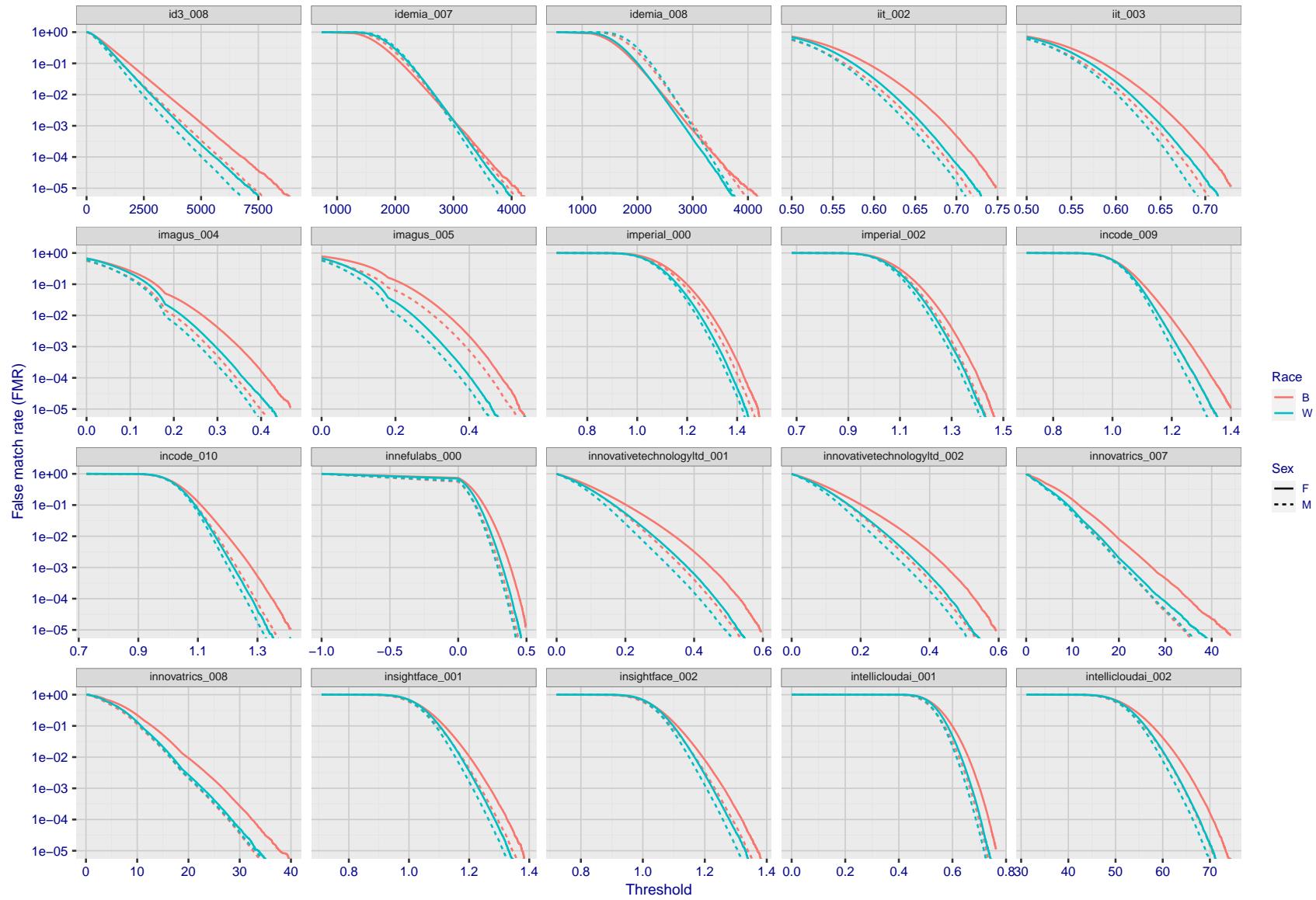


Figure 182: For the mugshot images, the false match calibration curves show false match rate vs. threshold. Separate curves appear for white females, black females, black males and white males.

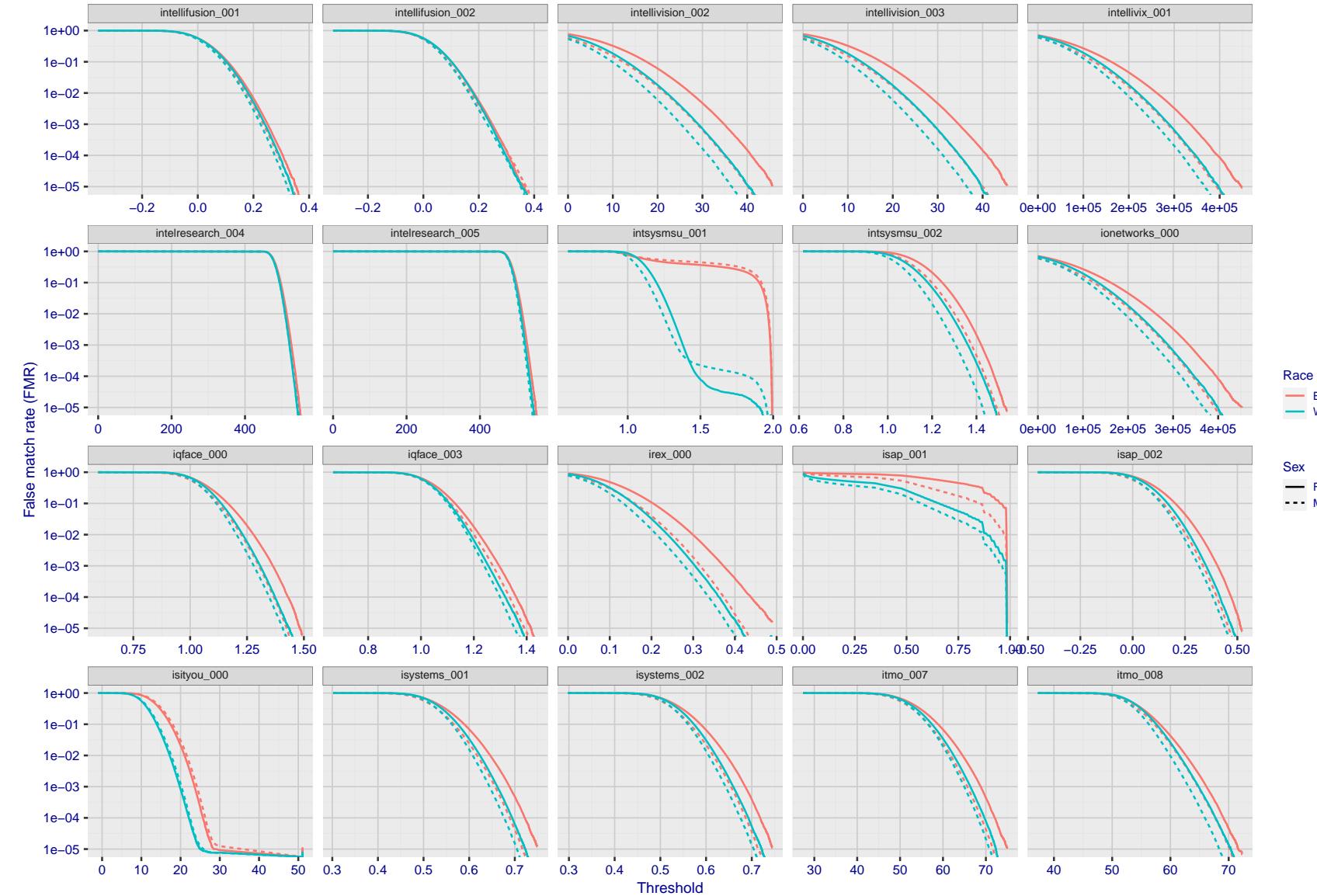


Figure 183: For the mugshot images, the false match calibration curves show false match rate vs. threshold. Separate curves appear for white females, black females, black males and white males.

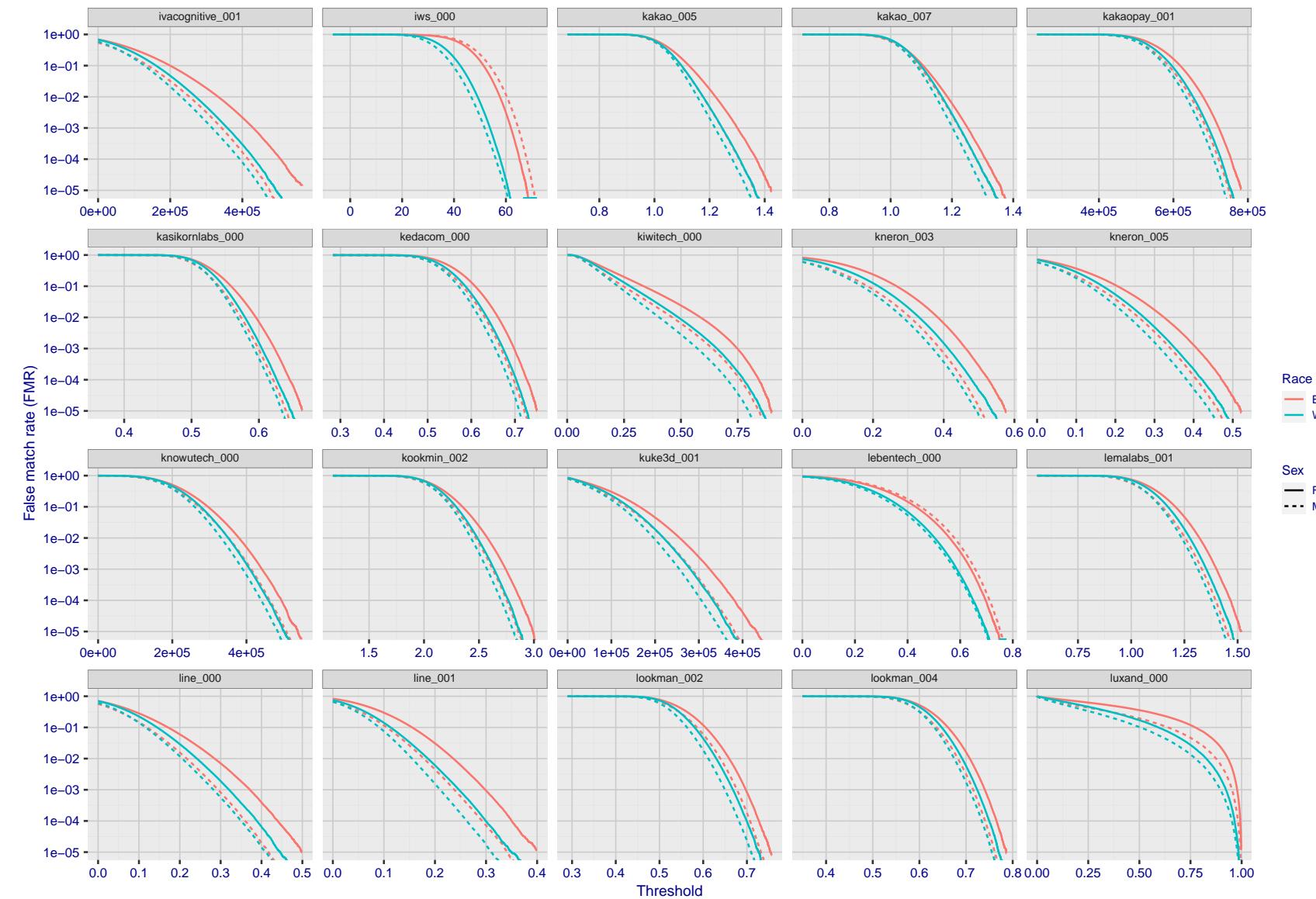


Figure 184: For the mugshot images, the false match calibration curves show false match rate vs. threshold. Separate curves appear for white females, black females, black males and white males.

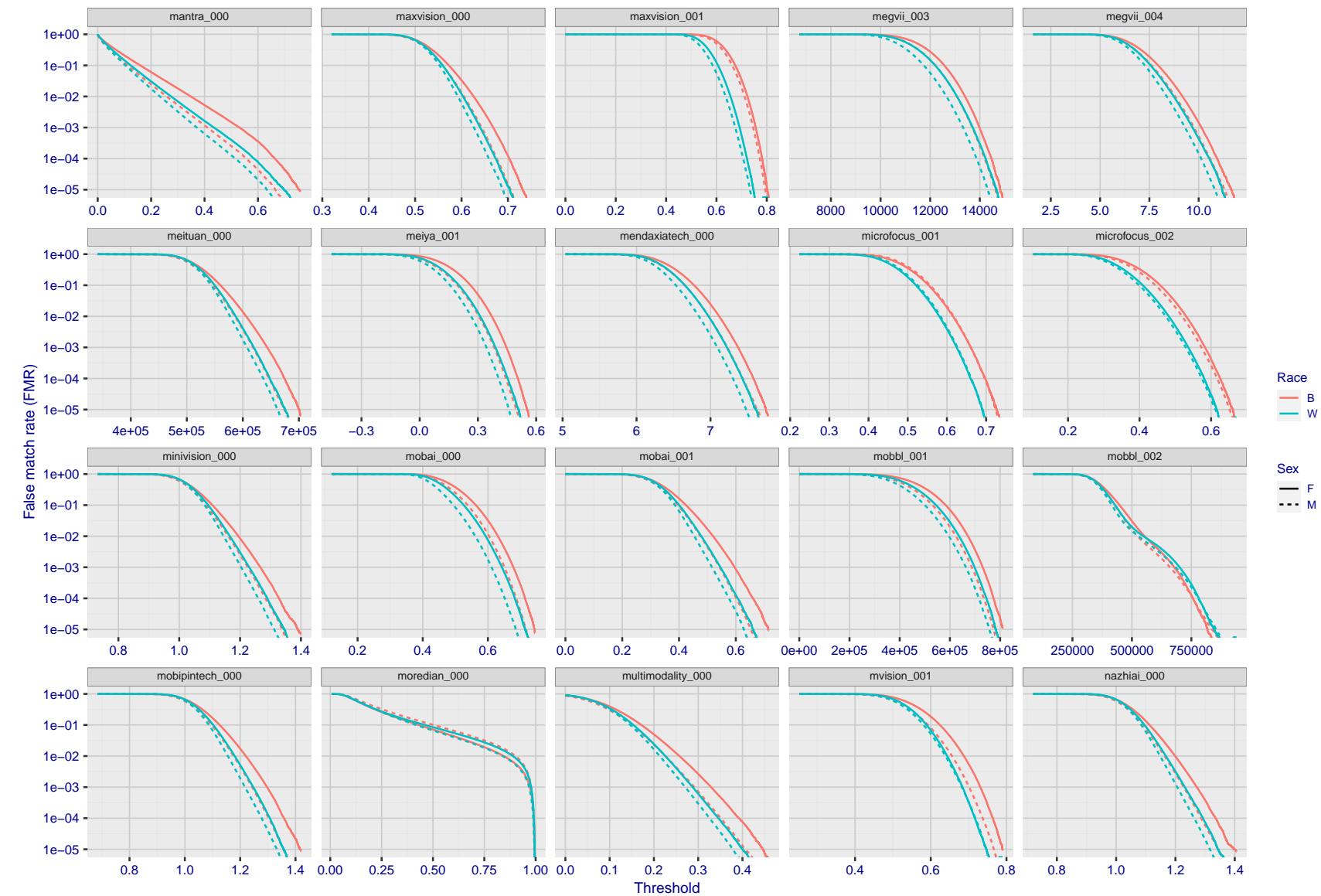


Figure 185: For the mugshot images, the false match calibration curves show false match rate vs. threshold. Separate curves appear for white females, black females, black males and white males.

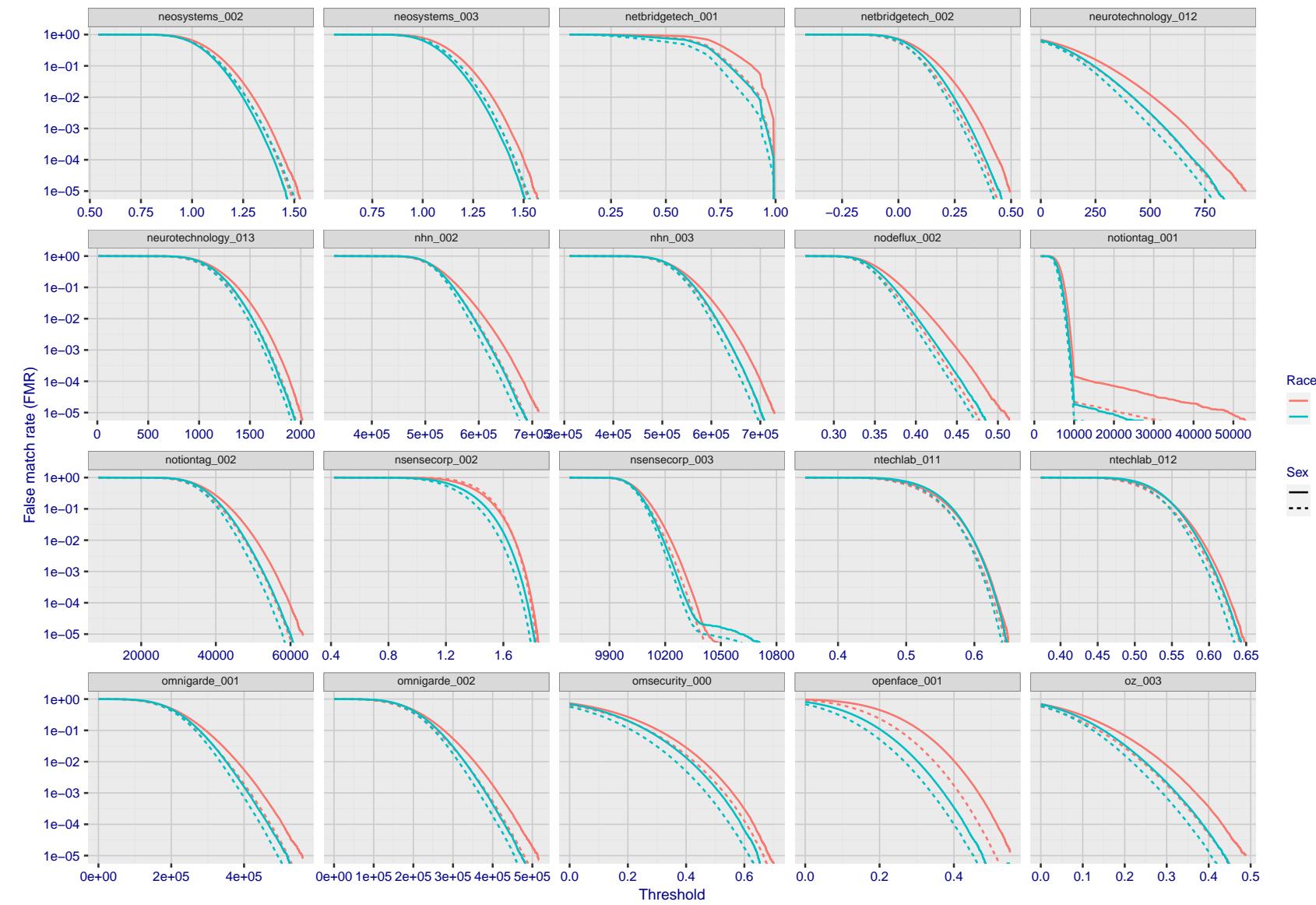


Figure 186: For the mugshot images, the false match calibration curves show false match rate vs. threshold. Separate curves appear for white females, black females, black males and white males.

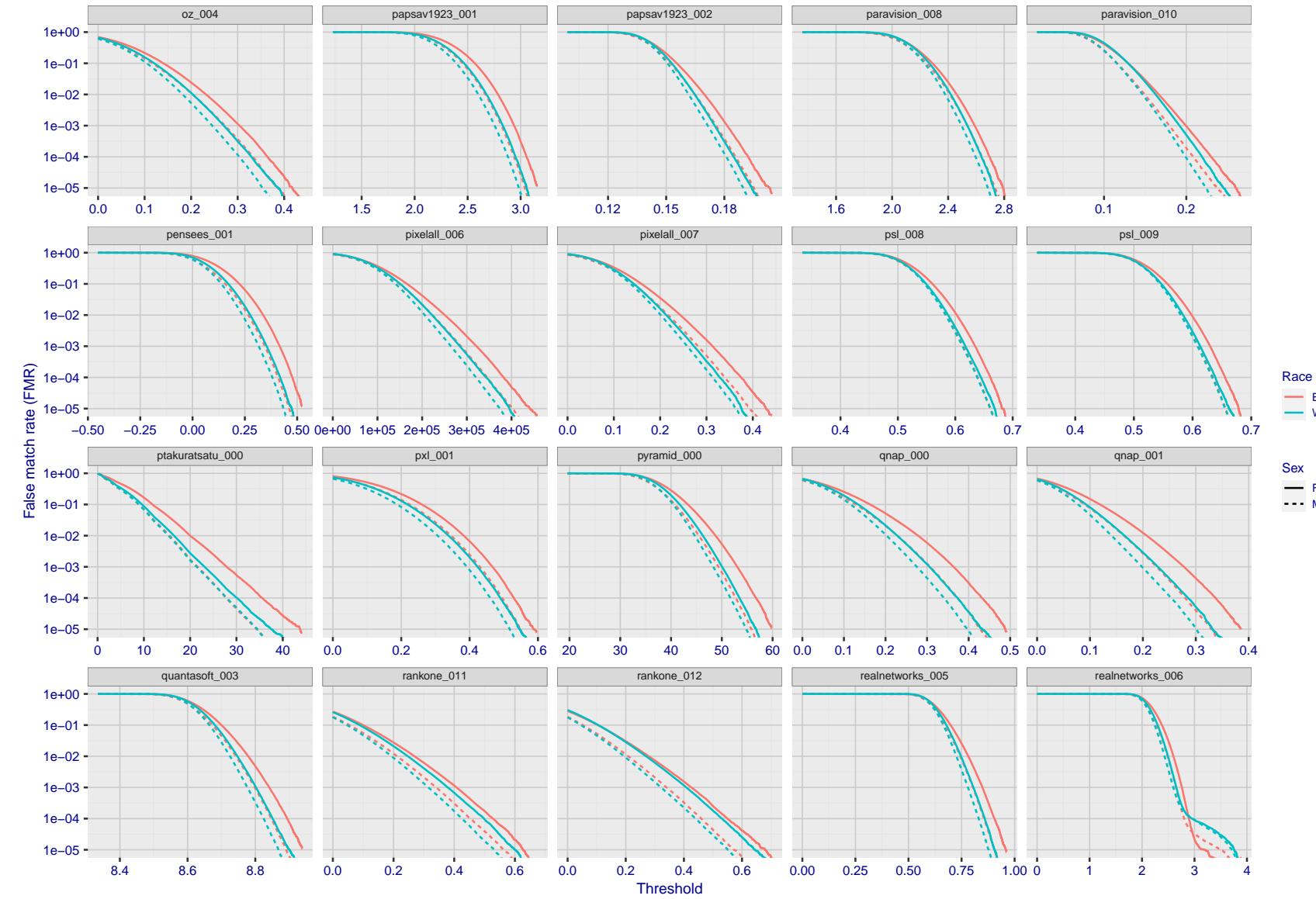


Figure 187: For the mugshot images, the false match calibration curves show false match rate vs. threshold. Separate curves appear for white females, black females, black males and white males.

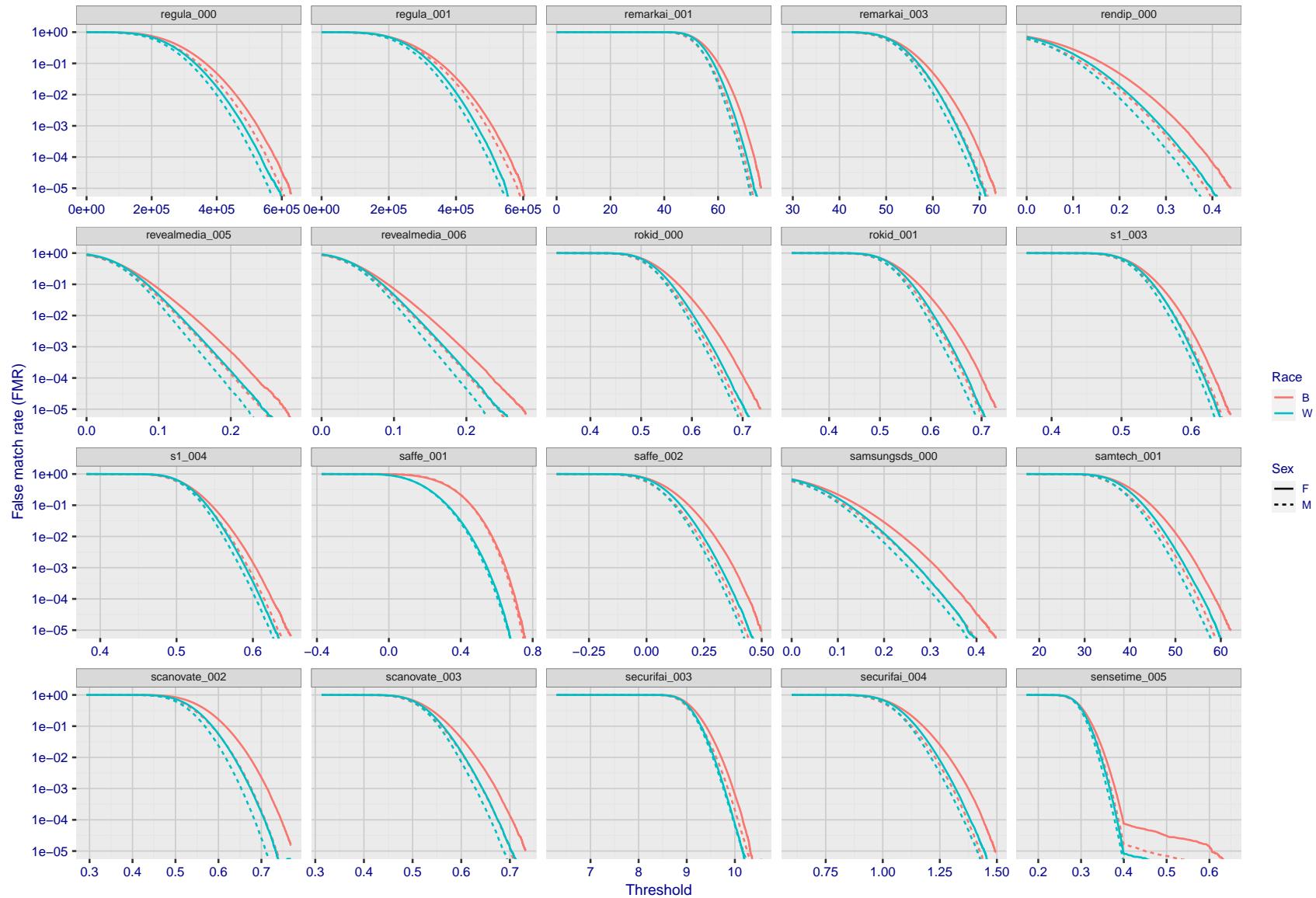


Figure 188: For the mugshot images, the false match calibration curves show false match rate vs. threshold. Separate curves appear for white females, black females, black males and white males.

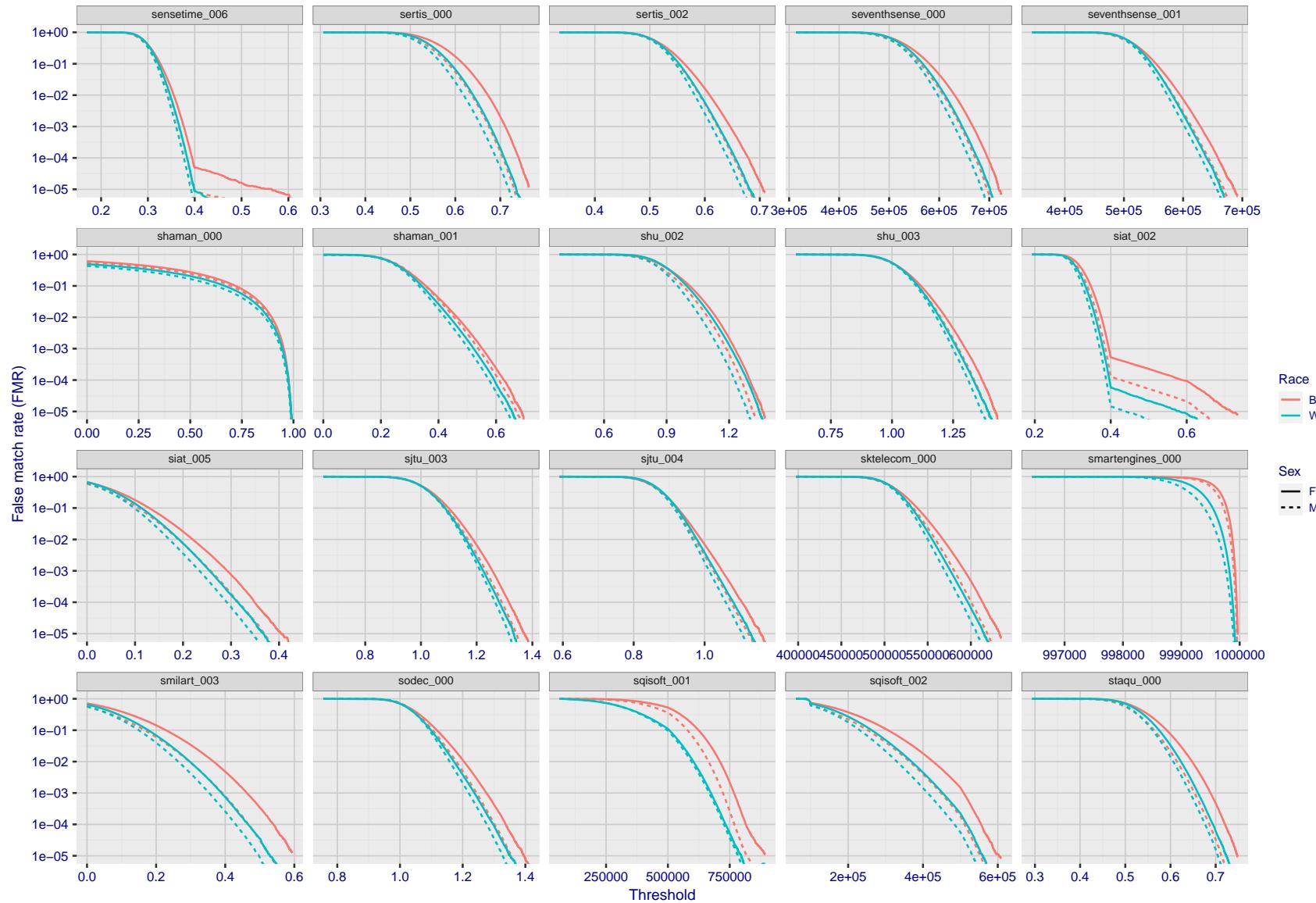


Figure 189: For the mugshot images, the false match calibration curves show false match rate vs. threshold. Separate curves appear for white females, black females, black males and white males.

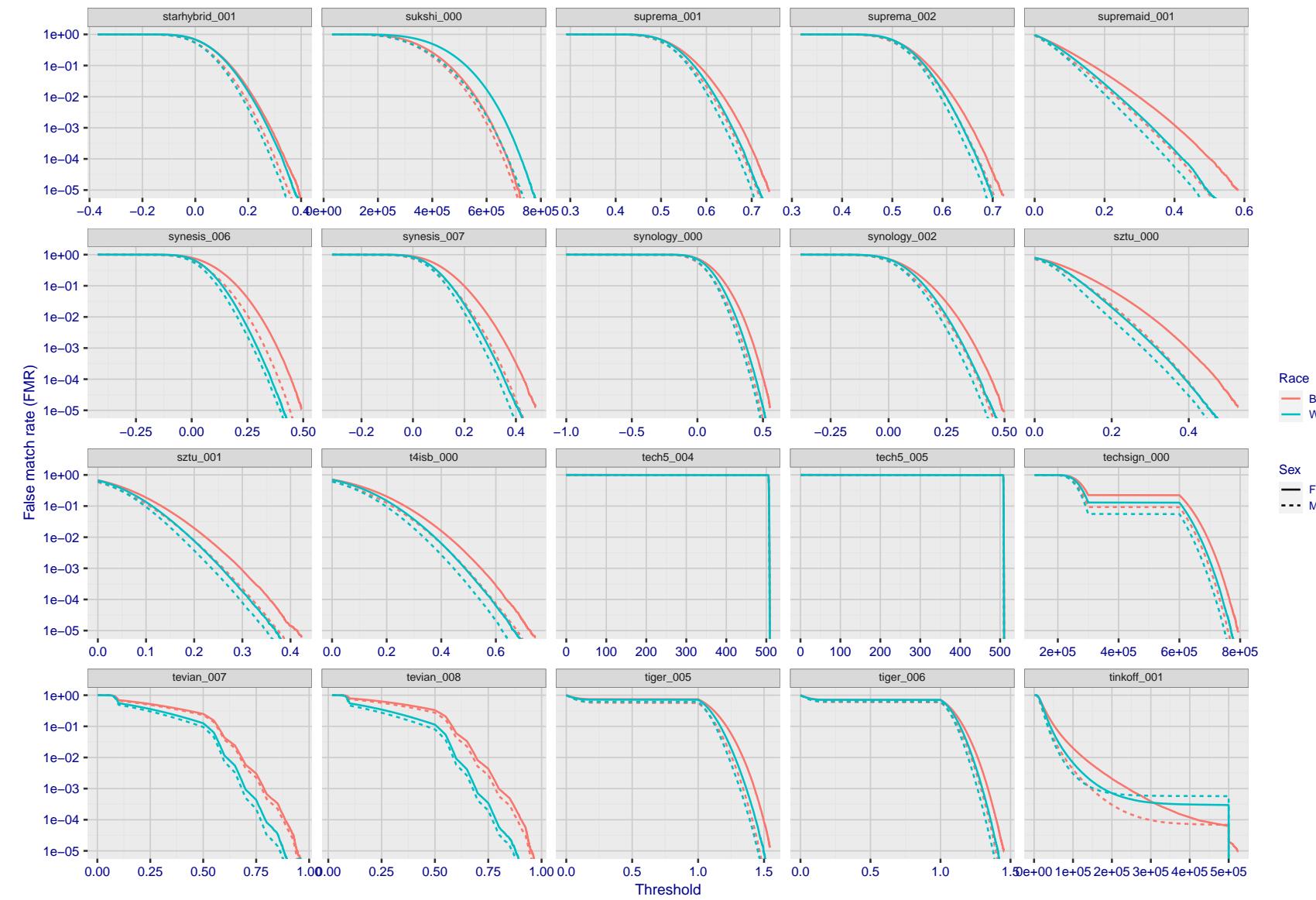


Figure 190: For the mugshot images, the false match calibration curves show false match rate vs. threshold. Separate curves appear for white females, black females, black males and white males.

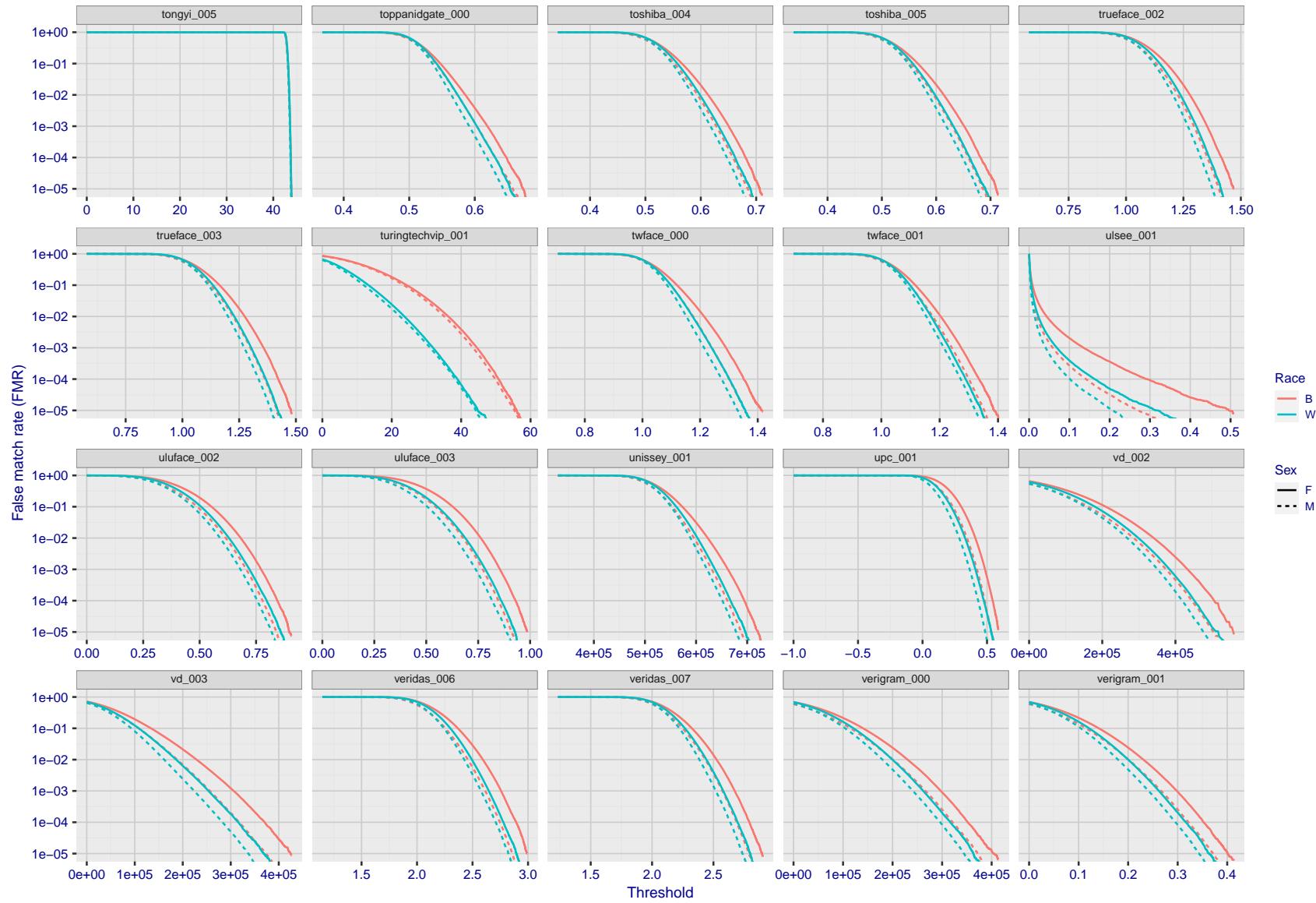


Figure 191: For the mugshot images, the false match calibration curves show false match rate vs. threshold. Separate curves appear for white females, black females, black males and white males.

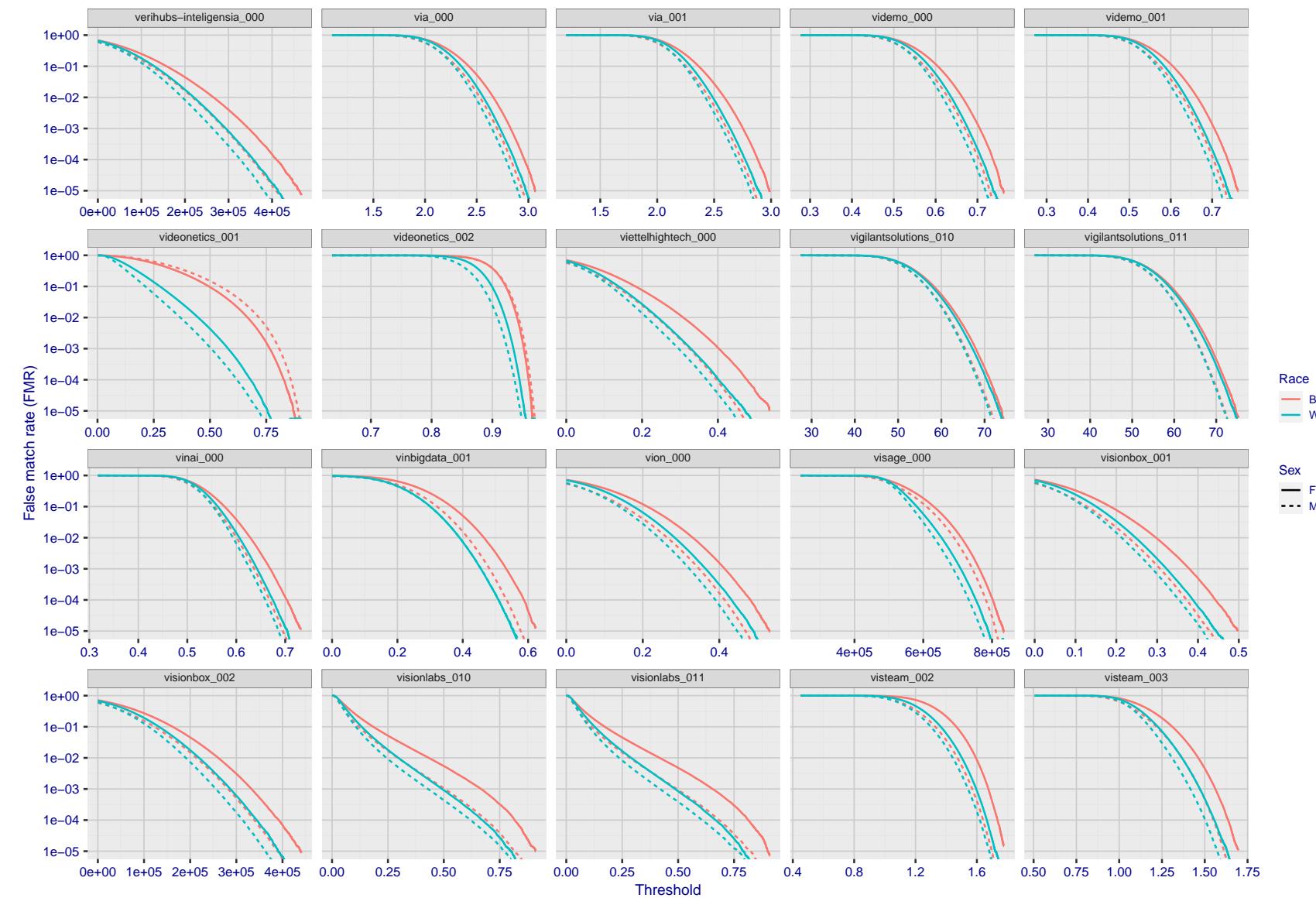


Figure 192: For the mugshot images, the false match calibration curves show false match rate vs. threshold. Separate curves appear for white females, black females, black males and white males.

2022/03/18 13:37:54

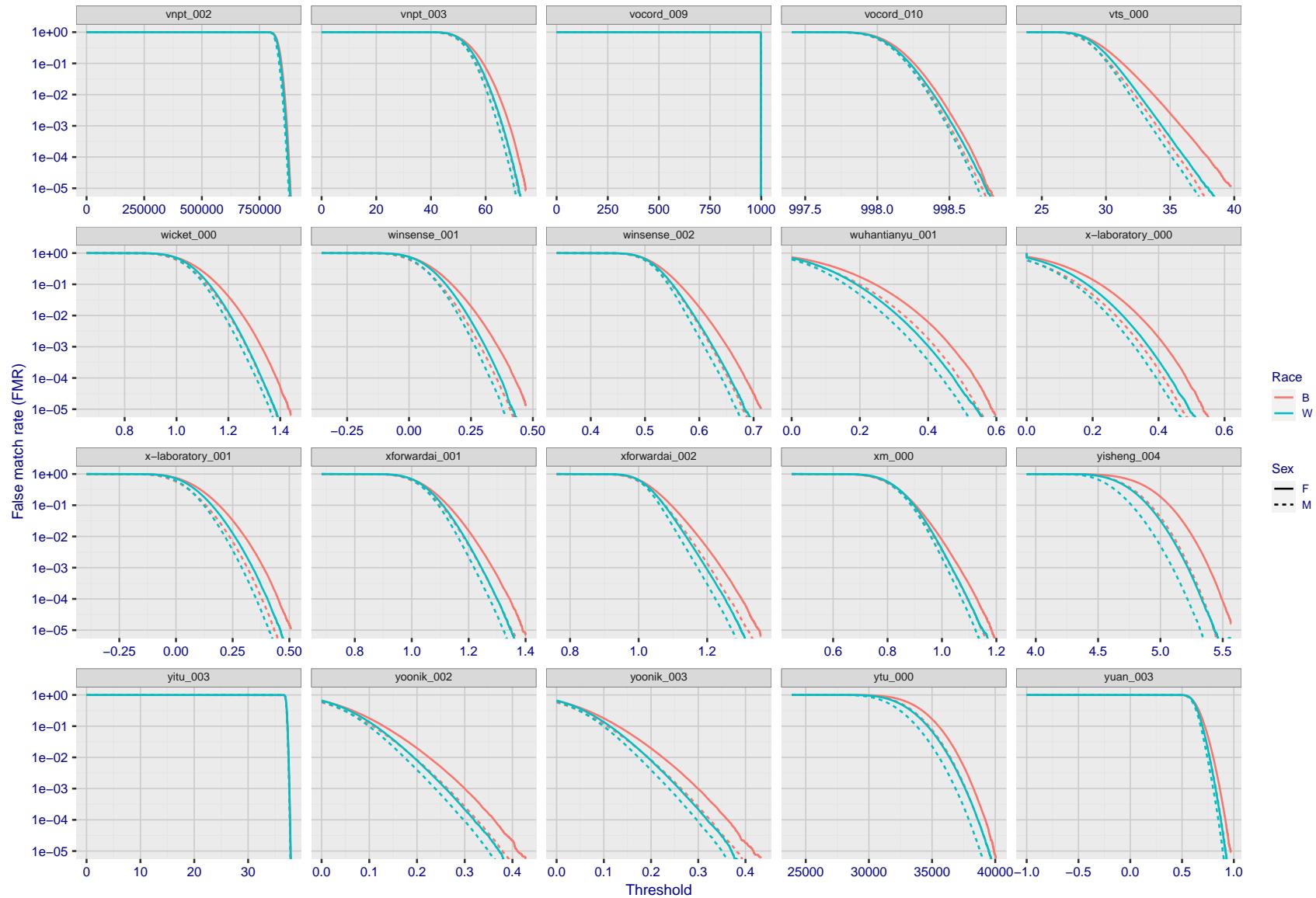


Figure 193: For the mugshot images, the false match calibration curves show false match rate vs. threshold. Separate curves appear for white females, black females, black males and white males.

FNMR(T)
"False non-match rate"
"False match rate"

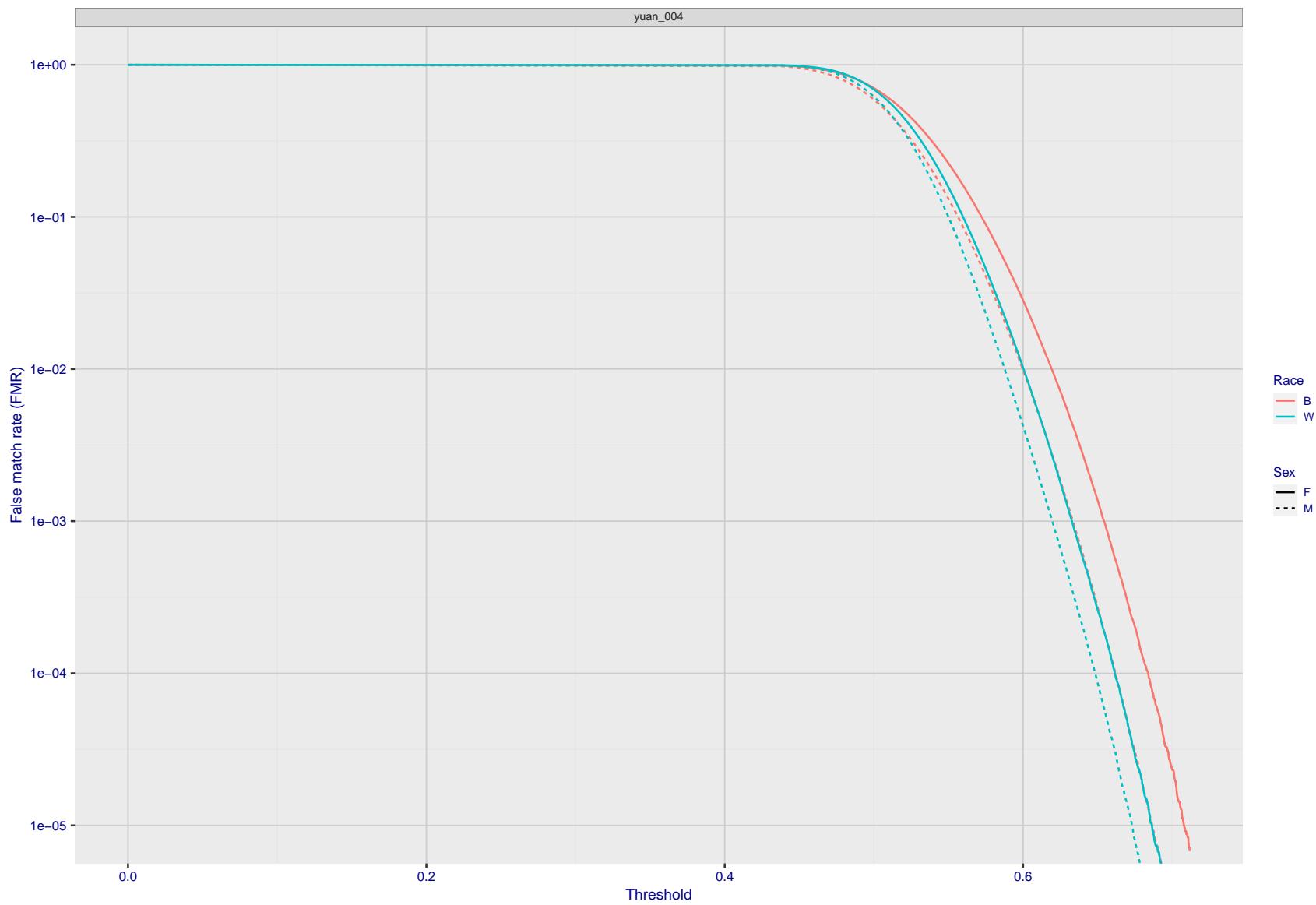


Figure 194: For the mugshot images, the false match calibration curves show false match rate vs. threshold. Separate curves appear for white females, black females, black males and white males.

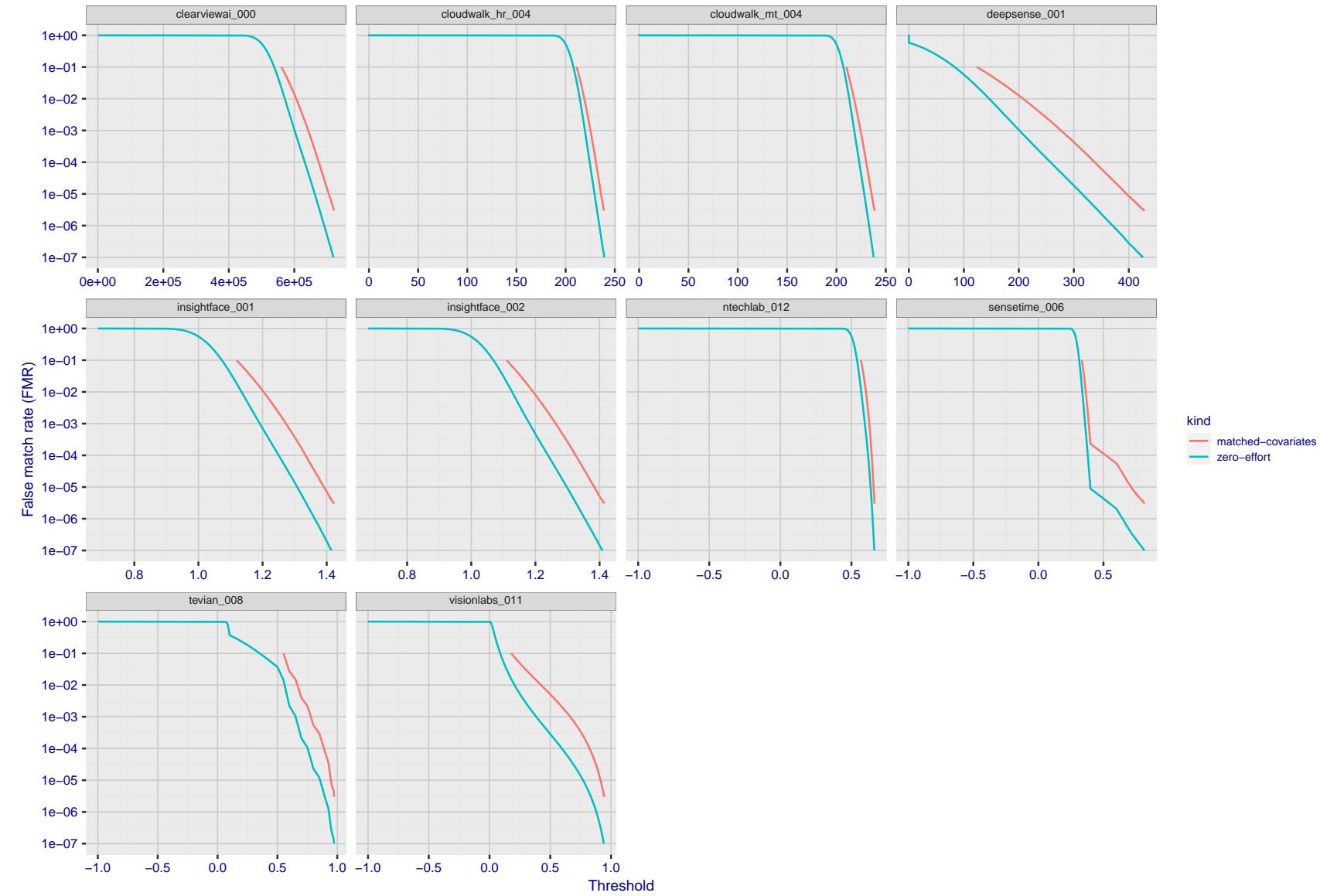


Figure 195: For the visa images, the false match calibration curves show FMR vs. threshold, T . The blue (lower) curves are for zero-effort impostors (i.e. comparing all images against all). The red (upper) curves are for persons of the same-sex, same-age, and same national-origin. This shows that FMR is underestimated (by a factor of 10 or more) by using a zero-effort impostor calculation to calibrate T . As shown later (sec. 3.6), FMR is higher for demographic-matched impostors.

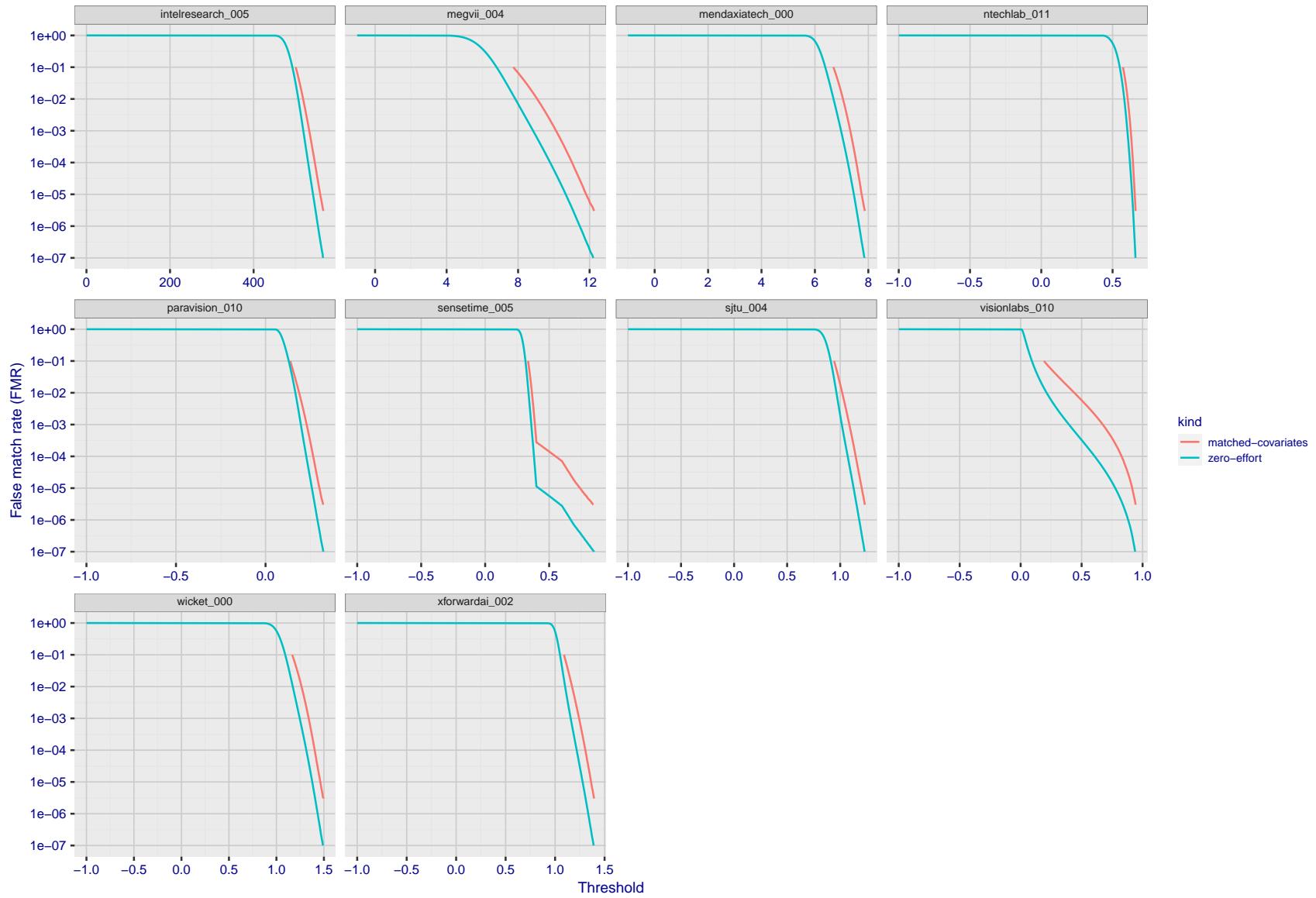


Figure 196: For the visa images, the false match calibration curves show FMR vs. threshold, T . The blue (lower) curves are for zero-effort impostors (i.e. comparing all images against all). The red (upper) curves are for persons of the same-sex, same-age, and same national-origin. This shows that FMR is underestimated (by a factor of 10 or more) by using a zero-effort impostor calculation to calibrate T . As shown later (sec. 3.6), FMR is higher for demographic-matched impostors.

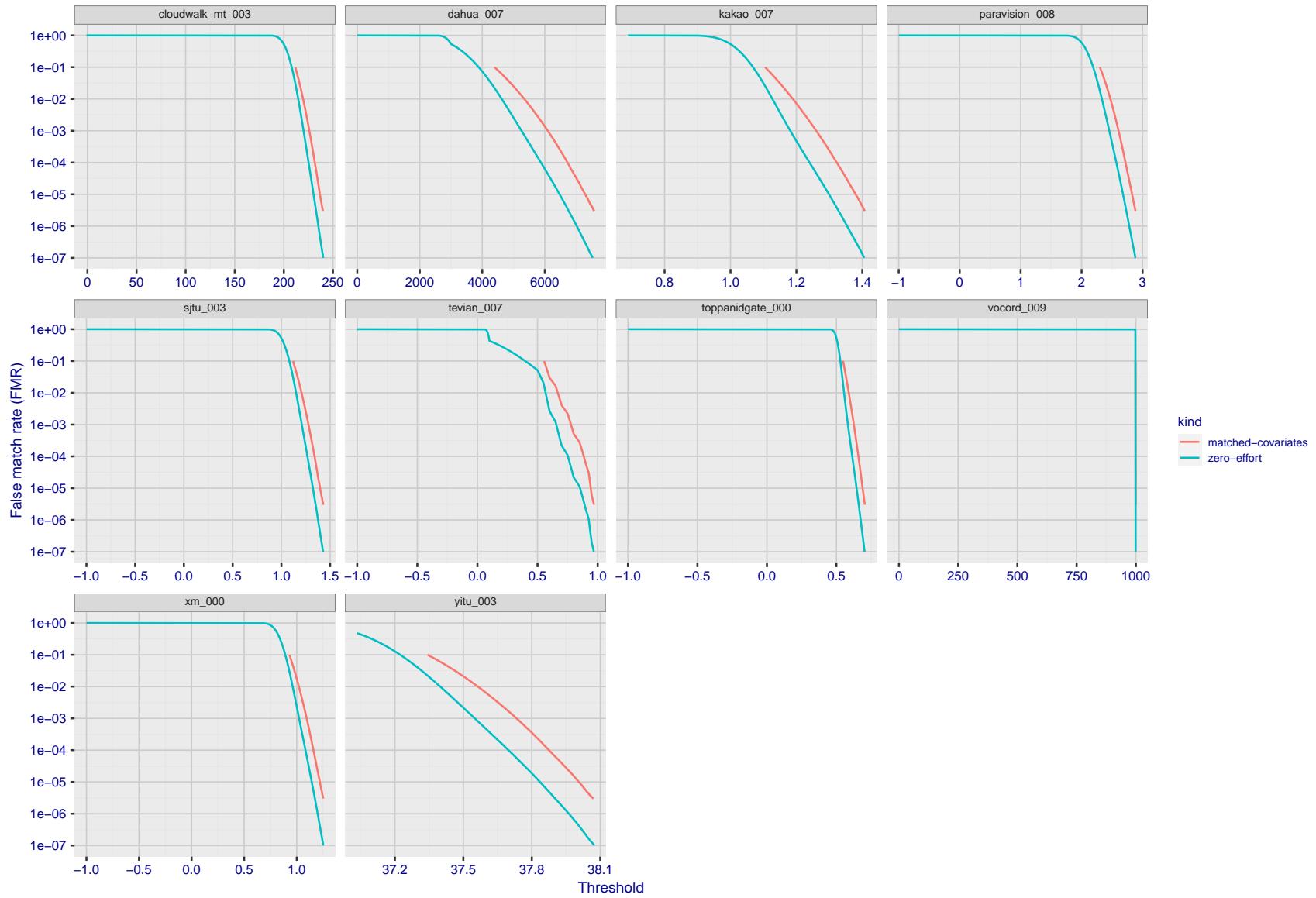


Figure 197: For the visa images, the false match calibration curves show FMR vs. threshold, T . The blue (lower) curves are for zero-effort impostors (i.e. comparing all images against all). The red (upper) curves are for persons of the same-sex, same-age, and same national-origin. This shows that FMR is underestimated (by a factor of 10 or more) by using a zero-effort impostor calculation to calibrate T . As shown later (sec. 3.6), FMR is higher for demographic-matched impostors.

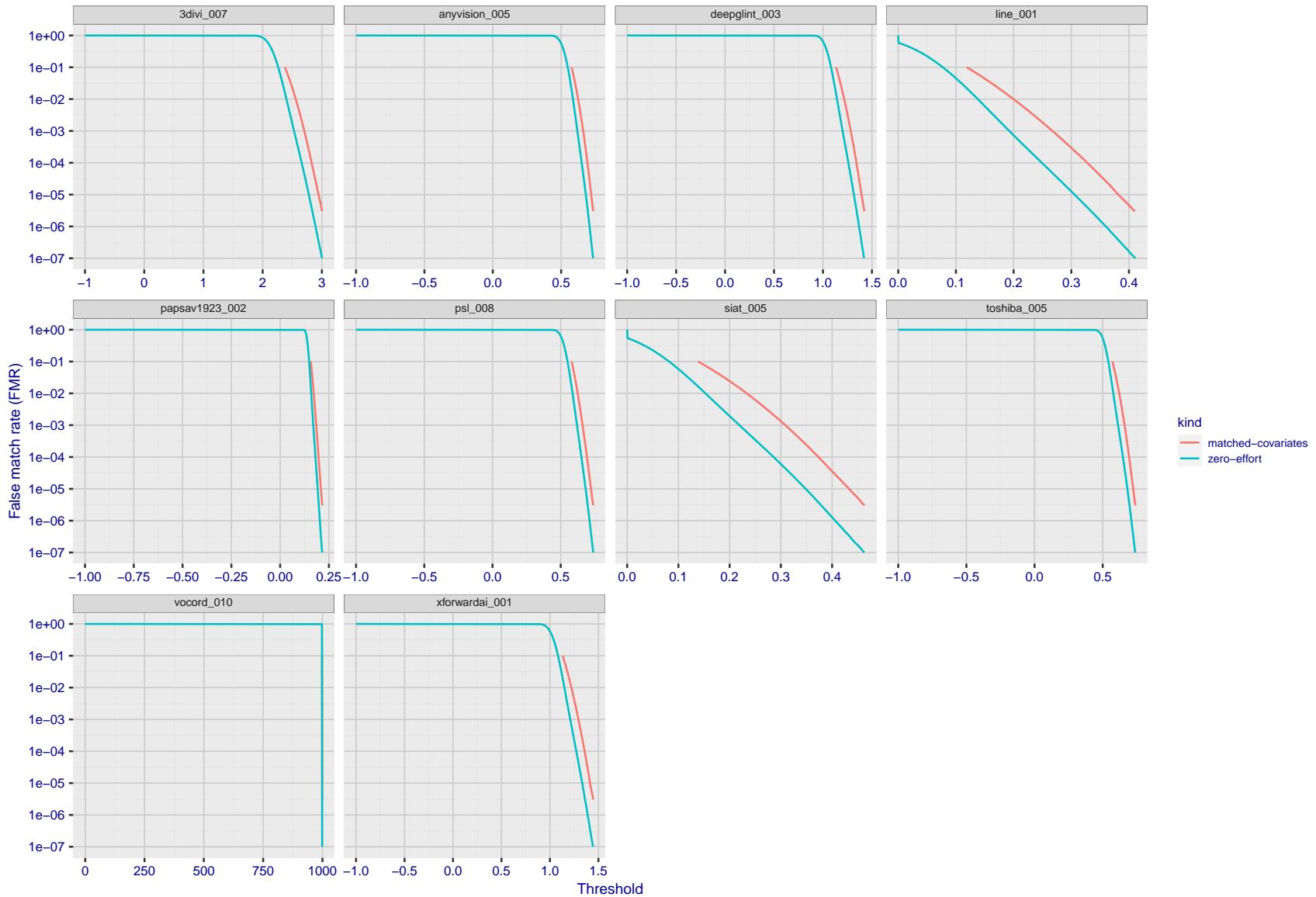


Figure 198: For the visa images, the false match calibration curves show FMR vs. threshold, T . The blue (lower) curves are for zero-effort impostors (i.e. comparing all images against all). The red (upper) curves are for persons of the same-sex, same-age, and same national-origin. This shows that FMR is underestimated (by a factor of 10 or more) by using a zero-effort impostor calculation to calibrate T . As shown later (sec. 3.6), FMR is higher for demographic-matched impostors.

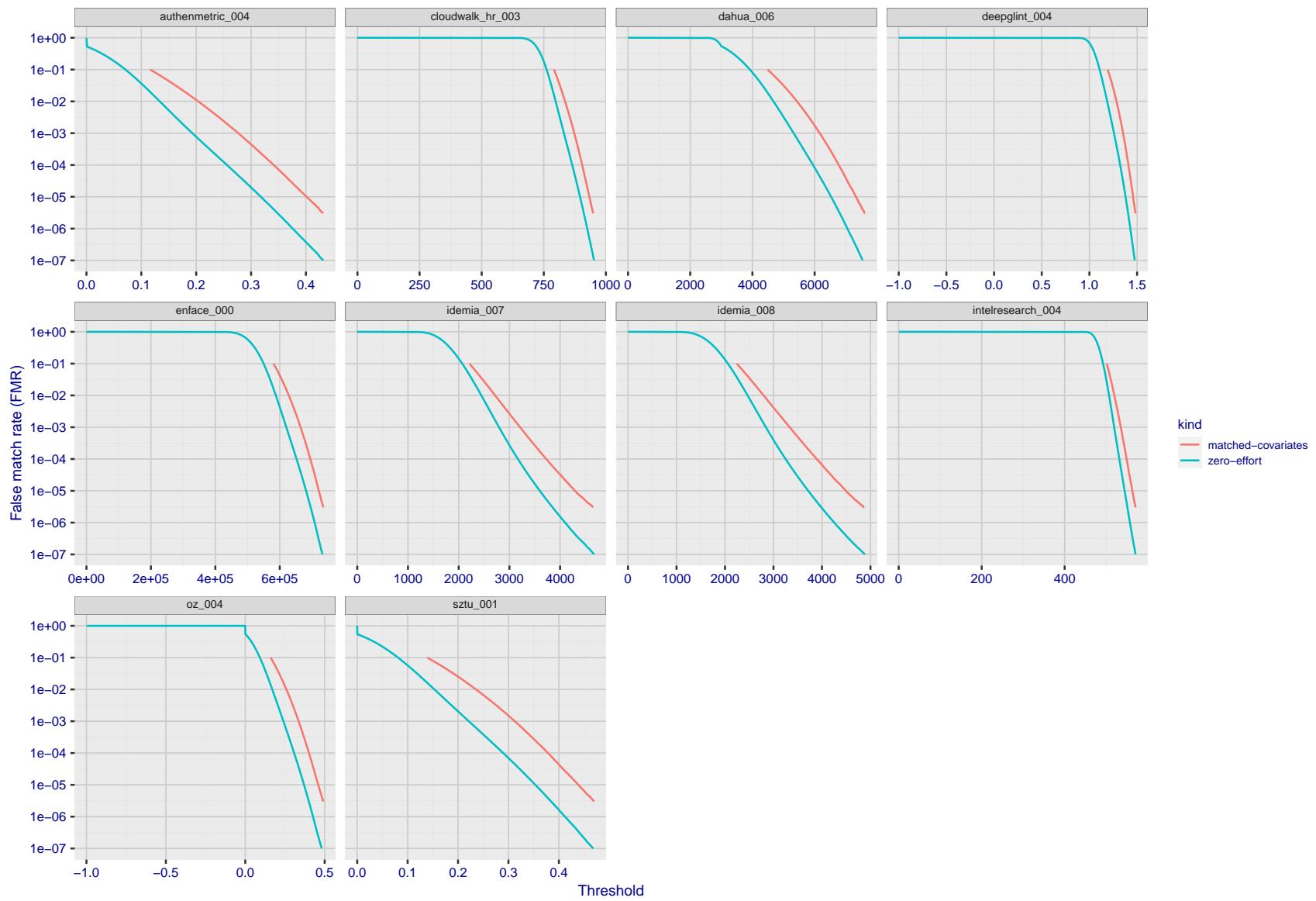


Figure 199: For the visa images, the false match calibration curves show FMR vs. threshold, T . The blue (lower) curves are for zero-effort impostors (i.e. comparing all images against all). The red (upper) curves are for persons of the same-sex, same-age, and same national-origin. This shows that FMR is underestimated (by a factor of 10 or more) by using a zero-effort impostor calculation to calibrate T . As shown later (sec. 3.6), FMR is higher for demographic-matched impostors.

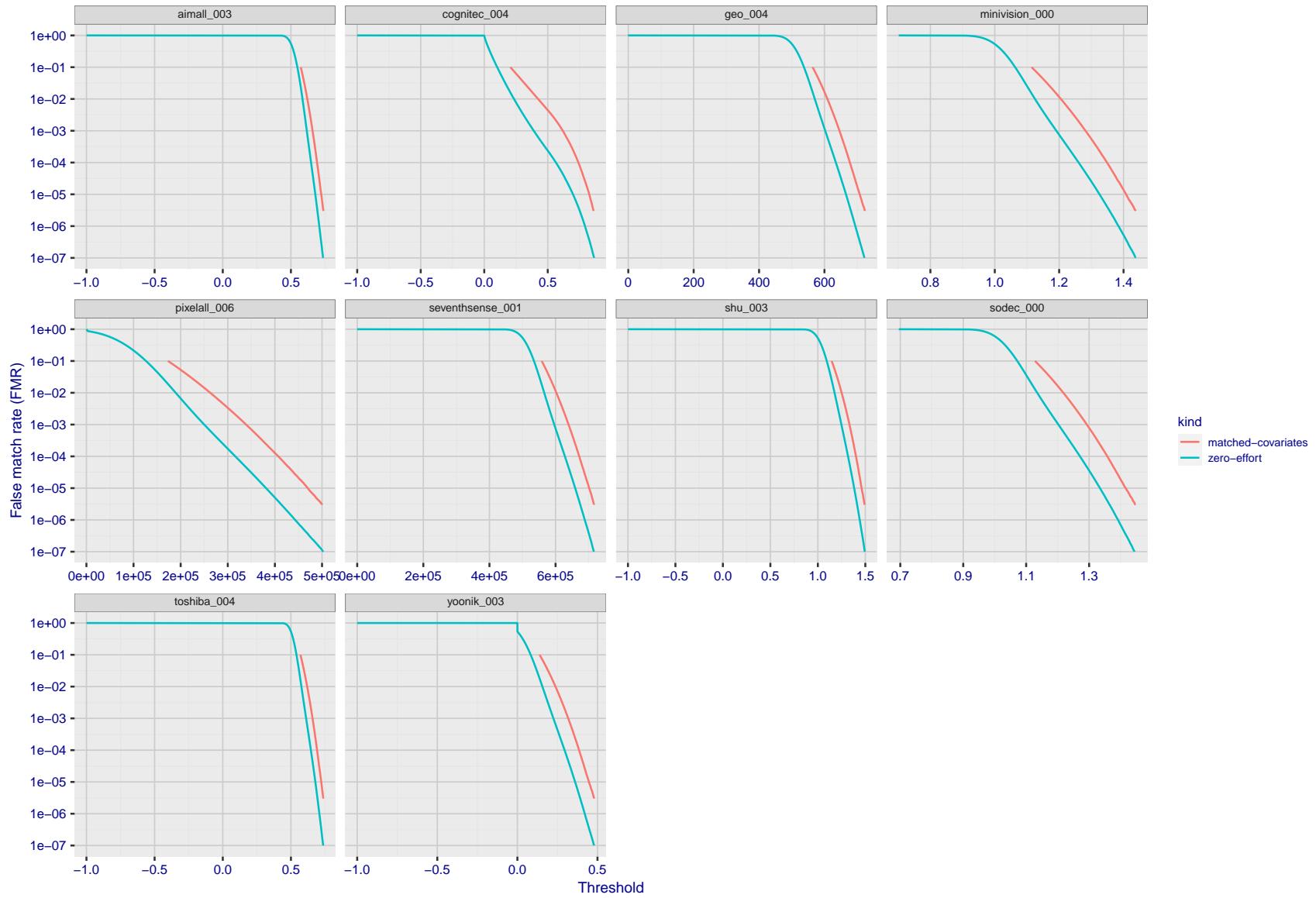


Figure 200: For the visa images, the false match calibration curves show FMR vs. threshold, T . The blue (lower) curves are for zero-effort impostors (i.e. comparing all images against all). The red (upper) curves are for persons of the same-sex, same-age, and same national-origin. This shows that FMR is underestimated (by a factor of 10 or more) by using a zero-effort impostor calculation to calibrate T . As shown later (sec. 3.6), FMR is higher for demographic-matched impostors.

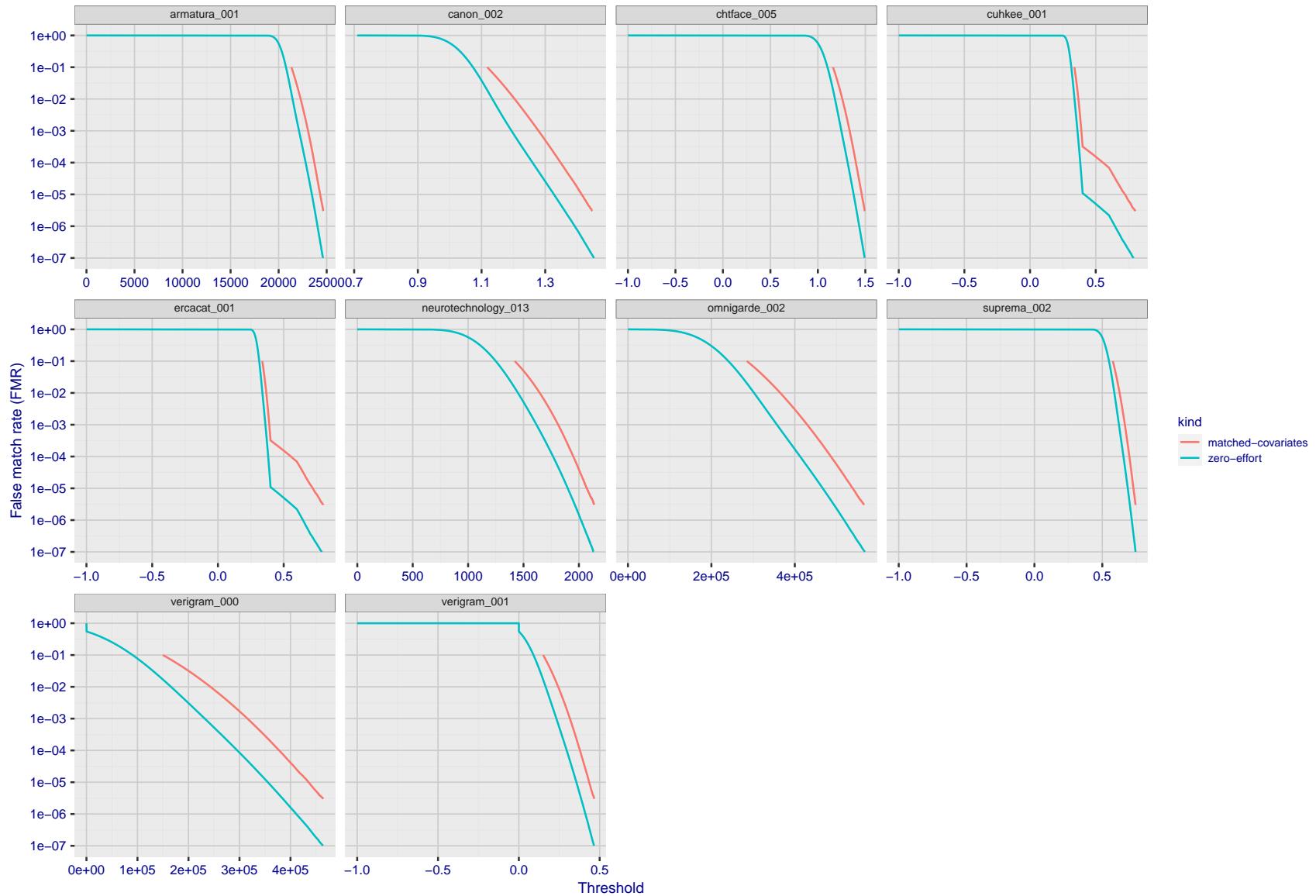


Figure 201: For the visa images, the false match calibration curves show FMR vs. threshold, T . The blue (lower) curves are for zero-effort impostors (i.e. comparing all images against all). The red (upper) curves are for persons of the same-sex, same-age, and same national-origin. This shows that FMR is underestimated (by a factor of 10 or more) by using a zero-effort impostor calculation to calibrate T . As shown later (sec. 3.6), FMR is higher for demographic-matched impostors.

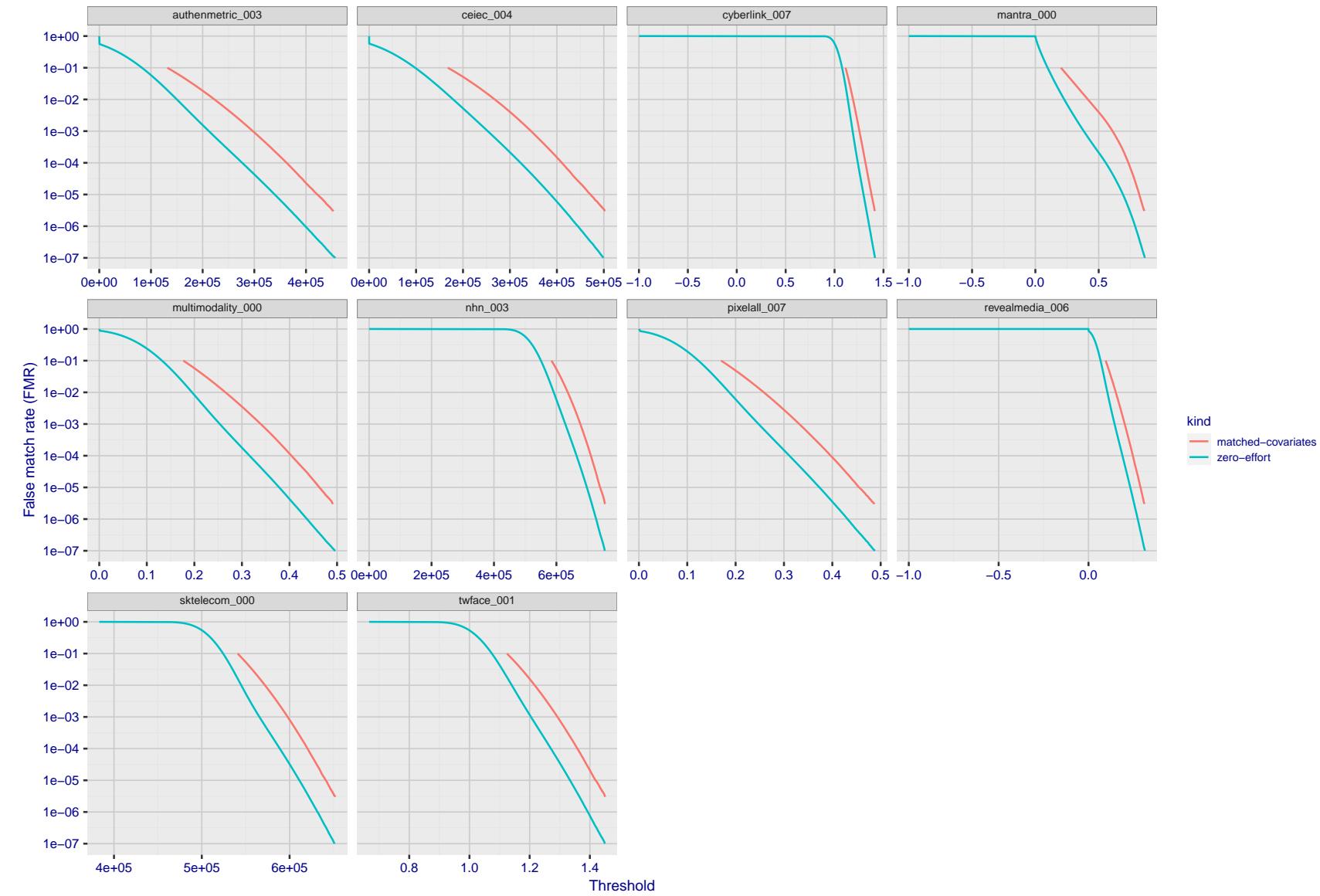


Figure 202: For the visa images, the false match calibration curves show FMR vs. threshold, T . The blue (lower) curves are for zero-effort impostors (i.e. comparing all images against all). The red (upper) curves are for persons of the same-sex, same-age, and same national-origin. This shows that FMR is underestimated (by a factor of 10 or more) by using a zero-effort impostor calculation to calibrate T . As shown later (sec. 3.6), FMR is higher for demographic-matched impostors.

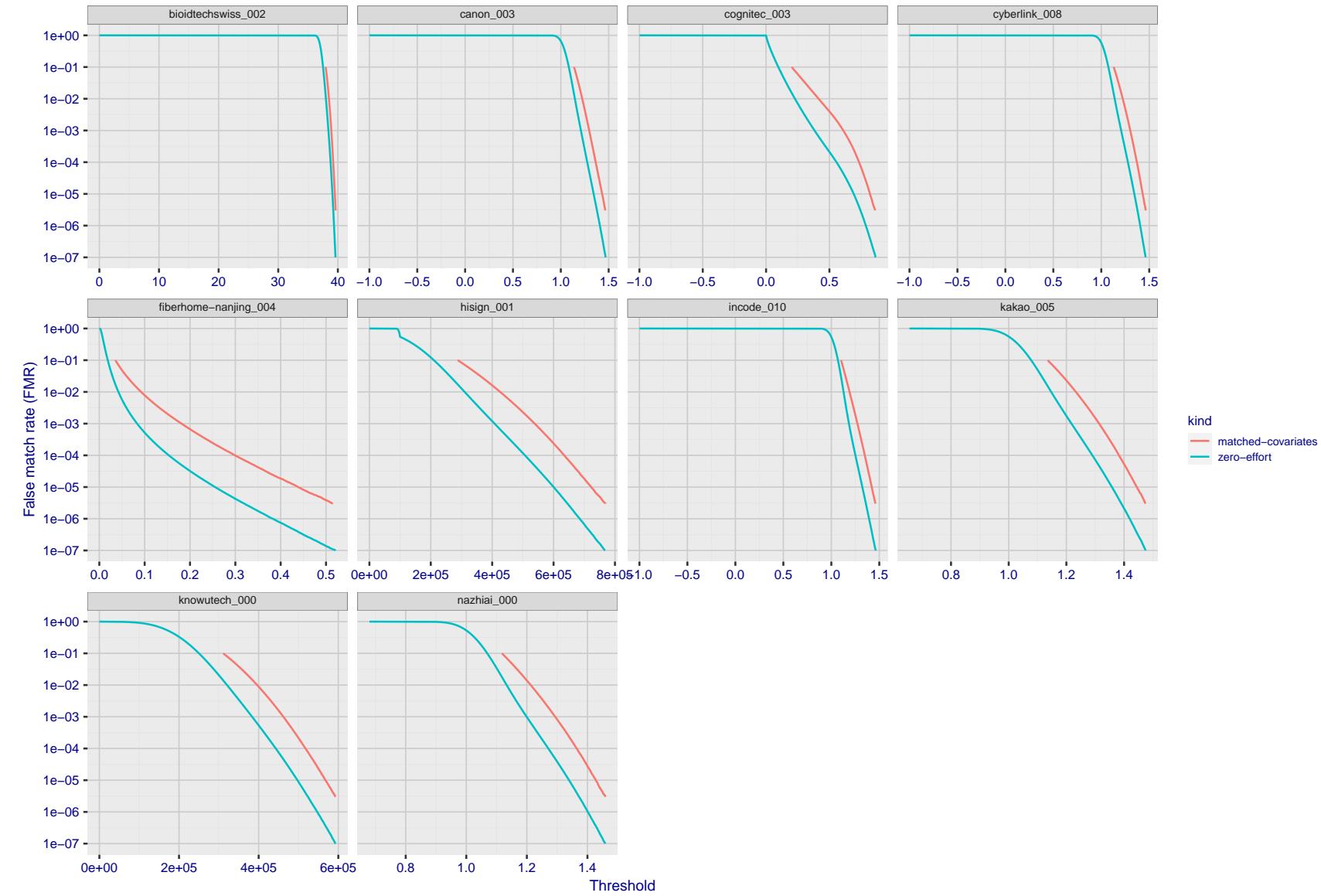


Figure 203: For the visa images, the false match calibration curves show FMR vs. threshold, T . The blue (lower) curves are for zero-effort impostors (i.e. comparing all images against all). The red (upper) curves are for persons of the same-sex, same-age, and same national-origin. This shows that FMR is underestimated (by a factor of 10 or more) by using a zero-effort impostor calculation to calibrate T . As shown later (sec. 3.6), FMR is higher for demographic-matched impostors.

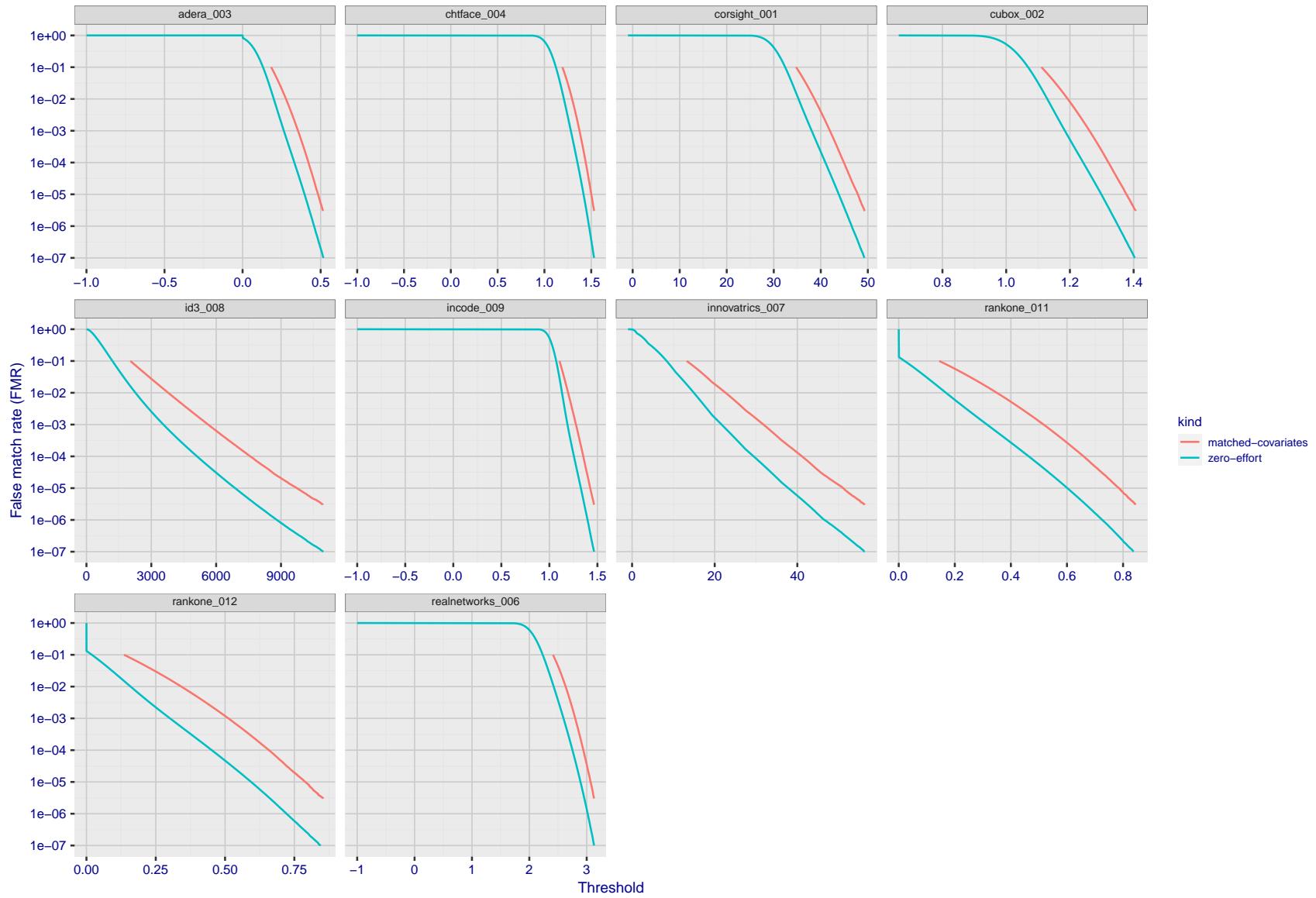


Figure 204: For the visa images, the false match calibration curves show FMR vs. threshold, T . The blue (lower) curves are for zero-effort impostors (i.e. comparing all images against all). The red (upper) curves are for persons of the same-sex, same-age, and same national-origin. This shows that FMR is underestimated (by a factor of 10 or more) by using a zero-effort impostor calculation to calibrate T . As shown later (sec. 3.6), FMR is higher for demographic-matched impostors.

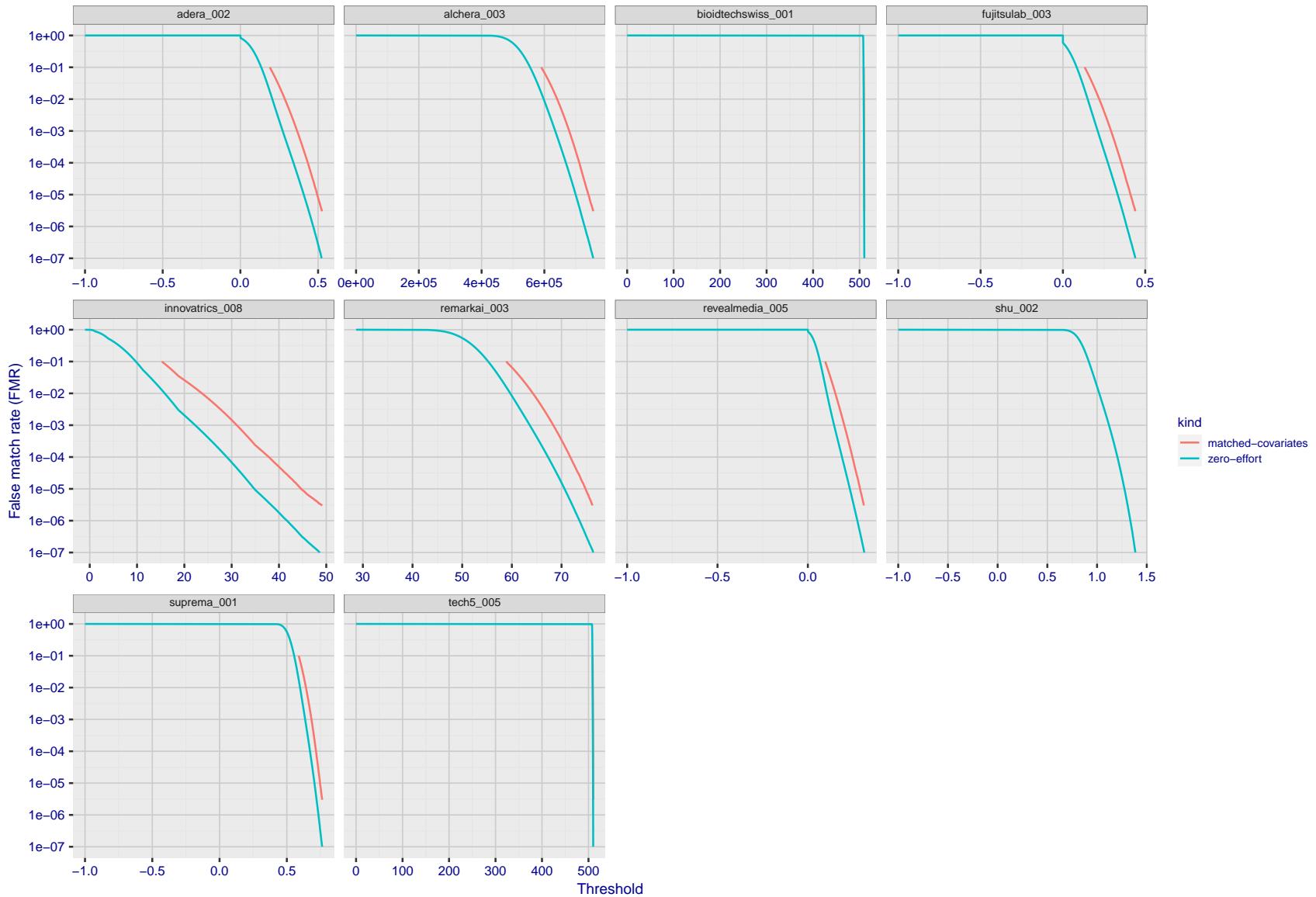


Figure 205: For the visa images, the false match calibration curves show FMR vs. threshold, T . The blue (lower) curves are for zero-effort impostors (i.e. comparing all images against all). The red (upper) curves are for persons of the same-sex, same-age, and same national-origin. This shows that FMR is underestimated (by a factor of 10 or more) by using a zero-effort impostor calculation to calibrate T . As shown later (sec. 3.6), FMR is higher for demographic-matched impostors.

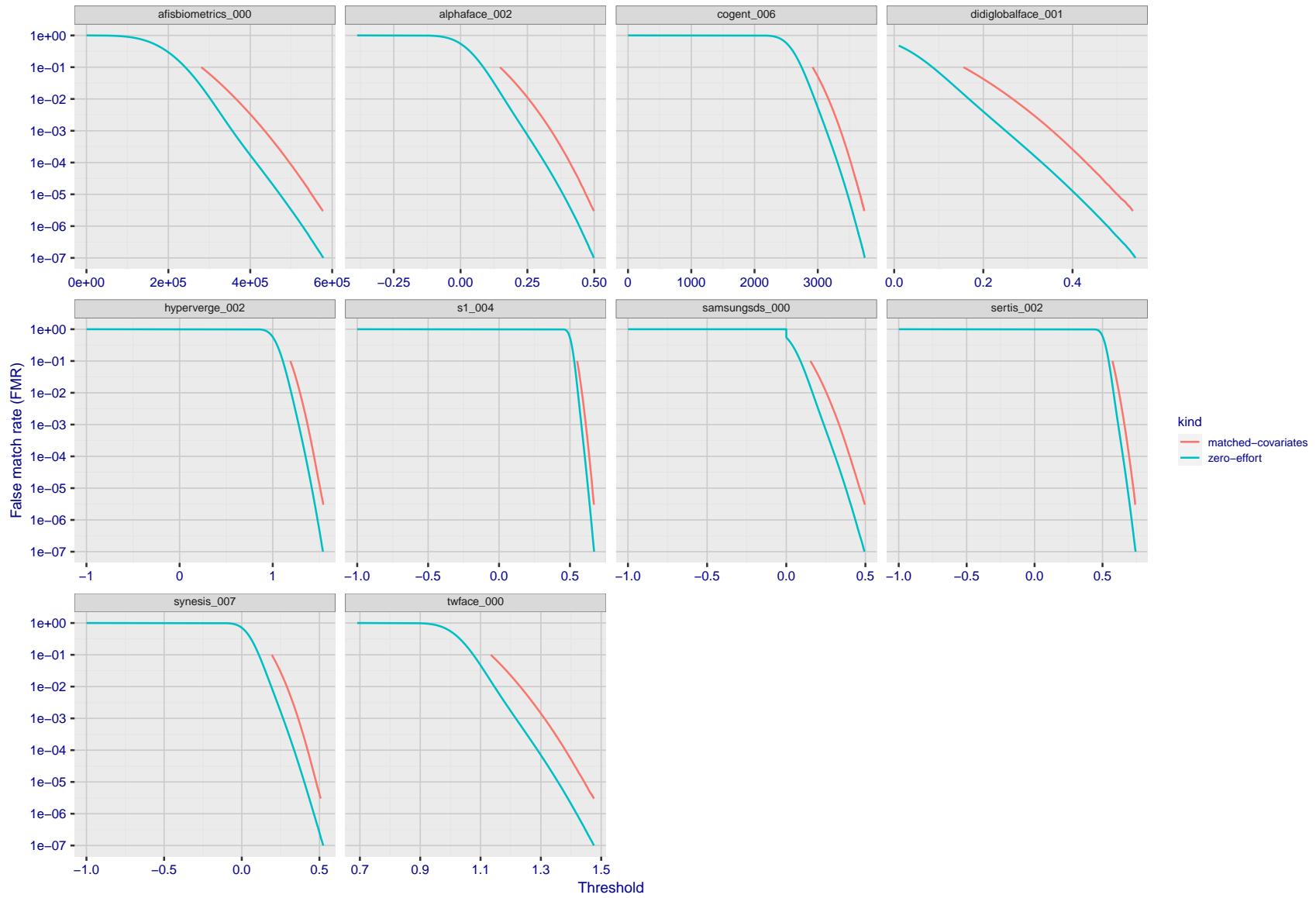


Figure 206: For the visa images, the false match calibration curves show FMR vs. threshold, T . The blue (lower) curves are for zero-effort impostors (i.e. comparing all images against all). The red (upper) curves are for persons of the same-sex, same-age, and same national-origin. This shows that FMR is underestimated (by a factor of 10 or more) by using a zero-effort impostor calculation to calibrate T . As shown later (sec. 3.6), FMR is higher for demographic-matched impostors.

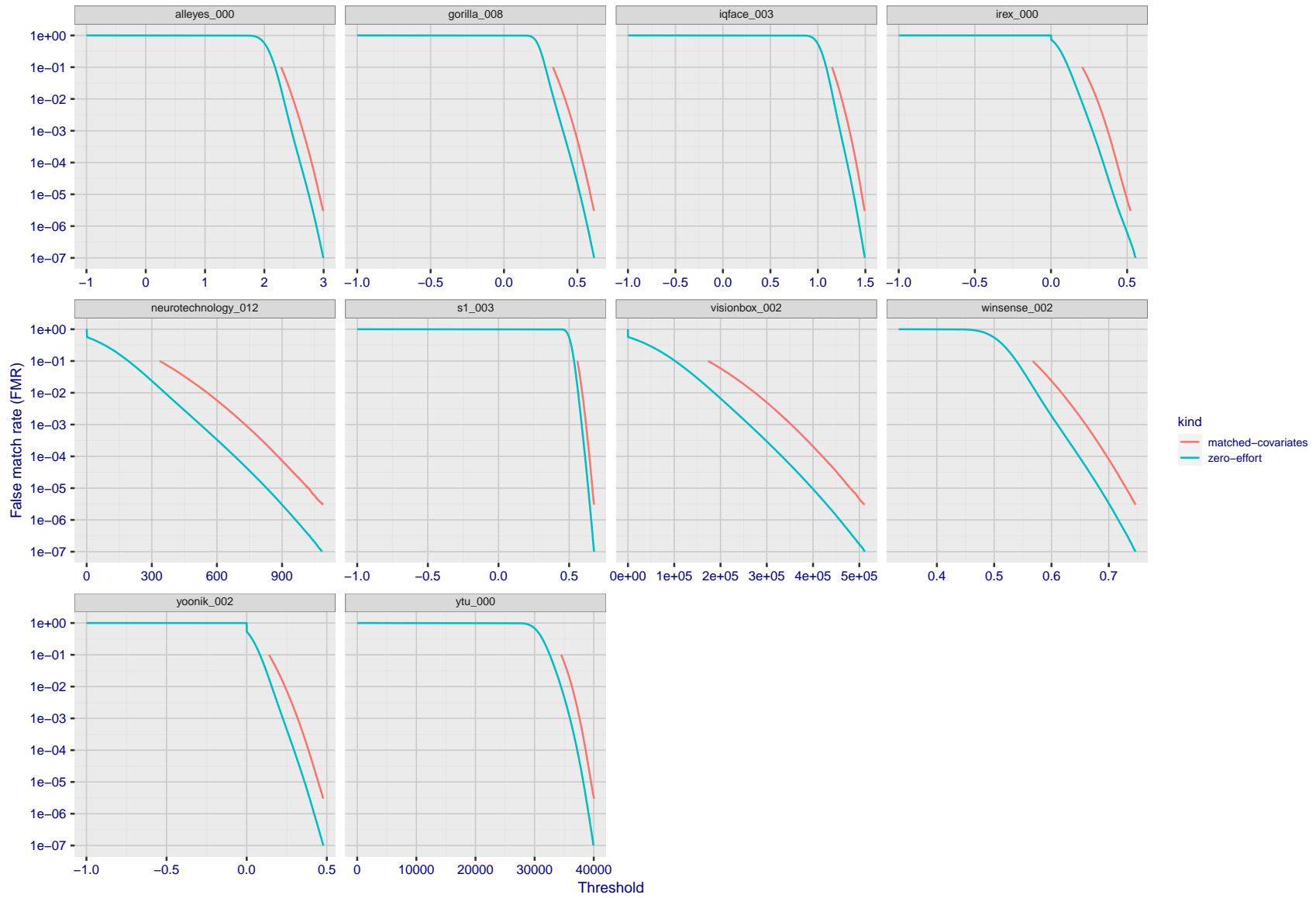


Figure 207: For the visa images, the false match calibration curves show FMR vs. threshold, T . The blue (lower) curves are for zero-effort impostors (i.e. comparing all images against all). The red (upper) curves are for persons of the same-sex, same-age, and same national-origin. This shows that FMR is underestimated (by a factor of 10 or more) by using a zero-effort impostor calculation to calibrate T . As shown later (sec. 3.6), FMR is higher for demographic-matched impostors.

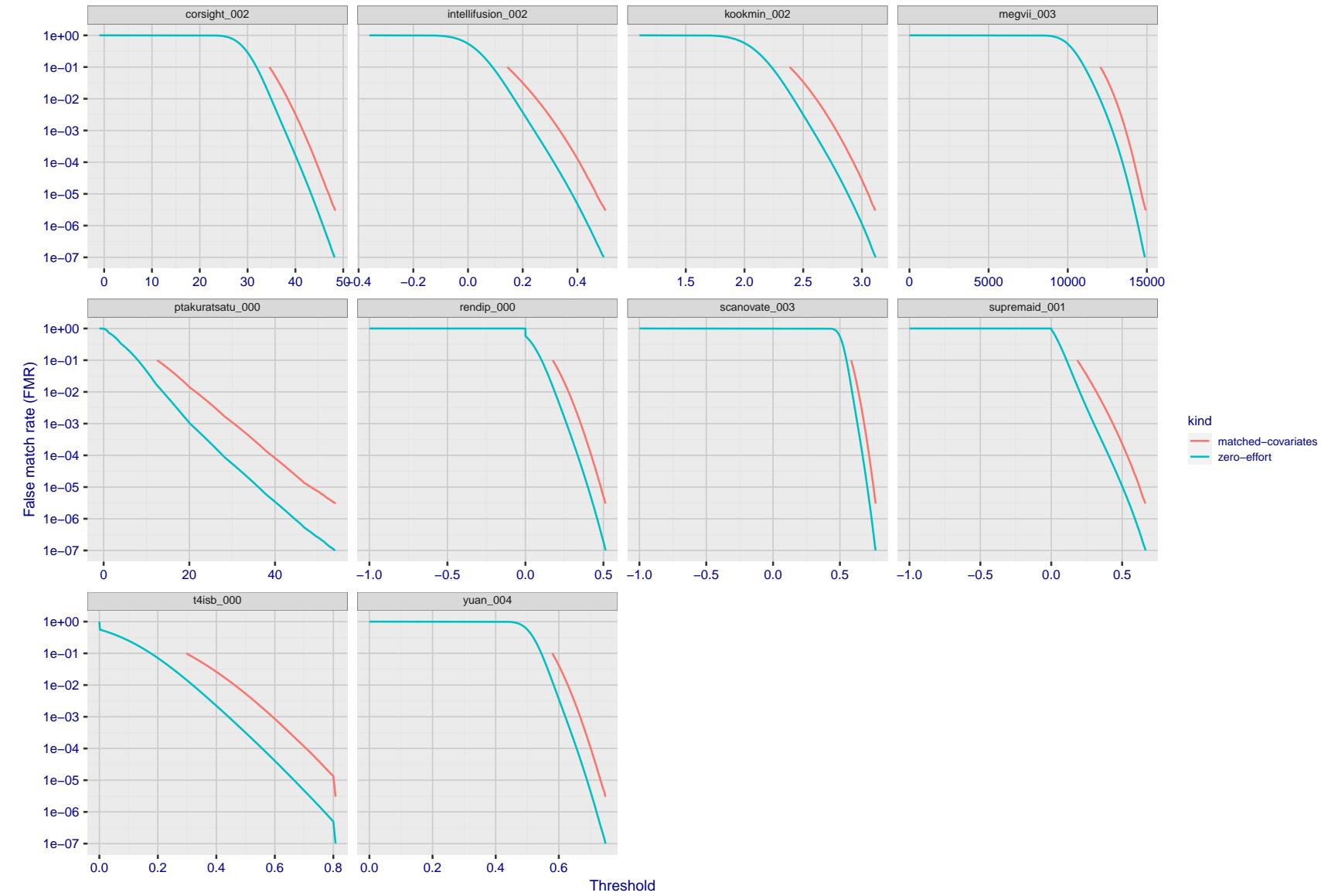


Figure 208: For the visa images, the false match calibration curves show FMR vs. threshold, T . The blue (lower) curves are for zero-effort impostors (i.e. comparing all images against all). The red (upper) curves are for persons of the same-sex, same-age, and same national-origin. This shows that FMR is underestimated (by a factor of 10 or more) by using a zero-effort impostor calculation to calibrate T . As shown later (sec. 3.6), FMR is higher for demographic-matched impostors.

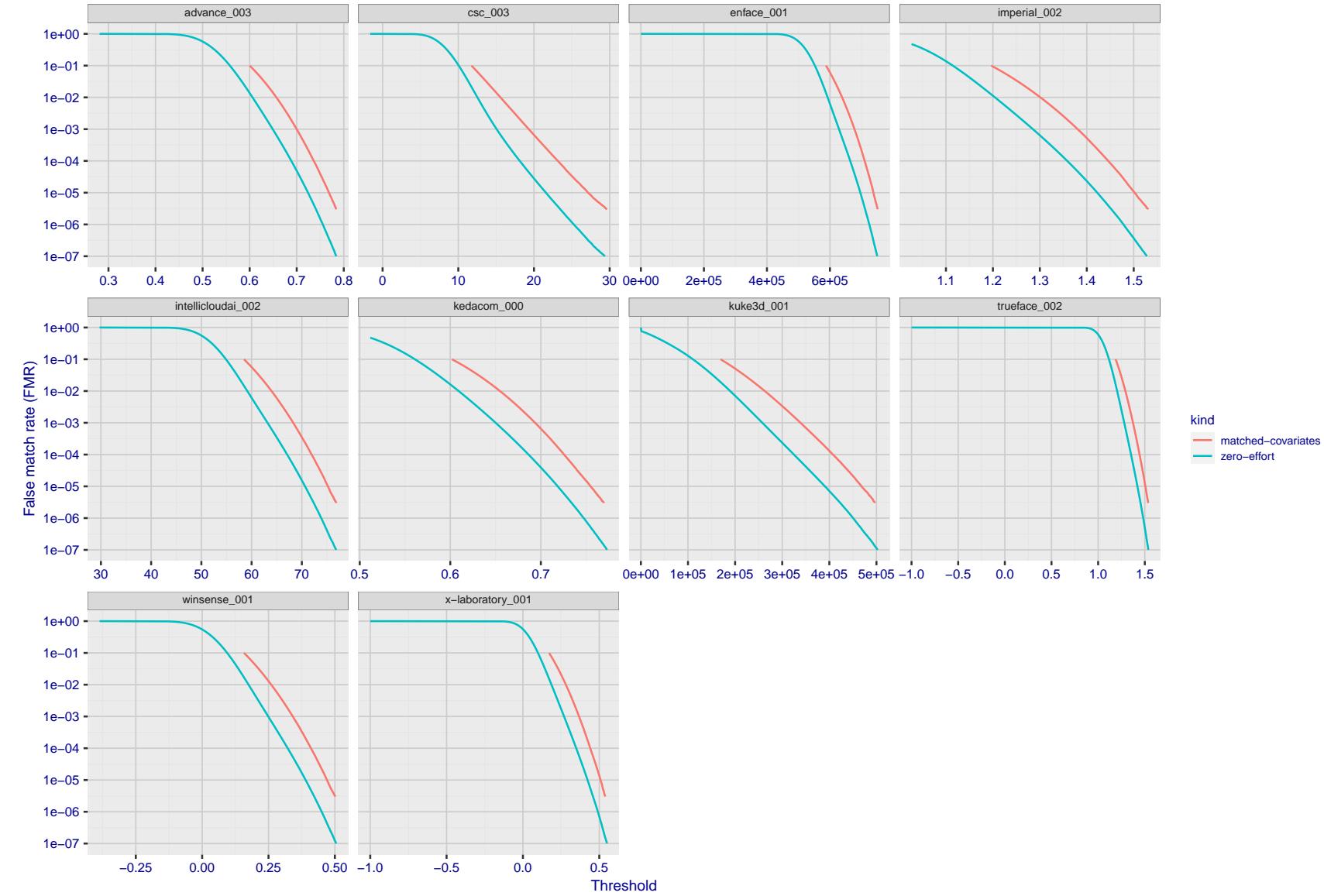


Figure 209: For the visa images, the false match calibration curves show FMR vs. threshold, T . The blue (lower) curves are for zero-effort impostors (i.e. comparing all images against all). The red (upper) curves are for persons of the same-sex, same-age, and same national-origin. This shows that FMR is underestimated (by a factor of 10 or more) by using a zero-effort impostor calculation to calibrate T . As shown later (sec. 3.6), FMR is higher for demographic-matched impostors.

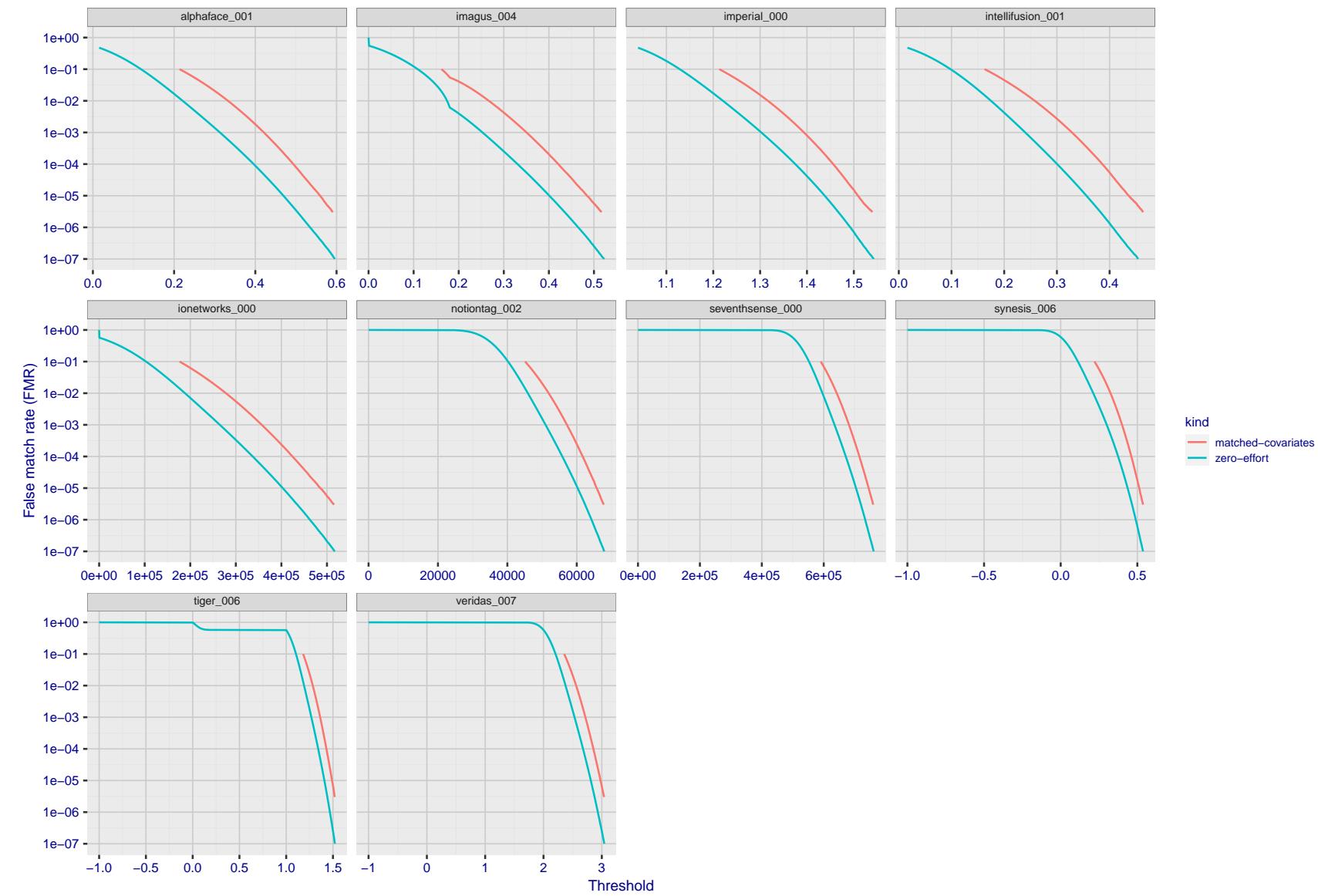


Figure 210: For the visa images, the false match calibration curves show FMR vs. threshold, T . The blue (lower) curves are for zero-effort impostors (i.e. comparing all images against all). The red (upper) curves are for persons of the same-sex, same-age, and same national-origin. This shows that FMR is underestimated (by a factor of 10 or more) by using a zero-effort impostor calculation to calibrate T . As shown later (sec. 3.6), FMR is higher for demographic-matched impostors.

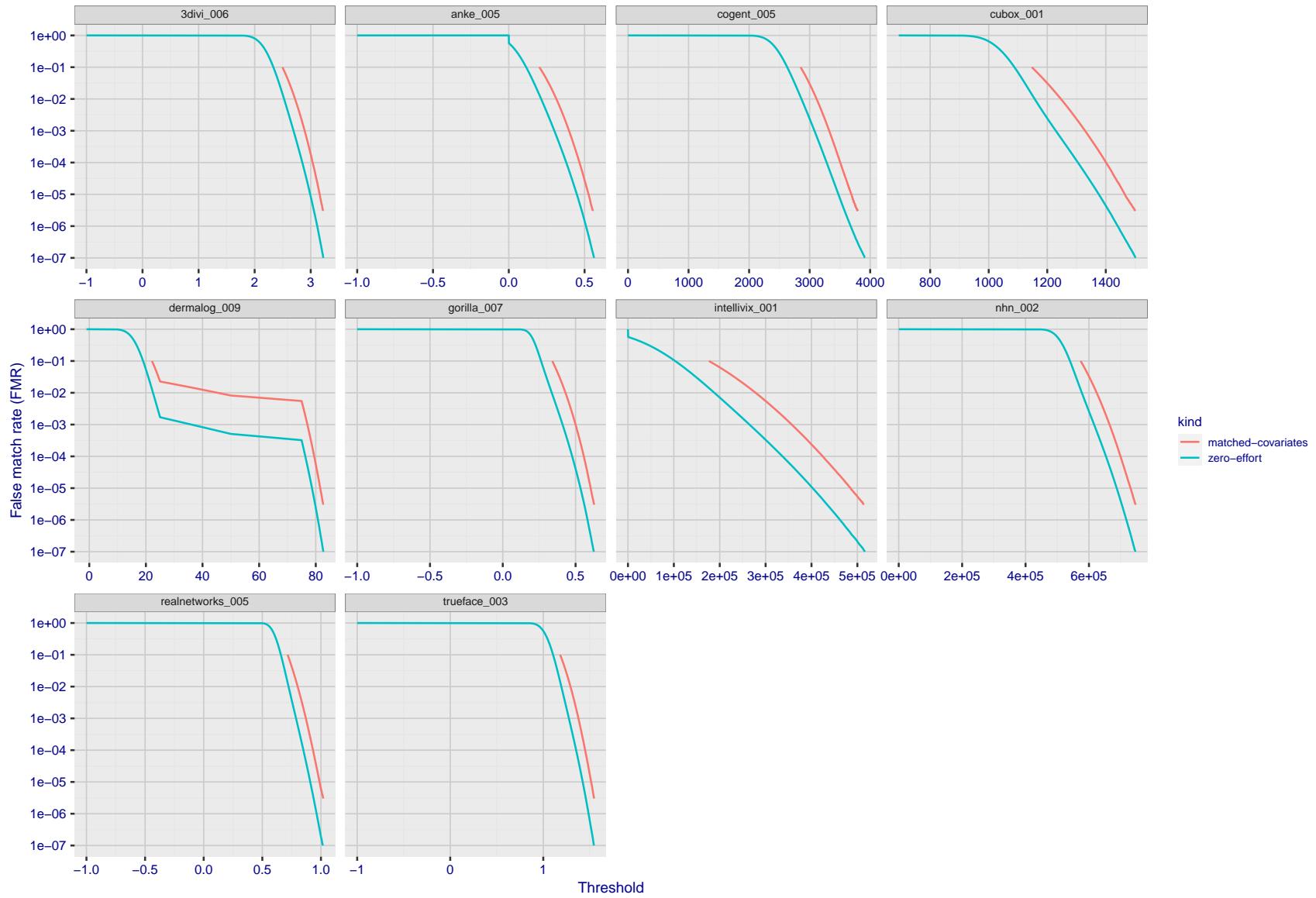


Figure 211: For the visa images, the false match calibration curves show FMR vs. threshold, T . The blue (lower) curves are for zero-effort impostors (i.e. comparing all images against all). The red (upper) curves are for persons of the same-sex, same-age, and same national-origin. This shows that FMR is underestimated (by a factor of 10 or more) by using a zero-effort impostor calculation to calibrate T . As shown later (sec. 3.6), FMR is higher for demographic-matched impostors.

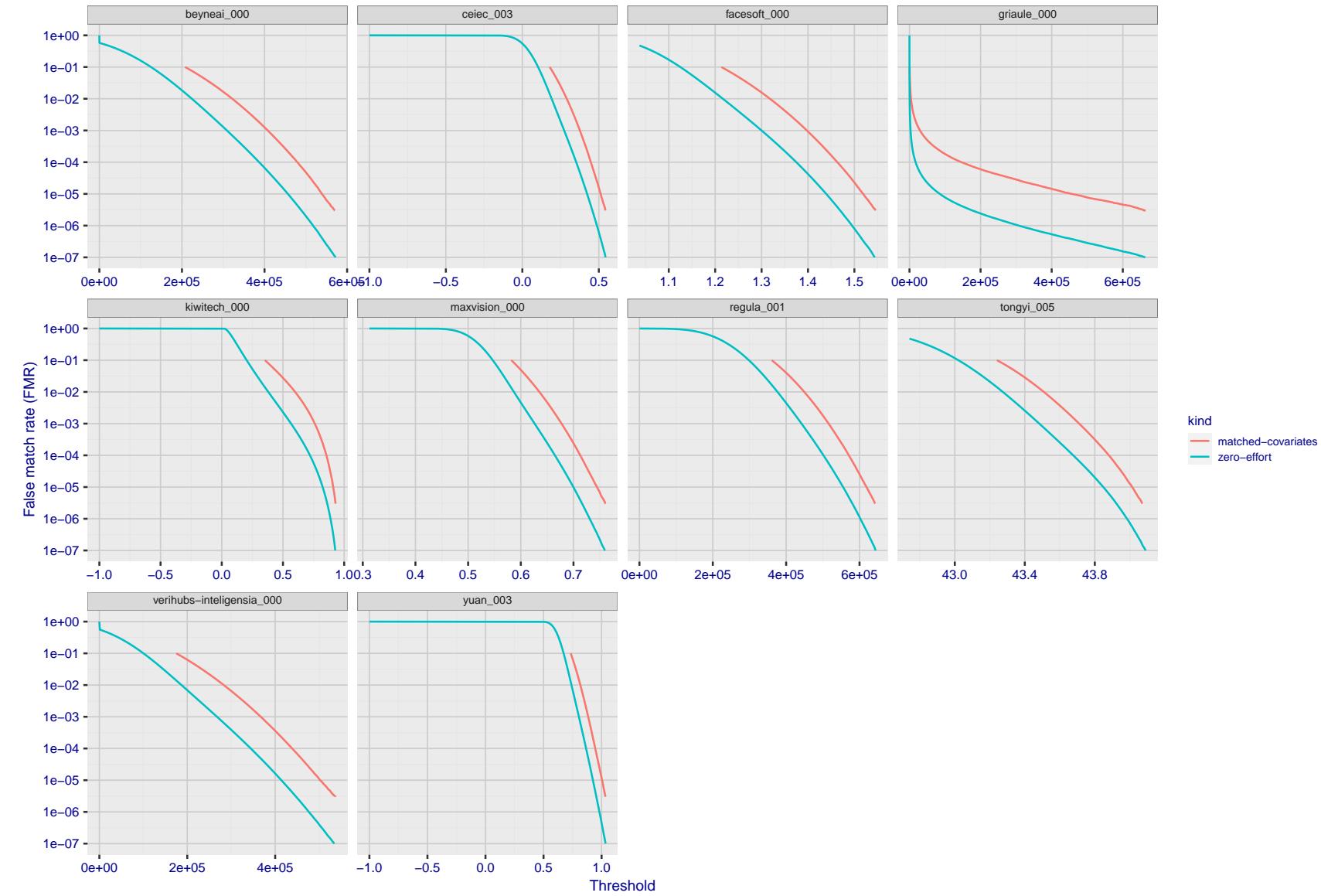


Figure 212: For the visa images, the false match calibration curves show FMR vs. threshold, T . The blue (lower) curves are for zero-effort impostors (i.e. comparing all images against all). The red (upper) curves are for persons of the same-sex, same-age, and same national-origin. This shows that FMR is underestimated (by a factor of 10 or more) by using a zero-effort impostor calculation to calibrate T . As shown later (sec. 3.6), FMR is higher for demographic-matched impostors.

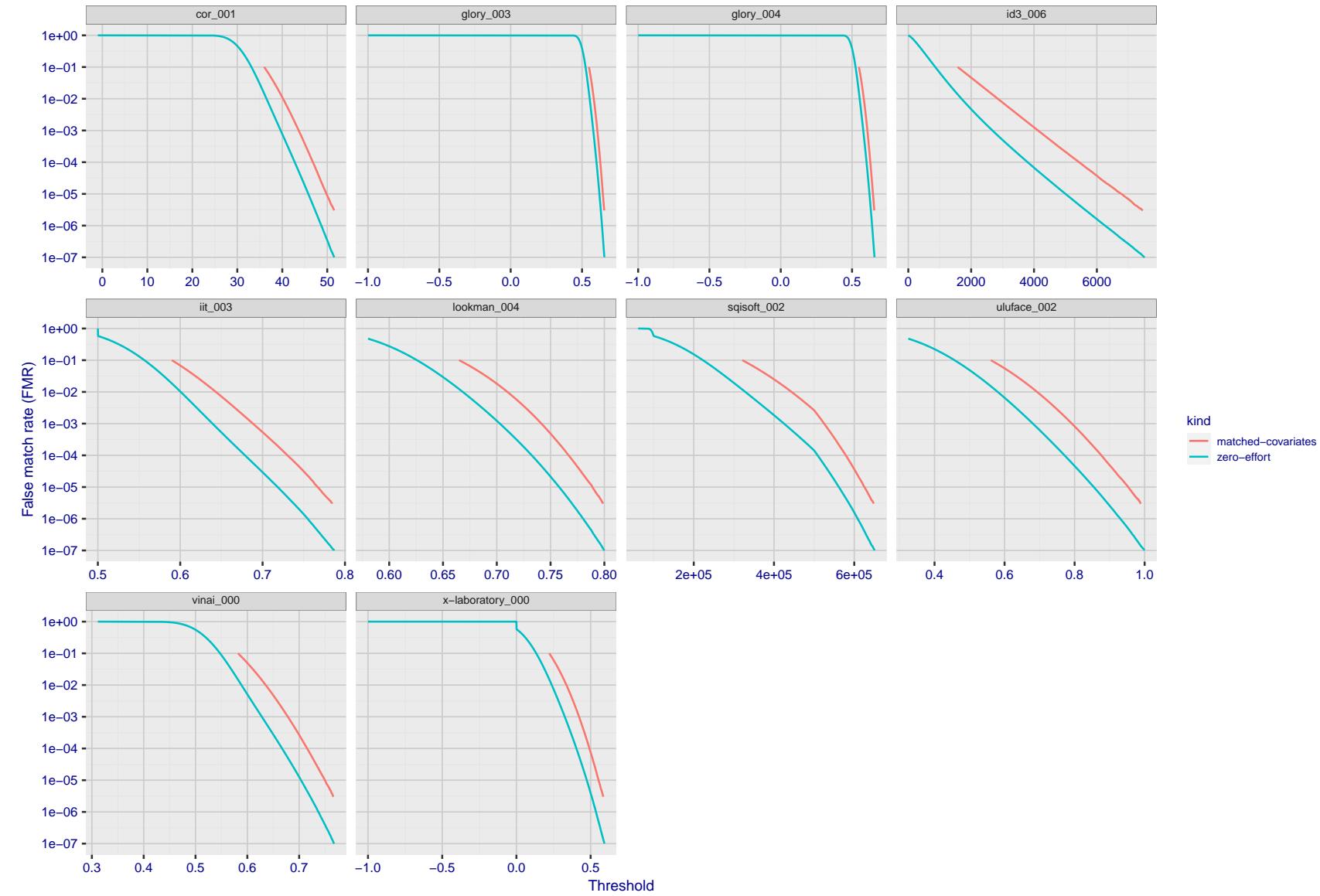


Figure 213: For the visa images, the false match calibration curves show FMR vs. threshold, T . The blue (lower) curves are for zero-effort impostors (i.e. comparing all images against all). The red (upper) curves are for persons of the same-sex, same-age, and same national-origin. This shows that FMR is underestimated (by a factor of 10 or more) by using a zero-effort impostor calculation to calibrate T . As shown later (sec. 3.6), FMR is higher for demographic-matched impostors.

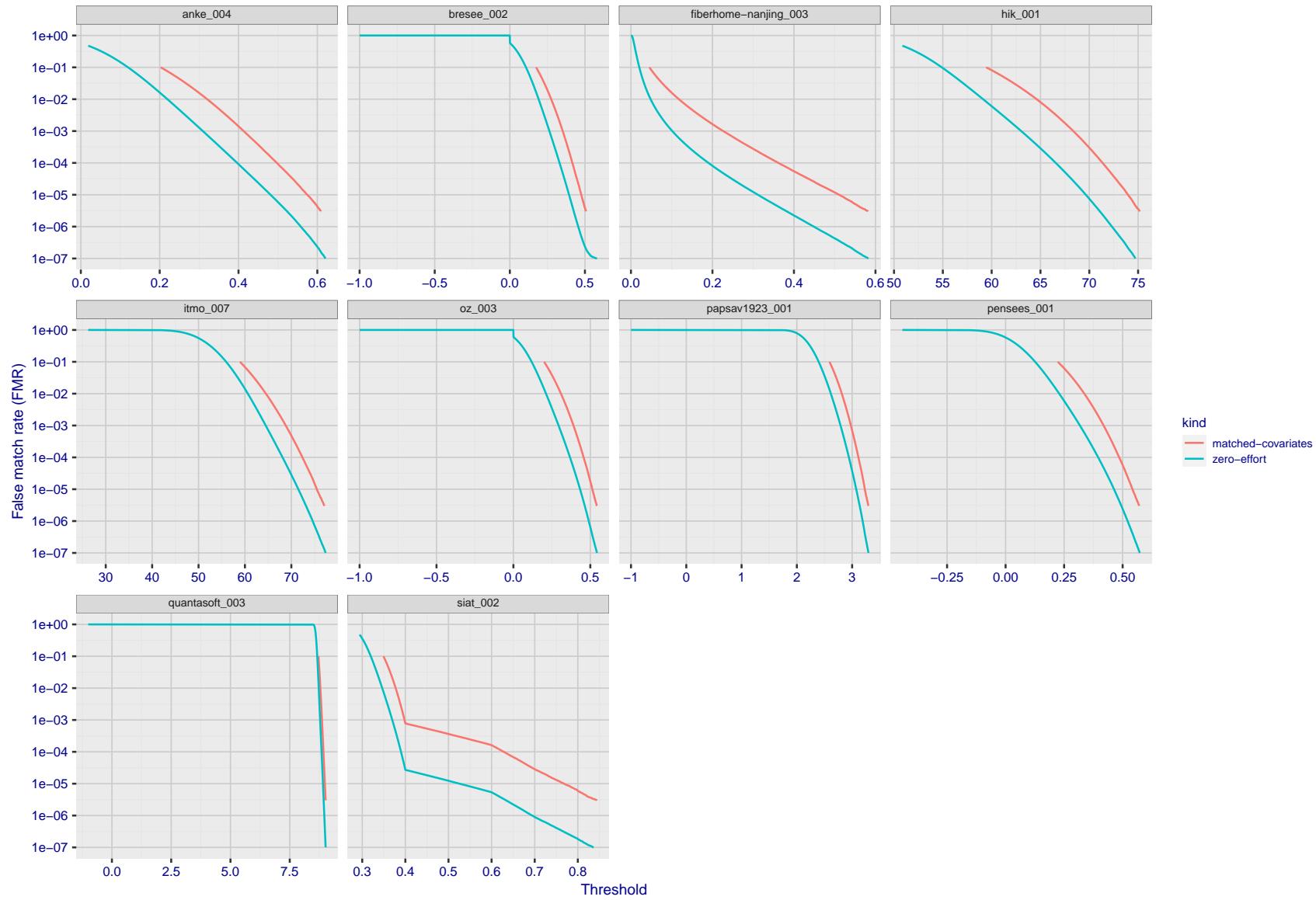


Figure 214: For the visa images, the false match calibration curves show FMR vs. threshold, T . The blue (lower) curves are for zero-effort impostors (i.e. comparing all images against all). The red (upper) curves are for persons of the same-sex, same-age, and same national-origin. This shows that FMR is underestimated (by a factor of 10 or more) by using a zero-effort impostor calculation to calibrate T . As shown later (sec. 3.6), FMR is higher for demographic-matched impostors.

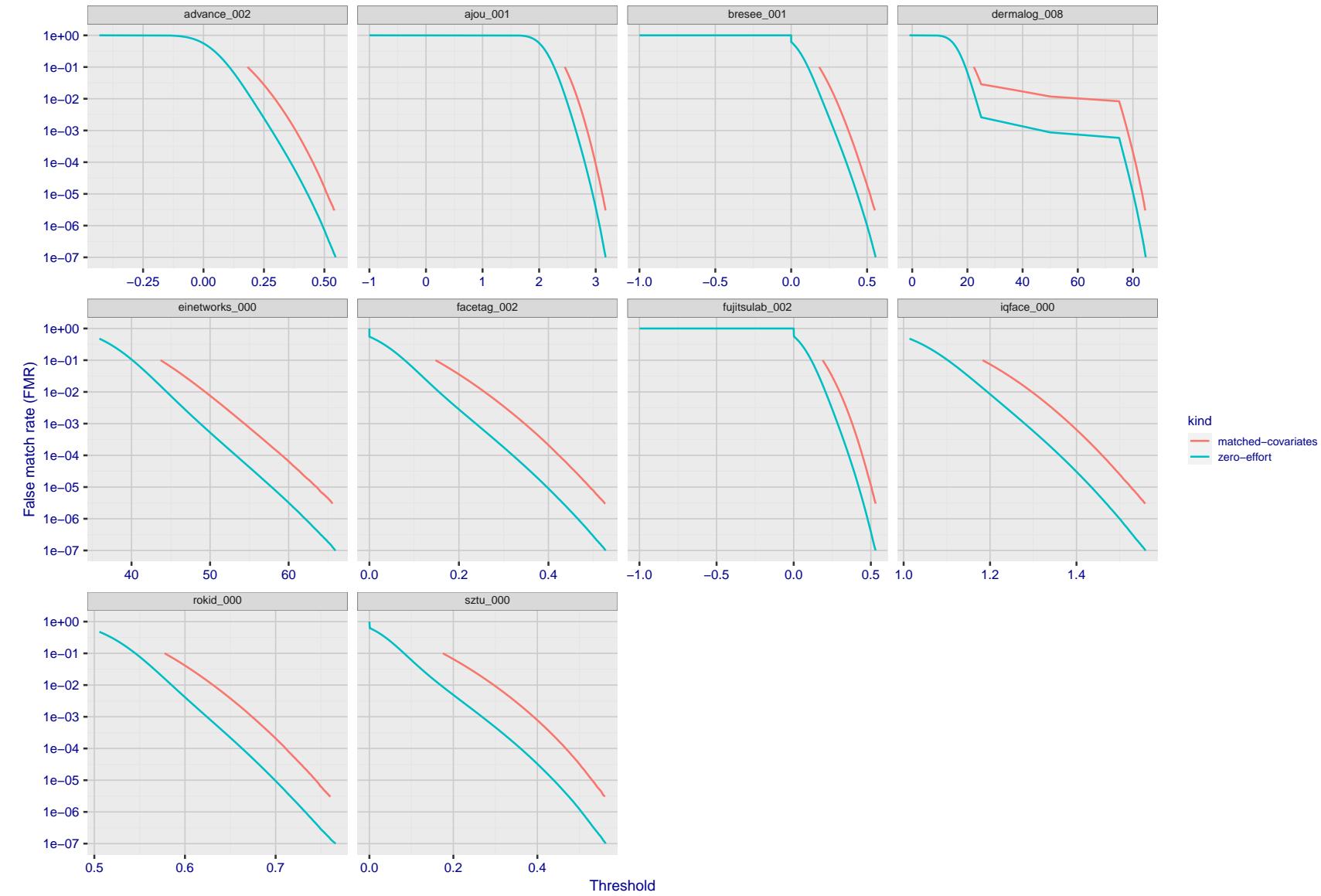


Figure 215: For the visa images, the false match calibration curves show FMR vs. threshold, T . The blue (lower) curves are for zero-effort impostors (i.e. comparing all images against all). The red (upper) curves are for persons of the same-sex, same-age, and same national-origin. This shows that FMR is underestimated (by a factor of 10 or more) by using a zero-effort impostor calculation to calibrate T . As shown later (sec. 3.6), FMR is higher for demographic-matched impostors.

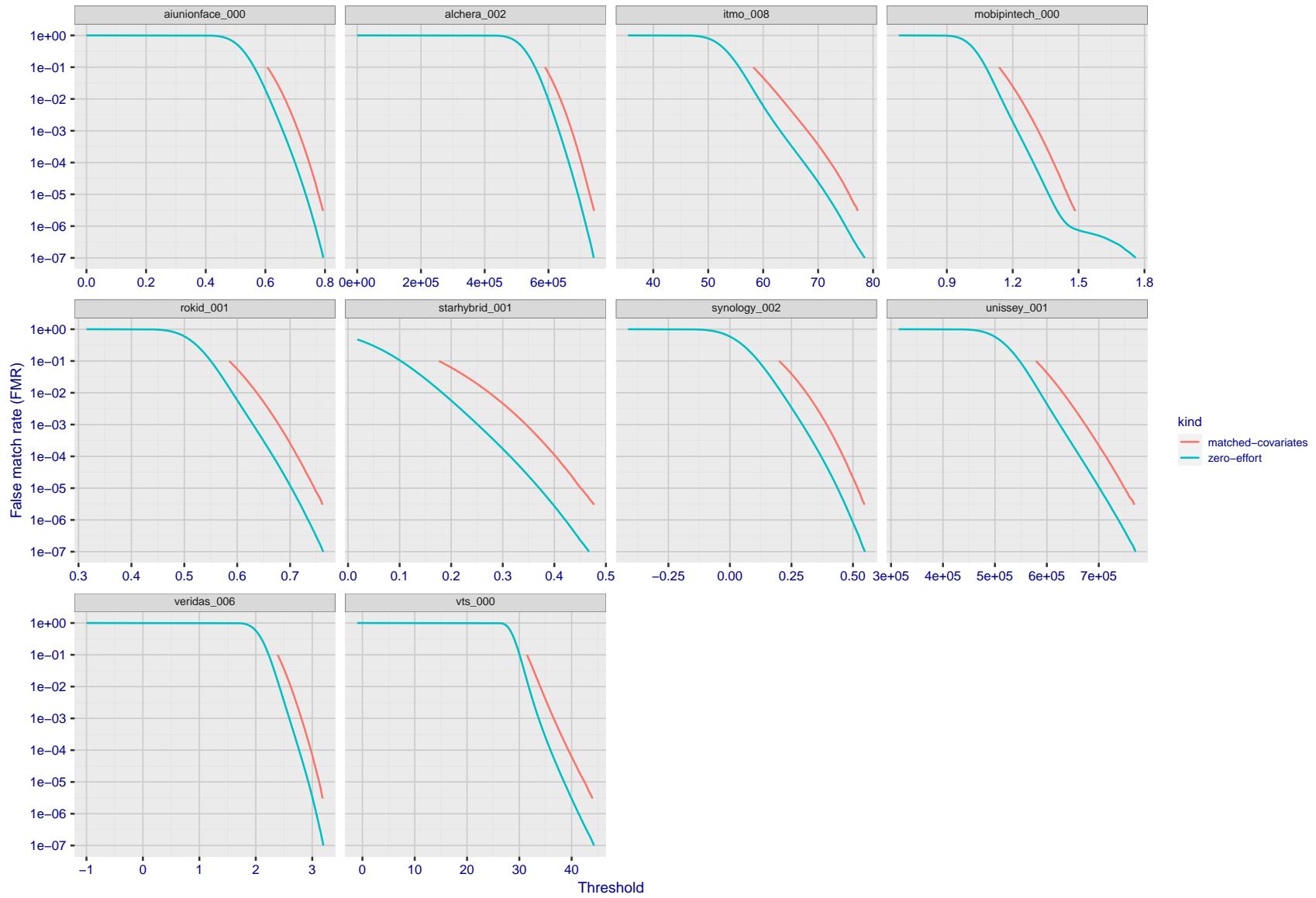


Figure 216: For the visa images, the false match calibration curves show FMR vs. threshold, T . The blue (lower) curves are for zero-effort impostors (i.e. comparing all images against all). The red (upper) curves are for persons of the same-sex, same-age, and same national-origin. This shows that FMR is underestimated (by a factor of 10 or more) by using a zero-effort impostor calculation to calibrate T . As shown later (sec. 3.6), FMR is higher for demographic-matched impostors.

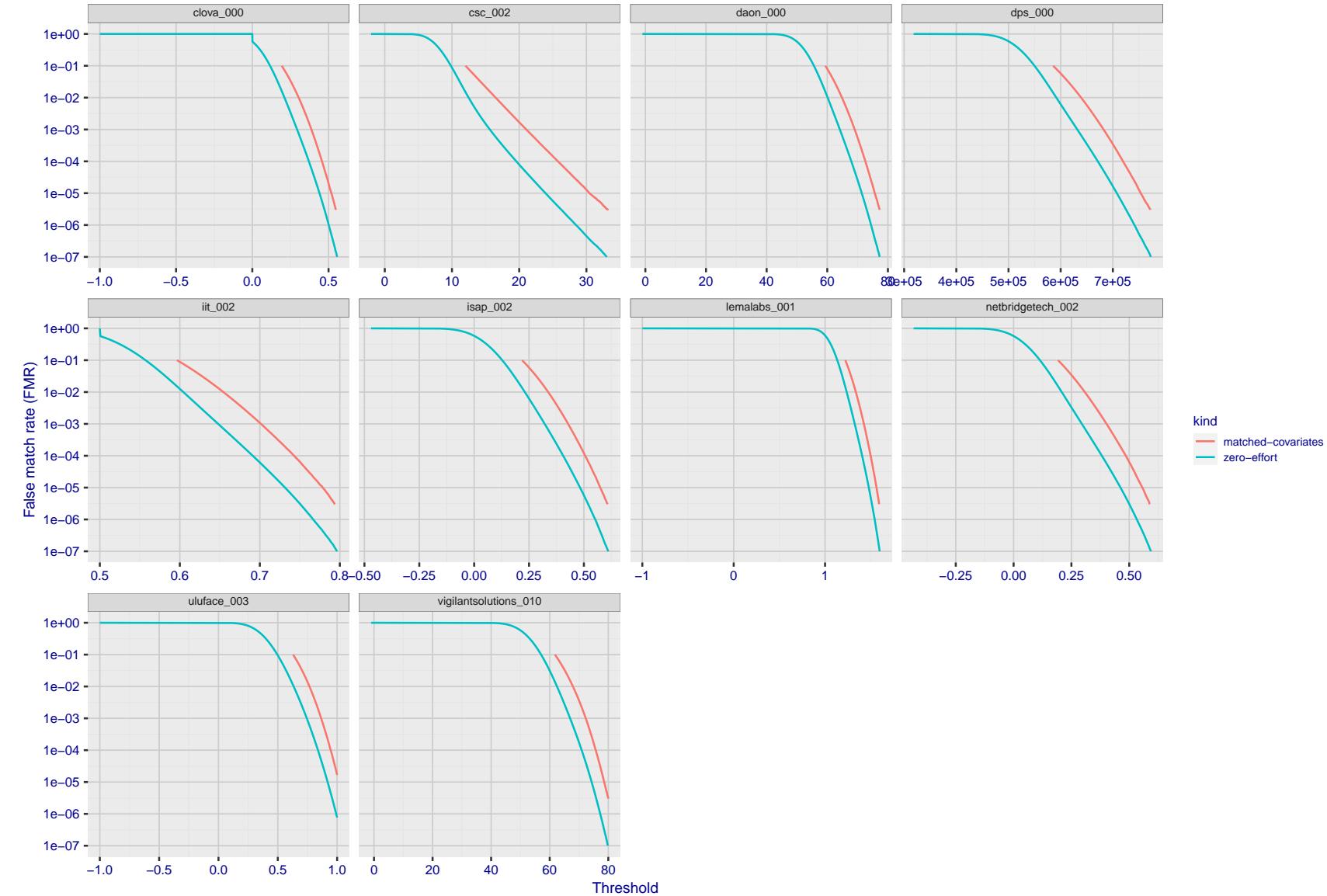


Figure 217: For the visa images, the false match calibration curves show FMR vs. threshold, T . The blue (lower) curves are for zero-effort impostors (i.e. comparing all images against all). The red (upper) curves are for persons of the same-sex, same-age, and same national-origin. This shows that FMR is underestimated (by a factor of 10 or more) by using a zero-effort impostor calculation to calibrate T . As shown later (sec. 3.6), FMR is higher for demographic-matched impostors.

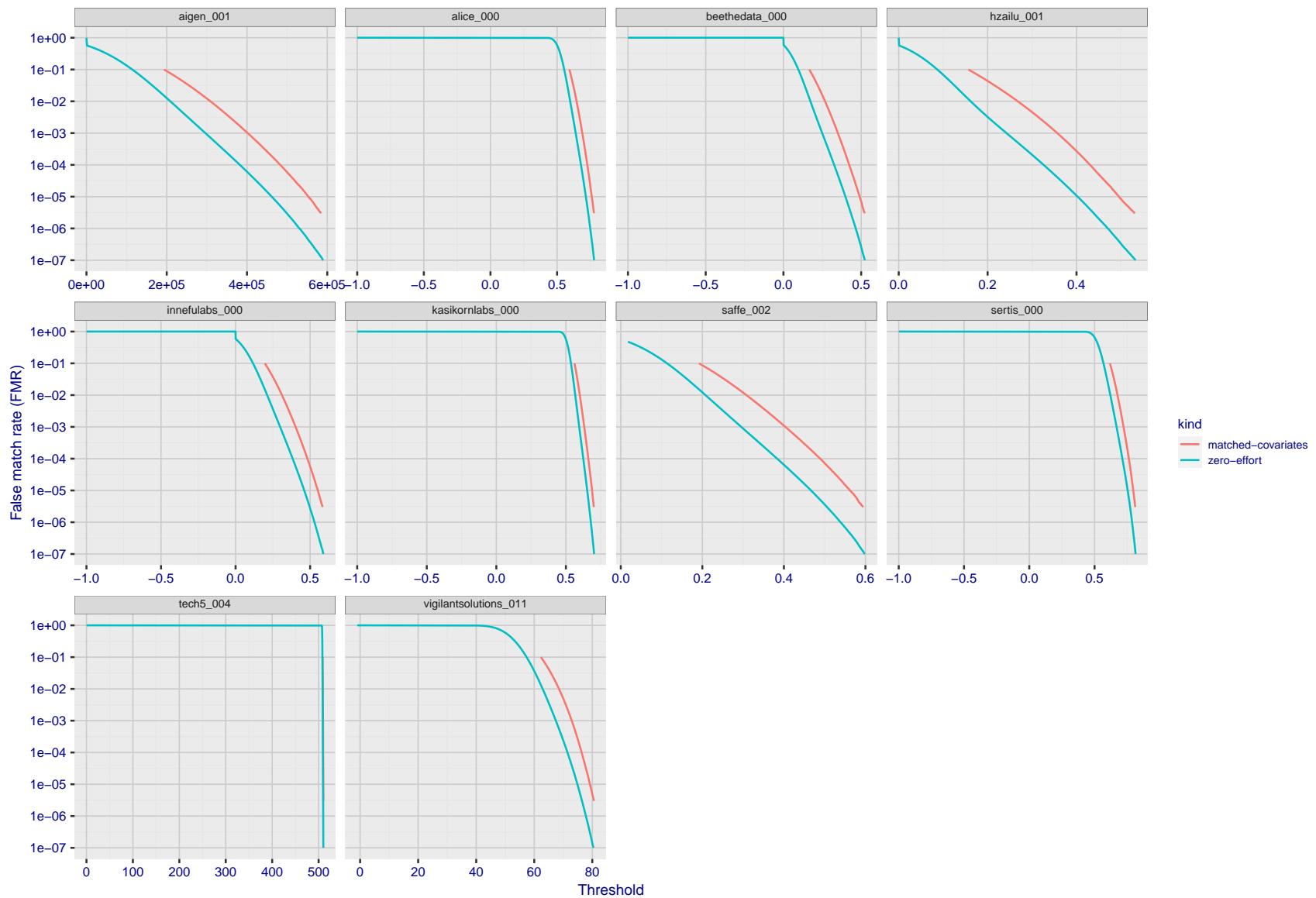


Figure 218: For the visa images, the false match calibration curves show FMR vs. threshold, T . The blue (lower) curves are for zero-effort impostors (i.e. comparing all images against all). The red (upper) curves are for persons of the same-sex, same-age, and same national-origin. This shows that FMR is underestimated (by a factor of 10 or more) by using a zero-effort impostor calculation to calibrate T . As shown later (sec. 3.6), FMR is higher for demographic-matched impostors.

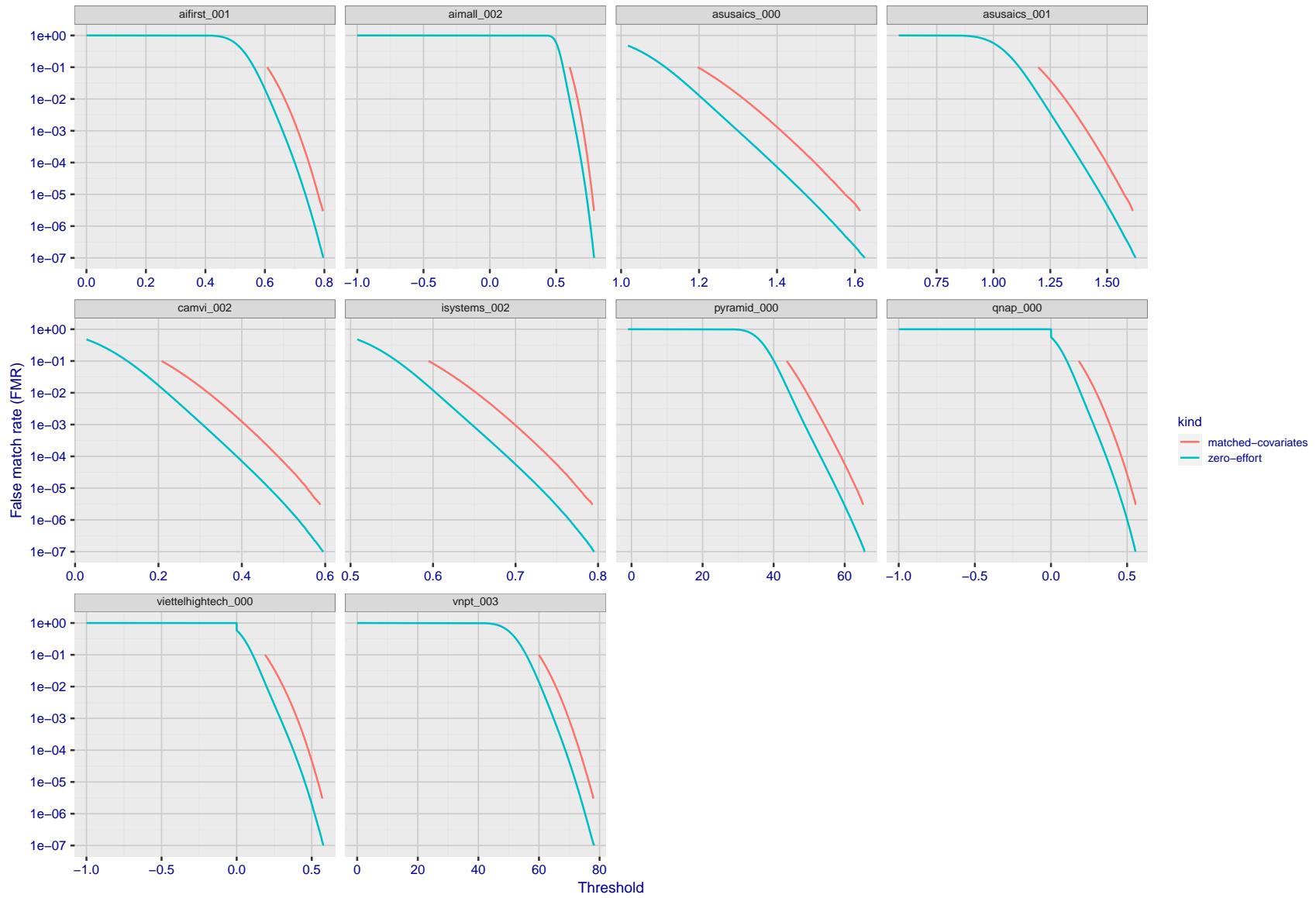


Figure 219: For the visa images, the false match calibration curves show FMR vs. threshold, T . The blue (lower) curves are for zero-effort impostors (i.e. comparing all images against all). The red (upper) curves are for persons of the same-sex, same-age, and same national-origin. This shows that FMR is underestimated (by a factor of 10 or more) by using a zero-effort impostor calculation to calibrate T . As shown later (sec. 3.6), FMR is higher for demographic-matched impostors.

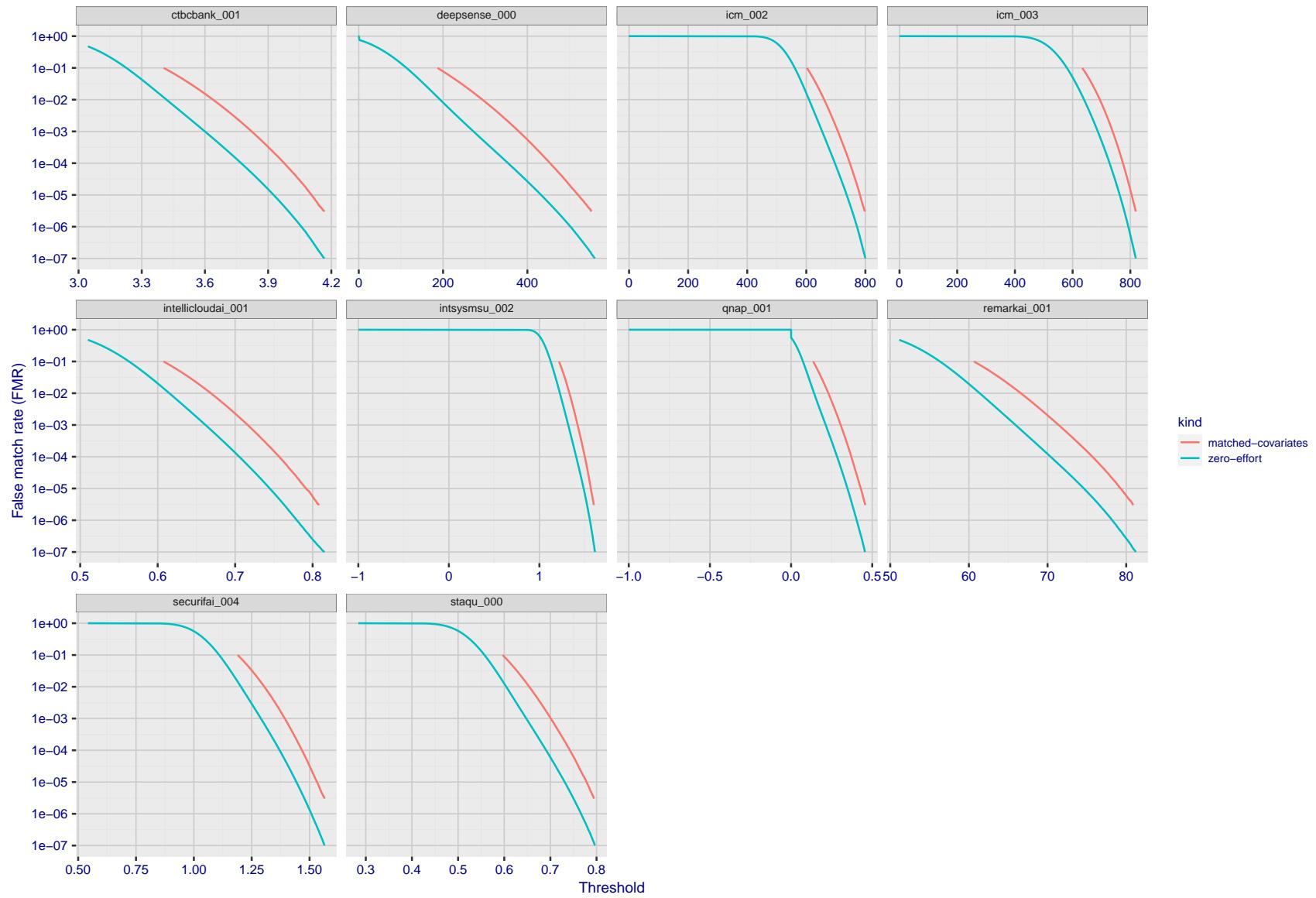


Figure 220: For the visa images, the false match calibration curves show FMR vs. threshold, T . The blue (lower) curves are for zero-effort impostors (i.e. comparing all images against all). The red (upper) curves are for persons of the same-sex, same-age, and same national-origin. This shows that FMR is underestimated (by a factor of 10 or more) by using a zero-effort impostor calculation to calibrate T . As shown later (sec. 3.6), FMR is higher for demographic-matched impostors.

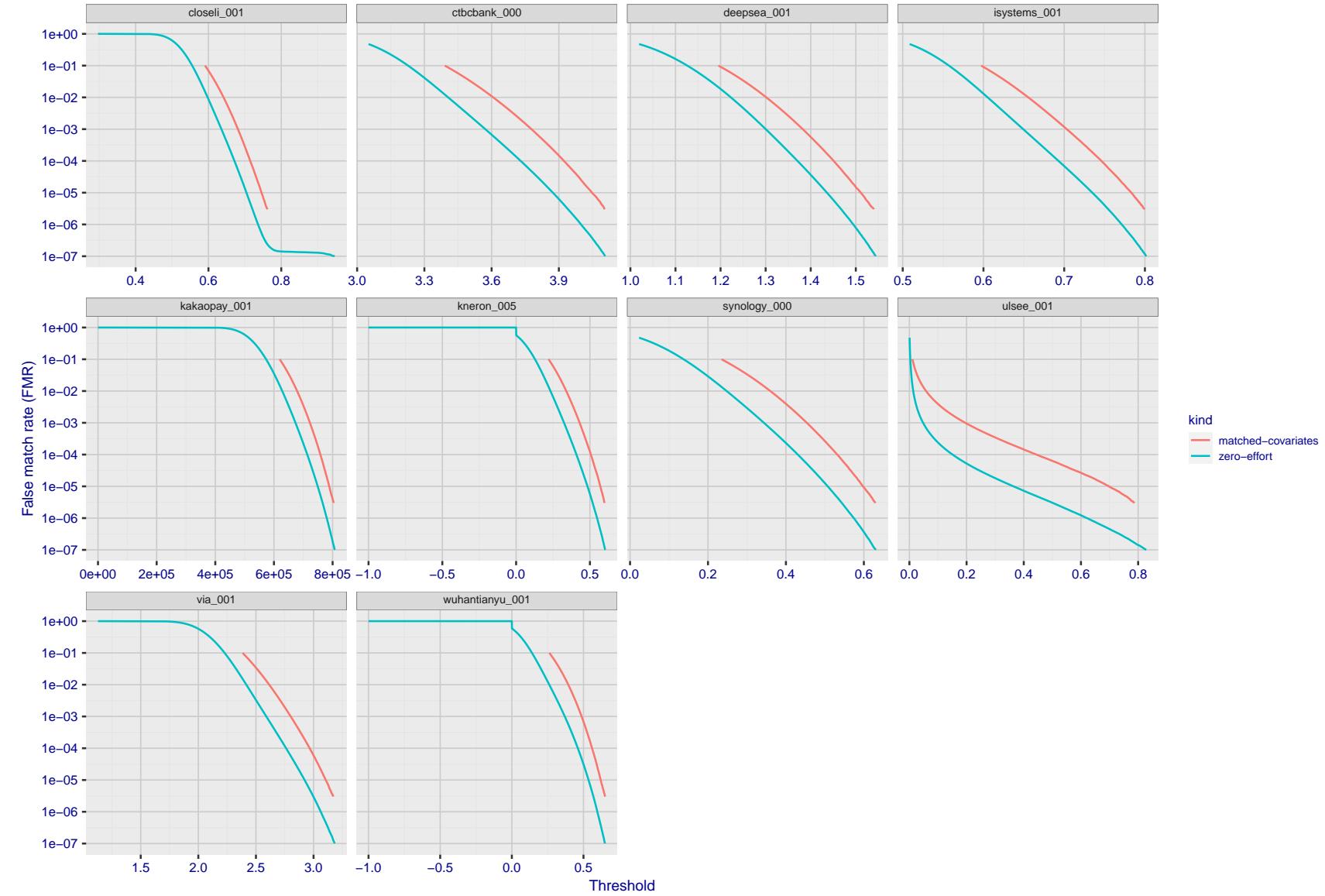


Figure 221: For the visa images, the false match calibration curves show FMR vs. threshold, T . The blue (lower) curves are for zero-effort impostors (i.e. comparing all images against all). The red (upper) curves are for persons of the same-sex, same-age, and same national-origin. This shows that FMR is underestimated (by a factor of 10 or more) by using a zero-effort impostor calculation to calibrate T . As shown later (sec. 3.6), FMR is higher for demographic-matched impostors.

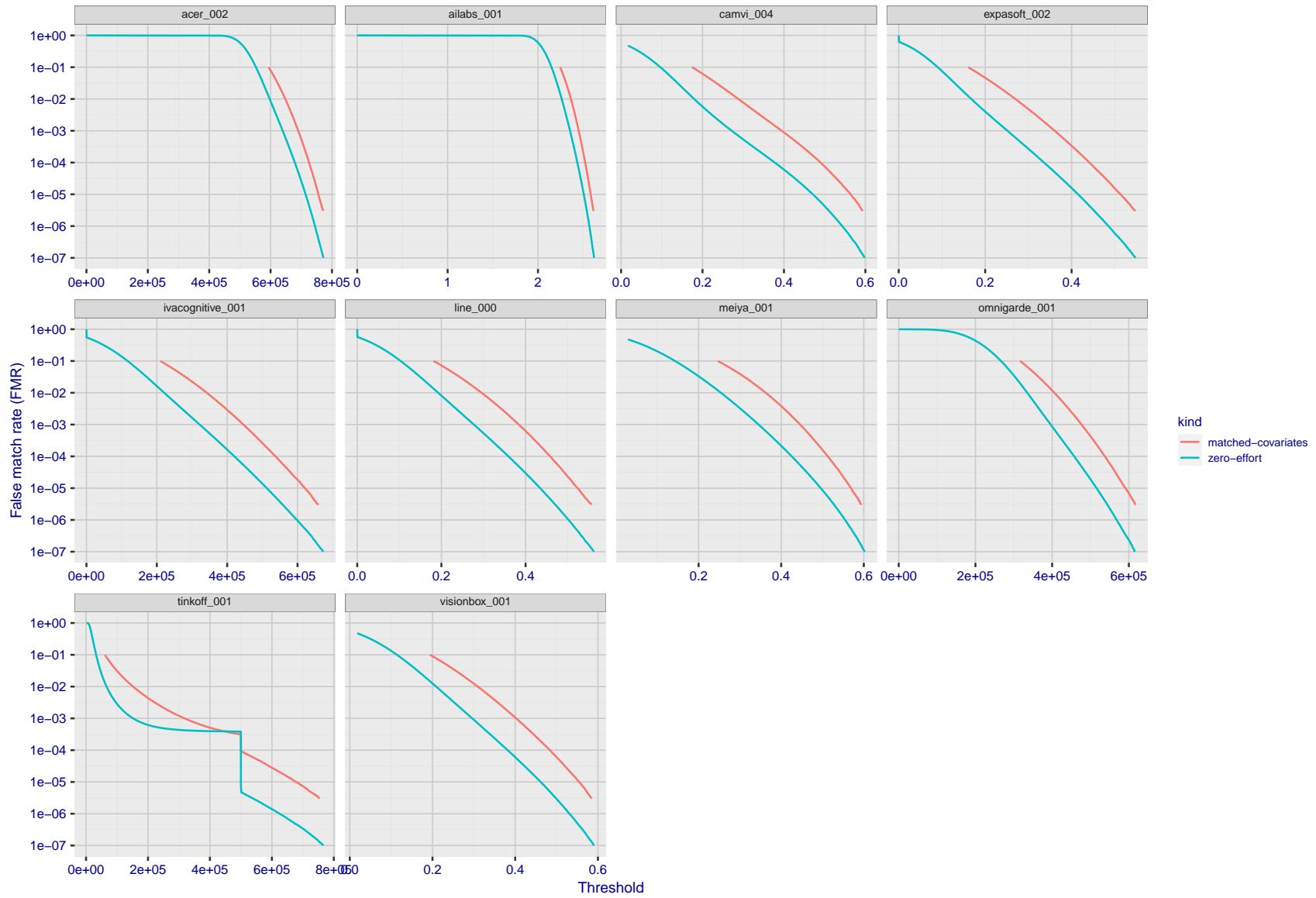


Figure 222: For the visa images, the false match calibration curves show FMR vs. threshold, T . The blue (lower) curves are for zero-effort impostors (i.e. comparing all images against all). The red (upper) curves are for persons of the same-sex, same-age, and same national-origin. This shows that FMR is underestimated (by a factor of 10 or more) by using a zero-effort impostor calculation to calibrate T . As shown later (sec. 3.6), FMR is higher for demographic-matched impostors.

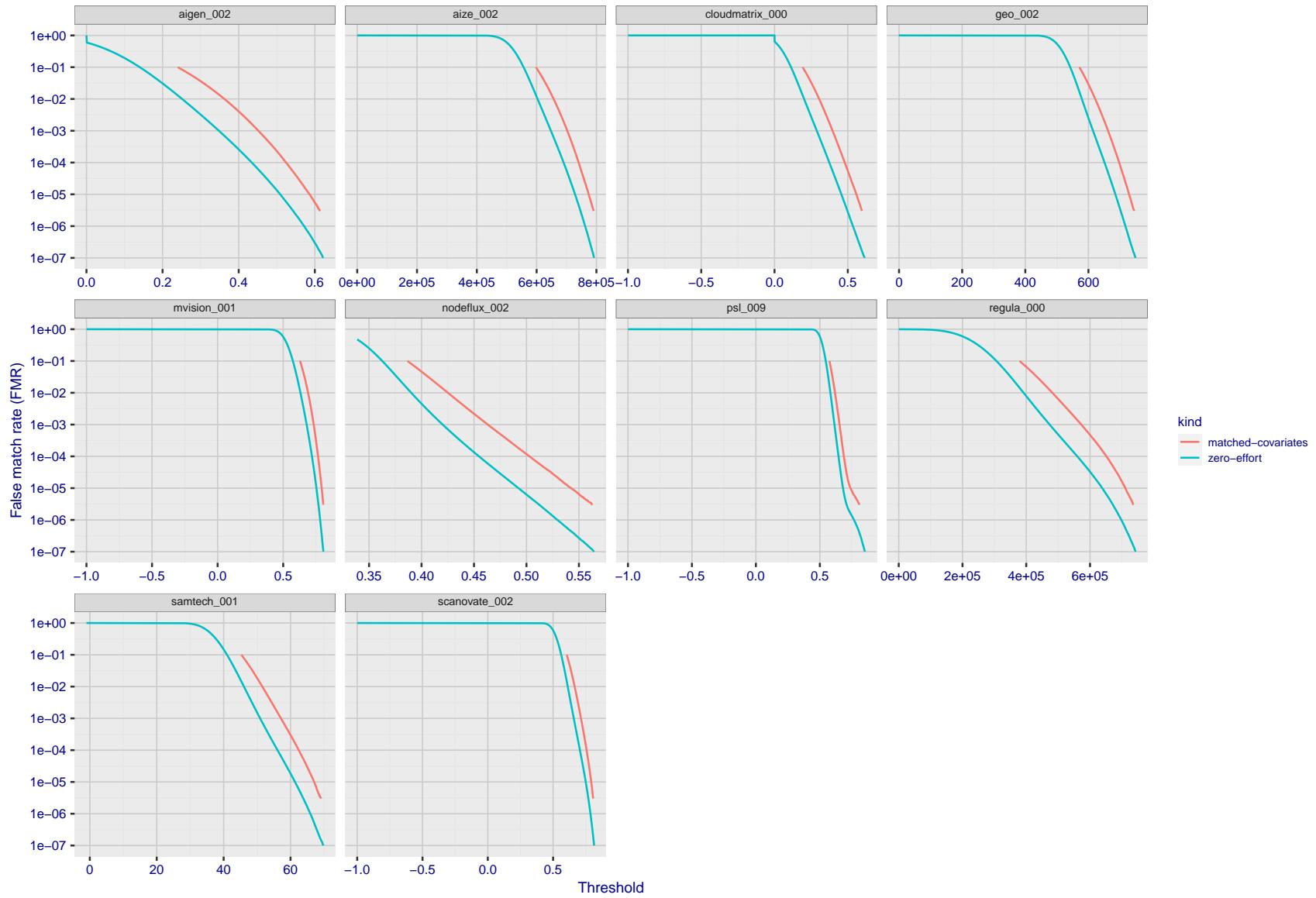


Figure 223: For the visa images, the false match calibration curves show FMR vs. threshold, T . The blue (lower) curves are for zero-effort impostors (i.e. comparing all images against all). The red (upper) curves are for persons of the same-sex, same-age, and same national-origin. This shows that FMR is underestimated (by a factor of 10 or more) by using a zero-effort impostor calculation to calibrate T . As shown later (sec. 3.6), FMR is higher for demographic-matched impostors.

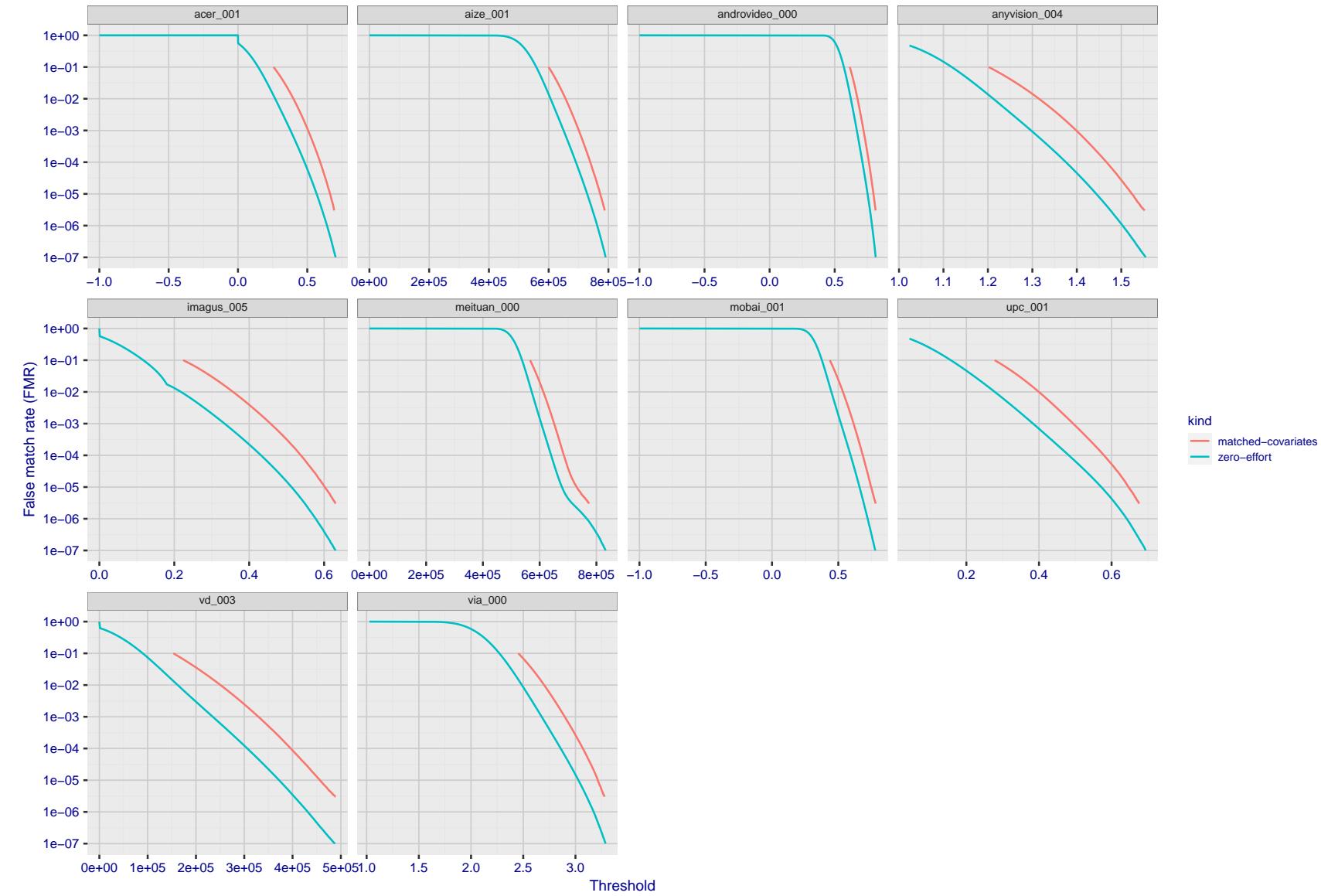


Figure 224: For the visa images, the false match calibration curves show FMR vs. threshold, T . The blue (lower) curves are for zero-effort impostors (i.e. comparing all images against all). The red (upper) curves are for persons of the same-sex, same-age, and same national-origin. This shows that FMR is underestimated (by a factor of 10 or more) by using a zero-effort impostor calculation to calibrate T . As shown later (sec. 3.6), FMR is higher for demographic-matched impostors.

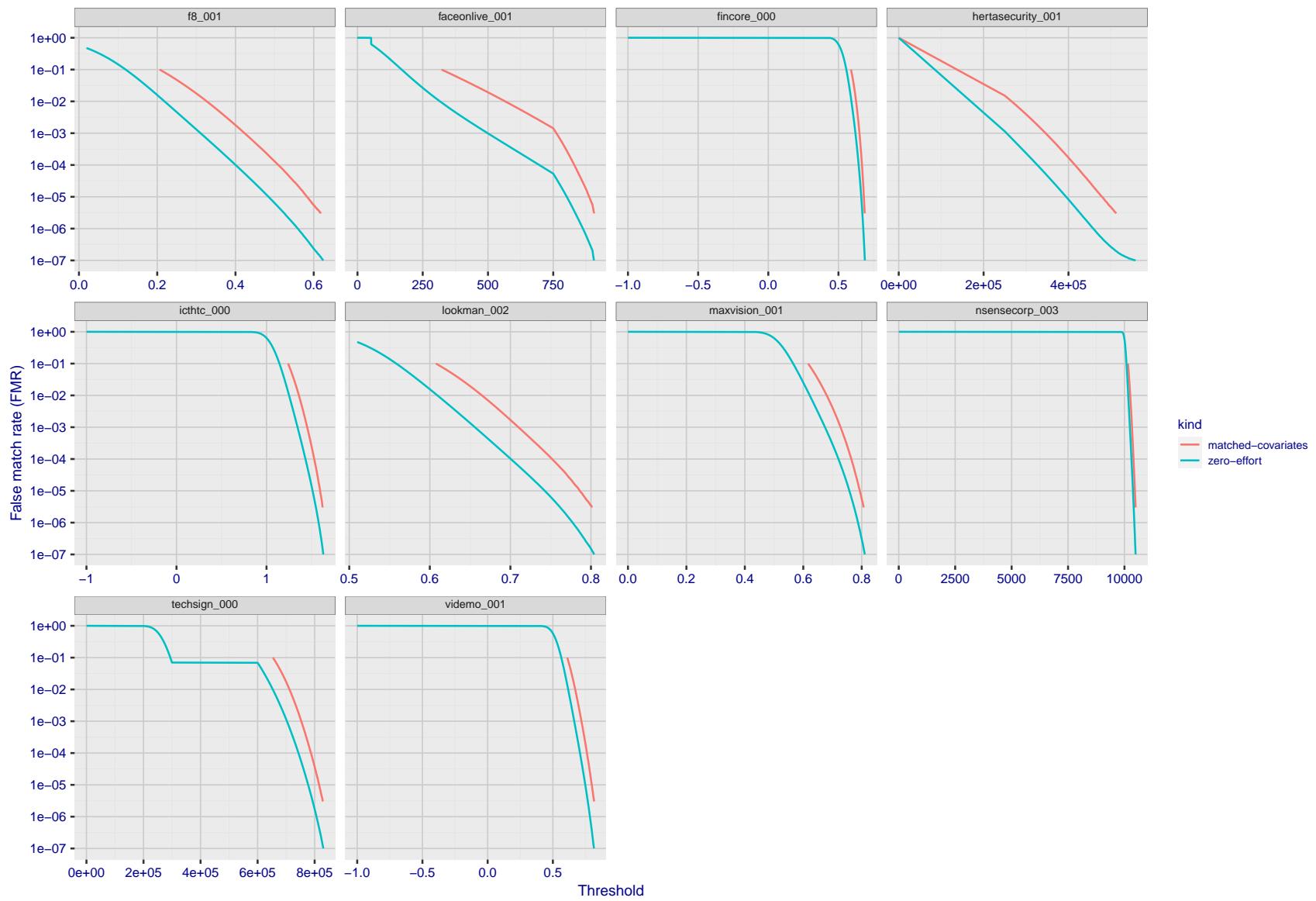


Figure 225: For the visa images, the false match calibration curves show FMR vs. threshold, T . The blue (lower) curves are for zero-effort impostors (i.e. comparing all images against all). The red (upper) curves are for persons of the same-sex, same-age, and same national-origin. This shows that FMR is underestimated (by a factor of 10 or more) by using a zero-effort impostor calculation to calibrate T . As shown later (sec. 3.6), FMR is higher for demographic-matched impostors.

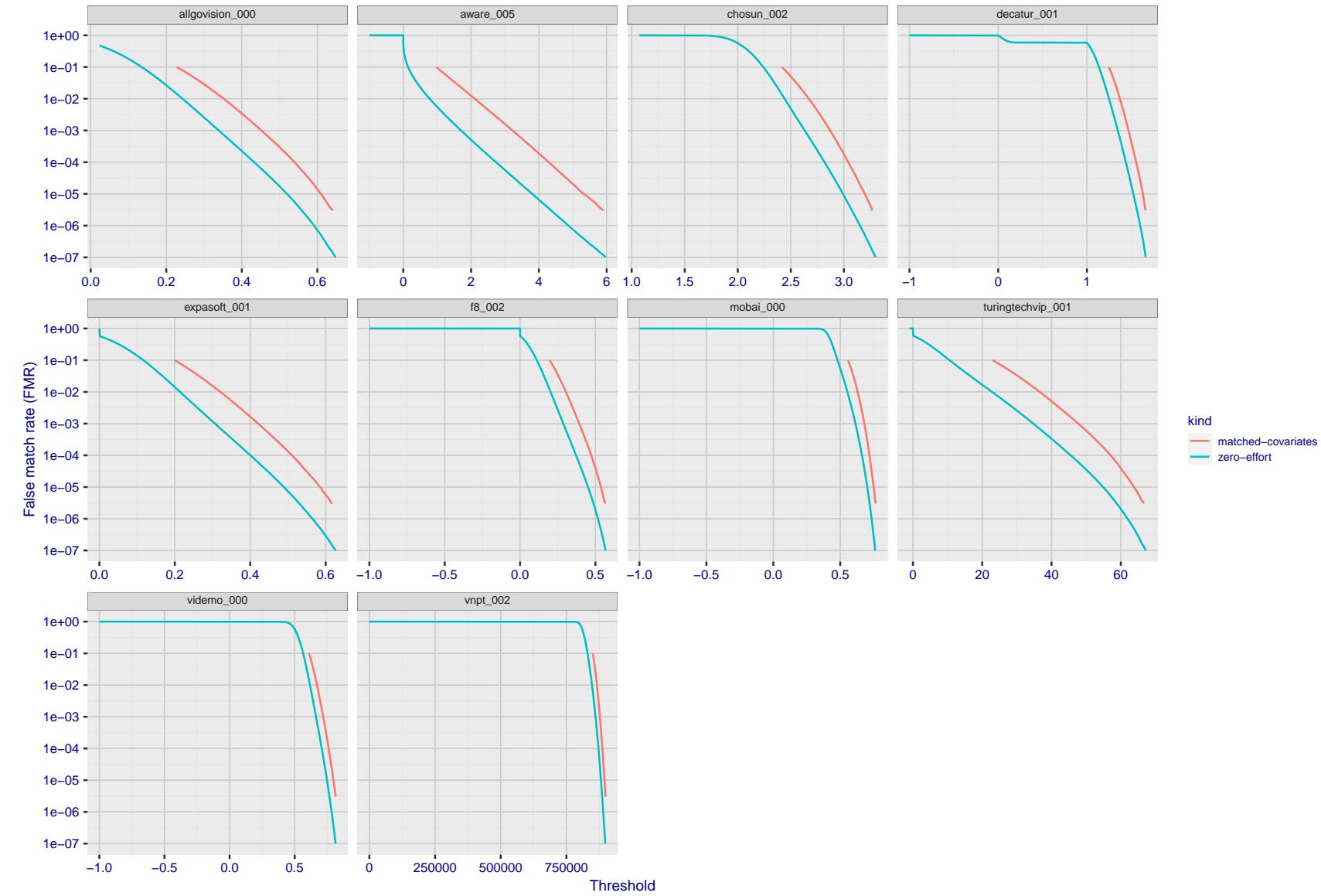


Figure 226: For the visa images, the false match calibration curves show FMR vs. threshold, T . The blue (lower) curves are for zero-effort impostors (i.e. comparing all images against all). The red (upper) curves are for persons of the same-sex, same-age, and same national-origin. This shows that FMR is underestimated (by a factor of 10 or more) by using a zero-effort impostor calculation to calibrate T . As shown later (sec. 3.6), FMR is higher for demographic-matched impostors.

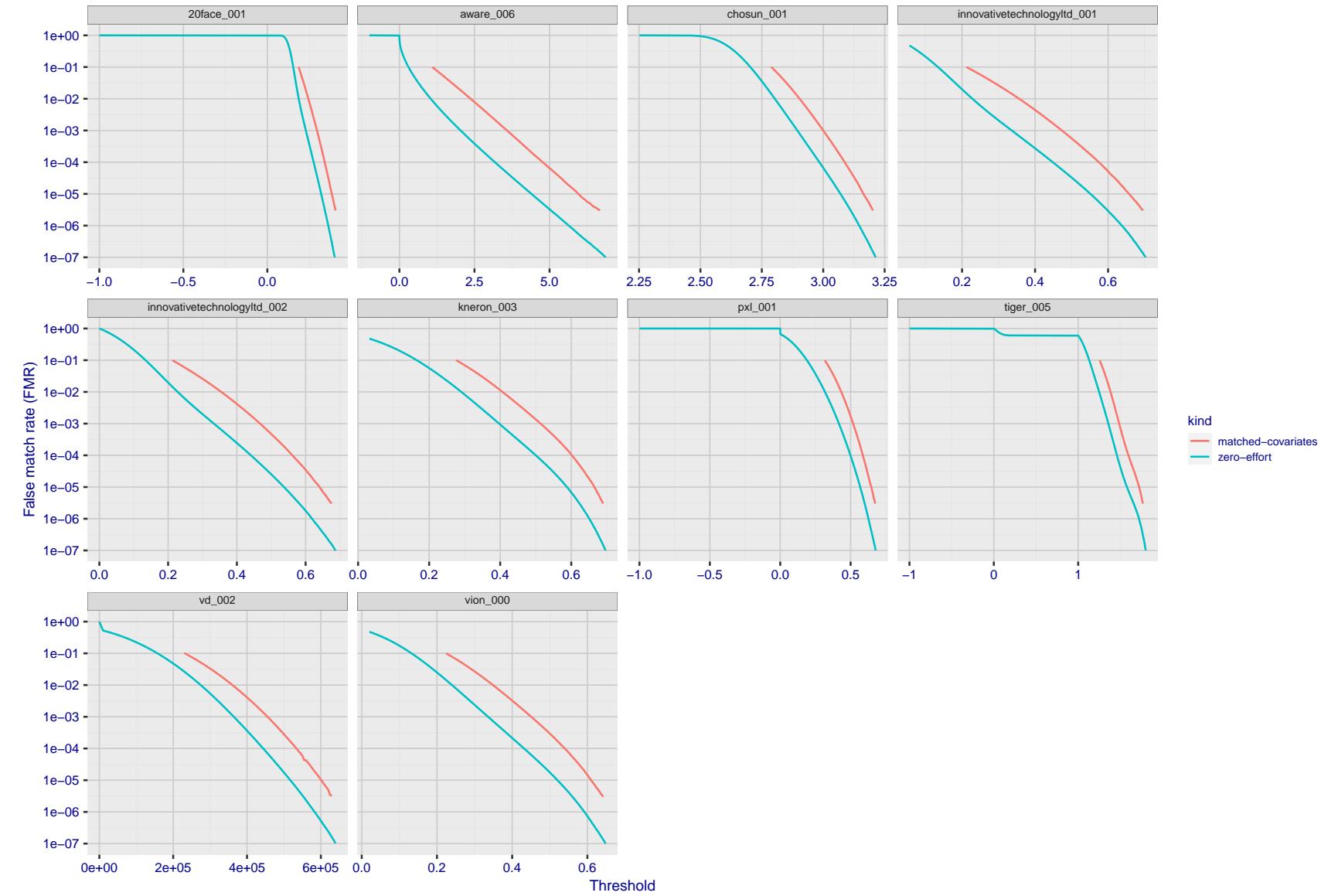


Figure 227: For the visa images, the false match calibration curves show FMR vs. threshold, T . The blue (lower) curves are for zero-effort impostors (i.e. comparing all images against all). The red (upper) curves are for persons of the same-sex, same-age, and same national-origin. This shows that FMR is underestimated (by a factor of 10 or more) by using a zero-effort impostor calculation to calibrate T . As shown later (sec. 3.6), FMR is higher for demographic-matched impostors.

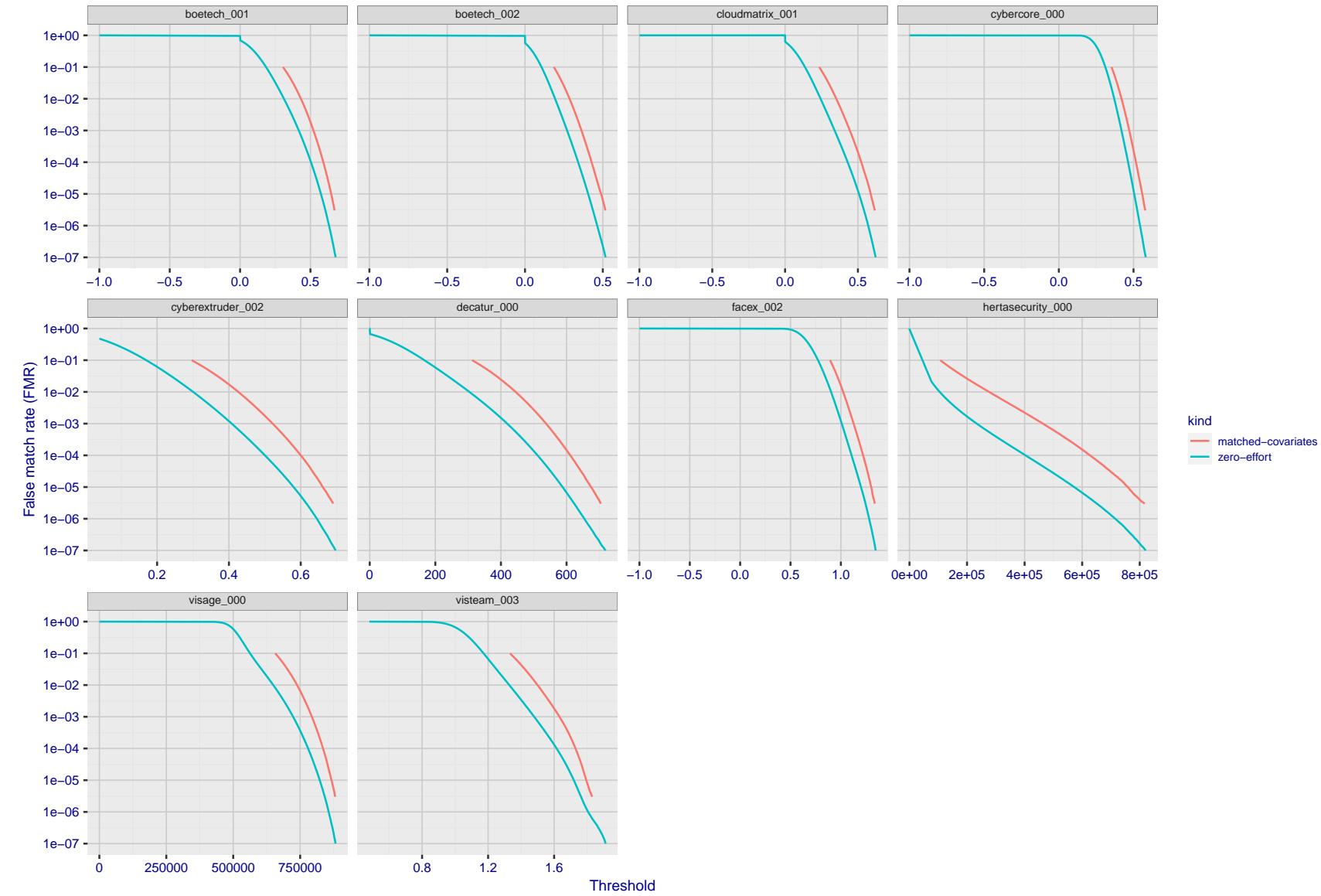


Figure 228: For the visa images, the false match calibration curves show FMR vs. threshold, T . The blue (lower) curves are for zero-effort impostors (i.e. comparing all images against all). The red (upper) curves are for persons of the same-sex, same-age, and same national-origin. This shows that FMR is underestimated (by a factor of 10 or more) by using a zero-effort impostor calculation to calibrate T . As shown later (sec. 3.6), FMR is higher for demographic-matched impostors.

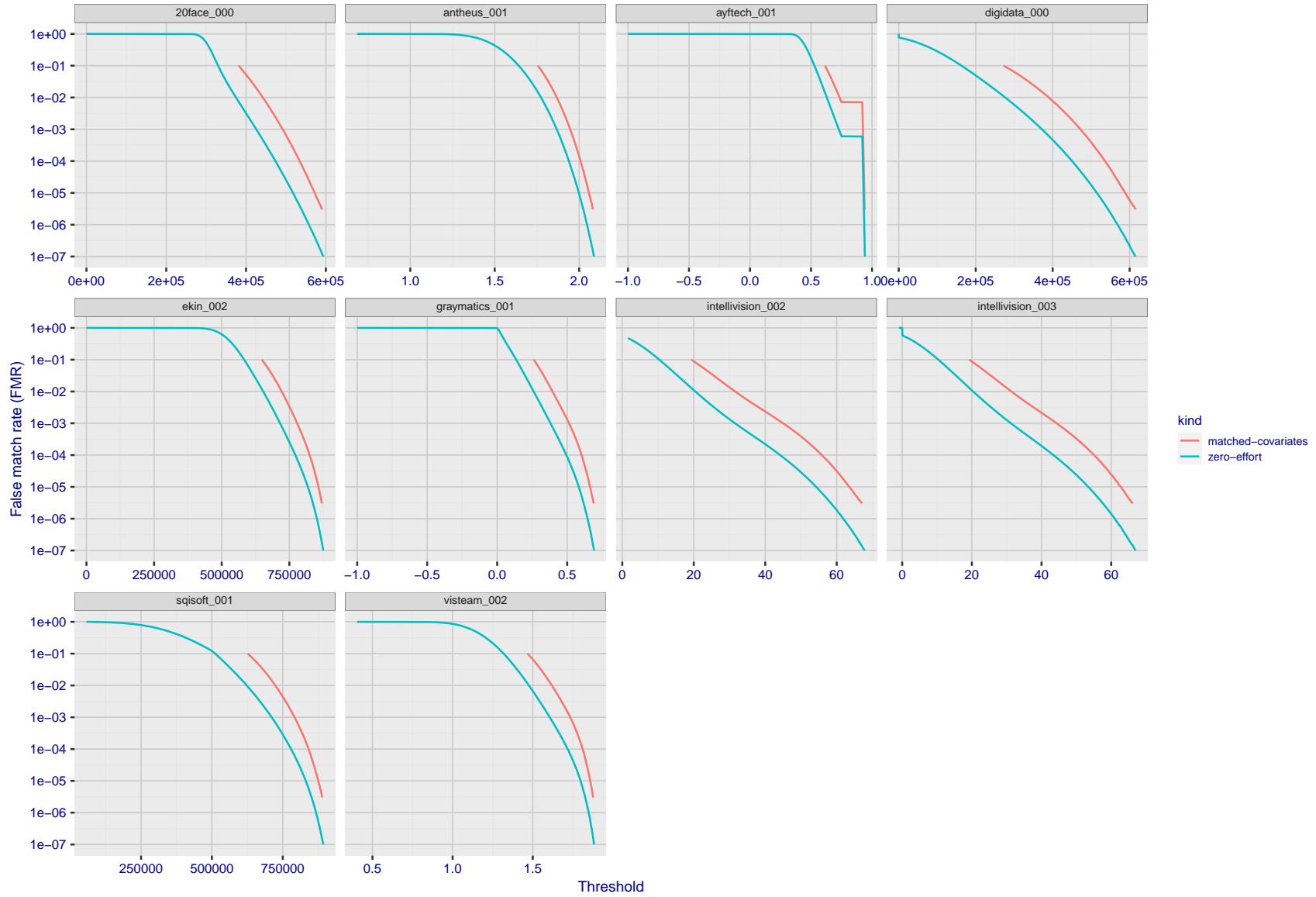


Figure 229: For the visa images, the false match calibration curves show FMR vs. threshold, T . The blue (lower) curves are for zero-effort impostors (i.e. comparing all images against all). The red (upper) curves are for persons of the same-sex, same-age, and same national-origin. This shows that FMR is underestimated (by a factor of 10 or more) by using a zero-effort impostor calculation to calibrate T . As shown later (sec. 3.6), FMR is higher for demographic-matched impostors.

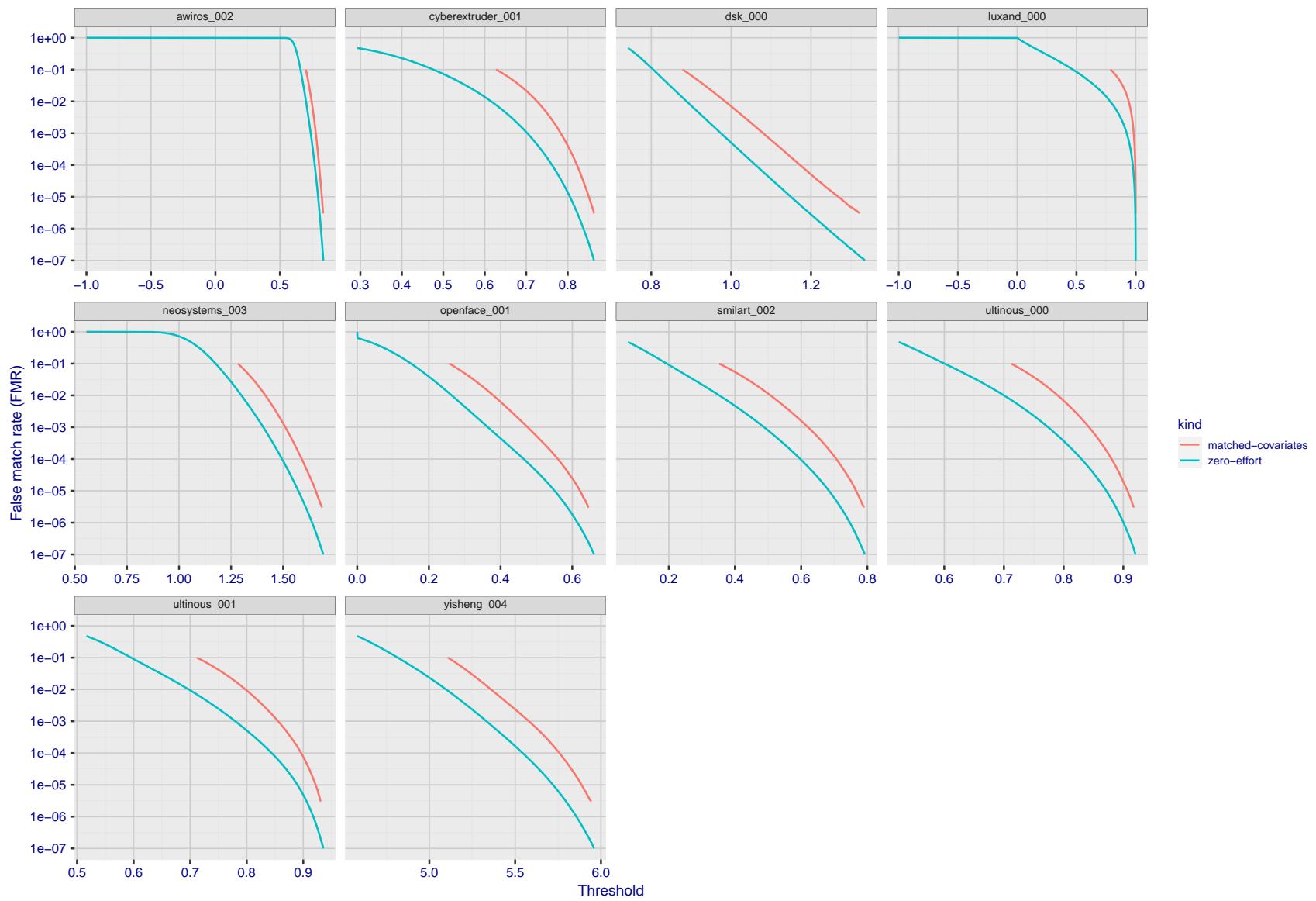


Figure 230: For the visa images, the false match calibration curves show FMR vs. threshold, T . The blue (lower) curves are for zero-effort impostors (i.e. comparing all images against all). The red (upper) curves are for persons of the same-sex, same-age, and same national-origin. This shows that FMR is underestimated (by a factor of 10 or more) by using a zero-effort impostor calculation to calibrate T . As shown later (sec. 3.6), FMR is higher for demographic-matched impostors.

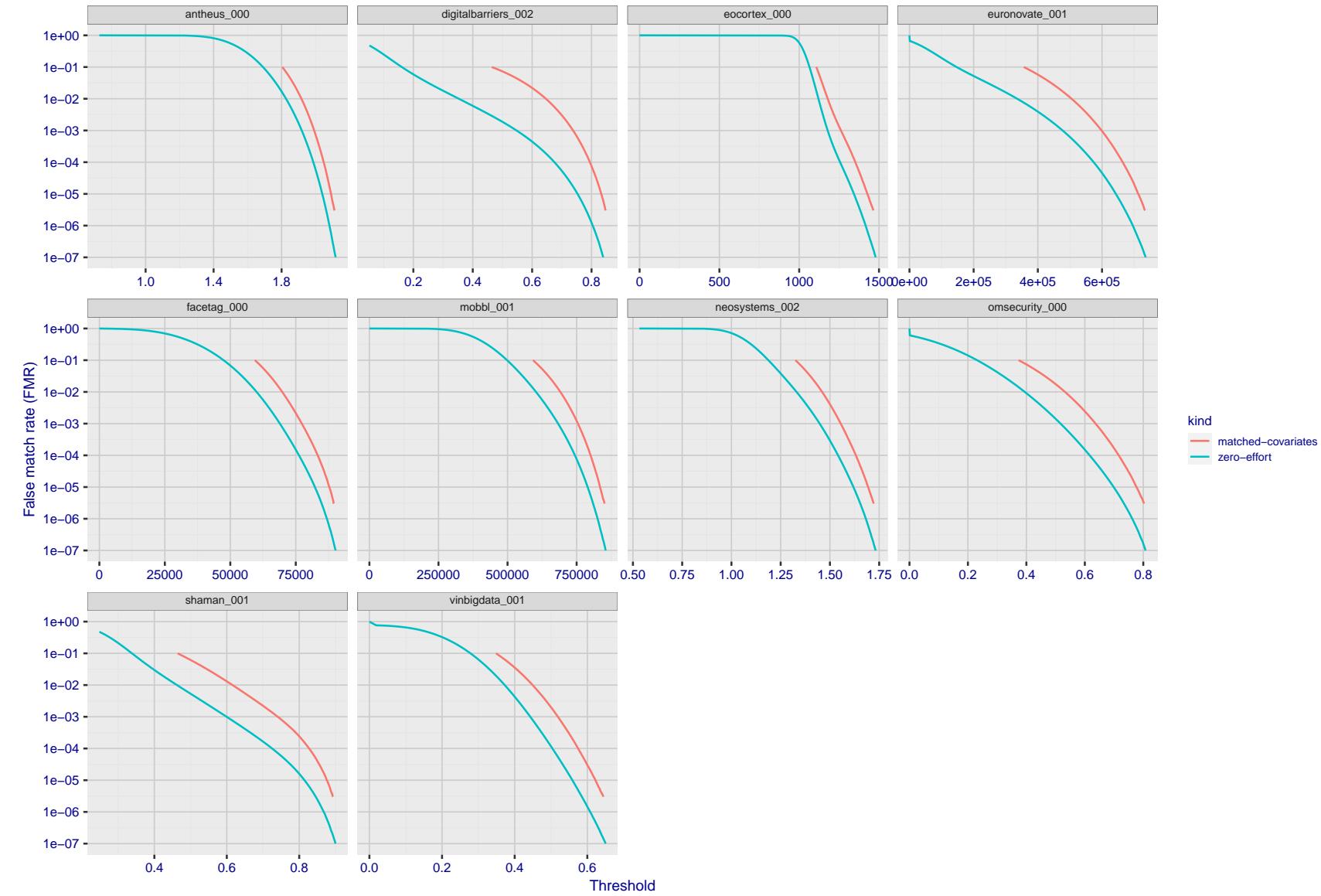


Figure 231: For the visa images, the false match calibration curves show FMR vs. threshold, T . The blue (lower) curves are for zero-effort impostors (i.e. comparing all images against all). The red (upper) curves are for persons of the same-sex, same-age, and same national-origin. This shows that FMR is underestimated (by a factor of 10 or more) by using a zero-effort impostor calculation to calibrate T . As shown later (sec. 3.6), FMR is higher for demographic-matched impostors.

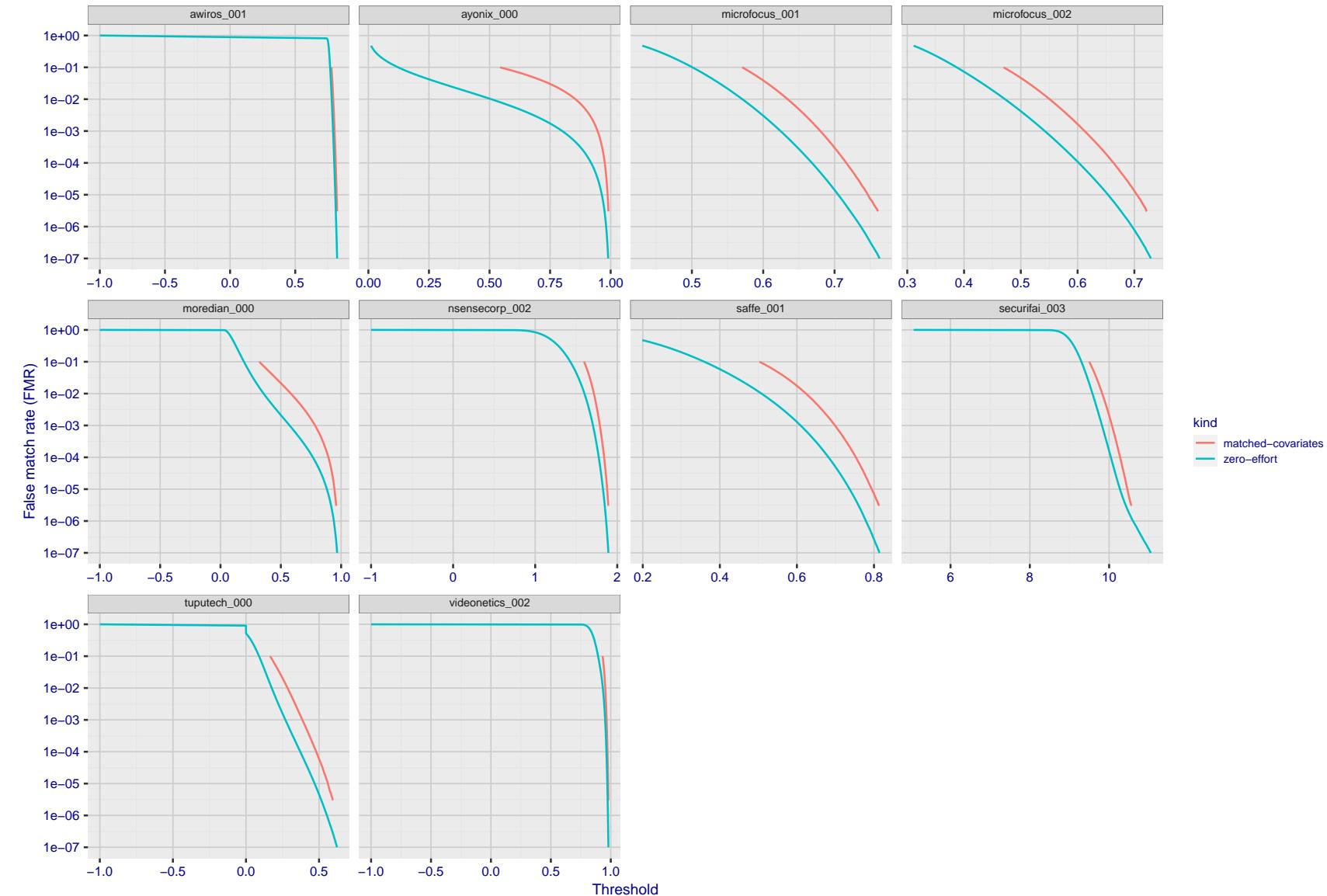


Figure 232: For the visa images, the false match calibration curves show FMR vs. threshold, T . The blue (lower) curves are for zero-effort impostors (i.e. comparing all images against all). The red (upper) curves are for persons of the same-sex, same-age, and same national-origin. This shows that FMR is underestimated (by a factor of 10 or more) by using a zero-effort impostor calculation to calibrate T . As shown later (sec. 3.6), FMR is higher for demographic-matched impostors.

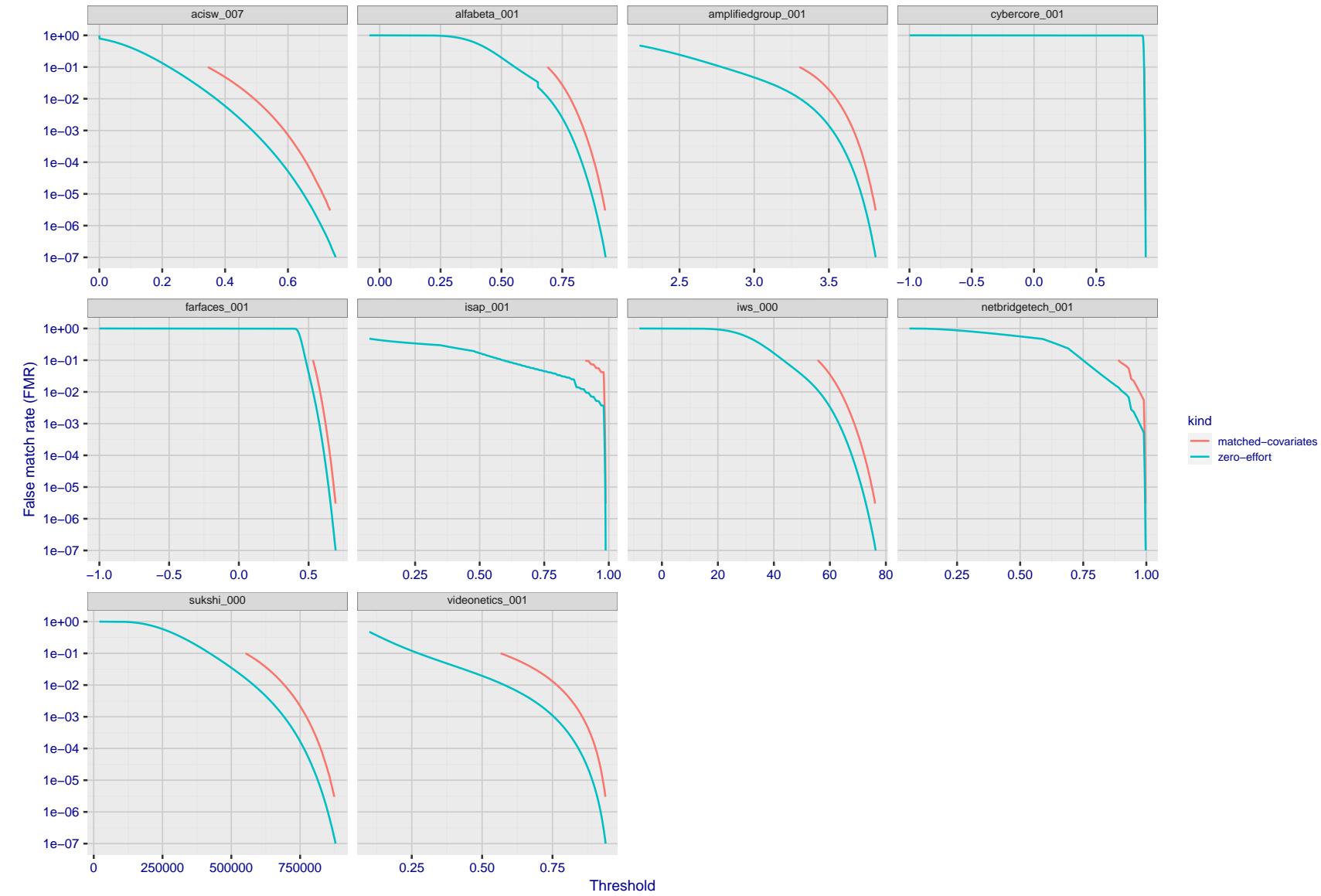


Figure 233: For the visa images, the false match calibration curves show FMR vs. threshold, T . The blue (lower) curves are for zero-effort impostors (i.e. comparing all images against all). The red (upper) curves are for persons of the same-sex, same-age, and same national-origin. This shows that FMR is underestimated (by a factor of 10 or more) by using a zero-effort impostor calculation to calibrate T . As shown later (sec. 3.6), FMR is higher for demographic-matched impostors.

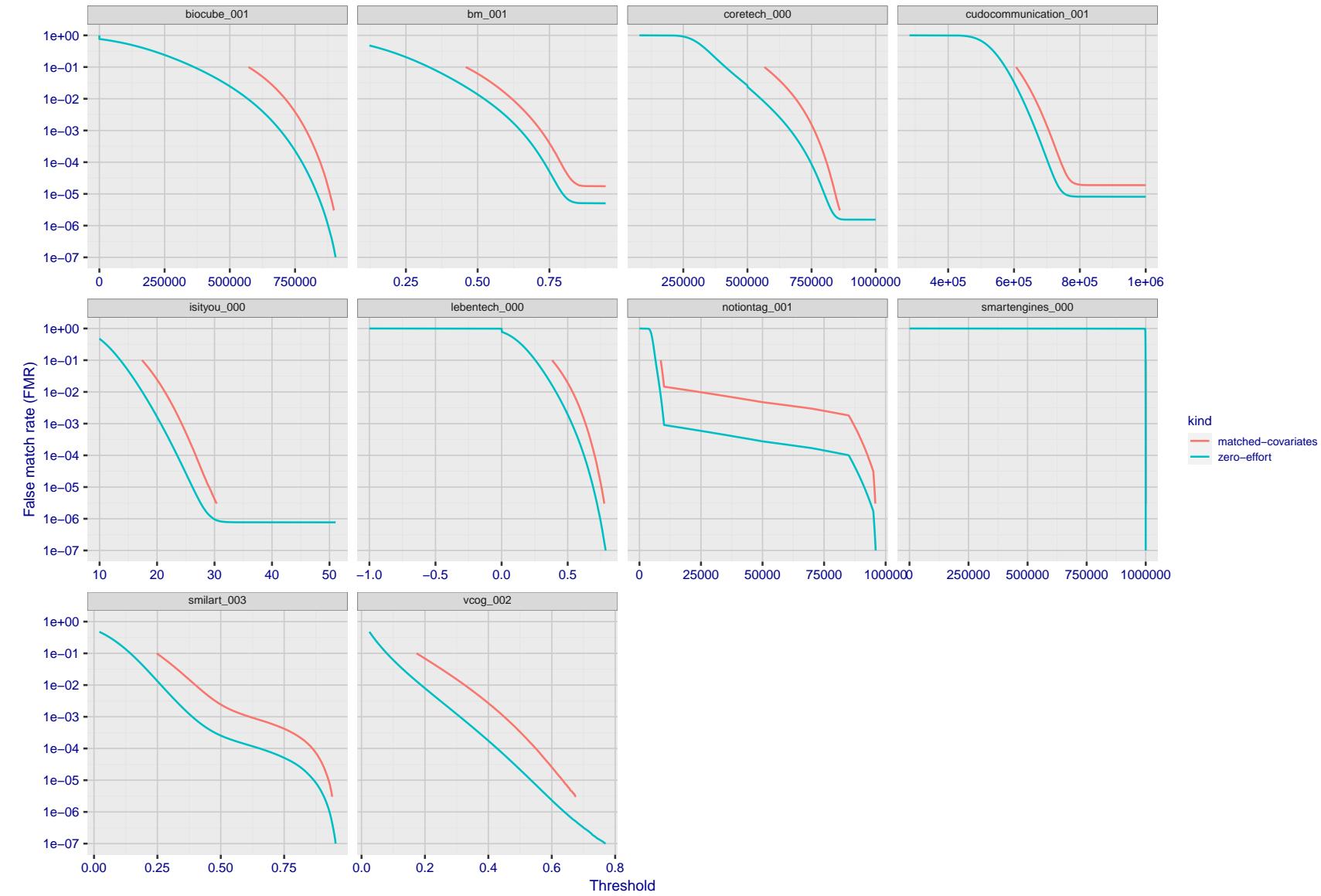


Figure 234: For the visa images, the false match calibration curves show FMR vs. threshold, T . The blue (lower) curves are for zero-effort impostors (i.e. comparing all images against all). The red (upper) curves are for persons of the same-sex, same-age, and same national-origin. This shows that FMR is underestimated (by a factor of 10 or more) by using a zero-effort impostor calculation to calibrate T . As shown later (sec. 3.6), FMR is higher for demographic-matched impostors.

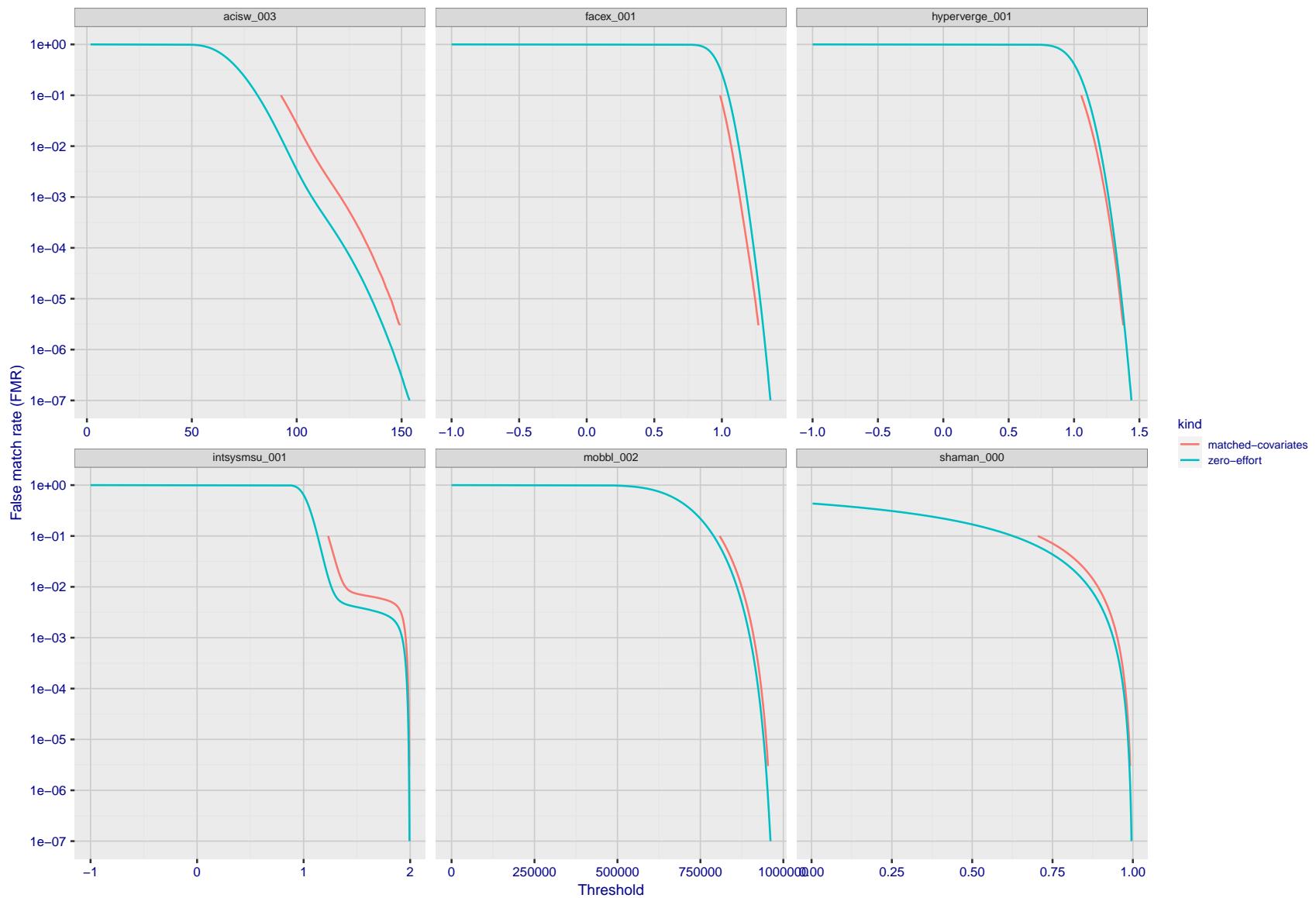


Figure 235: For the visa images, the false match calibration curves show FMR vs. threshold, T . The blue (lower) curves are for zero-effort impostors (i.e. comparing all images against all). The red (upper) curves are for persons of the same-sex, same-age, and same national-origin. This shows that FMR is underestimated (by a factor of 10 or more) by using a zero-effort impostor calculation to calibrate T . As shown later (sec. 3.6), FMR is higher for demographic-matched impostors.

3.5 Genuine distribution stability

3.5.1 Effect of birth place on the genuine distribution

Background: Both skin tone and bone structure vary geographically. Prior studies have reported variations in FNMR and FMR.

Goal: To measure false non-match rate (FNMR) variation with country of birth.

Methods: Thresholds are determined that give $FMR = \{0.001, 0.0001\}$ over the entire impostor set. Then FNMR is measured over 1000 bootstrap replications of the genuine scores. Only those countries with at least 140 individuals are included in the analysis.

Results: Figure 269 shows FNMR by country of birth for the two thresholds.

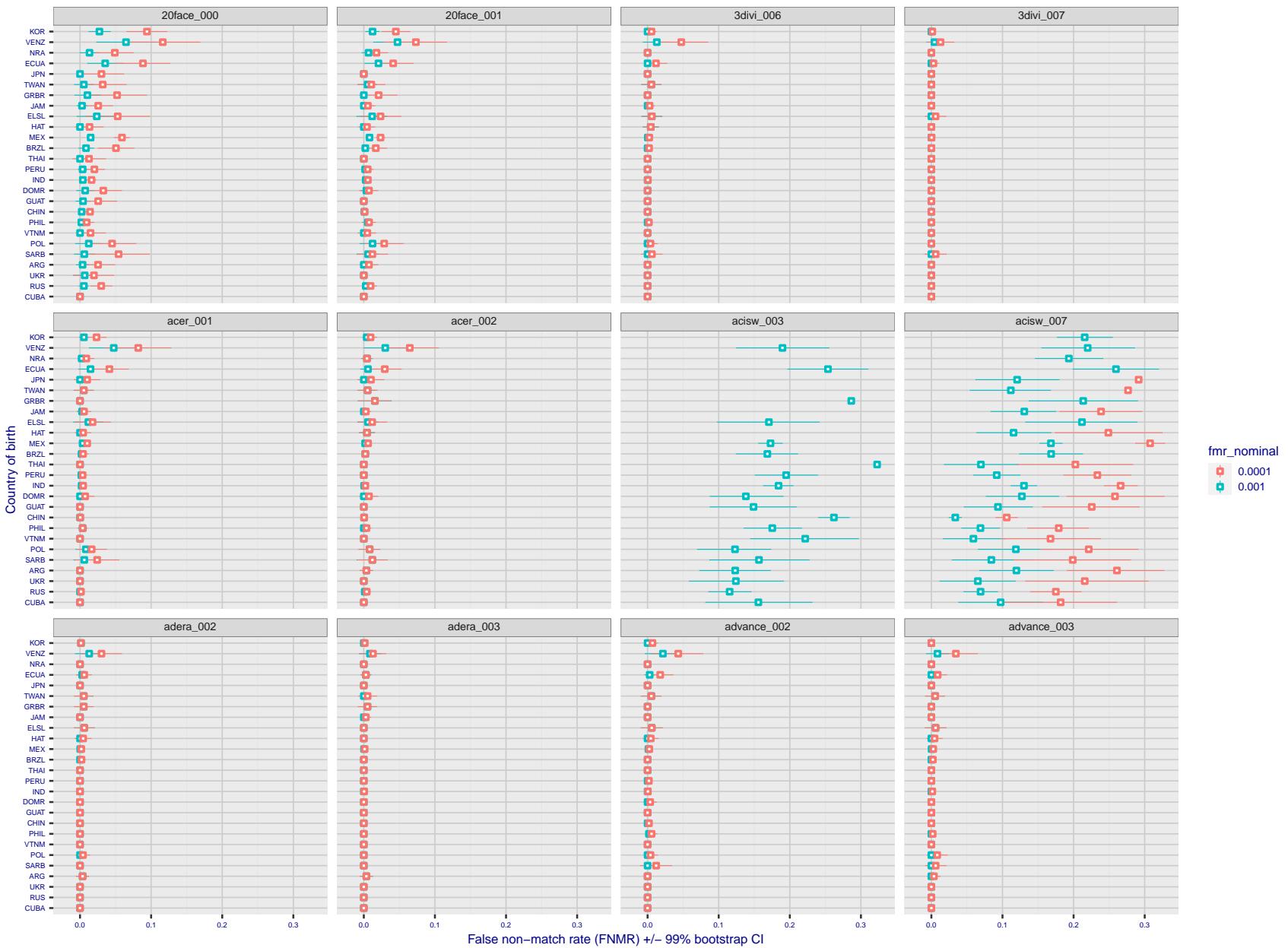


Figure 236: For the visa images, the dots show FNMR by country of birth for two globally set operating thresholds corresponding to $FMR = \{0.001, 0.0001\}$ computed over all on the order of 10^{10} impostor scores. The FMR in each bin will vary also - see subsequent impostor heatmaps in sec. 3.6.1. The figures shows an order of magnitude variation in FNMR across country of birth; these effects are likely due quality variations, then demographics like age and race. The error rates in some cases are zero, and in others the DET is flat so the error rates at the two thresholds are identical. The lines span 1% and 99% of bootstrap replicated FNMR estimates.

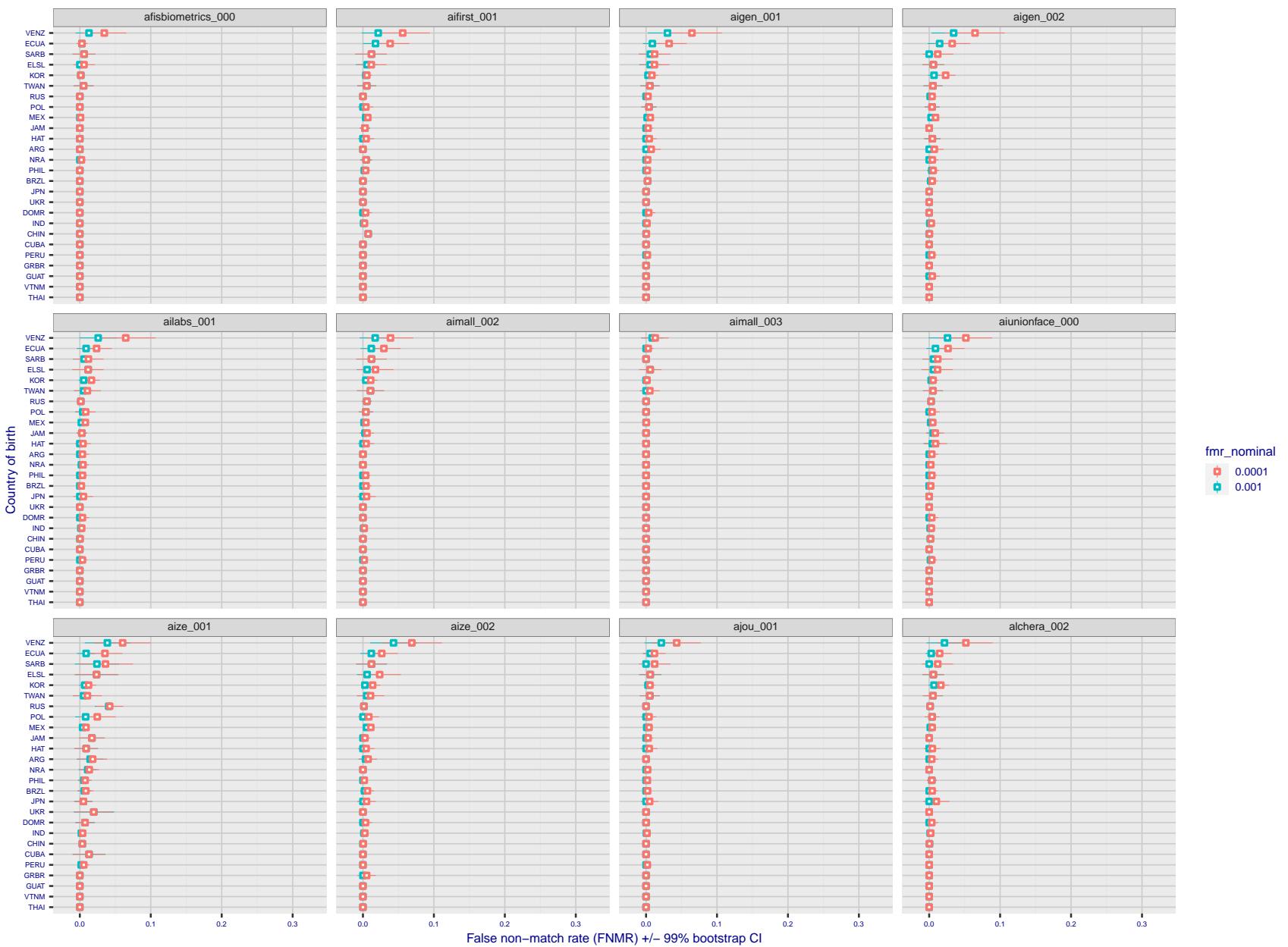


Figure 237: For the visa images, the dots show FNMR by country of birth for two globally set operating thresholds corresponding to $FMR = \{0.001, 0.0001\}$ computed over all on the order of 10^{10} impostor scores. The FMR in each bin will vary also - see subsequent impostor heatmaps in sec. 3.6.1. The figures shows an order of magnitude variation in FNMR across country of birth; these effects are likely due quality variations, then demographics like age and race. The error rates in some cases are zero, and in others the DET is flat so the error rates at the two thresholds are identical. The lines span 1% and 99% of bootstrap replicated FNMR estimates.

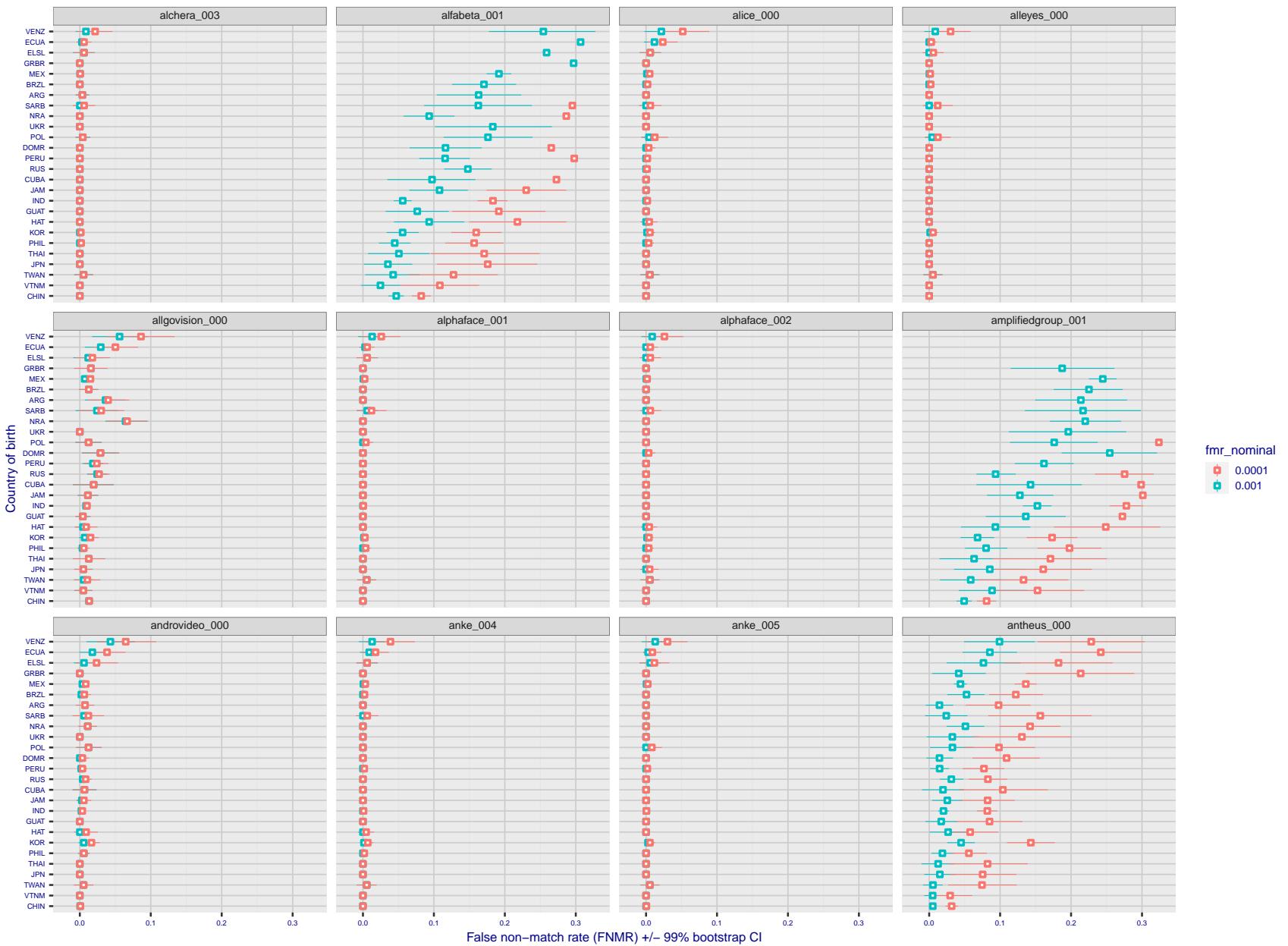


Figure 238: For the visa images, the dots show FNMR by country of birth for two globally set operating thresholds corresponding to $FMR = \{0.001, 0.0001\}$ computed over all on the order of 10^{10} impostor scores. The FMR in each bin will vary also - see subsequent impostor heatmaps in sec. 3.6.1. The figures shows an order of magnitude variation in FNMR across country of birth; these effects are likely due quality variations, then demographics like age and race. The error rates in some cases are zero, and in others the DET is flat so the error rates at the two thresholds are identical. The lines span 1% and 99% of bootstrap replicated FNMR estimates.

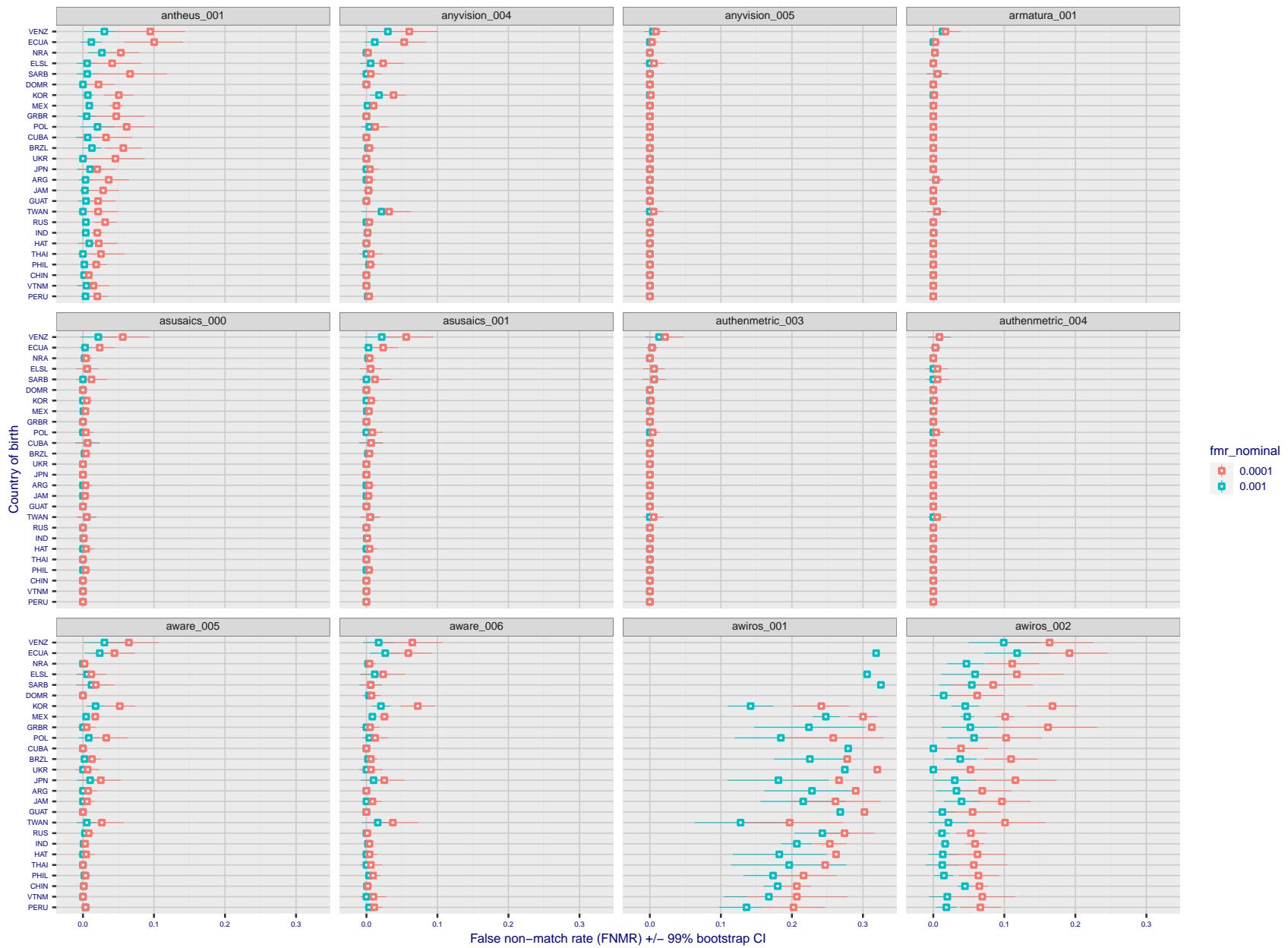


Figure 239: For the visa images, the dots show FNMR by country of birth for two globally set operating thresholds corresponding to $FMR = \{0.001, 0.0001\}$ computed over all on the order of 10^{10} impostor scores. The FMR in each bin will vary also - see subsequent impostor heatmaps in sec. 3.6.1. The figures shows an order of magnitude variation in FNMR across country of birth; these effects are likely due quality variations, then demographics like age and race. The error rates in some cases are zero, and in others the DET is flat so the error rates at the two thresholds are identical. The lines span 1% and 99% of bootstrap replicated FNMR estimates.

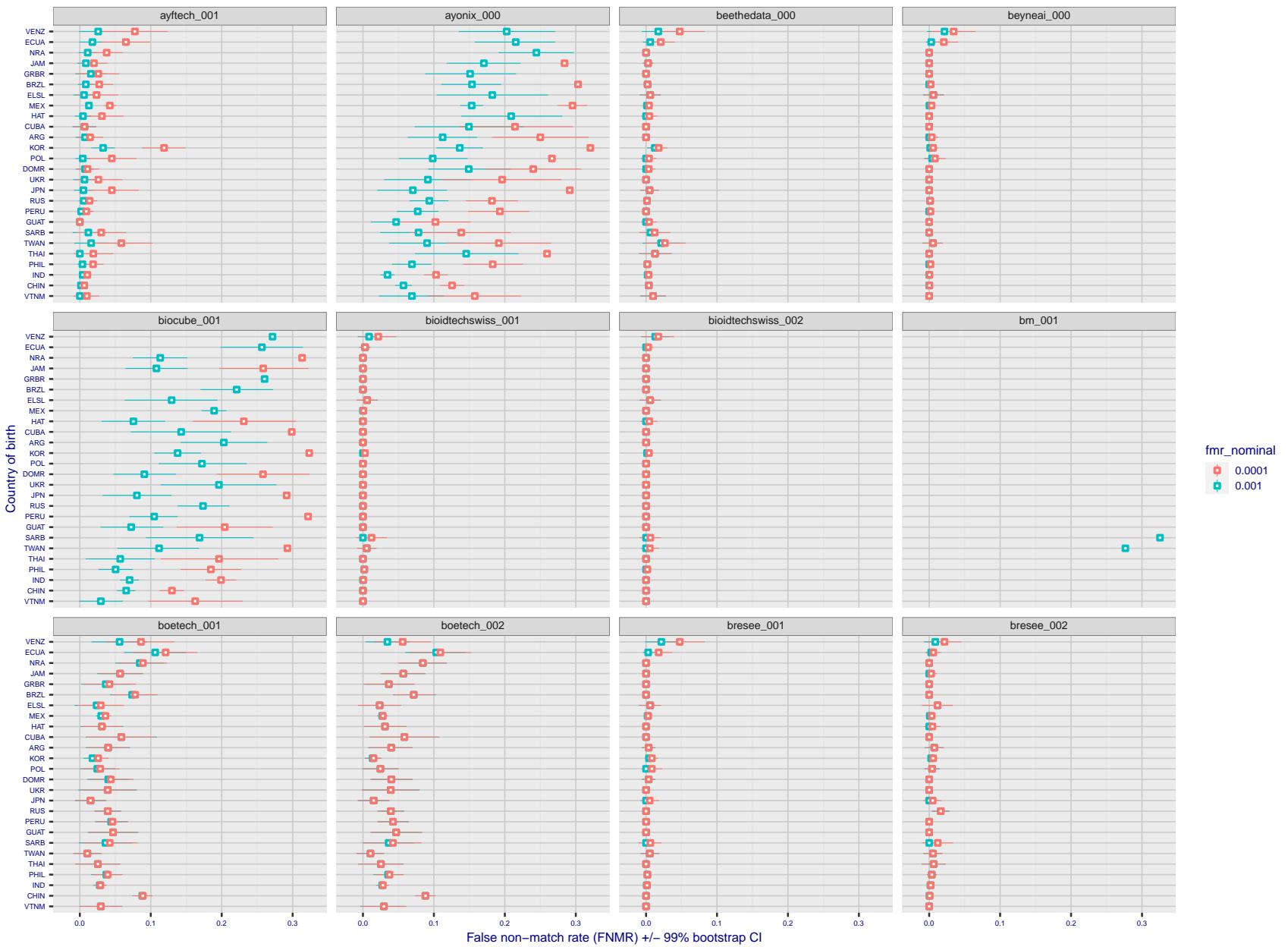


Figure 240: For the visa images, the dots show FNMR by country of birth for two globally set operating thresholds corresponding to $FMR = \{0.001, 0.0001\}$ computed over all on the order of 10^{10} impostor scores. The FMR in each bin will vary also - see subsequent impostor heatmaps in sec. 3.6.1. The figures shows an order of magnitude variation in FNMR across country of birth; these effects are likely due quality variations, then demographics like age and race. The error rates in some cases are zero, and in others the DET is flat so the error rates at the two thresholds are identical. The lines span 1% and 99% of bootstrap replicated FNMR estimates.

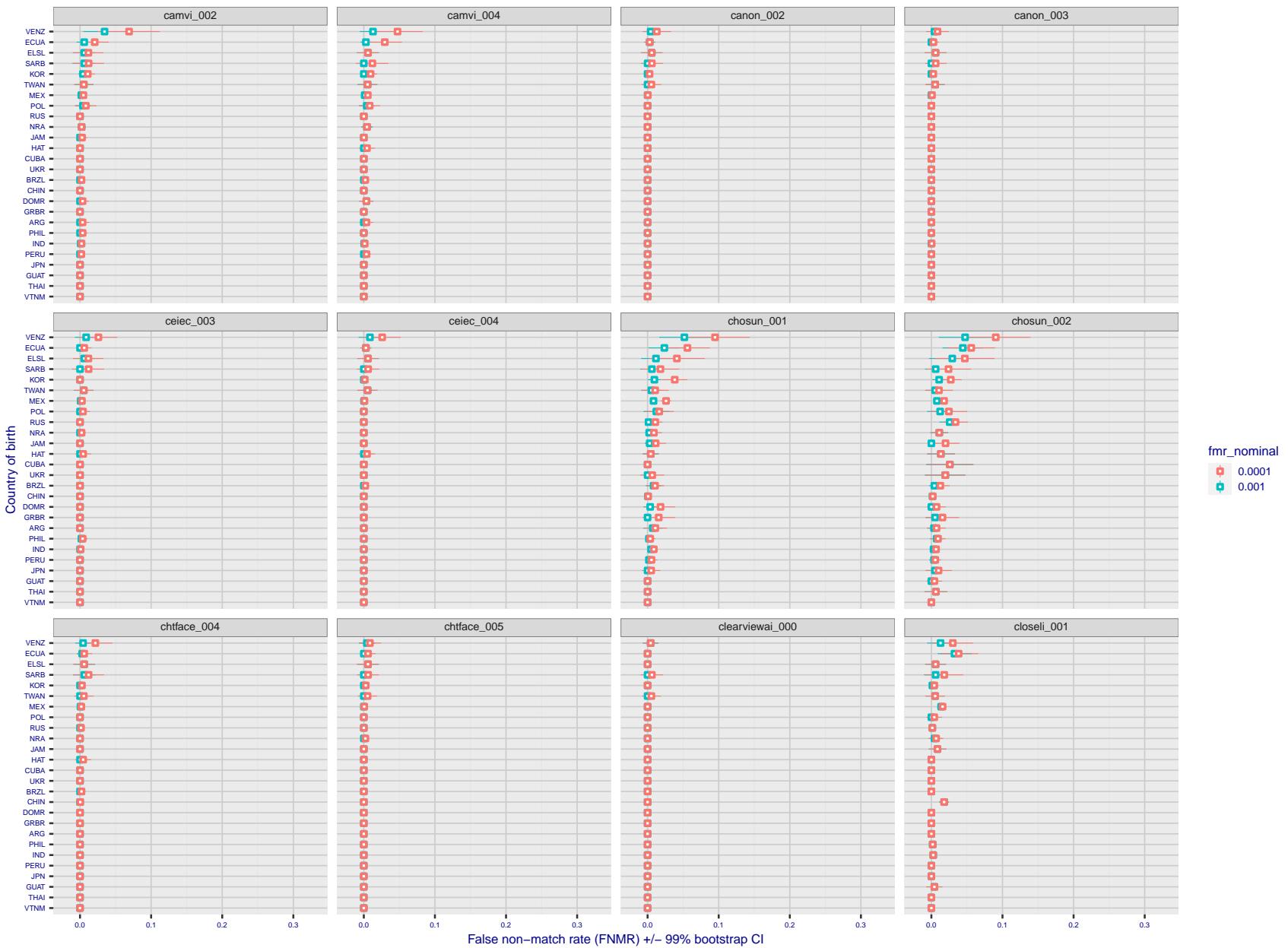


Figure 241: For the visa images, the dots show FNMR by country of birth for two globally set operating thresholds corresponding to $FMR = \{0.001, 0.0001\}$ computed over all on the order of 10^{10} impostor scores. The FMR in each bin will vary also - see subsequent impostor heatmaps in sec. 3.6.1. The figures shows an order of magnitude variation in FNMR across country of birth; these effects are likely due quality variations, then demographics like age and race. The error rates in some cases are zero, and in others the DET is flat so the error rates at the two thresholds are identical. The lines span 1% and 99% of bootstrap replicated FNMR estimates.

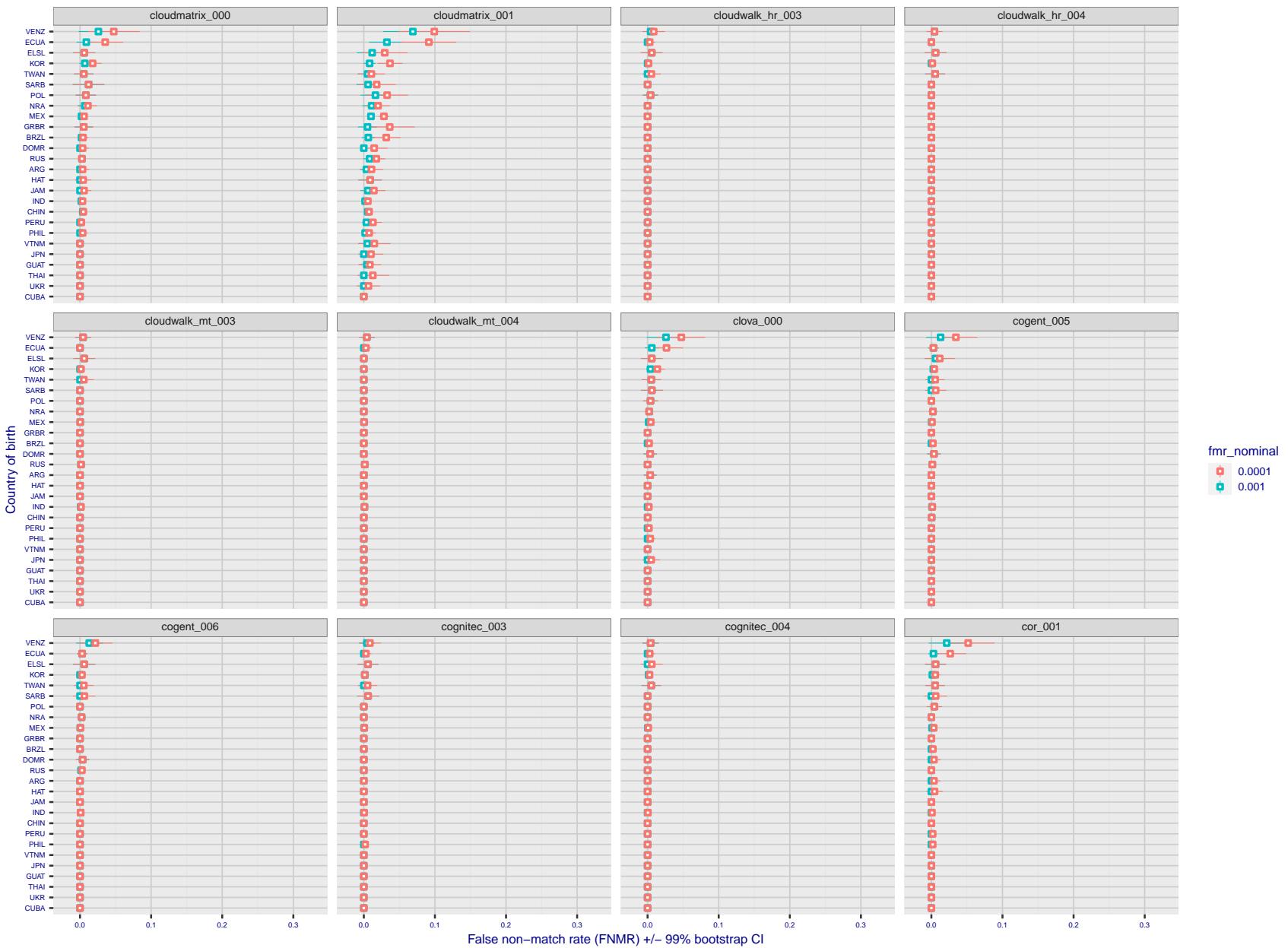


Figure 242: For the visa images, the dots show FNMR by country of birth for two globally set operating thresholds corresponding to $FMR = \{0.001, 0.0001\}$ computed over all on the order of 10^{10} impostor scores. The FMR in each bin will vary also - see subsequent impostor heatmaps in sec. 3.6.1. The figures shows an order of magnitude variation in FNMR across country of birth; these effects are likely due quality variations, then demographics like age and race. The error rates in some cases are zero, and in others the DET is flat so the error rates at the two thresholds are identical. The lines span 1% and 99% of bootstrap replicated FNMR estimates.

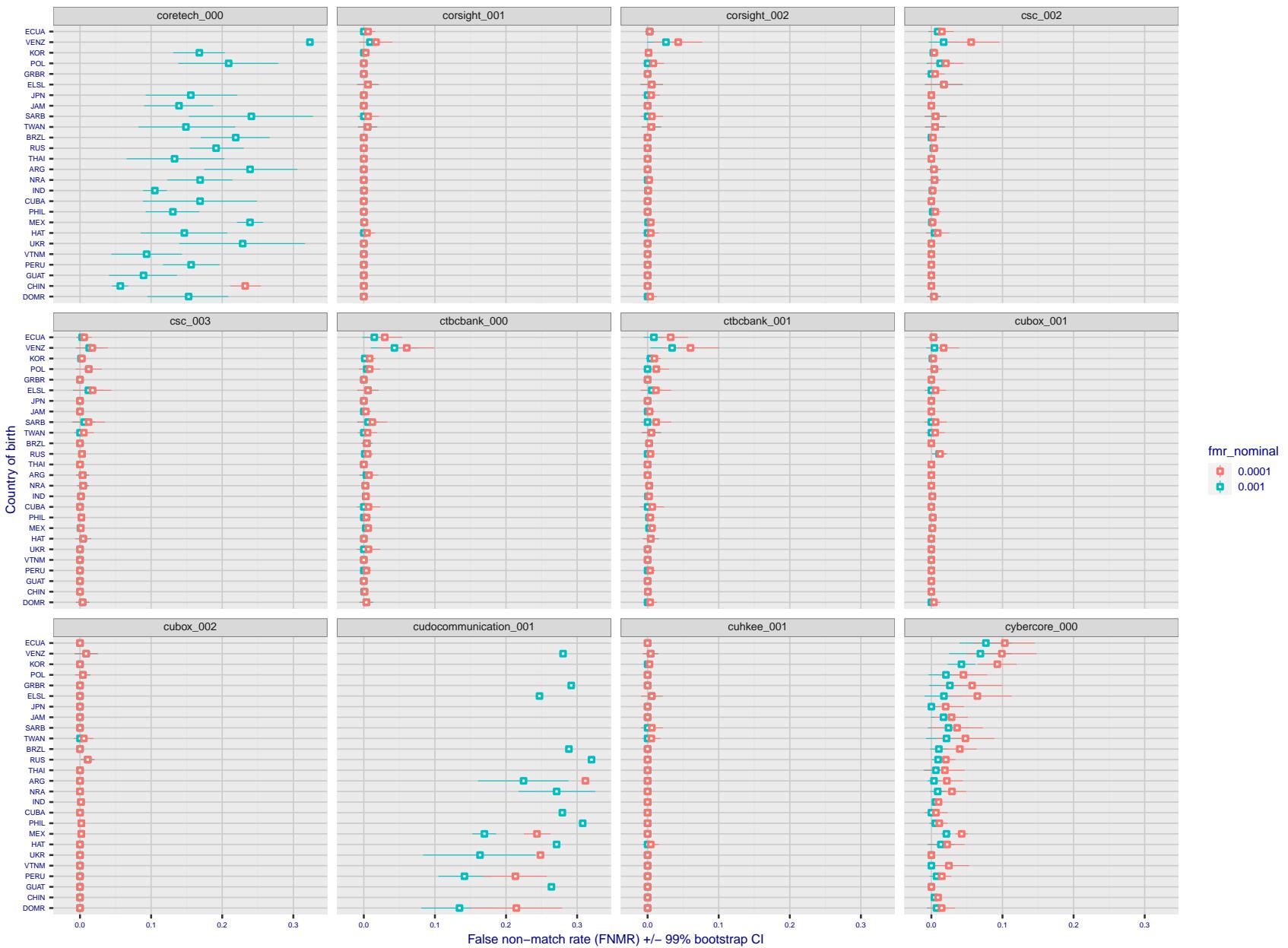


Figure 243: For the visa images, the dots show FNMR by country of birth for two globally set operating thresholds corresponding to $FMR = \{0.001, 0.0001\}$ computed over all on the order of 10^{10} impostor scores. The FMR in each bin will vary also - see subsequent impostor heatmaps in sec. 3.6.1. The figures shows an order of magnitude variation in FNMR across country of birth; these effects are likely due quality variations, then demographics like age and race. The error rates in some cases are zero, and in others the DET is flat so the error rates at the two thresholds are identical. The lines span 1% and 99% of bootstrap replicated FNMR estimates.

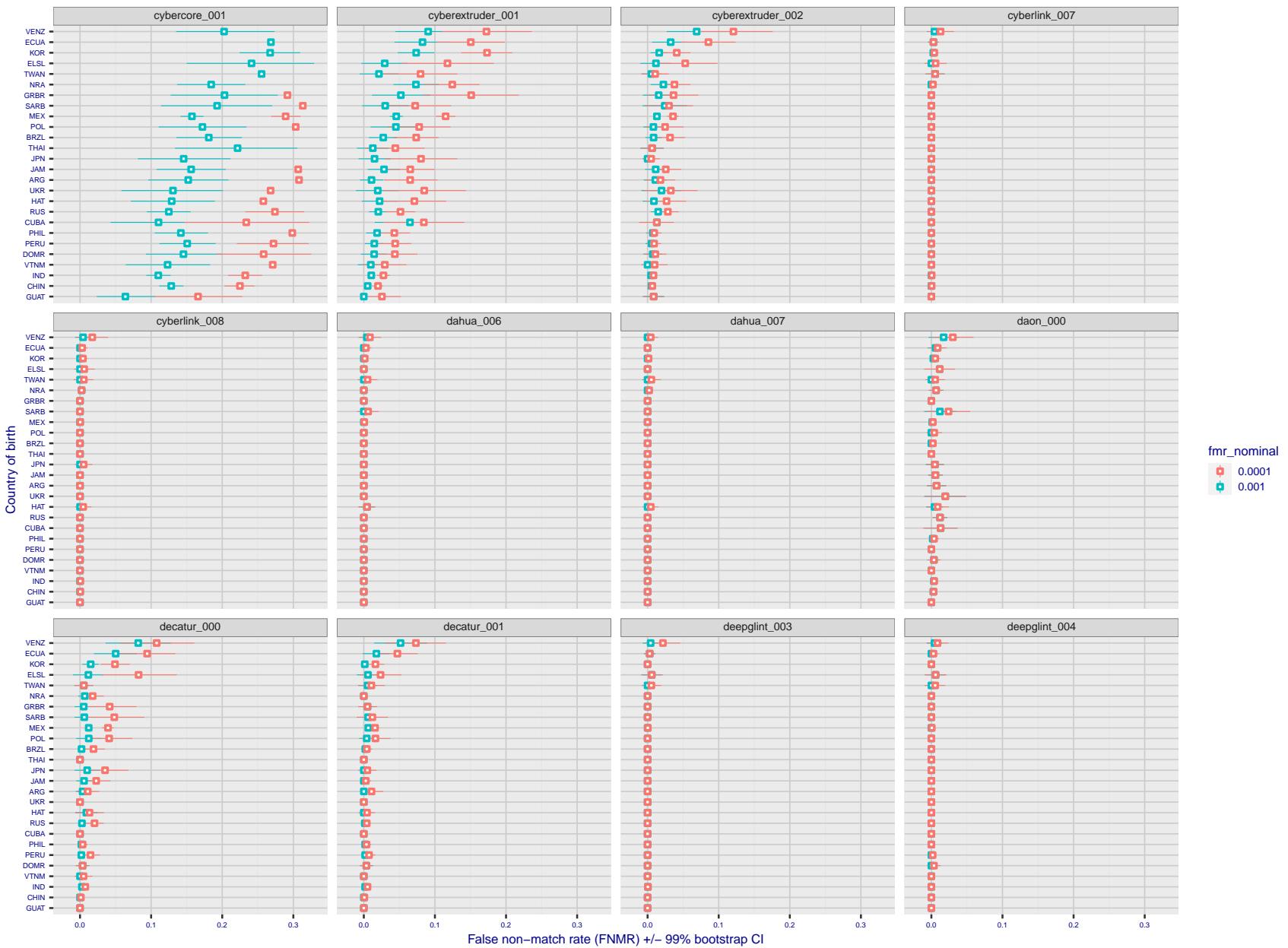


Figure 244: For the visa images, the dots show FNMR by country of birth for two globally set operating thresholds corresponding to $FMR = \{0.001, 0.0001\}$ computed over all on the order of 10^{10} impostor scores. The FMR in each bin will vary also - see subsequent impostor heatmaps in sec. 3.6.1. The figures shows an order of magnitude variation in FNMR across country of birth; these effects are likely due quality variations, then demographics like age and race. The error rates in some cases are zero, and in others the DET is flat so the error rates at the two thresholds are identical. The lines span 1% and 99% of bootstrap replicated FNMR estimates.

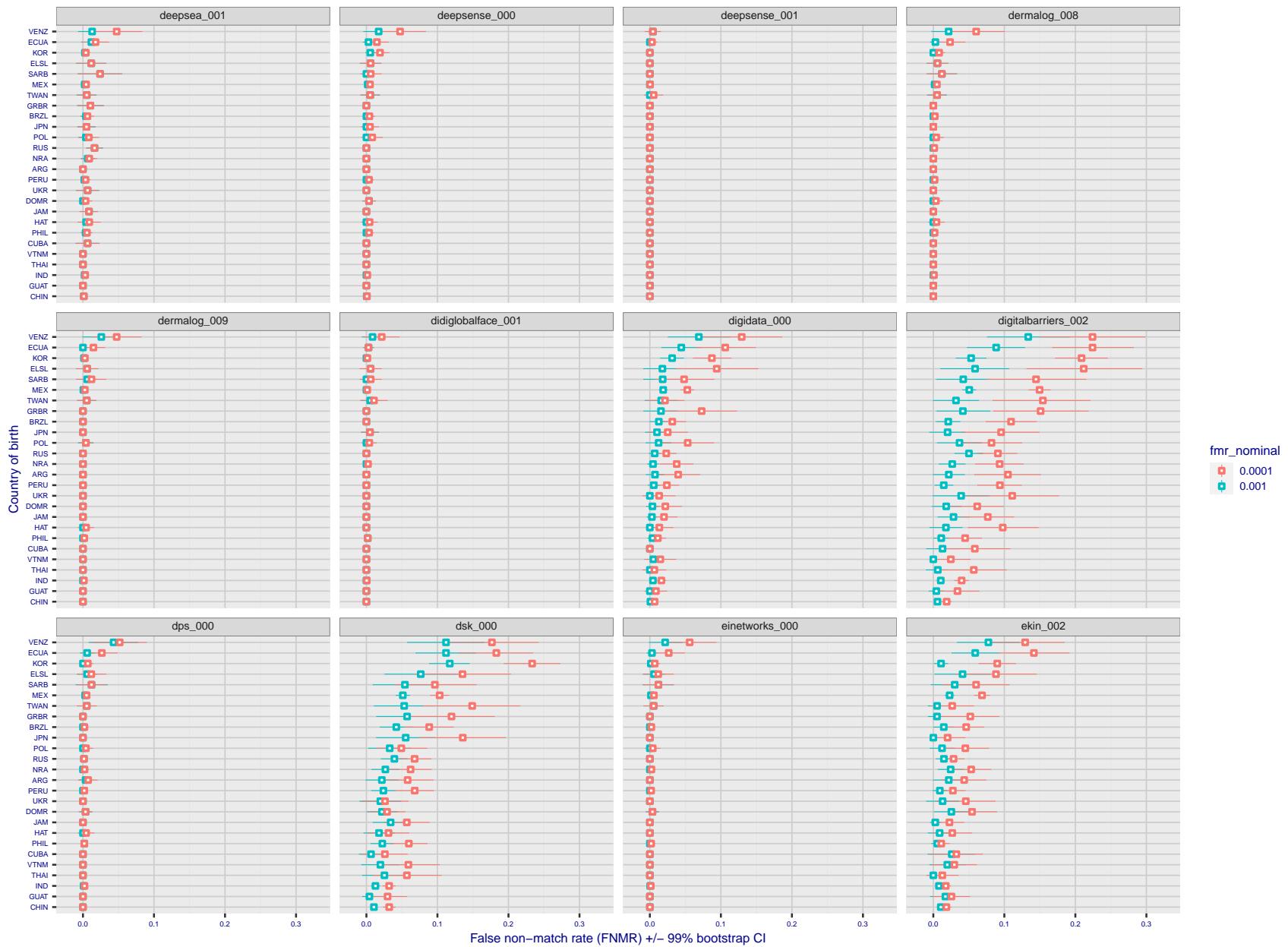


Figure 245: For the visa images, the dots show FNMR by country of birth for two globally set operating thresholds corresponding to $FMR = \{0.001, 0.0001\}$ computed over all on the order of 10^{10} impostor scores. The FMR in each bin will vary also - see subsequent impostor heatmaps in sec. 3.6.1. The figures shows an order of magnitude variation in FNMR across country of birth; these effects are likely due quality variations, then demographics like age and race. The error rates in some cases are zero, and in others the DET is flat so the error rates at the two thresholds are identical. The lines span 1% and 99% of bootstrap replicated FNMR estimates.

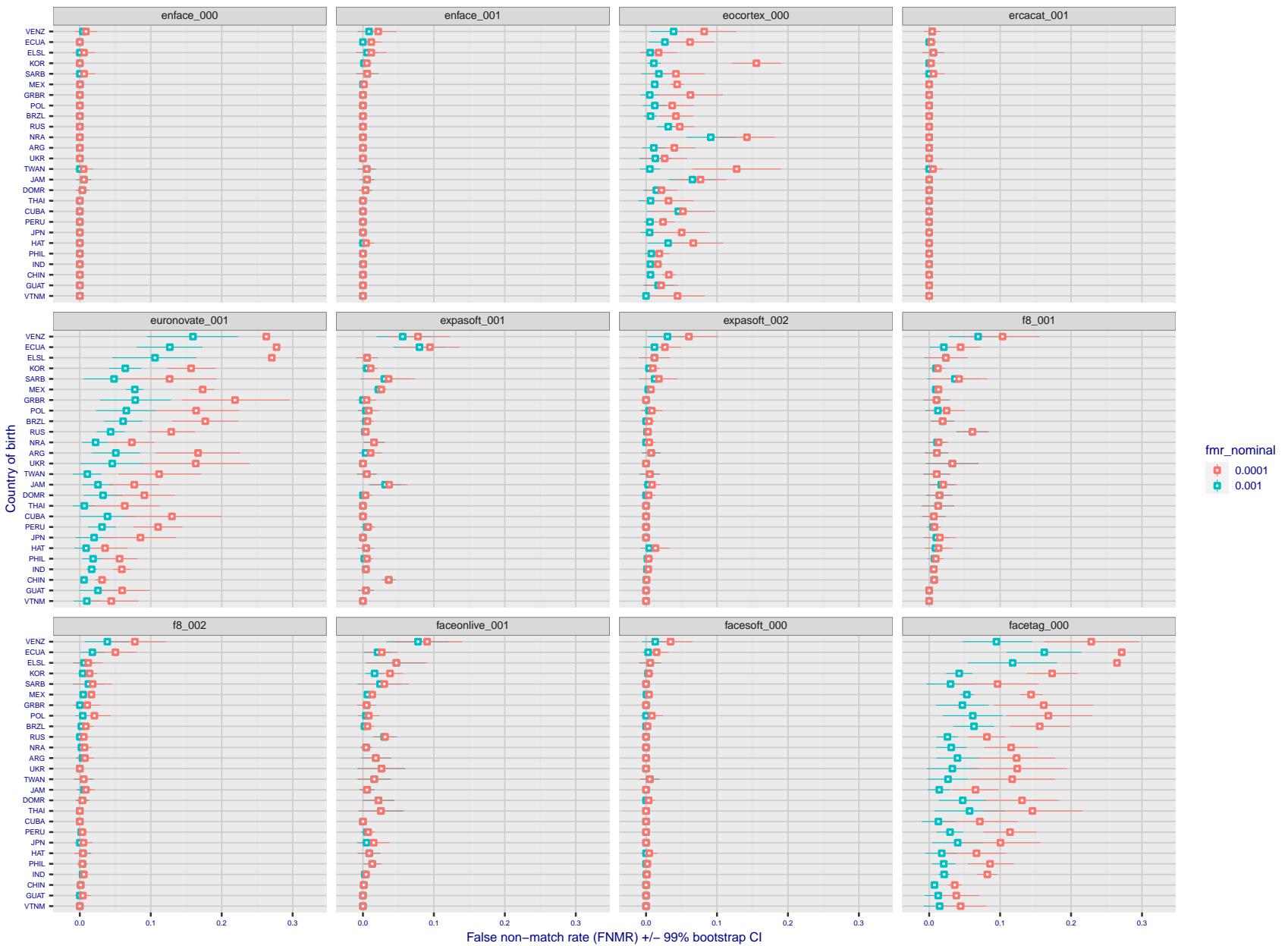


Figure 246: For the visa images, the dots show FNMR by country of birth for two globally set operating thresholds corresponding to $FMR = \{0.001, 0.0001\}$ computed over all on the order of 10^{10} impostor scores. The FMR in each bin will vary also - see subsequent impostor heatmaps in sec. 3.6.1. The figures shows an order of magnitude variation in FNMR across country of birth; these effects are likely due quality variations, then demographics like age and race. The error rates in some cases are zero, and in others the DET is flat so the error rates at the two thresholds are identical. The lines span 1% and 99% of bootstrap replicated FNMR estimates.

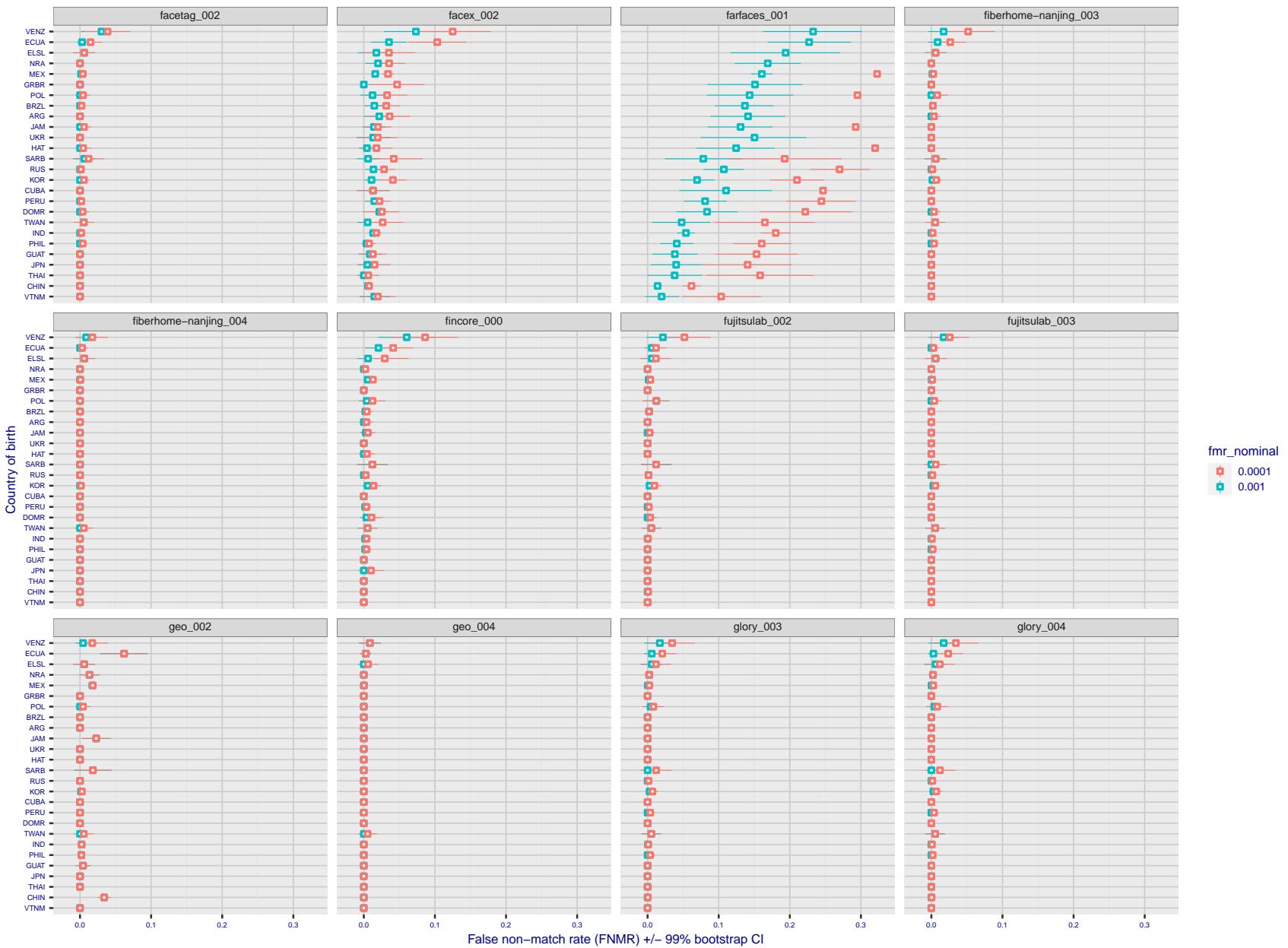


Figure 247: For the visa images, the dots show FNMR by country of birth for two globally set operating thresholds corresponding to $FMR = \{0.001, 0.0001\}$ computed over all on the order of 10^{10} impostor scores. The FMR in each bin will vary also - see subsequent impostor heatmaps in sec. 3.6.1. The figures shows an order of magnitude variation in FNMR across country of birth; these effects are likely due quality variations, then demographics like age and race. The error rates in some cases are zero, and in others the DET is flat so the error rates at the two thresholds are identical. The lines span 1% and 99% of bootstrap replicated FNMR estimates.

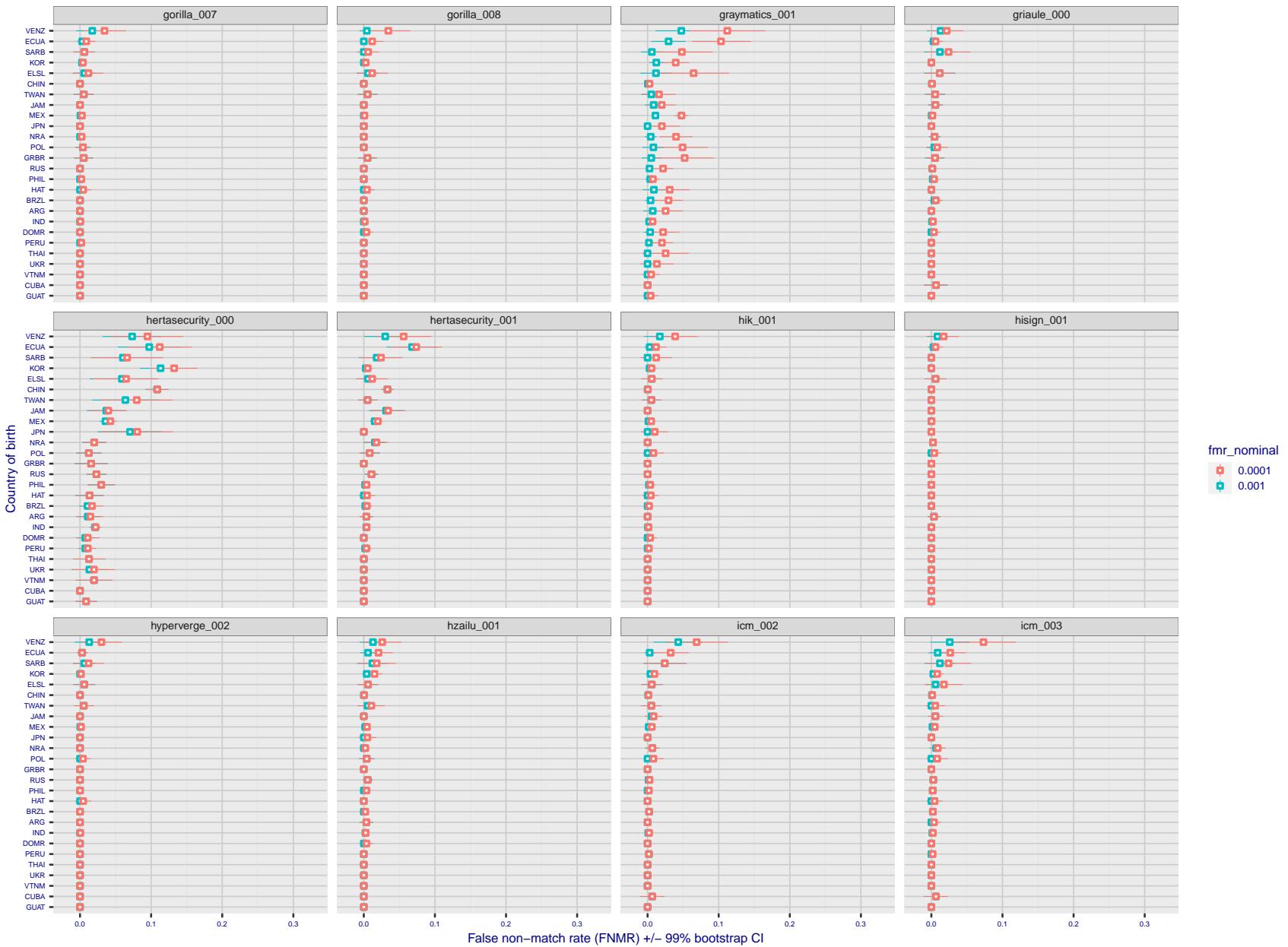


Figure 248: For the visa images, the dots show FNMR by country of birth for two globally set operating thresholds corresponding to $FMR = \{0.001, 0.0001\}$ computed over all on the order of 10^{10} impostor scores. The FMR in each bin will vary also - see subsequent impostor heatmaps in sec. 3.6.1. The figures shows an order of magnitude variation in FNMR across country of birth; these effects are likely due quality variations, then demographics like age and race. The error rates in some cases are zero, and in others the DET is flat so the error rates at the two thresholds are identical. The lines span 1% and 99% of bootstrap replicated FNMR estimates.

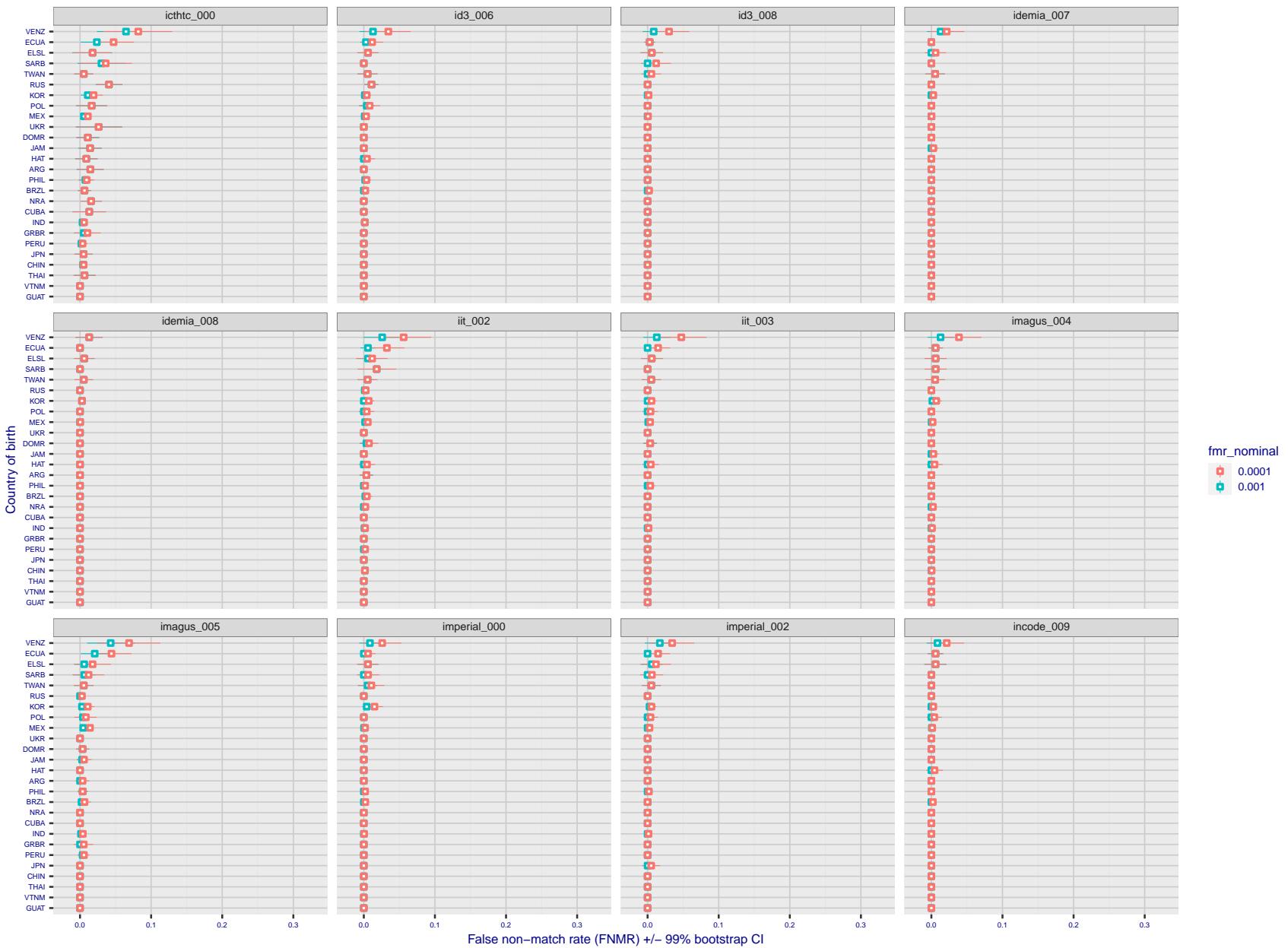


Figure 249: For the visa images, the dots show FNMR by country of birth for two globally set operating thresholds corresponding to $FMR = \{0.001, 0.0001\}$ computed over all on the order of 10^{10} impostor scores. The FMR in each bin will vary also - see subsequent impostor heatmaps in sec. 3.6.1. The figures shows an order of magnitude variation in FNMR across country of birth; these effects are likely due quality variations, then demographics like age and race. The error rates in some cases are zero, and in others the DET is flat so the error rates at the two thresholds are identical. The lines span 1% and 99% of bootstrap replicated FNMR estimates.

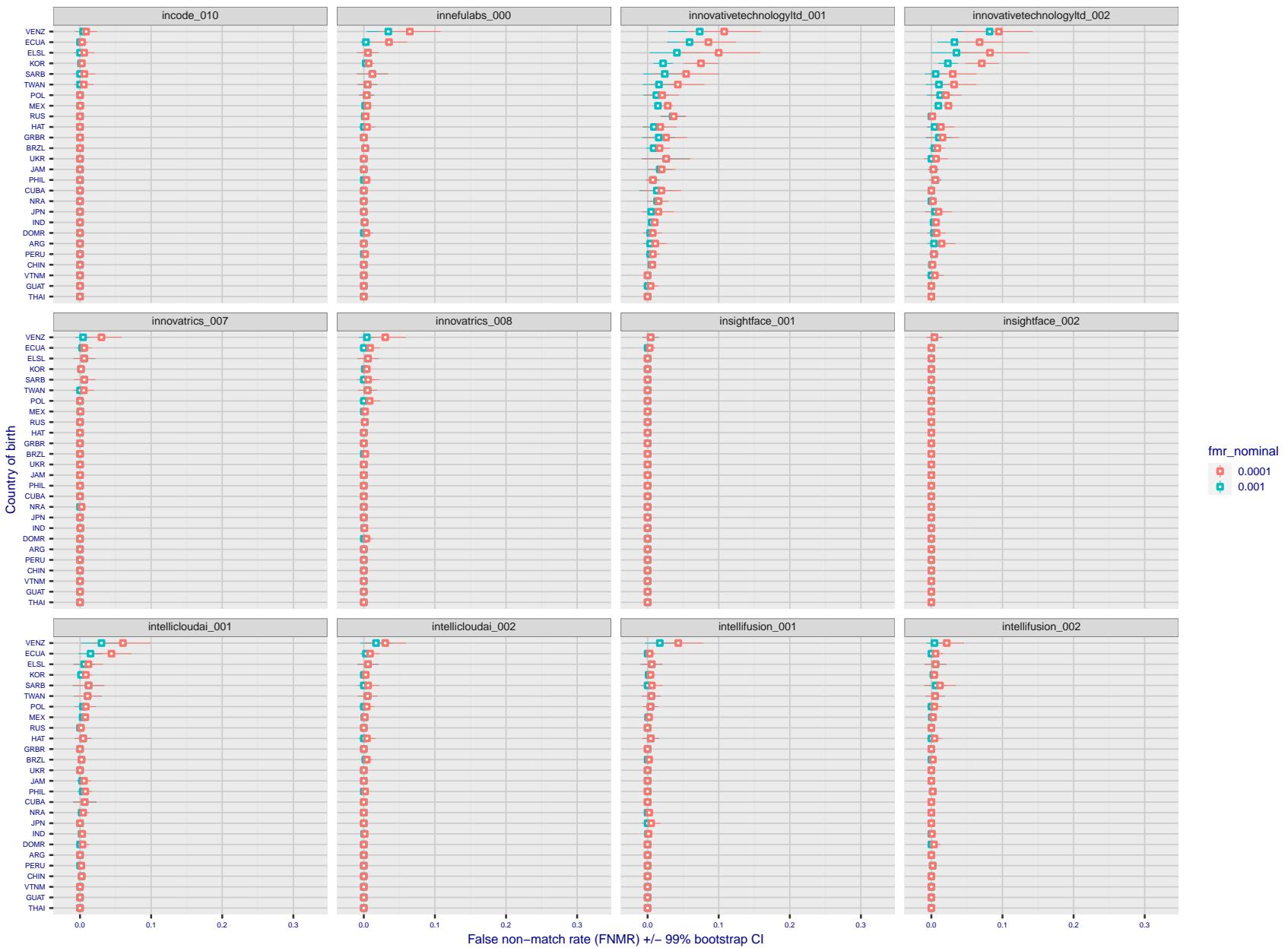


Figure 250: For the visa images, the dots show FNMR by country of birth for two globally set operating thresholds corresponding to $FMR = \{0.001, 0.0001\}$ computed over all on the order of 10^{10} impostor scores. The FMR in each bin will vary also - see subsequent impostor heatmaps in sec. 3.6.1. The figures shows an order of magnitude variation in FNMR across country of birth; these effects are likely due quality variations, then demographics like age and race. The error rates in some cases are zero, and in others the DET is flat so the error rates at the two thresholds are identical. The lines span 1% and 99% of bootstrap replicated FNMR estimates.

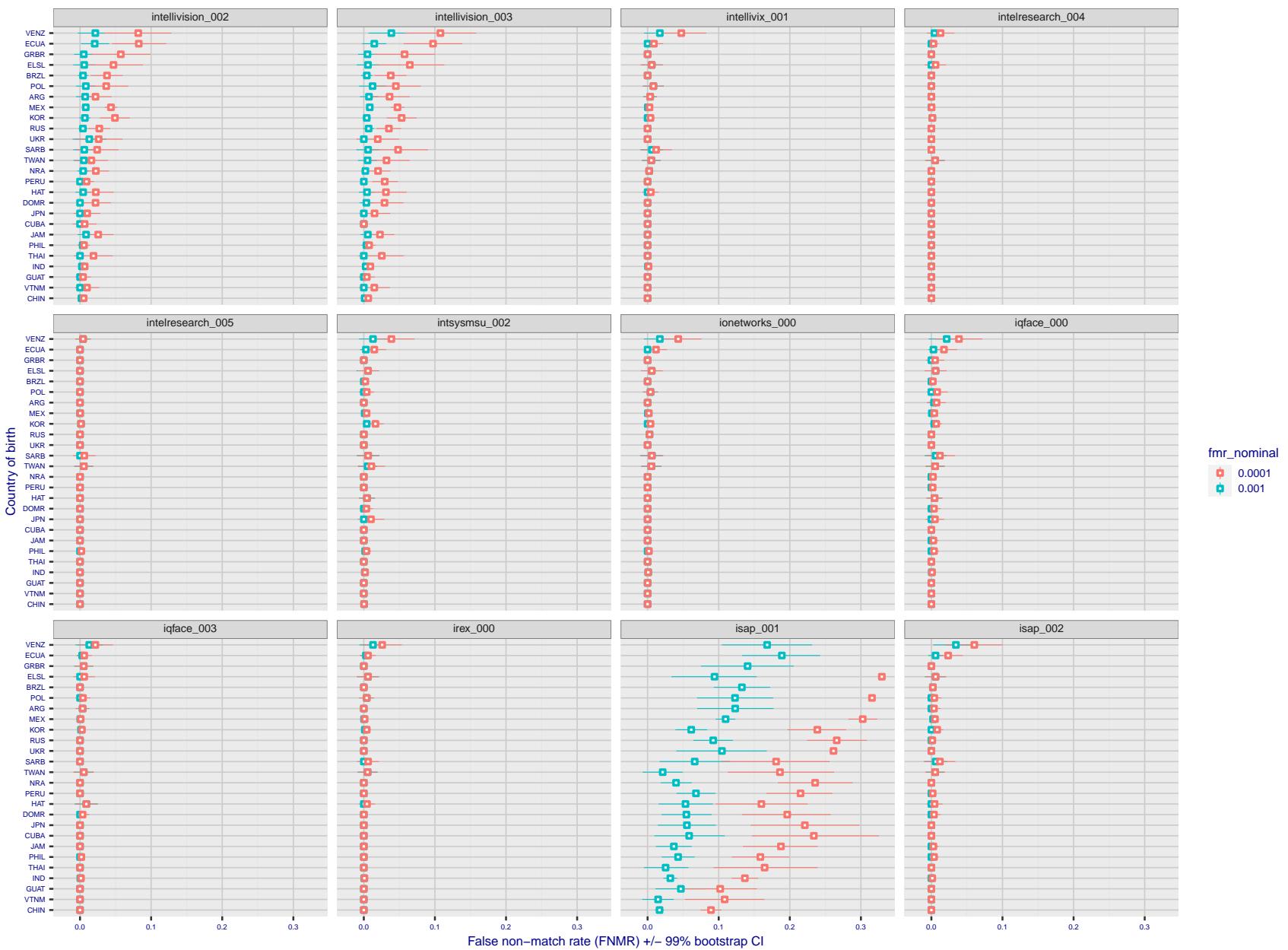


Figure 251: For the visa images, the dots show FNMR by country of birth for two globally set operating thresholds corresponding to $FMR = \{0.001, 0.0001\}$ computed over all on the order of 10^{10} impostor scores. The FMR in each bin will vary also - see subsequent impostor heatmaps in sec. 3.6.1. The figures shows an order of magnitude variation in FNMR across country of birth; these effects are likely due quality variations, then demographics like age and race. The error rates in some cases are zero, and in others the DET is flat so the error rates at the two thresholds are identical. The lines span 1% and 99% of bootstrap replicated FNMR estimates.

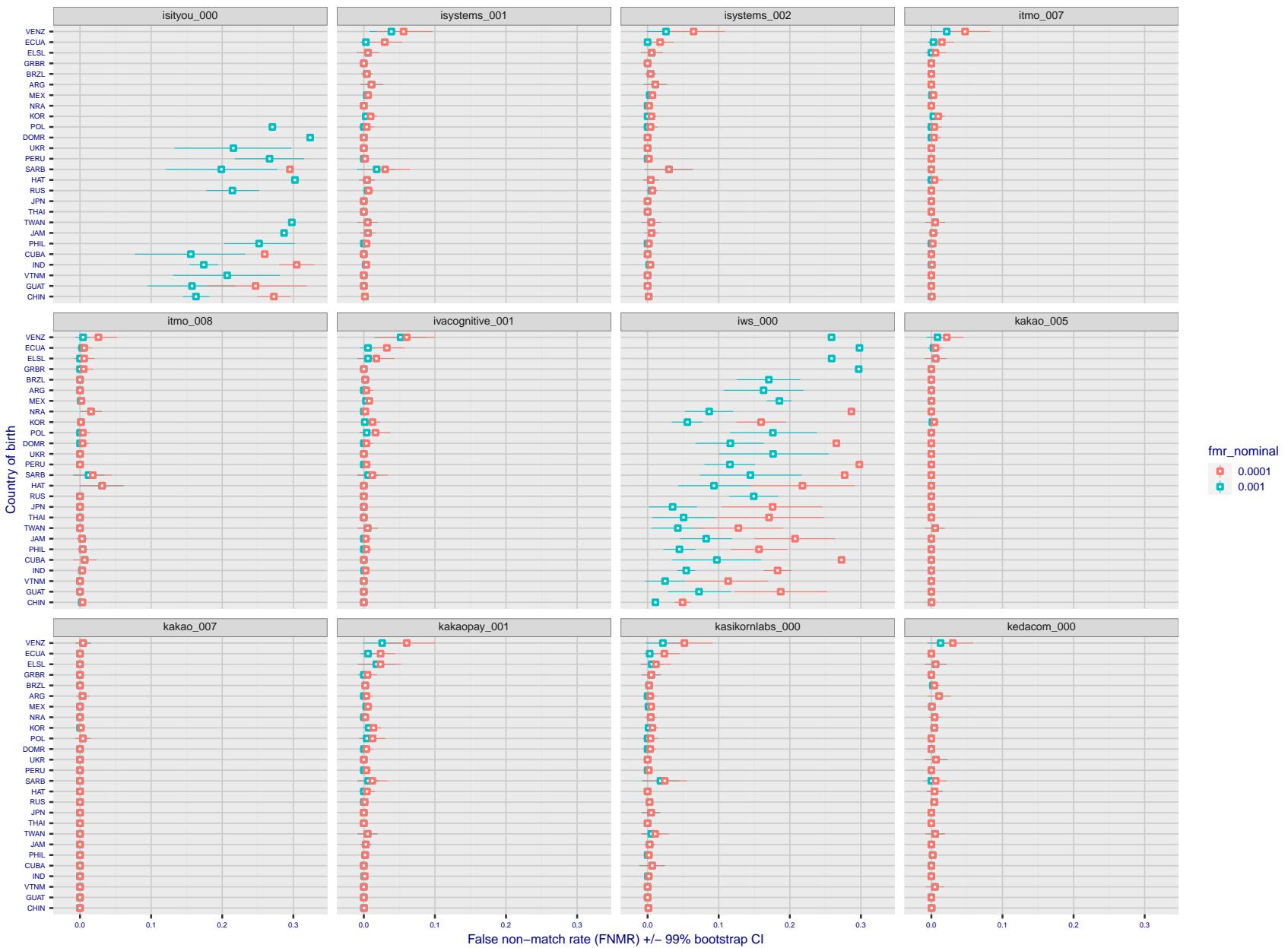


Figure 252: For the visa images, the dots show FNMR by country of birth for two globally set operating thresholds corresponding to $FMR = \{0.001, 0.0001\}$ computed over all on the order of 10^{10} impostor scores. The FMR in each bin will vary also - see subsequent impostor heatmaps in sec. 3.6.1. The figures shows an order of magnitude variation in FNMR across country of birth; these effects are likely due quality variations, then demographics like age and race. The error rates in some cases are zero, and in others the DET is flat so the error rates at the two thresholds are identical. The lines span 1% and 99% of bootstrap replicated FNMR estimates.

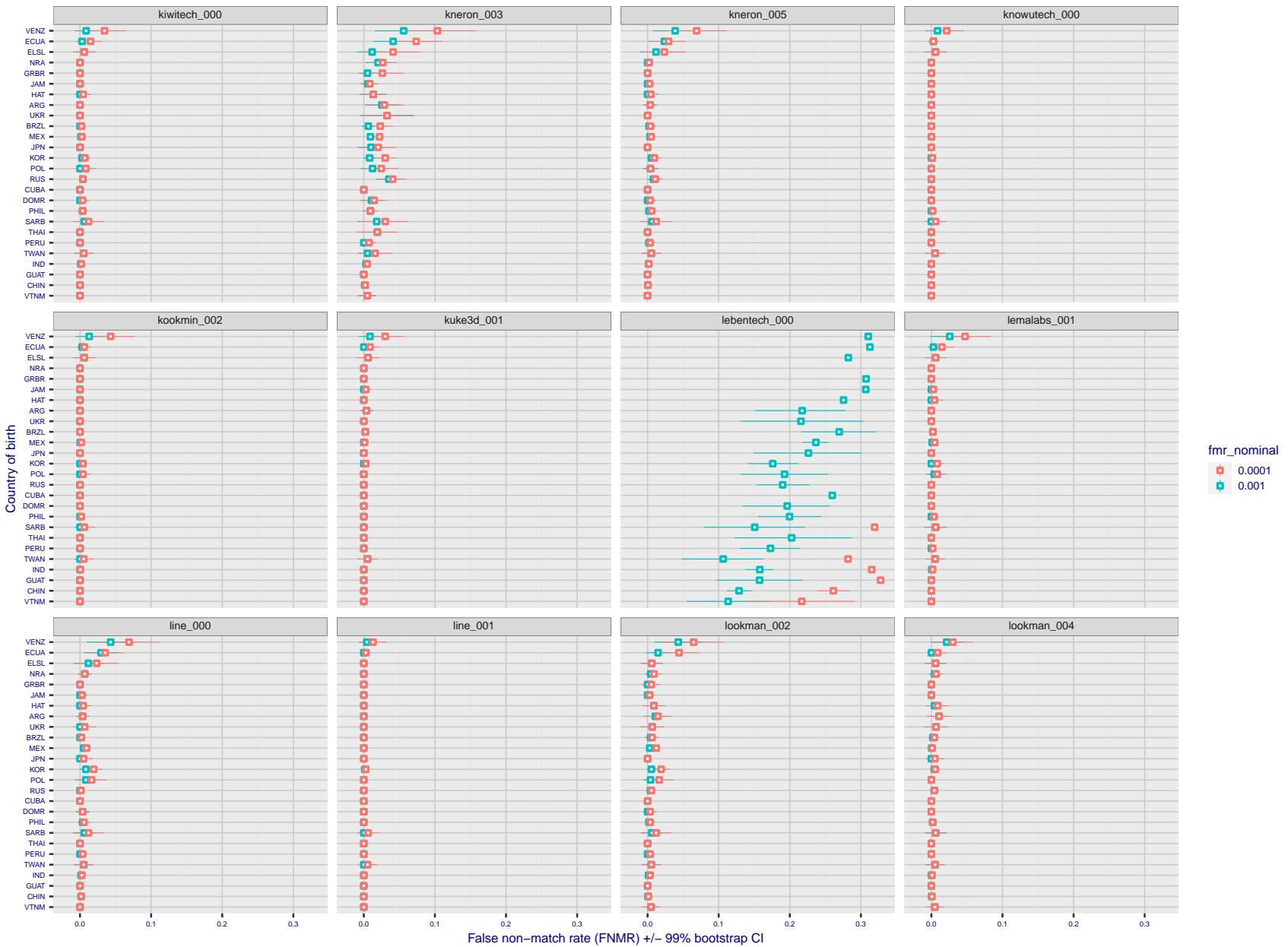


Figure 253: For the visa images, the dots show FNMR by country of birth for two globally set operating thresholds corresponding to $FMR = \{0.001, 0.0001\}$ computed over all on the order of 10^{10} impostor scores. The FMR in each bin will vary also - see subsequent impostor heatmaps in sec. 3.6.1. The figures shows an order of magnitude variation in FNMR across country of birth; these effects are likely due quality variations, then demographics like age and race. The error rates in some cases are zero, and in others the DET is flat so the error rates at the two thresholds are identical. The lines span 1% and 99% of bootstrap replicated FNMR estimates.

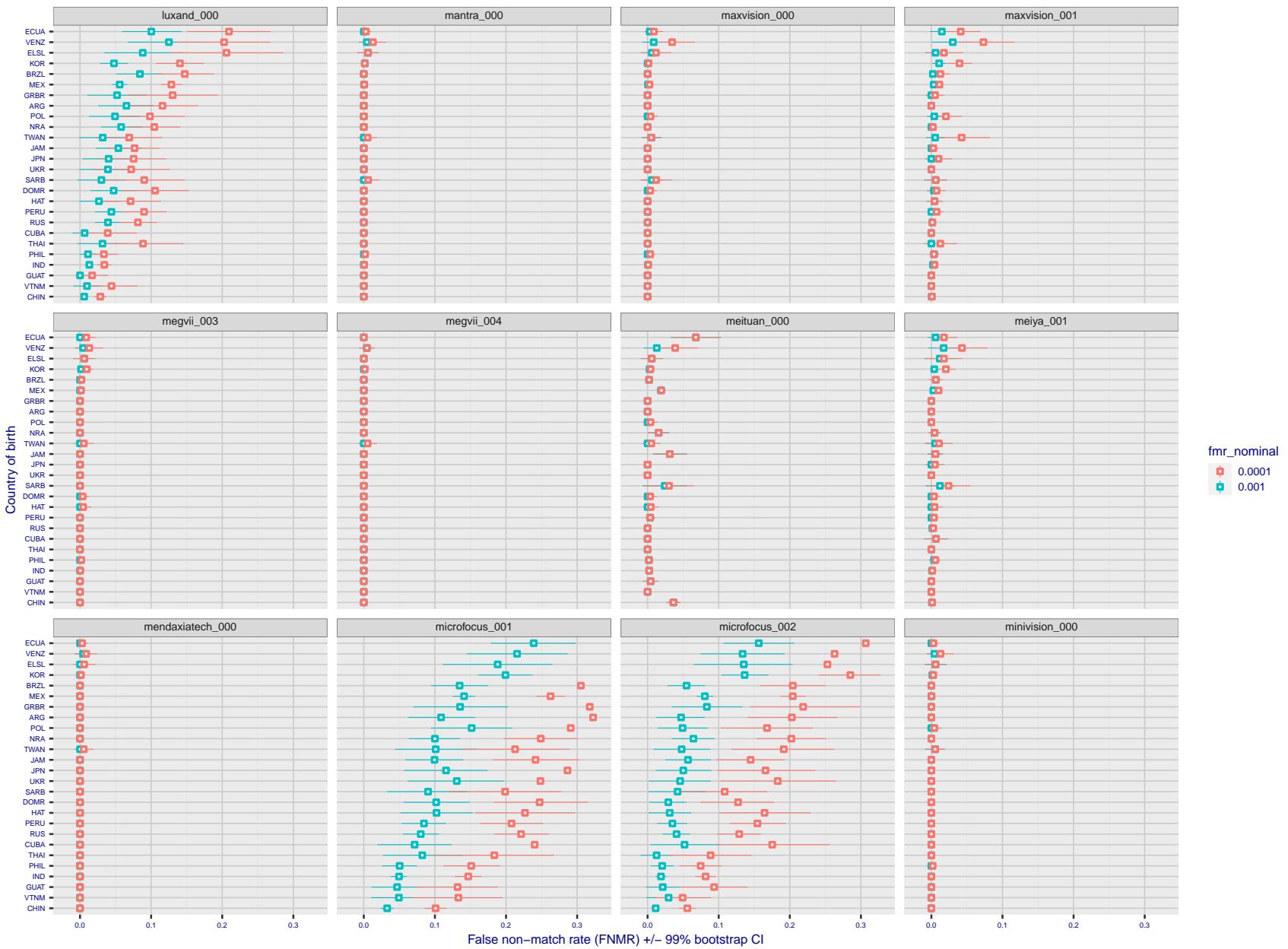


Figure 254: For the visa images, the dots show FNMR by country of birth for two globally set operating thresholds corresponding to $FMR = \{0.001, 0.0001\}$ computed over all on the order of 10^{10} impostor scores. The FMR in each bin will vary also - see subsequent impostor heatmaps in sec. 3.6.1. The figures shows an order of magnitude variation in FNMR across country of birth; these effects are likely due quality variations, then demographics like age and race. The error rates in some cases are zero, and in others the DET is flat so the error rates at the two thresholds are identical. The lines span 1% and 99% of bootstrap replicated FNMR estimates.

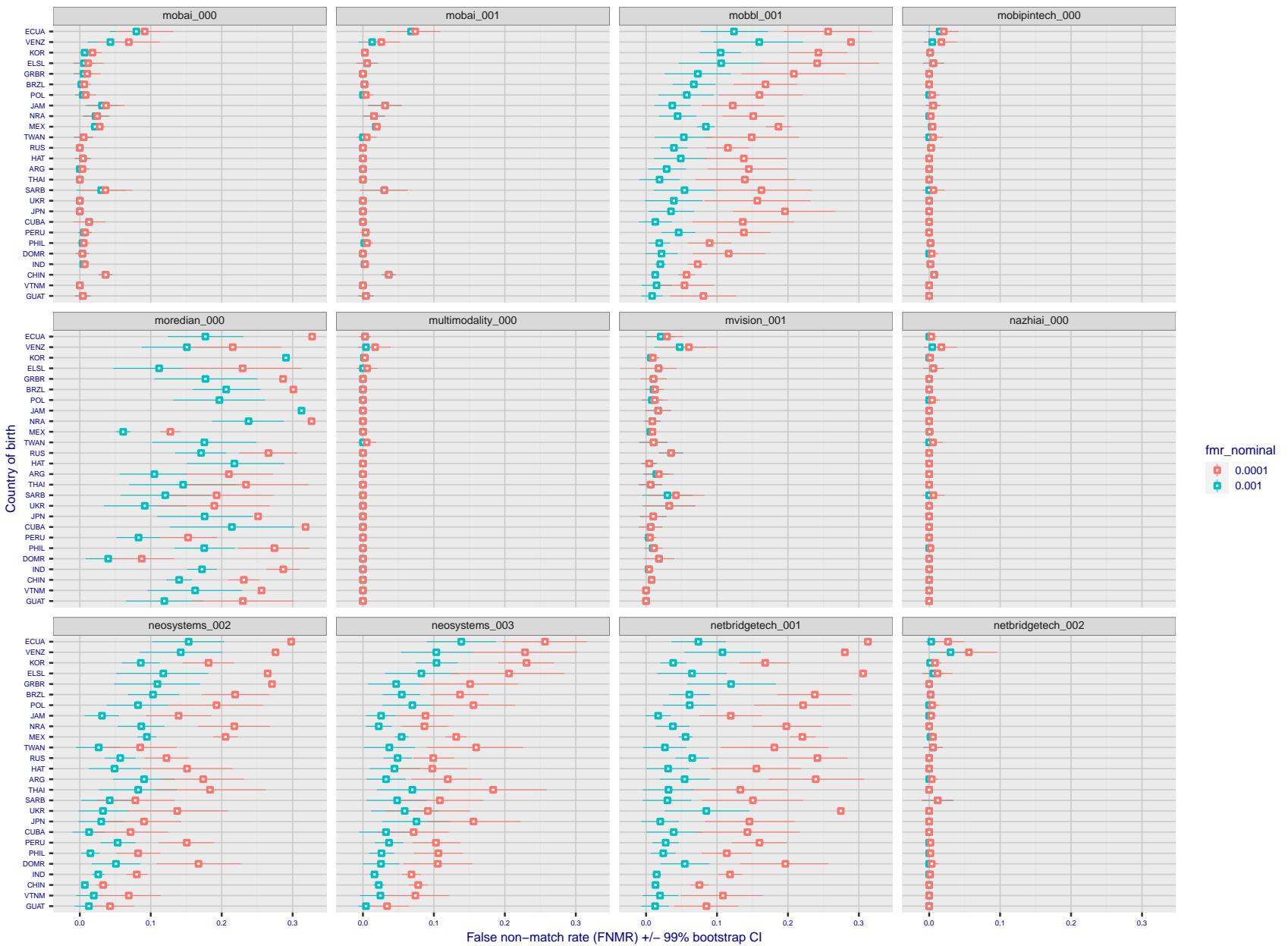


Figure 255: For the visa images, the dots show FNMR by country of birth for two globally set operating thresholds corresponding to $FMR = \{0.001, 0.0001\}$ computed over all on the order of 10^{10} impostor scores. The FMR in each bin will vary also - see subsequent impostor heatmaps in sec. 3.6.1. The figures shows an order of magnitude variation in FNMR across country of birth; these effects are likely due quality variations, then demographics like age and race. The error rates in some cases are zero, and in others the DET is flat so the error rates at the two thresholds are identical. The lines span 1% and 99% of bootstrap replicated FNMR estimates.

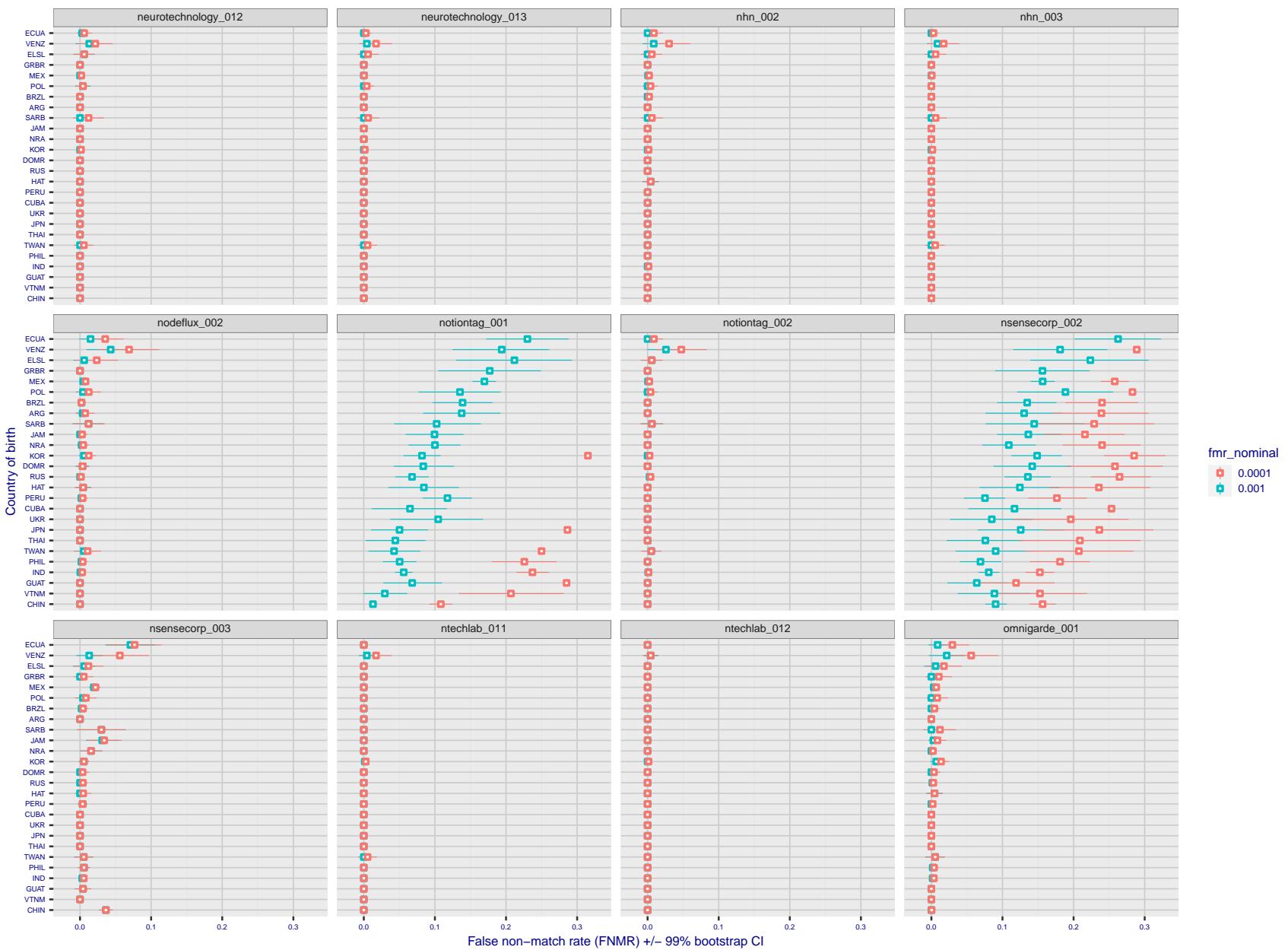


Figure 256: For the visa images, the dots show FNMR by country of birth for two globally set operating thresholds corresponding to $FMR = \{0.001, 0.0001\}$ computed over all on the order of 10^{10} impostor scores. The FMR in each bin will vary also - see subsequent impostor heatmaps in sec. 3.6.1. The figures shows an order of magnitude variation in FNMR across country of birth; these effects are likely due quality variations, then demographics like age and race. The error rates in some cases are zero, and in others the DET is flat so the error rates at the two thresholds are identical. The lines span 1% and 99% of bootstrap replicated FNMR estimates.

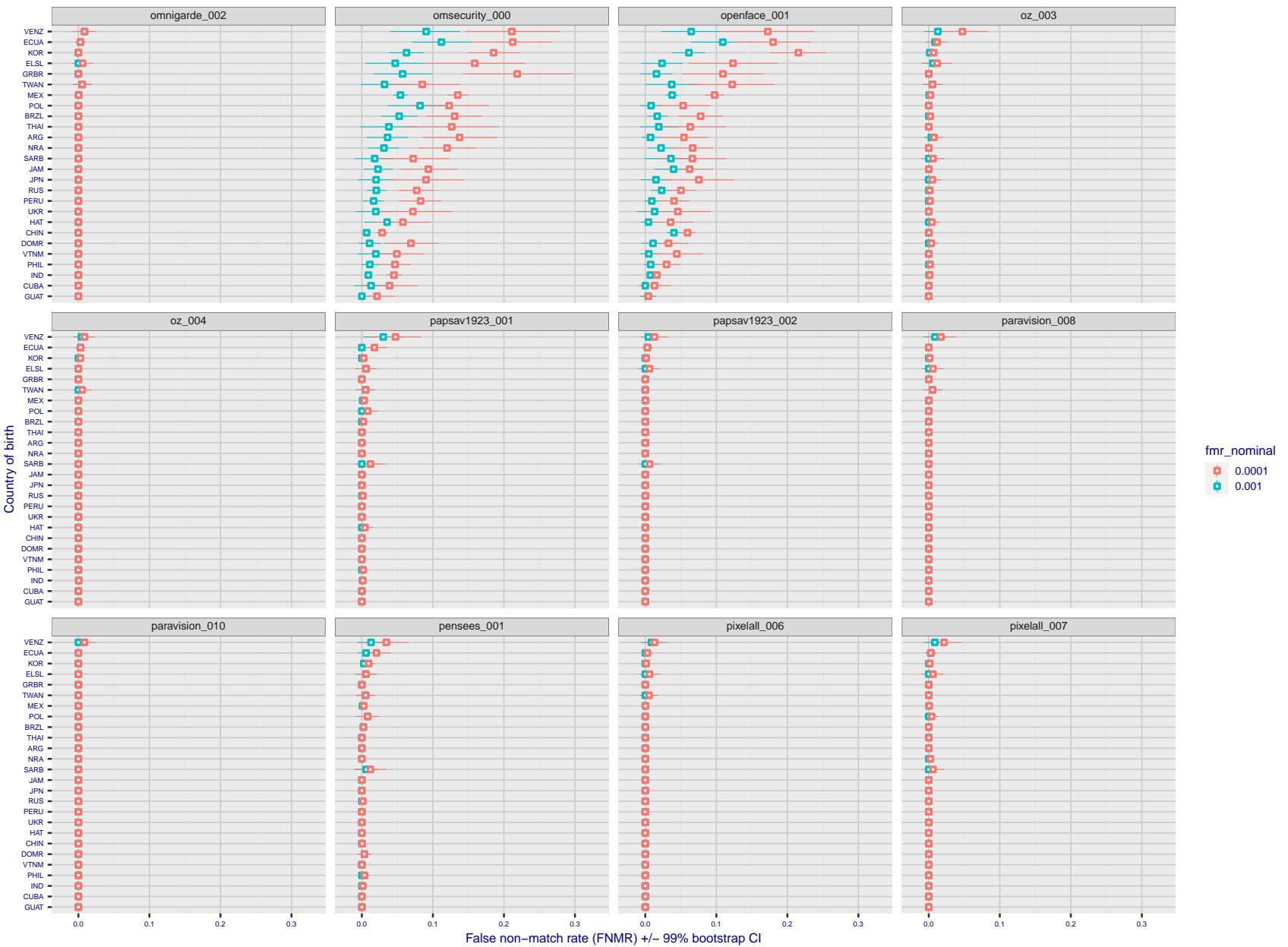


Figure 257: For the visa images, the dots show FNMR by country of birth for two globally set operating thresholds corresponding to $FMR = \{0.001, 0.0001\}$ computed over all on the order of 10^{10} impostor scores. The FMR in each bin will vary also - see subsequent impostor heatmaps in sec. 3.6.1. The figures shows an order of magnitude variation in FNMR across country of birth; these effects are likely due quality variations, then demographics like age and race. The error rates in some cases are zero, and in others the DET is flat so the error rates at the two thresholds are identical. The lines span 1% and 99% of bootstrap replicated FNMR estimates.

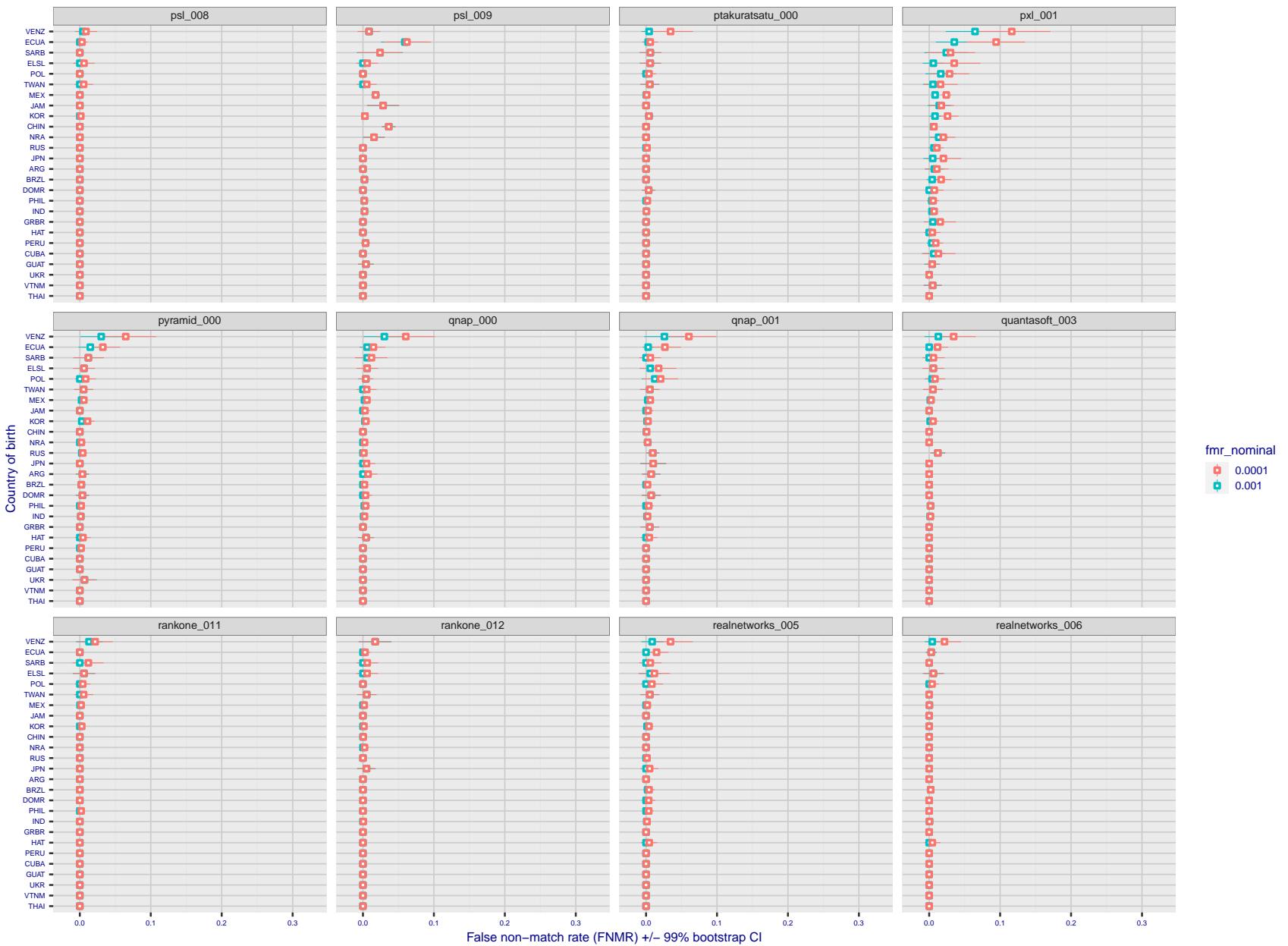


Figure 258: For the visa images, the dots show FNMR by country of birth for two globally set operating thresholds corresponding to $FMR = \{0.001, 0.0001\}$ computed over all on the order of 10^{10} impostor scores. The FMR in each bin will vary also - see subsequent impostor heatmaps in sec. 3.6.1. The figures shows an order of magnitude variation in FNMR across country of birth; these effects are likely due quality variations, then demographics like age and race. The error rates in some cases are zero, and in others the DET is flat so the error rates at the two thresholds are identical. The lines span 1% and 99% of bootstrap replicated FNMR estimates.

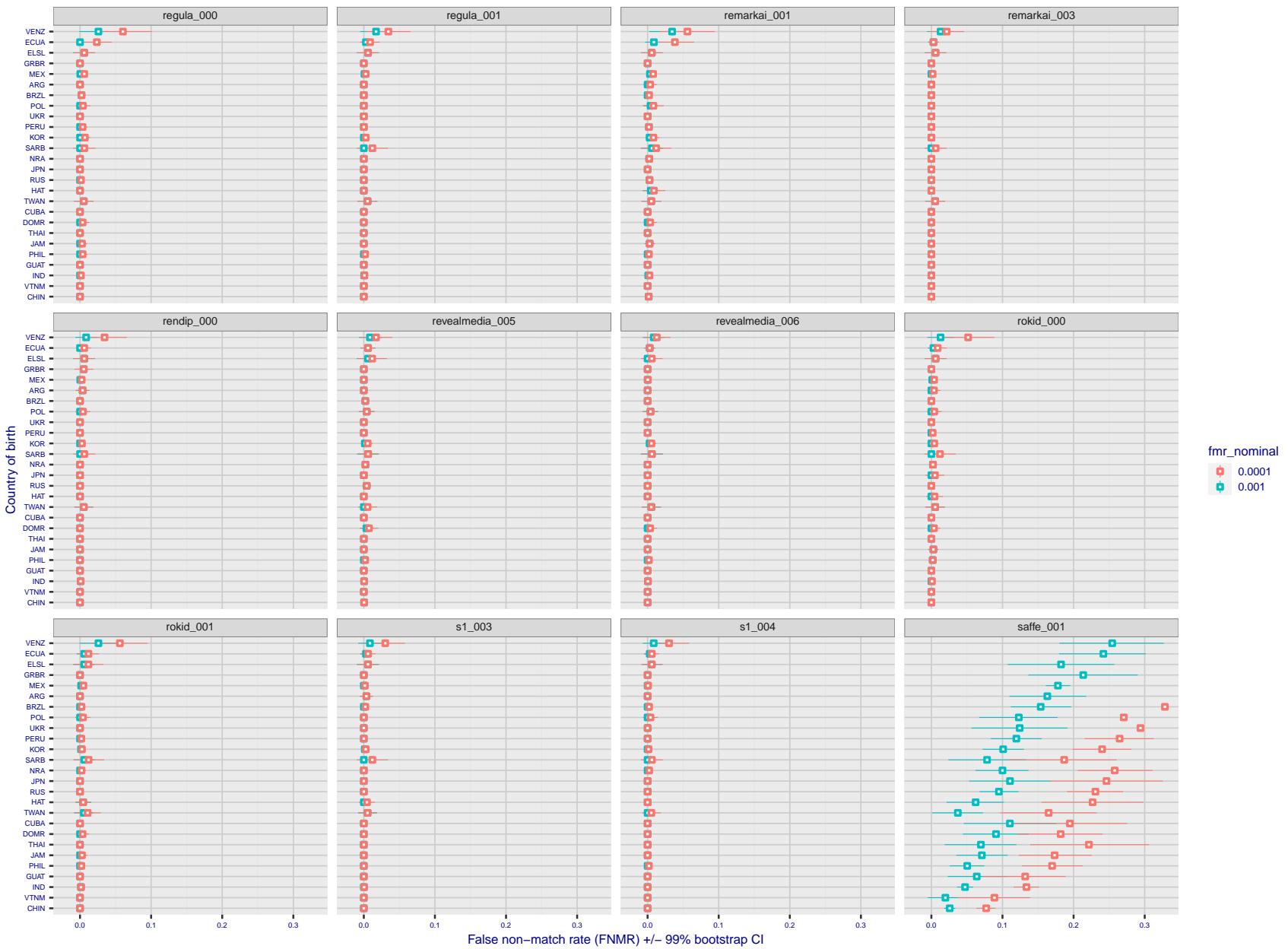


Figure 259: For the visa images, the dots show FNMR by country of birth for two globally set operating thresholds corresponding to $FMR = \{0.001, 0.0001\}$ computed over all on the order of 10^{10} impostor scores. The FMR in each bin will vary also - see subsequent impostor heatmaps in sec. 3.6.1. The figures shows an order of magnitude variation in FNMR across country of birth; these effects are likely due quality variations, then demographics like age and race. The error rates in some cases are zero, and in others the DET is flat so the error rates at the two thresholds are identical. The lines span 1% and 99% of bootstrap replicated FNMR estimates.

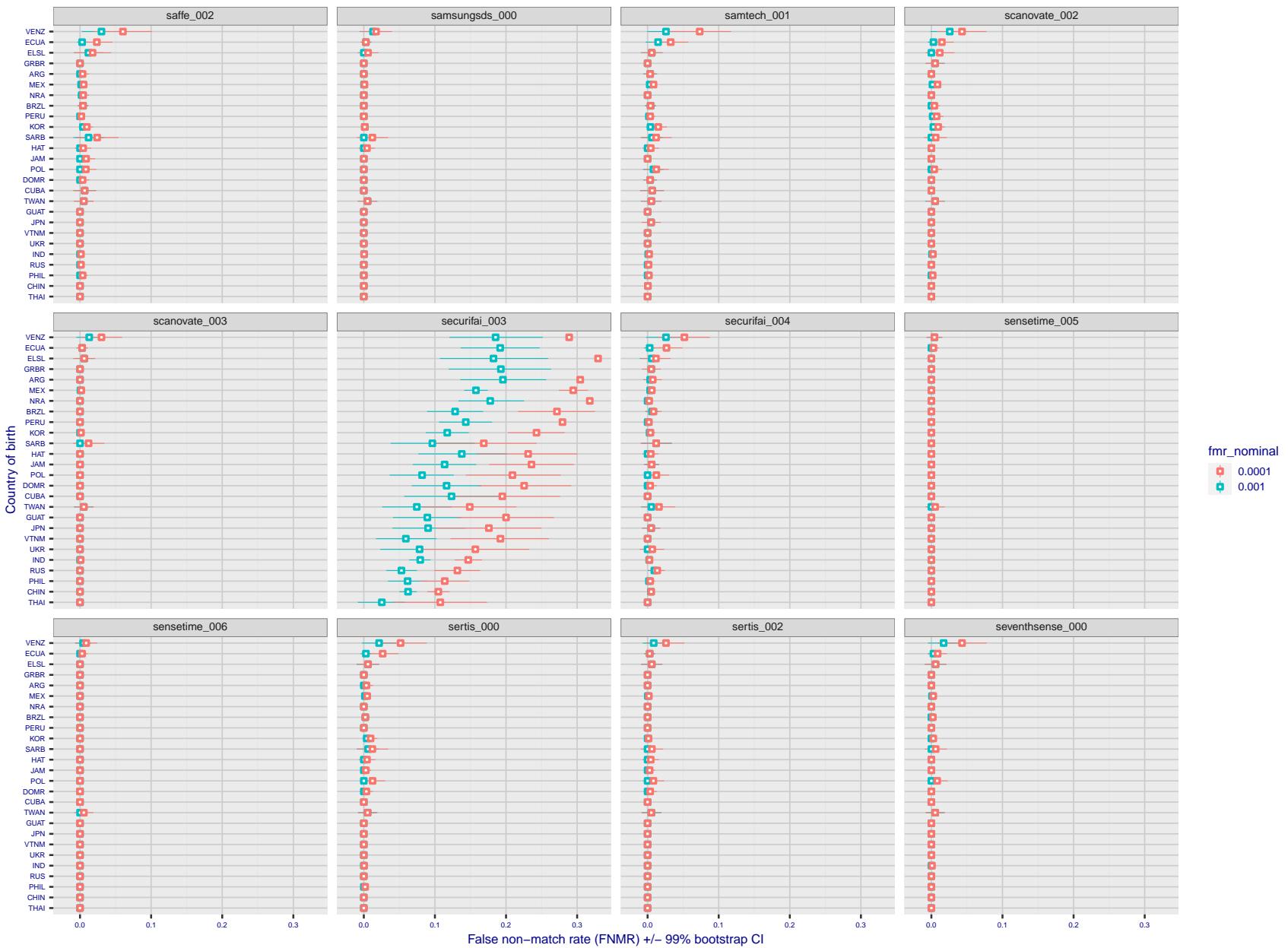


Figure 260: For the visa images, the dots show FNMR by country of birth for two globally set operating thresholds corresponding to $FMR = \{0.001, 0.0001\}$ computed over all on the order of 10^{10} impostor scores. The FMR in each bin will vary also - see subsequent impostor heatmaps in sec. 3.6.1. The figures shows an order of magnitude variation in FNMR across country of birth; these effects are likely due quality variations, then demographics like age and race. The error rates in some cases are zero, and in others the DET is flat so the error rates at the two thresholds are identical. The lines span 1% and 99% of bootstrap replicated FNMR estimates.

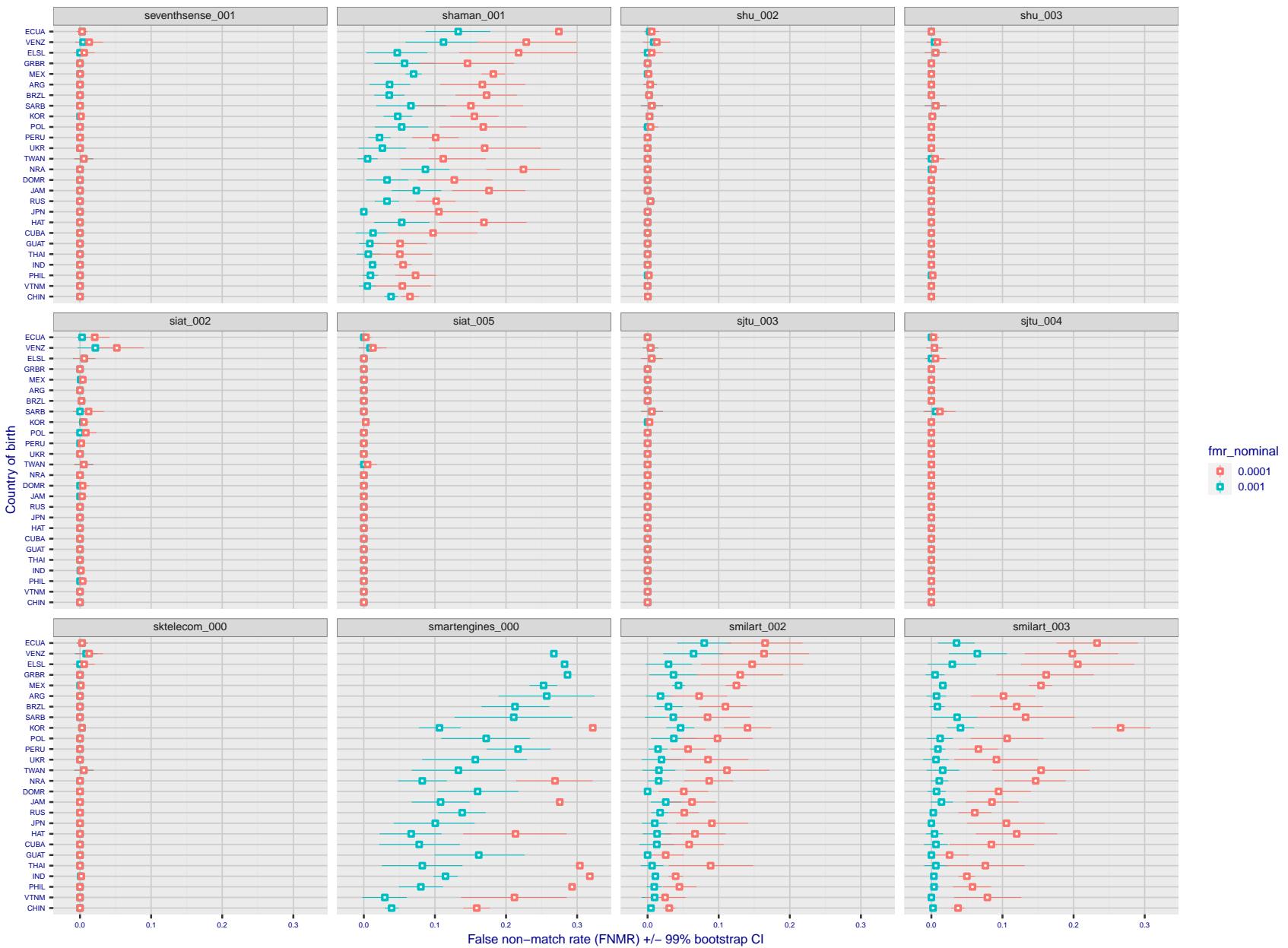


Figure 261: For the visa images, the dots show FNMR by country of birth for two globally set operating thresholds corresponding to $FMR = \{0.001, 0.0001\}$ computed over all on the order of 10^{10} impostor scores. The FMR in each bin will vary also - see subsequent impostor heatmaps in sec. 3.6.1. The figures shows an order of magnitude variation in FNMR across country of birth; these effects are likely due quality variations, then demographics like age and race. The error rates in some cases are zero, and in others the DET is flat so the error rates at the two thresholds are identical. The lines span 1% and 99% of bootstrap replicated FNMR estimates.

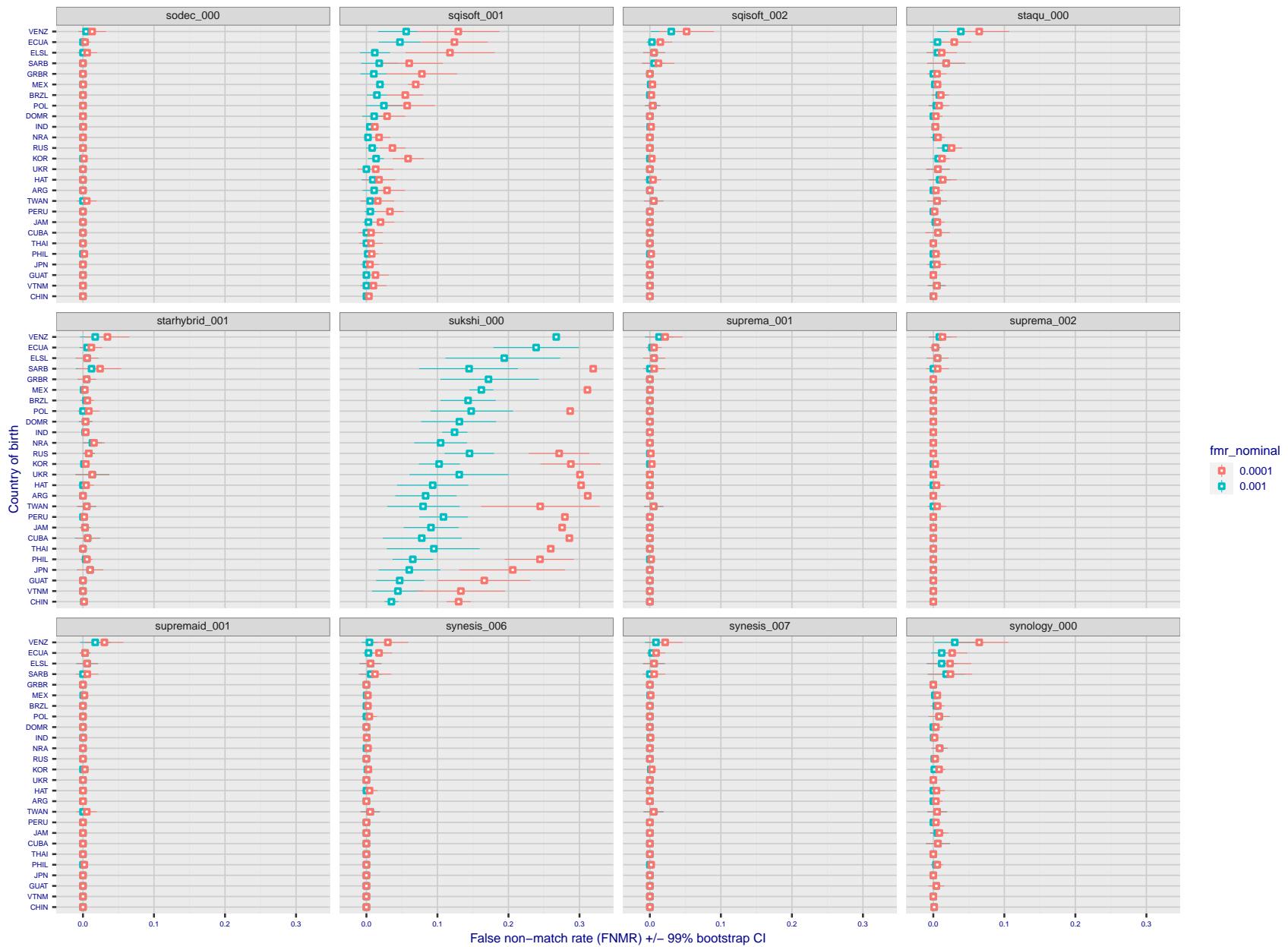


Figure 262: For the visa images, the dots show FNMR by country of birth for two globally set operating thresholds corresponding to $FMR = \{0.001, 0.0001\}$ computed over all on the order of 10^{10} impostor scores. The FMR in each bin will vary also - see subsequent impostor heatmaps in sec. 3.6.1. The figures shows an order of magnitude variation in FNMR across country of birth; these effects are likely due quality variations, then demographics like age and race. The error rates in some cases are zero, and in others the DET is flat so the error rates at the two thresholds are identical. The lines span 1% and 99% of bootstrap replicated FNMR estimates.

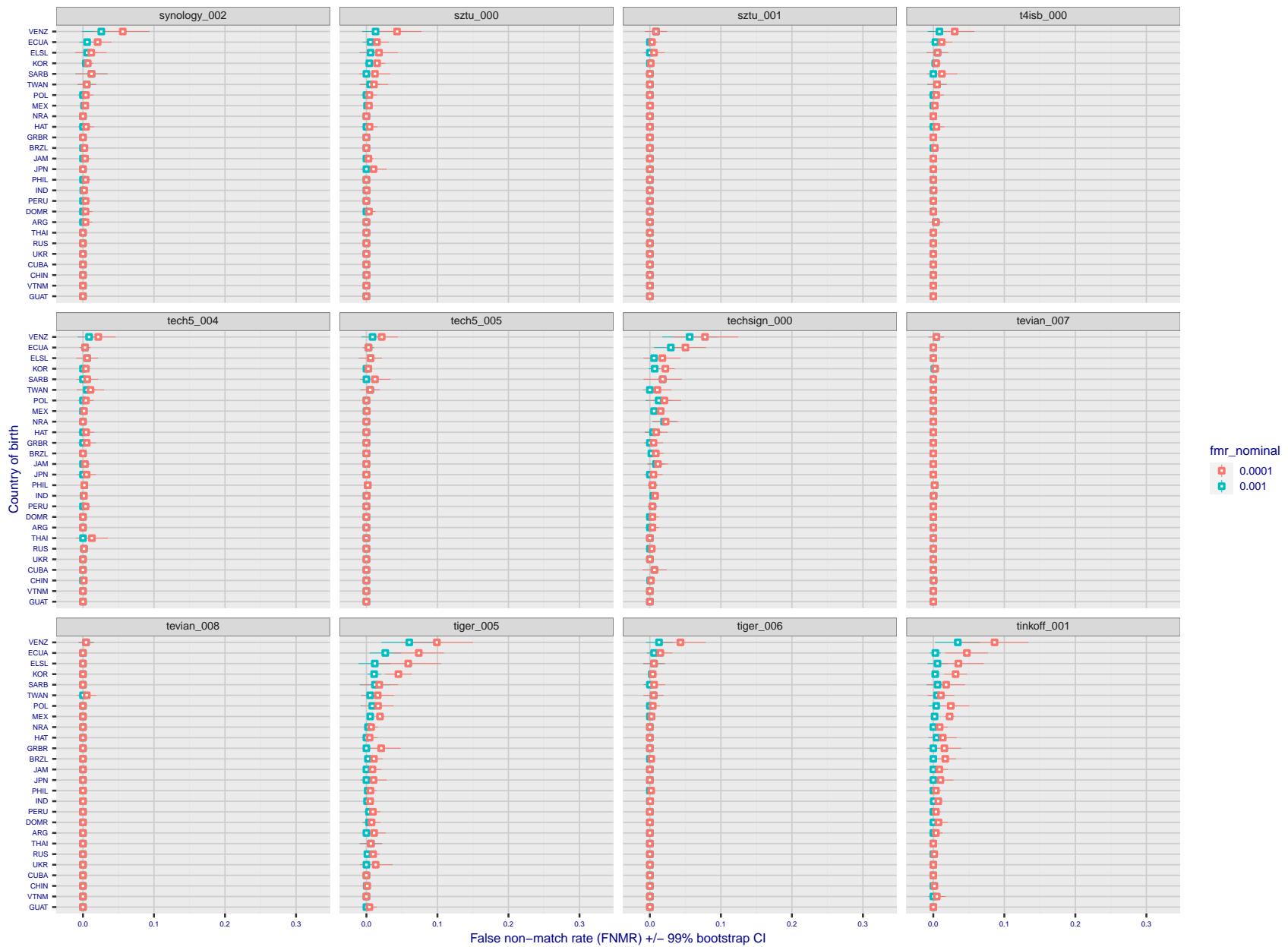


Figure 263: For the visa images, the dots show FNMR by country of birth for two globally set operating thresholds corresponding to $FMR = \{0.001, 0.0001\}$ computed over all on the order of 10^{10} impostor scores. The FMR in each bin will vary also - see subsequent impostor heatmaps in sec. 3.6.1. The figures shows an order of magnitude variation in FNMR across country of birth; these effects are likely due quality variations, then demographics like age and race. The error rates in some cases are zero, and in others the DET is flat so the error rates at the two thresholds are identical. The lines span 1% and 99% of bootstrap replicated FNMR estimates.

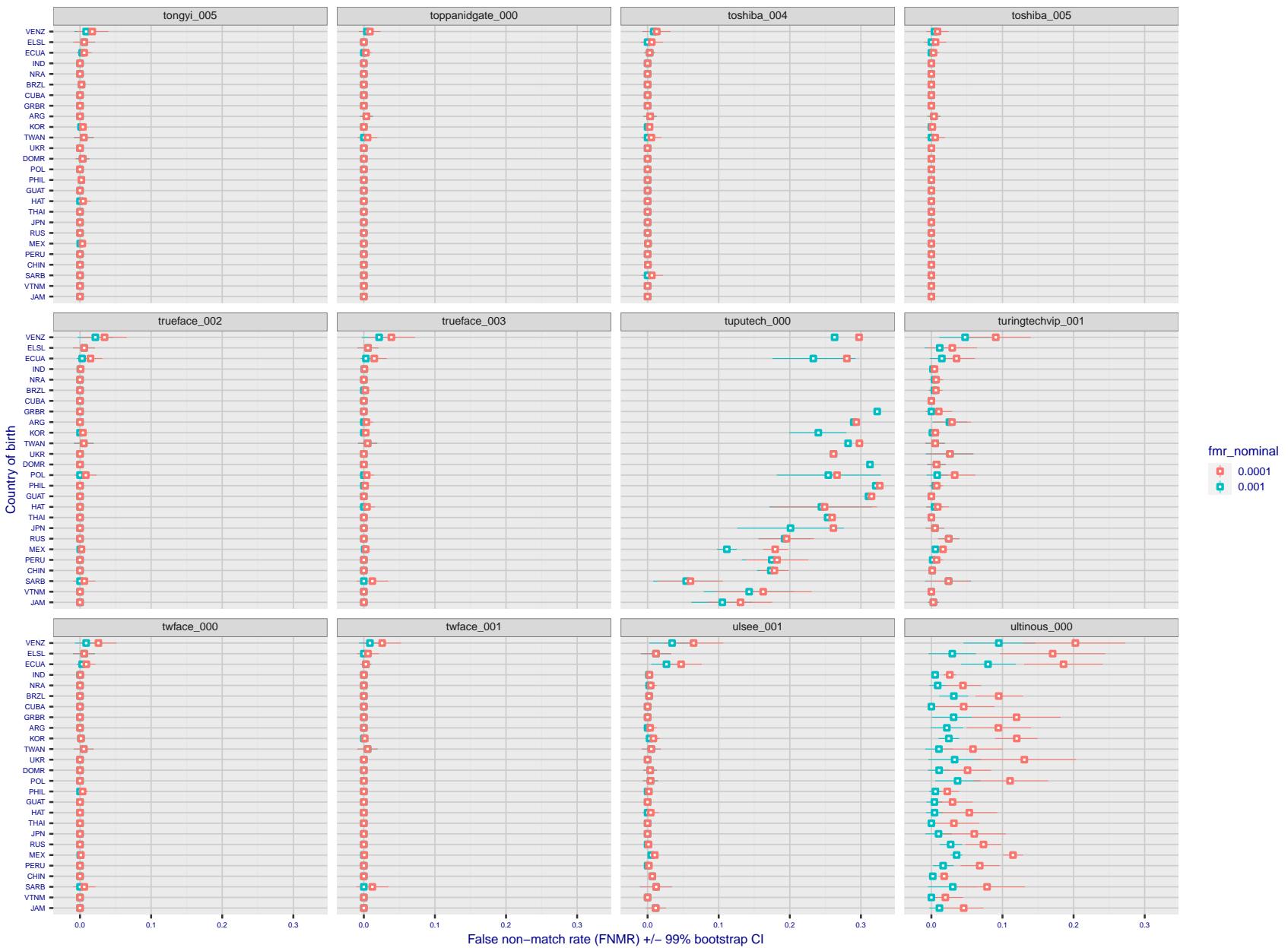


Figure 264: For the visa images, the dots show FNMR by country of birth for two globally set operating thresholds corresponding to $FMR = \{0.001, 0.0001\}$ computed over all on the order of 10^{10} impostor scores. The FMR in each bin will vary also - see subsequent impostor heatmaps in sec. 3.6.1. The figures shows an order of magnitude variation in FNMR across country of birth; these effects are likely due quality variations, then demographics like age and race. The error rates in some cases are zero, and in others the DET is flat so the error rates at the two thresholds are identical. The lines span 1% and 99% of bootstrap replicated FNMR estimates.

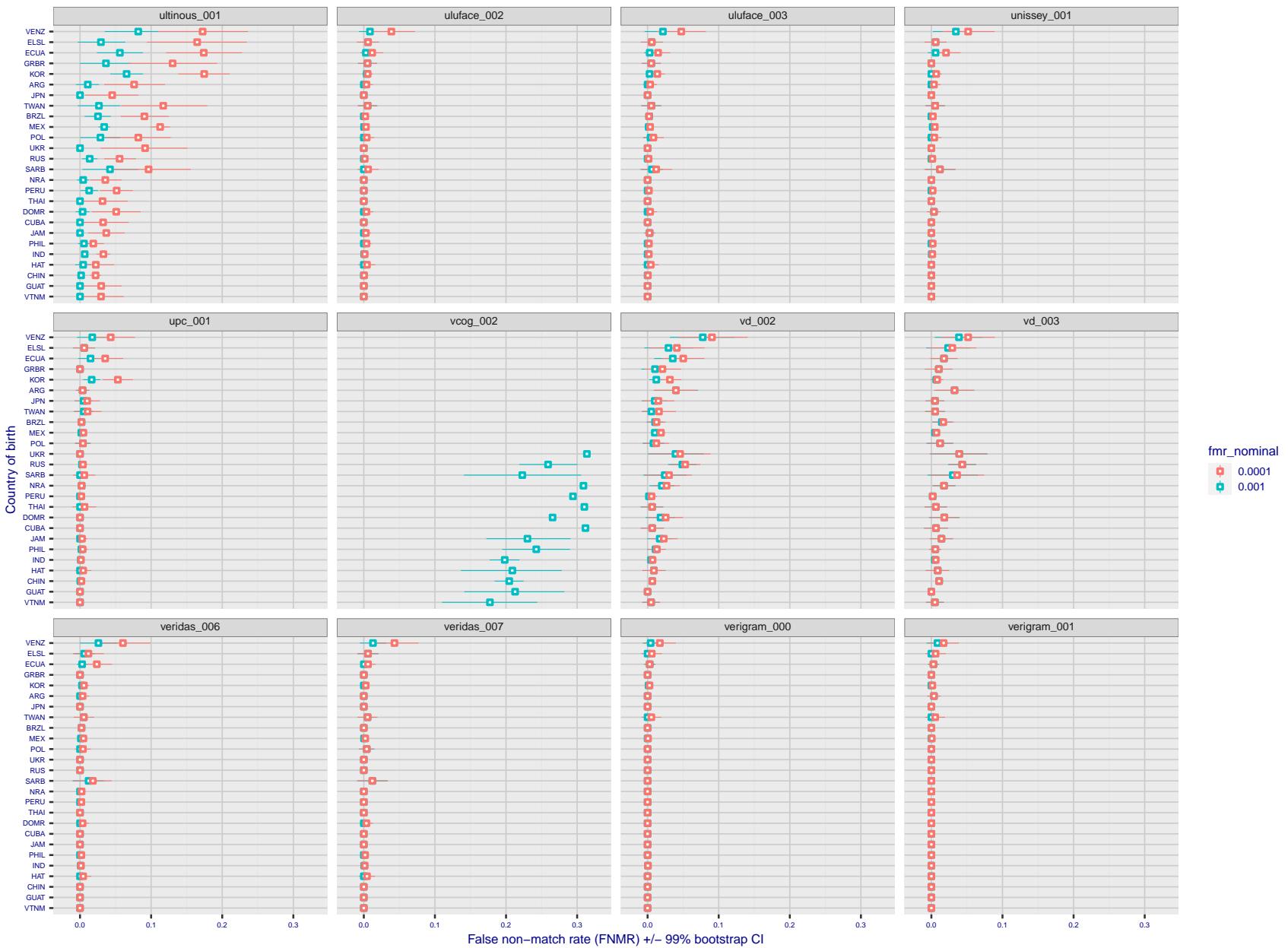


Figure 265: For the visa images, the dots show FNMR by country of birth for two globally set operating thresholds corresponding to $FMR = \{0.001, 0.0001\}$ computed over all on the order of 10^{10} impostor scores. The FMR in each bin will vary also - see subsequent impostor heatmaps in sec. 3.6.1. The figures shows an order of magnitude variation in FNMR across country of birth; these effects are likely due quality variations, then demographics like age and race. The error rates in some cases are zero, and in others the DET is flat so the error rates at the two thresholds are identical. The lines span 1% and 99% of bootstrap replicated FNMR estimates.

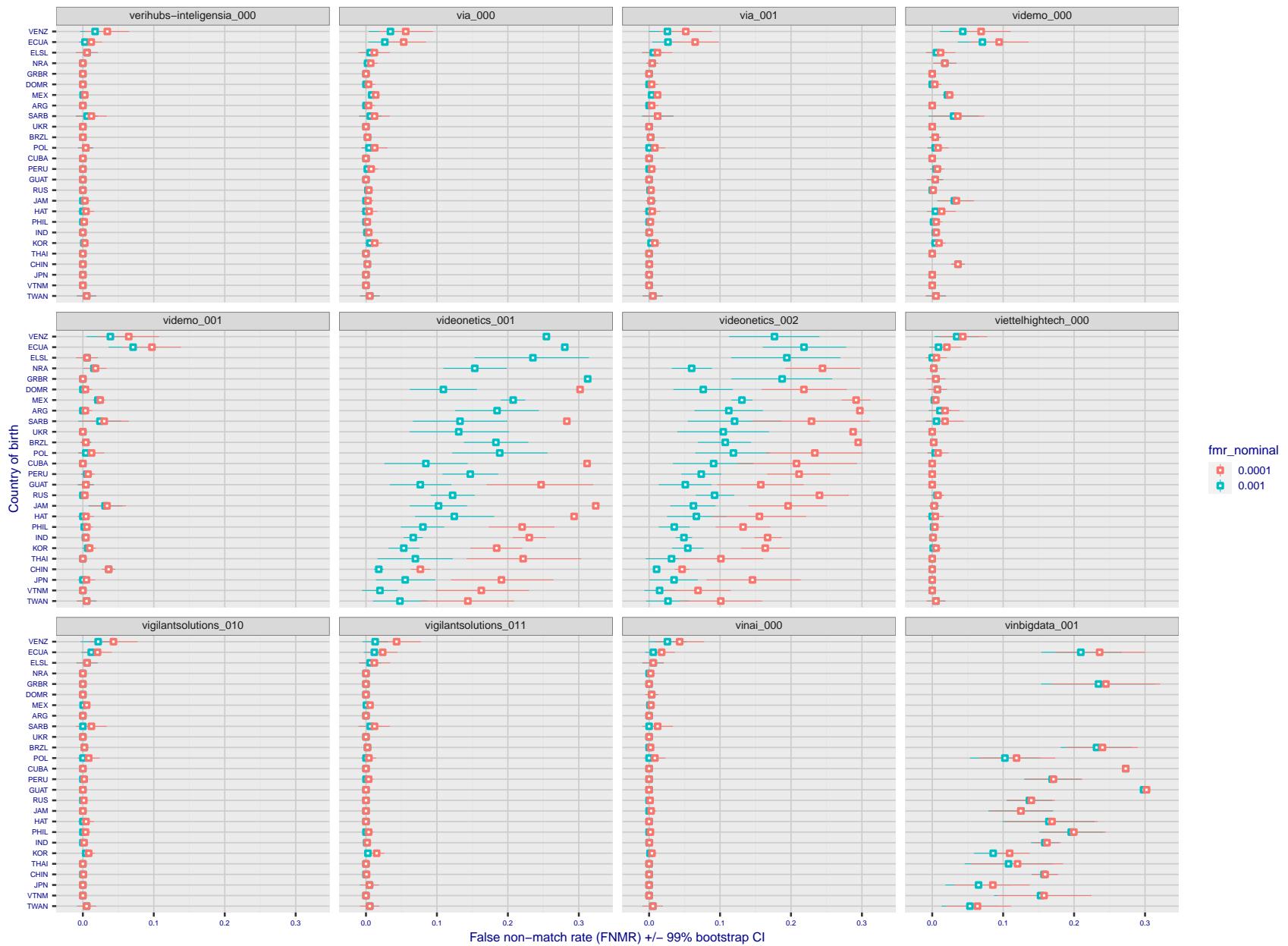
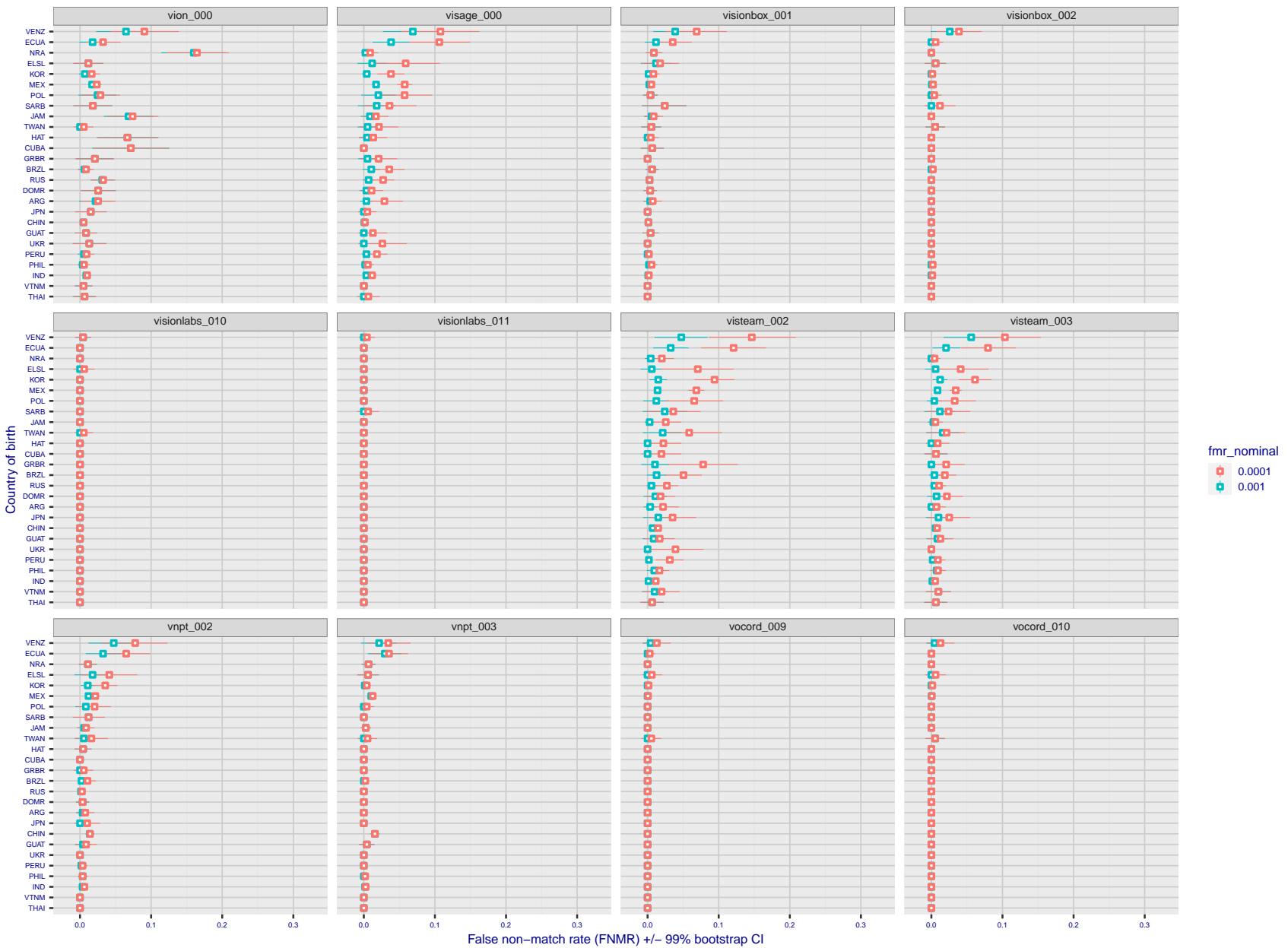


Figure 266: For the visa images, the dots show FNMR by country of birth for two globally set operating thresholds corresponding to $FMR = \{0.001, 0.0001\}$ computed over all on the order of 10^{10} impostor scores. The FMR in each bin will vary also - see subsequent impostor heatmaps in sec. 3.6.1. The figures shows an order of magnitude variation in FNMR across country of birth; these effects are likely due quality variations, then demographics like age and race. The error rates in some cases are zero, and in others the DET is flat so the error rates at the two thresholds are identical. The lines span 1% and 99% of bootstrap replicated FNMR estimates.



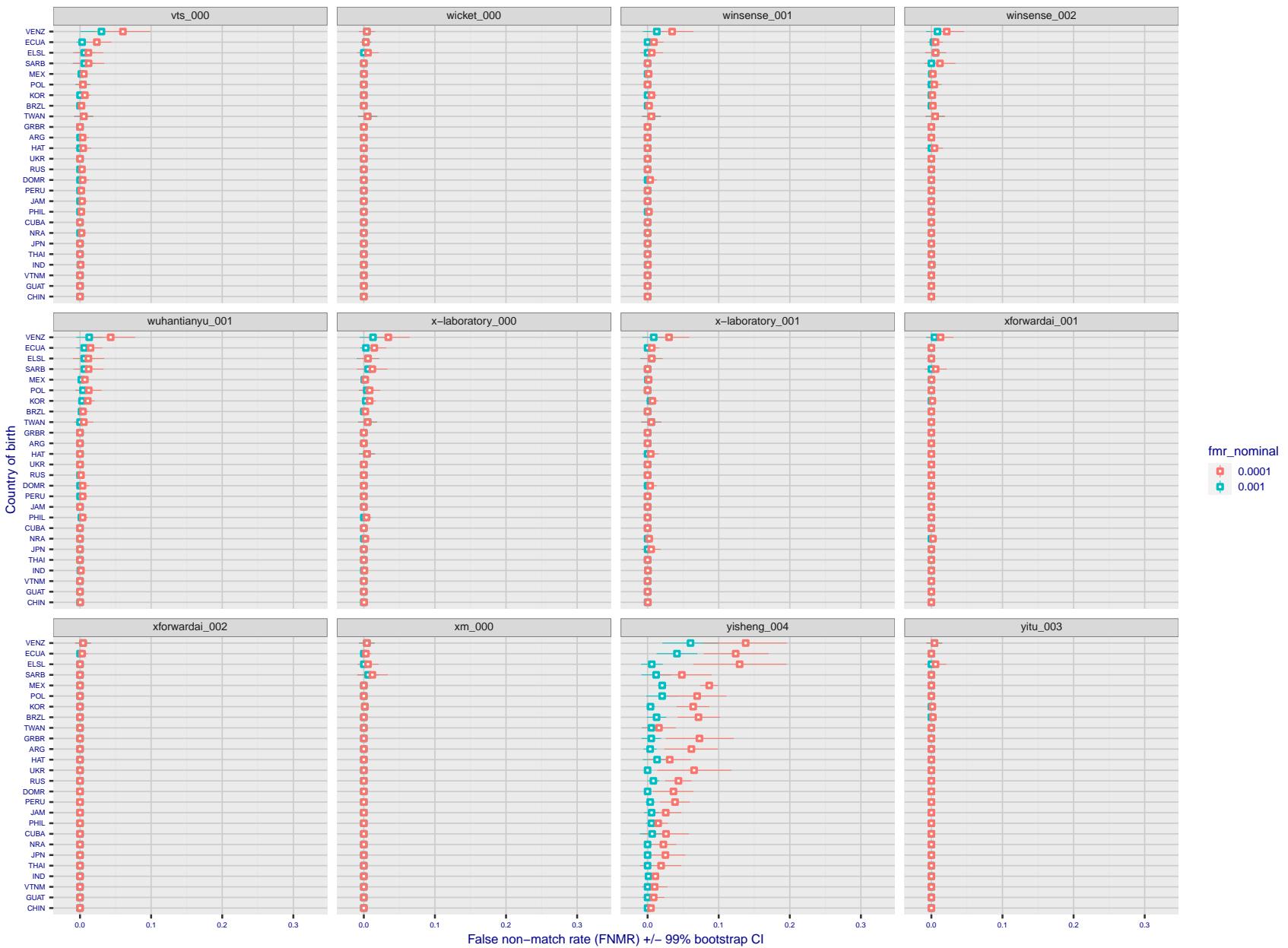


Figure 268: For the visa images, the dots show FNMR by country of birth for two globally set operating thresholds corresponding to $FMR = \{0.001, 0.0001\}$ computed over all on the order of 10^{10} impostor scores. The FMR in each bin will vary also - see subsequent impostor heatmaps in sec. 3.6.1. The figures shows an order of magnitude variation in FNMR across country of birth; these effects are likely due quality variations, then demographics like age and race. The error rates in some cases are zero, and in others the DET is flat so the error rates at the two thresholds are identical. The lines span 1% and 99% of bootstrap replicated FNMR estimates.

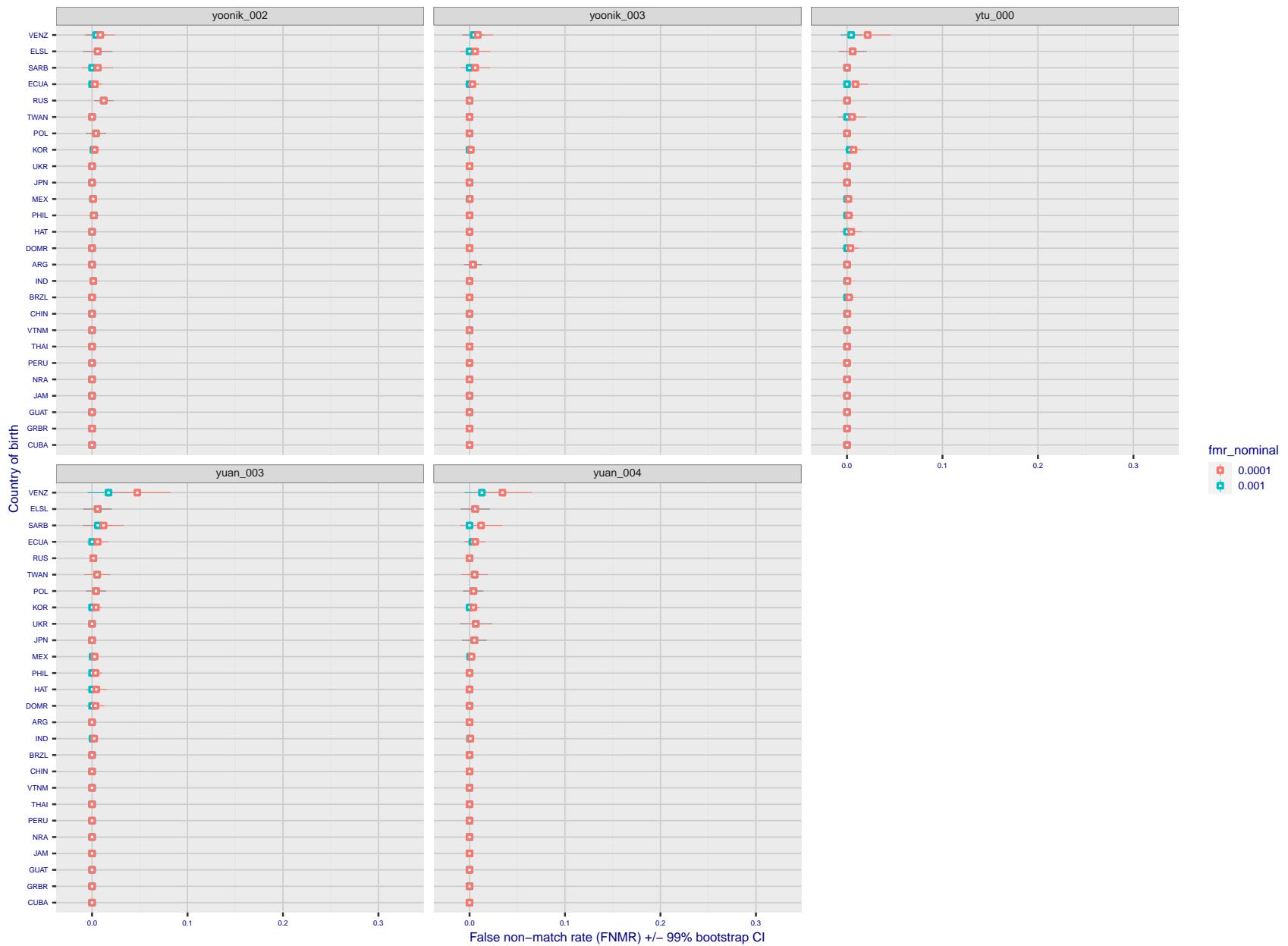


Figure 269: For the visa images, the dots show FNMR by country of birth for two globally set operating thresholds corresponding to $FMR = \{0.001, 0.0001\}$ computed over all on the order of 10^{10} impostor scores. The FMR in each bin will vary also - see subsequent impostor heatmaps in sec. 3.6.1. The figures shows an order of magnitude variation in FNMR across country of birth; these effects are likely due quality variations, then demographics like age and race. The error rates in some cases are zero, and in others the DET is flat so the error rates at the two thresholds are identical. The lines span 1% and 99% of bootstrap replicated FNMR estimates.

Caveats: The results may not relate to subject-specific properties. Instead they could reflect image-specific quality differences, which could occur due to collection protocol or software processing variations.

3.5.2 Effect of ageing

Background: Faces change appearance throughout life. This change gradually reduces similarity of a new image to an earlier image. Face recognition algorithms give reduced similarity scores and more frequent false rejections.

Goal: To quantify false non-match rates (FNMR) as a function of elapsed time in an adult population.

Methods: Using the mugshot images, a threshold is set to give FMR = 0.00001 over the entire impostor set. Then FNMR is measured over 1000 bootstrap replications of the genuine scores.

Results: For the visa images, Figure 294 shows how false non-match rates for genuine users, as a function of age group.

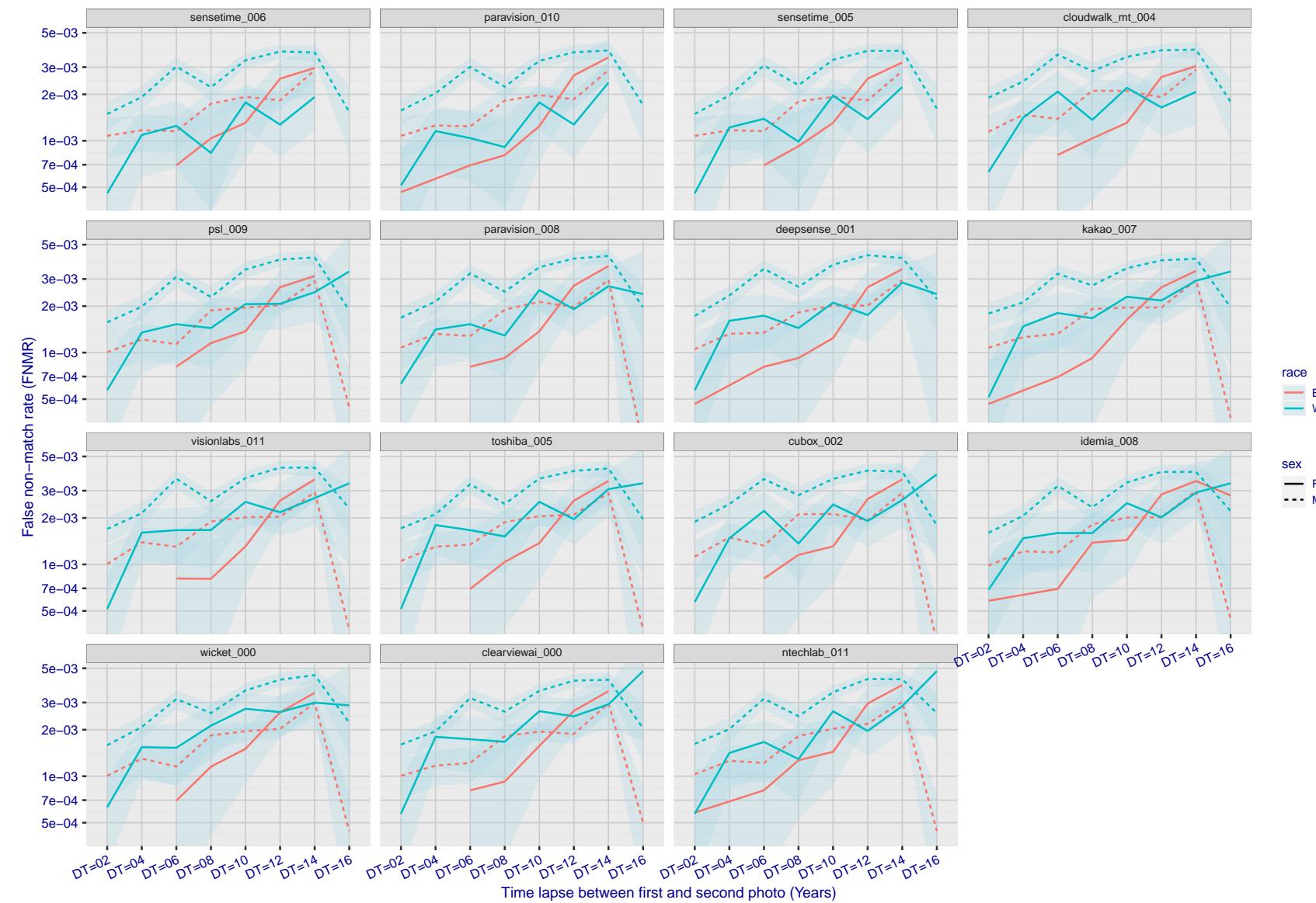


Figure 270: For the mugshot images, FNMR as a function of elapsed time between initial enrollment and second verification images. The panels appear most accurate first, and vertical scale changes on each page. The four traces correspond to images annotated with codes for black female, black male, white female, white male. The threshold is fixed for each algorithm to give FMR = 0.00001 over all (10^8) impostor comparisons. For short time-lapses, the most accurate algorithms give very few errors (FNMR < 0.001) so that the uncertainty estimates are high.

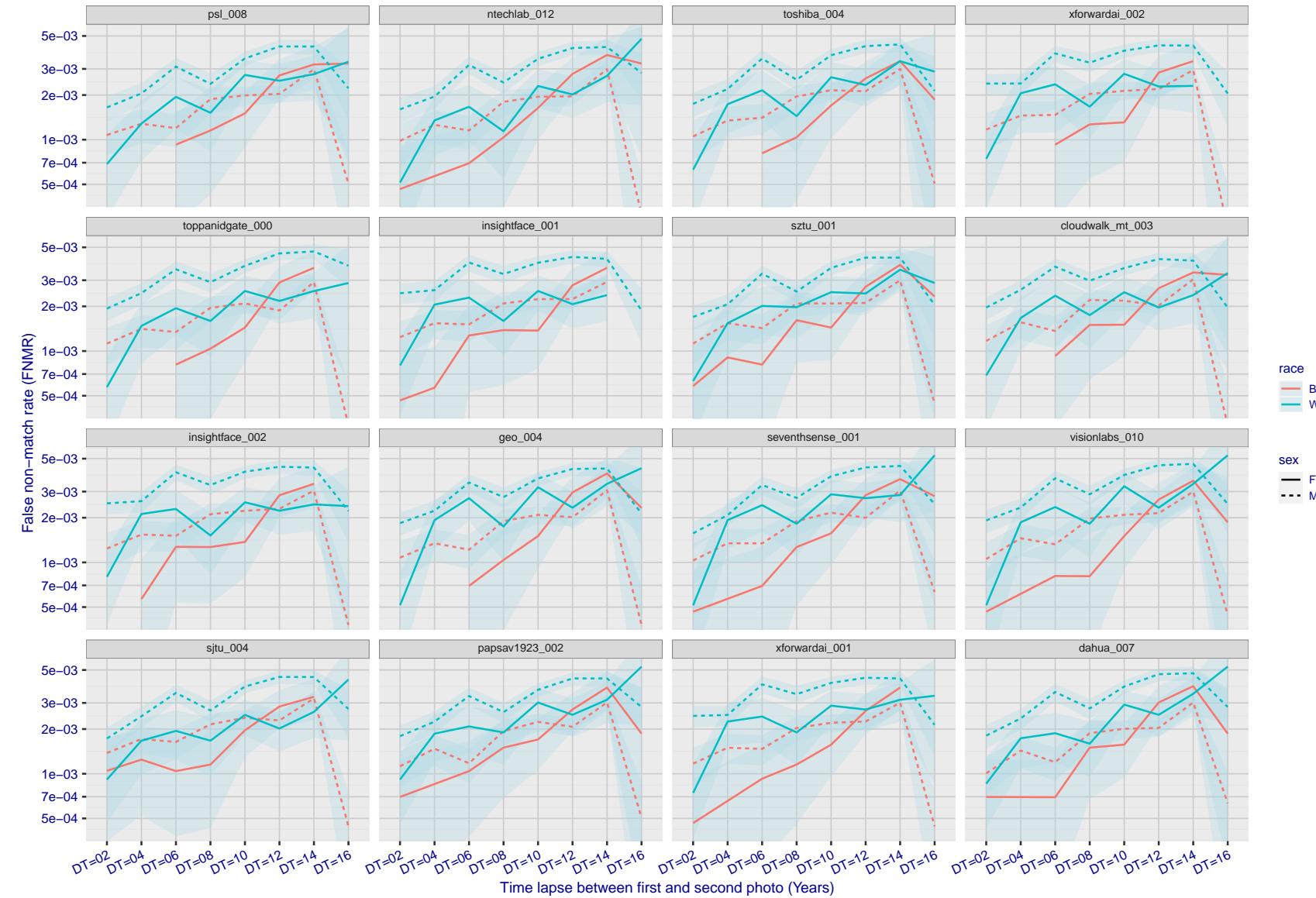


Figure 271: For the mugshot images, FNMR as a function of elapsed time between initial enrollment and second verification images. The panels appear most accurate first, and vertical scale changes on each page. The four traces correspond to images annotated with codes for black female, black male, white female, white male. The threshold is fixed for each algorithm to give FMR = 0.00001 over all (10^8) impostor comparisons. For short time-lapses, the most accurate algorithms give very few errors (FNMR < 0.001) so that the uncertainty estimates are high.

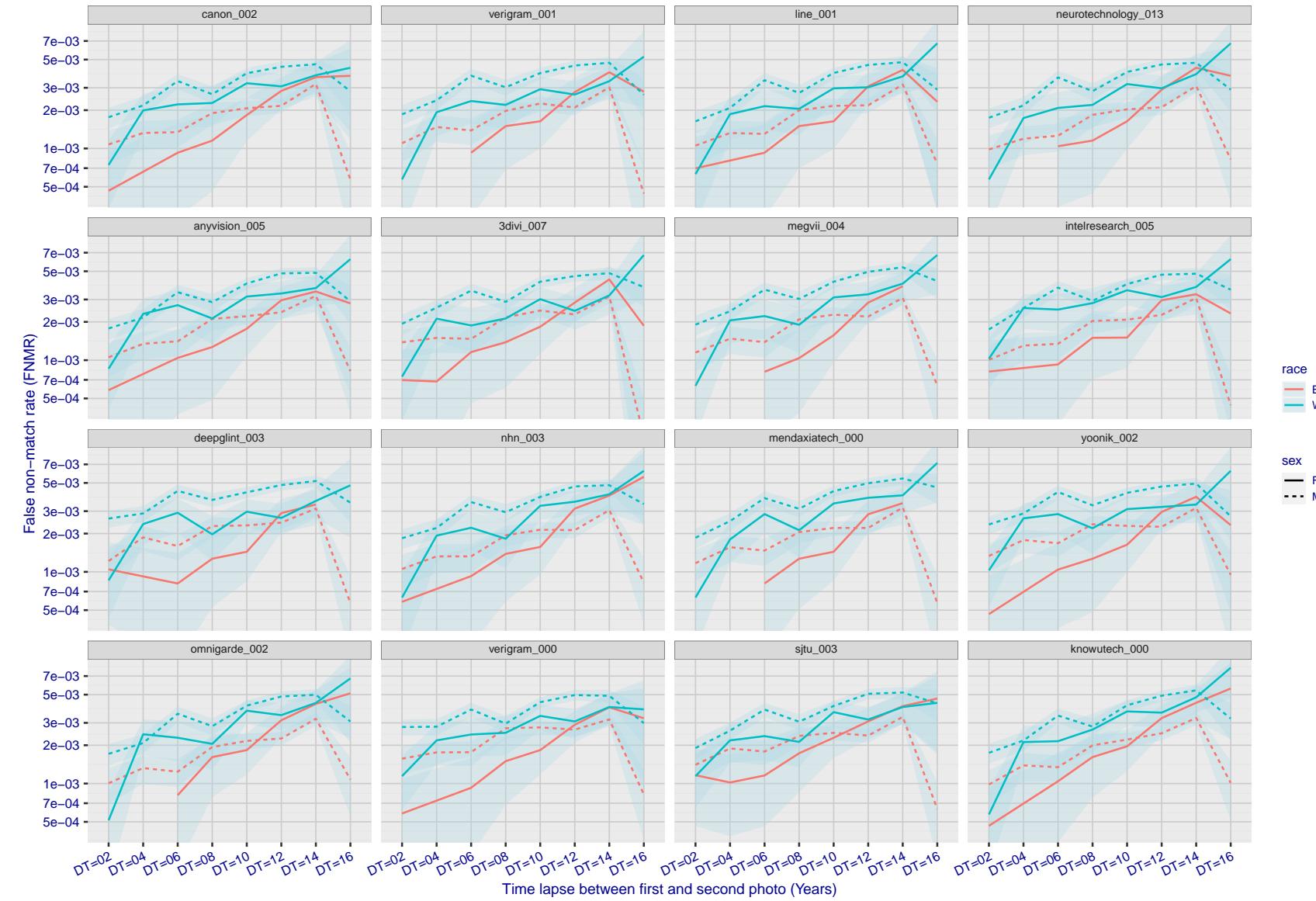


Figure 272: For the mugshot images, FNMR as a function of elapsed time between initial enrollment and second verification images. The panels appear most accurate first, and vertical scale changes on each page. The four traces correspond to images annotated with codes for black female, black male, white female, white male. The threshold is fixed for each algorithm to give $FMR = 0.00001$ over all (10^8) impostor comparisons. For short time-lapses, the most accurate algorithms give very few errors ($FNMR < 0.001$) so that the uncertainty estimates are high.

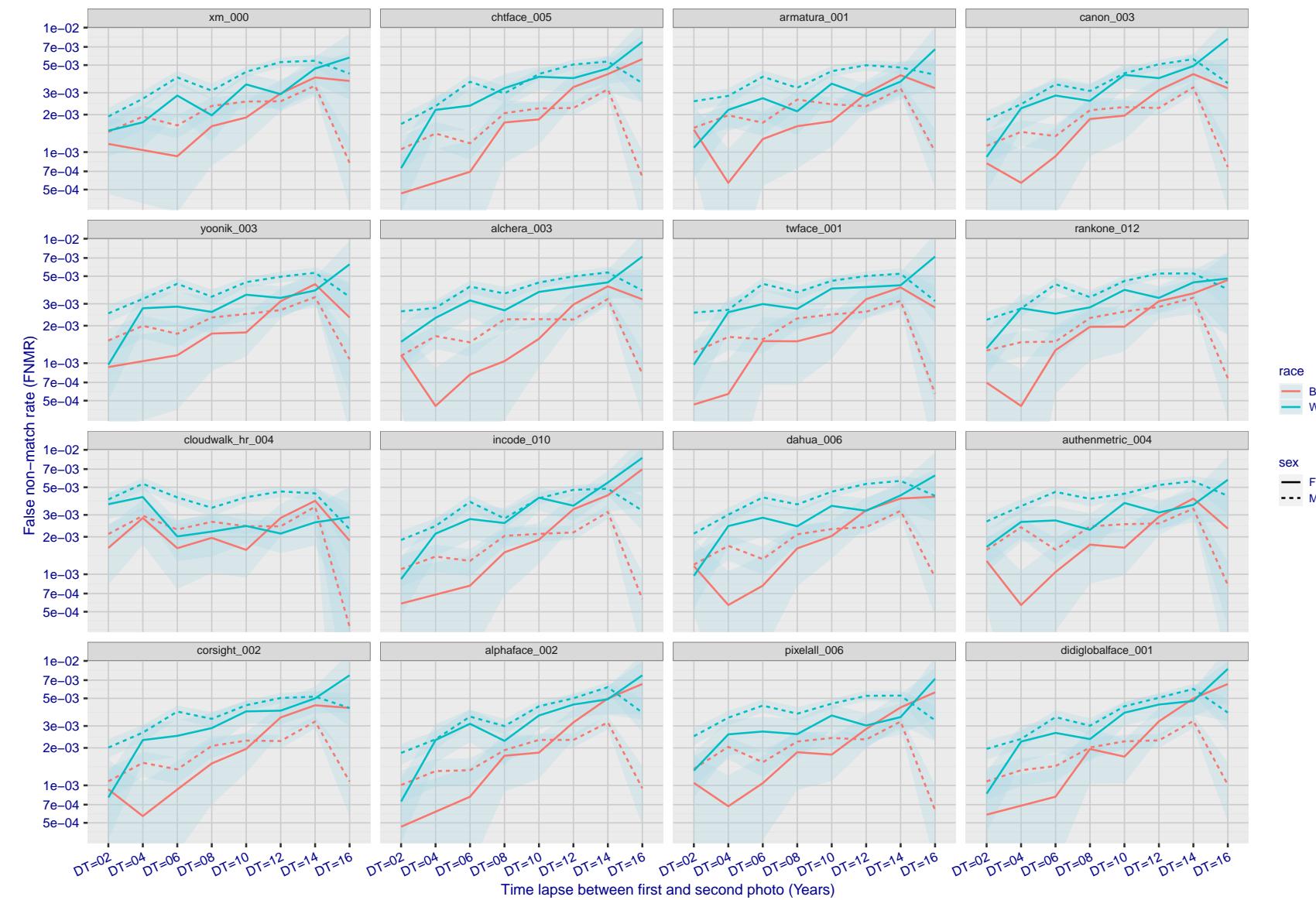


Figure 273: For the mugshot images, FNMR as a function of elapsed time between initial enrollment and second verification images. The panels appear most accurate first, and vertical scale changes on each page. The four traces correspond to images annotated with codes for black female, black male, white female, white male. The threshold is fixed for each algorithm to give $FMR = 0.00001$ over all (10^8) impostor comparisons. For short time-lapses, the most accurate algorithms give very few errors ($FNMR < 0.001$) so that the uncertainty estimates are high.

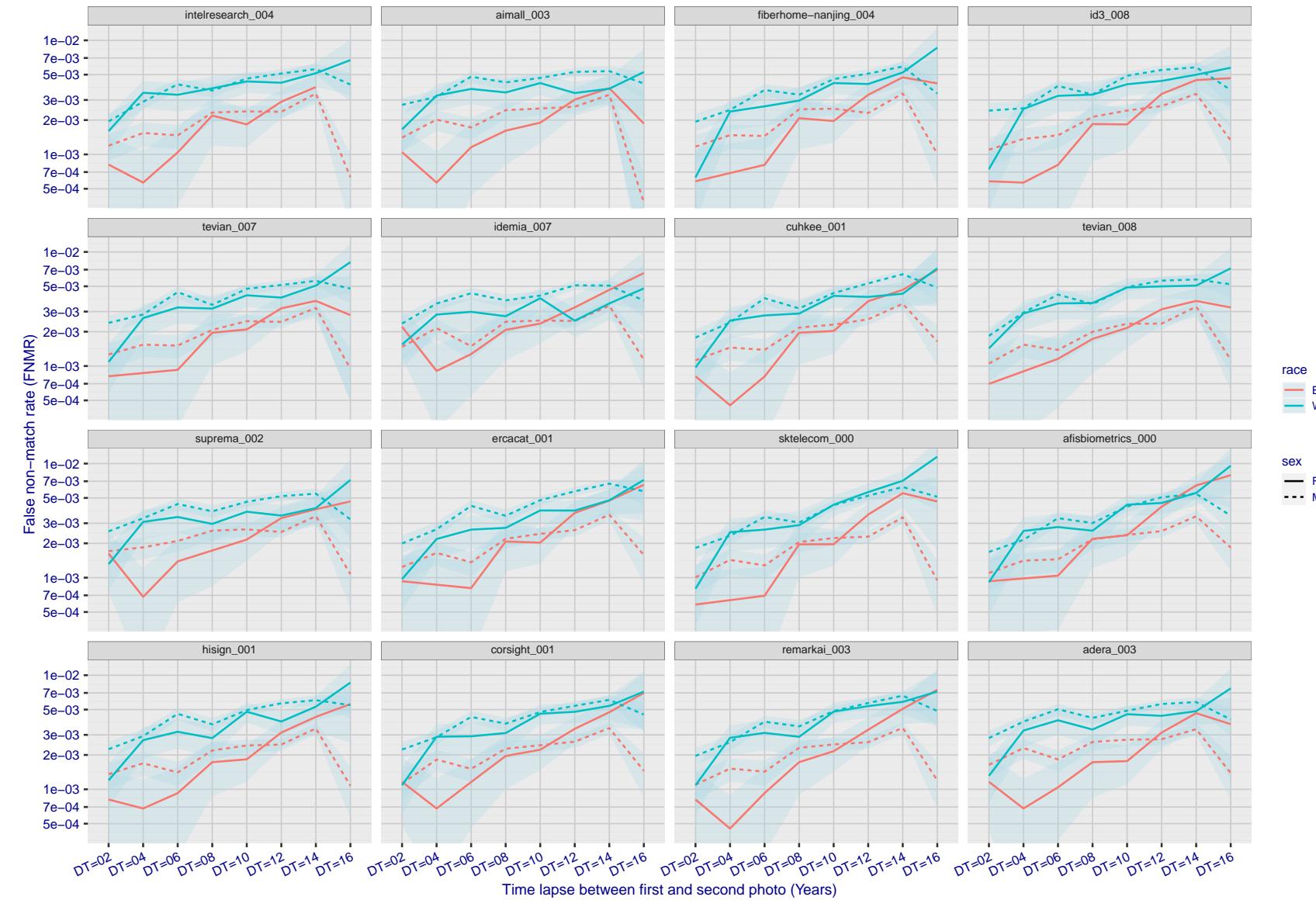


Figure 274: For the mugshot images, FNMR as a function of elapsed time between initial enrollment and second verification images. The panels appear most accurate first, and vertical scale changes on each page. The four traces correspond to images annotated with codes for black female, black male, white female, white male. The threshold is fixed for each algorithm to give $FMR = 0.00001$ over all (10^8) impostor comparisons. For short time-lapses, the most accurate algorithms give very few errors ($FNMR < 0.001$) so that the uncertainty estimates are high.

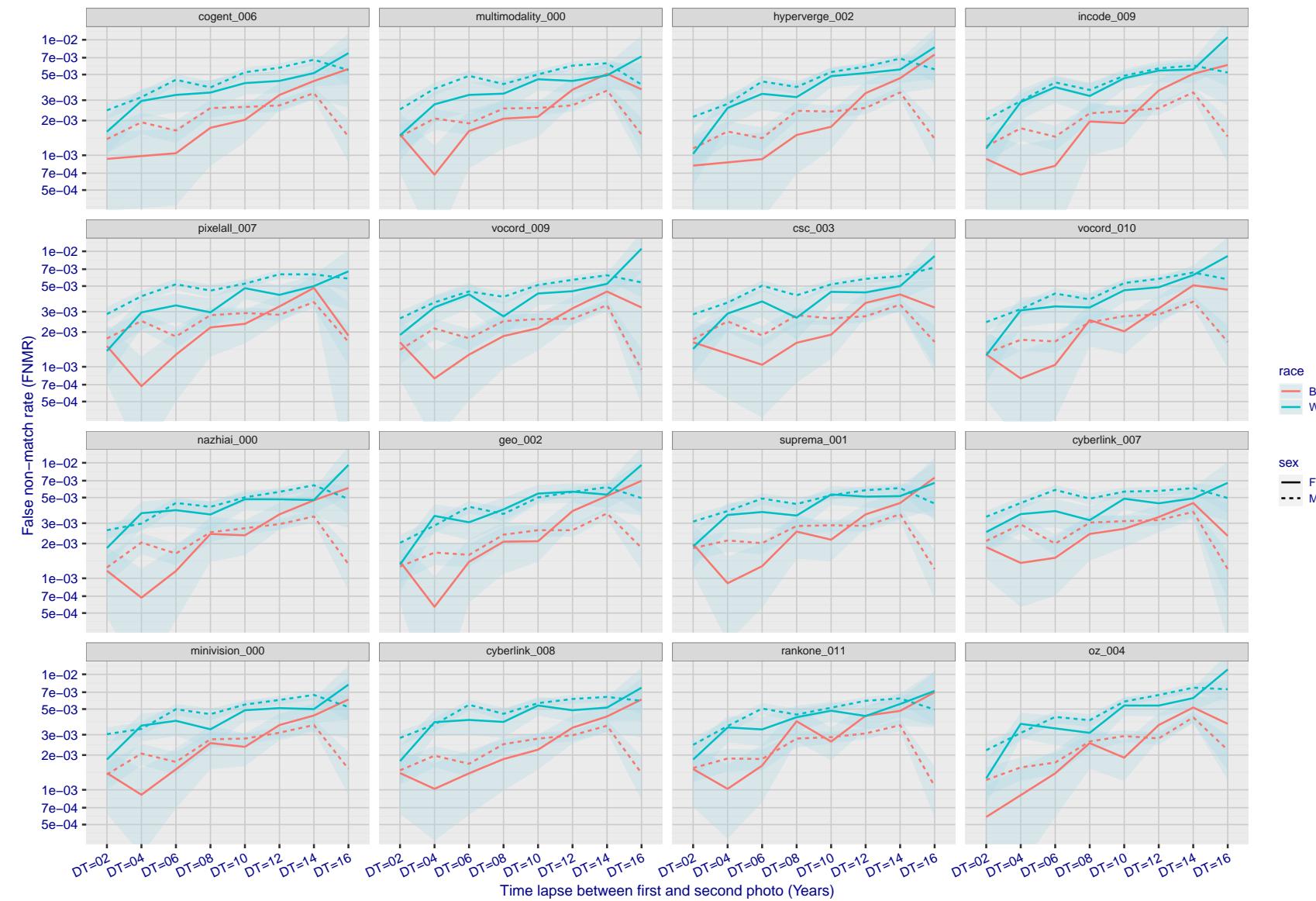


Figure 275: For the mugshot images, FNMR as a function of elapsed time between initial enrollment and second verification images. The panels appear most accurate first, and vertical scale changes on each page. The four traces correspond to images annotated with codes for black female, black male, white female, white male. The threshold is fixed for each algorithm to give FMR = 0.00001 over all (10^8) impostor comparisons. For short time-lapses, the most accurate algorithms give very few errors (FNMR < 0.001) so that the uncertainty estimates are high.

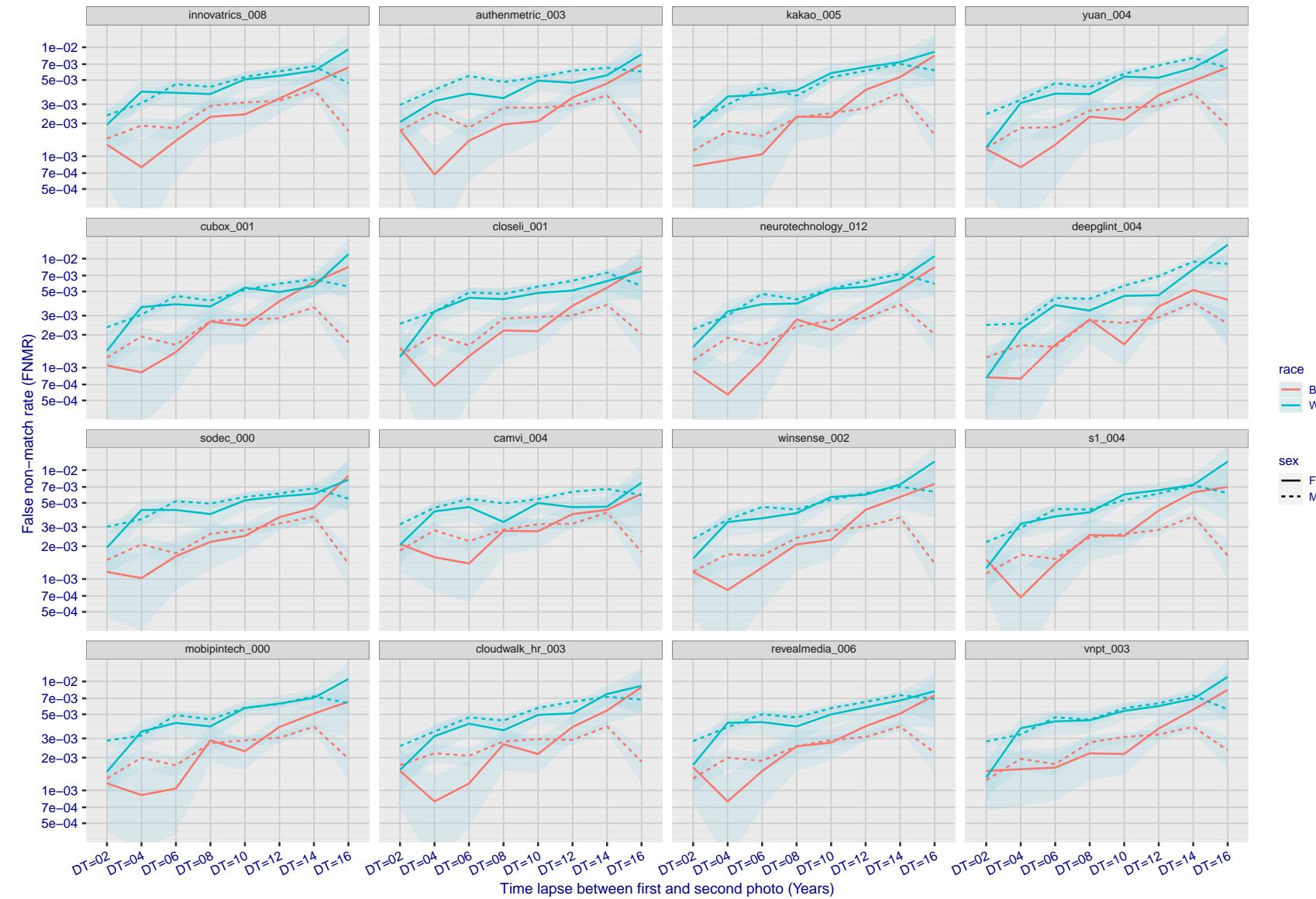


Figure 276: For the mugshot images, FNMR as a function of elapsed time between initial enrollment and second verification images. The panels appear most accurate first, and vertical scale changes on each page. The four traces correspond to images annotated with codes for black female, black male, white female, white male. The threshold is fixed for each algorithm to give $FMR = 0.00001$ over all (10^8) impostor comparisons. For short time-lapses, the most accurate algorithms give very few errors ($FNMR < 0.001$) so that the uncertainty estimates are high.

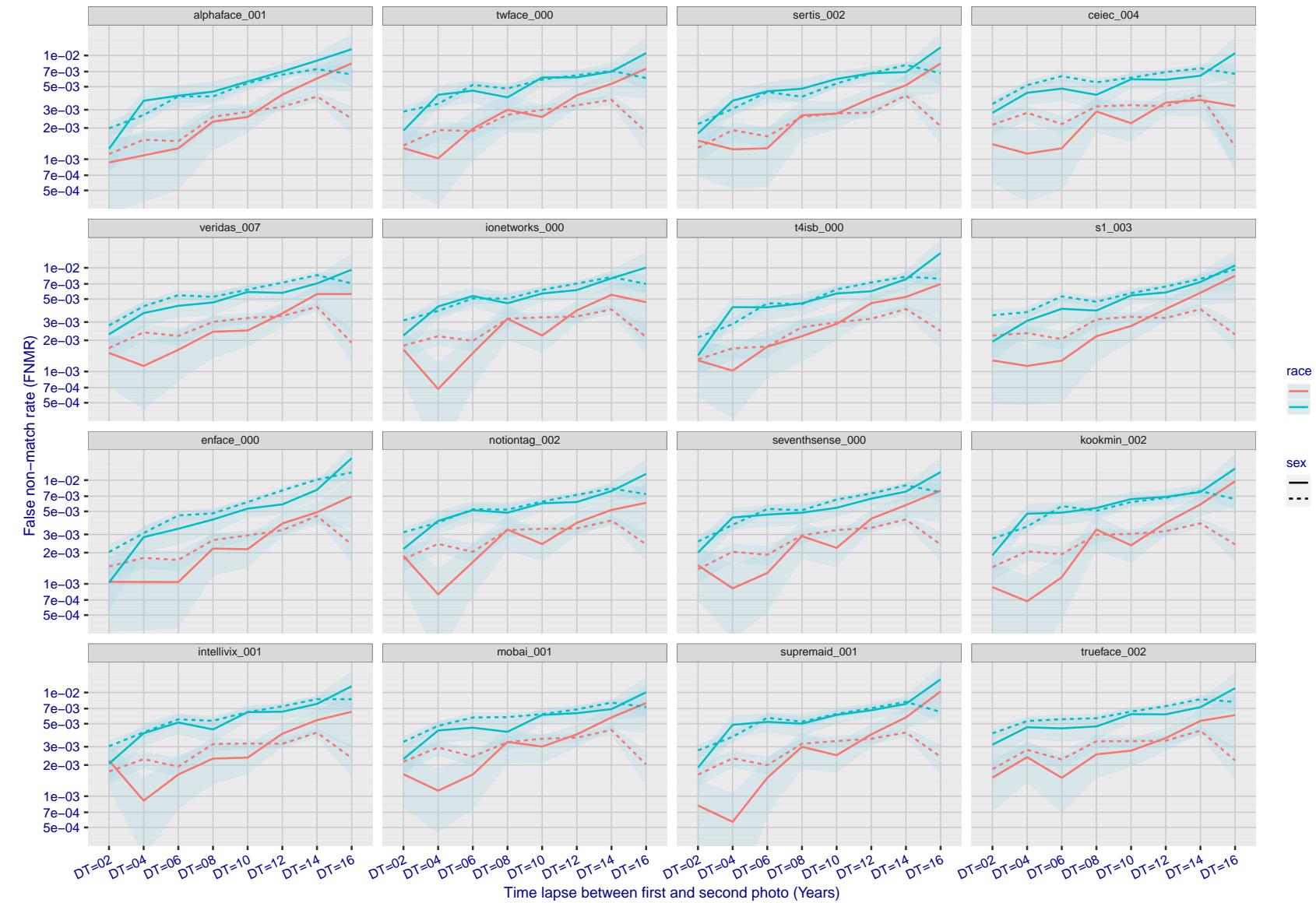


Figure 277: For the mugshot images, FNMR as a function of elapsed time between initial enrollment and second verification images. The panels appear most accurate first, and vertical scale changes on each page. The four traces correspond to images annotated with codes for black female, black male, white female, white male. The threshold is fixed for each algorithm to give $FMR = 0.00001$ over all (10^8) impostor comparisons. For short time-lapses, the most accurate algorithms give very few errors ($FNMR < 0.001$) so that the uncertainty estimates are high.

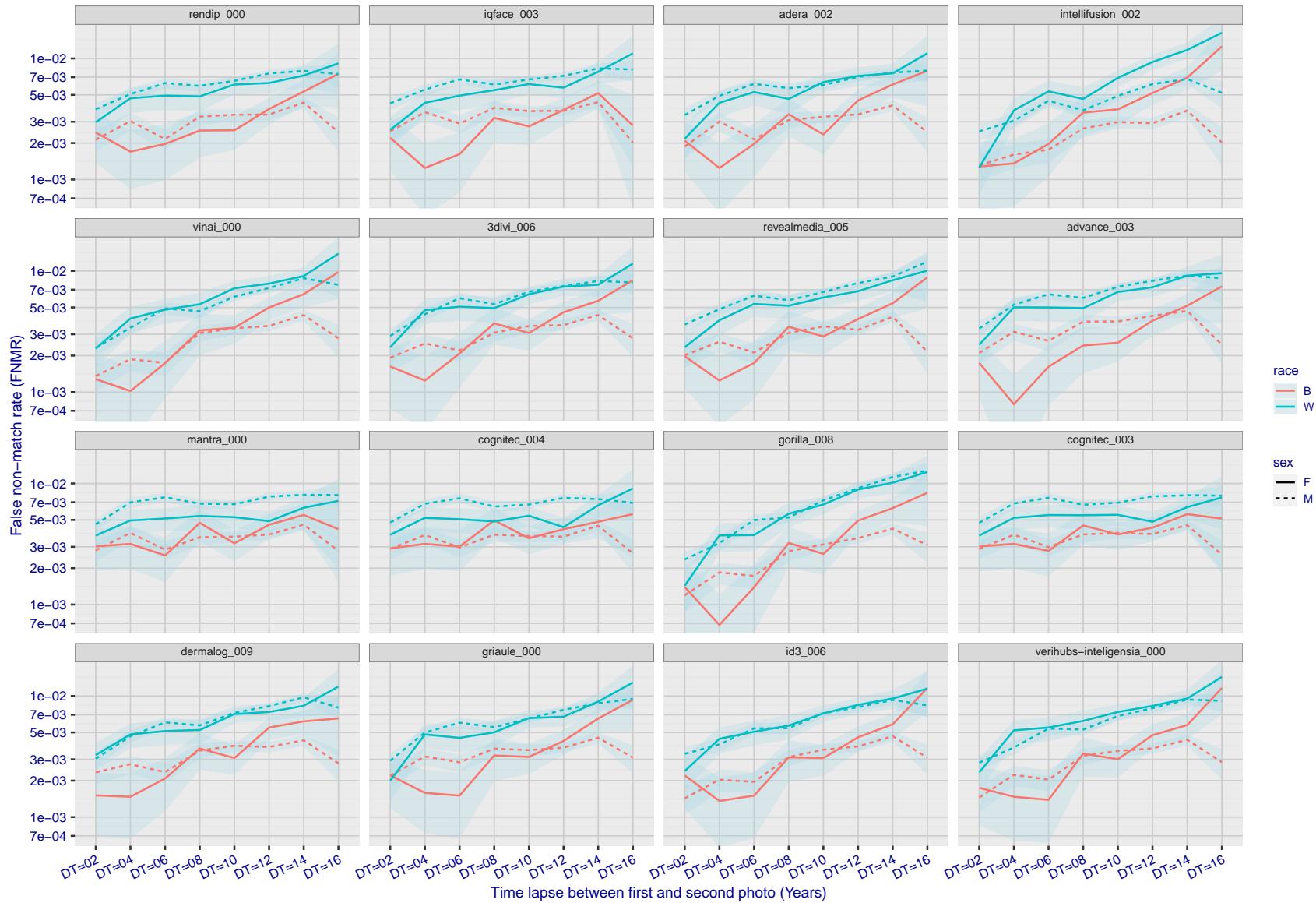


Figure 278: For the mugshot images, FNMR as a function of elapsed time between initial enrollment and second verification images. The panels appear most accurate first, and vertical scale changes on each page. The four traces correspond to images annotated with codes for black female, black male, white female, white male. The threshold is fixed for each algorithm to give $FMR = 0.00001$ over all (10^8) impostor comparisons. For short time-lapses, the most accurate algorithms give very few errors ($FNMR < 0.001$) so that the uncertainty estimates are high.

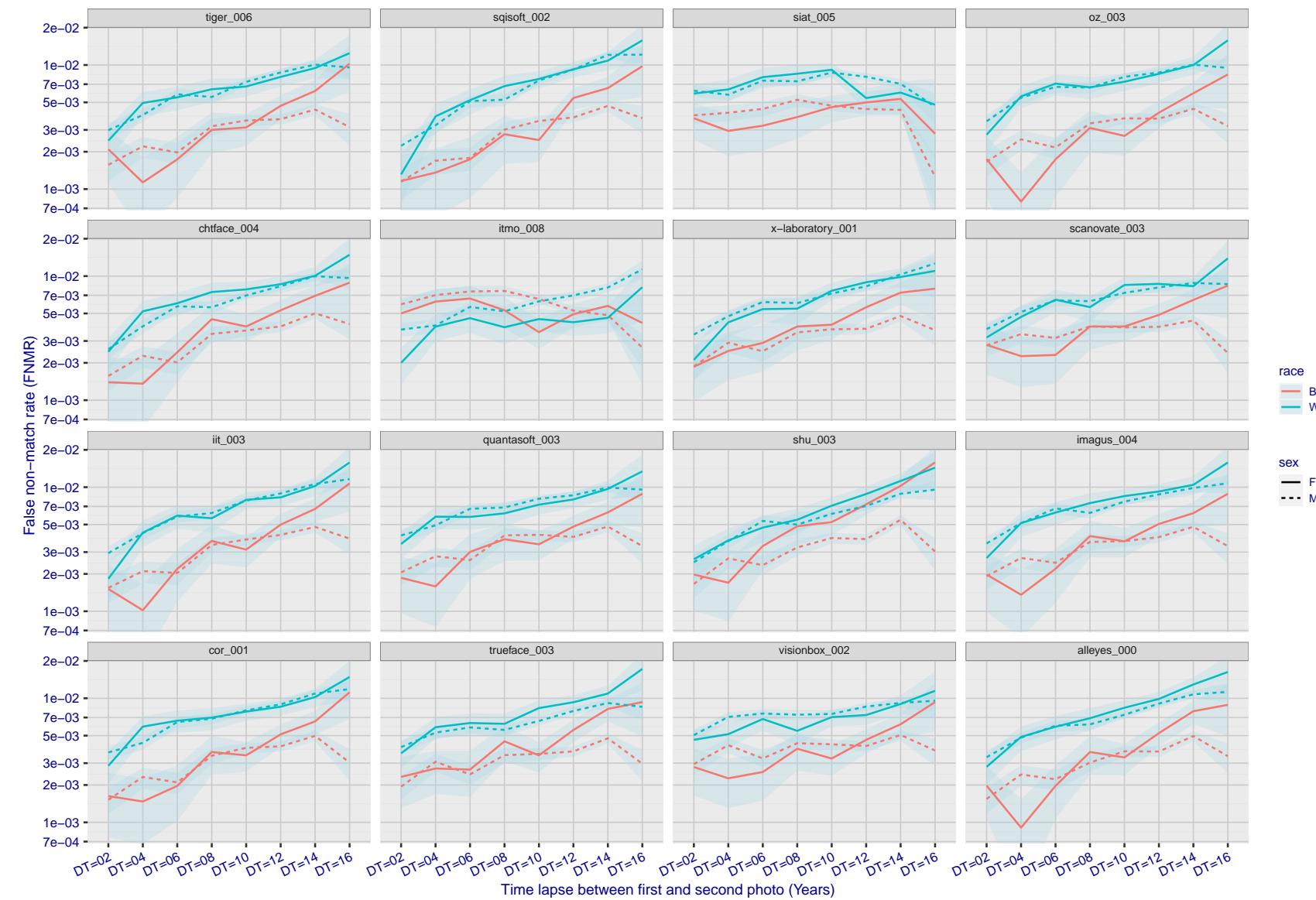


Figure 279: For the mugshot images, FNMR as a function of elapsed time between initial enrollment and second verification images. The panels appear most accurate first, and vertical scale changes on each page. The four traces correspond to images annotated with codes for black female, black male, white female, white male. The threshold is fixed for each algorithm to give $FMR = 0.00001$ over all (10^8) impostor comparisons. For short time-lapses, the most accurate algorithms give very few errors ($FNMR < 0.001$) so that the uncertainty estimates are high.

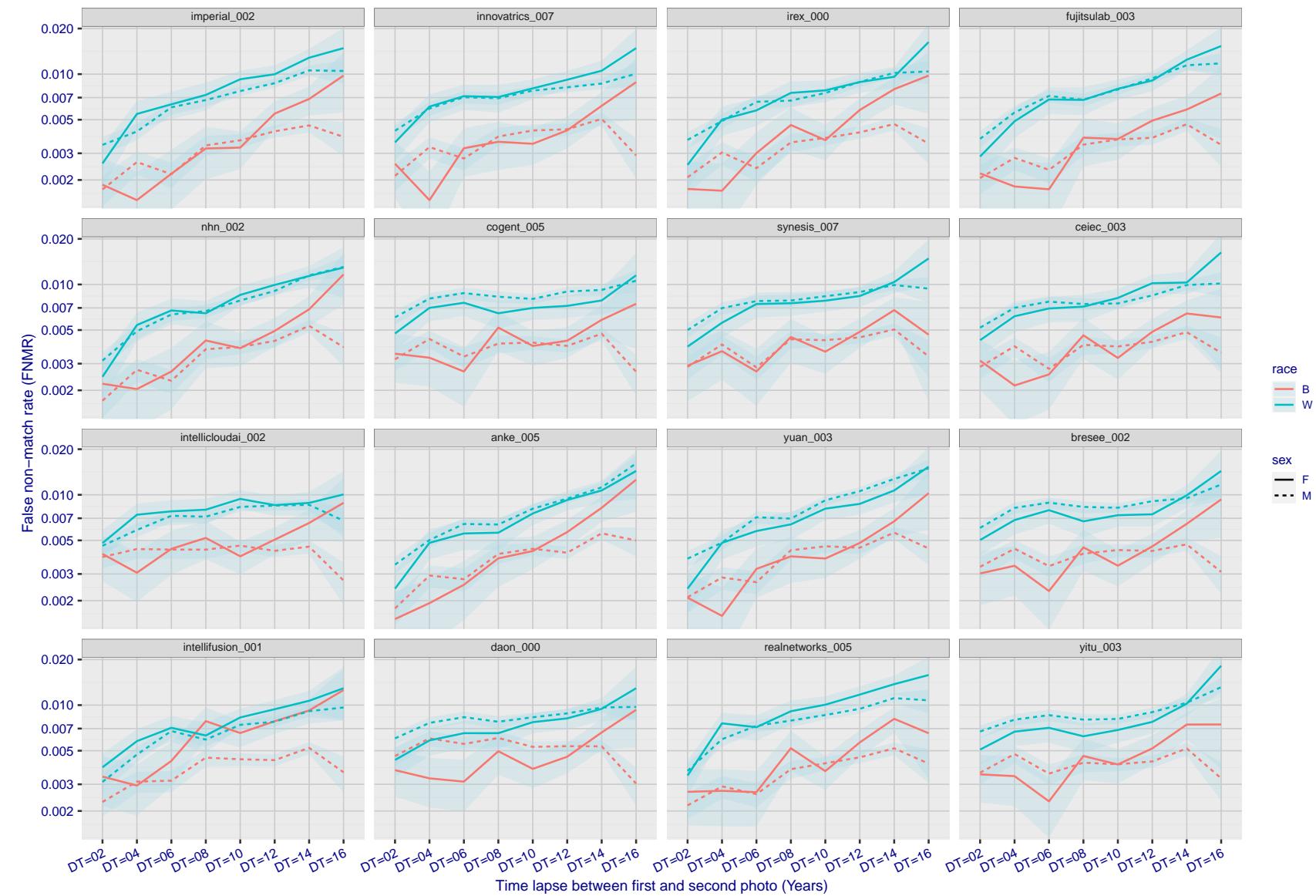


Figure 280: For the mugshot images, FNMR as a function of elapsed time between initial enrollment and second verification images. The panels appear most accurate first, and vertical scale changes on each page. The four traces correspond to images annotated with codes for black female, black male, white female, white male. The threshold is fixed for each algorithm to give FMR = 0.00001 over all (10^8) impostor comparisons. For short time-lapses, the most accurate algorithms give very few errors (FNMR < 0.001) so that the uncertainty estimates are high.

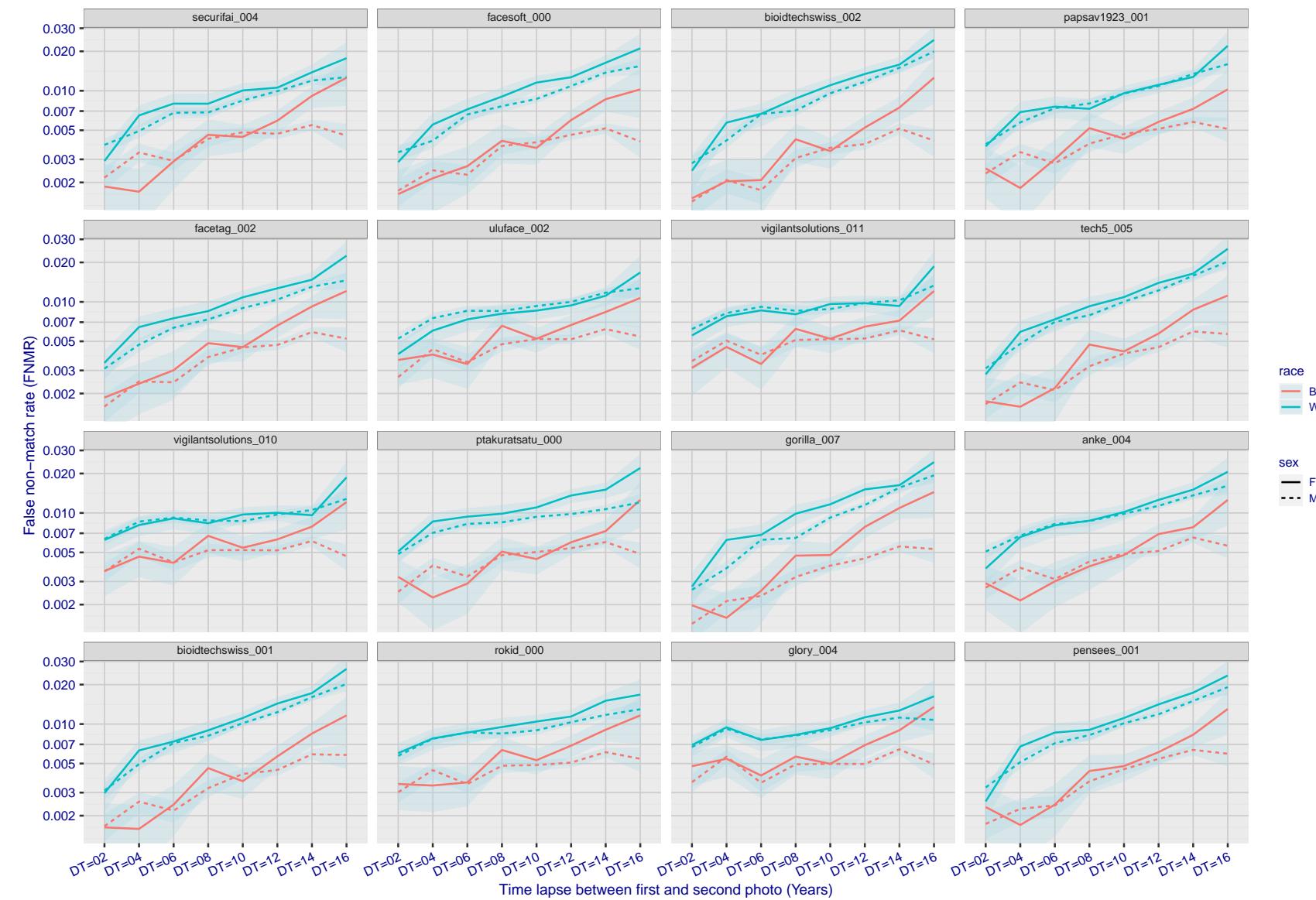


Figure 281: For the mugshot images, FNMR as a function of elapsed time between initial enrollment and second verification images. The panels appear most accurate first, and vertical scale changes on each page. The four traces correspond to images annotated with codes for black female, black male, white female, white male. The threshold is fixed for each algorithm to give FMR = 0.00001 over all (10^8) impostor comparisons. For short time-lapses, the most accurate algorithms give very few errors (FNMR < 0.001) so that the uncertainty estimates are high.

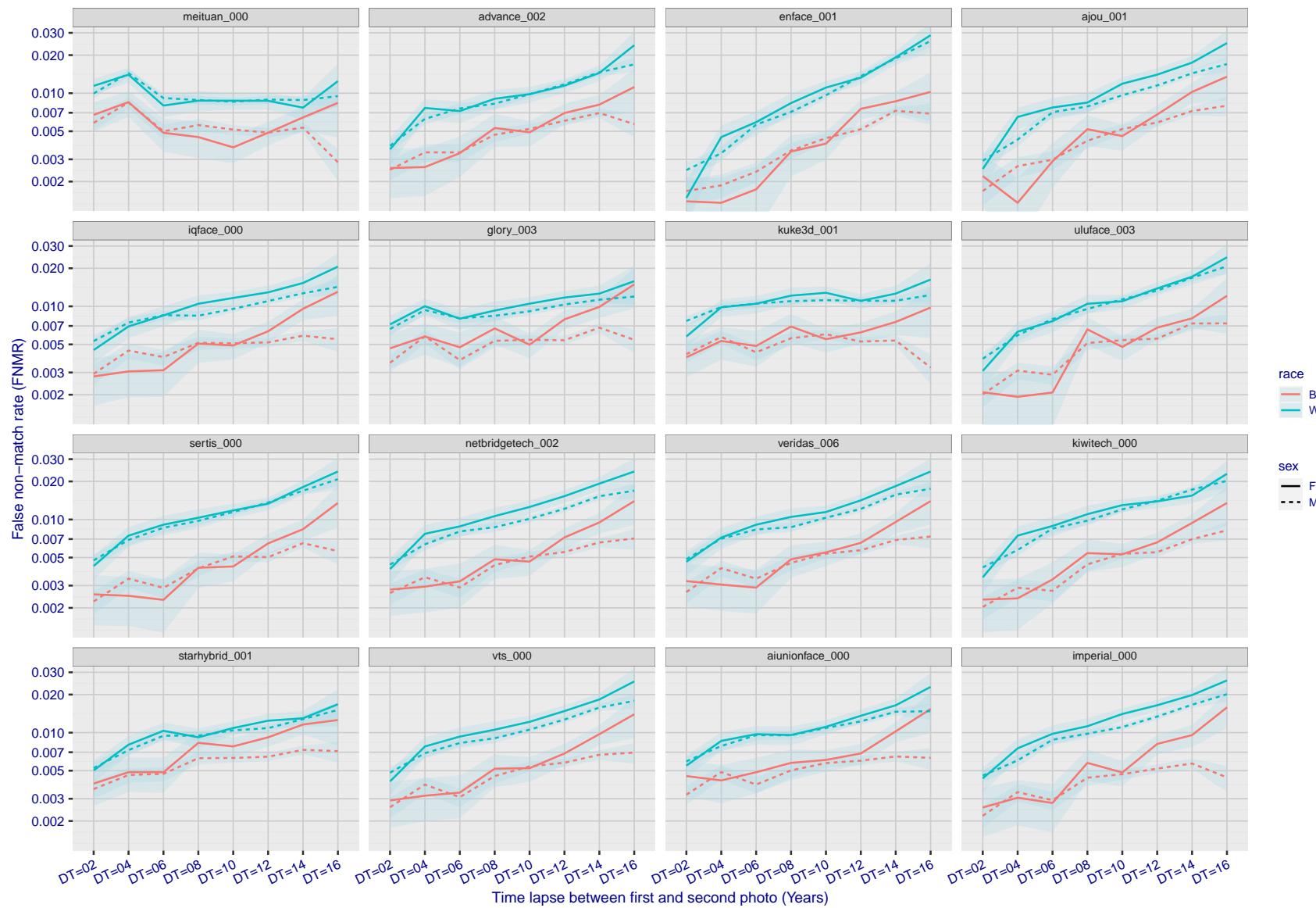


Figure 282: For the mugshot images, FNMR as a function of elapsed time between initial enrollment and second verification images. The panels appear most accurate first, and vertical scale changes on each page. The four traces correspond to images annotated with codes for black female, black male, white female, white male. The threshold is fixed for each algorithm to give FMR = 0.00001 over all (10^8) impostor comparisons. For short time-lapses, the most accurate algorithms give very few errors (FNMR < 0.001) so that the uncertainty estimates are high.

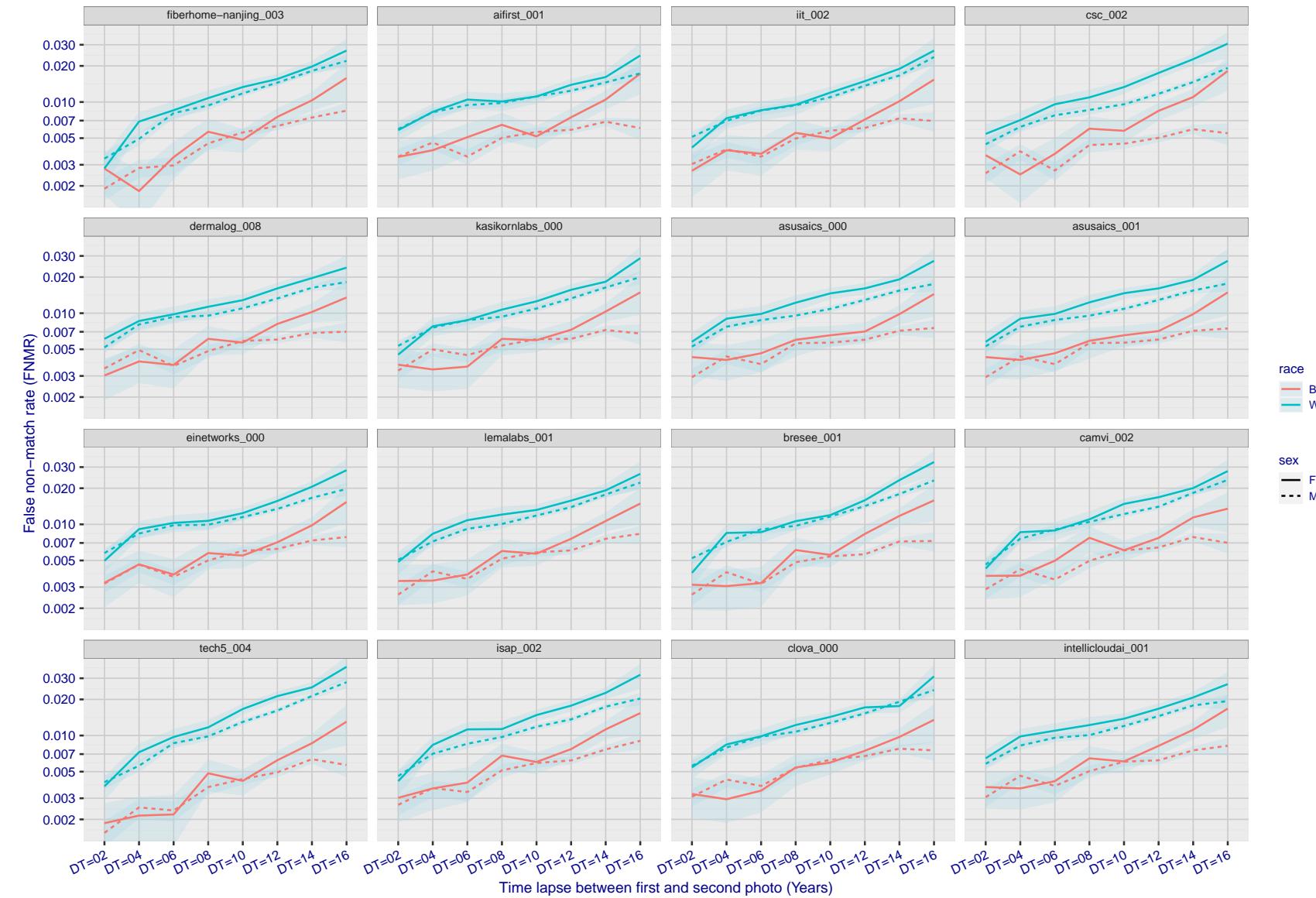


Figure 283: For the mugshot images, FNMR as a function of elapsed time between initial enrollment and second verification images. The panels appear most accurate first, and vertical scale changes on each page. The four traces correspond to images annotated with codes for black female, black male, white female, white male. The threshold is fixed for each algorithm to give FMR = 0.00001 over all (10^8) impostor comparisons. For short time-lapses, the most accurate algorithms give very few errors (FNMR < 0.001) so that the uncertainty estimates are high.

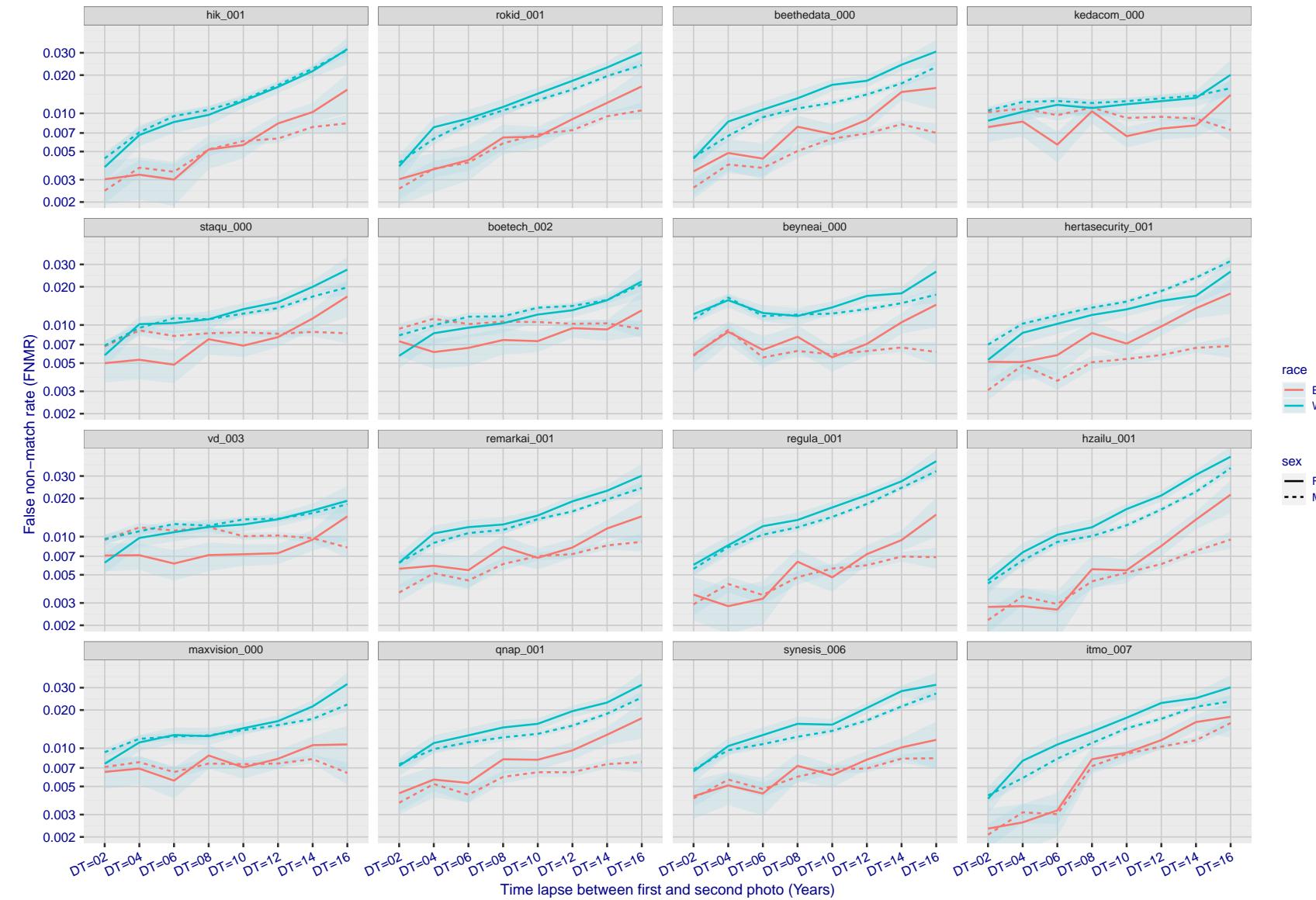


Figure 284: For the mugshot images, FNMR as a function of elapsed time between initial enrollment and second verification images. The panels appear most accurate first, and vertical scale changes on each page. The four traces correspond to images annotated with codes for black female, black male, white female, white male. The threshold is fixed for each algorithm to give FMR = 0.00001 over all (10^8) impostor comparisons. For short time-lapses, the most accurate algorithms give very few errors (FNMR < 0.001) so that the uncertainty estimates are high.

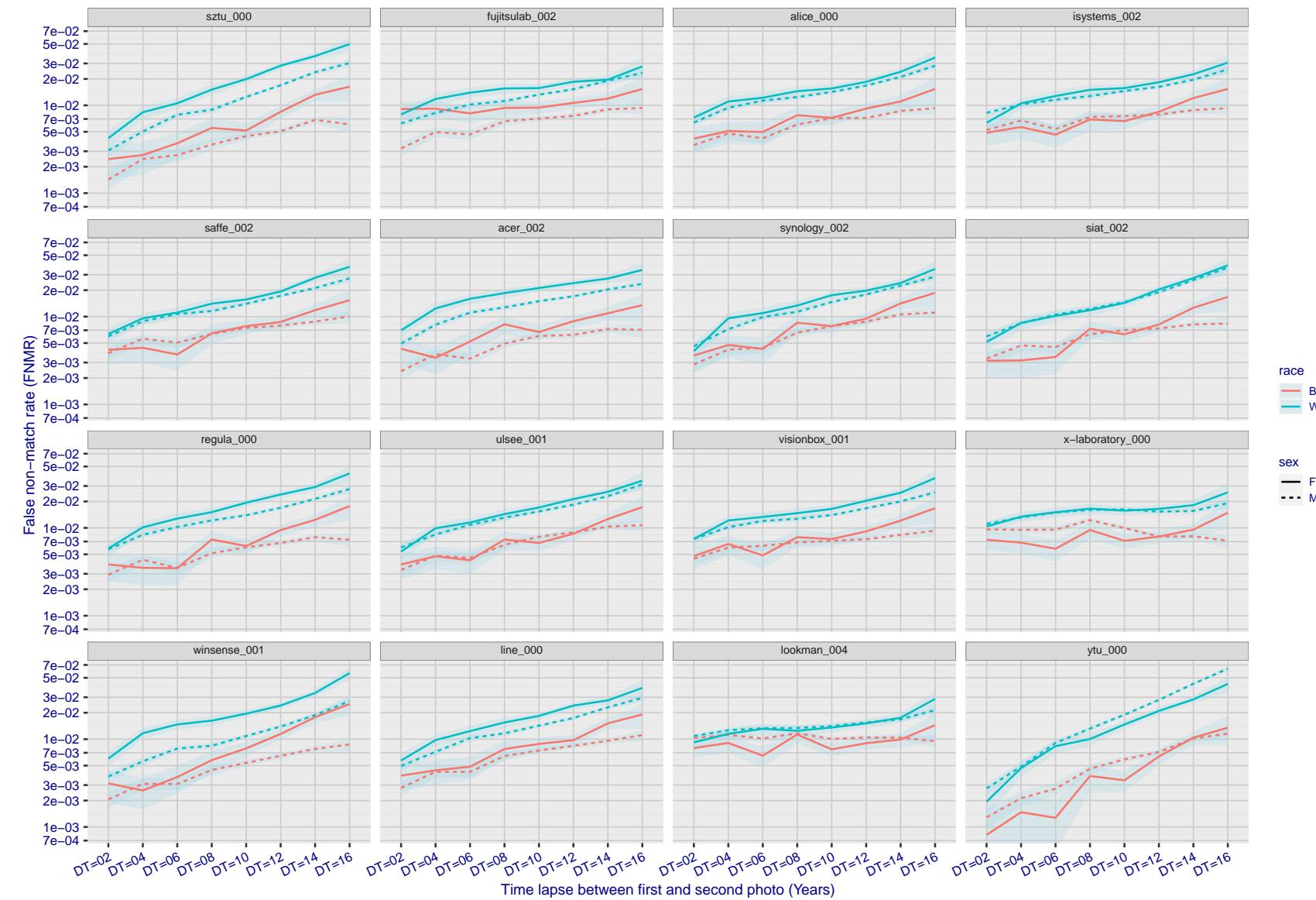


Figure 285: For the mugshot images, FNMR as a function of elapsed time between initial enrollment and second verification images. The panels appear most accurate first, and vertical scale changes on each page. The four traces correspond to images annotated with codes for black female, black male, white female, white male. The threshold is fixed for each algorithm to give $FMR = 0.00001$ over all (10^8) impostor comparisons. For short time-lapses, the most accurate algorithms give very few errors ($FNMR < 0.001$) so that the uncertainty estimates are high.

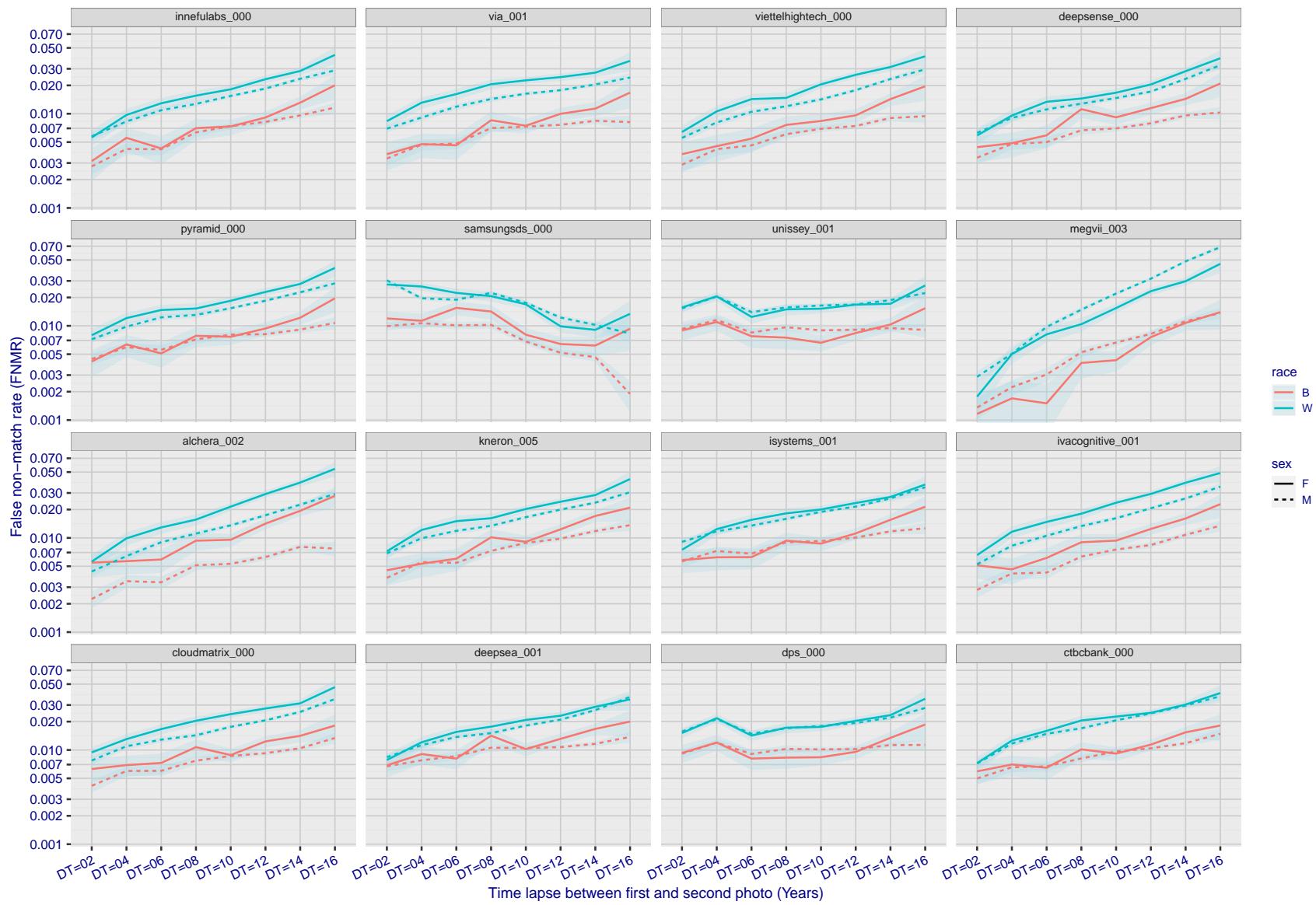


Figure 286: For the mugshot images, FNMR as a function of elapsed time between initial enrollment and second verification images. The panels appear most accurate first, and vertical scale changes on each page. The four traces correspond to images annotated with codes for black female, black male, white female, white male. The threshold is fixed for each algorithm to give FMR = 0.00001 over all (10^8) impostor comparisons. For short time-lapses, the most accurate algorithms give very few errors (FNMR < 0.001) so that the uncertainty estimates are high.

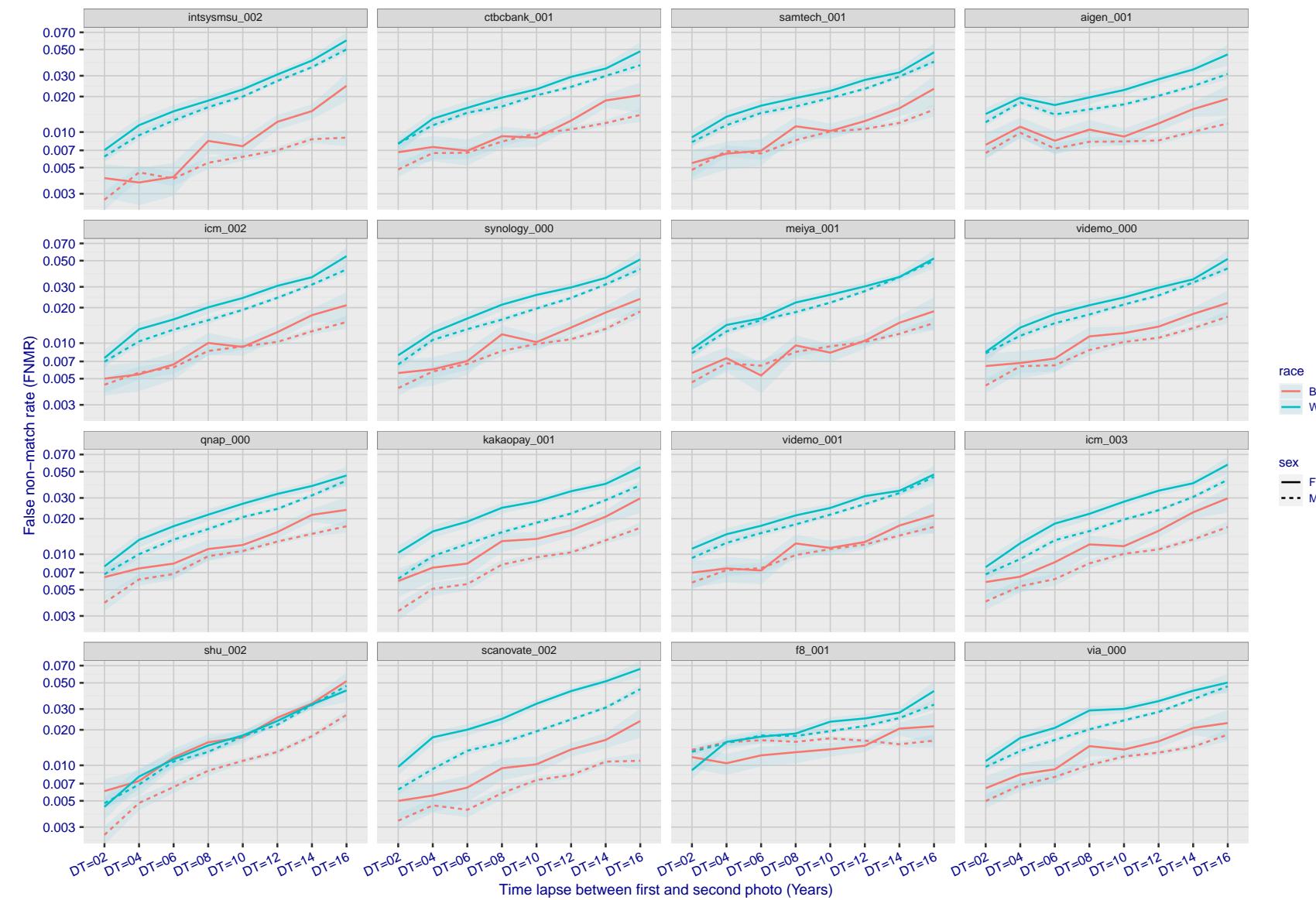


Figure 287: For the mugshot images, FNMR as a function of elapsed time between initial enrollment and second verification images. The panels appear most accurate first, and vertical scale changes on each page. The four traces correspond to images annotated with codes for black female, black male, white female, white male. The threshold is fixed for each algorithm to give FMR = 0.00001 over all (10^8) impostor comparisons. For short time-lapses, the most accurate algorithms give very few errors (FNMR < 0.001) so that the uncertainty estimates are high.

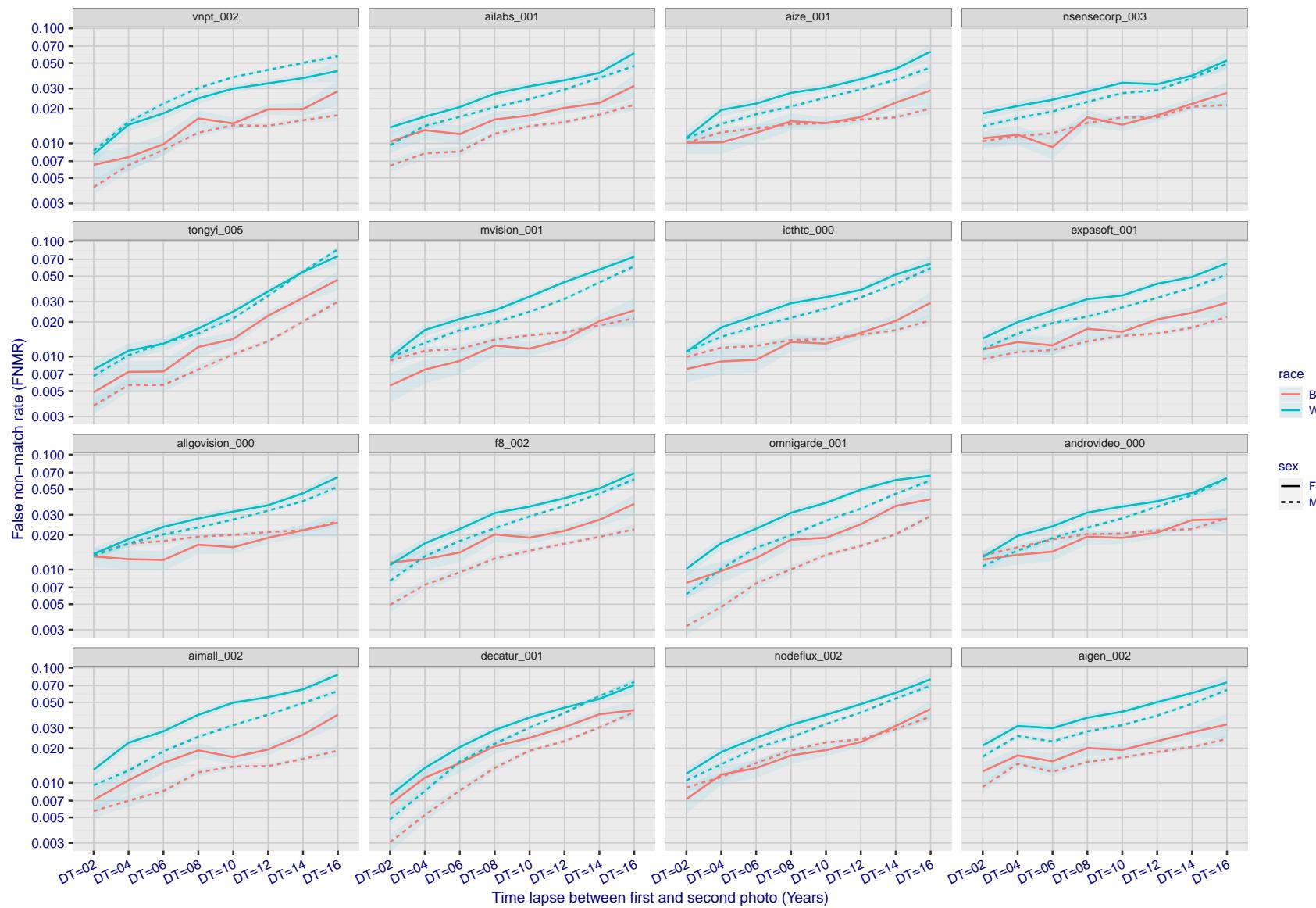


Figure 288: For the mugshot images, FNMR as a function of elapsed time between initial enrollment and second verification images. The panels appear most accurate first, and vertical scale changes on each page. The four traces correspond to images annotated with codes for black female, black male, white female, white male. The threshold is fixed for each algorithm to give $FMR = 0.00001$ over all (10^8) impostor comparisons. For short time-lapses, the most accurate algorithms give very few errors ($FNMR < 0.001$) so that the uncertainty estimates are high.

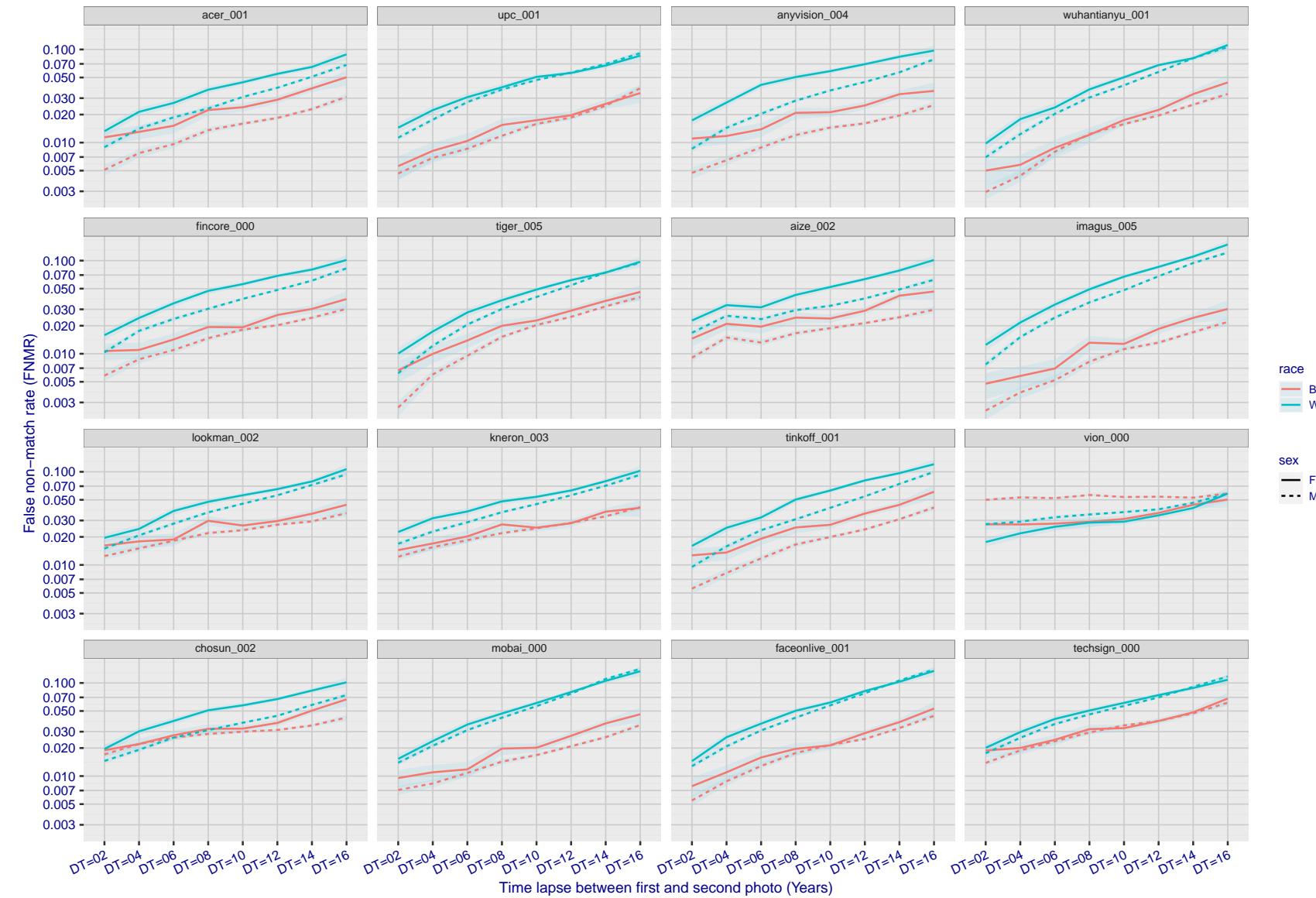


Figure 289: For the mugshot images, FNMR as a function of elapsed time between initial enrollment and second verification images. The panels appear most accurate first, and vertical scale changes on each page. The four traces correspond to images annotated with codes for black female, black male, white female, white male. The threshold is fixed for each algorithm to give FMR = 0.00001 over all (10^8) impostor comparisons. For short time-lapses, the most accurate algorithms give very few errors (FNMR < 0.001) so that the uncertainty estimates are high.

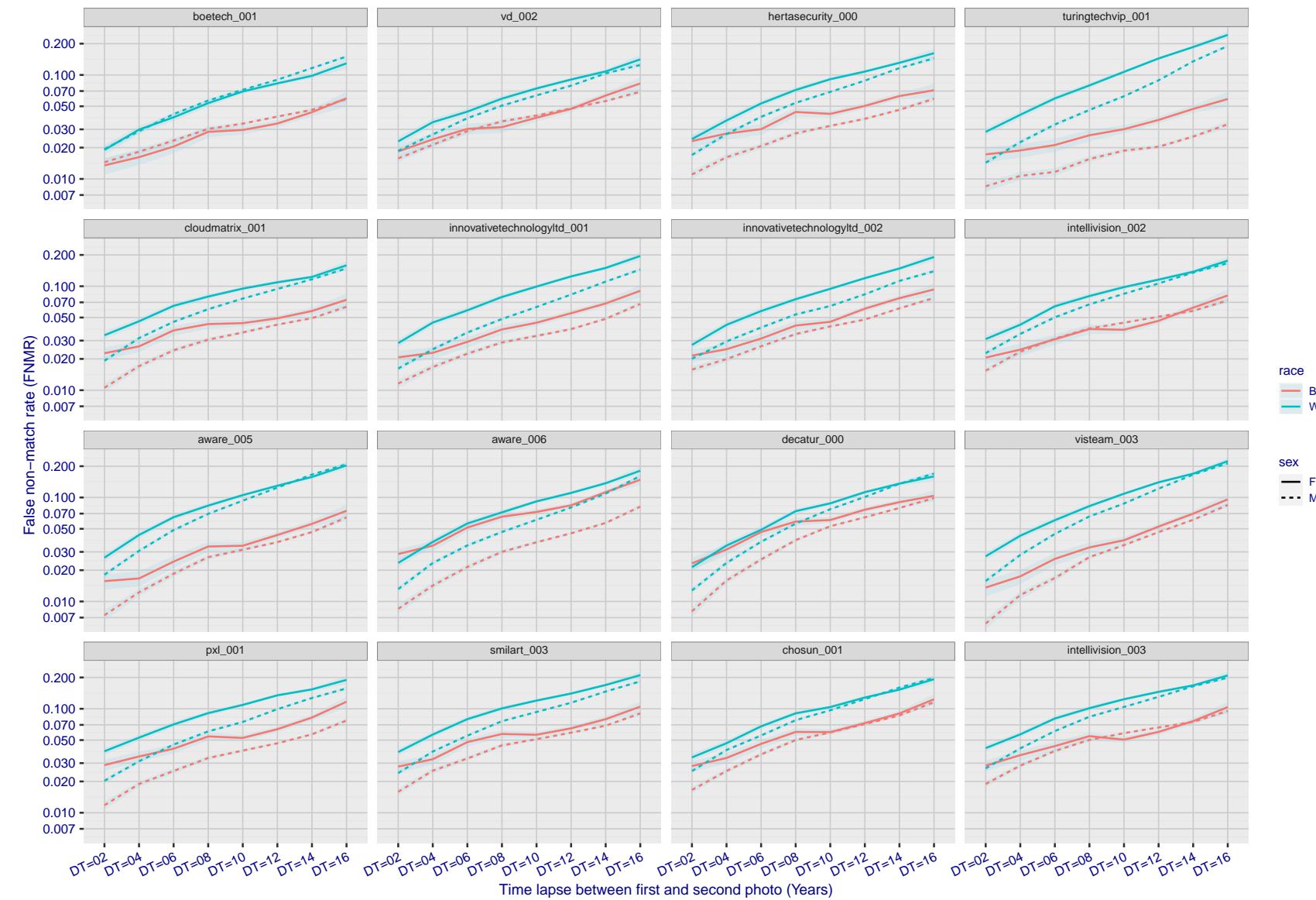


Figure 290: For the mugshot images, FNMR as a function of elapsed time between initial enrollment and second verification images. The panels appear most accurate first, and vertical scale changes on each page. The four traces correspond to images annotated with codes for black female, black male, white female, white male. The threshold is fixed for each algorithm to give FMR = 0.00001 over all (10^8) impostor comparisons. For short time-lapses, the most accurate algorithms give very few errors (FNMR < 0.001) so that the uncertainty estimates are high.

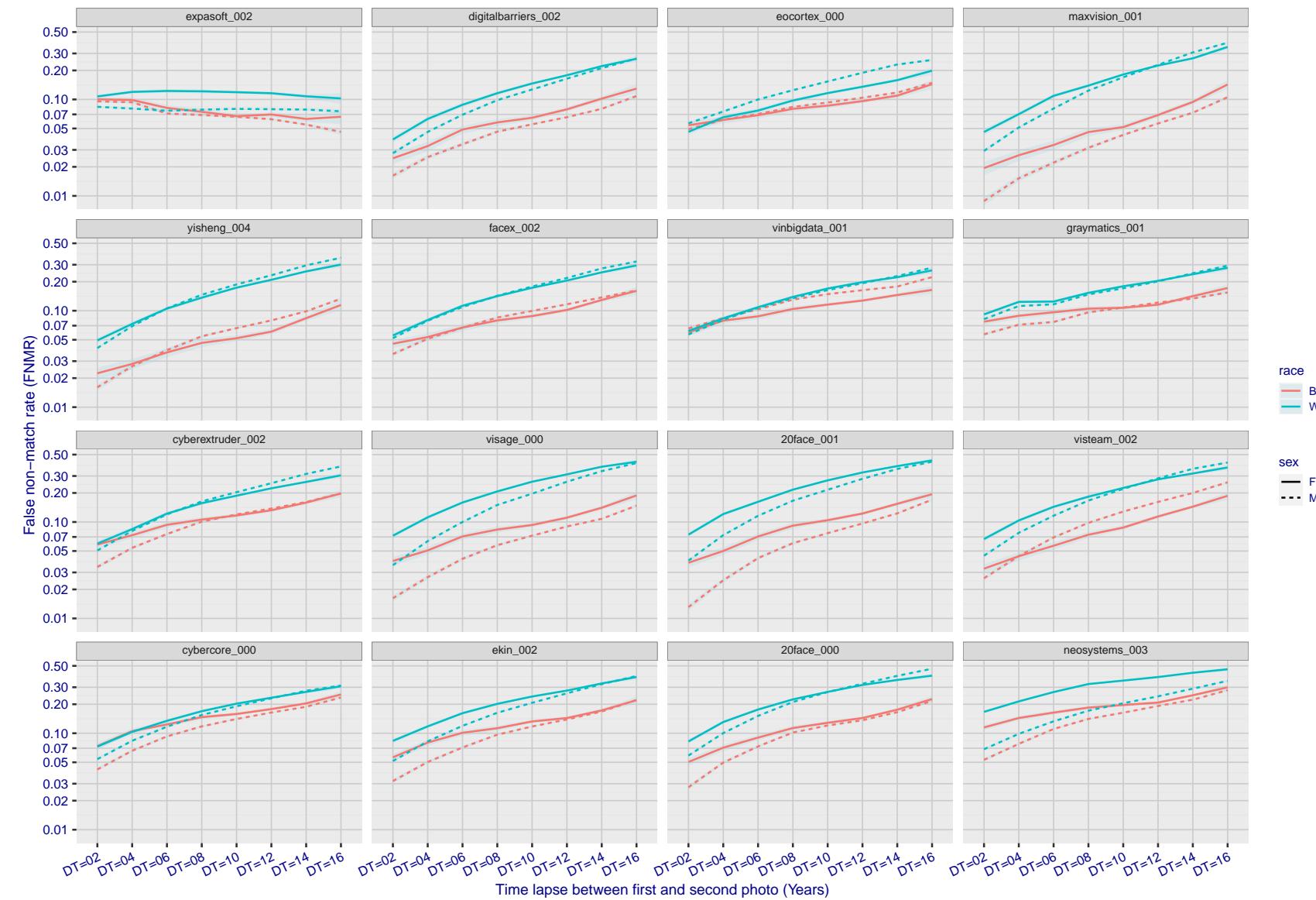


Figure 291: For the mugshot images, FNMR as a function of elapsed time between initial enrollment and second verification images. The panels appear most accurate first, and vertical scale changes on each page. The four traces correspond to images annotated with codes for black female, black male, white female, white male. The threshold is fixed for each algorithm to give FMR = 0.00001 over all (10^8) impostor comparisons. For short time-lapses, the most accurate algorithms give very few errors (FNMR < 0.001) so that the uncertainty estimates are high.

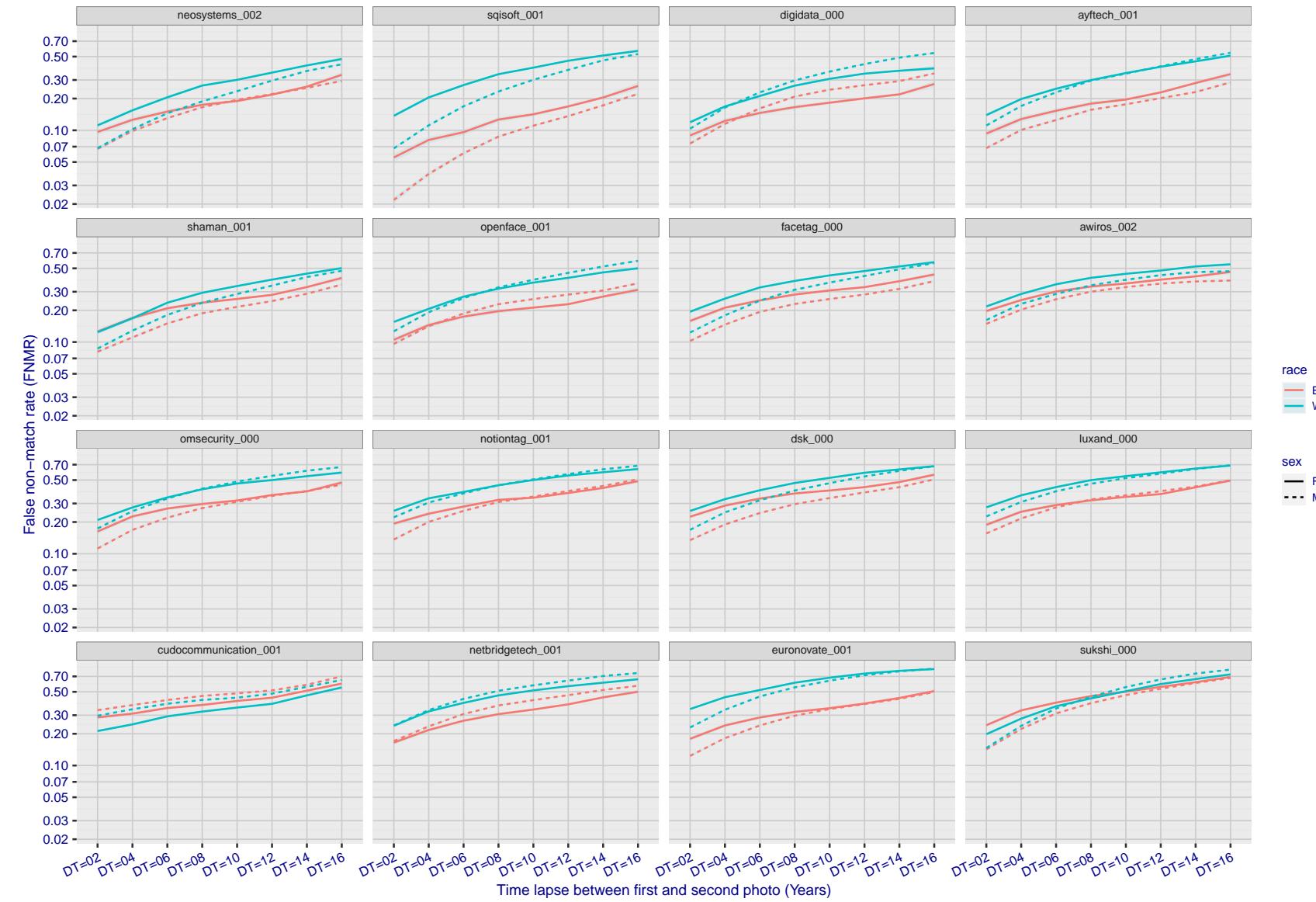


Figure 292: For the mugshot images, FNMR as a function of elapsed time between initial enrollment and second verification images. The panels appear most accurate first, and vertical scale changes on each page. The four traces correspond to images annotated with codes for black female, black male, white female, white male. The threshold is fixed for each algorithm to give FMR = 0.00001 over all (10^8) impostor comparisons. For short time-lapses, the most accurate algorithms give very few errors (FNMR < 0.001) so that the uncertainty estimates are high.

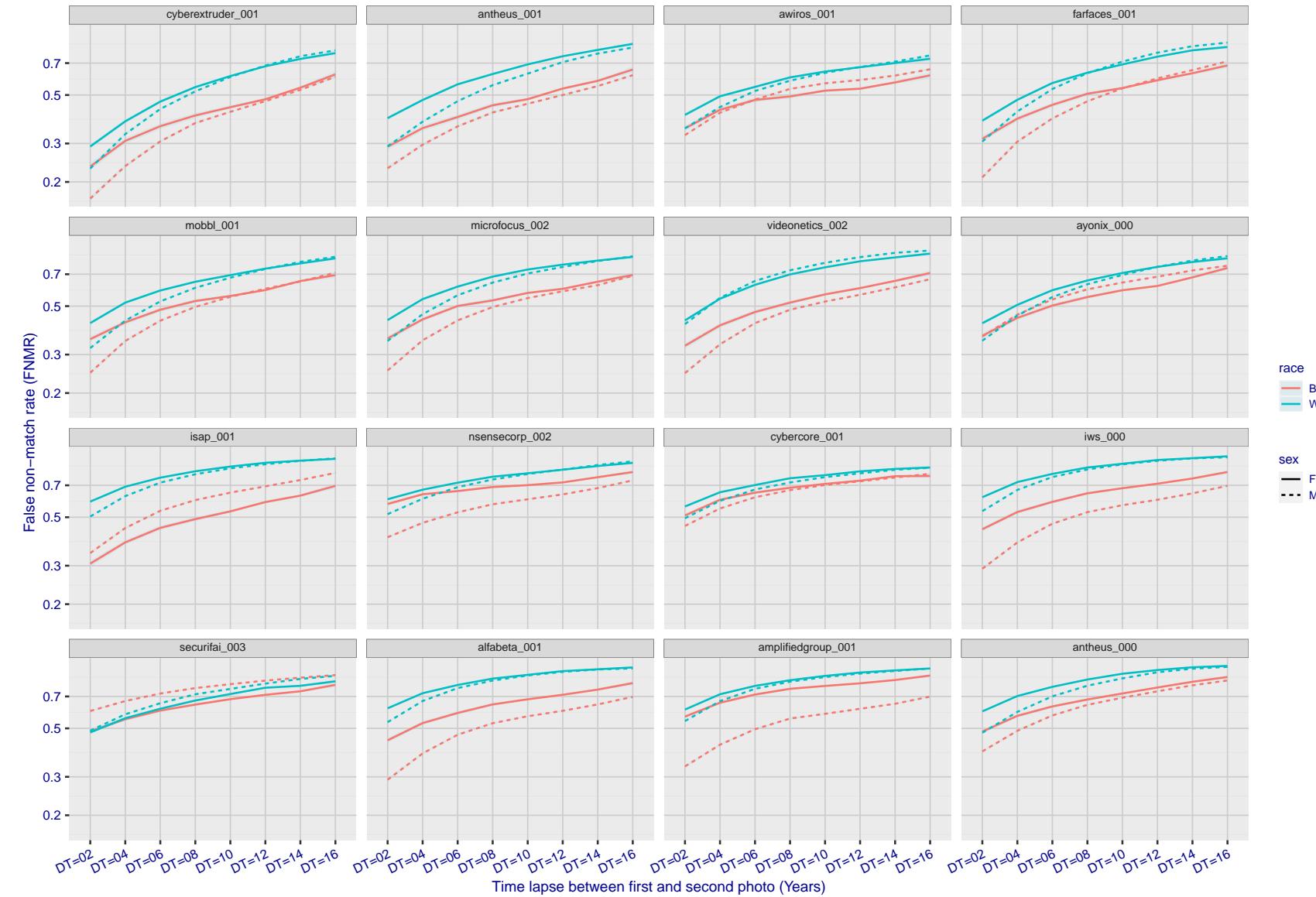


Figure 293: For the mugshot images, FNMR as a function of elapsed time between initial enrollment and second verification images. The panels appear most accurate first, and vertical scale changes on each page. The four traces correspond to images annotated with codes for black female, black male, white female, white male. The threshold is fixed for each algorithm to give FMR = 0.00001 over all (10^8) impostor comparisons. For short time-lapses, the most accurate algorithms give very few errors (FNMR < 0.001) so that the uncertainty estimates are high.

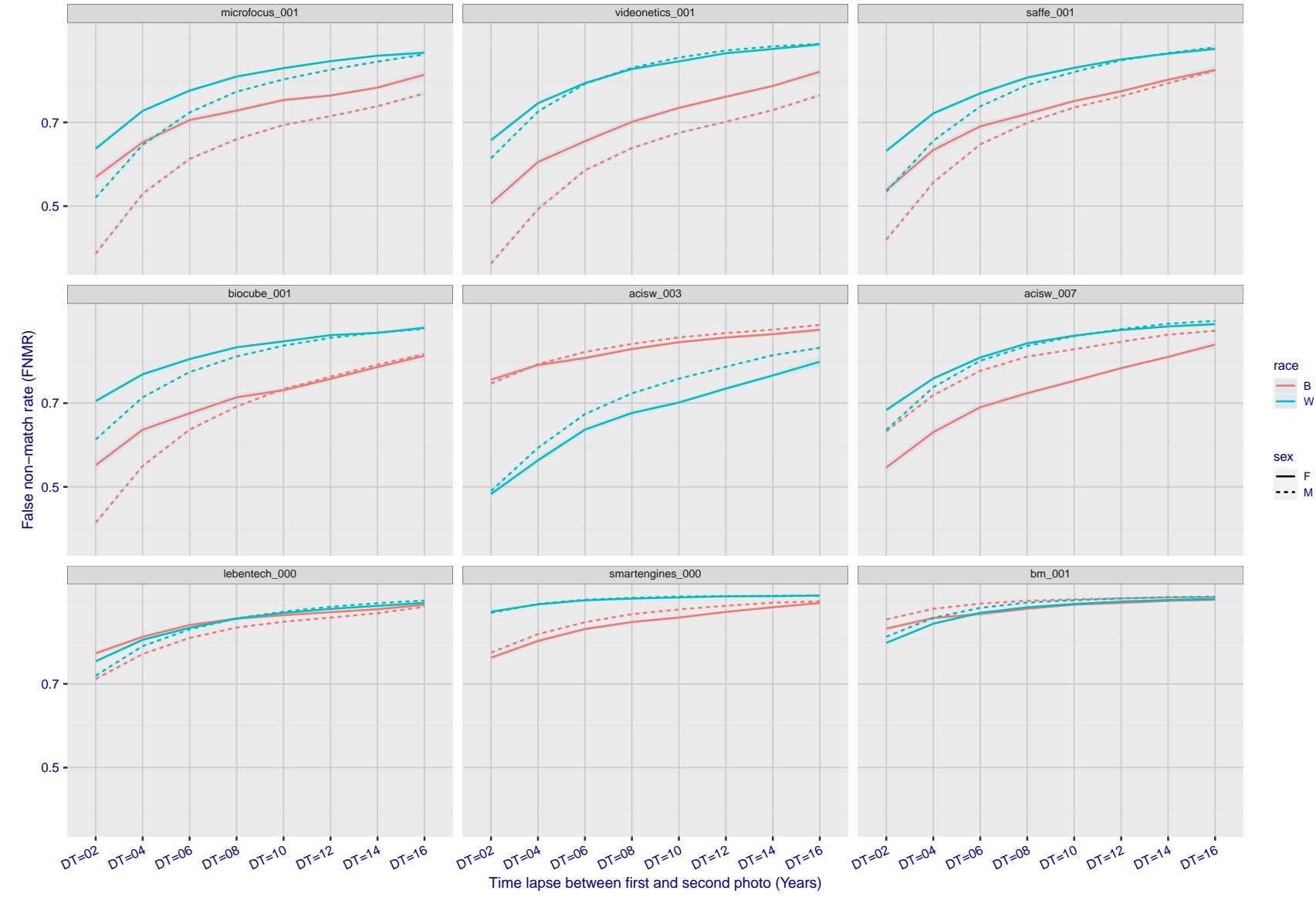


Figure 294: For the mugshot images, FNMR as a function of elapsed time between initial enrollment and second verification images. The panels appear most accurate first, and vertical scale changes on each page. The four traces correspond to images annotated with codes for black female, black male, white female, white male. The threshold is fixed for each algorithm to give FMR = 0.00001 over all (10^8) impostor comparisons. For short time-lapses, the most accurate algorithms give very few errors (FNMR < 0.001) so that the uncertainty estimates are high.

3.5.3 Effect of age on genuine subjects

Background: Faces change appearance throughout life. Face recognition algorithms have previously been reported to give better accuracy on older individuals (See NIST IR 8009).

Goal: To quantify false non-match rates (FNMR) as a function of age, without an ageing component.

Methods: Using the visa images, which span fewer than five years, thresholds are determined that give FMR = 0.001 and 0.0001 over the entire impostor set. Then FNMR is measured over 1000 bootstrap replications of the genuine scores.

Results: For the visa images, Figure 328 shows how false non-match rates for genuine users, as a function of age group.

The notable aspects are:

- ▷ Younger subjects give considerably higher FNMR. This is likely due to rapid growth and change in facial appearance.
- ▷ FNMR trends down throughout life. The last bin, AGE > 72, contains fewer than 140 mated pairs, and may be affected by small sample size.

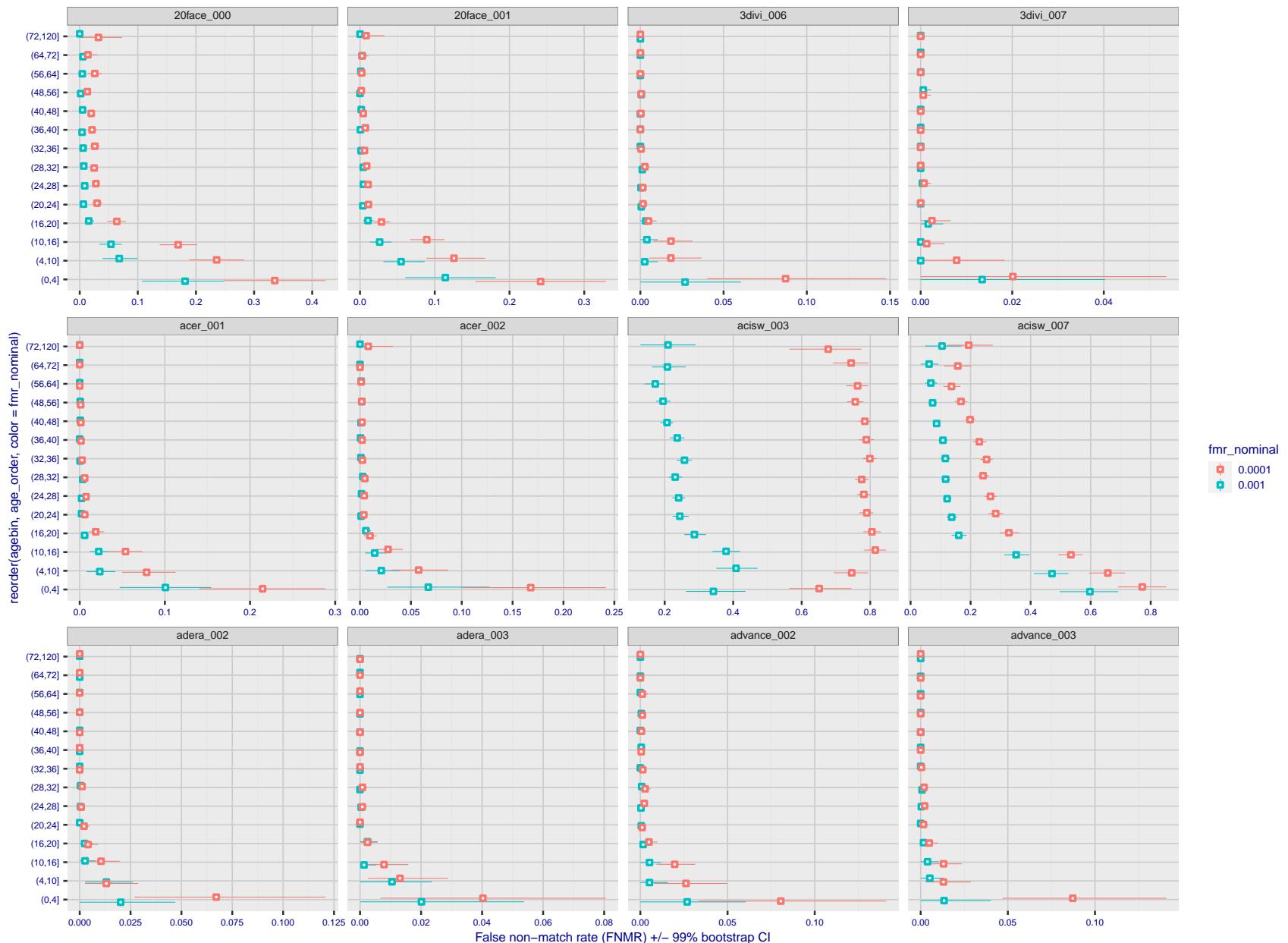


Figure 295: For the visa images, the dots show FNMR by age group for two operating thresholds corresponding to $FMR = \{0.001, 0.0001\}$ computed over all on the order of 10^{10} impostor scores. The FMR in each bin will vary also - see subsequent impostor heatmaps in sec. 3.6.2. Given a pair of face images taken at different times, we assign the comparison to the bin that is the arithmetic average of the subject's ages. This plot shows only the effect of age, not ageing. The number of comparisons in each bin is generally in the thousands, however the first and last bins are computed over 149 and 124 respectively. The error rates in some (adult) cases are zero, and in others the DET is flat so the error rates at the two thresholds are identical. The lines span 1% and 99% of bootstrap replicated FNMR estimates.

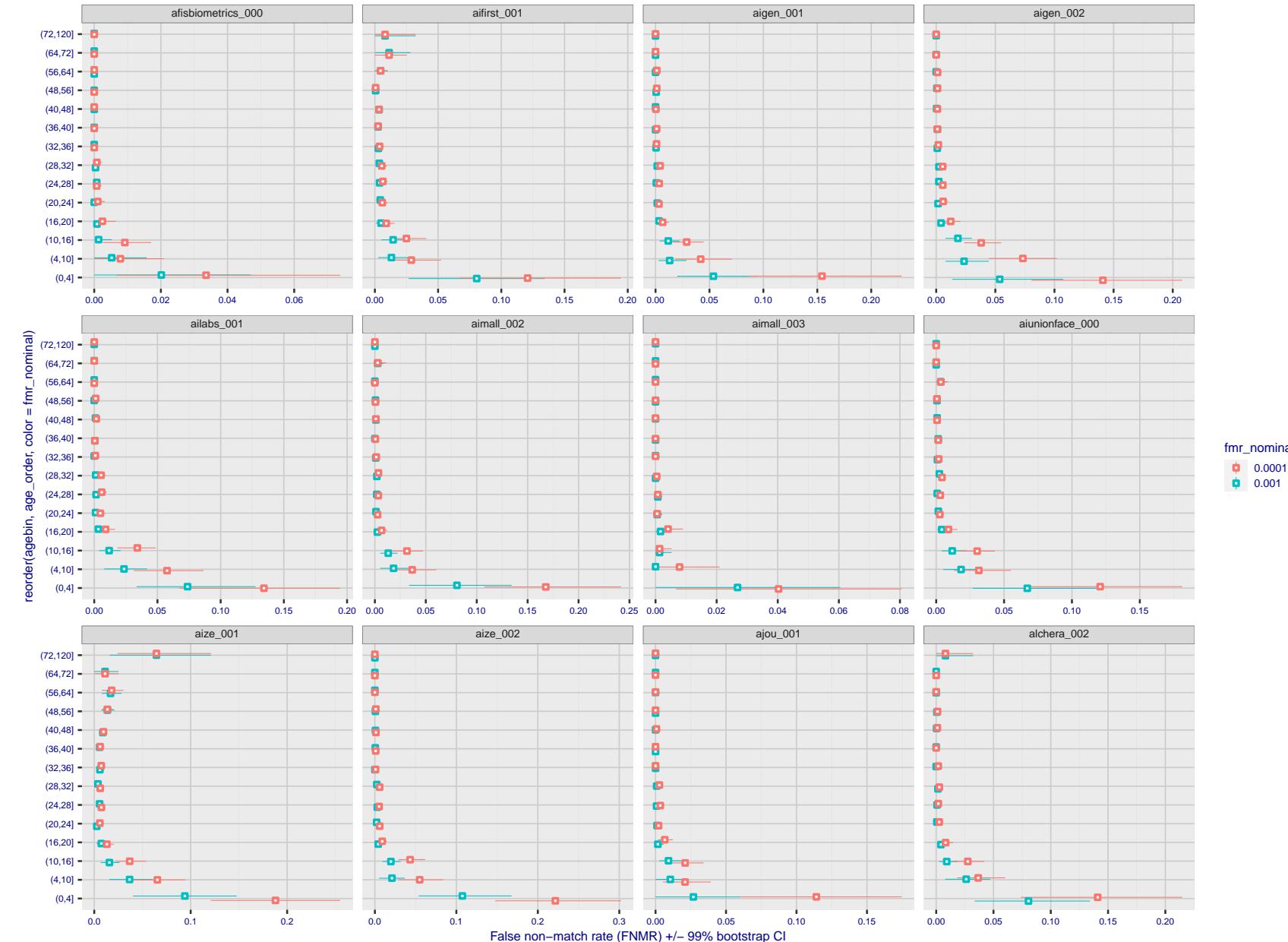


Figure 296: For the visa images, the dots show FNMR by age group for two operating thresholds corresponding to $FMR = \{0.001, 0.0001\}$ computed over all on the order of 10^{10} impostor scores. The FMR in each bin will vary also - see subsequent impostor heatmaps in sec. 3.6.2. Given a pair of face images taken at different times, we assign the comparison to the bin that is the arithmetic average of the subject's ages. This plot shows only the effect of age, not ageing. The number of comparisons in each bin is generally in the thousands, however the first and last bins are computed over 149 and 124 respectively. The error rates in some (adult) cases are zero, and in others the DET is flat so the error rates at the two thresholds are identical. The lines span 1% and 99% of bootstrap replicated FNMR estimates.

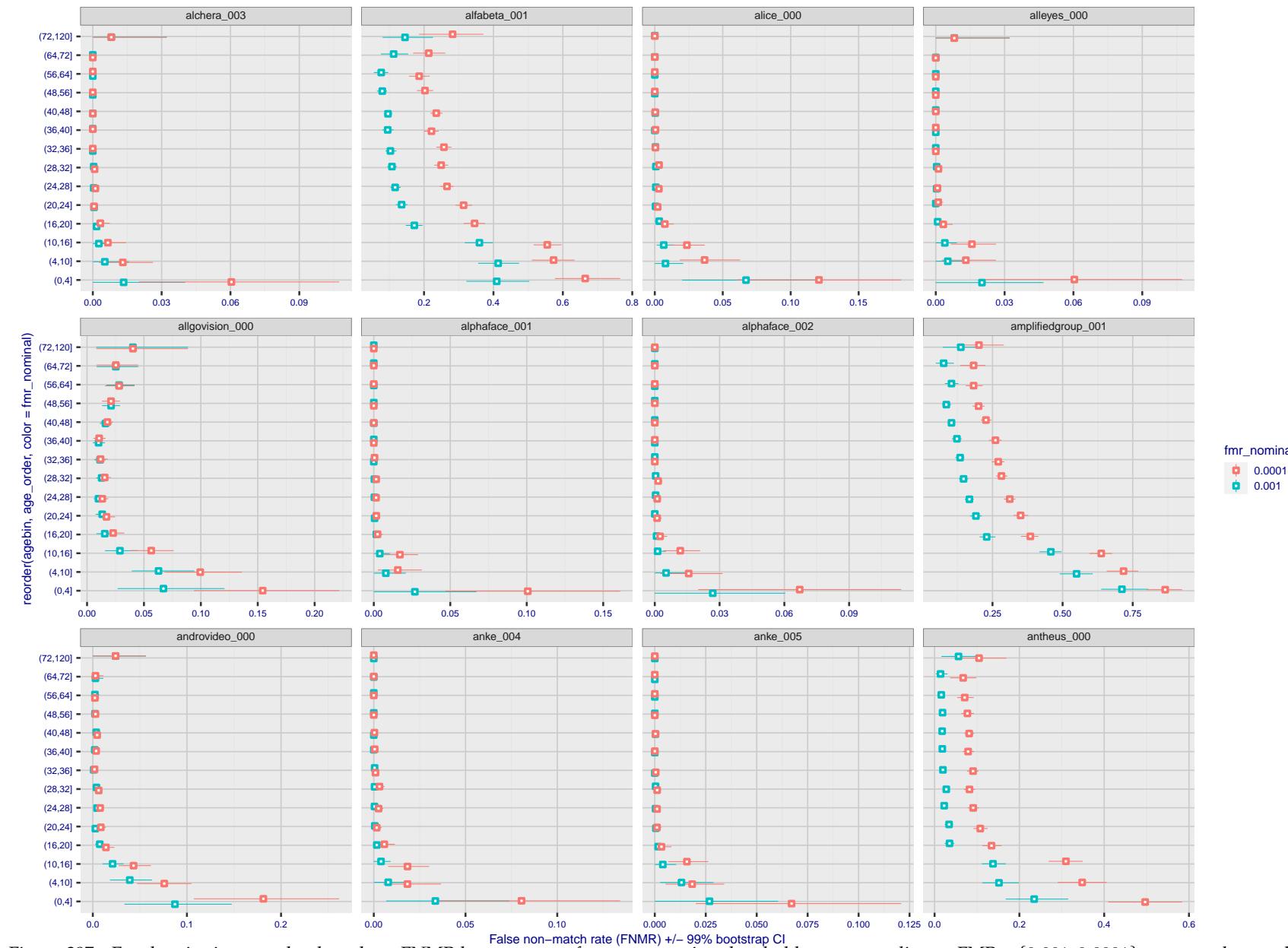


Figure 297: For the visa images, the dots show FNMR by age group for two operating thresholds corresponding to $FMR = \{0.001, 0.0001\}$ computed over all on the order of 10^{10} impostor scores. The FMR in each bin will vary also - see subsequent impostor heatmaps in sec. 3.6.2. Given a pair of face images taken at different times, we assign the comparison to the bin that is the arithmetic average of the subject's ages. This plot shows only the effect of age, not ageing. The number of comparisons in each bin is generally in the thousands, however the first and last bins are computed over 149 and 124 respectively. The error rates in some (adult) cases are zero, and in others the DET is flat so the error rates at the two thresholds are identical. The lines span 1% and 99% of bootstrap replicated FNMR estimates.

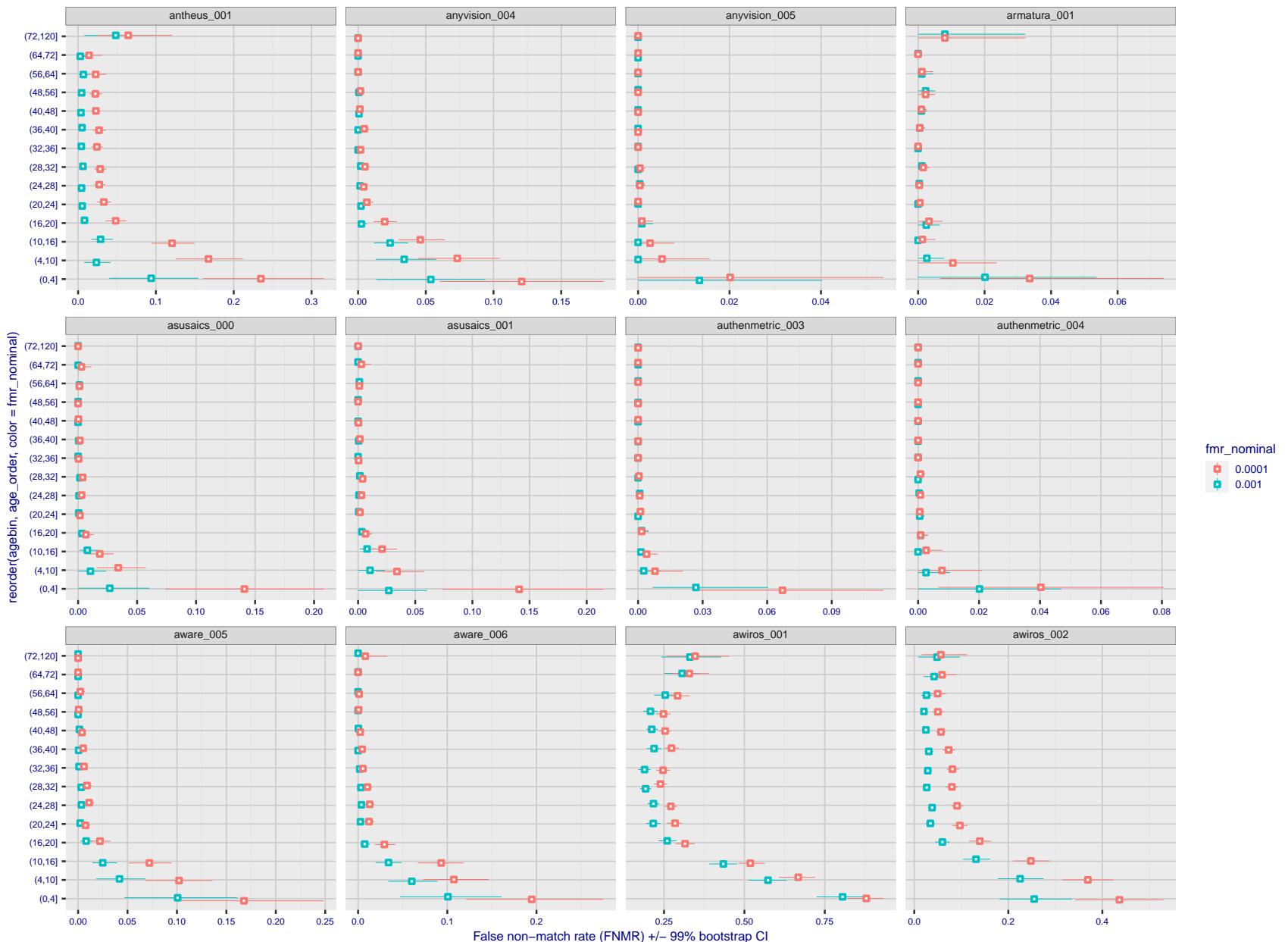


Figure 298: For the visa images, the dots show FNMR by age group for two operating thresholds corresponding to $FMR = \{0.001, 0.0001\}$ computed over all on the order of 10^{10} impostor scores. The FMR in each bin will vary also - see subsequent impostor heatmaps in sec. 3.6.2. Given a pair of face images taken at different times, we assign the comparison to the bin that is the arithmetic average of the subject's ages. This plot shows only the effect of age, not ageing. The number of comparisons in each bin is generally in the thousands, however the first and last bins are computed over 149 and 124 respectively. The error rates in some (adult) cases are zero, and in others the DET is flat so the error rates at the two thresholds are identical. The lines span 1% and 99% of bootstrap replicated FNMR estimates.

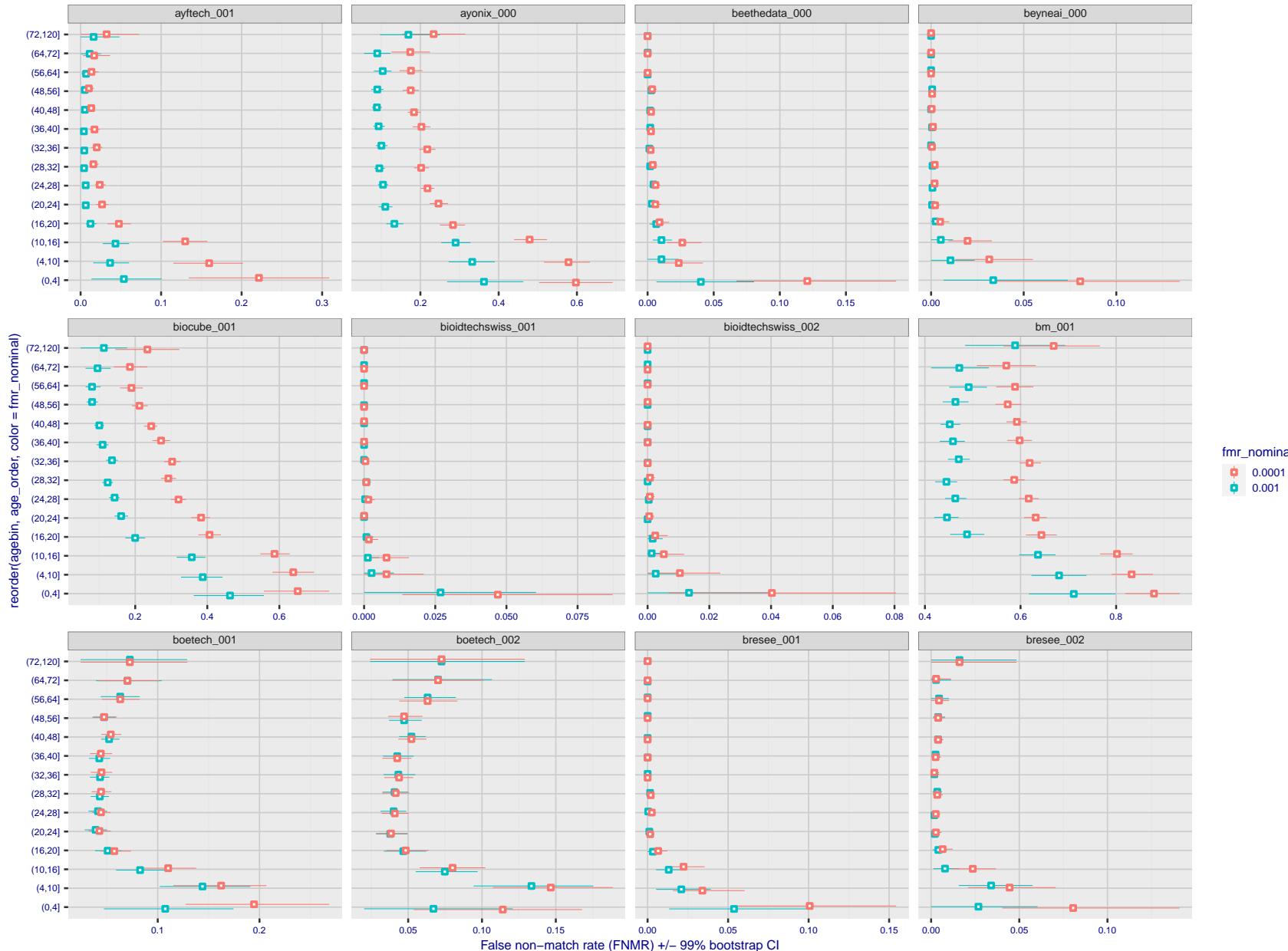


Figure 299: For the visa images, the dots show FNMR by age group for two operating thresholds corresponding to $FMR = \{0.001, 0.0001\}$ computed over all on the order of 10^{10} impostor scores. The FMR in each bin will vary also - see subsequent impostor heatmaps in sec. 3.6.2. Given a pair of face images taken at different times, we assign the comparison to the bin that is the arithmetic average of the subject's ages. This plot shows only the effect of age, not ageing. The number of comparisons in each bin is generally in the thousands, however the first and last bins are computed over 149 and 124 respectively. The error rates in some (adult) cases are zero, and in others the DET is flat so the error rates at the two thresholds are identical. The lines span 1% and 99% of bootstrap replicated FNMR estimates.



Figure 300: For the visa images, the dots show FNMR by age group for two operating thresholds corresponding to $FMR = \{0.001, 0.0001\}$ computed over all on the order of 10^{10} impostor scores. The FMR in each bin will vary also - see subsequent impostor heatmaps in sec. 3.6.2. Given a pair of face images taken at different times, we assign the comparison to the bin that is the arithmetic average of the subject's ages. This plot shows only the effect of age, not ageing. The number of comparisons in each bin is generally in the thousands, however the first and last bins are computed over 149 and 124 respectively. The error rates in some (adult) cases are zero, and in others the DET is flat so the error rates at the two thresholds are identical. The lines span 1% and 99% of bootstrap replicated FNMR estimates.

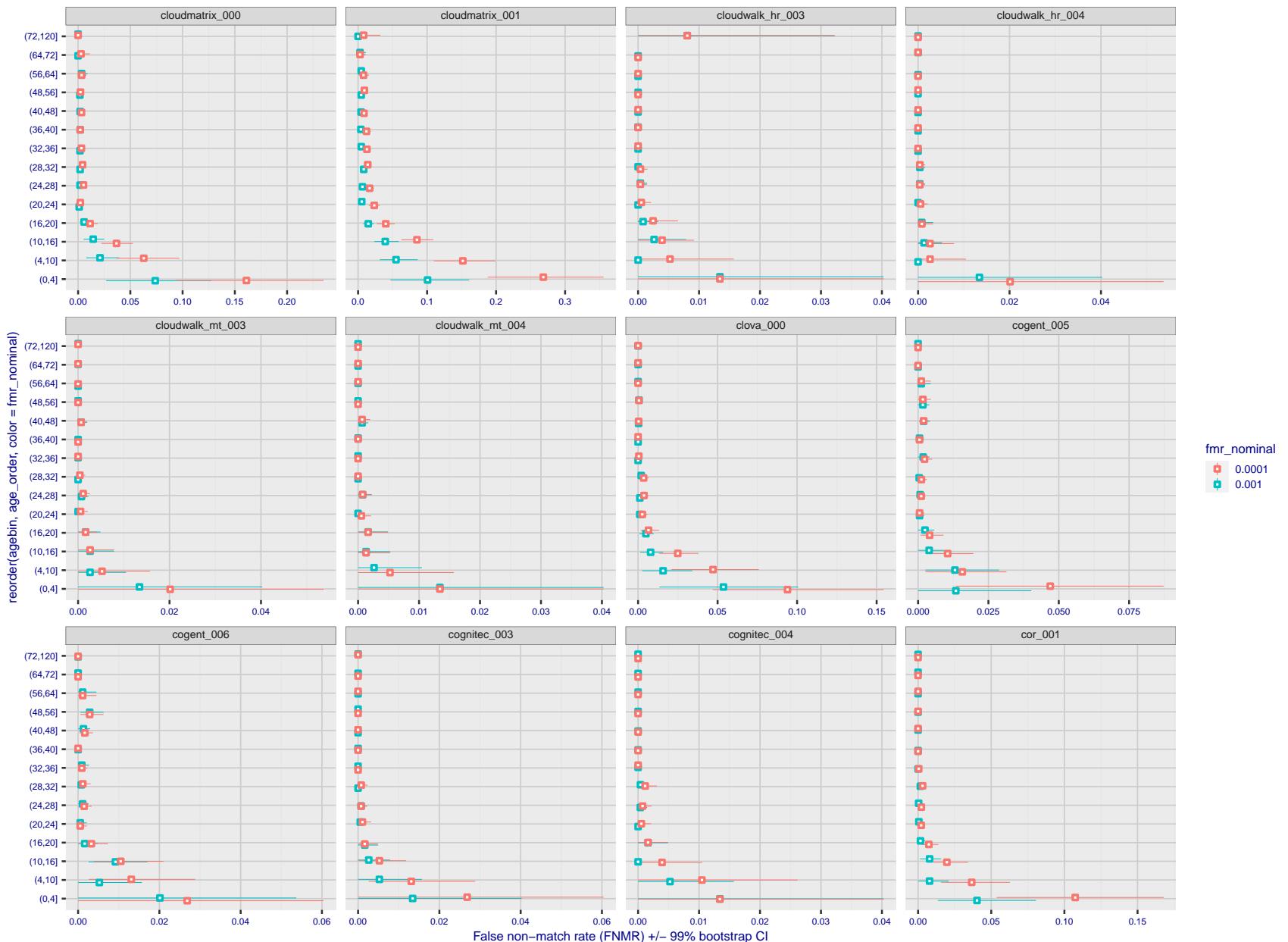


Figure 301: For the visa images, the dots show FNMR by age group for two operating thresholds corresponding to $FMR = \{0.001, 0.0001\}$ computed over all on the order of 10^{10} impostor scores. The FMR in each bin will vary also - see subsequent impostor heatmaps in sec. 3.6.2. Given a pair of face images taken at different times, we assign the comparison to the bin that is the arithmetic average of the subject's ages. This plot shows only the effect of age, not ageing. The number of comparisons in each bin is generally in the thousands, however the first and last bins are computed over 149 and 124 respectively. The error rates in some (adult) cases are zero, and in others the DET is flat so the error rates at the two thresholds are identical. The lines span 1% and 99% of bootstrap replicated FNMR estimates.

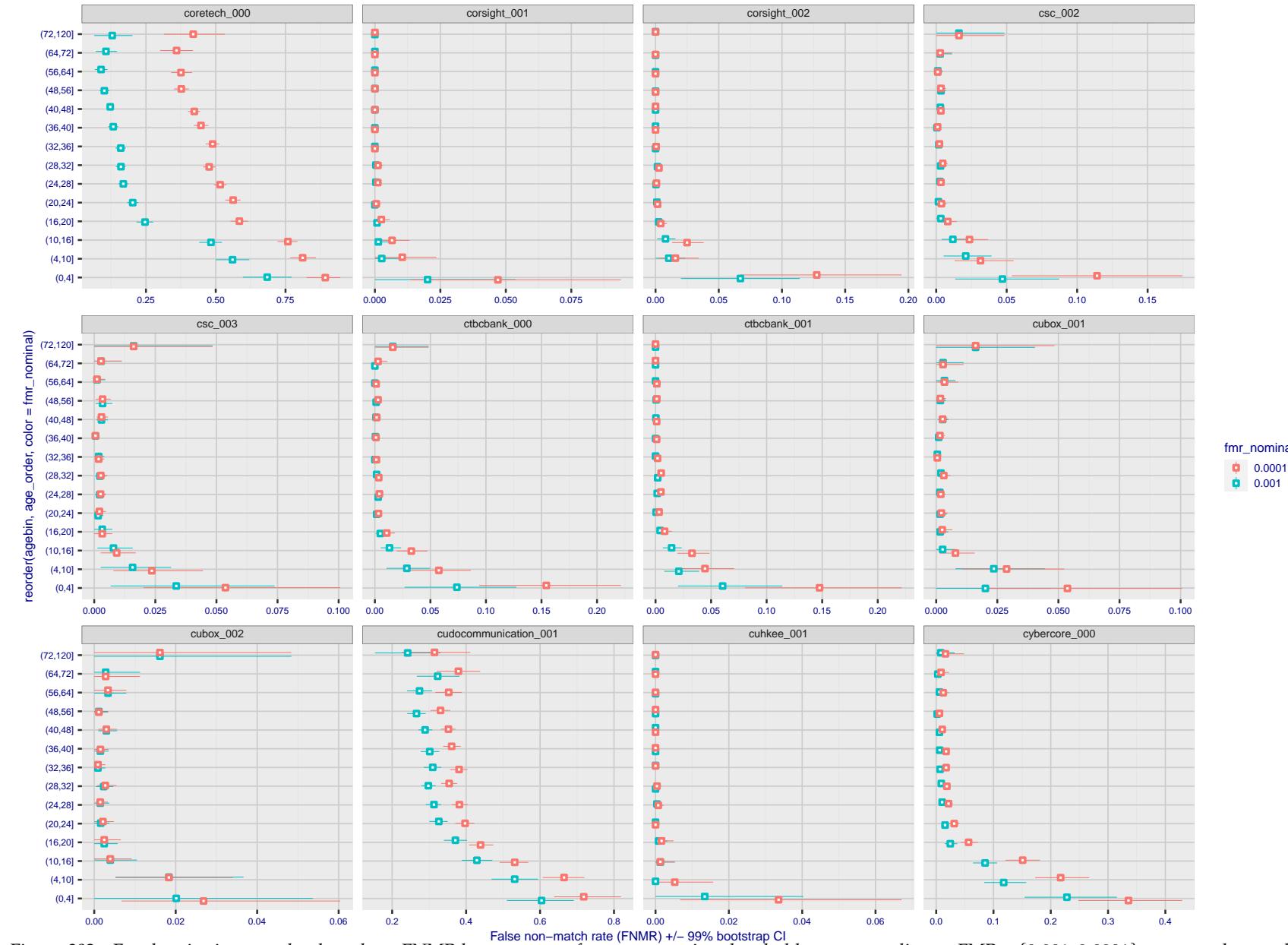


Figure 302: For the visa images, the dots show FNMR by age group for two operating thresholds corresponding to $FMR = \{0.001, 0.0001\}$ computed over all on the order of 10^{10} impostor scores. The FMR in each bin will vary also - see subsequent impostor heatmaps in sec. 3.6.2. Given a pair of face images taken at different times, we assign the comparison to the bin that is the arithmetic average of the subject's ages. This plot shows only the effect of age, not ageing. The number of comparisons in each bin is generally in the thousands, however the first and last bins are computed over 149 and 124 respectively. The error rates in some (adult) cases are zero, and in others the DET is flat so the error rates at the two thresholds are identical. The lines span 1% and 99% of bootstrap replicated FNMR estimates.

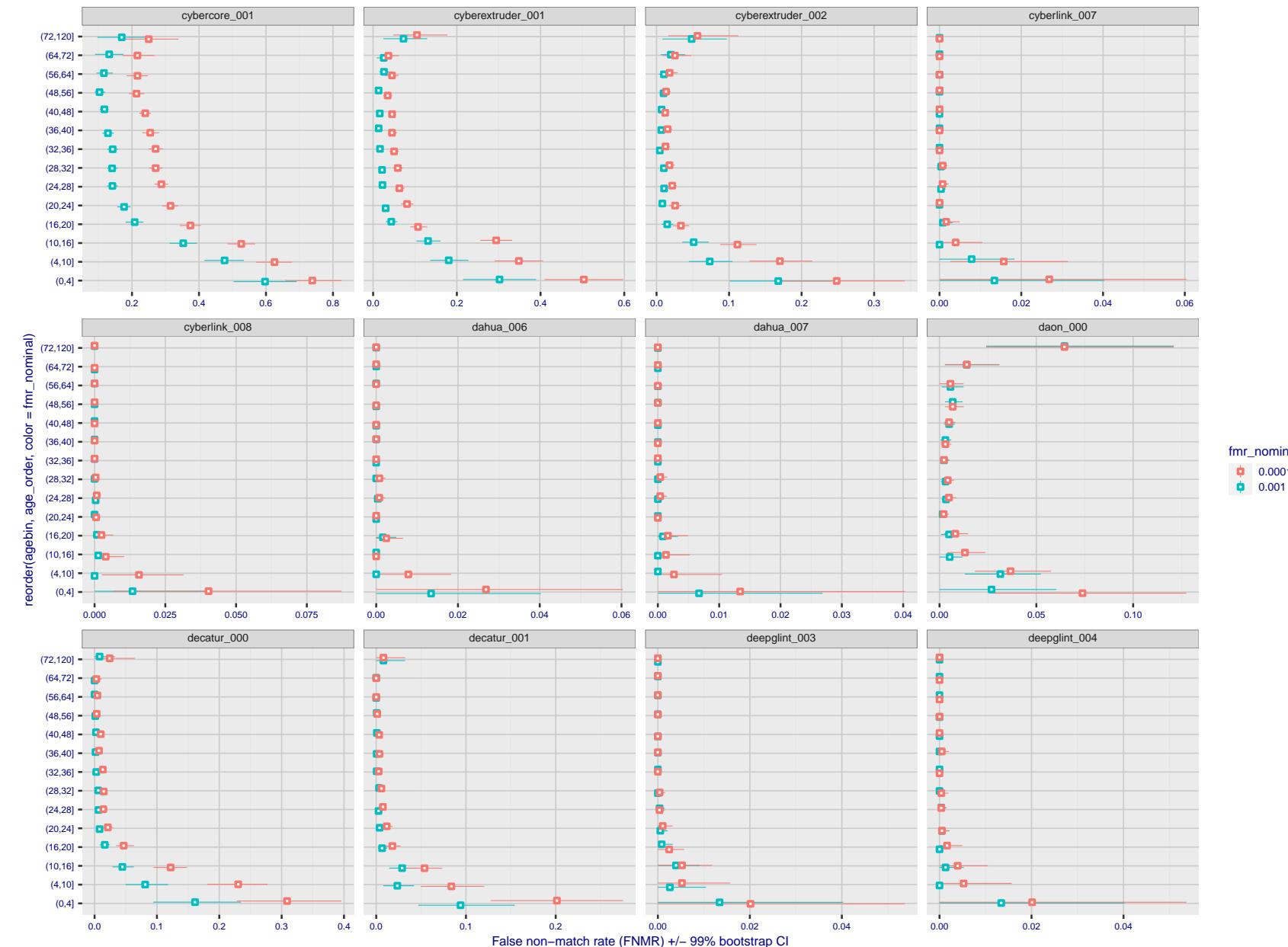


Figure 303: For the visa images, the dots show FNMR by age group for two operating thresholds corresponding to $FMR = \{0.001, 0.0001\}$ computed over all on the order of 10^{10} impostor scores. The FMR in each bin will vary also - see subsequent impostor heatmaps in sec. 3.6.2. Given a pair of face images taken at different times, we assign the comparison to the bin that is the arithmetic average of the subject's ages. This plot shows only the effect of age, not ageing. The number of comparisons in each bin is generally in the thousands, however the first and last bins are computed over 149 and 124 respectively. The error rates in some (adult) cases are zero, and in others the DET is flat so the error rates at the two thresholds are identical. The lines span 1% and 99% of bootstrap replicated FNMR estimates.

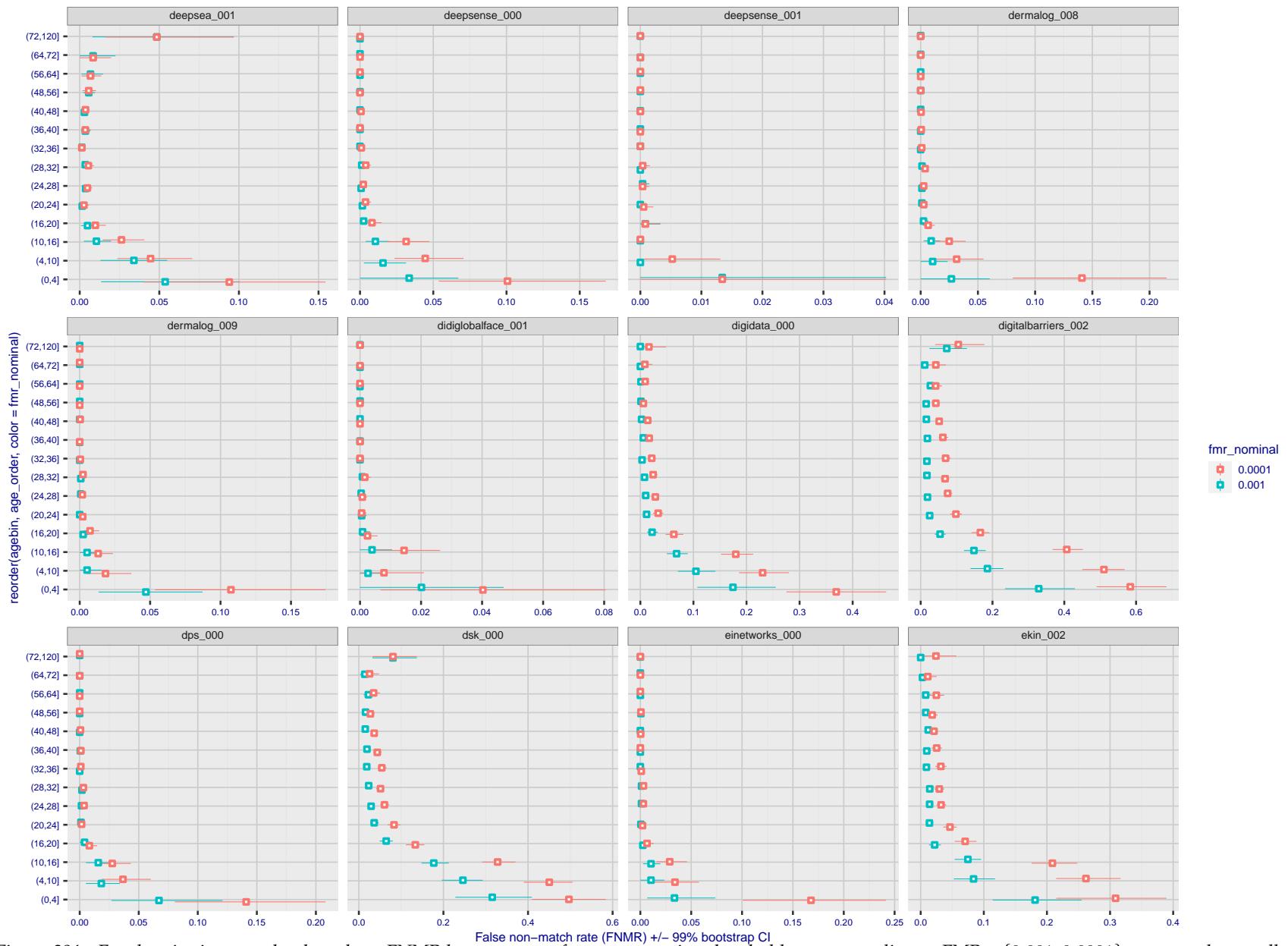


Figure 304: For the visa images, the dots show FNMR by age group for two operating thresholds corresponding to $FMR = \{0.001, 0.0001\}$ computed over all on the order of 10^{10} impostor scores. The FMR in each bin will vary also - see subsequent impostor heatmaps in sec. 3.6.2. Given a pair of face images taken at different times, we assign the comparison to the bin that is the arithmetic average of the subject's ages. This plot shows only the effect of age, not ageing. The number of comparisons in each bin is generally in the thousands, however the first and last bins are computed over 149 and 124 respectively. The error rates in some (adult) cases are zero, and in others the DET is flat so the error rates at the two thresholds are identical. The lines span 1% and 99% of bootstrap replicated FNMR estimates.

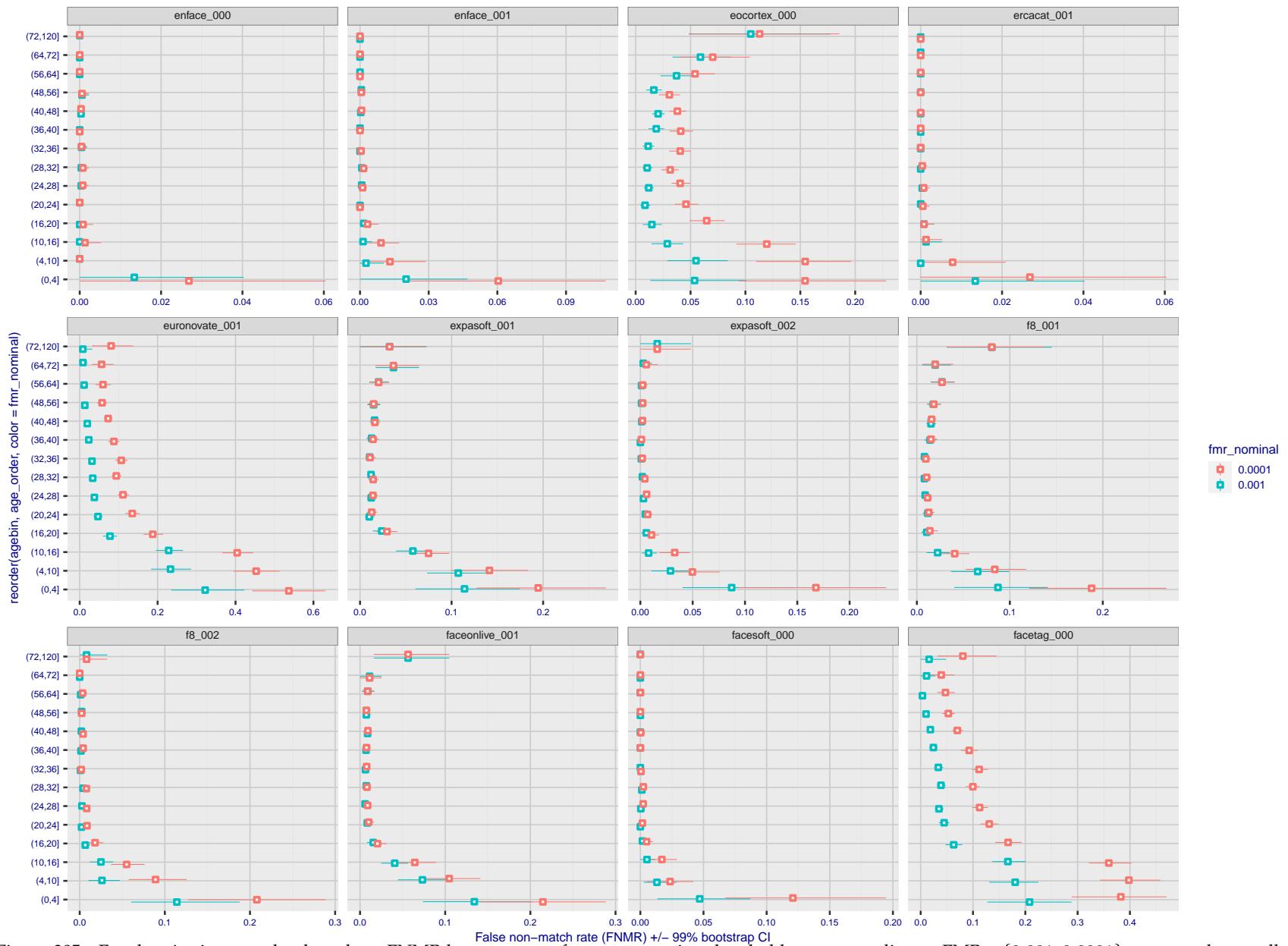


Figure 305: For the visa images, the dots show FNMR by age group for two operating thresholds corresponding to $FMR = \{0.001, 0.0001\}$ computed over all on the order of 10^{10} impostor scores. The FMR in each bin will vary also - see subsequent impostor heatmaps in sec. 3.6.2. Given a pair of face images taken at different times, we assign the comparison to the bin that is the arithmetic average of the subject's ages. This plot shows only the effect of age, not ageing. The number of comparisons in each bin is generally in the thousands, however the first and last bins are computed over 149 and 124 respectively. The error rates in some (adult) cases are zero, and in others the DET is flat so the error rates at the two thresholds are identical. The lines span 1% and 99% of bootstrap replicated FNMR estimates.

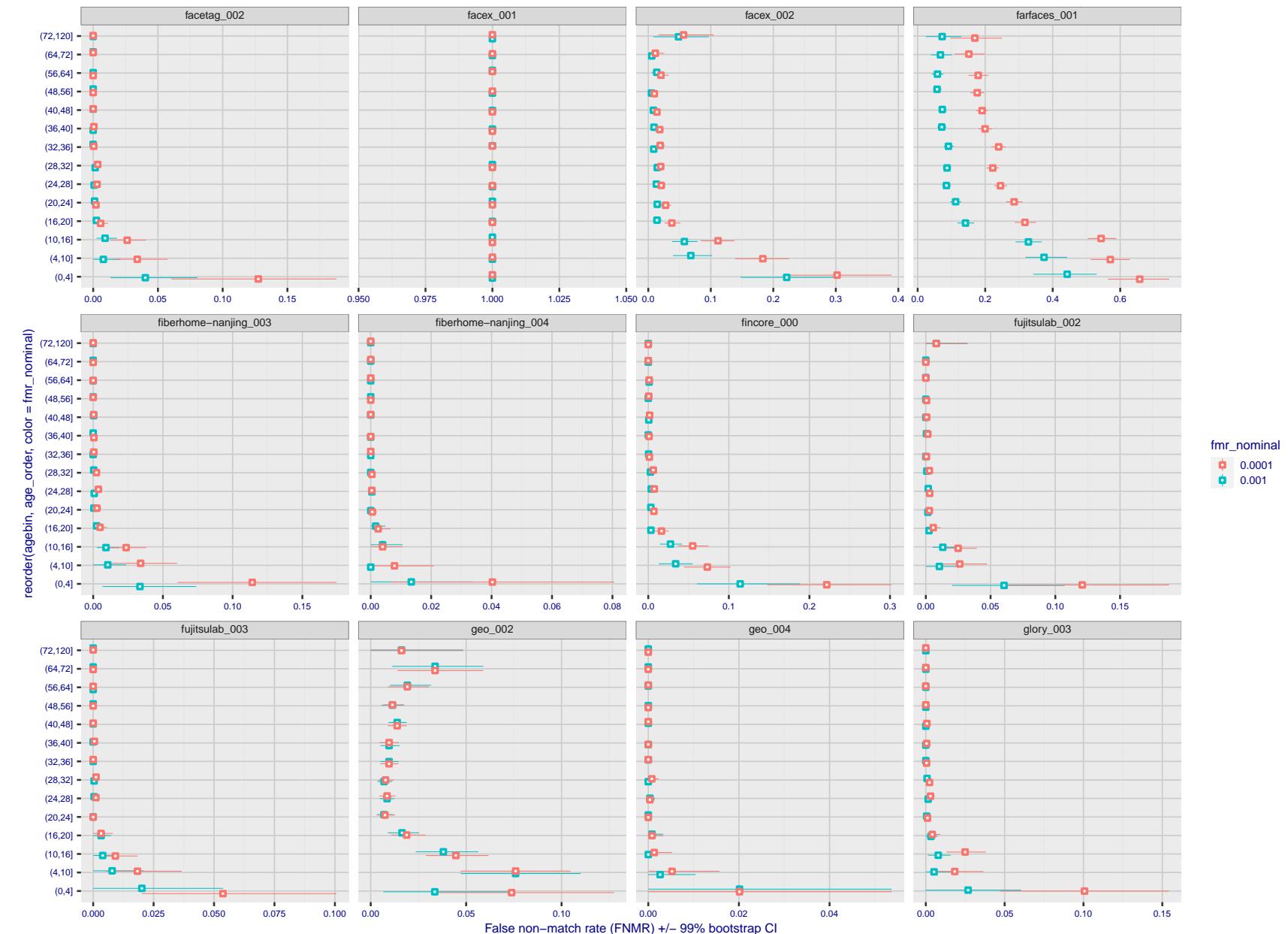


Figure 306: For the visa images, the dots show FNMR by age group for two operating thresholds corresponding to $FMR = \{0.001, 0.0001\}$ computed over all on the order of 10^{10} impostor scores. The FMR in each bin will vary also - see subsequent impostor heatmaps in sec. 3.6.2. Given a pair of face images taken at different times, we assign the comparison to the bin that is the arithmetic average of the subject's ages. This plot shows only the effect of age, not ageing. The number of comparisons in each bin is generally in the thousands, however the first and last bins are computed over 149 and 124 respectively. The error rates in some (adult) cases are zero, and in others the DET is flat so the error rates at the two thresholds are identical. The lines span 1% and 99% of bootstrap replicated FNMR estimates.

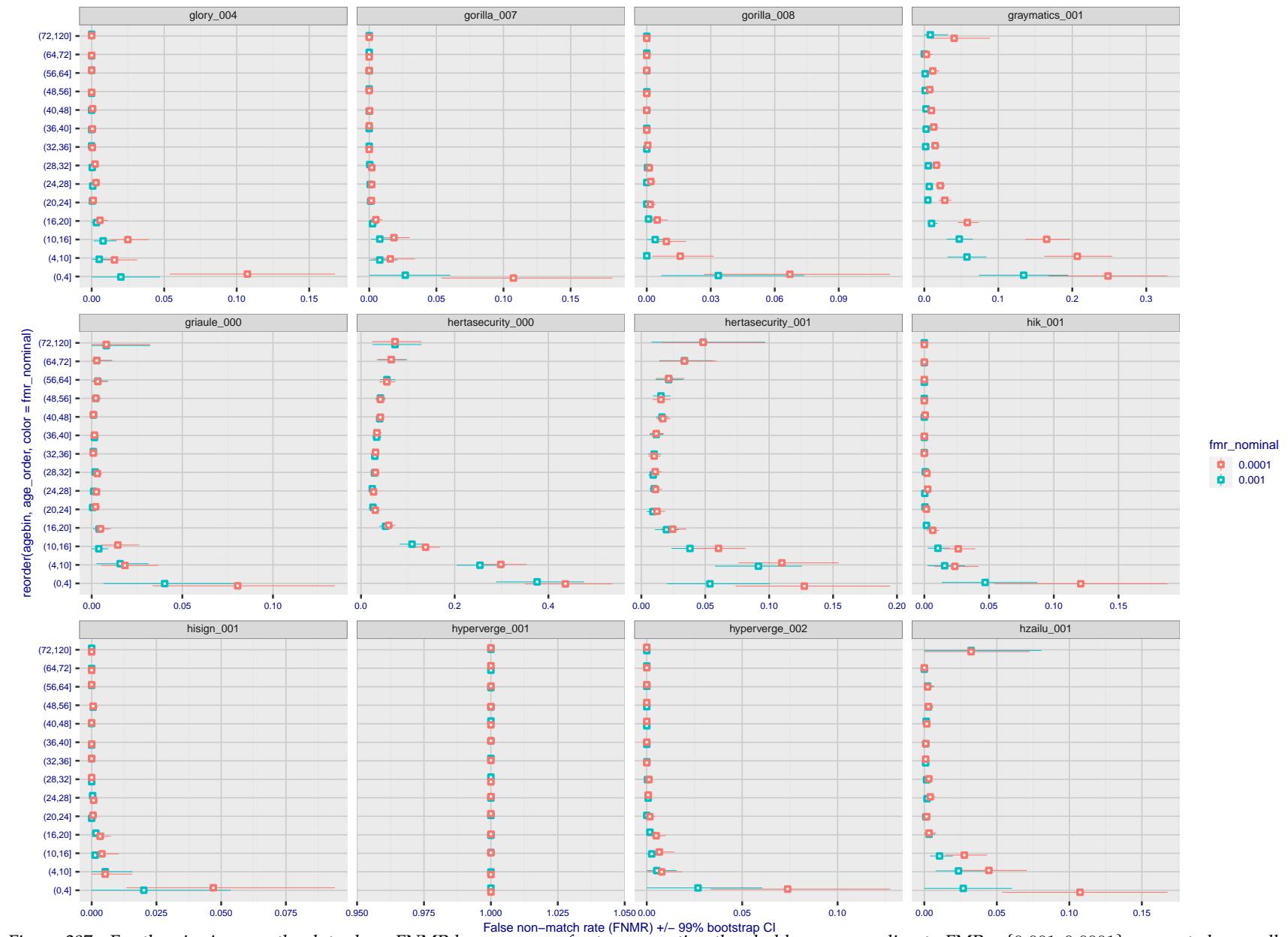


Figure 307: For the visa images, the dots show FNMR by age group for two operating thresholds corresponding to $FMR = \{0.001, 0.0001\}$ computed over all on the order of 10^{10} impostor scores. The FMR in each bin will vary also - see subsequent impostor heatmaps in sec. 3.6.2. Given a pair of face images taken at different times, we assign the comparison to the bin that is the arithmetic average of the subject's ages. This plot shows only the effect of age, not ageing. The number of comparisons in each bin is generally in the thousands, however the first and last bins are computed over 149 and 124 respectively. The error rates in some (adult) cases are zero, and in others the DET is flat so the error rates at the two thresholds are identical. The lines span 1% and 99% of bootstrap replicated FNMR estimates.

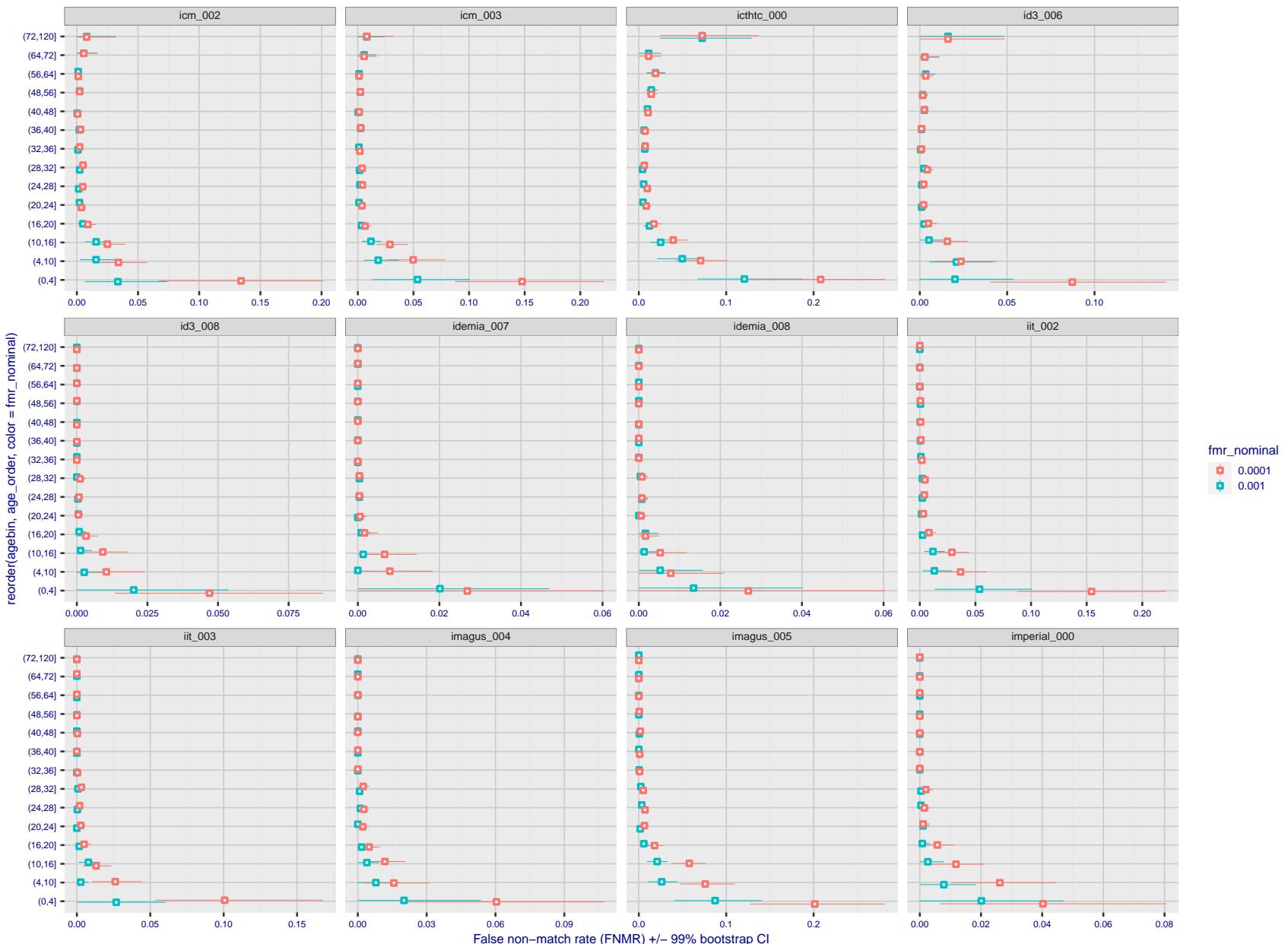


Figure 308: For the visa images, the dots show FNMR by age group for two operating thresholds corresponding to $FMR = \{0.001, 0.0001\}$ computed over all on the order of 10^{10} impostor scores. The FMR in each bin will vary also - see subsequent impostor heatmaps in sec. 3.6.2. Given a pair of face images taken at different times, we assign the comparison to the bin that is the arithmetic average of the subject's ages. This plot shows only the effect of age, not ageing. The number of comparisons in each bin is generally in the thousands, however the first and last bins are computed over 149 and 124 respectively. The error rates in some (adult) cases are zero, and in others the DET is flat so the error rates at the two thresholds are identical. The lines span 1% and 99% of bootstrap replicated FNMR estimates.



Figure 309: For the visa images, the dots show FNMR by age group for two operating thresholds corresponding to $FMR = \{0.001, 0.0001\}$ computed over all on the order of 10^{10} impostor scores. The FMR in each bin will vary also - see subsequent impostor heatmaps in sec. 3.6.2. Given a pair of face images taken at different times, we assign the comparison to the bin that is the arithmetic average of the subject's ages. This plot shows only the effect of age, not ageing. The number of comparisons in each bin is generally in the thousands, however the first and last bins are computed over 149 and 124 respectively. The error rates in some (adult) cases are zero, and in others the DET is flat so the error rates at the two thresholds are identical. The lines span 1% and 99% of bootstrap replicated FNMR estimates.

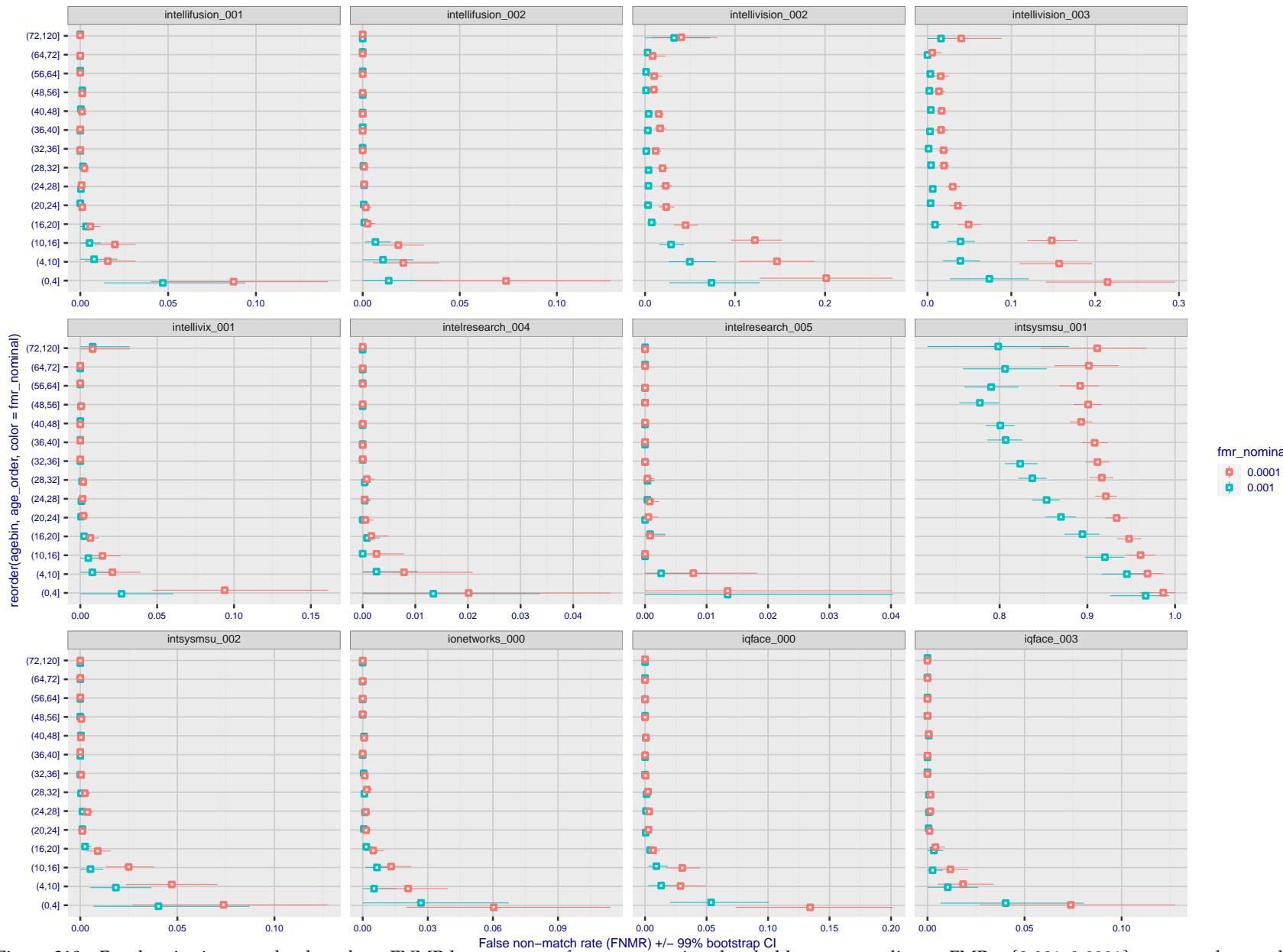


Figure 310: For the visa images, the dots show FNMR by age group for two operating thresholds corresponding to $FMR = \{0.001, 0.0001\}$ computed over all on the order of 10^{10} impostor scores. The FMR in each bin will vary also - see subsequent impostor heatmaps in sec. 3.6.2. Given a pair of face images taken at different times, we assign the comparison to the bin that is the arithmetic average of the subject's ages. This plot shows only the effect of age, not ageing. The number of comparisons in each bin is generally in the thousands, however the first and last bins are computed over 149 and 124 respectively. The error rates in some (adult) cases are zero, and in others the DET is flat so the error rates at the two thresholds are identical. The lines span 1% and 99% of bootstrap replicated FNMR estimates.

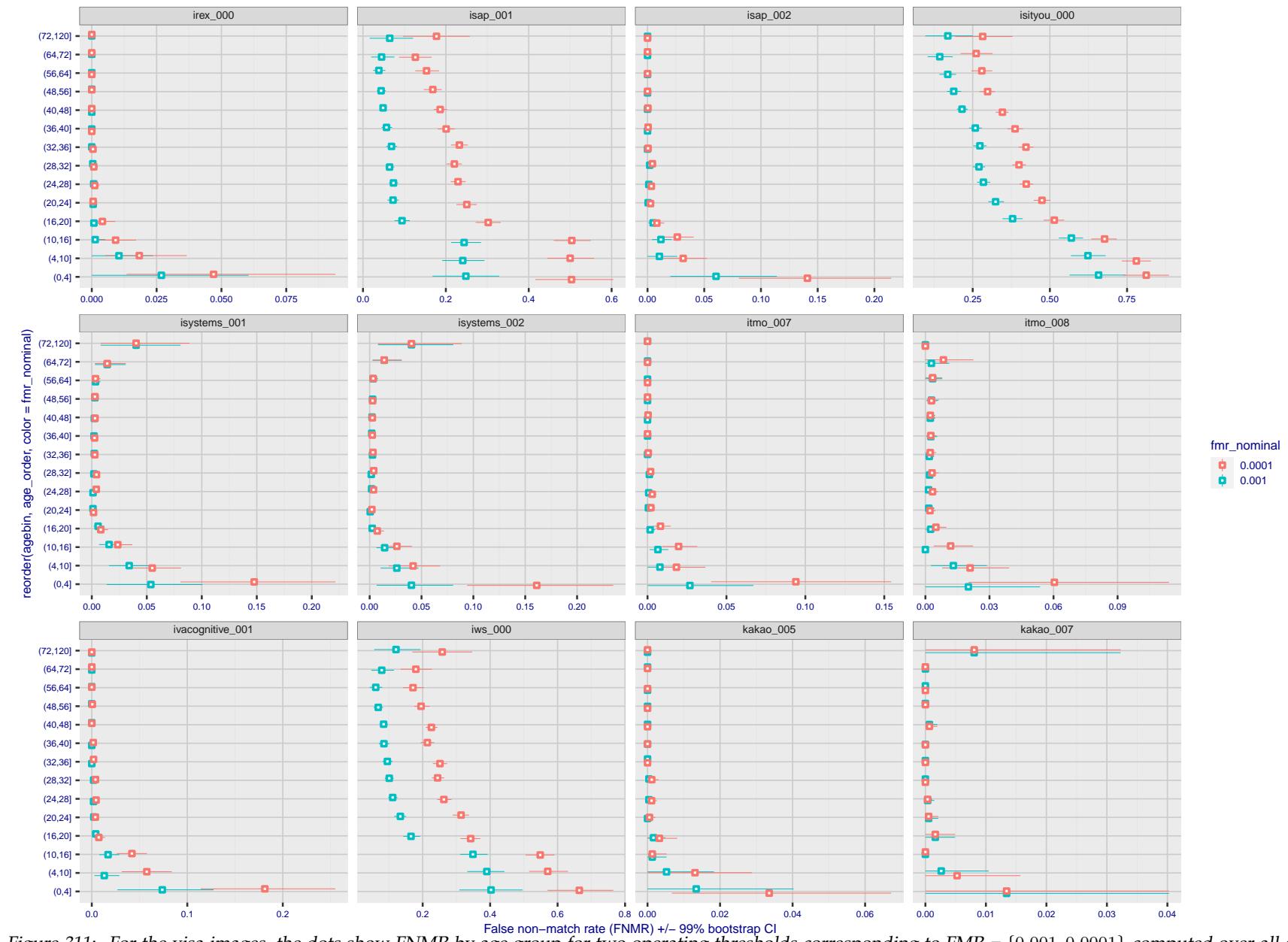


Figure 311: For the visa images, the dots show FNMR by age group for two operating thresholds corresponding to $FMR = \{0.001, 0.0001\}$ computed over all on the order of 10^{10} impostor scores. The FMR in each bin will vary also - see subsequent impostor heatmaps in sec. 3.6.2. Given a pair of face images taken at different times, we assign the comparison to the bin that is the arithmetic average of the subject's ages. This plot shows only the effect of age, not ageing. The number of comparisons in each bin is generally in the thousands, however the first and last bins are computed over 149 and 124 respectively. The error rates in some (adult) cases are zero, and in others the DET is flat so the error rates at the two thresholds are identical. The lines span 1% and 99% of bootstrap replicated FNMR estimates.



Figure 312: For the visa images, the dots show FNMR by age group for two operating thresholds corresponding to $FMR = \{0.001, 0.0001\}$ computed over all on the order of 10^{10} impostor scores. The FMR in each bin will vary also - see subsequent impostor heatmaps in sec. 3.6.2. Given a pair of face images taken at different times, we assign the comparison to the bin that is the arithmetic average of the subject's ages. This plot shows only the effect of age, not ageing. The number of comparisons in each bin is generally in the thousands, however the first and last bins are computed over 149 and 124 respectively. The error rates in some (adult) cases are zero, and in others the DET is flat so the error rates at the two thresholds are identical. The lines span 1% and 99% of bootstrap replicated FNMR estimates.

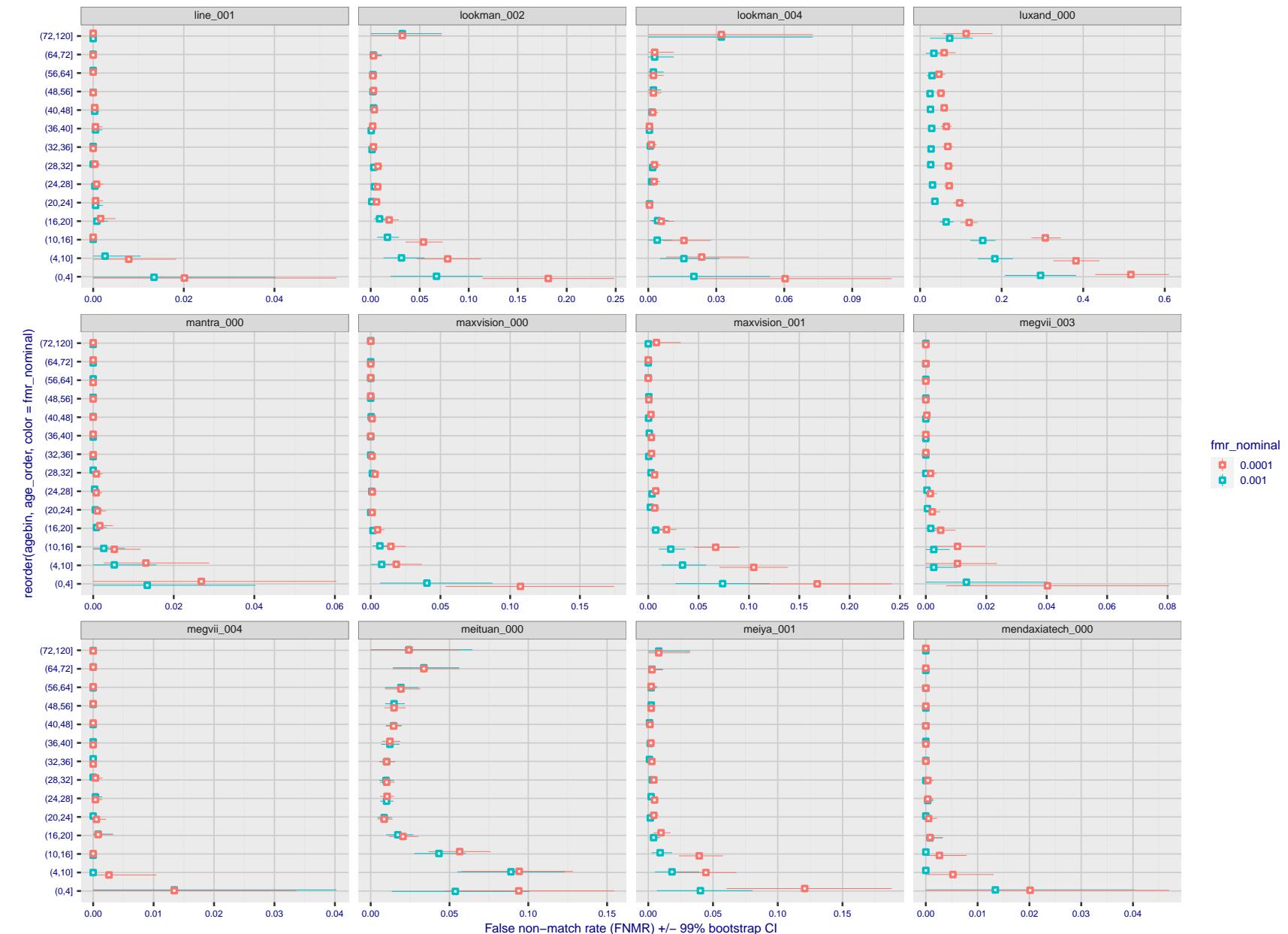


Figure 313: For the visa images, the dots show FNMR by age group for two operating thresholds corresponding to $FMR = \{0.001, 0.0001\}$ computed over all on the order of 10^{10} impostor scores. The FMR in each bin will vary also - see subsequent impostor heatmaps in sec. 3.6.2. Given a pair of face images taken at different times, we assign the comparison to the bin that is the arithmetic average of the subject's ages. This plot shows only the effect of age, not ageing. The number of comparisons in each bin is generally in the thousands, however the first and last bins are computed over 149 and 124 respectively. The error rates in some (adult) cases are zero, and in others the DET is flat so the error rates at the two thresholds are identical. The lines span 1% and 99% of bootstrap replicated FNMR estimates.

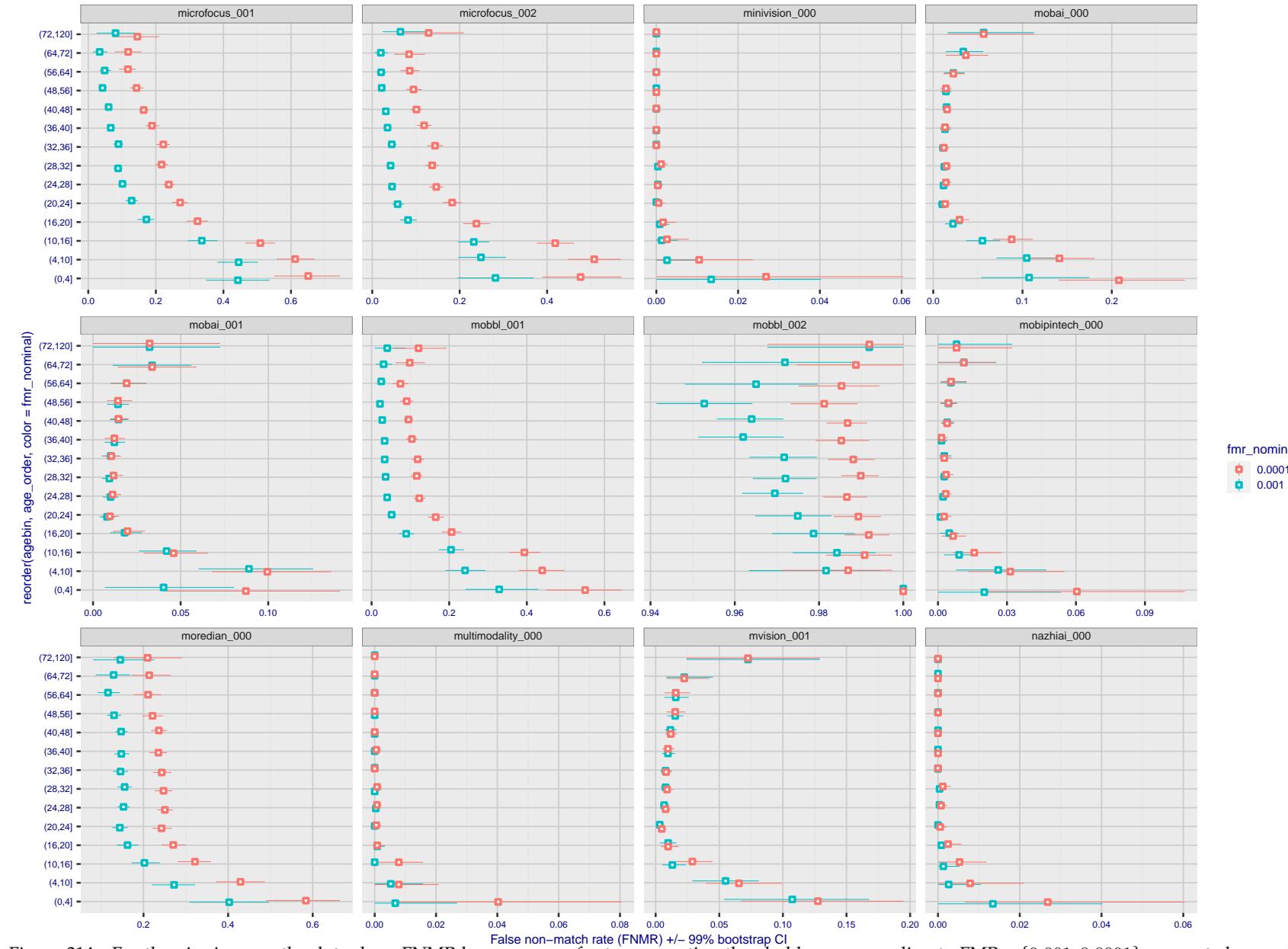


Figure 314: For the visa images, the dots show FNMR by age group for two operating thresholds corresponding to $FMR = \{0.001, 0.0001\}$ computed over all on the order of 10^{10} impostor scores. The FMR in each bin will vary also - see subsequent impostor heatmaps in sec. 3.6.2. Given a pair of face images taken at different times, we assign the comparison to the bin that is the arithmetic average of the subject's ages. This plot shows only the effect of age, not ageing. The number of comparisons in each bin is generally in the thousands, however the first and last bins are computed over 149 and 124 respectively. The error rates in some (adult) cases are zero, and in others the DET is flat so the error rates at the two thresholds are identical. The lines span 1% and 99% of bootstrap replicated FNMR estimates.

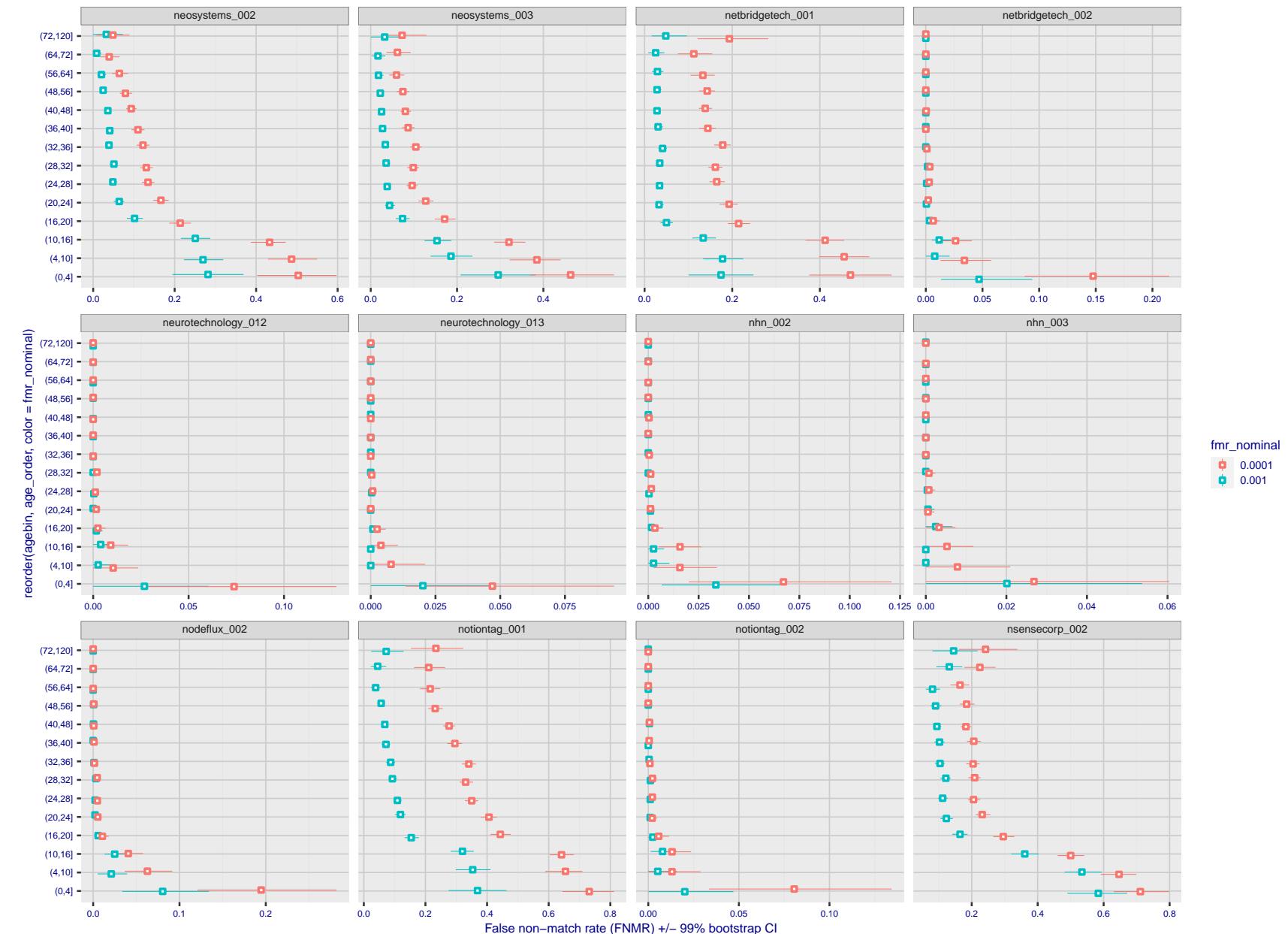


Figure 315: For the visa images, the dots show FNMR by age group for two operating thresholds corresponding to $\text{FMR} = \{0.001, 0.0001\}$ computed over all on the order of 10^{10} impostor scores. The FMR in each bin will vary also - see subsequent impostor heatmaps in sec. 3.6.2. Given a pair of face images taken at different times, we assign the comparison to the bin that is the arithmetic average of the subject's ages. This plot shows only the effect of age, not ageing. The number of comparisons in each bin is generally in the thousands, however the first and last bins are computed over 149 and 124 respectively. The error rates in some (adult) cases are zero, and in others the DET is flat so the error rates at the two thresholds are identical. The lines span 1% and 99% of bootstrap replicated FNMR estimates.

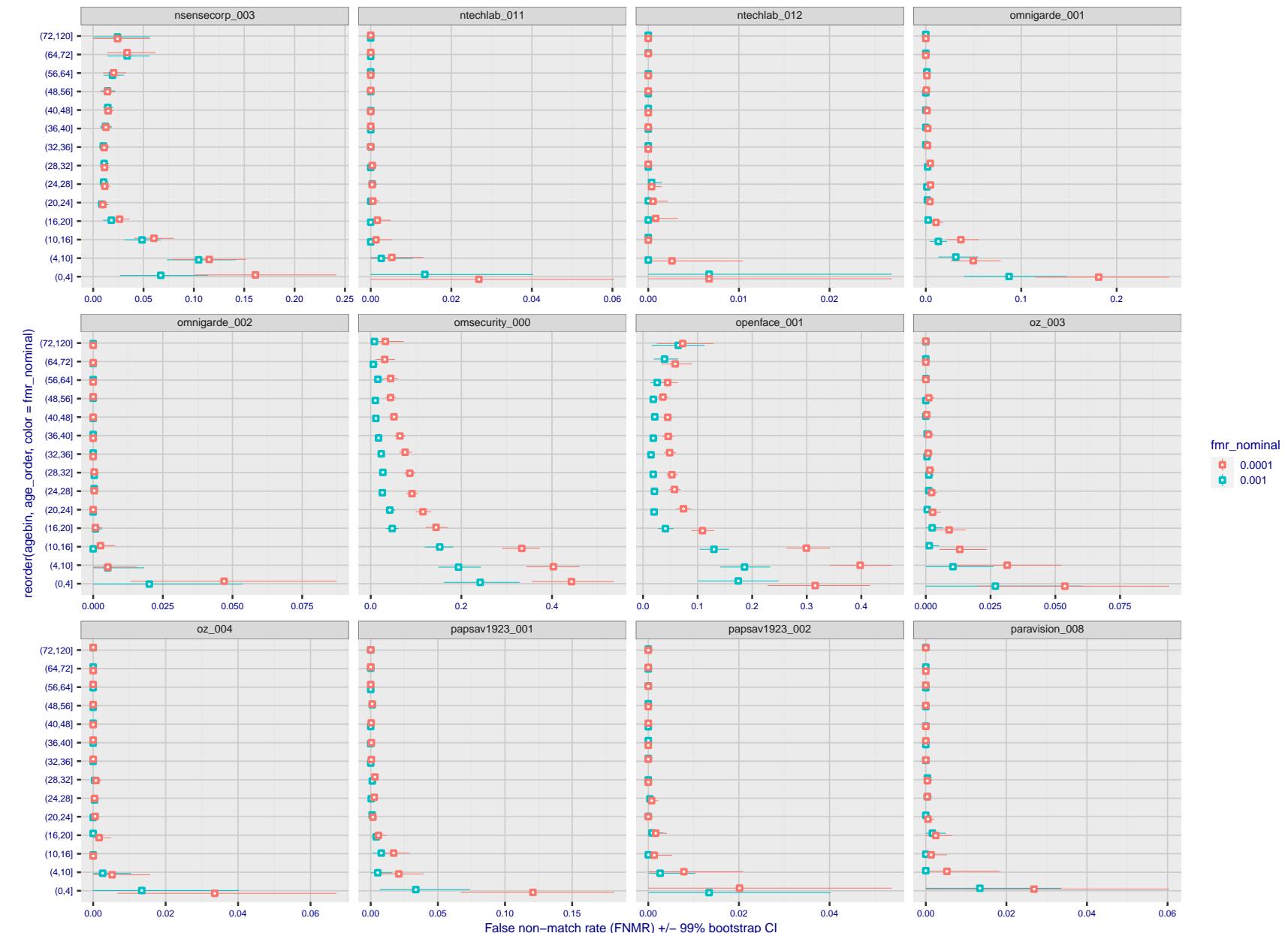


Figure 316: For the visa images, the dots show FNMR by age group for two operating thresholds corresponding to $FMR = \{0.001, 0.0001\}$ computed over all on the order of 10^{10} impostor scores. The FMR in each bin will vary also - see subsequent impostor heatmaps in sec. 3.6.2. Given a pair of face images taken at different times, we assign the comparison to the bin that is the arithmetic average of the subject's ages. This plot shows only the effect of age, not ageing. The number of comparisons in each bin is generally in the thousands, however the first and last bins are computed over 149 and 124 respectively. The error rates in some (adult) cases are zero, and in others the DET is flat so the error rates at the two thresholds are identical. The lines span 1% and 99% of bootstrap replicated FNMR estimates.

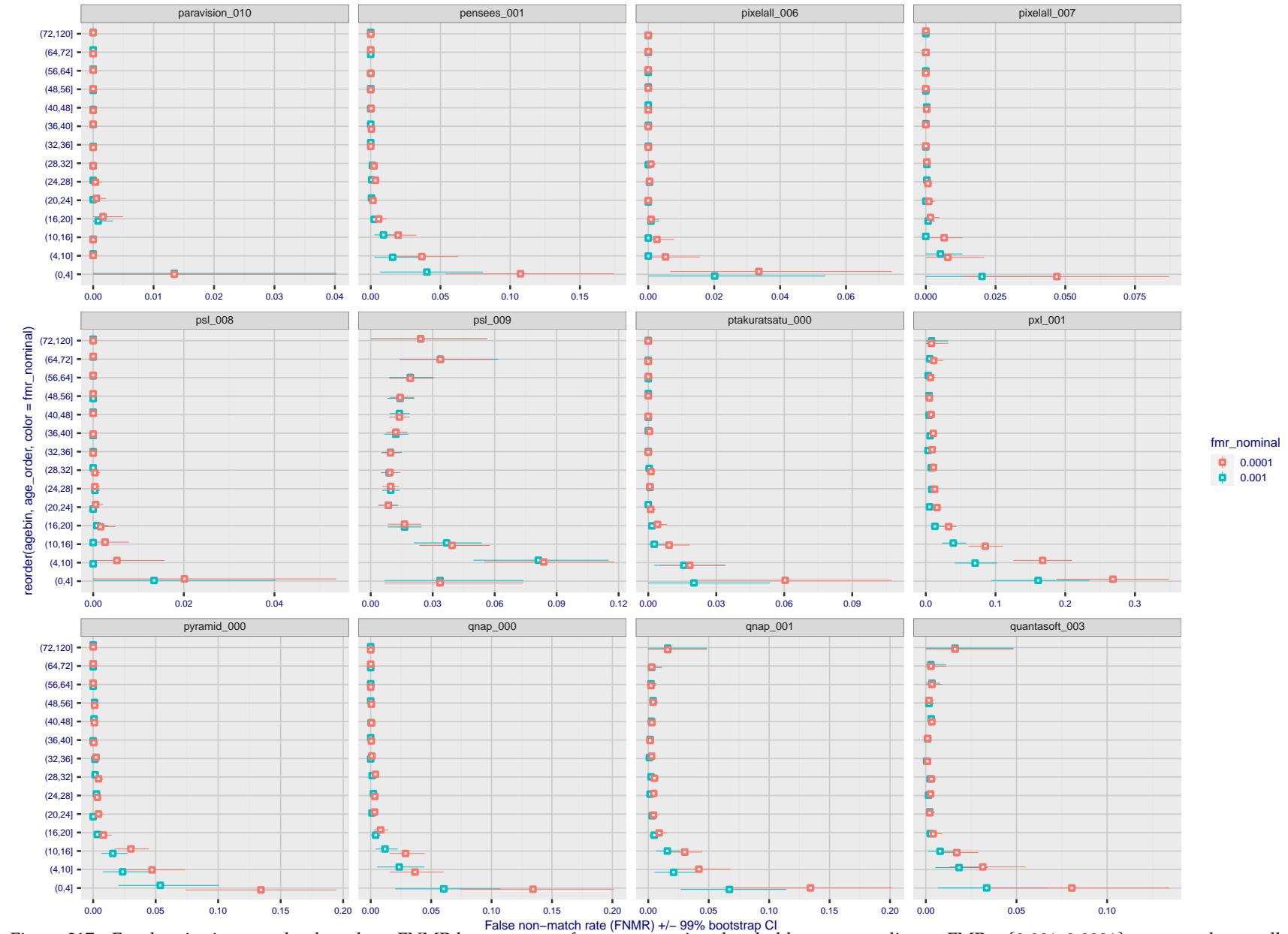


Figure 317: For the visa images, the dots show FNMR by age group for two operating thresholds corresponding to $FMR = \{0.001, 0.0001\}$ computed over all on the order of 10^{10} impostor scores. The FMR in each bin will vary also - see subsequent impostor heatmaps in sec. 3.6.2. Given a pair of face images taken at different times, we assign the comparison to the bin that is the arithmetic average of the subject's ages. This plot shows only the effect of age, not ageing. The number of comparisons in each bin is generally in the thousands, however the first and last bins are computed over 149 and 124 respectively. The error rates in some (adult) cases are zero, and in others the DET is flat so the error rates at the two thresholds are identical. The lines span 1% and 99% of bootstrap replicated FNMR estimates.

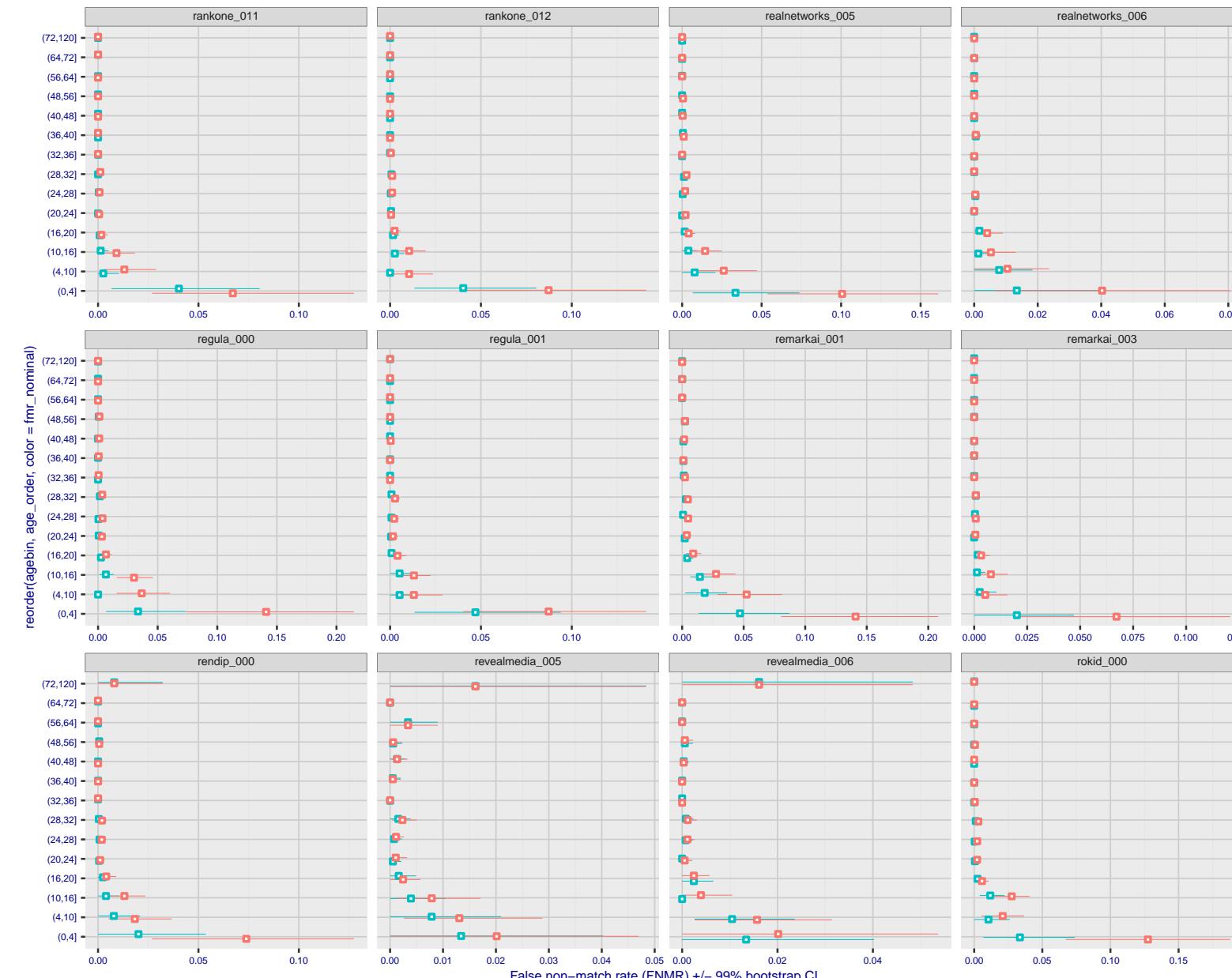


Figure 318: For the visa images, the dots show FNMR by age group for two operating thresholds corresponding to $FMR = \{0.001, 0.0001\}$ computed over all on the order of 10^{10} impostor scores. The FMR in each bin will vary also - see subsequent impostor heatmaps in sec. 3.6.2. Given a pair of face images taken at different times, we assign the comparison to the bin that is the arithmetic average of the subject's ages. This plot shows only the effect of age, not ageing. The number of comparisons in each bin is generally in the thousands, however the first and last bins are computed over 149 and 124 respectively. The error rates in some (adult) cases are zero, and in others the DET is flat so the error rates at the two thresholds are identical. The lines span 1% and 99% of bootstrap replicated FNMR estimates.

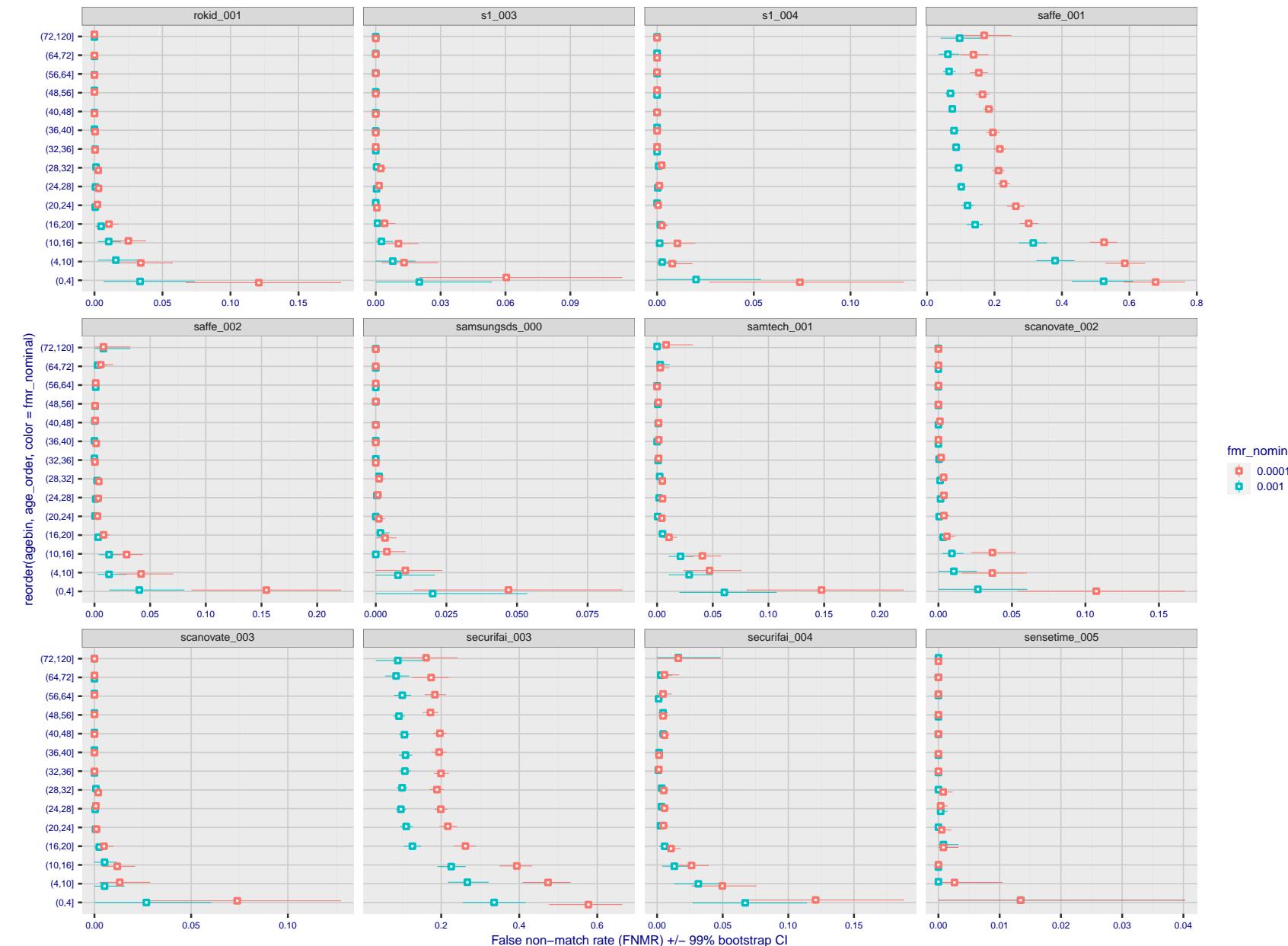


Figure 319: For the visa images, the dots show FNMR by age group for two operating thresholds corresponding to $FMR = \{0.001, 0.0001\}$ computed over all on the order of 10^{10} impostor scores. The FMR in each bin will vary also - see subsequent impostor heatmaps in sec. 3.6.2. Given a pair of face images taken at different times, we assign the comparison to the bin that is the arithmetic average of the subject's ages. This plot shows only the effect of age, not ageing. The number of comparisons in each bin is generally in the thousands, however the first and last bins are computed over 149 and 124 respectively. The error rates in some (adult) cases are zero, and in others the DET is flat so the error rates at the two thresholds are identical. The lines span 1% and 99% of bootstrap replicated FNMR estimates.

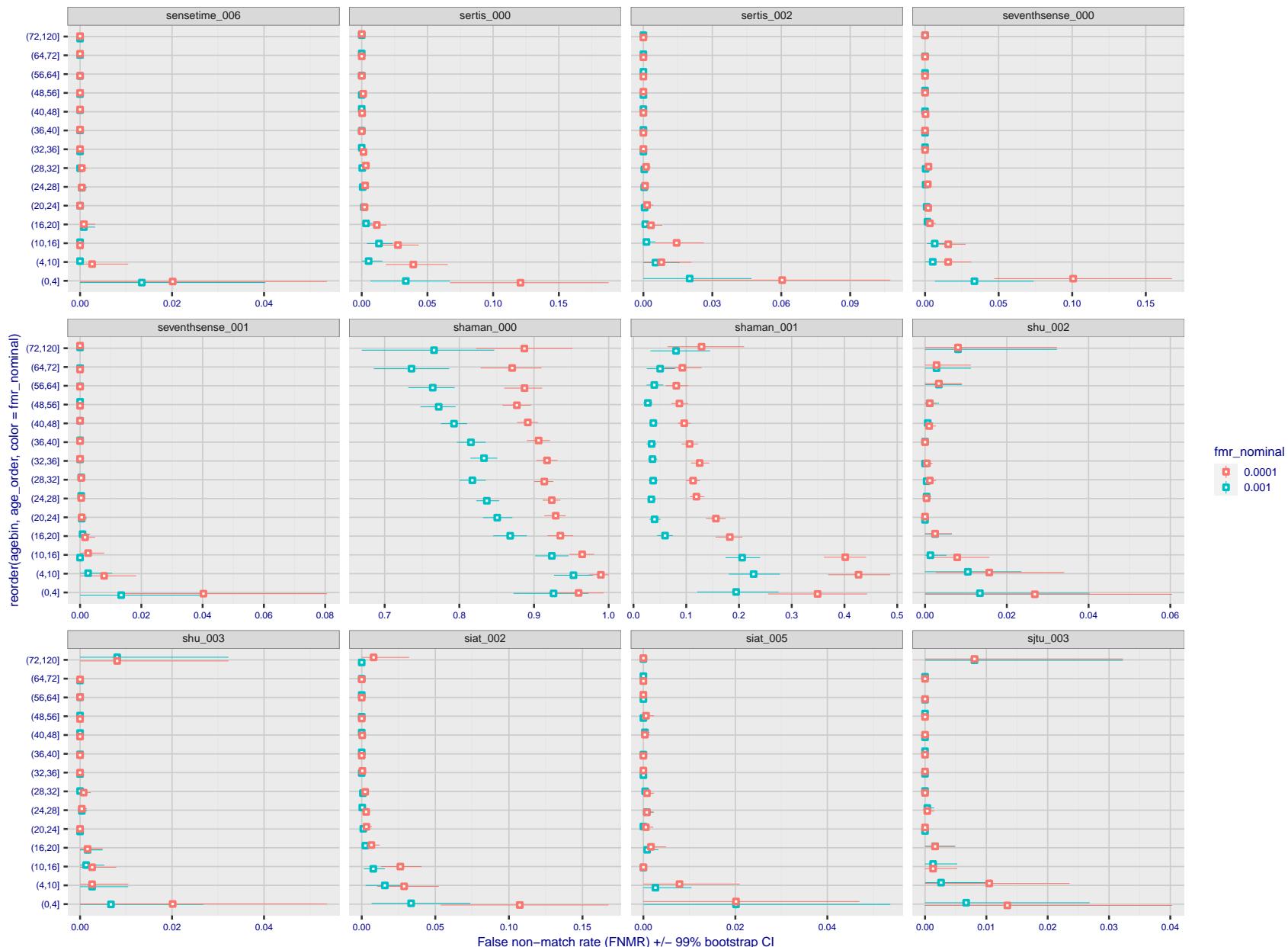


Figure 320: For the visa images, the dots show FNMR by age group for two operating thresholds corresponding to $FMR = \{0.001, 0.0001\}$ computed over all on the order of 10^{10} impostor scores. The FMR in each bin will vary also - see subsequent impostor heatmaps in sec. 3.6.2. Given a pair of face images taken at different times, we assign the comparison to the bin that is the arithmetic average of the subject's ages. This plot shows only the effect of age, not ageing. The number of comparisons in each bin is generally in the thousands, however the first and last bins are computed over 149 and 124 respectively. The error rates in some (adult) cases are zero, and in others the DET is flat so the error rates at the two thresholds are identical. The lines span 1% and 99% of bootstrap replicated FNMR estimates.

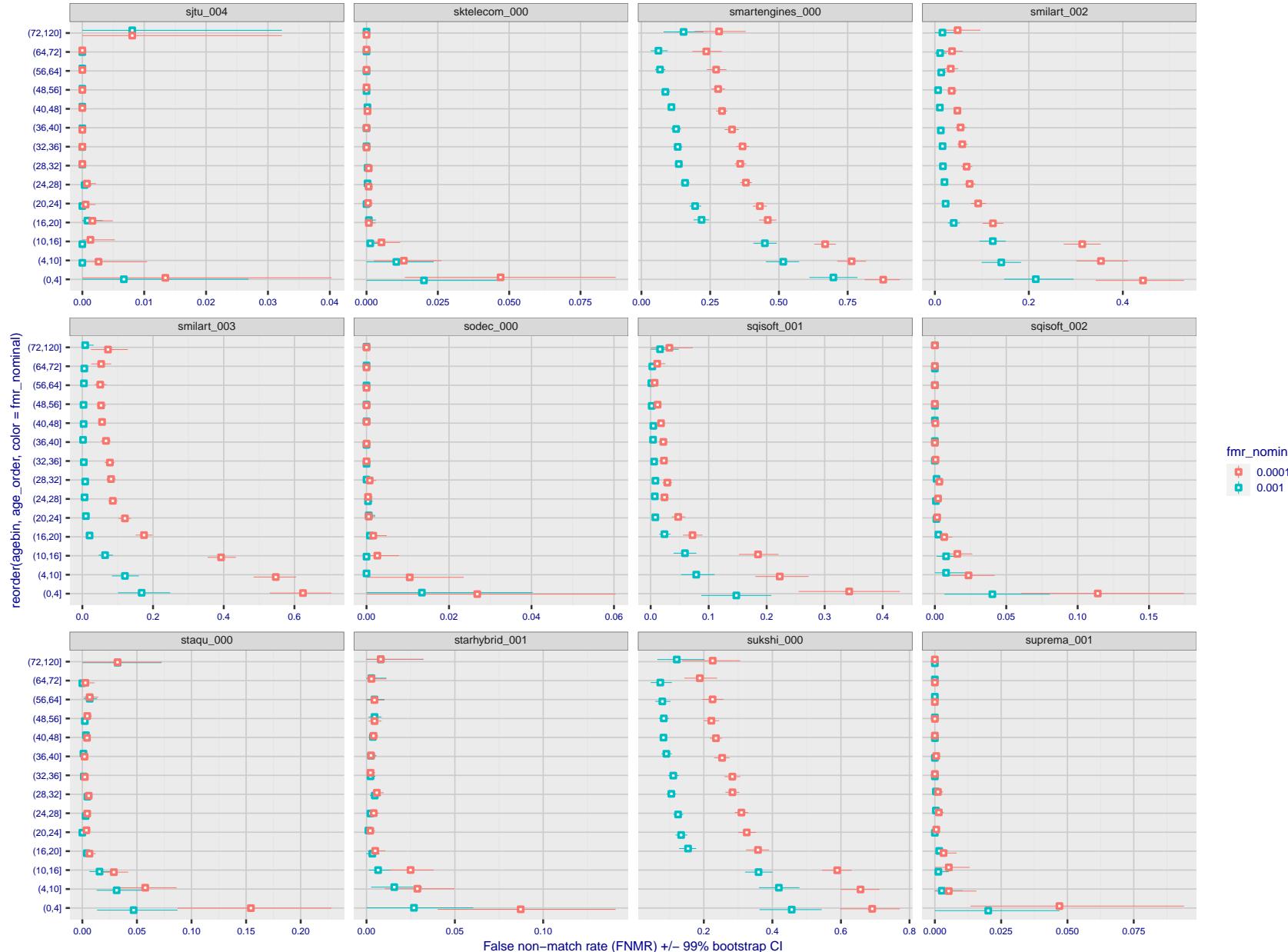


Figure 321: For the visa images, the dots show FNMR by age group for two operating thresholds corresponding to $FMR = \{0.001, 0.0001\}$ computed over all on the order of 10^{10} impostor scores. The FMR in each bin will vary also - see subsequent impostor heatmaps in sec. 3.6.2. Given a pair of face images taken at different times, we assign the comparison to the bin that is the arithmetic average of the subject's ages. This plot shows only the effect of age, not ageing. The number of comparisons in each bin is generally in the thousands, however the first and last bins are computed over 149 and 124 respectively. The error rates in some (adult) cases are zero, and in others the DET is flat so the error rates at the two thresholds are identical. The lines span 1% and 99% of bootstrap replicated FNMR estimates.

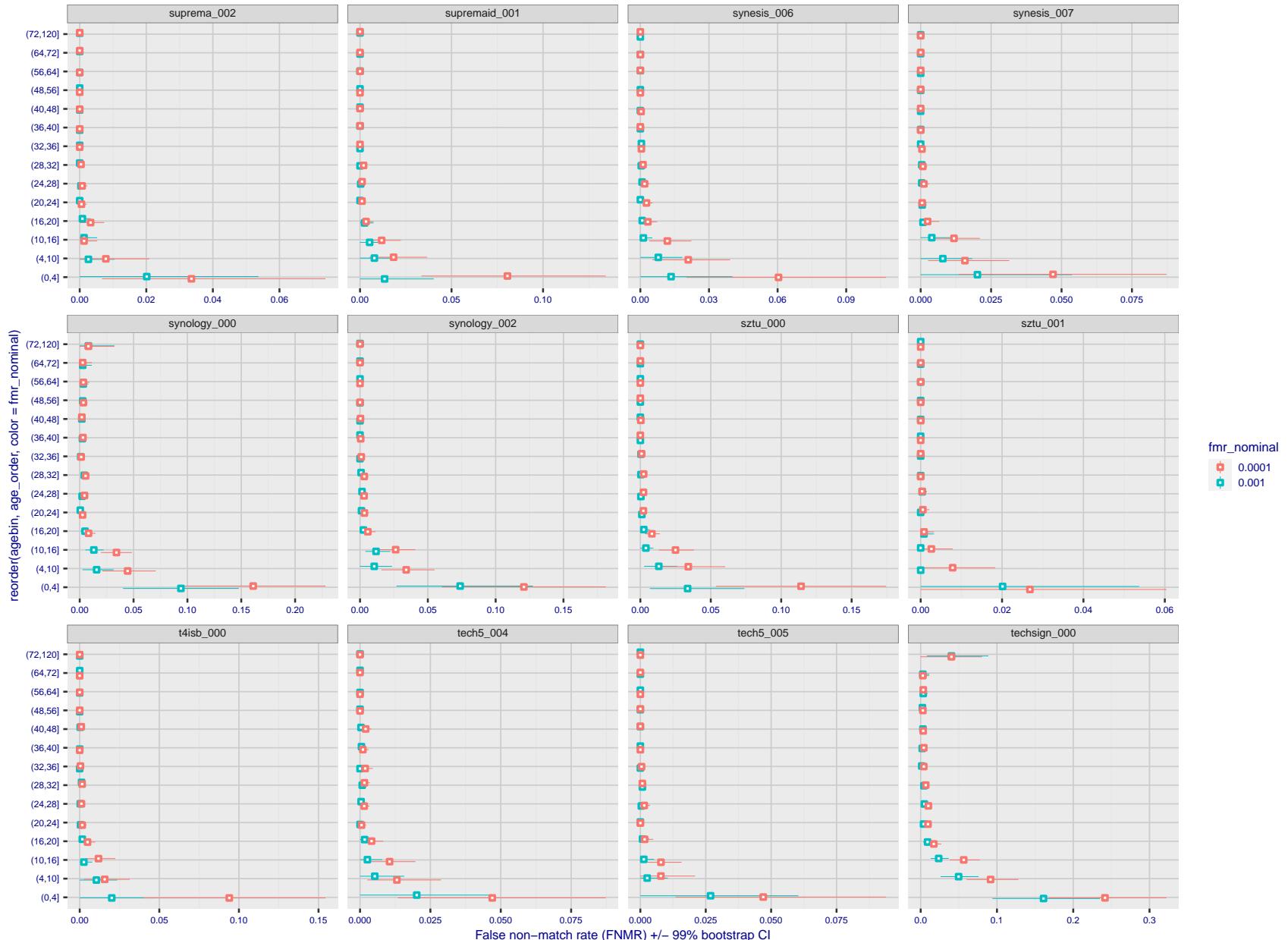


Figure 322: For the visa images, the dots show FNMR by age group for two operating thresholds corresponding to $FMR = \{0.001, 0.0001\}$ computed over all on the order of 10^{10} impostor scores. The FMR in each bin will vary also - see subsequent impostor heatmaps in sec. 3.6.2. Given a pair of face images taken at different times, we assign the comparison to the bin that is the arithmetic average of the subject's ages. This plot shows only the effect of age, not ageing. The number of comparisons in each bin is generally in the thousands, however the first and last bins are computed over 149 and 124 respectively. The error rates in some (adult) cases are zero, and in others the DET is flat so the error rates at the two thresholds are identical. The lines span 1% and 99% of bootstrap replicated FNMR estimates.



Figure 323: For the visa images, the dots show FNMR by age group for two operating thresholds corresponding to $FMR = \{0.001, 0.0001\}$ computed over all on the order of 10^{10} impostor scores. The FMR in each bin will vary also - see subsequent impostor heatmaps in sec. 3.6.2. Given a pair of face images taken at different times, we assign the comparison to the bin that is the arithmetic average of the subject's ages. This plot shows only the effect of age, not ageing. The number of comparisons in each bin is generally in the thousands, however the first and last bins are computed over 149 and 124 respectively. The error rates in some (adult) cases are zero, and in others the DET is flat so the error rates at the two thresholds are identical. The lines span 1% and 99% of bootstrap replicated FNMR estimates.



Figure 324: For the visa images, the dots show FNMR by age group for two operating thresholds corresponding to $FMR = \{0.001, 0.0001\}$ computed over all on the order of 10^{10} impostor scores. The FMR in each bin will vary also - see subsequent impostor heatmaps in sec. 3.6.2. Given a pair of face images taken at different times, we assign the comparison to the bin that is the arithmetic average of the subject's ages. This plot shows only the effect of age, not ageing. The number of comparisons in each bin is generally in the thousands, however the first and last bins are computed over 149 and 124 respectively. The error rates in some (adult) cases are zero, and in others the DET is flat so the error rates at the two thresholds are identical. The lines span 1% and 99% of bootstrap replicated FNMR estimates.

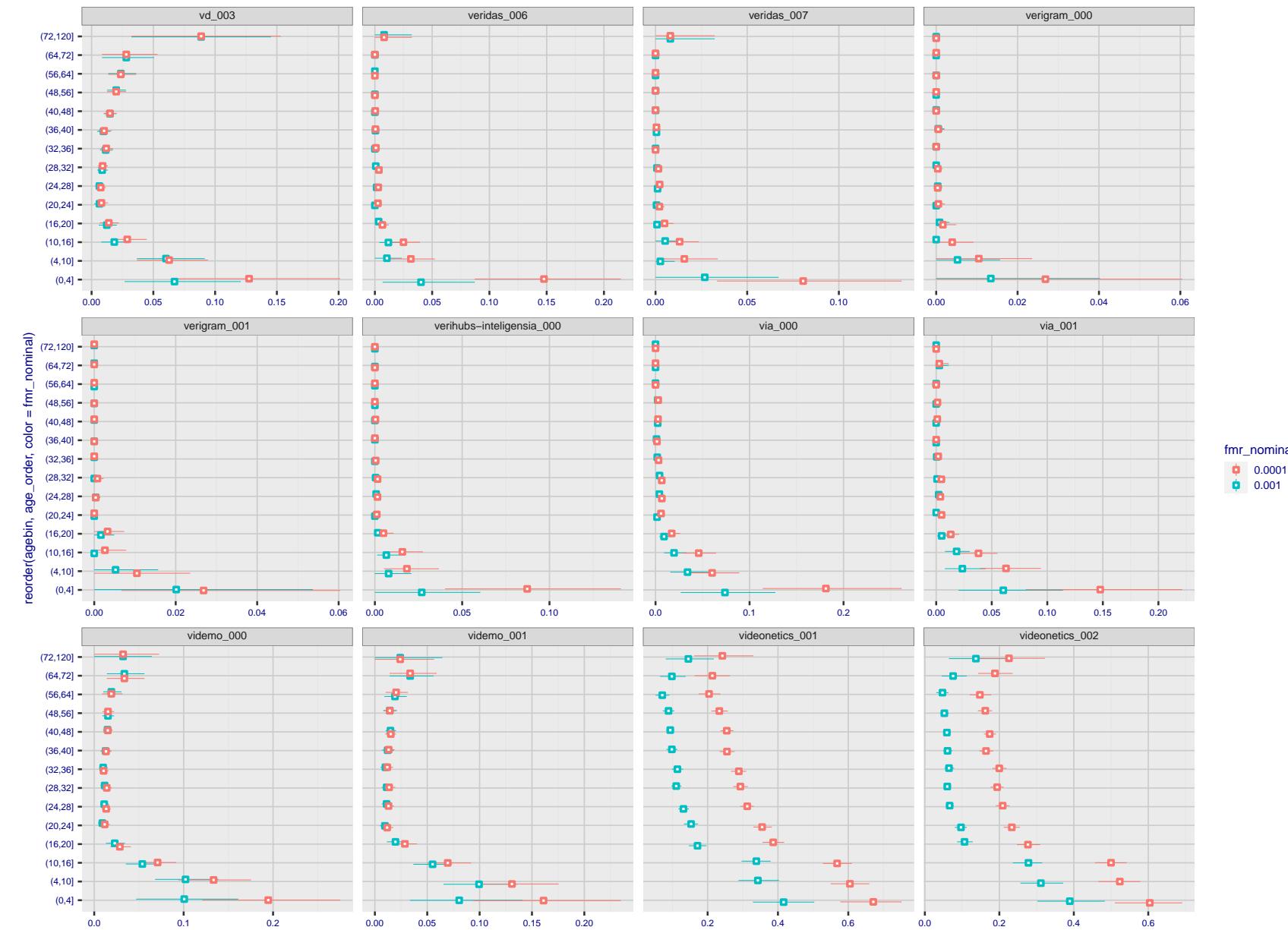


Figure 325: For the visa images, the dots show FNMR by age group for two operating thresholds corresponding to $FMR = \{0.001, 0.0001\}$ computed over all on the order of 10^{10} impostor scores. The FMR in each bin will vary also - see subsequent impostor heatmaps in sec. 3.6.2. Given a pair of face images taken at different times, we assign the comparison to the bin that is the arithmetic average of the subject's ages. This plot shows only the effect of age, not ageing. The number of comparisons in each bin is generally in the thousands, however the first and last bins are computed over 149 and 124 respectively. The error rates in some (adult) cases are zero, and in others the DET is flat so the error rates at the two thresholds are identical. The lines span 1% and 99% of bootstrap replicated FNMR estimates.

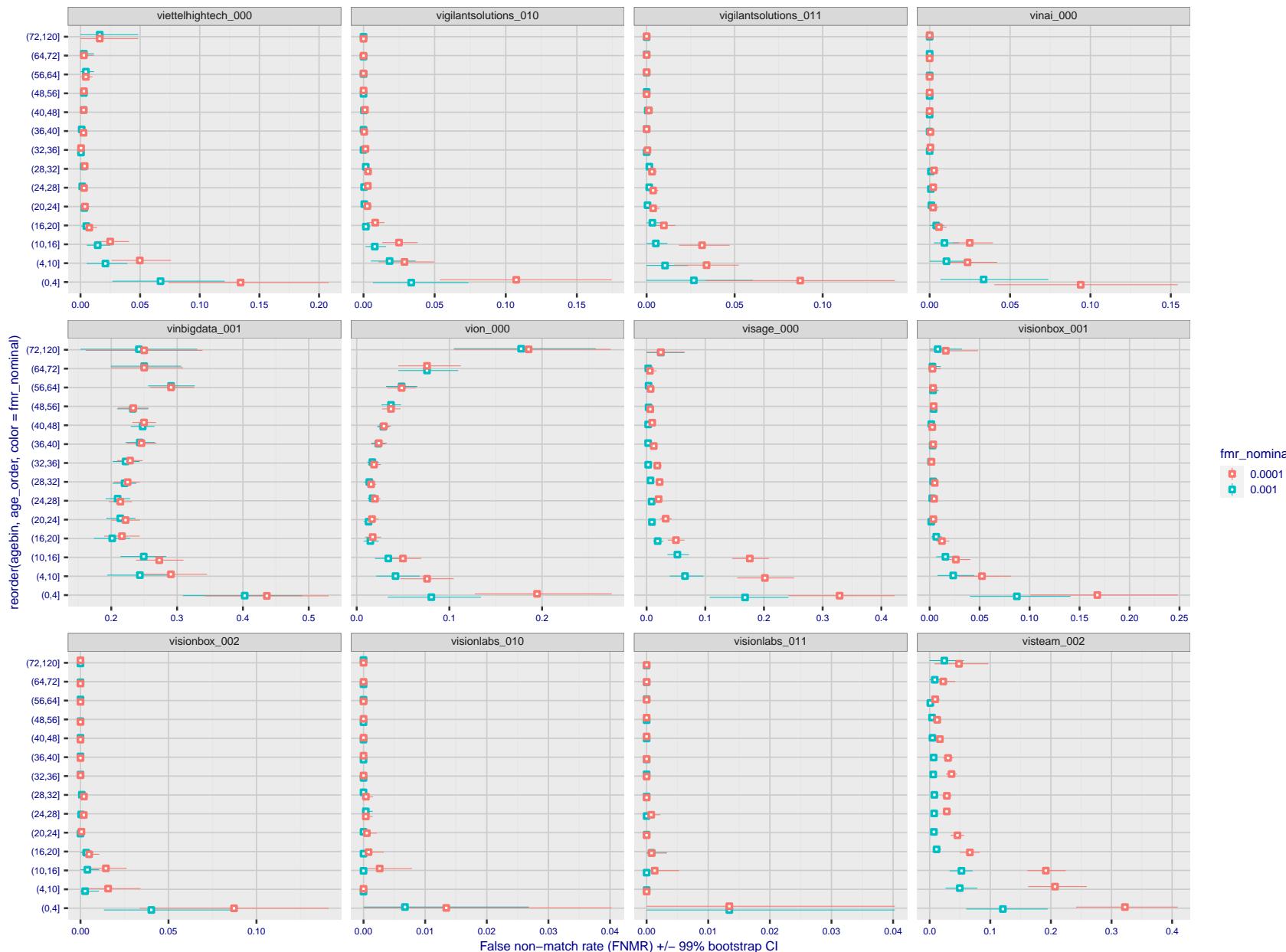


Figure 326: For the visa images, the dots show FNMR by age group for two operating thresholds corresponding to $FMR = \{0.001, 0.0001\}$ computed over all on the order of 10^{10} impostor scores. The FMR in each bin will vary also - see subsequent impostor heatmaps in sec. 3.6.2. Given a pair of face images taken at different times, we assign the comparison to the bin that is the arithmetic average of the subject's ages. This plot shows only the effect of age, not ageing. The number of comparisons in each bin is generally in the thousands, however the first and last bins are computed over 149 and 124 respectively. The error rates in some (adult) cases are zero, and in others the DET is flat so the error rates at the two thresholds are identical. The lines span 1% and 99% of bootstrap replicated FNMR estimates.

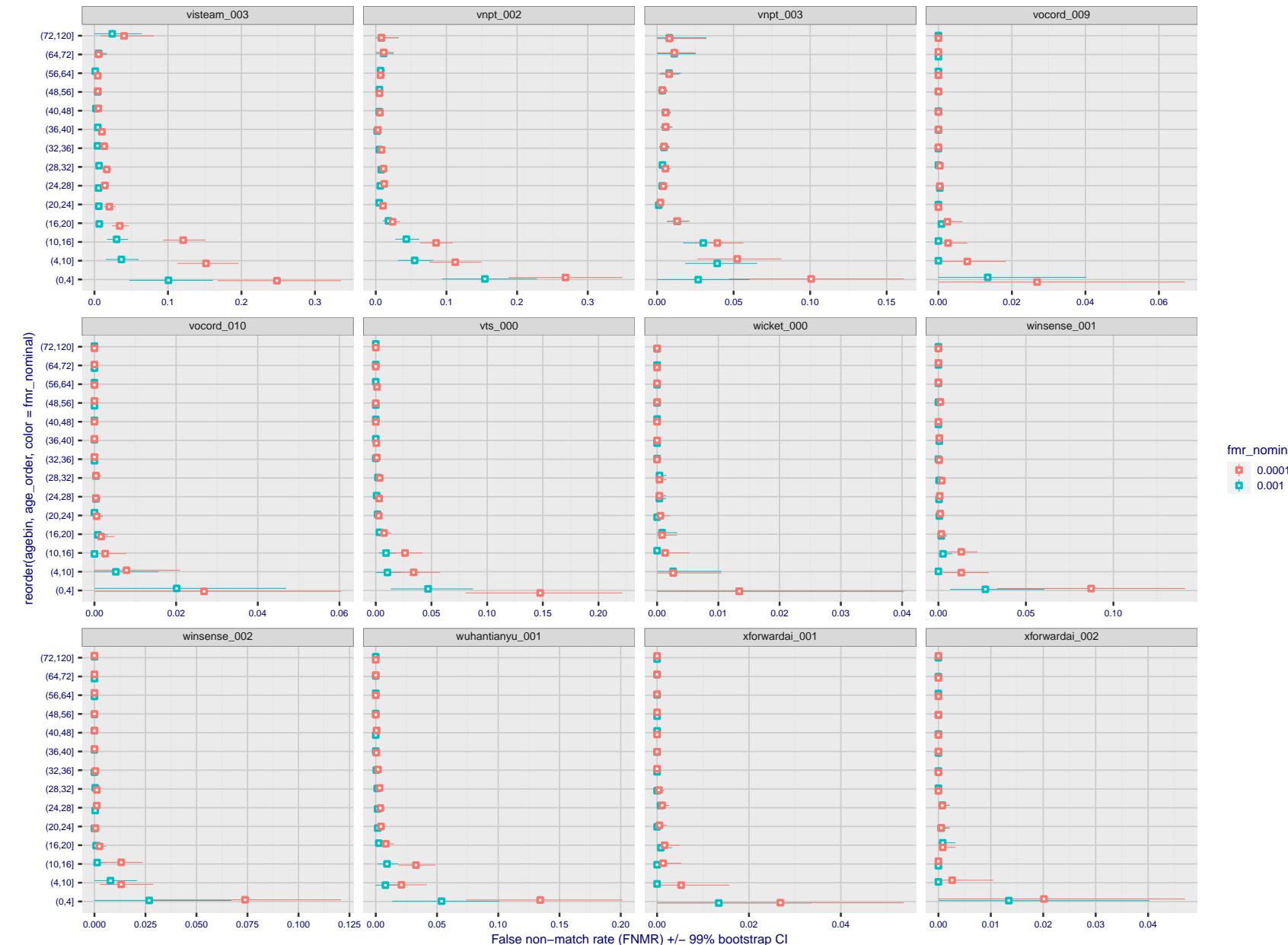


Figure 327: For the visa images, the dots show FNMR by age group for two operating thresholds corresponding to $FMR = \{0.001, 0.0001\}$ computed over all on the order of 10^{10} impostor scores. The FMR in each bin will vary also - see subsequent impostor heatmaps in sec. 3.6.2. Given a pair of face images taken at different times, we assign the comparison to the bin that is the arithmetic average of the subject's ages. This plot shows only the effect of age, not ageing. The number of comparisons in each bin is generally in the thousands, however the first and last bins are computed over 149 and 124 respectively. The error rates in some (adult) cases are zero, and in others the DET is flat so the error rates at the two thresholds are identical. The lines span 1% and 99% of bootstrap replicated FNMR estimates.



Caveats: None.

3.6 Impostor distribution stability

3.6.1 Effect of birth place on the impostor distribution

Background: Facial appearance varies geographically, both in terms of skin tone, cranio-facial structure and size. This section addresses whether false match rates vary intra- and inter-regionally.

Goals:

- ▷ To show the effect of birth region of the impostor and enrollee on false match rates.
- ▷ To determine whether some algorithms give better impostor distribution stability.

Methods:

- ▷ For the visa images, NIST defined 10 regions: Sub-Saharan Africa, South Asia, Polynesia, North Africa, Middle East, Europe, East Asia, Central and South America, Central Asia, and the Caribbean.
- ▷ For the visa images, NIST mapped each country of birth to a region. There is some arbitrariness to this. For example, Egypt could reasonably be assigned to the Middle East instead of North Africa. An alternative methodology could, for example, assign the Philippines to *both* Polynesia and East Asia.
- ▷ FMR is computed for cases where all face images of impostors born in region r_2 are compared with enrolled face images of persons born in region r_1 .

$$\text{FMR}(r_1, r_2, T) = \frac{\sum_{i=1}^{N_{r_1, r_2}} H(s_i - T)}{N_{r_1, r_2}} \quad (5)$$

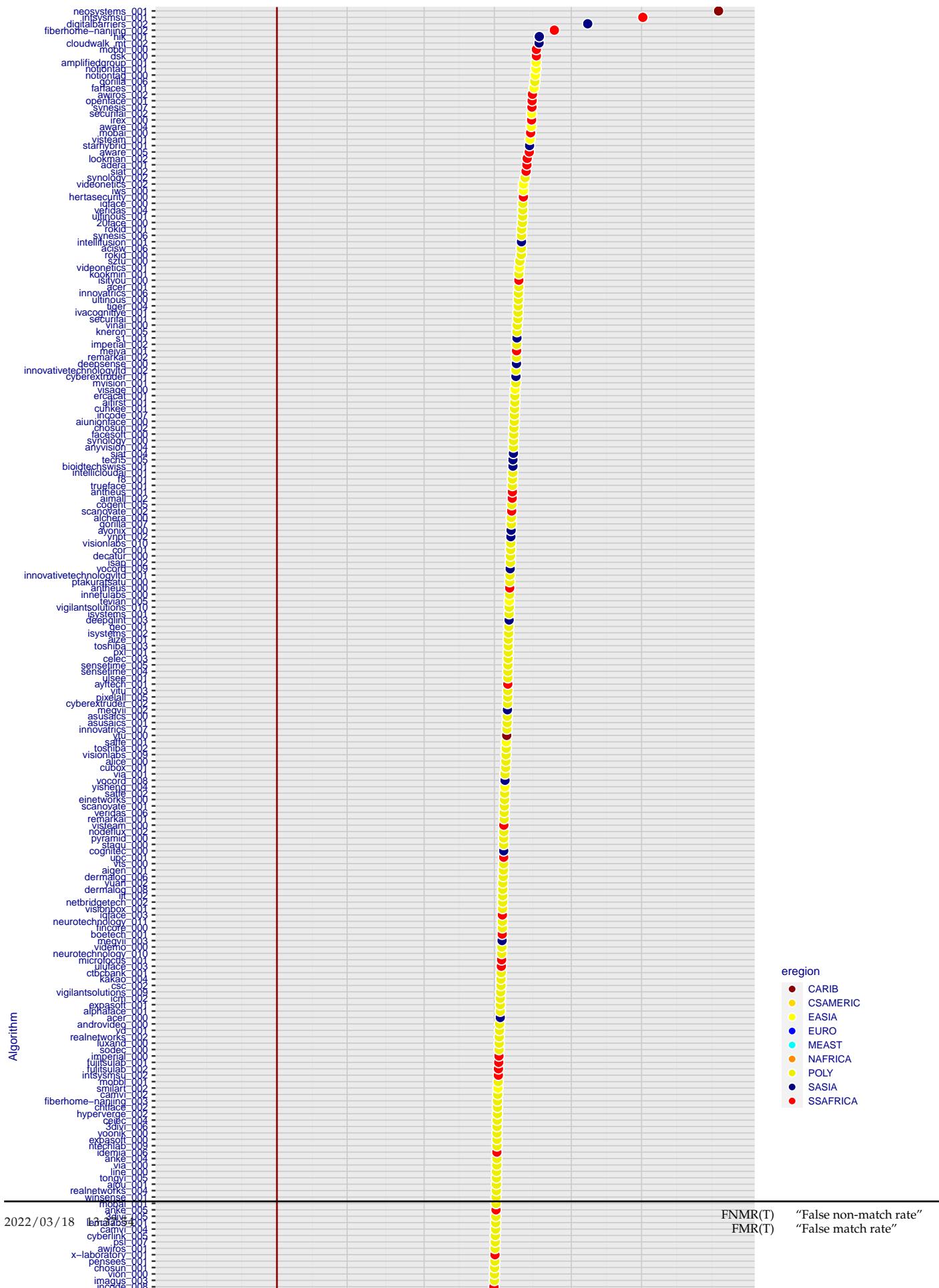
where the same threshold, T , is used in all cells, and H is the unit step function. The threshold is set to give $\text{FMR}(T) = 0.001$ over the entire set of visa image impostor comparisons.

- ▷ This analysis is then repeated by country-pair, but only for those country pairs where both have at least 1000 images available. The countries¹ appear in the axes of graphs that follow.
- ▷ The mean number of impostor scores in any cross-region bin is 33 million. The smallest number of impostor scores in any bin is 135000, for Central Asia - North Africa. While these counts are large enough to support reasonable significance, the number of individual faces is much smaller, on the order of $N^{0.5}$.
- ▷ The numbers of impostor scores in any cross-country bin is shown in Figure ??.

Results: Subsequent figures show heatmaps that use color to represent the base-10 logarithm of the false match rate. Red colors indicate high (bad) false match rates. Dark colors indicate benign false match rates. There are two series of graphs corresponding to aggregated geographical regions, and to countries. The notable observations are:

- ▷ The on-diagonal elements correspond to within-region impostors. FMR is generally above the nominal value of $\text{FMR} = 0.001$. Particularly there is usually higher FMR in, Sub-Saharan Africa, South Asia, and the Caribbean. Europe and Central Asia, on the other hand, usually give FMR closer to the nominal value.
- ▷ The off-diagonal elements correspond to across-region impostors. The highest FMR is produced between the Caribbean and Sub-Saharan Africa.
- ▷ Algorithms vary.

¹These are Argentina, Australia, Brazil, Chile, China, Costa Rica, Cuba, Czech Republic, Dominican Republic, Ecuador, Egypt, El Salvador, Germany, Ghana, Great Britain, Greece, Guatemala, Haiti, Hong Kong, Honduras, Indonesia, India, Israel, Jamaica, Japan, Kenya, Korea, Lebanon, Mexico, Malaysia, Nepal, Nigeria, Peru, Philippines, Pakistan, Poland, Romania, Russia, South Africa, Saudi Arabia, Thailand, Trinidad, Turkey, Taiwan, Ukraine, Venezuela, and Vietnam.



- ▷ We computed the same quantities for a global FMR = 0.0001. The effects are similar.

Caveats:

- ▷ The effects of variable impostor rates on one-to-many identification systems may well differ from what's implied by these one-to-one verification results. Two reasons for this are a) the enrollment galleries are usually imbalanced across countries of birth, age and sex; b) one-to-many identification algorithms often implement techniques aimed at stabilizing the impostor distribution. Further research is necessary.
- ▷ In principle, the effects seen in this subsection could be due to differences in the image capture process. We consider this unlikely since the effects are maintained across geography - e.g. Caribbean vs. Africa, or Japan vs. China.

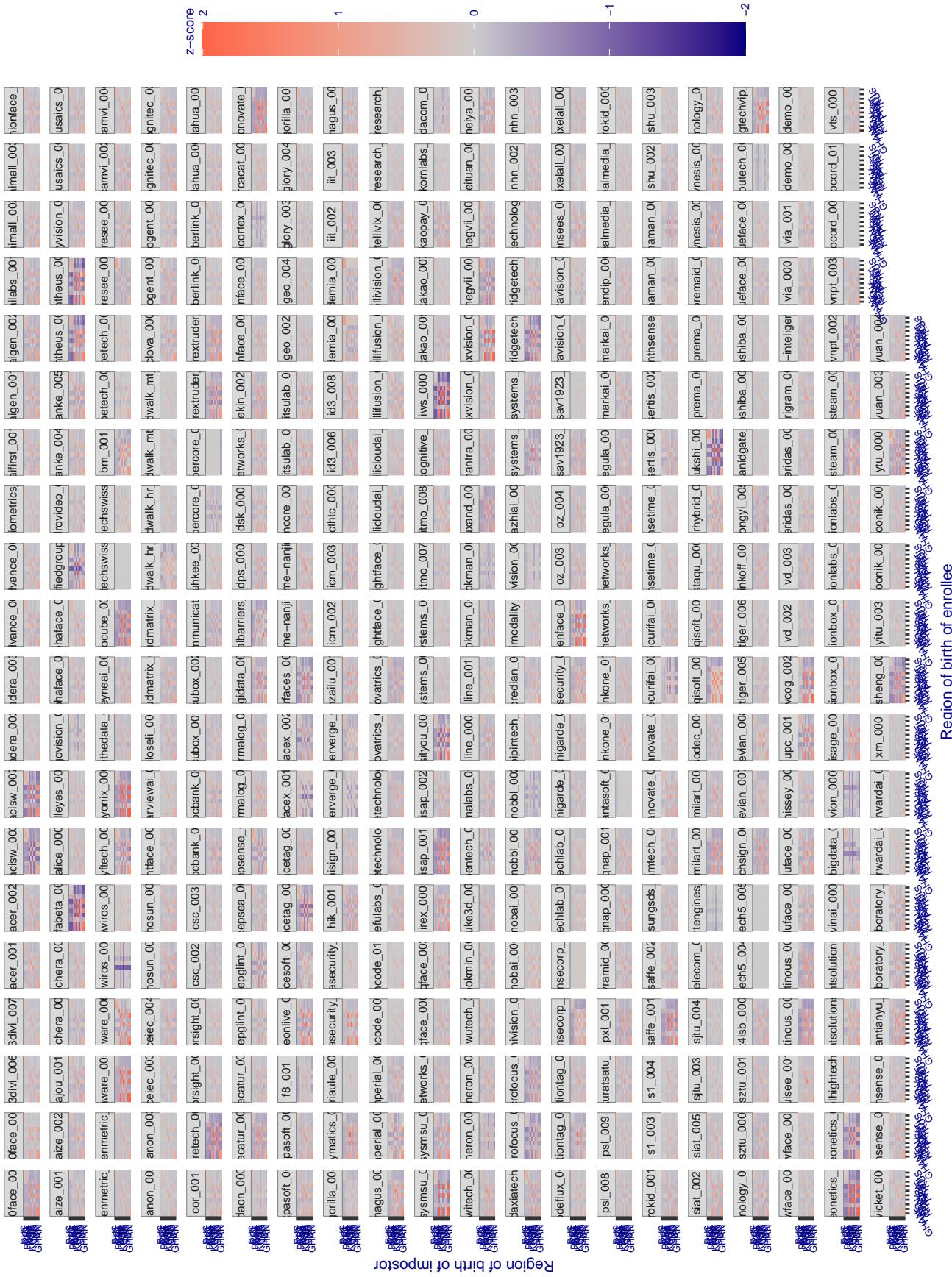


Figure 330: For visa images, the heatmap shows how the mean of the impostor distribution for the country pair (a,b) is shifted relative to the mean of the global impostor distribution, expressed as a number of standard deviations of the global impostor distribution. This statistic is designed to show shifts in the entire impostor distribution, not just tail effects that manifest as the anomalously high (or low) false match rates that appear in the subsequent figures. The countries are chosen to show that skin tone alone does not explain impostor distribution shifts. The reduced shift in Asian populations with the Yitu and Tong YiTrans algorithms, is accompanied by positive shifts in the European populations. This reversal relative to most other algorithms, may derive from use of nationally weighted training sets. The figure is computed from same-sex and same-age impostor pairs.

3.6.2 Effect of age on impostors

Background: This section shows the effect of age on the impostor distribution. The ideal behaviour is that the age of the enrollee and the impostor would not affect impostor scores. This would support FMR stability over sub-populations.

Goals:

- ▷ To show the effect of relative ages of the impostor and enrollee on false match rates.
- ▷ To determine whether some algorithms have better impostor distribution stability.

Methods:

- ▷ Define 14 age group bins, spanning 0 to over 100 years old.
- ▷ Compute FMR over all impostor comparisons for which the subjects in the enrollee and impostor images have ages in two bins.
- ▷ Compute FMR over all impostor comparisons for which the subjects are additionally of the same sex, and born in the same geographic region.

Results:

The notable aspects are:

- ▷ Diagonal dominance: Impostors are more likely to be matched against their same age group.
- ▷ Same sex and same region impostors are more successful. On the diagonal, an impostor is more likely to succeed by posing as someone of the same sex. If $\Delta \log_{10} \text{FMR} = 0.2$, then same-sex same-region FMR exceeds the all-pairs FMR by factor of $10^{0.2} = 1.6$.
- ▷ Young children impostors give elevated FMR against young children. Older adult impostor give elevated FMR against older adults. These effects are quite large, for example if $\Delta \log_{10} \text{FMR} = 1.0$ larger than a 32 year old, then these groups have higher FMR by a factor of $10^1 = 10$. This would imply an FMR above 0.01 for a nominal (global) FMR = 0.001.
- ▷ Algorithms vary.
- ▷ We computed the same quantities for a global FMR = 0.0001. The effects are similar.

Note the calculations in this section include impostors paired across all countries of birth.

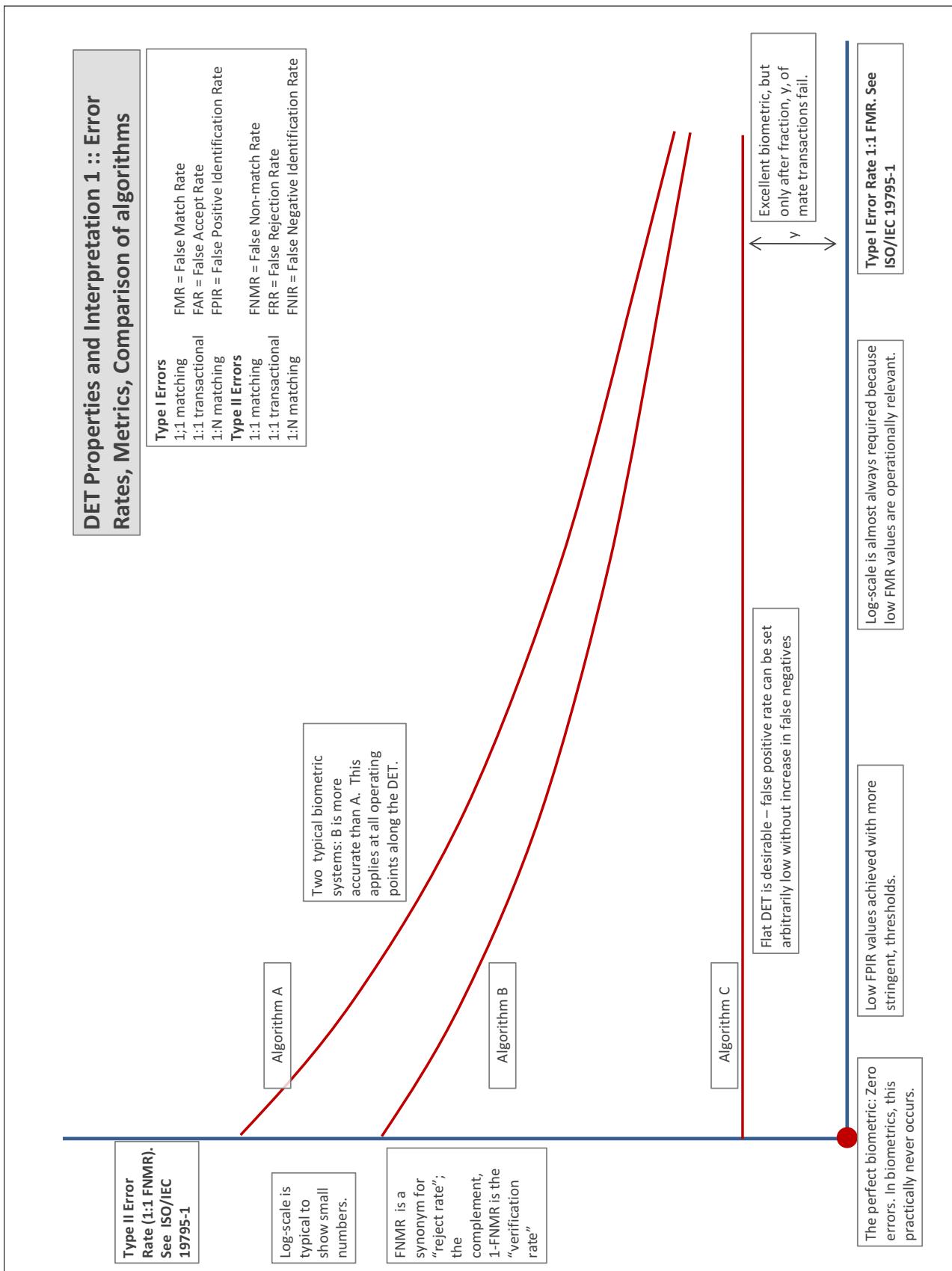
Accuracy Terms + Definitions

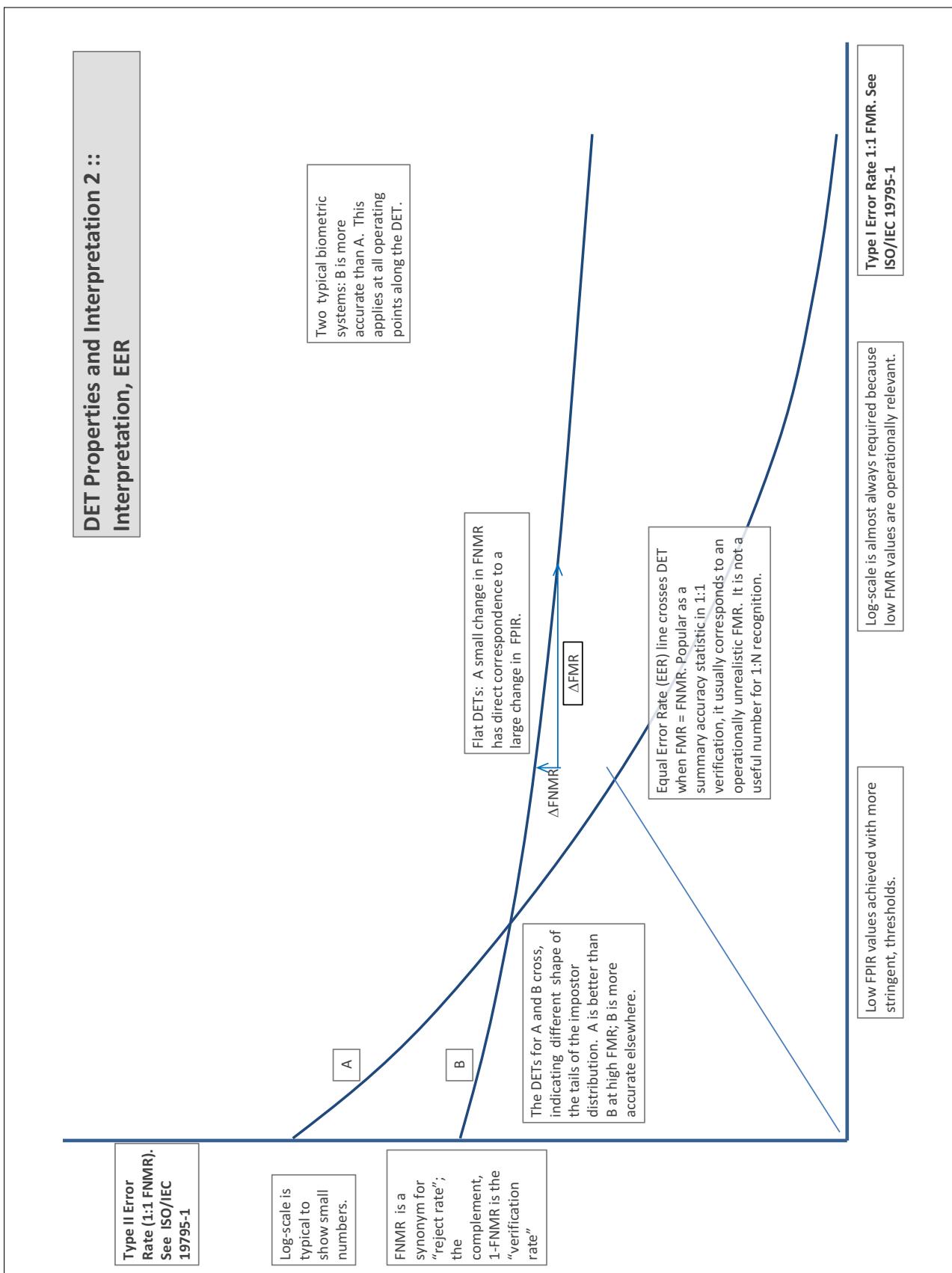
In biometrics, Type II errors occur when two samples of one person do not match – this is called a **false negative**. Correspondingly, Type I errors occur when samples from two persons do match – this is called a **false positive**. Matches are declared by a biometric system when the native comparison score from the recognition algorithm meets some **threshold**. Comparison scores can be either **similarity scores**, in which case higher values indicate that the samples are more likely to come from the same person, or **dissimilarity scores**, in which case higher values indicate different people. Similarity scores are traditionally computed by **fingerprint** and **face** recognition algorithms, while dissimilarities are used in **iris recognition**. In some cases, the dissimilarity score is a distance; this applies only when **metric** properties are obeyed. In any case, scores can be either **mate** scores, coming from a comparison of one person's samples, or **nonmate** scores, coming from comparison of different persons' samples. The words **genuine** or **authentic** are synonyms for mate, and the word **impostor** is used as a synonym for nonmatch. The words mate and nonmatch are traditionally used in identification applications (such as law enforcement search, or background checks) while genuine and impostor are used in verification applications (such as access control).

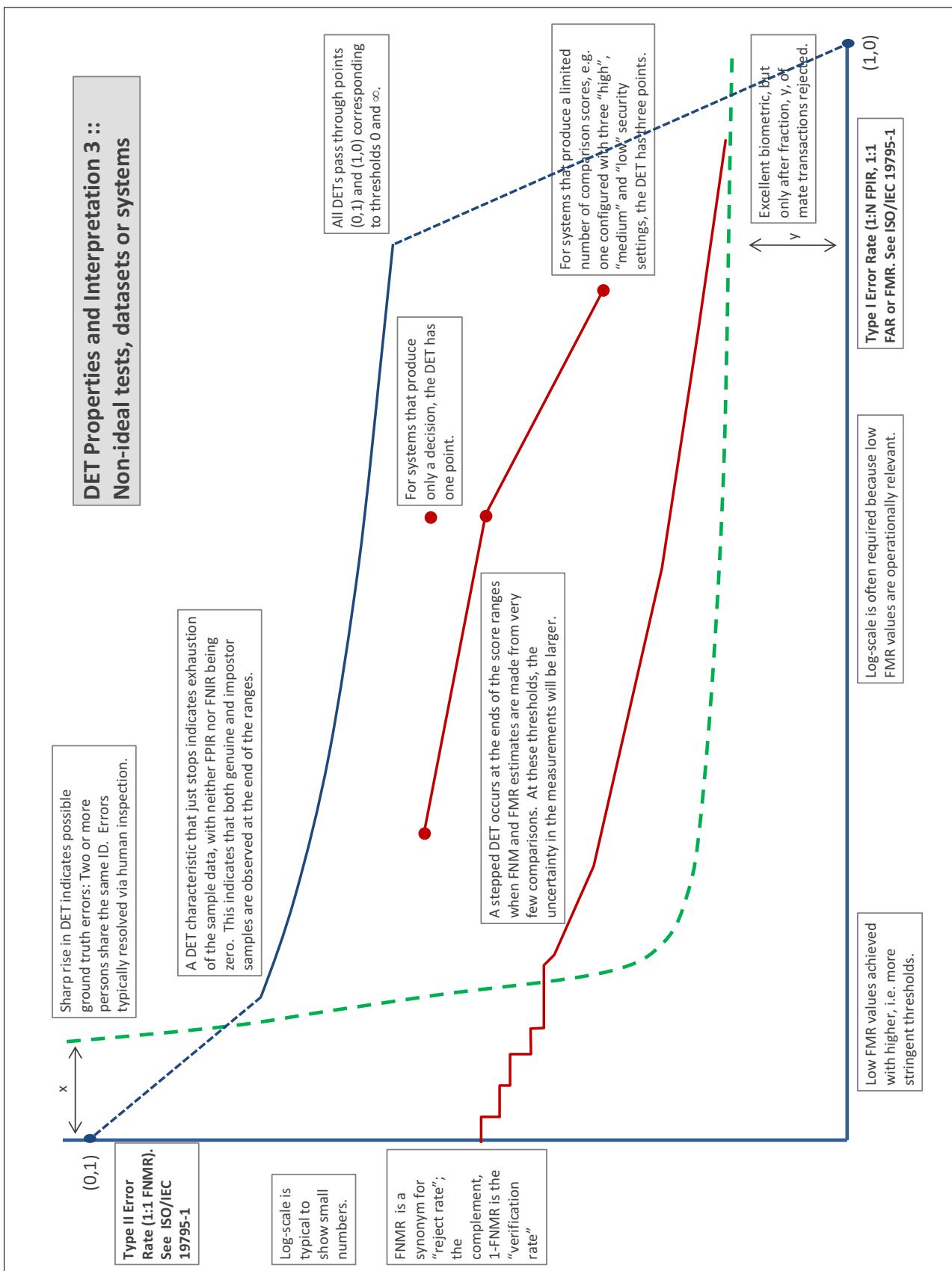
A **error tradeoff** characteristic represents the tradeoff between Type II and Type I classification errors. For verification this plots false non-match rate (FNMR) vs. false match rate (FMR) parametrically with T.

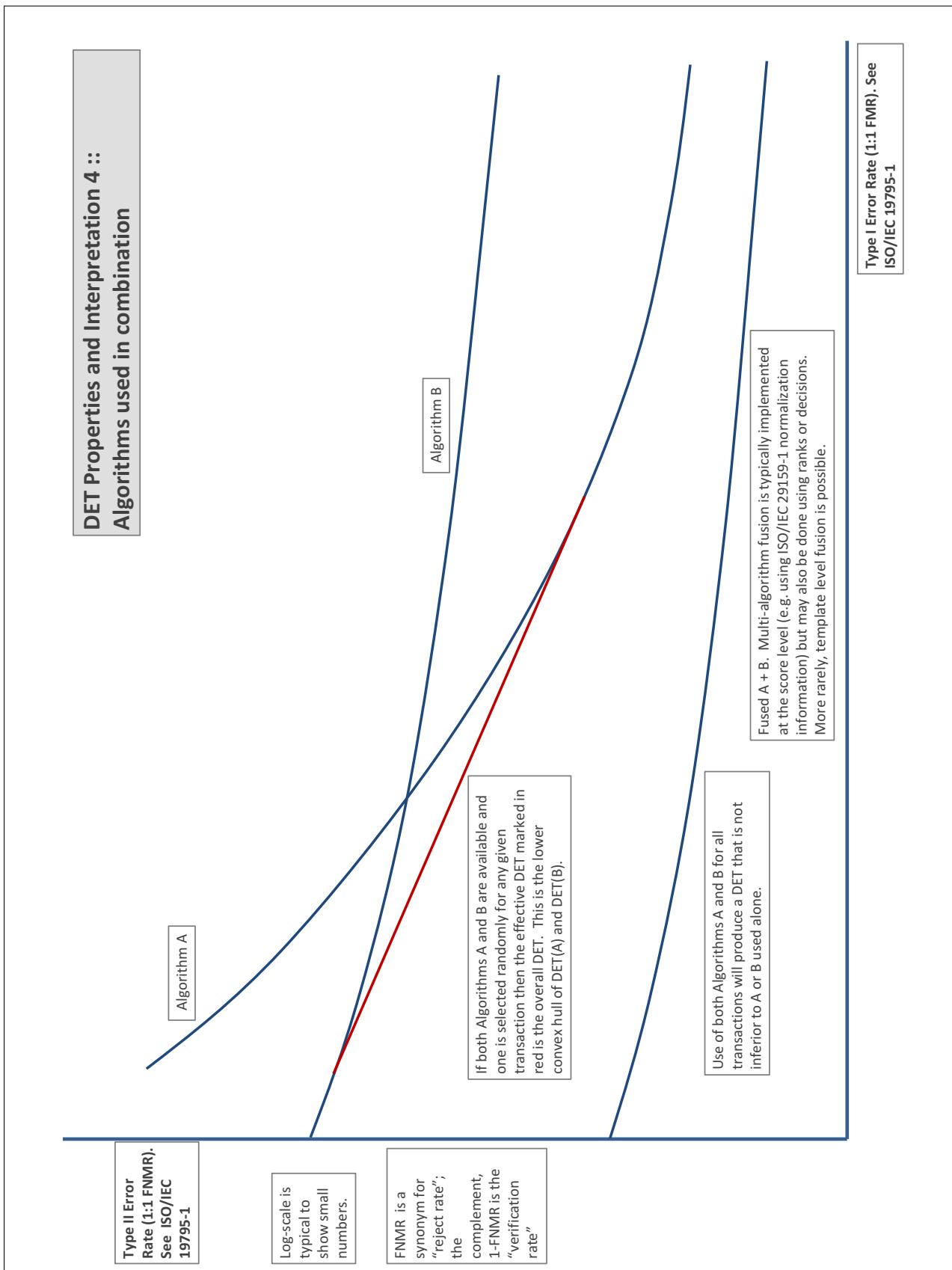
The error tradeoff plots are often called **detection error tradeoff (DET)** characteristics or **receiver operating characteristic (ROC)**. These serve the same function but differ, for example, in plotting the complement of an error rate (e.g., $TMR = 1 - FNMR$) and in transforming the axes most commonly using logarithms, to show multiple decades of FMR. More rarely, the function might be the inverse Gaussian function.

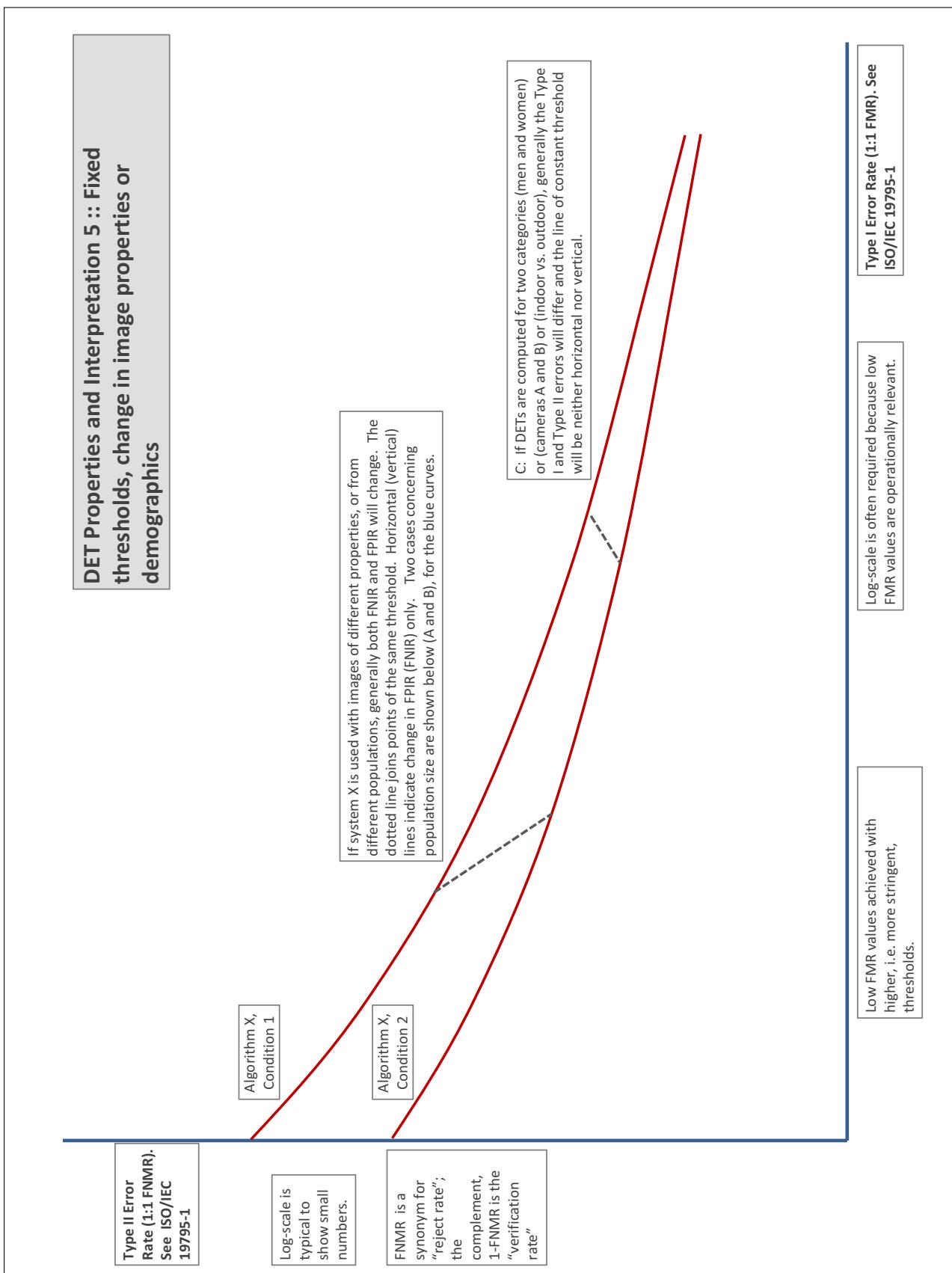
More detail and generality is provided in formal biometrics testing standards, see the various parts of [ISO/IEC 19795 Biometrics Testing and Reporting](#). More terms, including and beyond those to do with accuracy, see [ISO/IEC 2382-37 Information technology -- Vocabulary -- Part 37: Harmonized biometric vocabulary](#)











References

- [1] P. Jonathon Phillips, Amy N. Yates, Ying Hu, Carina A. Hahn, Eilidh Noyes, Kelsey Jackson, Jacqueline G. Cavazos, Géraldine Jeckeln, Rajeev Ranjan, Swami Sankaranarayanan, Jun-Cheng Chen, Carlos D. Castillo, Rama Chellappa, David White, and Alice J. O'Toole. Face recognition accuracy of forensic examiners, superrecognizers, and face recognition algorithms. *Proceedings of the National Academy of Sciences*, 115(24):6171–6176, 2018.